



**AALBORG UNIVERSITY**  
DENMARK

**Aalborg Universitet**

## **Optimization of large-scale offshore wind farm**

Hou, Peng

*DOI (link to publication from Publisher):*  
[10.5278/vbn.phd.eng.00005](https://doi.org/10.5278/vbn.phd.eng.00005)

*Publication date:*  
2017

*Document Version*  
Publisher's PDF, also known as Version of record

[Link to publication from Aalborg University](#)

*Citation for published version (APA):*

Hou, P. (2017). *Optimization of large-scale offshore wind farm*. Aalborg Universitetsforlag. PhD Series, Faculty of Engineering and Science, Aalborg University <https://doi.org/10.5278/vbn.phd.eng.00005>

### **General rights**

Copyright and moral rights for the publications made accessible in the public portal are retained by the authors and/or other copyright owners and it is a condition of accessing publications that users recognise and abide by the legal requirements associated with these rights.

- ? Users may download and print one copy of any publication from the public portal for the purpose of private study or research.
- ? You may not further distribute the material or use it for any profit-making activity or commercial gain
- ? You may freely distribute the URL identifying the publication in the public portal ?

### **Take down policy**

If you believe that this document breaches copyright please contact us at [vbn@aub.aau.dk](mailto:vbn@aub.aau.dk) providing details, and we will remove access to the work immediately and investigate your claim.



# **OPTIMIZATION OF LARGE-SCALE OFFSHORE WIND FARM**

**BY  
PENG HOU**

DISSERTATION SUBMITTED 2017



**AALBORG UNIVERSITY**  
DENMARK





# OPTIMIZATION OF LARGE-SCALE OFFSHORE WIND FARM

PH.D. THESIS

by

Peng Hou

Department of Energy Technology

Aalborg University, Denmark

May, 2017



**AALBORG UNIVERSITY**  
DENMARK

Dissertation submitted: May 2017

PhD supervisor: Professor Zhe Chen  
Aalborg University  
Assistant PhD supervisor: Associate Professor  
Weihao Hu  
Aalborg University

PhD committee: Associate Professor Jayakrishnan R. Pilai  
(Chairman)  
Aalborg University  
Professor Constantine (Costas) D. Vournas  
National Technical University of Athens  
Professor Surya Santoso  
The University of Texas at Austin

PhD Series Faculty of Engineering and Science, Aalborg  
University

ISSN (online): 2446-1636

ISBN (online): 978-87-7112-900-7

Published by:  
Aalborg University Press  
Skjernvej 4A, 2nd floor  
DK – 9220 Aalborg Ø  
Phone: +45 99407140  
aauf@forlag.aau.dk  
forlag.aau.dk

© Copyright: Peng Hou

Printed in Denmark by Rosendahls, 2017



## CV

Peng Hou received the B. Sc. degree in electrical engineering and automation from the Hebei University of Technology, China in 2008 and M. Sc. degree in electric power engineering from Chalmers University of Technology, Sweden in 2010. He is working toward the PhD degree in the department of Energy Technology, Aalborg University Denmark. His research interests are wind farm optimization, electricity market, integrated energy system, hydrogen storage system and algorithm application and development.

# ABSTRACT

As one of the renewable resources, wind energy has drawn more and more attention worldwide. Compared with onshore case, there is always more wind with less turbulence exists offshore which promotes the development of offshore wind farm. Presently, the capacity of offshore wind farm has been over 1 GW. In such a large scale wind farm, hundreds of wind turbines (WT) and plenty of equipment are required to be installed which highlights the significance of optimization for offshore wind farm.

The wake loss is one of the dominant factors that influence the power reached at the onshore substation. It can be described as the impacts of the upstream WTs to the downstream ones which reduce the total energy yield of the wind farm due to the wind speed drop downstream. If larger spacing is arranged between each pair of WTs then the wake losses can be reduced. However, this could result in a bad investment due to the increase on the cost of connection. In addition, the design of the electrical system as the selection of electrical equipment, substation design regarding location and quantity, cable connection topology design significantly contributes to the overall performance of the wind farm. Hence, it is necessary to develop a method and procedure to optimize wind farm layout as well as the system topologies to make a cost-effective wind farm.

This dissertation studies the optimization of offshore wind farm with the objective of minimizing the Levelized Production Cost (LPC) which cares three aspects: the energy yields considering the wake losses, power losses within the electrical system as well as the investment. Many works has been done on optimizing the WT positions to increase the energy production. However, the restriction zone offshore which was formulated due to existing gas pipe or oil well was not taken into consideration. In addition, the electrical system layout which is correlated to wind farm layout has not yet accounted in the WT locating work. On the other hand, the electrical system (the cost of which could take up to 30% of capital investment) optimization including voltage selection, cable connection scheme determination and offshore substation design was done in some previous work. However, no the existing works took uncrossed cable connection layout as one constraint and the proposed algorithms were applied in a simplified searching domain where some potential solutions are neglected due to computational cost. A new algorithm should be proposed to find a better layout to benefit the wind farm owner. The above problems were analyzed and solved in this thesis work step by step as follows: a. Optimization of offshore wind farm layout was done either for a regular distribution strategy or irregular one to minimize the wake losses. b. The electrical system design was improved for offshore wind farm to realize the reduced cost of energy by minimizing system cost and loss, improving energy production, while meet the operational requirements of power systems. c. The optimized control strategy was

## ABSTRACT

investigated to further benefit the offshore wind farm owner. d. The overall optimization work which takes a and b or a and c into account so that a co-optimization work can be done.

This research work gives an overall optimization of offshore wind farm. It firstly proposed two methods of wake losses estimation corresponding to offshore wind farm with homogeneous and mixed types of WTs respectively. Then the wind farm layout was optimized to minimize the wake losses based on the proposed method. Afterwards, this dissertation comes up with the novel way of electrical system design which concerns the voltage selection, offshore substation locating and quantity determination as well as the cable connection layout design. At last the thesis concludes the whole research work and outlook the future development trends.

## DANSK RESUME

Som en af de vedvarende ressourcer, har vindenergi trukket mere og mere opmærksomhed i hele verden. Sammenlignet med onshore tilfælde, er der altid mere vind med mindre turbulens findes offshore som fremmer udviklingen af havmølleparken. I øjeblikket har kapacitet havmølleparken været over 1 GW. I en sådan storstilet vindmøllepark, er hundredvis af vindmøller (WT) og masser af udstyr, der kræves for at blive installeret der fremhæver betydningen af optimering for havvindmøllepark.

Den kølvandet tab er en af de dominerende faktorer, der påvirker strømmen nået på onshore transformerstationen. Det kan beskrives som virkningerne af de opstrøms wts til de efterfølgende dem, der reducerer det samlede udbytte af vindmølleparken energi på grund af vindhastigheden drop nedstrøms. Hvis større rum er anbragt mellem hvert par af WTS derefter tab wake kan reduceres. Imidlertid kunne dette resultere i en dårlig investering på grund af stigningen på prisen på forbindelsen. Hertil kommer, at udformningen af det elektriske system som udvælgelsen af elektrisk udstyr, understation design med hensyn til placering og mængde, kabeltilslutning topologi design bidrager væsentligt til de samlede resultater af vindmølleparken. Derfor er det nødvendigt at udvikle en fremgangsmåde og procedure til at optimere vindmøllepark layout samt systemet topologier til at gøre en omkostningseffektiv vindmøllepark.

Denne afhandling undersøger optimering af havmølleparken med det formål at minimere udjævnedede Production Cost (LPC), som bekymrer sig tre aspekter: den energi udbytter overvejer tab wake, effekttab i det elektriske system samt investeringen. Mange værker er blevet gjort på at optimere de WT positioner for at øge energiproduktionen, men begrænsningen zone offshore som blev formuleret på grund af den eksisterende gasledning eller olie kilde blev ikke taget i betragtning. Desuden har det elektriske system layout, som er korreleret til vindmølleparken layout endnu ikke tegnede i WT lokalisering arbejde. På den anden side, det elektriske system (og omkostningerne herved kan tage op til 30% af investeringskapital) optimering herunder spænding udvælgelse, ordning kabelforbindelse beslutsomhed og offshore transformerstation design blev gjort i nogle tidligere arbejde. Dog ingen af de eksisterende værker tog uncrossed kabeltilslutning layout som en begrænsning, og de foreslåede algoritmer blev anvendt i en forenklet søgning domænenavn nogle potentielle løsninger er forsømt på grund af beregningsmæssige omkostninger. En ny algoritme bør foreslås for at finde en bedre layout til gavn vindmølleparken ejer. De ovennævnte problemer blev analyseret og løst i denne afhandling arbejde skridt for skridt som følger: a. Optimering af havmølleparken layout blev gjort enten for en regelmæssig distributionsstrategi eller uregelmæssig en til at minimere tabene morgenvækning. b. Det elektriske system design blev forbedret for havmøllepark at realisere den

reducerede energiomkostninger ved at minimere systemets omkostninger og tab, forbedre energiproduktion, mens opfylde de operationelle krav elsystemer. c. Den optimerede kontrolstrategi blev undersøgt for yderligere gavne havvindmølleparken ejer. d. Den samlede optimering arbejde, som tager a og b eller a og c i betragtning, således at en co-design Arbejdet kan udføres.

Denne forskning giver en samlet optimering af havmølleparken. Det første foreslået to metoder til tab morgenvækning estimering svarende til havmøllepark med homogene og blandede typer af WTS hhv. Så vindmølleparken layout blev optimeret til at minimere tabene wake baseret på den foreslåede metode. Bagefter denne afhandling kommer op med den ny måde elektriske system design, der vedrører spændingen udvælgelse, offshore transformerstation lokalisering og mængde beslutsomhed samt kabelforbindelsen layout design. Omsider afhandlingen konkluderer hele forskningsarbejde og udsigterne de fremtidige udviklingstendenser.

# THESIS DETAILS AND PUBLICATIONS

**Thesis Title:** Optimization of large-scale offshore wind farm

**Ph.D. Student:** Peng Hou

**Supervisor:** Zhe Chen

**Co-supervisor:** Weihao Hu

## **List of Publications:**

### **Journal papers**

J1 Peng Hou, Weihao Hu, Mohsen Soltani, Zhe Chen, “Optimized Placement of Wind Turbines in Large Scale Offshore Wind Farm using Particle Swarm Optimization Algorithm,” *IEEE Transactions on Sustainable Energy*, Vol. 6, Issue 4, pp.1272-1282, 2015.

J2 Peng Hou, Weihao Hu, Mohsen Soltani, Zhe Chen, “Optimization of Offshore Wind Farm Layout Considering Restriction Zone,” *Energy*, Vol. 113, pp. 487-496, 15 Oct. 2016.

J3 Peng Hou, Weihao Hu, Mohsen Soltani, Cong Chen, Baohua Zhang, Zhe Chen, “Offshore Wind Farm Layout Design Considering Optimized Power Dispatch Strategy,” *IEEE Transaction on Sustainable Energy*, Vol. 8, Issue 2, pp. 638-647, 2016.

J4 Peng Hou, Weihao Hu, Baohua Zhang, Mohsen Soltani, Cong Chen, Zhe Chen, “Optimised Power Dispatch Strategy for Offshore Wind Farms,” *IET Renewable Power Generation*, Vol. 10, Issue 3, pp. 399-409, 2016.



J5 Peng Hou, Weihao Hu, Cong Chen, Zhe Chen, “Optimization of Offshore Wind Farm Cable Connection Layout Considering Levelised Production Cost Using Dynamic Minimum Spanning Tree Algorithm,” *IET Renewable Power Generation*, Vol. 10, Issue 2, pp. 175-183, Feb. 2016.

J6 Peng Hou, Weihao Hu, Zhe Chen, “Optimization for Offshore Wind Farm Cable Connection Layout using Adaptive Particle Swarm Optimisation Minimum Spanning Tree Method,” *IET Renewable Power Generation*, Vol. 10, Issue 5, pp. 694-702, 2016.

J7 Peng Hou, Weihao Hu, Cong Chen, Mohsen Soltani, Zhe Chen, “A Novel Way for Offshore Wind Farm Cable Connection Layout Design with Meta-heuristic Optimization,” *Renewable energy*, first revision.

J8 Peng Hou, Weihao Hu, Cong Chen, Zhe Chen, “Overall Optimization for Offshore Wind Farm Electrical System,” *Wind energy*, 2016, DOI: [10.1002/we.2077](https://doi.org/10.1002/we.2077).

J9 Peng Hou, Weihao Hu, Mohsen Soltani, Cong Chen, Zhe Chen, “Combined Optimization for Offshore Wind Farm Planning,” *Applied energy*, Vol. 189, pp. 271-282, March 2017.

J10 Peng Hou, Peter Enevoldsen, Weihao Hu, Zhe Chen, “Offshore Wind Farm Repowering Optimization,” *Applied Energy*, submitted.

J11 Peng Hou, Peter Enevoldsen, Joshua Eichman, Weihao Hu, Mark Z. Jacobson, Zhe Chen, “Optimizing Investments in Coupled Offshore Wind -Electrolytic Hydrogen Storage Systems in Denmark,” *Journal of power sources*, 1<sup>st</sup> revision.

J12 Peng Hou, Weihao Hu, Zhe Chen, “A Review of Offshore Wind Farm Layout Optimization and Electrical System Design,” *Renewable & Sustainable Energy Reviews*, submitted.

J13 Baohua Zhang, Weihao Hu, Peng Hou, Mohsen Soltani, Cong Chen, Zhe Chen, “A Reactive Power Dispatch Strategy with Loss Minimization for a DFIG Based Wind Farm,” *IEEE Transactions on Sustainable Energy*, Vol. 7, pp. 914-923, July 2016.

J14 Nuri Gökmen, Weihao Hu, Peng Hou, Zhe Chen, Dezso Sera, Sergiu Spataru, “Investigation of wind speed cooling effect on PV panels in windy locations,” *Renewable Energy*, pp. 283-290, 2016.

J15 Thomas Bak, Angus Graham, Alla Saprionova, Mihai Florian, John Sorensen, Torben Knudsen, Peng Hou, Zhe Chen, “Baseline Layout and Design of a 0.8 GW Reference Wind farm in the North Sea,” *Wind Energy*, 2017.

J16 Baohua Zhang, Mohsen Soltani, Weihao Hu, Peng Hou, Zhe Chen, “Optimized Power Dispatch in Wind Farms for Power Maximizing Considering Fatigue Loads,” *IEEE Transactions on Sustainable Energy*, 1<sup>st</sup> revision.

J17 Baohua Zhang, Weihao Hu, Peng Hou, Jin Tan, Mohsen Soltani, Zhe Chen, “Review of Reactive Power Dispatch Strategies for Loss Minimization in a DFIG based Wind Farm,” *IEEE Transactions on Sustainable Energy*, submitted.

### **Conference papers:**

C1 Peng Hou, Weihao Hu, Zhe Chen, “Offshore Substation Locating in Wind Farms Based on Prim Algorithm,” *Power and Energy Society General Meeting 2015*, pp. 1-5, 26-30 July 2015. (Best Paper Award)

C2 Peng Hou, Weihao Hu, Zhe Chen, “Offshore Wind Farm Cable Connection Configuration Optimization using Dynamic Minimum Spinning

Tree Algorithm,” *50th IEEE International Universities Power Engineering Conference, UPEC 2015*, England, UK, pp.1-5, 2015.

C3 Peng Hou, Weihao Hu, Mohsen Soltani and Zhe Chen, “A Novel Energy Yields Calculation Method for Irregular Wind Farm Layout,” *41th Annual Conference of the IEEE Industrial Electronics Society (IECON 2015)*, Yokohama, Japan, pp. 000380-000385, 2015, doi: [10.1109/IECON.2015.7392129](https://doi.org/10.1109/IECON.2015.7392129).

C4 Peng Hou, Weihao Hu, Mohsen Soltani, Baohua Zhang, Zhe Chen, “Optimization of Decommission Strategy for Offshore Wind Farms,” *Proceedings of the 2016 IEEE Power & Energy Society General Meeting 2016*, pp. 1-5, 2016.

C5 Peng Hou, Weihao Hu, Mohsen Soltani and Zhe Chen, “A New Approach for Offshore Wind Farm Energy Yields Calculation with Mixed Hub Height Wind Turbines,” *Proceedings of the 2016 IEEE Power & Energy Society General Meeting 2016*, pp. 1-5, 2016.

C6 Peng Hou, Peter Enevoldsen, Weihao Hu, Zhe Chen, “Operational Optimization of Wind Energy Based Hydrogen Electrolysis Storage System Considering Electricity Market’s Influence,” *IEEE PES Asia-Pacific Power and Energy Engineering Conference 2016*, pp. 466-471, 2016.

C7 Peng Hou, Weihao Hu, Zhe Chen, “Optimal Selection of AC cables for Large Scale Offshore Wind Farms,” *IECON 2014 - 40th Annual Conference of the IEEE Industrial Electronics Society*, pp. 2206-2212, 2014.

C8 Baohua Zhang, Weihao Hu, Peng Hou, Zhe Chen, “Reactive Power Dispatch for Loss Minimization of a Doubly Fed Induction Generator

Based Wind Farm,” *2014 17th International Conference on Electrical Machines and Systems (ICEMS)*, pp. 1373 – 1378, 2014.

C9 Baohua Zhang, Weihao Hu, Peng Hou, Cong Chen, Mohsen Soltani, Zhe Chen, “Wind Farm Active Power Dispatch for Output Power Maximizing Based on a Wind Turbine Control Strategy for Load Minimizing,” *Proceedings of the International Conference on Sustainable Mobility Applications, Renewables and Technology 2015*, Kuwait, Nov. 2015.

C10 Baohua Zhang, Weihao Hu, Peng Hou, Mohsen Soltani, Zhe Chen, “Coordinated Power Dispatch of a PMSG based Wind Farm for Output Power Maximizing Considering the Wake Effect and Losses to the PESGM2016 Submission Site,” *Proceedings of the 2016 IEEE Power & Energy Society General Meeting 2016*, pp. 1-5, 2016.

C11 Baohua Zhang, Mohsen Soltani, Weihao Hu, Peng Hou, Zhe Chen, “A Wind Farm Active Power Dispatch Strategy for Fatigue Load Reduction,” *2016 American Control Conference*, pp. 1-5, 2016.

This thesis has been submitted for assessment in partial fulfilment of the PhD degree. The thesis is based on the submitted or published scientific papers which are listed above. Parts of the papers are used directly or indirectly in the extended summary of the thesis. As part of the assessment, co-author statements have been made available to the assessment committee and are also available at the Faculty.

# ACKNOWLEDGEMENTS

The Ph.D. study on the topic of “optimization of large scale offshore wind farm” is carried out at the Department of Energy Technology, Aalborg University, under the supervision of Prof. Zhe Chen and Associate Prof. Weihao Hu. This study is co-funded by Norwegian Centre for Offshore Wind Energy (NORCOWE) under grant 193821/S60 from Research Council of Norway (RCN) and the Department of Energy Technology, Aalborg University (ET-AAU), Denmark. Hereby, I would like to express my sincere thanks to NORCOWE and the department for giving me this precious research opportunity.

I would like to show grateful thanks to my supervisor Prof. Zhe Chen. Thank you for offering me this precious opportunity to pursue my Ph.D. study, as well as the instructive and fruitful supervision during my PhD study. Your constructive advices, suggestive discussions and patient corrections for every paper not only contribute to this work but also have a deep influence on my enhancement of researching ability, managing and even supervising. Furthermore, I would like to sincerely acknowledge my co-supervisor, Associated Prof. Weihao Hu for his inspired suggestions and invaluable help to both of my research and career. It is lucky to work under such a patient co-supervisor. I always have a discussion with him once I met some problem or got a new idea which took him a lot of time. However, he is always glad to supervise me any time.

Thanks for Dr. Angus Graham and Associate Prof. Birgitte Rugaard Furevik for their generous help and supports on wind data.

Also I would like to thank Associate Prof. Mohsen Soltani for his continuous help for academic discussion and paper corrections. Dr. Josh Eichman, Ph.D. fellow Baohua Zhang, Peter Enevoldsen and Nuri Gökmen, are thanked here for the great cooperation with you. Then I want to thank some researchers in our department, assistant professor Chi Su, Jiakun Fang and Dr. Dong Wang, thanks you all for the help on my research work. All you guys make the Ph.D. time with great enrichment.

Special thanks to my parents, who spare no effort to support me. I love you all so much just as you do all the time.

## ACKNOWLEDGEMENTS

Then I want to specially thank my beloved wife, Miao Yu who supports me and motivates me, then I can enjoy the research and life in a better way, as well as being a better man.

Finally but significantly, I want to thank my colleagues and all my best friends here. I cannot list your names one by one, but will write them in my heart. Thank you all for making our life so wonderful in this peaceful place. I will cherish the golden time we are together in my life.

Peng Hou

April 2017

Aalborg

# LIST OF ACRONYMS

<b>Abbreviation</b>	<b>Decsription</b>
WT	Wind Turbine
NORCOWE	Norwegian Centre for Offshore Wind Energy
NRWF	NORCOWE Reference Wind Farm
WFLO	Wind Farm Layout Optimization
PSO	Particle Swarm Optimization
GA	Genetic Algorithm
DE	Differential Evolution
ACO	Ant Colony Optimization
OS	Offshore Substation
MST	Minimum Spanning Tree
TSP	Travelling Salesman Problem
OVRP	Open Vehicle Routing Problem
AEP	Annual Energy Production
WFLOP	Wind Farm Layout Optimization Problem
LPC	Levelised Production Cost
CFD	Computational Fluid Dynamic
WAsP	Wind Atlas Analysis and Application software
D	Rotor Diameter
BPSO-TVAC	Binary Particle Swarm Optimization with Time-Varying Acceleration Coefficients
QIP	Quadratic Integer Programming
MILP	Mix-integer Linear Programming
MDPSO	Mixed-Discrete Particle Swarm Optimization
LCOE	Levelised Cost of Energy
RS	Random Search
MPPT	Maximum Power Point Tracking
CCLOP	Cable Connection Layout Optimization Problem
FCM	Fuzzy C-Means
GPSO	Global version PSO
TCS	Traditional Control Straetgy
OPD	Optimal Power Dispatch Strategy

LIST OF ACRONYMS

<b>Abbreviation</b>	<b>Description</b>
ESE	Evolutionary State Estimation
PSO-MAM	PSO with Multiple Adaptive Methods



# LIST OF SYMBOLS

Symbol	Description
$N_s$	Number of possible solutions
$N_{cell}$	Number of generated grids
$N_{WT}$	Number of WTs that is going to be installed
$S_{partial} [m^2]$	Effective wake area
$S_0 [m^2]$	Swpet area by WT blade
$V_w [m/s]$	Wind speed in the wake
$R(x) [m]$	Generated wake radius at x distance
$R_0 [m]$	WT's rotor radius
$V_x [m/s]$	Wind speed in the wake at a distance x
$V_0 [m/s]$	Incoming wind speed of wind farm
$C_t$	Thrust coefficient
k	Decay constant
$V_{ij} [m/s]$	Wake speed generated by the WT at $i^{th}$ row, $j^{th}$ column of wind farm
$N_{row}$	Number of WTs in a row
$N_{col}$	Number of WTs in a column
$V_{nm} [m/s]$	Wind velocity reached at the WT at row $n^{th}$ , column $m^{th}$ of wind farm
$V_j(\alpha, V_0) [m/s]$	Wind speed reached at the downstream WT j when the inflow wind velocity is $V_0$ and direction angle is $\alpha$
$M(i, j)$	Element of matrix M at row $i^{th}$ , column $j^{th}$
$z_{ij} [m]$	Hub height of WT at row $i^{th}$ , column $j^{th}$
$z_{ref} [m]$	Reference height for the measured wind speed
$h_0$	Surface roughness
$V_{0,ij} [m/s]$	Wind velocity at the blade of WT at $i^{th}$ row, $j^{th}$ column of wind farm
w	Inertia weight
$w_{initial}$	Initial inertia weight at the start of a given run
$w_{final}$	Final inertia weight at the end of a given run
n	Nonlinear modulation index
$I_{max}$	Maximum number of iteration
$l_1, l_2$	Learning factors

LIST OF SYMBOLS

<b>Symbol</b>	<b>Decsription</b>
$\text{rand}_1, \text{rand}_2$	Stochastic numbers that can generate some random
$\mathbf{x}_i^k, \mathbf{x}_i^{k+1}$	Position of particle $i$ at iteration $k$ and $k + 1$ , respectively
$\mathbf{v}_i^k, \mathbf{v}_i^{k+1}$	Speed of particle $i$ at iteration $k$ and $k + 1$ , respectively
$\text{local}_i^k$	Best position of particle $i$ at iteration $k$ .
$\text{glocal}_i^k$	Best position of all particles at iteration $k$
$P_{\text{mec}}$ [MW]	Power extracted from the wind
$V$ [m/s]	Inflow wind speed
$\rho$ [kg/m <sup>3</sup> ]	Air density
$R$ [m]	Blade radius
$\lambda$	Tip speed ratio
$\beta$ [°]	Blade pitch angle
$\omega_{\text{rot}}$ [r/min]	Rotor speed of generator
$C_p(\beta, \lambda)$	Power coefficient of WT with pitch angle $\beta$ and tip speed ratio $\lambda$
$C_i$ [MDKK/km]	Cable $i$ 's unit cost
$S_{n,i}$ [W]	Cable $i$ 's rated apparent power
$N$	Total quantity of cables in a wind farm
$A_p, B_p, C_p$	Coefficient of cable cost model
$I_{i,\text{rated}}$ [A]	Cable $i$ 's rated current
$U_{i,\text{rated}}$ [V]	Cable $i$ 's rated voltage
$L_i$ [km]	Cable $i$ 's length
$Q_i$	Quantity of cable $i$
$\text{CAPt}$ [MDkk]	Net present value of investment in year $t$
$C_0$ [MDkk]	Net present value of capital investment
$F_r(L_i)$	Distance between WT pair $L_i$
$\phi(L_i)$	Pental function of WT pair $L_i$
$d_x$	Spacing of WTs in $x$ axis
$d_y$	Spacing of WTs in $y$ axis

# TABLE OF CONTENTS

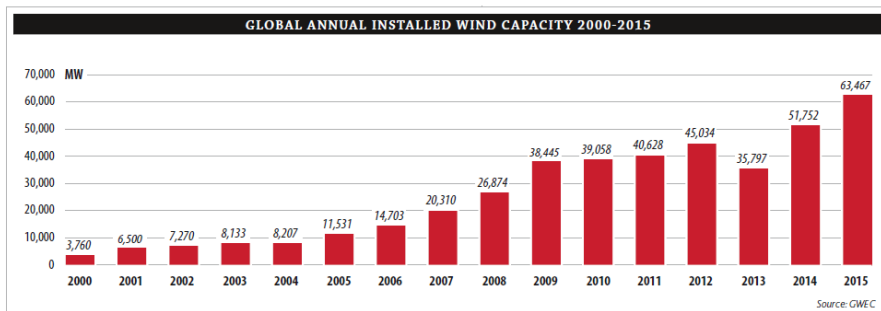
<b>Chapter 1. Introduction.....</b>	<b>1</b>
1.1. Background .....	1
1.2. Literature survey and motivation .....	4
1.2.1. Offshore wind farm micro siting .....	8
1.2.2. Optimized control strategy for offshore wind farm.....	11
1.2.3. Electrical system design for large scale offshore wind farm .....	12
1.2.4. Co-design concept of offshore wind farm .....	15
1.2.5. Future strategy: offshore wind farm repowering optimization .....	16
1.3. Research questions/hypothesis .....	17
1.4. Research objective and methodology .....	17
1.5. Technical contribution of the thesis .....	18
1.6. Project limitations .....	18
1.7. Organization of thesis .....	19
<b>Chapter 2. Energy production estimation for offshore wind farms .....</b>	<b>22</b>
2.1. State of art of wake loss estimation.....	22
2.2. Energy production estimation for offshore wind farms considering wake effect .....	22
2.2.1. Wake combination .....	23
2.2.2. Wake losses estimation by binary matrix method .....	25
2.2.3. Results and discussion.....	27
2.3. Wake losses estimation for offshore wind farm with mixed hub height wind turbines.....	29
2.3.1. Wind shear effect .....	29
2.3.2. Modified wake model for mixed hub height wind turbine offshore wind farm .....	29
2.3.3. Results and discussions .....	31
2.4. Summary .....	33
<b>Chapter 3. Optimized control strategy for offshore wind farms .....</b>	<b>35</b>
3.1. State of art of optimized wind farm control strategy .....	35
3.2. Optimization method.....	36

3.2.1. Particle swarm optimization (PSO).....	36
3.2.2. Mathematical expression.....	37
3.3. Optimized control strategy for offshore wind farms .....	38
3.3.1. Mathematical models .....	38
3.3.2. Objective function.....	40
3.4. Results and discussions .....	41
3.5. Summary .....	44
<b>Chapter 4. Offshore wind farm layout optimization.....</b>	<b>45</b>
4.1. State of art of WFLO.....	45
4.2. Regular shaped offshore WFLO .....	45
4.3. Irregular shaped offshore WFLO .....	49
4.4. Co-optimization of offshore wind farm layout.....	51
4.5. Summary .....	55
<b>Chapter 5. Electrical system design for large-scale offshore wind farms .....</b>	<b>57</b>
5.1. State of art of electrical system optimizatoin for offshore wind farm .....	57
5.2. Cable connection layout optimization using deterministic algorithms.....	57
5.3. Cable connection layout optimization using heuristic algorithm .....	60
5.4. Electrical system optimization for offshore wind farm .....	66
5.5. Summary .....	68
<b>Chapter 6. Offshore wind farm repowering optimization.....</b>	<b>70</b>
6.1. State of art of offshore wind farm decomissioning .....	70
6.2. Wind farm repowering optimization .....	71
6.3. Methodologies.....	72
6.4. Results and discussions .....	72
6.5. Summary .....	75
<b>Chapter 7. Conclusions and future works .....</b>	<b>76</b>
7.1. Conclusions.....	76
7.2. Future works .....	78
<b>Literature list.....</b>	<b>80</b>
<b>Appendix Paper A~O.....</b>	<b>89</b>

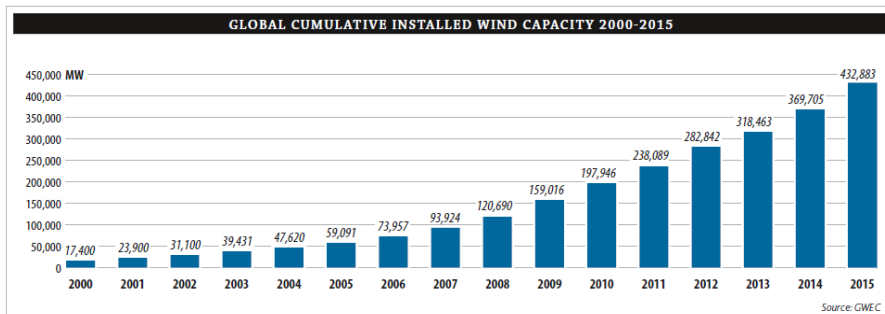
# CHAPTER 1. INTRODUCTION

## 1.1. BACKGROUND

Due to the increasing demand from clean energy, the utilization of prolific renewable energy such as wind energy becomes more and more popular. In 2015, the wind energy installation worldwide was over 63GW, a 22% increase. On the other hand, wind energy dominated more than 40% market share among the newly installed renewable energy. Both evidents demonstrated the significance of wind energy in meeting the energy requirement all over the world. The wind energy continues its rapid rising rate during the last 15 years as shown in Fig. 1.1 [1].



(a)



(b)

Figure 1.1 Wind power installation statistics. (a) Global annual installed capacity of wind from 2000 to 2015. (b) Global cumulative installed capacity of wind from 2000 to 2015. [1].

From Figure 1.1, it can be concluded that more than 43GW wind capacity was installed worldwide in 2015 which shows 22% enhancement compared with 2014. Except the suddenly drop of annual installed wind capacity in 2013, which is due to the unexpected situation in United State (merely 1GW installed), the annual installed wind power capacity continues its increasing trend during last 15 years. Wind power

has already provided more new power generation than any other forms of energies [1].

Presently, there are two forms of wind energy based generation technology, as offshore and onshore wind generation. The wind generation process can be simply described as the procedure of mechanical power conversion into electrical power by using wind to drive the rotation of WT blades. As to this process, there is no difference between onshore and offshore wind generation. However, it is not until 1991 that the first offshore wind farm (Vindeby) was commissioned and is about to be dismantled now [2] while the onshore wind farm technology has a longer history. Though much more investment is required for offshore wind farm, it still attracts more interests of researchers all over the world. For one thing that the wind offshore always has less turbulence and stable, for another it has no noise pollution to surrounding residents. In addition, it is a relatively new technology, there should be more space left for the researchers to investigate the method of planning a cost effective wind farm. The main characteristics of both onshore and offshore wind farm are concluded in table 1.1.

*Table 1.1 Differences comparison between onshore and offshore wind farm [3]*

<b>Offshore</b>		<b>Onshore</b>	
<i>Pros</i>	<i>Cons</i>	<i>Pros</i>	<i>Cons</i>
Wind speed increase in the afternoon which corresponds to the increase trend of power demand	Complex structures are needed to support the turbines in the sea	Simpler and cheaper technologies compared with offshore wind generation	WT operated at low efficiency
	Additional wear and tear from higher wind speeds or even storms makes the WTs more expensive than onshore ones		Long transmission lines are always required
O&M is more complicated and expensive. Skilled technicians with experiences are required			Harder to estimate AEP, due to complexity of terrain and surface – leading to an unsecure investment [4]
	Higher and consistent wind speed	Overall lower invest	Marring landscapes
Little impacts on residents	Impacts on humans (noise and flicker effect)		
		Wind speed increase in the night	

The purpose of wind farm layout optimization (WFLO) is to minimize the wake losses by optimizing the positions of each WT within the predefined area. The wake losses estimation for both onshore and offshore wind farms are relied on the same

model whereas with different wake model parameter setting. The wake model parameter settings for different conditions are concluded in table 1.2 as follows:

*Table 1.2 Wake parameter settings comparison among different conditions [5]*

<b>Terrain type</b>	<b>Wake Decay Constant</b>	<b>Description of application</b>
Offshore/Water areas	0.04	Water areas, seas or large lakes
Mixed water and land	0.052	Mixed water and land or very smooth terrain
Very open farmland	0.063	1. No crossing hedges. 2. decentralized buildings. 3. Smooth hills.
Open farmland	0.075	Fewer buildings. 8 m height crossing hedges and separated with 1250m.
Mixed farmland	0.083	Fewer buildings. 8 m height crossing hedges and separated with 800m.
Trees and farmland	0.092	Closed appearance. Thick vegetation. 8 m hedges 250 m separation.

The decay constant is one dominant parameter that influences the wake losses; it should be changed according to different conditions (terrain type). Larger wake decay constant indicates a stronger the wake effect. In table 1.2, the common terrain types for wind farms and the corresponding wake decay constants are listed. It can be seen that, the more open the terrain is, the lower the wake decay constant will be. Also, the water area has a lower wake decay constant than land area. This also explains why offshore wind farms have higher energy production efficiency than onshore wind farms.

Commonly, the wake decay constant is set as 0.04 for offshore wind farm and 0.075 for onshore wind farm in wake losses calculation process [6]. Due to the complex terrain of onshore wind farm, the topographic influence on the wake losses estimation, that is, the terrain effect model [7] should also be considered for onshore WFLO. In addition, the noise restriction is a hard constraint that should be counted which is another difference between offshore and onshore WFLO.

For electrical system design, both onshore and offshore wind farm concerns the locating of substations on site, the cable connection scheme optimization as well as the combinatory optimization of electrical components in terms of voltage level and type. In offshore wind farm, the total invest for electrical infrastructure can be raised up to 30% and the cost for installation and transport are also higher compared with onshore one [8]. Besides, the overall investment for offshore wind farm is twice as onshore one [9][10] which means that even a small improvement in the WT placement or electrical system topology design would lead to a large sum of money saving, thus the offshore configuration of wind power has experienced a dramatic

innovation focus in recent decades, when compared to its onshore counterpart [11]. Besides, our funding organization, Norwegian Centre for Offshore Wind Energy (NORCOWE) requires us to contribute to the deliverable of NORCOWE reference wind farm (NRWF) which is assumed to be constructed 80 km away from the shore of Sylt. Hence, in this thesis work, we only focused on the optimization of large scale offshore wind farm.

## 1.2. LITERATURE SURVEY AND MOTIVATION

When the wind passed the WT rotor, the wind speed will suddenly drop and recovered to certain extend after some distance. As a result, the upstream WT would incur the wind speed deficit on the wind speed reached at downstream WTs' blade and thereby the total power production of whole wind farm will be reduced. This is the so called wake effect [12] which is a dominant factor that is taken into account for WT micro siting optimization problem, in other term, WFLO [13].

The wind speed deficit calculation is a complex process which is related to the positions of WTs, the wind condition (wind velocity and direction) as well as the control strategy of wind farm. The analytical model of wind in a wake involves a mass of constraints that makes the WFLO problem as a NP-hard optimization problem [14]. For solving such problem, the classic optimization algorithm would flop because of excessive computation time. Hence, the heuristic optimization algorithm becomes popular in solving large-scale WFLO problem [15]. Within this algorithms, genetic algorithm (GA) [16]-[17] and particle swarm optimization (PSO) algorithm [18]-[27] were most frequently used while the simulated annealing, differential evolution (DE) [28], ant colony optimization (ACO) [29] and Monte Carlo simulation [30] were also adopted to solve WFLO in some publications.

Compared with WFLO, the electrical system design concerns about the selection of electrical components including voltage level selection [31]-[35], the cable connection layout [36]-[53] as well as the determination of offshore substation (OS) in terms of quantity and location [36][47][48][52][53]. Those works are mainly done by deterministic algorithm as minimum spanning tree algorithm [54], travelling salesman problem [55][56] algorithm and Open Vehicle Routing Problem (OVRP) [57] which are the classic algorithms in graphic theory [58] or hybrid method which used GA or PSO combined with deterministic algorithm [54]-[58].

In addition, some commerical softwares have already showed up which were focused on the annual energy production (AEP) estimation [59]-[61] In [59], it is demonstrated that WAsP has a higher accuracy in energy production estimation by comparing the simulation results with the real wind farm output and this software is widely used for wake losses estimation for a specific wind farm. The WFLO can also be solved by some commercial software [62]-[63] whereas no detailed information are given for the optimization methods. To our knowledge, no mature



software can be applied for the electrical system design for offshore wind farms. It can be expected that the performance of the offshore wind farm would be further enhanced by adopting some newly proposed methodology.

Considering the huge investment that are required for offshore wind farm construction, methodologies and procedures which can make the wind power more competitive in energy market should be investigated. Due to the wake effect, the WT location is highly related to the energy production of the wind farm. The extremely non-convexity of wind farm layout optimization problem (WFLOP) makes heuristic optimization technology widely used to make a good wind farm layout so that more profits can be obtained by help the wind farm owner.

Instead of making more profits, electrical system optimization can reduce the capital investment which will also contribute to a cost-effective wind farm. Since the increasing size of the offshore wind farm, more than one OS could be installed in one wind farm. Taking the number of OSs, the voltage level of collection and transmission system as well as the cable connection scheme into consideration, the electrical system design is a mixed integer optimization problem. The synergic relation of those factors should be analyzed so that a good decision can be made to benefit the wind farm owner. The author's works involve both two aspects are in the 15 papers attached in the collection. It is expected that an offshore wind farm optimization platform can be formulated as shown in figure 1.2

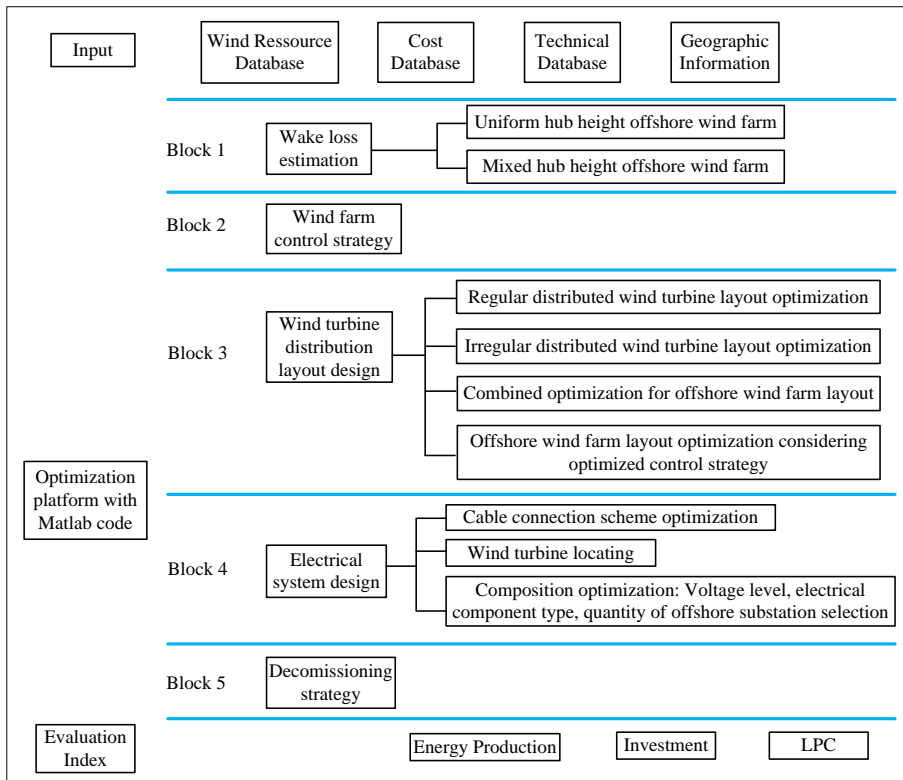


Figure 1.2 The structure of proposed offshore wind farm optimization platform.

The achievement of this Ph.D. project can be concluded as an overall optimization platform for large scale offshore wind farm. As illustrated in Fig. 1.2, there are several blocks within the optimization platform and each corresponds to one or several different tasks. To get the desired outcome, the customers need to trigger the program in different block according to their own requirement. The detailed descriptions of the optimization platform are summarized as follows:

Input: Four databases can be defined in this part. Wind Resource Database contains the time series wind speed which is the base for power production calculation of wind farm. Cost Database contains the cost of main electrical system components including transformer, cable and substation structure. Technical Database collects the specification of different types of WT as power curve, hub height, rotor diameter, the information of different types of cable in terms of sectional area, capacitance and inductance per km (which is the necessarily parameter for  $\pi$  model). The coordinate of each WT, OSs and onshore substation, the construction boundary of wind farm and the construction forbidden area within the wind farm are defined in Geographic

Information database. The above databases will be partly or fully adopted according to different optimization target (customer requirement).

1. Evaluation Index: There are totally three evaluation indexes in this optimization platform as Energy Production, Investment and the well-known evaluation index LPC respectively which are used for composing the objective function for each task in different block.
2. Block 1: The programs designed in this block are used for wake losses or energy production calculation for the offshore wind farm with either uniform (Task 1) or mixed hub height offshore wind farm (Task 2). The input data for this block should be the Wind Resource Database, Technical Database as well as Geographic Information while the outcome or in other words, evaluation index for this block is Energy Production of whole wind farm.
3. Block 2: In this block, only one task is defined, that is the wind farm control strategy optimization. By intelligently tuning the pitch angle of each WT, the performance of the existing offshore wind farm can be enhanced in this task which is evaluated by LPC. The input data for this block should be the Wind Resource database, Technical Database, Cost Database as well as Geographic Information database.
4. Block 3: The program for WT micro-siting optimization is implemented in this block. Four tasks are defined as regular<sup>a</sup>/irregular<sup>b</sup> distributed WT micro siting optimization, combined optimization for offshore wind farm layout<sup>c</sup> and offshore WFLO considering optimized control strategy<sup>d</sup>. The input data for task a should be Wind Resource Database, Technical Database, Cost Database as well as Geographic Information database (only the location of OS and onshore substation) with LPC as the evaluation index. For task b, the evaluation index is Energy Production with Wind Resource Database, Technical Database (only the specification of adopted WT as power curve, hub height and rotor diameter) as well as Geographic Information database (only the construction boundary of wind farm and the construction forbidden area within the wind farm) as the input data. Task c is aiming at minimizing the LPC so the input data are Wind Resource Database, Technical Database, Cost Database and Geographic Information database (without inputting the location of WTs). Task d uses the same evaluation index and input data as task c.
5. Block 4: The programs completed in this block are used for electrical system optimization for large scale offshore wind farm. There are totally three tasks defined which can be used separately or combined according to different objectives. In the first task, the evaluation index can be selected as either investment with input data of Technical Database, Cost Database (only cost of tables) or LPC with input database as Wind Resource Database, Technical Database, Cost Database (only cost of

tables) and Geographic Information database. Task b uses investment as the evaluation index with input data as Technical Database, Cost Database (only cost of tables). The last task needs input data as Wind Resource Database, Technical Database, Cost Database (only cost of tables) and Geographic Information database with the evaluation index as LPC.

6. Block 5: In this block, only one task is defined for offshore wind farm repowering optimization. The LPC is also adopted as the evaluation index with input data as Wind Resource database, Technical Database, Cost Database and Geographic Information database.

This Ph.D. project aims at proposing new methods of the wind turbine micro-siting optimization and electrical system design for large scale offshore wind farm to realize the minimized LPC by minimizing system cost and loss, improving energy production, while meet the operational requirements of power systems. The methodologies and procedures to locate OSs and WTs will be developed. The system topologies and voltage levels for various power levels will be optimized by some proposed methods. The control strategy will also be investigated for improving the energy production of existing offshore wind farm. The wake effect which is the main factor that incurs energy losses within the wind farm will be considered. Further, the interactions between either wind farm layout and energy production or wind farm layout and electrical system topology will be fully explored. In addition to that, a design program will be developed; the system costs, power losses of the cable associated with a wind farm, and the connection between wind farms and the electric system will be evaluated. The NRWF, which may represent the future large scale offshore wind farm in some ways, is chosen as the studied offshore wind farm. The significance of this project includes formulation the mathematical analytical models for wake losses estimation, development of the methods for WFLO, wind farm control strategy and electrical system design. The motivations for each problem will be specified in the following sub sections.

### **1.2.1. OFFSHORE WIND FARM MICRO SITING**

The wake losses can take up to 10-15% [64] of AEP which will make the wind farm owner lost a large sum of money. Hence, it is critical to estimate the energy yields of offshore wind farm considering wake losses accurately so that a solid background and basis can be provided to the wind farm optimization research. Lots of works have been proposed for wake modelling which can be categorized into two sorts: One is using computational fluid dynamic (CFD) technology which can obtain the dynamic wind flow characteristic accurately by discretizing the continuous field, however, the computational time is quite long [65], the other is using analytical model instead of differential equations to estimate the wind speed deficit [66]-[70], [62]-[63]. Based on the existing wake models, some commercial software has already come out as Wind Atlas Analysis and Application software) [59] (which is

the most popular one [13]), WindSim [60] and Meteodyn [61]. However, those softwares can only be used for energy production estimation, As presented in [13], Jensen model has higher accuracy and less computational cost compared with other analytical wake models, thus most of the offshore wind farm optimization works were implemented by using Jensen mode. The energy production estimation of whole wind farm is a complex process which involved superposition and judgement. Hence, the wake losses calculation for whole wind farm should be specified analytically before the WFLO can be done.

### **1.2.1.1 Optimization of regular shaped large scale offshore wind farm layout**

In earlier time, some simple rule was given for regular shaped wind farm layout design, 8 times rotor diameter ( $D$ ) to  $12D$  in the main direction of wind flowing and  $3D$  to  $5D$  in the crossing direction [71]. The placements of WTs were done based on this empirical conclusion at that time. However, the positions of WTs were actually not in the optimization procedure, a mathematical derivation between WT positions and objective function (annual energy production or cost of energy) should be specified so that a clear rule for wind farm layout design can be further determined. Currently, the wind farm layout design works were mostly done on minimizing the wake losses or cost of energy or using net present value of constructing wind farm to assess the economic performance of wind farm [72]. The overall cost of an offshore wind farm was given estimated using an integrated cost model which is related to the capacity of the wind farm. The relationship between WT location and electrical system cost were not investigated. Moreover, the recent research are always focused on irregular shaped WFLO (WT distributed scattered at sea) since it has a higher energy capacity compared with regular shaped wind farm layout while regular shaped wind farm design should also be an interest since its good appearance which is one consideration in practice.

In order to solve the problems mentioned above, the wind speed deficit calculation process should be specified which is the basis for WFLO. The optimized spacing for WTs in a regular shaped wind farm should be decided by considering the cost variation from different layout designs.

### **1.2.1.2 Irregular shaped wind farm layout design**

At earlier time, the WFLOP was solved by dividing the whole construction area into a number of squares. The WTs were assumed to be installed in the center of selected squares. Then the problem was converted into finding the proper squares from a given region which is an integer optimization problem. The smaller the size of square, the more computational cost should be paid, in other words, the final solution was highly related to the size of the generated grids. The grid model is shown as Fig. 1.3.

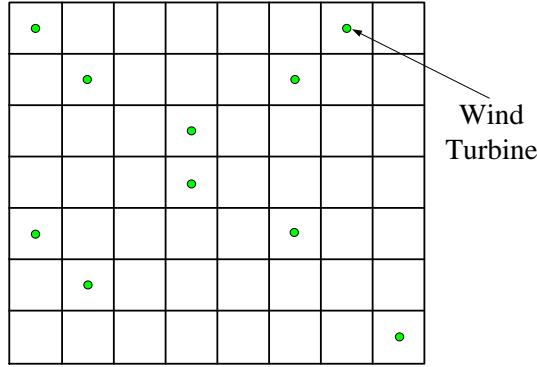


Fig. 1.3 Grid model example for WFLO

In 1994, G. Mosetti et al. proposed a method to minimize the cost of energy for offshore wind farm using genetic algorithm (GA) [73] which is the beginning of offshore WFLO. After that, several works has been published using the optimized layout in [74] as a benchmark [75]-[77]. Similarly, a binary particle swarm optimization with time-varying acceleration coefficients (BPSO-TVAC) algorithm to solve the WFLO was presented and compared with 5 other heuristic algorithms [78]. Also, using GA to solve the WFLO problem was done in [79], however, another wake model was adopted and the final result was compared with commercial software WindFarmer instead of benmark [74]. A layout design for a real offshore wind farm was addressed in [80] using evolutionary computational approach, it should be noticed that the final design is still with an array layout though many researches has been done on making a scattered WT placement. Hence, the same authors adopted coral reefs optimization method to make a better design which can generate more power production compared with the layouts obtained by evolutionary approach, differential evolution and harmony search algorithm [81]. In addition to use heuristic algorithms, mathematical programming (quadratic integer programming (QIP) and mix-integer linear programming (MILP) in [82] while sequential optimization in [83]) were also adopted to solve WFLOP.

In the above papers, the micro siting of offshore wind farm was done by separating the construction area into a number of grids which simplified the problem and thus reduced the computational cost. As indicated in [7], the number of possible solutions ( $N_s$ ) can be expressed in the following.

$$N_s = \frac{N_{cell}!}{N_{WT}!(N_{cell}! - N_{WT}!)} \quad (1)$$

In (1),  $N_{cell}$  is the number of generated grids while  $N_{WT}$  is the number of WTs that is going to be installed. By using the grid model, the complexity of WFLO can be simplified. However, some potential solutions will certainly be neglected. In order to

get an even cost effective wind farm layout, some works solve the WFLO problem by using coordinate form to represent the position of WT [84]-[95]. Under the constraint that the distance between every two WTs should be larger than  $4D$ , an evolutionary algorithm was used in [84] to find the coordinate of WTs within a circular boundary profile wind farm. Compared with [84], ant colony algorithm was proved to be more outstanding by getting a layout which can produce more power in [85]. Two advanced PSO techniques (Gaussian PSO algorithm in [86] and Mixed-Discrete Particle Swarm Optimization (MDPSO) algorithm in [87]) were also implemented to solve WFLO problem. GA was again used to get an optimized layout in [88][89], however, end up with a more realistic layout since some practical aspects as load-bearing capacity, WT hub height, sea bed condition and irregular outline of wind farm were taken into account in [88] while a scattered layout was proved to be with best performance within three common layout regarding levelised cost of energy (LCOE): aligned, staggered, scattered which selected an offshore wind farm in Hong Kong as the study case [89]. Based on Jensen model, a continuous wake model was proposed in [90] to formulate the wind farm power function and calibrated using CFD simulation data, moreover, the optimized layout was found by sequential convex programming which was demonstrated to be efficient enough to tackle the large offshore wind farm optimization problem with large number of WTs. Using Horns Rev I as the benchmark which is the same to [90], [91] used random search (RS) algorithm to get the optimized layout. Due to the non-convex characteristic of WFLO, no evidence shows that the existing work can ensure the optimality. Hence, researchers took efforts in improving the optimization algorithm to get a near optimal solution which can benefit the wind farm owner more. In [92], a combined optimization method was introduced which used heuristic method to set an initial layout and the local optimal solution under each initial layout was obtained using nonlinear mathematical programming techniques. A comparative study in terms of layout model (grid model and coordinate model) and cost model (model in [74] and Chen's model [94]) was done in [93] by GA.

Though many works have been done for solving WFLO using heuristic optimization technology, mathematical programming or hybrid method, the focus was mainly on harvest the output of an offshore wind farm while the availability of sea area and its impact on the final layout has not been addressed. In reality, the WTs can be persuaded to install in some sea area due to natural reserve, oil well, existing natural gas pipe, etc. Those aspects should be defined as a restricted region and considered in the WFLO. An efficient algorithm which can optimize the WT locations in consideration of restricted area offshore should be proposed.

### **1.2.2. OPTIMIZED CONTROL STRATEGY FOR OFFSHORE WIND FARM**

In planning stage, the WTs should be intelligently placed to maximize the overall power production while it is also possible to further minimize the wake losses for a constructed wind farm by improving the control strategy. Traditionally, the wind

farm are controlled by maximum power point tracking strategy (MPPT) [95] which changes WT's pitch angle and/or tip speed ratio so that the optimal power coefficient can be reached. This strategy is the best control strategy for single WT in terms of maximizing the power output. However, considering the wake effect, there is a possibility of resetting the power point coefficient of each WT within a wind farm so that total power production can be maximized. This idea has been demonstrated in several works [96]-[98]. However, there are still some limitations.

1. All the works are focus on achieving the maximum power production of a regular distributed wind farm with a regular or irregular outline. The application of such method for scattered wind farm layout should be investigated.
2. All the works mentioned above were aimed at maximization of power production of wind farm. The power losses within the wind farm are neglected.

In this work, the optimized control strategy which was fulfilled by changing the pitch angle was proposed for a scattered distribution wind farm layout. The investment, power losses as well as energy production considering wake effect which constitutes the so called levelized production cost (LPC) were utilized as the evaluation index.

### **1.2.3. ELECTRICAL SYSTEM DESIGN FOR LARGE SCALE OFFSHORE WIND FARM**

Due to the development of offshore wind energy technology, the offshore WTs become bigger and bigger which requires a larger sea area for minimizing the wake effect. On the other side, the offshore wind farm is moving further to the sea. Both factors indicates that a large number of submarine cables and electrical components would be needed so that the power generated by WTs can be effectively transferred to the grid. For offshore wind farm, the electrical system cost has already been taken up to 30% which signified the imporatnce of electrical system optimization work [7].

#### **1.2.3.1 Cable connection scheme optimization for offshore wind farm**

From the practical point of view, the cable connection scheme should concern two aspects: the crossed cable connection layout should not be permitted and the current in each cable under full load condition should not over the current carrying capability of responding cable. Some classical mathematical problem has been introduced to solve the cable connection layout optimization problem (CCLOP) as Minimum Spanning Tree (MST) problem [58], Travelling Salesman Problem (TSP) [56], Open Vehicle Routing Problem (OVRP) [54]. The cable connection layout was optimized based on the concept of MST in [37][49][53][99][99]. A capacitated MST



was introduced in [53] to help find the cable connection layout using mixed integer linear programming method while MST was applied in [99] to connect WTs in each WT group which was decided by k-clustering algorithm with the radial angle criterion, moreover, local search method was used to find some alternative layouts by which a better layout with lower cost compared with the layout obtained with MST algorithm was also found. Considering the seabed condition, some sea area will be not suitable or costly to lay cables. This problem was described and solved by a convex hull based bypassing algorithm combined with MST algorithm in [99] while MST was modified by introducing external splice locations in [37]. The same authors [37] also proposed a quality threshold clustering algorithm to solve the same problem [44]. The CCLOP was formulated as a well-known OVRP with unit demands in [52] and solved by Clarke and Wright savings heuristic algorithm. Similarly, the cable connection layout can also be optimized by TSP [38][41]. It should be notice that the CCLOP is non-convex, which means the deterministic method can help find a better layout compared with manual designed. Hence, some authors tried to use heuristic algorithm as GA or PSO [39]-[42], [37][50] to make a better design. The cable connection layout of a 4 substation offshore wind farm was optimized with GA in [41] and was treated as the benchmark to be compared with in [39]. Though some improvement of reducing cost was obtained by the layout proposed in [39], some crossed cables which contribute to a higher cost is not into account. In addition to that, some other methods as linear programming and ant colony system algorithm were also adopted [45][47]. The OS is usually located away from the WT construction area or in the center of offshore wind farm, the impact of OS location was not introduced until the presentation of [48]. In [48], the benefit of central located OS was analyzed from a practical point of view. Later, the real OS location optimization was done by making a best decision from a series of given positions in [47]. Recently, ref [49] specified the significant impact of OS location on the cost of offshore wind farm cable connection layout optimization which permitted more freedom area for OS, however , the cable connection layout was merely generated with MST.

In the above literatures, some limitations can be summarized as follow:

1. The cable connection layout optimization was mostly done by minimizing overall cost while the economic performance should be evaluated with a more comprehensive index, for instance LPC.
2. In [39], a GA-TSP algorithm was proposed to formulate the cable connection layout. However, the number of WTs in one feeder is designed to be the same. To our knowledge, there is no existing work used PSO (which was proved to have a better performance than GA [101]) combined with graphic theory (tree concept) to formulate the cable connection layout. This should be an interesting topic since the tree concept allows different numbers of WTs in a feeder which gives the designer more options to select.

3. The crossed cable connection layout will incur the cost increase which should be a constraint in the optimization problem. This constraint has not yet discussed in any paper.
4. The OS location has a significant impact on the cable connection layout formulation. This problem should be specified and investigated.

In order to overcome the above limitations, a new method which can generate an uncrossed cable connection layout with minimal LPC should be proposed. In addition to that, the impact of the cable crossing area and OS location on the cable connection layout formulation should also be investigated.

### **1.2.3.2 Overall electrical system optimization for large- scale offshore wind farm**

In 2003, Stefan [102] completed his master thesis on a comparative study of wind farm electrical system which is the initial work related to wind farm electrical system design. Similar comparisons have also been done in [35][108], some typical AC and DC wind farm topology was compared and investigated in terms of power losses, cost as well as reliability in [34] while different collection system designs for offshore wind farm was analyzed and compared in [103]. The above works concerned about the finding the best electrical system design for offshore wind farm within a limited selection and no optimization method was applied whereas there are many factors that can have an impact on the performance of offshore wind farm as voltage level, electrical equipment type, cable connection layout, etc. If the input database is so big that the traditional ergodic method will make the computer out of memory, then some optimization method should be considered to reduce the computational cost and increase the computational efficiency. By thinking of solving the problem efficiently, Zhao. et al presented a heuristic optimization method which can help get an optimized offshore wind farm electrical system with lower cost and higher reliability [33][34][104]-[106]. However, the optimization is actually done based on the selection of electrical equipment regarding voltage level and type, the cable connection scheme is decided based on several typical schemes (string clustering, star clustering, with redundancy or not). It should be noticed that the cable connection layout in [33]-[35], [102]-[106] is selected from a variety of empirically designed layouts. If the cable connection layout can be designed using some specific and suitable algorithm, then the cost of whole electrical system can be expected to be further reduced. Ref. [40] tried to make an overall optimization work which can take voltage level and electrical equipment type selection, OS determination regarding locations and quantity as well as collection system cable connection layout design into consideration, the fuzzy c-means (FCM) clustering method was adopted to decide the number of WT groups. However in each group the OS will be central located and the cable connection layout was obtained merely by MST.

Considering the problem proposed in section 1.2.3.1, the electrical system optimization for large scale offshore wind farm should be done by taking cable connection layout, OS location and quantity and electrical equipment selection into account so that an overall electrical system optimization framework can be presented.

## **1.2.4. CO-DESIGN CONCEPT OF OFFSHORE WIND FARM**

### **1.2.4.1 Wind turbine micro-siting optimization considering optimized control strategy**

As introduced in section 1.2.1, the energy yield of wind farm can be increased by placing the WT's intelligently. Presently, the WFLO works always target to minimize the wake losses within the wind farm under the assumption that all the WT's are controlled by MPPT control strategy. However, the energy yield of wind farm could be further increased for a given wind farm layout by adopting new control strategy of entire wind farm. As presented in section 1.2.2, this new control strategy was realized by changing the tip speed ratio, pitch angle or both of each WT. It is imaged that if this new control strategy is adopted in new offshore wind farm layout planning phase then the overall economic performance could be increased compared with the traditional method (optimize the WT locations at first and then adopted optimized control strategy based on the well-designed layout).

This simultaneous optimization which considers WT placement as well as control strategy of whole wind farm composes a co-design problem of offshore wind farm. To our knowledge, this co-design optimization work has not been investigated and presented in any work. Hence, a breakthrough is expected to be made in this work regarding the problem mentioned above.

### **1.2.4.2 Combined offshore wind farm optimization**

The works introduced in section 1.2.1 show more interests in harvesting the offshore wind farm without considering the invest on the electrical system while the CCLOP was solved by the methods proposed in section 1.2.3.1 with a predefined wind farm layout. It could be imagined that if two aspects of optimization work can be combined and solved simultaneously, then a better wind farm design could be decided. The overall optimization in terms of WT positions as well as the cable connection layout was conducted in [107] to reach the target of a cost-effective wind farm. However, the highlighted innovation was not well demonstrated through the case study, the wind farm layout was optimized using grid model while the optimized cable connection layout was obviously crossed. More efforts could be put in to get a better layout.

In this work, a combined optimization work which optimizes the WT's positions and cable connection layout at the same time will be proposed. Some new contributions will be presented as follows:

1. Improving the WFLO part compared with the work presented in [107] by using coordinate model.
2. The uncrossed layout should be converted into one constraint in the CCLOP. A new method that can generate more economic cable connection layout should be proposed.
3. The number and location of OS should be decided intelligently and its impact on the optimized cable connection layout should be specified.

### **1.2.5. FUTURE STRATEGY: OFFSHORE WIND FARM REPOWERING OPTIMIZATION**

The wind farm is usually estimated to be operated for about 20 years for the sake of WT's lifetime. However, not all WTs are out of service at the same time, some may continue to operate till 30 years [108]. It has been 25 years since the first offshore wind farm commissioned which indicated that plenty of WTs need to be decommissioned from now on. The idea of replacing old WTs with new type ones has been presented in [109], which shows advantages in saving land use and reduce social against. However, it focused on onshore wind farm. Though [110] investigate the decommission expenses regarding some main component offshore as foundation and cable, no explicit procedure was proposed for repowering offshore wind farm by the existing components. In this work, an optimization framework for offshore wind farm decommission will be proposed which have potential commercial value as follow:

1. Make best use of available components within offshore wind farm to construct a new offshore wind farm can reduce the overall investment which is an incentive for small investor to participate in.
2. As indicated in [111], the WTs distributed in the boundary of wind farm are expected to have a higher power output than others. Hence, it could be one solution to increase the efficiency of original wind farm by repowering the original wind farm with different types of WTs with different hub height
3. Integrating optimization technology into offshore wind farm decommission can help to quantify the economic performance of a planned decommission strategy which can help wind farm owner make a good decision.

### 1.3. RESEARCH QUESTIONS/HYPOTHESIS

Improve the energy production of offshore wind farm and make it cost-effective is expected for the planning offshore wind project. The research questions/hypothesis is

*How to optimize the large scale offshore wind farm including equipment type and voltage level selection, wind farm layout, cable connection scheme, wind farm control strategy and repowering so that more benefits can be obtained by the wind farm owner?*

### 1.4. RESEARCH OBJECTIVE AND METHODOLOGY

This three-year Ph.D. project “Electrical System Optimization for Offshore Wind Farms” was initiated by the Department of Energy Technology at Aalborg University in collaboration with Norwegian Centre for Offshore Wind Energy (NORCOWE).

The impacts of wake effect on the energy production of large scale offshore wind farm should be investigated. The WT micro siting and electrical system topology’s influence on the economic performance of offshore wind farm should be studied. Different algorithms are also needed to be studied and compared to give a cost effective wind farm layout. Specially, the objectives of this project are as follows:

1. To develop models to calculate the energy production of large scale offshore wind farm considering wake effect. The models can be used for wake losses calculation for uniform hub height as well as mixed hub height WT’s offshore wind farm with regular or irregular distributed WT layout.
2. To improve the energy production of existing offshore wind farm by optimizing the pitch angle of each WT using meta-heuristic optimization algorithm.
3. Comparison of deterministic algorithm and heuristic algorithm and propose new methods for cable connection layout design of offshore wind farm.
4. To propose a method for solving WFLOP.
5. To optimize offshore wind farm electrical system design on account of electrical component selection, voltage level selection, cable connection scheme design and OS quantity and location selection.
6. To propose an optimization method for offshore wind farm repowering.

In this thesis, the methodology includes modelling, simulation and optimization. In particular, PSO method is used and compared with GA. The MST concept is adopted and further developed as new algorithms as DMST, PSO-MST. The FCM

algorithm is adopted to divide the whole wind farm into sub regions. All the programs are compiled by Matlab software.

## 1.5. TECHNICAL CONTRIBUTION OF THE THESIS

The main technical contribution of the thesis is concluded as follows:

1. A new method of wake losses calculation for random distributed WT offshore wind farm layout is proposed and validated through commercial wake losses estimation software-WAsP.
2. A new wake model which can estimate the wake losses within an offshore wind farm with mixed hub height WTs are proposed.
3. A deterministic algorithm, dynamic MST (DMST), which can be used for cable connection layout design of offshore wind farm, is proposed and demonstrated can help reduce the overall investment compared with traditional deterministic algorithm MST algorithm.
4. A heuristic algorithm for cable connection layout optimization is represented and demonstrated to be outperformed than DMST and MST in finding an even lower investment cable connection layout.
5. Different types of meta-heuristic algorithms are investigated and compared so that the most suitable algorithm can be selected for offshore wind farm optimization to find a better solution.
6. A WT micro-siting optimization method based on heuristic algorithm is proposed to minimize the LPC or increase the energy production of offshore wind farm. The concept of forbidden area within the wind farm is proposed and fulfilled by introducing a penalty function.
7. The meta-heuristic algorithm is modified and combined with FCM algorithm to solve the mixed integer optimization problem of electrical system design for offshore wind farm.
8. An overall optimization procedure which optimizes the wind farm layout, cable connection scheme and OSs location simultaneously is proposed.
9. An optimization method for offshore wind farm repowering is proposed to help wind farm owner decide where and what WT should be installed in the existing offshore wind farm.

## 1.6. PROJECT LIMITATIONS

The limitations of this research are in the following.

1. This research focuses on the optimization of offshore wind farm; due to the requirement from the funding organization that onshore wind farm optimization is not involved. However, by adopting a new wake model and properly adding more constraints. The method proposed in this work can also be adapted to solve onshore wind farm optimization problem.

2. The cost model for electrical components is theoretical and may not reflect the real situation.
3. The foundation cost take a large proportion of overall investment and it is related to installed WT positions. The seabed condition has an impact on the foundation and installation cost. Due to the difficulty in obtaining the marine information, the foundation and installation cost is not considered in the WT micro-siting optimization.
4. The power losses along the cables are calculated by assuming all WTs are operated in one per unit.
5. The cable length is calculated according to the geometrical distance between each pair of WTs.
6. The yaw misalignment's impact on the energy production of offshore wind farm is neglected.
7. The LPC of offshore wind farm is calculated without considering the impacts of wind curtailment.

## **1.7. ORGNIZATION OF THESIS**

The thesis contains 7 chapters presented as a paper collection format and back up by 15 published or submitted papers.

Chapter 1 presents the introduction and motivation of the thesis, where the state of art, research questions/hypothesis, contributions and limitations are included.

Chapter 2 presented the energy production estimation approaches for offshore wind farm. The mathematical equations for wake model are given and results are discussed in the end of this chapter.

In Chapter 3, the optimized control strategy of entire wind farm is introduced. The relation between tip speed ratio, pitch angle and power coefficient are presented at first and then the meta-heuristic algorithm is specified. Based on these, the approach for improving the energy production of an existing wind farm is given.

In Chapter 4, the WFLOP is introduced at first. The criteria for evaluating the performance of offshore wind farm is discussed and the approach for WT micro-siting optimization considering forbidden area is presented

Chapter 5 presents the approaches related to the electrical system design of large-scale offshore wind farm. The deterministic and heuristic methods are introduced and the advantages of meta-heuristic methodology are highlighted through comparison.

In Chapter 6, the repowering optimization methods of offshore wind farm are introduced. Instead of dismantling the whole wind farm, the WTs can be repowered

using different types of new WTs. The quantitative analysis of the repowering approach is given.

Finally, the conclusions and contributions of the thesis and some future proposals are made in Chapter 7.

The 15 attached papers selected from the publications to support the thesis are listed as follows:

- [A1] Peng Hou, Weihao Hu, Mohsen Soltani and Zhe Chen, “A Novel Energy Yields Calculation Method for Irregular Wind Farm Layout,” *41th Annual Conference of the IEEE Industrial Electronics Society (IECON 2015)*, Yokohama, Japan, pp. 000380-000385, 2015, doi: 10.1109/IECON.2015.7392129.
- [A2] Peng Hou, Weihao Hu, Mohsen Soltani and Zhe Chen, “A New Approach for Offshore Wind Farm Energy Yields Calculation with Mixed Hub Height Wind Turbines,” *Proceedings of the 2016 IEEE Power & Energy Society General Meeting 2016*, pp. 1-5, 2016.
- [A3] Peng Hou, Weihao Hu, Baohua Zhang, Mohsen Soltani, Cong Chen, Zhe Chen, “Optimised Power dispatch Strategy for Offshore Wind Farms,” *IET Renewable Power Generation*, Vol. 10, Issue 3, pp. 399-409, 2016.
- [A4] Peng Hou, Weihao Hu, Mohsen Soltani, Zhe Chen, “Optimized Placement of Wind Turbines in Large Scale Offshore Wind Farm using Particle Swarm Optimization Algorithm,” *IEEE Transactions on Sustainable Energy*, Vol. 6, Issue 4, pp.1272-1282, 2015.
- [A5] Peng Hou, Weihao Hu, Mohsen Soltani, Zhe Chen, “Optimization of Offshore Wind Farm Layout Considering Restriction Zone,” *Energy*, Vol. 113, pp. 487-496, 15 Oct. 2016.
- [A6] Peng Hou, Weihao Hu, Mohsen Soltani, Cong Chen, Baohua Zhang, Zhe Chen, “Offshore Wind Farm Layout Design Considering Optimized Power Dispatch Strategy,” *IEEE Transactions on Sustainable Energy*, Vol. 8, Issue 2, pp. 638-647, 2016.
- [A7] Peng Hou, Weihao Hu, Mohsen Soltani, Cong Chen, Zhe Chen, “Combined Optimization for Offshore wind farm Planning,” *Applied energy*, Vol. 189, pp. 271-282, March 2017.
- [A8] Peng Hou, Weihao Hu, Cong Chen, Zhe Chen, “Optimization of Offshore Wind Farm Cable Connection Layout Considering Levelised Production Cost Using Dynamic Minimum Spanning Tree Algorithm,” *IET Renewable Power Generation*, Vol. 10, Issue 2, pp. 175-183, Feb. 2016.
- [A9] Peng Hou, Weihao Hu, Zhe Chen, “Optimization for Offshore Wind Farm Cable Connection Layout using Adaptive Particle Swarm Optimisation Minimum Spanning Tree Method,” *IET Renewable Power Generation*, Vol. 10, Issue 5, pp. 694-702, 2016.



- [A10] Peng Hou, Weihao Hu, Cong Chen, Mohsen Soltani, Zhe Chen, “A Novel Way for Offshore Wind Farm Cable Connection Layout Design with Meta-heuristic Optimization,” *Renewable Energy*, 1<sup>st</sup> revision.
- [A11] Peng Hou, Weihao Hu, Cong Chen, Zhe Chen, “Overall Optimization for Offshore Wind Farm Electrical system,” *Wind energy*, 2016, DOI: 10.1002/we.2077.
- [A12] Peng Hou, Weihao Hu, Zhe Chen, “Offshore Substation Locating in Wind Farms Based on Prim Algorithm,” *Power and Energy Society General Meeting 2015*, pp. 1-5, 26-30 July 2015. (Best Paper Award)
- [A13] Peng Hou, Weihao Hu, Zhe Chen, “Offshore Wind Farm Cable Connection Configuration Optimization using Dynamic Minimum Spinning Tree Algorithm,” *50th IEEE International Universities Power Engineering Conference (UPEC 2015)*, England, UK, pp.1-5, 2015.
- [A14] Peng Hou, Peter Enevoldsen, Weihao Hu, Zhe Chen, “Offshore Wind Farm Repowering Optimization,” *Applied Energy*, submitted.
- [A15] Peng Hou, Weihao Hu, Mohsen Soltani, Baohua Zhang, Zhe Chen, “Optimization of Decommission Strategy for Offshore Wind Farms,” *Proceedings of the 2016 IEEE Power & Energy Society General Meeting 2016*, pp. 1-5, 2016.

# CHAPTER 2. ENERGY PRODUCTION ESTIMATION FOR OFFSHORE WIND FARMS

In this chapter the state of art wake models are firstly introduced and discussed. Afterwards, two wake models for offshore wind farm energy production estimation are specified.

## 2.1. STATE OF ART OF WAKE LOSS ESTIMATION

The wake deficit is defined as the impact of the upstream WT to the downstream ones which results in the total energy yields reduction of the wind farm [12]. With the increasing size of offshore wind farm, more than one hundred wind turbines may be involved in one wind farm. In such a large wind farm, the wake effect's influence on the energy production should be counted and estimated accurately as far as possible. For one thing, a good estimation on energy yields of the whole wind farm can help the wind farm owner to make a good bidding strategy in the electricity market, for another the WFLO was essentially focused on minimizing the wake losses. Presently, many wake models have been presented as Jensen model, Ainslie model, G. C. Larsen model [66] which are widely adopted, and some other models [64], [65], [67]-[70]. Within these models, Jensen model is widely selected for solving WFLOP since it needs less computational time and shows good accuracy [66][72].

## 2.2. ENERGY PRODUCTION ESTIMATION FOR OFFSHORE WIND FARMS CONSIDERING WAKE EFFECT

In Jensen model, the wake is assumed to expand linearly after encounter the WT's blade and due to the relative position of WT pair, the downstream WT could be fully, partially influenced or even not influenced. The development of wake bypassing the WT and its impact on downstream WT is illustrated in Figure 2.1.

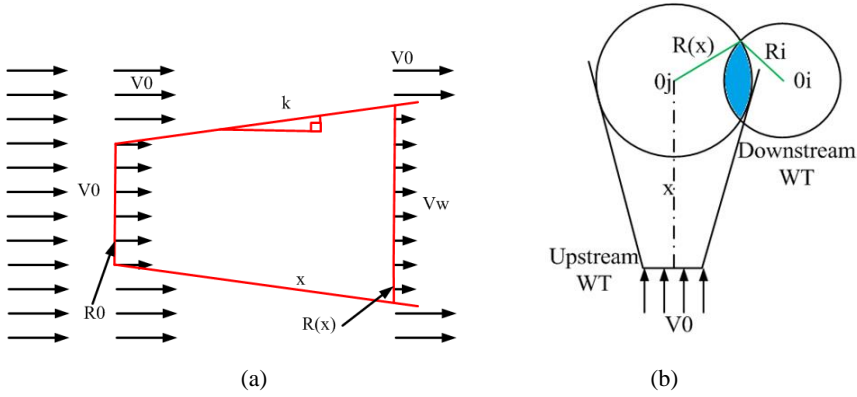


Figure 2.1 Jensen wake model. (a) Single wake expansion. (b) Partial wake effect.

As can be seen in Figure 2.1, the red line in Figure 2.1 (a) shows the development of wake and the blue area in (b) is the effective wake area,  $S_{partial}$ . Based on this model, the wind speed reached at the downstream WT blade can be derived as follows.

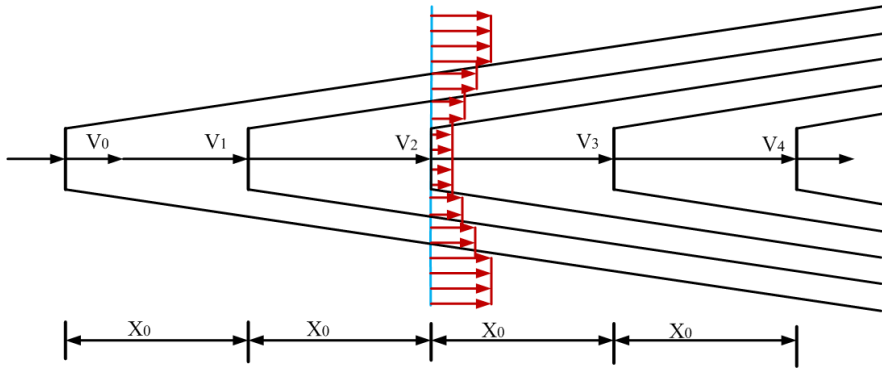
$$V_x = V_0 - V_0 \left(1 - \sqrt{1 - C_t}\right) \left(\frac{R_0}{R(x)}\right)^2 \left(\frac{S_{partial}}{S_0}\right) \quad (2)$$

$$R(x) = R_0 + kx \quad (3)$$

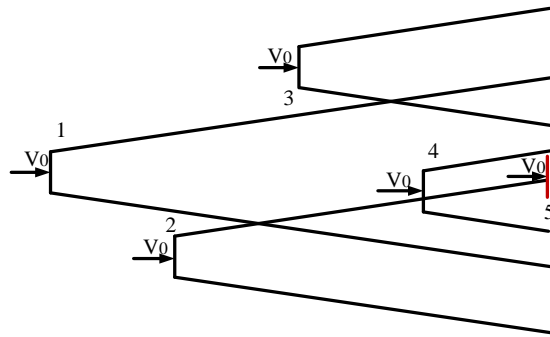
Where  $C_t$  is the thrust coefficient of WT and  $k$  is the wake decay constant which has been specified in section 1.1.

### 2.2.1. WAKE COMBINATION

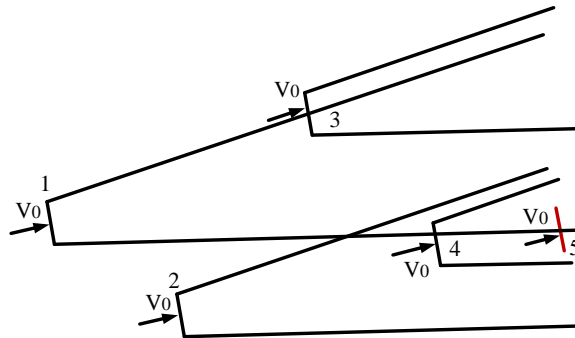
The model mentioned above can be used to calculate the wind speed within the wake as figure 2.1 (a) or the wind speed reached at downstream WT as figure 2.1 (b). However, in a large-scale offshore wind farm, one downstream WT could be affected by the wakes generated by several upstream WTs as illustrated in Figure 2.2.



(a)



(b)



(c)

Figure 2.2 Illustration of multiple wake effect. (a) Several WTs in a line. (b) Scattered WTs distribution with same incoming wind direction as (a). (c) Same WTs distribution as (b) with different incoming wind direction.

Figure 2.1 (a) shows the condition when several WTs are aligned in a line along the wind blowing direction. The length of red arrows show the wind speed in different positions, it can be know that the last WT in this line is fully affected by the wakes generated by the four upstream WTs while this situation will be more complex as in figure 2.2 (b), since it is required to judge whether the downstream WT is fully or partially influenced by the wakes generated from upstream WTs. For instance the WT indicated with red line (WT No. 5) is fully influenced by the wake generated by WT No.4 and 1 and partially influenced by the wake generated by WT 2 while WT 3 does not have any impact on WT 5. This situation will be changed when the incoming wind speed direction is varying. As illustrated in Figure 2.2 (c), for the same wind farm layout, when the wind speed direction changes the WT 5 will be fully influenced by WT 2 and 4 while partially influenced by WT 1. WT 3 still does not influence WT5. In order to evaluate the wake effects of corresponding WTs, a “sum of squares of velocity deficits” method was proposed by Katic et al which can be expressed in the following.

$$V_{n,m} = V_0 \left[ I - \sqrt{\sum_{i=1}^{N_{row}} \sum_{j=1}^{N_{col}} \left[ I - \left( \frac{V_{ij}}{V_0} \right) \right]^2} \right] \quad (4)$$

As can be seen in (4), in order to calculate the wind speed reached at each WT, the wake effects from corresponding upstream WTs to the downstream one should all be counted which means that a lot of judgements' and superposition's processes should be involved in the calculation process. Considering the changing wind direction, mainly four key points should be paid attention to in the AEP calculation process for an offshore wind farm as follows:

1. Identify the upstream and downstream WTs according to different wind direction.
2. Identify the wake developed distance between the downstream WT and each corresponding upstream WT.
3. Judgement and calculation of partial fully wake effect for each pair of related WTs.
4. Update the thrust coefficient,  $C_t$ , according to the wind speed reached at each downstream WT.

## 2.2.2. WAKE LOSSES ESTIMATION BY BINARY MATRIX METHOD

It can be imagine that for a regular distributed wind farm, the wake losses estimation is relatively simple since the distance between each pair of WT is the same. Hence, it is easy to identify the upstream and downstream WTs respectively and calculate the distance from upstream WT to downstream WT according to different wind direction. Recently, more and more offshore wind farm layouts are designed to be scattered since the wake losses can be significantly reduced. In order to estimate the

wake losses for any wind farm, a binary matrix method was proposed in [70] which can help simplify the calculation process. The method is illustrated below.

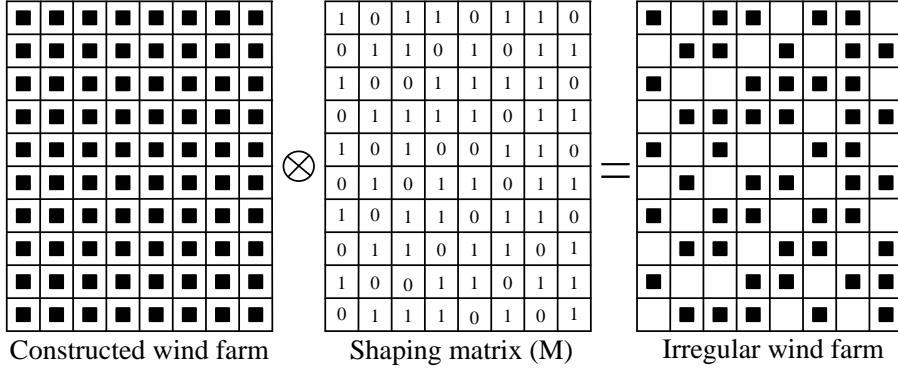


Figure 2.3 The illustration of binary matrix method.

As shown in figure 2.3, the black squares show the WT. The shaping matrix is designed to contain binary number, that is, 0 and 1. Number 1 represents the existence of WT in this position while 0 means this position is empty. It can be noticed that the original constructed wind farm which is a regular wind farm layout can be easily transferred into an irregular wind farm one by the shaping matrix. Combining (2) to (4), the wind speed reached at downstream WT can be shown as follow:

$$V_{n,m}(\alpha, V_0) = V_0 \left[ 1 - \sqrt{\sum_{i=1}^{N_{row}} \sum_{j=1}^{N_{col}} \left[ I-M(i, j) \left[ \frac{V_{ij}}{V_0} \frac{S_{partial,ij}}{S_0} \right]^2 \right]} \right] \quad (5)$$

Based on the binary matrix method, the energy production of whole wind farm can be calculated. The calculation flowchart is shown in figure 2.4.

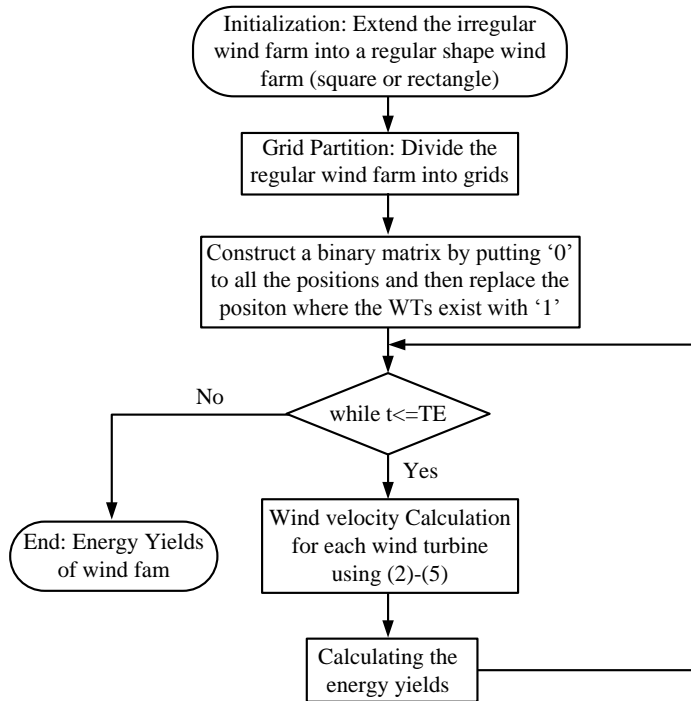


Figure 2.4 Calculation flowchart [70].

As can be seen in figure 2.4, the irregular shaped wind farm will be divided into small grids and the binary numbers are adopted to represent the existence of WT in each position. Then the energy production of the wind farm can be calculated using Jensen model which specified above. The detailed information of this method was presented in [A1].

### 2.2.3. RESULTS AND DISCUSSION

The effectiveness of the proposed model is validated by comparing the results obtained through commercial software WAsP. Two reference wind farm are selected as the study cases, the layouts are shown in Figure 2.5.

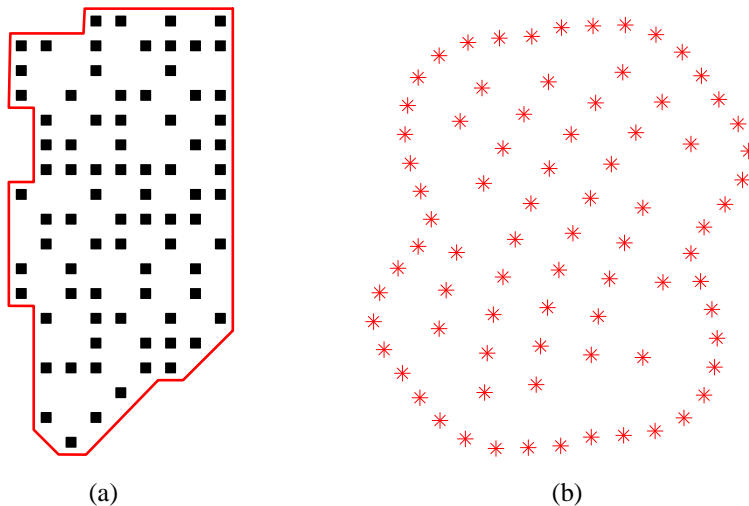


Figure 2.5 Reference wind farms. (a) Irregular shaped reference wind farm. (b) Extremely irregular shaped reference wind farm [A1].

The first study case is shown in figure 2.5 (a). Though it is with irregular boundary, some WTs are still distributed in a line with the same distance between each pair of WTs. In order to further validate the proposed model, another study case is adopted as shown in figure 2.5 (b) with an elliptic boundary and the WTs are distributed more scattered in this reference wind farm. The final results are listed in table 2.1.

Table 2.1 Simulation results for two cases [A1]

		Energy yields by Matlab (GWh)	Energy yields by WAsP (GWh)	Error (%)
<b>Case I</b>	<i>Without considering wake effect</i>	4164.91	4214.40	1.17%
	<i>Considering wake effect</i>	3460.70	3394.46	2.84%
<b>Case II</b>	<i>Without considering wake effect</i>	4164.91	4219.09	0.045%
	<i>Considering wake effect</i>	3951.80	3926.71	0.55%

The error listed in table 2.1 shows the difference between the proposed method and WAsP which indicates that effectiveness of the proposed method. The proposed method can be used for wake losses estimation for any wind farm layouts.



### 2.3. WAKE LOSSES ESTIMATION FOR OFFSHORE WIND FARM WITH MIXED HUB HEIGHT WIND TURBINES

The wind speed will be greatly reduced after bypassing the WT due to wake effect and then the wake will recover and expand before meeting the other WTs. Hence, it can be imagined that the WTs installed in the outer boundary of wind farm can generate more energy than the inner WTs when the incoming wind speed is between the cut-in and cut-out wind speed. On the other hand, the higher capacity the WT is the more investment should be paid. So if the bigger WTs are installed in the outer layer while use the smaller WTs inside the wind farm, then the power production efficiency of such a mixed hub height wind farm might be increased. Based on this hypothesis, a new method to estimate the energy yields of whole wind farm is proposed in A2. In order to evaluate the impact of hub height difference on the energy production of whole wind farm, the shear effect should be taken into consideration.

#### 2.3.1. WIND SHEAR EFFECT

The friction against the ground has barely impacts on the atmosphere at the height of more than 1 km whereas this effect cannot be neglected in the lower layers where the wind speed increases along with the height of air. This is called wind shear effect [112]. So if the height of some WTs is different, this effect should be also incorporated. Then, the wind speed can be rewritten as:

$$V_{0,ij} = V_{ref} \frac{\ln\left(\frac{z_{ij}}{h_0}\right)}{\ln\left(\frac{z_{ref}}{h_0}\right)} \quad (6)$$

#### 2.3.2. MODIFIED WAKE MODEL FOR MIXED HUB HEIGHT WIND TURBINE OFFSHORE WIND FARM

Assumed that there are two types of WTs with different hub heights are in the same offshore wind farm. Taken the shear wake effect into account, the effected wake area which contributes to the wind speed deficit is illustrated with a simple example in figure 2.6.

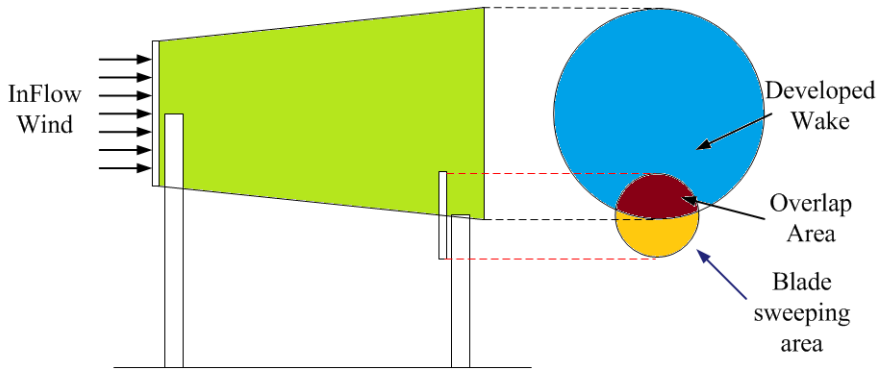


Figure 2.6 Partial wake effect for two WT's with different hub height [113].

In figure 2.6, the red color area indicates the effect wake area. It can be seen in figure 2.6, even the WT's are aligned in a line the downstream WT is still not fully influenced by the wake generated by the upstream WT. So the model presented in section 2.2.1 cannot be used directly, a modified model is required to take the shear effect into consideration. This problem has been solved by the proposed method in the attached paper [A2]. Based on the work [A1], the energy production of the wind farm with mixed hub height WT's can be calculated by using a modified matrix, hub height matrix. The calculation framework can then be modified in the following.

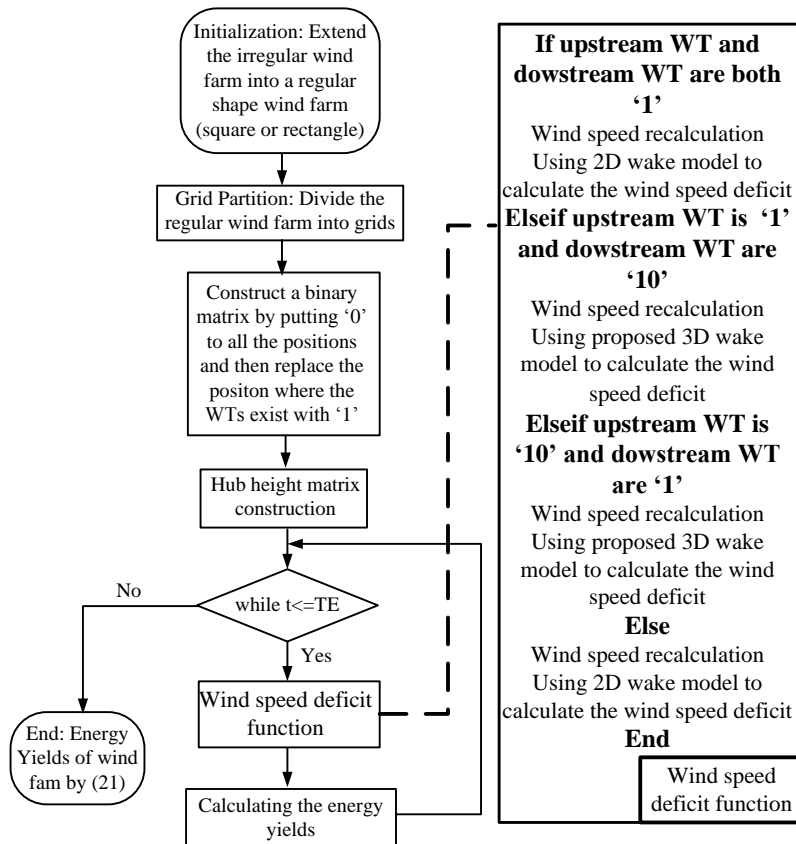


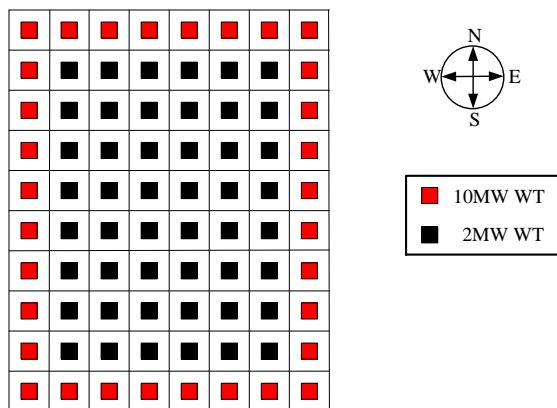
Figure 2.7 Calculation framework for energy production of wind farm with two hub height WTs [A2].

Similarly, the binary matrix will be used at first to shape the wind farm into the wanted wind farm layout. Then, the hub height matrix will be defined to identify the type of WT existed in the present position based on the information of binary matrix. In hub height matrix, number ‘10’ represents the second type WT and ‘1’ indicates the first type WT while ‘0’ means no WT in this position. Hence, based on the hub height matrix, not only the positions of installed WTs can be identified but also the type of WT in each position can be obtained. After that, the energy yields of mixed hub height WTs wind farm can then be calculated based on the similar procedure presented in section 2.2.2.

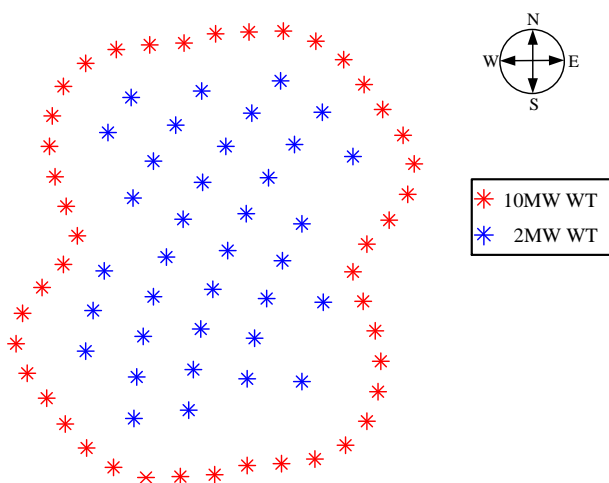
### 2.3.3. RESULTS AND DISCUSSIONS

In attached paper [A2], two study cases are given to validate the proposed method. It is assumed that there are two types of WTs in this case study, that is, Vestas V90-2.0

[114] and DTU 10MW reference WT [115]. The layouts of two reference wind farms are shown in figure 2.8.



(a)



(b)

Figure 2.8 Reference wind farms of two study cases. (a) Regular distributed wind farm layout. (b) Scattered wind farm layout [A2].

As can be seen in figure 2.8 (a), the black squares represent the 2MW WT while red squares indicate the 10MW WT. Similarly, the red stars in figure 2.8 (b) mean the 10MW WT while blue stars mean 2MW WT. The simulation results using proposed method are listed in table 2.2.

Table 2.2 Simulation results for two cases [A2]

		Wind farm capacity (MW)	Energy yields (GWh)	Capacity factor (%)	Energy yields without wake effect (GWh)	Capacity factor (no wakes) (%)	Wake losses efficiency (%)
<b>Case I</b>	<i>Mixed WT farm</i>	416	1813.4	49.76	2220.3	60.93	18.33
	<i>10MW WT farm</i>	800	3393.29	48.42	4386.12	62.59	22.64
	<i>2MW WT farm</i>	160	704.97	50.30	776.38	55.39	9.20
<b>Case II</b>	<i>Mixed WT farm</i>	512	2321.3	51.76	2761.7	61.58	15.95
	<i>10MW WT farm</i>	800	3870.68	55.23	4386.12	62.59	11.75
	<i>2MW WT farm</i>	160	684.57	48.84	776.38	55.39	11.83

In both cases, there are totally 3 scenarios as mixed WT farm, 10MW WT farm and 2MW WT farm respectively. In scenario 1 of case I, the wake losses can take up to 18.33% of total energy yields. Compared with scenario 1, the 10MW WT farm has the highest wake losses efficiency. This is because bigger WTs are installed in the reference wind farm which is designed for smaller WT wind farm. With a smaller distance between each pair of WT, the wake effect becomes more significant. By merely installing several bigger WTs in the outer layer of wind farm, the capacity factor can be improved by 1.5% and 2.9% in case I and II respectively.

## 2.4. SUMMARY

The wake effect contributes to the energy loss of offshore wind farm. The wake losses can take more than 10% of overall energy production of whole wind farm. In order to minimize this energy loss and give more benefits to the wind farm owner, the wind farm layout should be optimized and a good estimation of wake losses is the basis for solving WFLOP. Considering the variation in both wind velocity and direction, the wake losses calculation becomes more complex. In addition, the capacity of newly constructed wind farm is higher and higher which could involve hundreds of WTs. To minimize the wake loss, the wind farms are designed to be more and more scattered distributed which also brings challenges to the wake losses estimation work.

The formulation of wind speed deficit is described in this chapter. The proposed binary matrix method can evaluate the wake loss of any offshore wind farm which is demonstrated to be effective by comparing the results obtained from commercial energy production estimation software, WAsP. Besides, a novel method of estimating the wake loss for an offshore wind farm with mixed hub height WTs is also presented in this chapter which is expected to help optimize the future wind farm layout with multiple types of WTs.

The main work of this chapter has been presented in the author's previous publications [A1][A2].

### **Relevant attached papers**

- [A1] Peng Hou, Weihao Hu, Mohsen Soltani and Zhe Chen, "A Novel Energy Yields Calculation Method for Irregular Wind Farm Layout," *41th Annual Conference of the IEEE Industrial Electronics Society (IECON 2015)*, Yokohama, Japan, pp. 000380-000385, 2015, doi: 10.1109/IECON.2015.7392129.
- [A2] Peng Hou, Weihao Hu, Mohsen Soltani and Zhe Chen, "A New Approach for Offshore Wind Farm Energy Yields Calculation with Mixed Hub Height Wind Turbines," *Proceedings of the 2016 IEEE Power & Energy Society General Meeting 2016*, pp. 1-5, 2016.

# CHAPTER 3. OPTIMIZED CONTROL STRATEGY FOR OFFSHORE WIND FARMS

Chapter 3 presents the paper B, which has been published in IET Renewable Power Generation. This paper proposed an optimized control approach for entire wind farm which can reduce the LPC compared with traditional MPPT method. The proposed control strategy was also implemented in an extremely irregular shaped wind farm for demonstration.

## 3.1. STATE OF ART OF OPTIMIZED WIND FARM CONTROL STRATEGY

For an existing wind farm, the energy production is decided not only by the wind condition but also the applied control strategy. Commonly, the MPPT control strategy is adopted to control each wind turbine. By tracking the optimal power coefficient ( $C_p$ ), it can ensure the maximum energy production of a single wind turbine. However, considering the wake effect, the optimal wind turbine control strategy may not be the optimal control strategy for the whole wind farm. The mechanism can be explained with a simple example as shown in Figure 3.1.

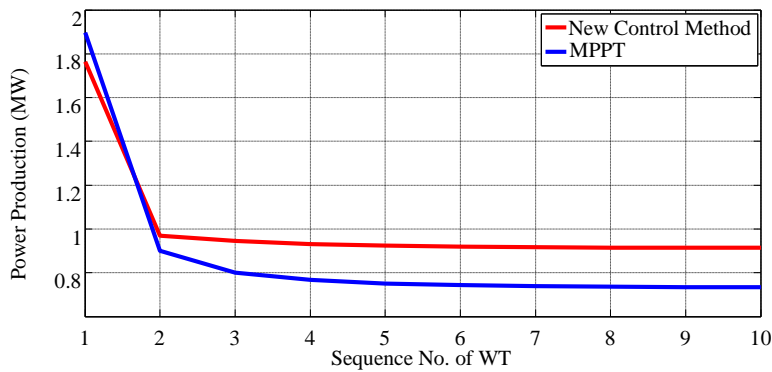


Figure 3.1 Power production comparisons between two methods when inflow wind speed is 8m/s and wind direction equals to  $0^\circ$ .

It is assumed that there are totally 10 WTs installed in a lone along the incoming wind direction. The power production for each WT using either MPPT (blue line) or optimized control method (red line) is shown in figure 3.1. The x axis is the sequence No. of each WT. It can be seen that if we tune the control parameters of

the first WT in a line and let it extract less energy from the wind then there is a chance to increase the power productions of the rest WTs. This simple example shows the basic idea of optimized control strategy.

Several works [96][116] have been done based on the idea presented above which intelligently changing the pitch angles or tip speed ratio of each WT. However, the existing works of control strategy optimization are at initial stage. The selected wind farm for case study is just 4 by 4 regular distributed wind farm and the objective function is merely the total power production from WTs within the wind farm while the power losses are neglected. The work can be improved by using LPC as the objective and select a well-designed offshore wind farm as the study case. This part of work will be specified in the following.

### **3.2. OPTIMIZATION METHOD**

The optimization algorithm can be mainly divided into two branches. The gradient based optimization method and non-gradient based method. For non-convex optimization problem with a large searching domain, it is impossible to enumerate to find the optimal solution and for some problem the gradient of the objective function cannot be derived. Hence, some researchers proposed meta-heuristic algorithm to help find an optimized solution without using the gradient information. Some meta-heuristic methods have already been used in WFLO as PSO [18]-[27], GA[16][17], DE [28] , ACO [29]. Within these methods, PSO and GA are widely used. In this work, PSO is selected since it outperformed than GA in finding a better solution [101]. The detailed description of PSO is specified in the following.

#### **3.2.1. PARTICLE SWARM OPTIMIZATION (PSO)**

Mimicking the social behavior of fish foraging and bird flocking, an evolutionary algorithm was proposed by Kennedy and Eberhart in 1995 [18]. It was proposed to solve non-convex optimization problem and demonstrated to have a good performance. The mechanism of PSO is illustrated in figure 3.2.



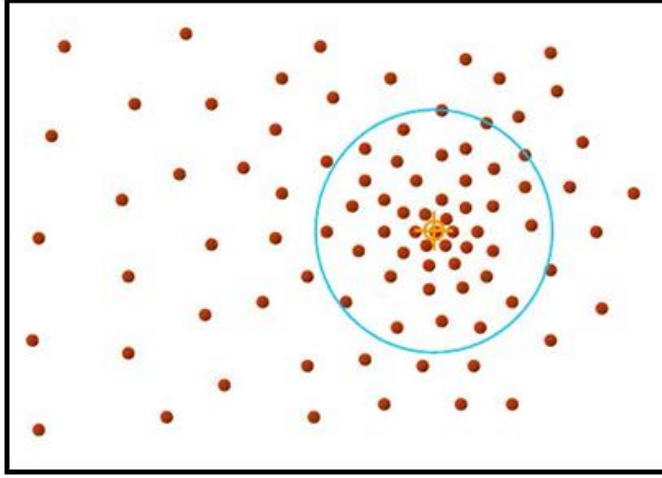


Figure 3.2 Illustration of PSO [18].

In PSO, each possible solution is defined as a particle which is illustrated with red dot in figure 3.2. The swarm size or particle population is the number of particles, in other words, the total number of red dots in figure 3.2. It can be seen from figure 3.2 that all the red dots (particles) are intended to move to the position where the yellow cross pattern exists. The red dot indicated by the yellow cross pattern is called the “global” optimal solution.

### 3.2.2. MATHEMATICAL EXPRESSION

Actually, the global optimal solution defined in PSO is just the best solution that PSO can found; it is not the optimal solution in theory. The global version PSO (GPSO) can be expressed as follows [A3]:

$$v_i^{k+1} = wv_i^k + l_1 \text{rand}_1 \left( \text{local}_i^k - x_i^k \right) + l_2 \text{rand}_2 \left( \text{global}^k - x_i^k \right) \quad (7)$$

$$x_i^{k+1} = x_i^k + v_i^{k+1} \quad (8)$$

As can be seen in (7), there are three parts in PSO. The first part represents the velocity of previous particle and  $w$  is inertial weight. The value of  $w$  represents the searching ability of PSO. For one thing, a larger  $w$  indicates a stronger global searching ability for another smaller  $w$  ensures the local searching ability. The rest two terms in (7) are used to ensure the local convergence ability of PSO. It can be seen that the final result is sensitive to the setting of the control parameters ( $l_1$ ,  $l_2$  and  $w$ ).

For different problem, the control parameters should be tuned so that a better solution can be found. However, it is not wise to use trial and error method to decide the value of control parameters for each problem. Hence, lots of works have been conducted to reduce the sensitivity of the global optimal solution to control parameters by changing  $w$  smartly. These works can be categorized into two sorts [20]: time-varying parameter control strategy [21]-[24] and adaptive parameter control strategy [25]. By using linear increasing/decreasing, non-linear changing or fuzzy rule inertia weight, the performance of PSO can be improved which is the first part control strategy while the second control strategy introduced evolutionary state estimation (ESE) technique [26] to increase the PSO performance. In addition, a PSO with multiple adaptive methods (PSO-MAM) was recently proposed and demonstrated to have an outstanding performance in finding a near optimal solution [117]. In this work, the non-linear inertia weight [21] control method is adopted which is shown as follow:

$$w = w_{final} + (w_{initial} - w_{final}) \left( \frac{I_{max} - t}{I_{max}} \right)^n \quad (9)$$

### 3.3. OPTIMIZED CONTROL STRATEGY FOR OFFSHORE WIND FARMS

As mentioned in section 3.1, the energy production of existing wind farm can be further increased by optimizing the power set point for each WT. In order to meet the requirement, the pitch angle or tip speed ratio should be controlled to follow the order from wind farm operator. On the other hand, changing pitching angle or tip speed ratio will change the performance of wake effect which influences the final power production of whole wind farm. In this chapter, the mathematical model for wind farm control optimization problem is introduced at first. The new control strategy is compared by MPPT at last.

#### 3.3.1. MATHEMATICAL MODELS

For the wind farm control strategy optimization, the wake model, power captured model and cost model are required. The wake model has been specified in section 2.2. The power captured model is as follow [A3]:

$$P_{mec} = \frac{1}{2} \rho \pi R^2 V^3 C_p(\beta, \lambda) \quad (10)$$

The power captured by a WT can be expressed as (10) and can be drawn as a curve in its whole operation region which is called power curve [118] as shown in figure 3.3.

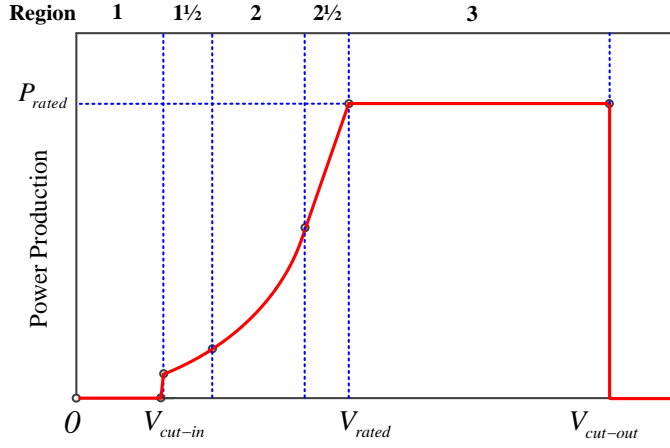


Figure 3.3 WT power curve [A3].

As can be seen in figure 3.3, there are totally four parts in this power curve. Region 1 is the first part, in which the wind speed is lower than cut-in speed. Hence the WT does not start to generate power. Region 2 is the second part where the MPPT control strategy [119] works. In this region, the pitch angle and tip speed ratio are both set to their optimal value as  $\beta_{opt}$  and  $\lambda_{opt}$  respectively by tuning the rotor speed to its reference [120]. Region 3 is the third part where the wind speed is over the rated wind speed, the reference rotor speed will be the nominal rotor speed,  $\omega_{rot}^{nom}$ , [120] and the tip speed ratio will not be its optimal value any more. Hence, the tip speed ratio and power coefficient should be recalculated as follows:

$$\lambda = \frac{\omega_{rot}^{nom} R}{V} \quad (11)$$

$$C_p(\beta, \lambda) = \frac{2 \times 10^6 P_{mec}^{rated}}{\rho \pi R^2 V^3} \quad (12)$$

The pitch angle,  $\beta$ , can be obtained by interpolating the power coefficient table  $C_p(\beta, \lambda)$  when  $C_p(\beta, \lambda)$  and  $\lambda$  are calculated by (11) and (12). The last part contains the transition regions 1/2 and 2/2. In both regions, the generator rotational speed will be the lower limit  $\omega_{rot}^{min}$  for Region 1/2 and the nominal value  $\omega_{rot}^{nom}$  for Region 2/2 which is kept at a fixed value. Similarly,  $\lambda$  can be determined by (11) for a certain wind speed and based on this value the optimal power coefficient value  $C_p^{opt}(\beta, \lambda)$  and then the corresponding pitch angle  $\beta$  can be found in the look-up table  $C_p(\beta, \lambda)$  [120] by interpolation.

In this work, only the cable cost is considered and also only the cable's power losses are considered. The cost model of cable can be expressed as [102]:

$$C_i = A_p + B_p \exp\left(\frac{C_p S_{n,i}}{10^8}\right)^2 \quad (13)$$

$$S_{n,i} = \sqrt{3} I_{i,rated} U_{i,rated} \quad (14)$$

### 3.3.2. OBJECTIVE FUNCTION

As discussed above, the four parameters  $\beta$ ,  $\lambda$ ,  $C_p$  and  $C_t$  are interrelated. Hence, by changing the blade pitch angle of each WT the overall power production of wind farm could be increase. However, it should also be noticed that the profits is decided by the power reached at the onshore substation which means that the power losses should also be considered. Thus, LPC is adopted as the evaluation index which takes both total discounted costs and the total discounted energy output (considering the power loss in each cable) into account. The expressions are as follows [A3]:

$$CAP_t = \sum_i^N C_i L_i Q_i \quad (15)$$

$$C_0 = \sum_{t=1}^{Ny} CAP_t (1+r)^{-t} \quad (16)$$

$$\text{Obj.: } \min_{\beta_{mn}} \left\{ LPC = \frac{C_0 r (1+r)^{Ny}}{(1+r)^{Ny} - 1} \frac{1}{\sum_n \sum_m^{Num\_col \text{ Num\_row}} 0.5 \rho C_{p,mn}(\beta_{mn}, \lambda_{mn}) \pi R^2 v_{mn}^3} \right\} \quad (17)$$

$$\text{Constraints: } \beta_{min} \leq \beta_{ij} \leq \beta_{max} \quad (18)$$

$$P_{ij} \leq P_{rated} \quad (19)$$

$$\omega \leq \omega_{max} \quad (20)$$

$$\frac{\partial C_p(\beta_{mn}, \lambda)}{\partial \lambda} \leq 0 \quad (21)$$

Where  $C_0$  is the total investment and assumed to be made in the first year and paid off during the lifetime of the wind farm. The last constraint (21) is used to ensure WT not to fall into stall region, in other words, the  $\lambda$  has to limit to be in the right side of  $C_p$ - $\lambda$  curve.

### 3.4. RESULTS AND DISCUSSIONS

Two study cases are presented in [A3]. One is a regular shaped wind farm which is similar to the layout of Horns Rev I and the other is NORCOWE reference wind farm [121]. The layouts are shown in figure 3.4 [A3].

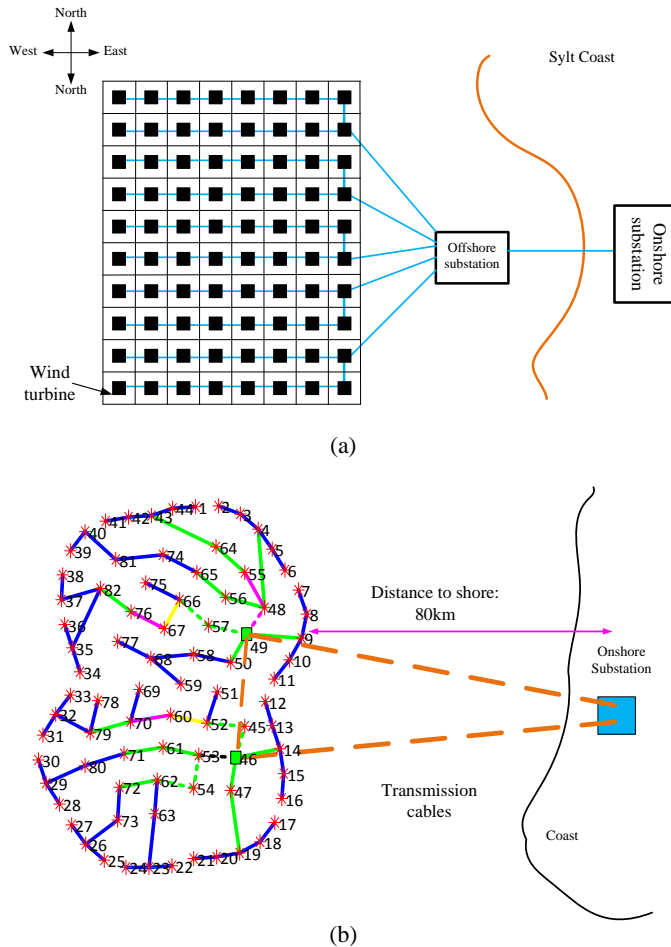


Figure 3.4 Reference wind farm layout. (a) Regular shaped wind farm layout. (b) NRWF layout.

The first reference wind farm is with a regular wind farm layout while the WTs in NRWF are distributed more randomly. For the first case study, the optimized power dispatch (OPD) control strategy was tested with a small example at first. It is assumed that the wind velocity is 6m/s and  $0^\circ$  wind direction. Since the spacing between each WT columns or rows is with 7 D which is large enough to avoid wake intersection, there is no wake effect between rows. Also, the upwind speed reached

at the first WT of each row is assumed to be the same. Hence, only one row WT's power production is shown and compared with the results obtained by MPPT control strategy in figure 3.5.

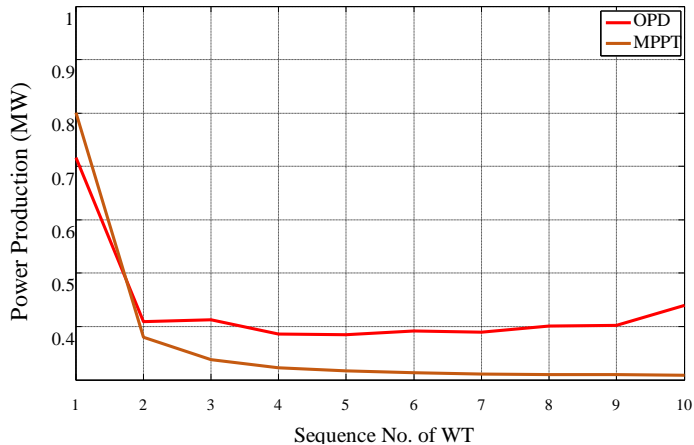


Figure 3.5 Power production comparisons between OPD and MPPT when incoming wind velocity is 6m/s and wind direction equals to 0° [A3].

It can be seen that by forcing the first WT generating less power, there is a significant power enhancement from other WTs. The detailed results are shown in table 3.1.

Table 3.1 Simulation results for test example [A3]

Sequence No. of WT column	TCS				OPD			
	$\lambda$	$\beta$	$\omega$	$v$	$\lambda$	$\beta$	$\omega$	$v$
1	7.5	0	6.82	6	7.5	3.12	6.82	6
2	7.5	0	5.32	4.68	7.5	3.16	5.78	5.09
3	7.5	0	5.12	4.50	7.5	3.14	5.74	5.05
4	7.5	0	5.04	4.44	7.5	3.03	5.67	4.99
5	7.5	0	5.01	4.41	7.5	3.51	5.69	5.00
6	7.5	0	4.99	4.39	7.5	2.97	5.70	5.02
7	7.5	0	4.98	4.38	7.5	2.96	5.69	5.01
8	7.5	0	4.98	4.38	7.5	3.40	5.69	5.00
9	7.5	0	4.97	4.37	7.5	3.97	5.64	4.96
10	7.5	0	4.07	4.37	7.5	3.69	5.59	4.91
Power production	29.70 MW				34.66 MW			
LPC	2794.7 Dkk/MW				2395.8 Dkk/MW			

It can be seen that by using the OPD strategy, the overall power production can be increased by 16.7% which results in 14.3% LPC reduction compared with MPPT strategy.

The simple example shows the effectiveness of the proposed method. However, it should also be noticed that the proposed method is essentially minimizing the overall wake losses by control each WT. In this example, the wind direction is aligned with the WTs row which makes the wake losses higher than other situation (different wind directions). Hence, it is interesting to see the performance of the proposed method in different situations. Based on this idea, several scenarios have been done for different wind velocities and directions in [A3]. Also, the energy production is calculated over a year base on the OPD and the results are presented as a wind rose as follows:

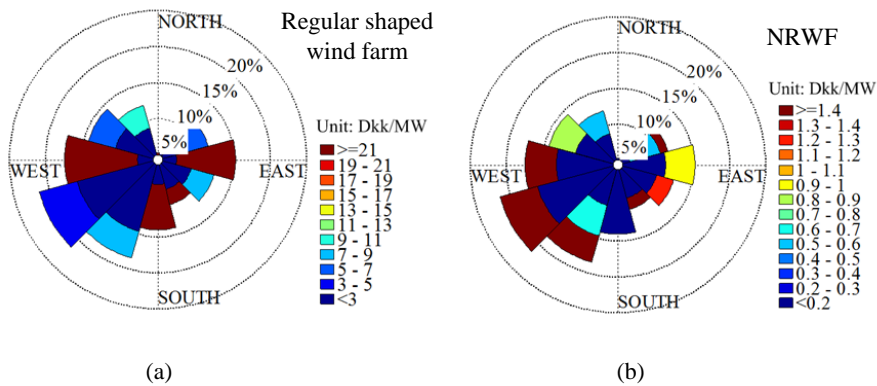


Figure 3.6 Simulation results illustration by wind rose. (a) LPC reduction percentage for regular shape wind farm layout in one year. (b) LPC reduction for NRWF in one year [A3].

From figure 3.6, it is shown that the LPC of both regular and irregular shaped wind farm can be reduced by OPD method and the reduction of LPC of the irregular shaped wind farm was lower than that of the regular shaped wind farm. The reason is that irregular shaped wind farm has been designed to minimize the wake compared with regular shaped wind farm, that is to say, there are less wake losses in this irregular shaped wind farm compared with regular shaped wind farm.

Table 3.2 Simulation results for two cases [A3]

Name	MPPT control strategy	OPD control strategy	LPC reduction proportion
Regular shaped wind farm	375.37 Dkk/MW	367.13 Dkk/MW	2.20%
NRWF	338.5788 Dkk/MW	338.0733 Dkk/MW	0.15%

From table 3.2, it can be seen that the OPD method can reduce the LPC of regular shaped wind farm and irregular shaped wind farm by 2.20% and 0.15% respectively compared with the MPPT control strategy. It is an effective way of improving the economic performance of an existing offshore wind farm.

### 3.5. SUMMARY

In order to make more profit, the wake losses should be minimized. In design phase, the wind farm layout can be optimized to maximize the energy yields while for an existing wind farm; it is also possible to increase the power reached at the onshore substation by optimizing the power production reference of each WT within the offshore wind farm.

By using the OPD strategy instead of traditional MPPT control strategy, the LPC of regular/irregular shaped wind farm can be reduced. By tuning the pitch angle of WT, the power reference given by the wind farm operator can be met. Since the problem is non-convex and the gradient information of the objective function is hard to obtain, meta-heuristic algorithm, PSO is adopted and demonstrated to be an effective tool of finding a better solution.

#### Relevant attached papers

[A3] Peng Hou, Weihao Hu, Baohua Zhang, Mohsen Soltani, Cong Chen, Zhe Chen, "Optimised Power Dispatch Strategy for Offshore Wind Farms," *IET Renewable Power Generation*, Vol. 10, Issue 3, pp. 399-409, 2016.



# CHAPTER 4. OFFSHORE WIND FARM LAYOUT OPTIMIZATION

This chapter discusses the criteria for evaluating the economic performance of offshore wind farm layout. The concept of forbidden area offshore in WFLOP is given and solved by penalty function method. A wind farm layout co-optimization problem is also at last.

## 4.1. STATE OF ART OF WFLO

At early times, the wind farm is always designed based on the empirical data, for instance, 8 to 12 D separation between two WTs in prevailing wind blowing direction while 3D to 5D in orthotropic direction. Then, several researches showed that scattered WT distribution layout can benefit the wind farm owner more by reducing the wake losses. Presently, the WFLOP can be classified into two sorts: grid model based optimization [73]-[83] and coordinate model based optimization [82]-[93]. Using the coordinate model, the wake losses can be further minimized compared with grid model. However, the complexity of the problem will be significantly increased which emphasis the importance on the performance of optimization algorithm. The majority of the WFLO works are solved by meta-heuristic optimization works as PSO [78][86][87][A4]-[A7], GA [73][79][88][89][93], evolutionary algorithm [81][84], random search algorithm [91], colony algorithm [85] and some new research works began to use gradient based optimization method [82][83][90][92] instead.

## 4.2. REGULAR SHAPED OFFSHORE WFLO

The objective of WFLO is to decide the WTs' positions within the wind farm so that more benefits can be obtained by the wind farm owner. Increasing the energy production can bring more profits to the wind farm owner while reducing the investment can also make the wind farm cost effective. Due to the wake effect, a larger spacing between WTs means more energy production. However, more investment should be paid on electrical system, especially the cables. Hence, there should be a tradeoff. Based on this idea, index is selected as the evaluation index in this work. The wake losses estimation is based on the work presented in 2.2. The cost model in 3.3.1 is adopted. The study case is a regular shaped wind farm which is shown in figure 4.1.

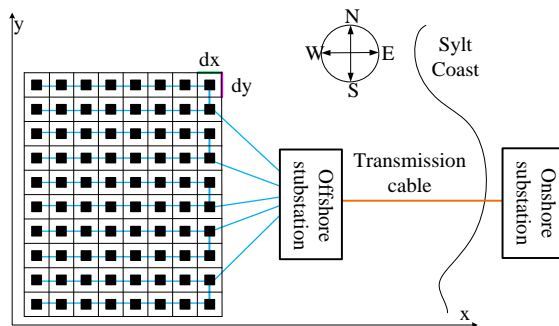


Figure 4.1 Regular shaped wind farm layout [A4].

The blue lines indicate the collection system cable layout while brown line shows the transmission cable. The reference wind farm is composed by 80 DTU 10MW WT, the detailed information is listed in table 4.1.

Table 4.1 DTU 10MW WT information [115]

Name	Value
Cut-in wind speed	4 m/s
Cut-out wind speed	11.4 m/s
Rated wind speed	25 m/s
Rotor diameter	178.3m
Rated power	10 MW

In this work, the wind farm layout is optimized in terms of spacing's between WT rows and columns using the optimization algorithm presented in section 3.2.2, that is GPSO with nonlinear weight control. The optimized WT positions for each layout are illustrated in figure 4.2.

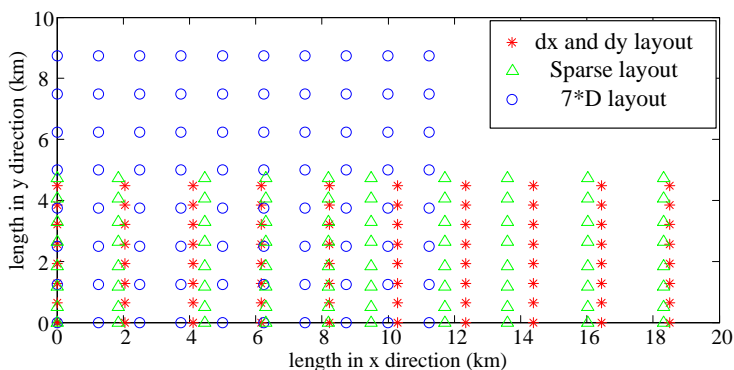


Figure 4.2 WT positions for optimized wind farm layouts [A4].

In figure 4.2, the 7D layout is the benchmark. The spacing between each WT row and column is 7D in this layout where the WT positions are illustrated with blue circles. The red stars show the WT positions for  $d_x$  and  $d_y$  layout, in which the distances between each pair of WT in a row and the distances between each pair of WT in a column is assumed to be the same. The GPSO is only used to optimize these two distances while in sparse layout the distances between each pair of WT in a column is assumed to be different, so do the row distances. The WT positions for this layout are indicated with green triangles in figure 4.2. The final results are listed in table 4.2.

Table 4.2 Simulation results for regular shaped WFLO [A4]

Name	Optimal layout for constant $d_x$ and $d_y$	Sparse optimal layout	7D layout
Annual power losses	45.28 GWh	46.80 GWh	51.71 GWh
Annual energy yields	3556.46 GWh	3637.96 GWh	3839.94 GWh
Cable cost	837.01 MDKK	848.36 MDKK	959.41 MDKK
LPC	238.4549 DKK/MWh	236.3054 DKK/MWh	253.3376 DKK/MWh
Layout	4.99km*8.84km	4.99km*12.45km	8.73km*11.23km

It can be seen that GPSO can help find an optimized layout which reduces LPC by 5.87% and 6.72% respectively compared with benchmark, and occupy less sea area.

Usually, the WFLOP will be solved by assuming that all WTs are under the MPPT control strategy. In chapter 3, an optimized control strategy has already been introduced which was demonstrated to be outperformed than MPPT in reducing the LPC of offshore wind farm. It can be imagined that if the optimized control strategy can be considered in the WFLO process, the designed wind farm layout would be more cost effective. In addition to that, the dominant inflow wind for a specific location is different. The empirical results show that the spacing between each pair of WT along the dominant inflow wind direction should be larger other directions so that the wake losses can be reduced which means that the geographic direction of regular shaped wind farm has an impact on the wake losses and should be considered in the WFLOP.

Based on the same reference wind farm as shown in figure 4.1, the WFLO considering the above two aspects is proposed in [A6]. The optimized layouts are shown in figure 4.3.

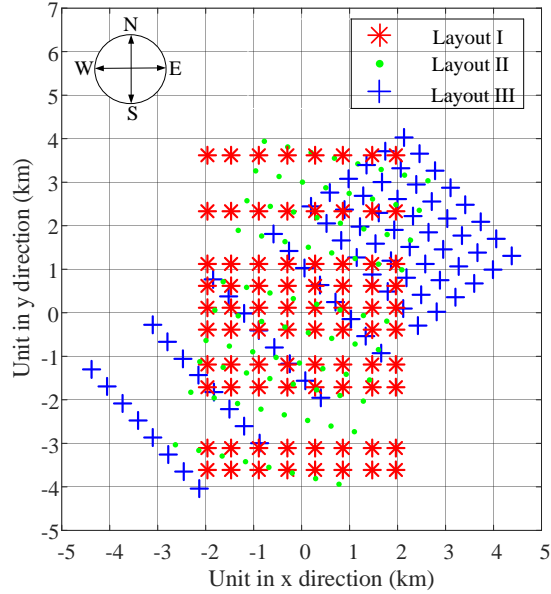


Figure 4.3 WT positions for each optimized wind farm layout [A6].

For this problem, the spacing between WTs in a row and the spacing between WTs in a column, the wind farm direction and control strategy should be optimized simultaneously. In each layout, the WTs are connected with the same cable connection configuration. In order to improve the performance of PSO and get a better result, an adaptive inertia weight control strategy was applied [25]. In figure 4.3, several layouts which correspond to different optimization objectives are shown as follows:

- Layout I: Optimizing the spacing of each WT row and column which is the same work as proposed in [A4]. (Scenario I)
- Layout II: Part a. Optimizing the WT interval and wind farm direction simultaneously. (Scenario II) Part b. control strategy optimization based on layout obtained from Part a. (Scenario III)
- Layout III: Combining the work mentioned in Layout II which is optimizing the wind farm layout and control strategy at the same time. (Scenario IV)

The specification of each layout is in listed table 4.3 as follows.

Table 4.3 Simulation results for wind farm layout co-optimization [A6]

	Wind farm direction (°)	Energy yields (GWh)	Cost of cables (MDkk)	LPC (DKK/MWh)
Benchmark	0	1972.9	345.25	178.14
Scenario I	0	1884.3	317.75	171.55
Scenario II	-14.89	2143.9	314.67	149.45
Scenario III	-14.89	2147.2	314.67	149.23
Scenario IV	-50.63	2096.4	306.70	148.95

In table 4.3, the benchmark is the performance of the wind farm before optimization; the layout is shown in figure 4.1. It can be seen that the optimized layouts in Scenarios I to IV can reduce the LPC by 3.70%, 16.10%, 16.23% and 16.38% respectively compared with the benchmark. The aims of optimizing the wind farm direction or spacing between WTs are both finding the tradeoff between wake losses reduction and cable investment reduction. Considering the wind farm direction into optimization can further reduced the LPC by 13% which demonstrated that wind farm direction is an important factor for regular shaped WFLO.

By simultaneously optimizing the control strategy and wind farm layout as in Scenario III and IV, the LPC can be merely improved by 0.15% and 0.33% respectively compared with Scenario II. This corresponds to the conclusion in chapter 3 that the optimized control strategy is essentially aiming at redistributing the wake losses among the WTs within the wind farm. For a well-designed wind farm, this strategy cannot improve the performance of wind farm significantly.

### 4.3. IRREGULAR SHAPED OFFSHORE WFLO

As mentioned above, the wake losses can be further minimized if coordinate model is adopted. However, the total number of potential solutions will be greatly increased compared with the optimization using grid model. Hence, the performance of optimization method should be improved to help find a near optimal solution. For the irregular shaped wind farm layout design, a PSO-MAM algorithm is adopted. The detailed information for PSO-MAM is specified in [20].

The position of each WT should be optimized to minimize wake losses within a predefined construction sea area. However, there could be some offshore regions that exists some facilities as oil well, pipelines or shipwreck, etc. which make these regions impossible to install WTs. In order to ensure all the WTs are installed out of the restriction regions, a penalty function method is applied to simplify the numerical calculation. The mathematical expression is in the following.

$$\phi(L_i) = \left| \min \{0, F_r(L_i)\} \right| \quad (22)$$

The purpose of this work is to maximize the energy production of the whole wind farm. Based on (22), the objective function of this work can be written as:

$$\max \left( E_{tot}(L) - PF \sum_{i=1}^c \phi(L_i) \right) \quad (23)$$

Once a potential solution (all WT positions) is found by PSO-MAM, the program will check if there is any of WTs is within the predefined restriction area and if so the penalty function will penalize the present solution (in other word,  $\Phi(L_i)$  will not equal to 0 anymore) by reducing the total energy production as (23). In such a way, PSO program will update its present solution by avoiding WTs enter into forbidden area by and by since the solution without triggering the penalty function will have a higher energy production.

In this work, NRWF is selected as the benchmark which has been shown in figure 3.4 (b). In order to test the performance of PSO-MAM, the final results obtained by PSO-MAM was also compared with the results obtained by GA. The predefined restriction zones are shown in figure 4.4 and the optimized wind farm layouts are shown in figure 4.5.

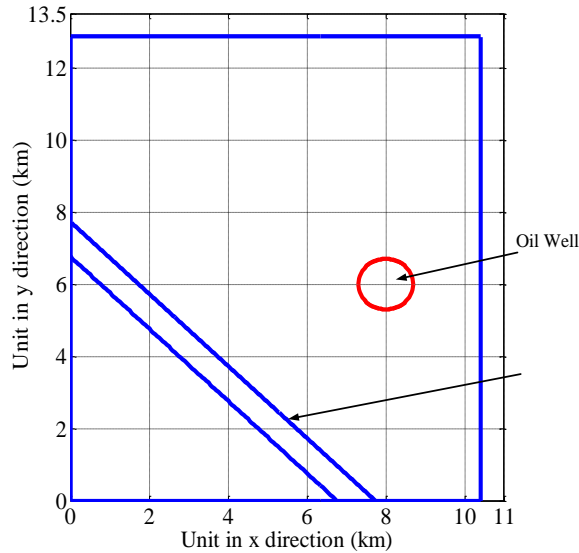


Figure 4.4 Illustration of restriction region [A5].

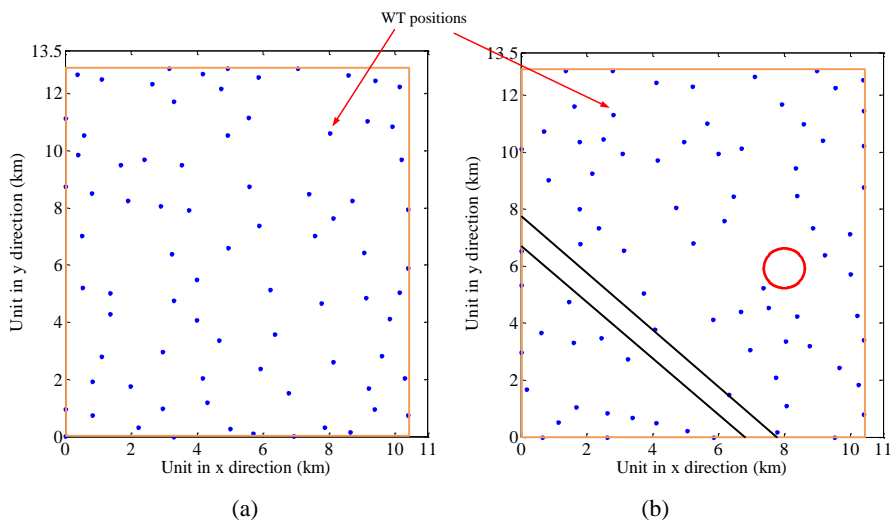


Figure 4.5 Optimized wind farm layouts for irregular shaped wind farm. (a) Optimized layout for unrestricted region. (b) Optimized layout for restricted regions [A5].

It can be seen that the optimized layout is more scattered and some WTs are installed on the boundary of wind farm. The penalty function helps PSO find an optimized layout where all WTs are located outside the restriction area as shown in figure 4.5 (b). The simulation results are concluded in table 4.4.

Table 4.4 Simulation results for WFLO considering restriction area [A5]

Name	Energy yields (GWh)		Capacity factor (%)	
	PSO-MAM	GA	PSO-MAM	GA
NRWF	4015.17		57.29	
Scenario I	4169.24	4048.23	59.49	57.76
Scenario II	4151.95	3892.02	59.25	55.54

From table 4.4, it can be seen that the optimized layout in scenario I can increase the energy yield by 3.84% compared with NRWF layout. Even if a restriction area is assumed as in scenario II, the energy yield is still 3.41% higher than the NRWF layout. Compared PSO-MAM with GA, it can also be seen that PSO-MAM outperformed than GA in finding an optimized wind farm layout which generated 2.99% and 6.68% more energy in the respective scenarios.

#### 4.4. CO-OPTIMIZATION OF OFFSHORE WIND FARM LAYOUT

The WTs extract the power from wind and transmitted to the onshore substation by a series of submarine cables. With the increasing capacity of offshore wind farm, the

cost of electrical system can take up to 30% of overall investment while a large proportion is invested on cables. Hence, it is critical to optimize the cable connection scheme to deliver the power to shore efficiently. Traditionally, the wind farm layout will be firstly designed according to the local wind resource with the purpose of minimizing wake losses. After that, the electrical system including equipment type, voltage level, quantity and location of OS as well as cable connection scheme will be designed to realize a cost effective wind farm.

As introduced in 4.1, the investment on cables related to the wind farm layout which means that there is a possibility of optimizing the wind farm layout and electrical system simultaneously so that a more cost effective wind farm can be created.

In our previous works, the regular shaped WFLO and irregular WFLO have been done [A4]-[A6]. For the co-optimization of wind farm layout and cable connection scheme, more variables which are either integer (cable connection scheme) or continuous (WT positions, OS positions) are needed to be optimized. The recent proposed PSO-MAM method has good performance compared with other versions of PSO. However, it can only be applied to solve continuous optimization problem. Thus, the mixed integer PSO with adaptive inertial weight control optimization method is adopted in this work. To cope with integer optimization problem, the PSO can be modified by taking the integer value of the updated particle (solution) in each iteration. The mathematical expression is written as follows:

$$x_i^{k+1} = \text{int}(x_i^k + v_i^{k+1}) \quad (24)$$

The LPC is also adopted as the evaluation index in this work. The minimum distance between each pair of WT cannot be smaller than 4D [72], this constraint has been satisfied by using the penalty function method which is introduced in 4.3. The APSO-MST algorithm is adopted for solving the cable connection scheme optimization problem. This algorithm will be specified in chapter 5.

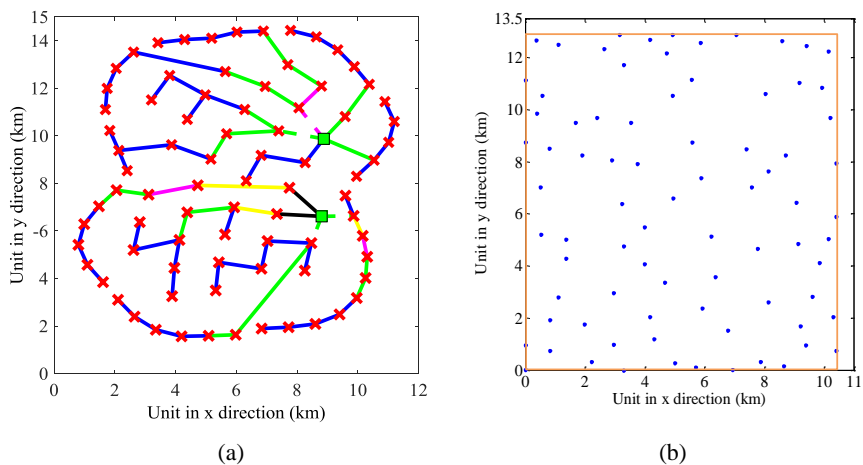
The NRWF is also selected as the reference wind farm which is composed by 80 10MW WT as specified in table 4.1. In figure 3.4 (b), the WT positions, the cable connection layout as well as the selected cable types are all illustrated. The color lines indicate different sectional cable areas which are specified in table 4.5.



Table 4.5 Cables' sectional areas specification by color [A7]

Name	Collection line				
Voltage	66kV				
Type	AC				
Color	Blue	Green	Purple	Yellow	Black
Cable sectional area (mm <sup>2</sup> )	95/150	240/300	400/500	630/800	1000

The optimized wind farm layout performance is compared with NRWF layout. In order to see the performance of the co-optimization method, the proposed method procedure was compared with three other optimization procedures and the results are presented in scenario I through IV. The optimized wind farm layouts with cable connection scheme are shown in figure 4.6.



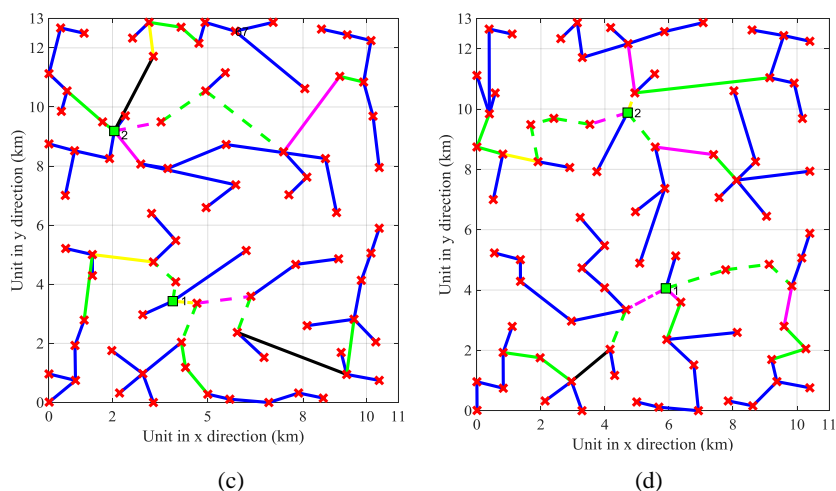


Figure 4.6 Wind farm layouts comparison. (a) Scenario I: Cable connection layout optimization for NRWF layout. (b) Scenario II: Wind farm layout from [A6]. (c) Scenario II: Cable connection layout optimization for the wind farm layout given in (b). (d) Scenario III: The wind farm layout design by proposed co-optimization procedure.

In figure 4.6, the red crosses represent the WT, color lines indicates different sectional area cables which correspond to the information given in table 4.5. The simulation results of three scenarios as well as the benchmark are listed in table 4.6 as follows.

Table 4.6 Simulation results for wind farm layout co-optimization [A7]

Name	Cost of link cables	Cost of collection system cables	Total cost	Energy yields from all WTs	Energy reached at onshore sub-station	LPC
Benchmark	30.86 MDkk	229.25 MDkk	1417.18 MDkk	4010.93 GWh	3927.68 GWh	360.92 Dkk/MWh
Scenario I	22.85 MDkk	215.24 MDkk	1392.60 MDkk	4010.93 GWh	3928.56 GWh	354.59 Dkk/MWh
Scenario II	42.37 MDkk	250.99 MDkk	1450.18 MDkk	4169.24 GWh	4078.53 GWh	355.67 Dkk/MWh
Scenario III	41.69 MDkk	230.30 MDkk	1397.14 MDkk	4164.08 GWh	4075.84 GWh	342.89 Dkk/MWh

In table 4.6, the link cables are the cables between two OSs and the cost of collection system cables are the overall cost of cables for connecting WTs. Compared with benchmark (NRWF layout), it can be seen that the LPC in scenarios I through III has been reduce by 1.75%, 1.45% and 5.00% respectively. The highest energy yields are from scenario II which has a 3.95% enhancement compared with benchmark. However, the total cost is also increased by 2.33%. As a result, the LPC is only reduced by 1.45% and this is also the reason why scenario III is the best layout which achieved a further 3.59% reduction in LPC compared with scenario II. The scenario II is the tradition method which optimizes the wind turbine positions at first and then optimizes the cable connection layout, the simulation demonstrated that it is the best method to minimize the overall losses. However, it is not the best method for planning an overall cost effective wind farm. The best layout is from scenario III which is the proposed co-optimization method.

#### 4.5. SUMMARY

With the increasing capacity of offshore wind farm, the investment of electrical system become larger and larger, this could take up to 30%. As one part of electrical system, submarine cables take a large proportion of overall investment on electrical system. To make a cost effective wind farm, two aspects should be concerned: energy production and investment. The WFLO is with the purpose of optimizing the WT positions to minimize wake losses while electrical system design concerns about how to deliver the power generated by each WT to shore economically. These two aspects are inevitably correlated and should be considered simultaneously in the wind farm planning stage.

In this chapter, several optimized wind farm layouts has been presented. The co-optimization procedure which optimizes the wind turbine positions together with cable connection layout is demonstrated to be the best method in terms of delivering a cost effective offshore wind farm. The control strategy can also be optimized together with wind farm layout. However, due to the limitation in the accuracy of wake model and technology for wind speed forecasting, more research should be done to make it into real application.

The main work of this chapter has been presented in the author's previous publications [A4]-[A7].

#### Relevant attached papers

[A4] Peng Hou, Weihao Hu, Mohsen Soltani, Zhe Chen, "Optimized Placement of Wind Turbines in Large Scale Offshore Wind Farm using Particle Swarm

- Optimization Algorithm,” *IEEE Transactions on Sustainable Energy*, Vol. 6, Issue 4, pp.1272-1282, 2015.
- [A5] Peng Hou, Weihao Hu, Mohsen Soltani, Zhe Chen, “Optimization of Offshore Wind Farm Layout Considering Restriction Zone,” *Energy*, Vol. 113, pp. 487-496, 15 Oct. 2016.
- [A6] Peng Hou, Weihao Hu, Mohsen Soltani, Cong Chen, Baohua Zhang, Zhe Chen, “Offshore Wind Farm Layout Design Considering Optimized Power Dispatch Strategy,” *IEEE Transactions on Sustainable Energy*, Vol. 8, Issue 2, pp. 638-647, 2016.
- [A7] Peng Hou, Weihao Hu, Mohsen Soltani, Cong Chen, Zhe Chen, “Combined Optimization for Offshore wind farm Planning,” *Applied energy*, Vol. 189, pp. 271-282, March 2017.

# CHAPTER 5. ELECTRICAL SYSTEM DESIGN FOR LARGE-SCALE OFFSHORE WIND FARMS

In this chapter, several methods for cable connection layout optimization are presented. The overall electrical system optimization problem including, cable connection layout optimization, voltage level selection and OS locating is investigated and solved by a mixed integer APSO-MST algorithm.

## 5.1. STATE OF ART OF ELECTRICAL SYSTEM OPTIMIZATION FOR OFFSHORE WIND FARM

The electrical system optimization for offshore wind farm can be categorized into three parts: the locating of OS [48][49], the cable connection scheme design [37]-[47], [52][53][99][100] the electrical components selection including voltage level selection [50]. The cable connection scheme optimization problem can be solved using classic mathematical models as MST [39][49][53][99][100], TSP [38][41], OVRP [52] or meta-heuristic optimization method as GA [39]-[42], PSO [37][40]. Recently, linear programming was also applied in solving CCLOP [45][47]. The locations of OSs have an obvious impact on the formulation of cable connection layout. So does the components selection. Hence, the correlation among these three aspects should be investigated and considered in the electrical design of offshore wind farm.

## 5.2. CABLE CONNECTION LAYOUT OPTIMIZATION USING DETERMINISTIC ALGORITHMS

Since the crossed cable connection layout will increase the investment on installation, it is desirable to make an uncrossed layout which minimizes the investment. If each WT location is regarded as a vertex, while the cost of cable between each pair of WT is considered as the weight of the line, then the problem can be easily transformed into a classic mathematical problem of finding a MST from a weighted graph. However, in MST, the weight of each line is always given. So the final layout found by MST will be the optimal solution. As for CCLOP, the cable costs are decided by both distance between two WTs and the cable sectional area which is decided by voltage level and current carrying capacity. If more WTs are connected to one feeder, then the cables in previous arrangement might have to be changed which means the weight of each line is not fixed and thus the MST cannot ensure the optimal solution for this problem anymore. In order to further reduce the investment, a deterministic algorithm, Dynamic MST (DMST) is

proposed in [A13] which can be explained by a simple example as shown in figure 5.1.

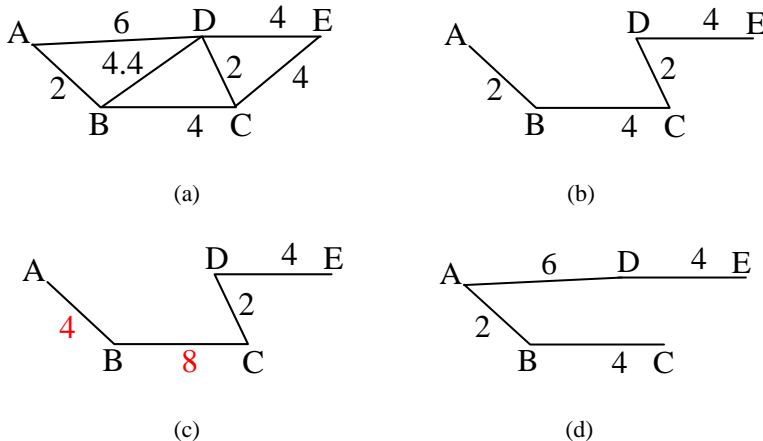


Figure 5.1 Simple example for DMST method. (a) Weighted graph (b) Layout obtained by MST. (c) MST layout with updated weights. (d) Layout obtained by DMST [A13].

In figure 5.1 there are totally 5 vertices. Assuming A is the starting point where the tree shaped layout begins to formulate. The full information of this weighted graph is shown in (a) where the number besides each line indicates the value of weight and the layout formulated by MST method is shown in (b). It can be seen that the total weights using MST is  $2+4+2+4=6$ . If this weight only represents the distance between each pair of WT then it is the optimal solution. However, if the weight in previous arrangement is assumed to be doubled when more than 2 vertices are connected after one branch (which simulating the situation that bigger sectional area (also more expensive) cable should be used when more WTs are connected in one feeder). Then the weights in layout (b) should be updated as (c) and in this case the total weight should be  $4+8+2+4=18$ . (d) is the layout found by DMST method which considers the impact of the vertices that is about to be added into the present layout on the previous layout's weight. Thus, a layout with less total weight (that is  $2+6+4+4=16$ ) can be found by DMST compared with MST.

The DMST method has been applied on a reference wind farm which has a similar layout as Anholt offshore wind farm. The cable costs are calculated based on the cost model presented in section 3.3.1. The layout of the reference wind farm is shown in figure 4.7 (a). The cable sectional area and corresponding current carrying capability is decided according to the information provided in table 5.1.

Table 5.1 Cable sectional area V.S. current carrying capacity [A13]

10-90 kV XLPE 3-core cables		100-300 kV XLPE 3-core cables	
Cross section (mm <sup>2</sup> )	Current carrying capacity (A)	Cross section (mm <sup>2</sup> )	Current carrying capacity (A)
95	300	300	530
120	340	400	590
150	375	500	655
185	420	630	715
240	480	800	775
300	530	1000	825
400	590		
500	655		
630	715		
800	775		
1000	825		

In table 5.1, all available cables for both collection and transmission system cables are listed. This is the database for solving the following CCLOP.

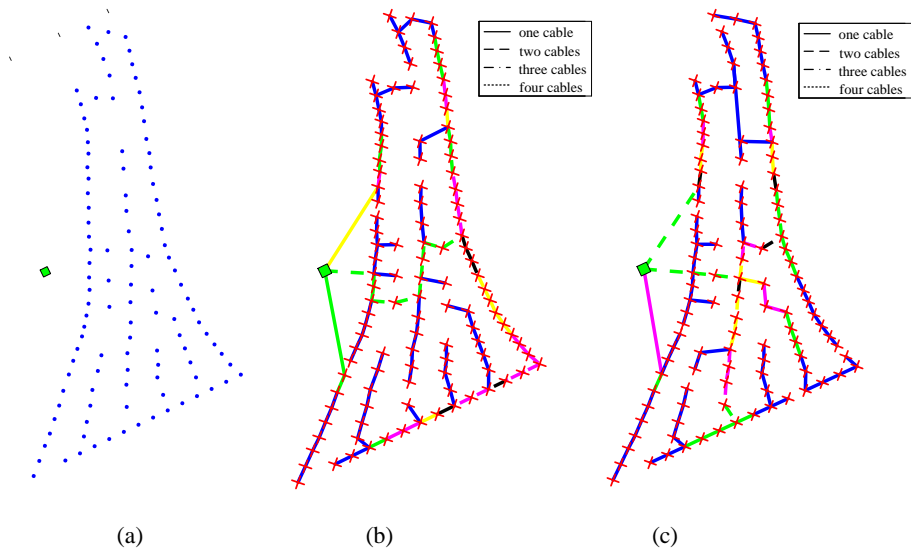


Figure 5.2 Layouts for case study. (a) Reference wind farm layout. (b) Optimized layout found by MST method. (c) Optimized layout found by DMST method [A13].

The blue dots in figure 5.2 (a) show the WTs' positions of reference wind farm and the same wind farm layout was illustrated with red crosses in (b) and (c). The color

lines represent different cable sectional area cables which have been specified in table 4.5. The simulation results are concluded in table 5.2.

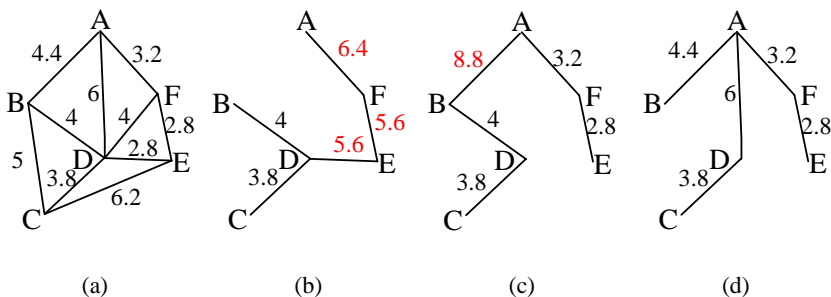
Table 5.2 Simulation results comparison between MST and DMST [A13]

Name	MST	DMST
Investment on cables (MDKK)	399.06	374.70
Total length of cables for collection system (km)	99.215	98.785
Trenching length for collection system (km)	69.741	78.214

It can be seen in table 5.2 that the total investment on collection system cables can be reduced by 6.10% using DMST method compared with MST method. However, the minimum trenching length was found by MST method instead of DMST method with a 10.83% reduction. This is because between some pairs of WTs there could be more than one laid cables. As a result, the overall cable length found using MST was longer than that obtained by DMST. In addition, some thicker cables are used in the layout found by MST which can be seen from the colors of figure 5.2 (b) and (c). As a result, the overall investment needed for MST layout is higher than DMST layout.

### 5.3. CABLE CONNECTION LAYOUT OPTIMIZATION USING HEURISTIC ALGORITHM

As mentioned in section 5.2, the CCLOP can be solved using deterministic algorithms as MST and DMST algorithm. However, these methods make decisions step by step and once a decision is made it cannot be changed any more, this means that some potential solutions are neglected. By using heuristic method, there is a possibility of finding a better layout among these potential solutions and this is the basic idea of APSO-MST method. The differences among these methods are compared through a simple example as illustrated in figure 5.3.





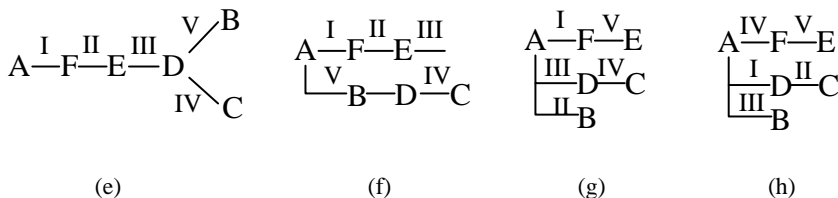


Figure 5.3 Comparison of three cable connection layout optimization methods. (a) Weighted graph with 6 vertices and 10 branches with different weight. (b) Layout found by MST. (c) Layout found by DMST. (d) Layout found by APSO-MST. (e) The layout formulation procedure by MST. (f) The layout formulation procedure by DMST. (g) and (h) The layout formulation procedure by APSO-MST. [A9].

Similar to the example shown in figure 5.1, it is assumed that there are totally six vertices are to be connected. (a) is the graph which contains 10 weighted branches. The number besides the line shows the weight value. Also, A is selected as the searching start point and in this example it is also assumed that the weights in previous arrangement will be doubled when more than 2 nodes are connected after one feeder. The doubled weights are illustrated with red color in figure (b) and (c). The layout found by MST method is shown in (b) and the total weight is  $3.2*2+2.8*2+2.8*2+2+1.9=21.5$ . As introduced in section 5.2, the layout found by DMST method is shown in (c), the total weight is  $4.4*2+2+1.9+1.6+1.4=15.7$ . The APSO-MST can randomly select the vertex to add into the present formulated layout, one possible solution found by APSO-MST is shown in (d). The total weight of graph (d) is  $2.2+1.6+1.4+3+1.9=10.1$ . In figure 5.3 (e) through (h), the tree graphic formulation sequence is indicated by the Greek numerals I to V. As introduced above, MST and DMST are deterministic algorithms. Thus, the layout formulation process is unique as shown in figure 5.3 (e) and (f). Compared with deterministic algorithm, the heuristic method, APSO-MST will random select a branch in each tree formulation step. Therefore, the layout formulation process is not unique. Figure 5.3 (g) and (h) shows two layout formulation processes. Though the layout formulation sequence is different, the final layout is the same. Due to this release in the freedom of branch selection, the lowest weight layout can be found by the APSO-MST method compared with MST and DMST methods in this example.

Based on this idea, a case study is made to validate the effectiveness of proposed algorithm. With the purpose of demonstrating the performance of APSO-MST method, a randomly designed reference wind farm is selected which is shown in figure 5.4.

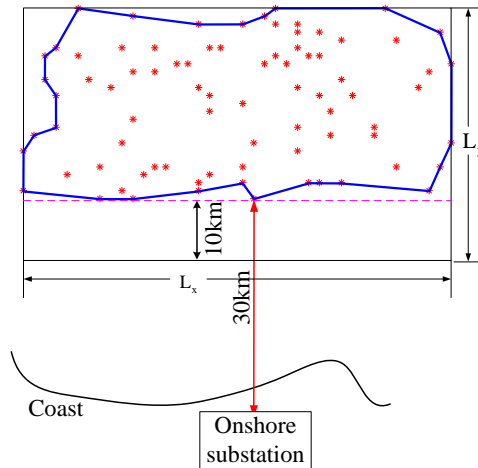
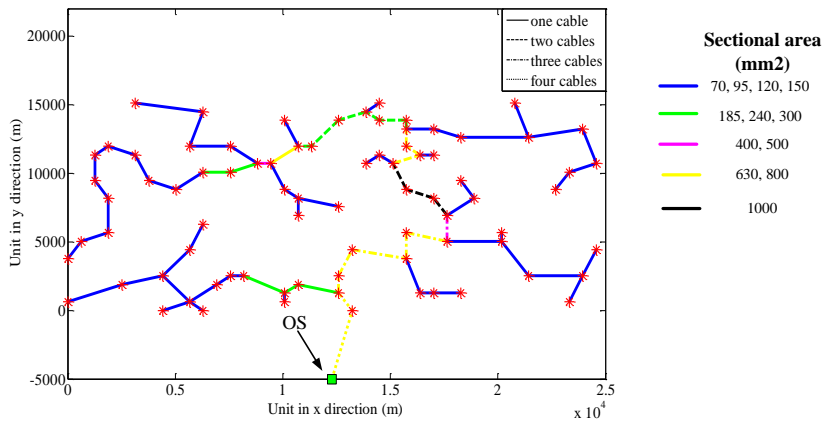


Figure 5.4 Reference wind farm layout illustration for case I.

In figure 5.4, the black square is the boundary for locating OS while the red stars represent the WT. In order to investigate the OS's impact on the layout formulation, three scenarios are considered in this case, that is, cable connection layout optimization with OS near shore, cable connection layout optimization with central located OS and simultaneous optimization of cable connection layout and OS location. The optimized layouts for each scenario using three methods are illustrated in figure 5.5 to 5.7 respectively.



(a)

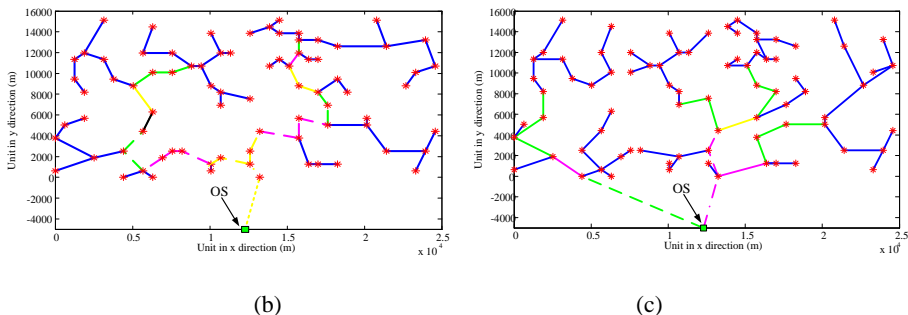


Figure 5.5 Optimized cable connection layouts with near shore OS for case I. (a) Layout found by MST when OS near shore. (b) Layout found by DMST when OS near shore. (c) Layout found by APSO-MST when OS near shore.

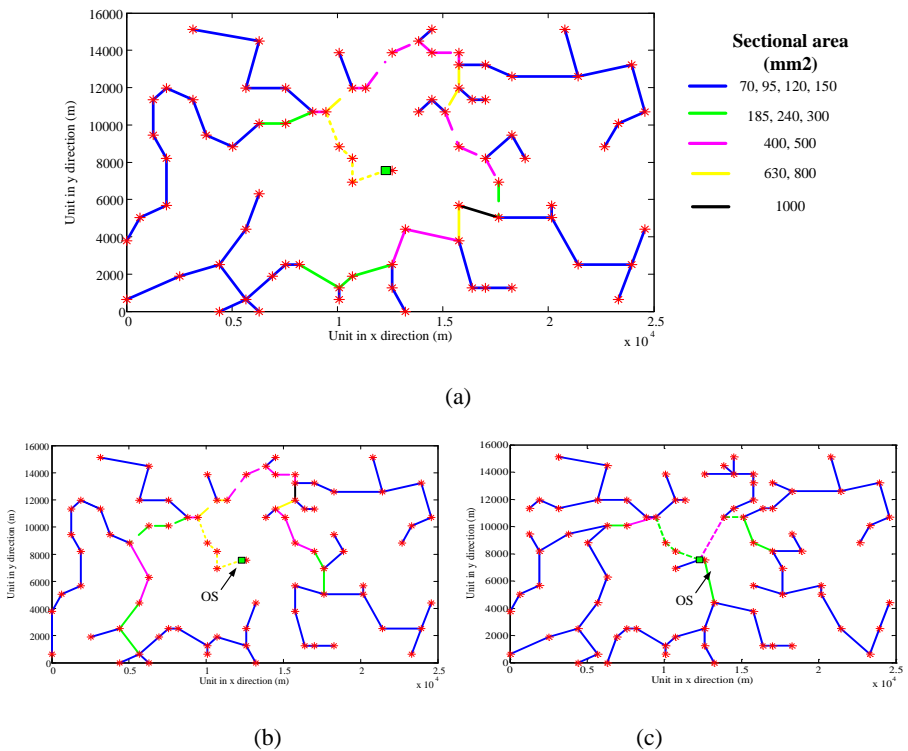


Figure 5.6 Optimized cable connection layouts with near shore OS for case I. (a) Layout found by MST when OS near shore. (b) Layout found by DMST when OS near shore. (c) Layout found by APSO-MST when OS near shore.

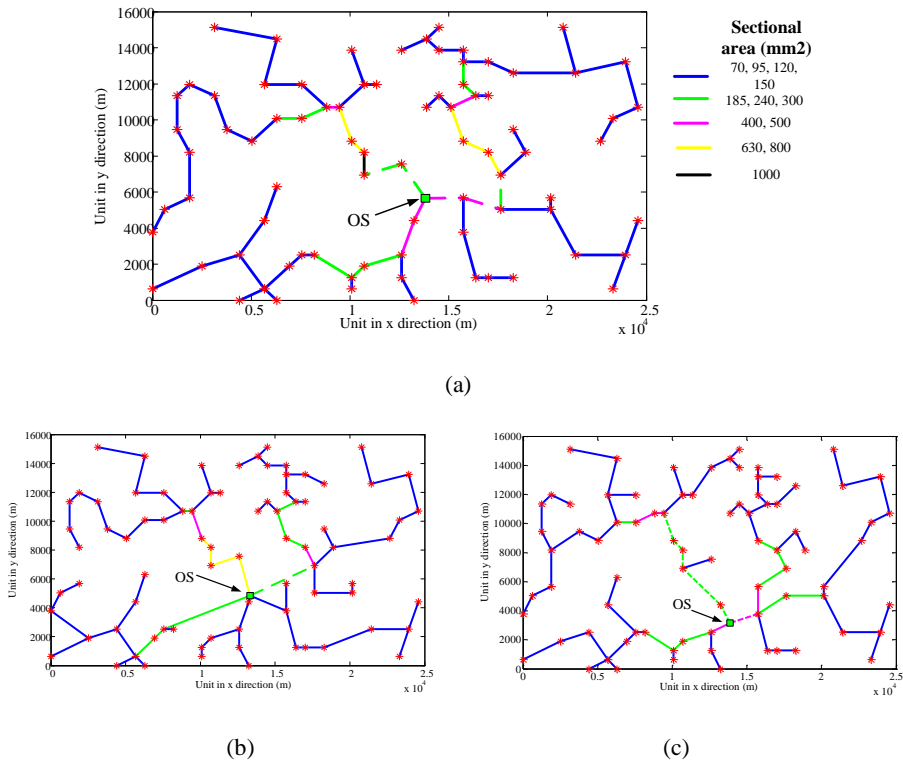


Figure 5.7 Optimized cable connection layouts with near shore OS for case I. (a) Layout found by MST when OS near shore. (b) Layout found by DMST when OS near shore. (c) Layout found by APSO-MST when OS near shore.

The available cable types that can be used for layout optimization is illustrated with different colors through figure 5.5 to 5.7. The simulation results are listed in table 5.3.

Table 5.3 Layout performance comparison among three cable connection optimization methods [A13]

	OS near shore			Central located OS			Simultaneous		
	<i>MS T</i>	<i>DM ST</i>	<i>APSO -MST</i>	<i>MST</i>	<i>DM ST</i>	<i>APSO -MST</i>	<i>MST</i>	<i>DMS T</i>	<i>APSO- MST</i>
Total cable length for CS (km)	193.20	181.88	185.22	174.57	161.96	149.80	140.70	144.37	146.35
Total trenching length for CS (km)	135	136.36	161.12	129.93	130.94	140.44	130.61	139.58	135.24
Cable to shore (km)	25	25	25	37.56	37.56	37.56	35.67	37.30	33.19
Cable costs for CS (MDkk)	390.79	349.71	294.68	330.50	295.94	210.89	222.99	215.38	215.79
Cable costs for TS (MDkk)	103.75	103.75	103.75	155.87	155.87	155.87	148.04	154.80	137.73
Total cable invest (MDkk)	494.54	453.46	398.43	486.37	451.81	366.76	371.03	370.18	353.52
Sub-staion location	(12.29,-5)			(12.29,7.56)			(13.81,5.64)	(13.7,5.26)	(13.86,3.15)

From table 5.3 it can be seen that APSO-MST method can find the best layout in each scenario while DMST method is better than MST in finding a cheaper cable connection layout. Compared with MST and DMST, the APSO-MST method can reduce the cost by 19.4% and 12.1% respectively in scenario I, 24.6% and 18.8% in scenario II, 4.7% and 4.5% in scenario III. When the OS location is considered in the optimization process, it can be seen that no matter which method is adopted, the

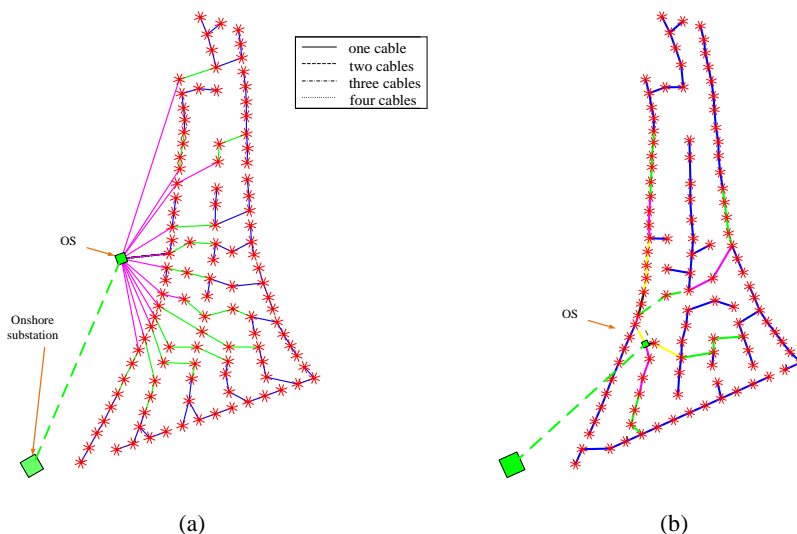
cost in each scenario can all be reduced which show the importance of considering OS location in cable connection layout optimization. It can also be noticed that when the OS is located within the wind farm as scenario II and III, the cost can be reduced which corresponds to the conclusion that central located OS can help make a more cost effective cable connection layout design.

#### 5.4. ELECTRICAL SYSTEM OPTIMIZATION FOR OFFSHORE WIND FARM

With the increasing capacity of offshore wind farm, more than one OS would be required. The power collected by collection systems will be first transmitted the corresponding OS and then to the onshore substation. Hence, it is meaningful to optimize the quantity of OSs and the cable connection layout related to each OS. Also, the electrical components and voltage level selection have an impact on the layout formulation. The above aspects should all be considered so that an overall optimization for offshore wind farm electrical system can be fulfilled.

In order to decide the quantity of OSs, the FCM algorithm is adopted to partition the whole wind farm into several sub regions and the number of sub regions is the same to the number of OSs. The APSO-MST algorithm presented in section 5.4 is adopted to optimize the cable connection layout and the voltage level and equipment selection is through MIAPSO which is introduced in section 4.4.

The reference wind farm layout is the same as figure 5.2 (a) and the cable connection layout is shown in figure 5.8 (a).



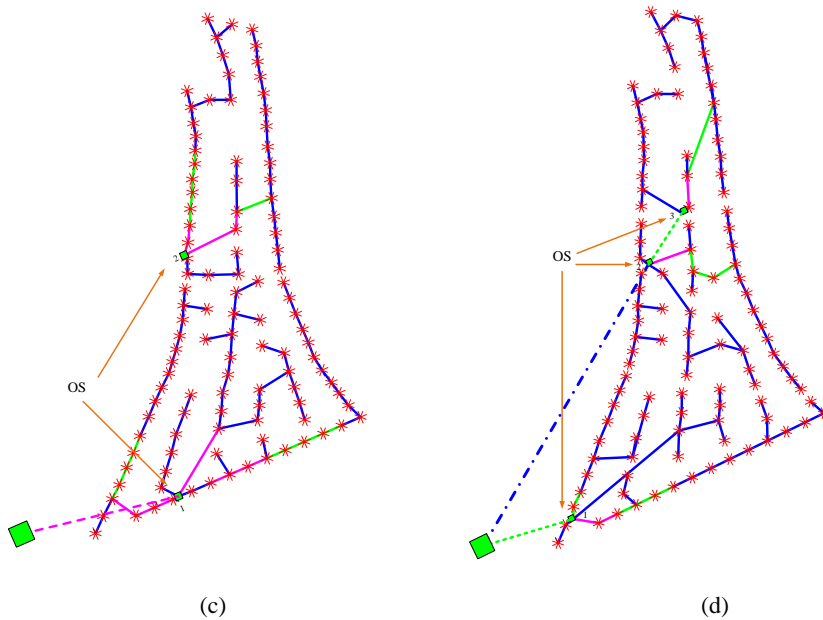


Figure 5.8 Cable connection layout illustrations. (a) Industrial layout for reference wind farm (Layout 1). (b) Cable connection layout optimization result with one OS through APSO-MST (Layout 2). (c) Cable connection layout optimization result with two OSs through APSO-MST (Layout 3). (d) Cable connection layout optimization result with three OSs through APSO-MST (Layout 4). [A11].

The selected cable size is illustrated using different color lines which has already been specified in table 4.5. An industrial layout is selected as the benchmark which is similar to the Anholt wind farm layout [122]. The optimized cable connection layout with different number of OSs is shown in figure (b) to (d). The detailed information of each optimized layout is specified in table 5.4.

Table 5.4 simulation results for overall electrical system optimization [A11]

	<b>Layout 1</b>	<b>Layout 2</b>	<b>Layout 3</b>	<b>Layout 4</b>
Transformer type	33/220 kV, 220 MVA	66/220 kV, 220 MVA	66/220kV, 140, 85 MVA	66/220, 60, 80, 85 MVA
Quantity of platform	1	1	2	3
Cost of CS	26.25 M€	19.81 M€	17.36 M€	18.56 M€
Cost of TS	23.02 M€	22.63 M€	23.98 M€	25.47 M€
Cost of cable installation	28.70 M€	32.05 M€	31.22 M€	33.42 M€
Total length of cables	14.77 km	16.48 km	16.06 km	17.19 km
Transformer cost	2.25 M€	2.25 M€	3.17 M€	3.86 M€
Platform	35.73 M€	35.73 M€	38.67 M€	40.85 M€
Total cost	115.95 M€	112.46 M€	114.40 M€	122.16 M€
Energy losses along cables	23.42 GWh	15.89 GWh	9.64 GWh	1.92 GWh
Energy yields at onshore substation	1887.89 GWh	1895.42 GWh	1901.67 GWh	1902.39 GWh
Cost of energy	61.42 €/MWh	59.33 €/MWh	60.16 €/MWh	64.21 €/MWh

In table 5.4, the energy yields at onshore substation are calculated by taking wake effect and the losses along the cables into account. The wake losses calculation is based on the previous work [A1] which has been specified in section 2.2. The cost of energy is defined as the total cost over energy yields. Layout 2 to 4 are obtained by proposed method, it can be seen that the total cost can be reduced by 3.01% and 1.33% in layout 2 and 4 compared with layout 4. Though the CS cable costs was reduced by layout 4, the big increase on the cost of platforms and transformers results in a 5.35% higher total cost compared with layout 1. Layout 3 and 4 can deliver more energy to shore. However, the lowest cost of energy layout is layout 2 which is the most cost effective layout in this work.

## 5.5. SUMMARY

With the increasing proportion of electrical system investment in the capital investment, more and more research focused on the electrical system optimization of large scale offshore wind farm to help deliver a cost effective wind farm. The



electrical system optimization problem includes several aspects: cable size selection and connection layout design, voltage selection for both CS and TS, transformer type selection, OSs' quantity and locations' optimization. The optimization variables are either integer or continuous. Though PSO-MAM is demonstrated to have a better performance, the APSO method is adopted instead to solve this problem since PSO-MAM can only solve continuous optimization problem. The cable connection layout optimization can be solved by heuristic optimization method or using deterministic algorithms as MST or DMST. Though the heuristic optimization method can find a cable connection layout with lower cost or LPC, it cannot ensure the robustness of the final solution which is a drawback compared with deterministic algorithm. The FCM algorithm can be adopted to help partition the wind farm into sub regions and the proposed APSO-MST method can help connect the WTs in each sub region. However, in FCM method the OS is planned to be central located which is proved to be not the best solution by [A12]. Hence, this algorithm has been modified to optimize the OS location in each sub region and shows better performance.

The main work of this chapter has been presented in the author's previous publications [A8]-[A13].

### Relevant attached papers

- [A8] Peng Hou, Weihao Hu, Cong Chen, Zhe Chen, "Optimization of Offshore Wind Farm Cable Connection Layout Considering Levelised Production Cost Using Dynamic Minimum Spanning Tree Algorithm," *IET Renewable Power Generation*, Vol. 10, Issue 2, pp. 175-183, Feb. 2016.
- [A9] Peng Hou, Weihao Hu, Zhe Chen, "Optimization for Offshore Wind Farm Cable Connection Layout using Adaptive Particle Swarm Optimisation Minimum Spanning Tree Method," *IET Renewable Power Generation*, Vol. 10, Issue 5, pp. 694-702, 2016.
- [A10] Peng Hou, Weihao Hu, Cong Chen, Mohsen Soltani, Zhe Chen, "A Novel Way for Offshore Wind Farm Cable Connection Layout Design with Meta-heuristic Optimization," *Renewable Energy*, 1<sup>st</sup> revision.
- [A11] Peng Hou, Weihao Hu, Cong Chen, Zhe Chen, "Overall Optimization for Offshore Wind Farm Electrical system," *Wind energy*, 2016, DOI: 10.1002/we.2077.
- [A12] Peng Hou, Weihao Hu, Zhe Chen, "Offshore Substation Locating in Wind Farms Based on Prim Algorithm," *Power and Energy Society General Meeting 2015*, pp. 1-5, 26-30 July 2015. (Best Paper Award)
- [A13] Peng Hou, Weihao Hu, Zhe Chen, "Offshore Wind Farm Cable Connection Configuration Optimization using Dynamic Minimum Spinning Tree Algorithm," *50th IEEE International Universities Power Engineering Conference (UPEC 2015)*, England, UK, pp.1-5, 2015.

# CHAPTER 6. OFFSHORE WIND FARM REPOWERING OPTIMIZATION

This chapter investigates the repowering strategy of offshore wind farm which makes the best use of the present component within the wind farm. The problem will be introduced in the following and the criteria for WT type selection for making a mixed type WT offshore wind farm will be investigated.

## 6.1. STATE OF ART OF OFFSHORE WIND FARM DECOMMISSIONING

Decommissioning is considered to be the last step of the project. According to [123], decommissioning can be defined as the reverse of the installation phase; the objective of decommissioning is to return the site to its condition before project deployment as far as possible. The first offshore wind farm decommissioning on record (Yttre Stengrud wind project) happened in 2016 [124]. This project only operated for 15 years [125]. However, due to the difficulty of finding spare parts and huge cost of repairs and upgrades, the wind farm owner decided to dismantle it [124].

Instead of fully dismantling the whole wind farm, repowering could be another way which can reduce the impacts of the offshore wind farm on the local marine environment [126][127]. Since some components within the wind farm usually have a longer life time. For example, the foundation has a life time over 100 years [128] and the cables can last over 40 years [129]. Based on this, some wind farm owner decided to repower the offshore wind farm which use the majority of the original electrical system (or foundations) to install bigger wind turbines or change some component so that the production efficiency can be increased [130]-[132], [126], [133], [128][129][134][135]. However, the profitability of the repowering option was not demonstrated until [136] which evaluated the lucrativeness of repowering wind farm by net present value (NPV). It can be concluded that full repowering will be attractive after 20-25 years of operation. Before this time, the benefits of repowering are insignificant. Moreover, partial repowering shows only about 10% cost savings compared with full repowering, so it is not preferable unless advanced technology can be applied to promote generation efficiency or minimize operating costs. However, not all wind turbines will be out of order at the exact same time as [136] assumed. The replacement of merely one wind turbine within a wind farm will cause changes in the wind conditions observed for the other wind turbines, due to changes in wakes. It is therefore worth considering which wind turbine to remove and which type of WT to install instead to maximize the energy output of the remaining wind turbines.

## 6.2. WIND FARM REPOWERING OPTIMIZATION

The repowering strategy intends to make best use of the existing facilities, However, the conditions in each wind farm are different (wind condition, original wind turbine type, wind turbine layout, etc.). The quantitative analysis is required to evaluate the profitability of repowering strategy. Therefore an optimized repowering strategy is proposed in this paper to help the wind farm owner make the decision. The concept is elaborated with a simple example as shown in figure 6.1.

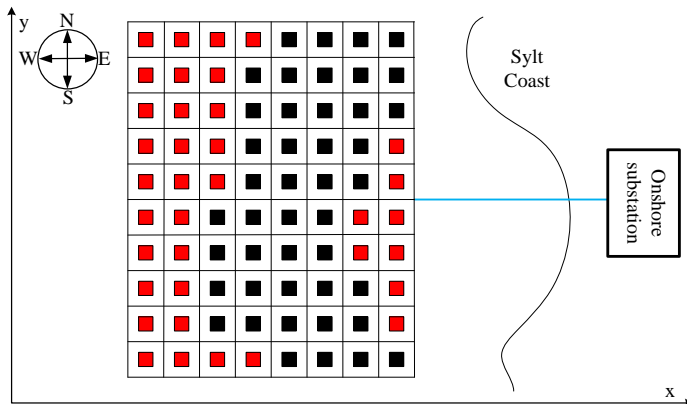


Figure 6.1 The reference wind farm layout for simple example.

In figure 6.1, the squares represent the WTs. It can be imagined that not all WTs “break” at the same time. In this work, it is assumed that the old WTs will be dismantled over several generations. The WTs marked with red in figure 2 are assumed to be dismantled or repowered after 20 years’ operation, which is the first generation of repowering. Several types of WTs can be selected to replace the original WTs in this research. It is assumed that if the original type of WT (Vestas V80-2.0 MW) or a smaller WT is selected, then no further costs for foundations would be needed, while installation of bigger WTs will incur higher costs of both WT and foundation. After the first repowering generation is completed, the remaining old WTs may need to be operated together with the new WTs, which are expected to improve production efficiency. In this research, it is also assumed that 4 years after the first repowering generation, the WTs represented by black squares are required to be replaced as well. In the first repowering generation, there is a possibility that a few locations exist where no new WTs were installed. Hence, the optimization process at this time will involve not only the selection of WTs for the remaining locations but also the locations where no WTs were installed in the first repowering generation. Finally, a new wind farm with mixed types of WTs may be constructed.

It can be known that using bigger WT's to repower wind farm will result in a higher energy production. However, more investment is needed since the larger the WT the more expensive it is. The proposed wind farm repowering strategy should help find this tradeoff by minimizing the LCoE for offshore energy.

### 6.3. METHODOLOGIES

In order to help select the locations to dismantle or install new WT's, the integer PSO (IPSO) which introduced in section 4.4 is adopted. The 4D distance between each pair of WT's (bigger WT's could be installed which has a bigger rotor diameter) can be satisfied by using the penalty function method specified in 4.3. The evaluation index is LCoE in this research. The energy production considering wake losses for this work is based on the model presented in section 2.3.

### 6.4. RESULTS AND DISCUSSIONS

The information of available WT types is listed in table 6.1. The Horns Rev I wind farm is selected as the reference wind farm for simulation which has been introduced and shown in 4.1. The wind farm is with the capacity of 160 MW based on 80 wind turbines with a hub height of 70 m.

Table 6.1 Specification of WT's [A14]

Type	Siemens 1.3 (I)	Vestas V90- 1.8 (II)	Vestas V80-2.0 (III)	Siemens 2.3 (IV)	Siemens 3.6 (V)	NREL 5MW (VI)	DTU 10 MW (VII)
Rated power	1.3MW	1.8 MW	2 MW	2.3 MW	3.6 MW	5 MW	10 MW
Cut-in wind speed	4 m/s					3 m/s	4 m/s
Rated wind Speed	17 m/s	13 m/s	14.5 m/s	16 m/s	17 m/s	11.4 m/s	11.4 m/s
Cut-out wind Speed	25 m/s						
Rotor diameter	62m	90m	80m	93m	107m	126m	178.3m
Hub height	60m	80m	67m	80m	80m	90m	119m

The WTs listed in table 6.1 is the database which is used for constructing the new wind farm. Two cases are presented to demonstrate the effectiveness of the proposed repowering optimization strategy. In case I, the original WTs will be replaced with the same type WT in each repowering process so the energy yields after each repowering optimization are the same (“new for old” repowering optimization strategy). Case II uses the proposed repowering optimization method to select which type of WT should be used to replace the original one. The final optimized layouts are shown in figure 6.2.

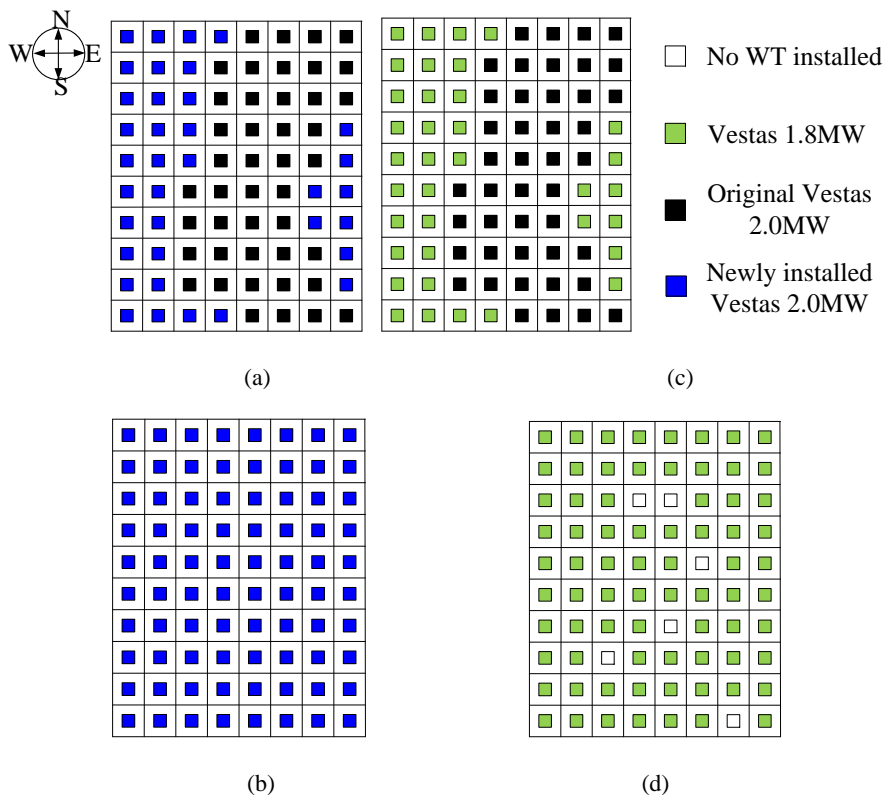


Figure 6.2 Repowering result after each replacing period. (a) the wind turbine selection after first repowering in case I. (b) the wind turbine selection after second repowering in case I. (c) the wind turbine selection after first repowering in case II. (d) the wind turbine selection after second repowering in case II [A14].

Figure 6.2 (a) and (c) shows the results after first repowering phase, the black blocks are the original WTs and the newly installed WTs are illustrated in blue (scenario I) or green (scenario II) while figure 6 (b) and (d) shows the result after the second repowering phase, assumed to take place 4 years after the first repowering has been

finalized. The energy productions of the wind farm after each repowering process in each scenario are concluded in table 6.2.

Table 6.2 Comparison of different repowering strategies for each repowering process [A14]

		Capacity	Original 2MW WT Left	Number of 2MW WT Newly Installed	Power Production	Capacity Factor (%)
Case I	1st repowering	160 MW	44	36	81.74 MW	51.08
	2nd repowering	160 MW	0	44	81.74 MW	51.08
Case II	1st repowering	152.8 MW	44	36	77.38 MW	50.64
	2nd repowering	133.2 MW	0	44	73.47 MW	55.16

It can be seen in table 6.2 that the capacity factor of case I after 1<sup>st</sup> repowering is just a little bit higher compared with the result of case II while after 2<sup>nd</sup> repowering, the capacity factor of case I becomes 7.99% lower than case II. This is because in this case the original wind farm layout is designed according to 2MW WT which is larger than the newly installed WT. The wake losses in the new constructed wind farm would have less wake losses and thus the capacity factor is increased. It is interesting to see that bigger WT is not selected in case II which contradicts with the common sense that it is more profitable to install bigger WT. The reason is that the reference wind farm in this case is designed for 2.0 MW WT which means the distances between pair of WTs are relatively smaller for bigger wind turbine. If bigger WT are adopted, the wake losses will be greatly increased or even violated the 4D distance constraint. On the other side, the original wind farm is always designed according to the onsite wind resource which is not enough to drive bigger WT. Hence, the 1.8MW WT is selected by the program.

Table 6.3 Economic performance comparison of different repowering strategies [A14]

	LCoE	Net Present Value of Total Cost related to foundations	Net Present Value of Total cost of WTs	Net Present Value of overall cost
Case I	204.08 Dkk/MW	0	1973.1 MDkk	1973.1 MDkk
Case II	175.44 Dkk/MW	0	1652.9 MDkk	1652.9 MDkk

As can be seen from table 6.3, the new constructed wind farm using the proposed repowering strategy has a 14.03% lower LCoE compared with the “new for old”

repowering strategy. Also, the overall investment is reduced by 16.23%. It is more lucrative to invest in such way.

## 6.5. SUMMARY

The life time of offshore wind farm can last for about 20 years. After that, the wind farm owner has to decide decommission or repowering the wind farm. Different from standard offshore wind farm decommissioning, the “recycling idea”, that is, repowering is quantitatively analyzed in this work. The simulation results showed that the proposed optimized repowering strategy for offshore wind farms can reduce the LCoE by 14.03% compared with the common replacing method.

The advantage of applying the proposed method is for one thing if a recycled wind farm project can be launched, it would encourage more investors to participate since the proposed strategy requires less capital investment and construction time compared with the construction of a new wind farm, which might not only be a barrier for some investors who do not have enough funds, but also not decrease the levelized cost of wind energy, for another reduce the impacts on the marine ecosystem.

The main work of this chapter has been presented in the author’s previous publications [A14][A15].

[A14] Peng Hou, Peter Enevoldsen, Weihao Hu, Zhe Chen, “Offshore Wind Farm Repowering Optimization,” *Applied Energy*, submitted.

[A15] Peng Hou, Weihao Hu, Mohsen Soltani, Baohua Zhang, Zhe Chen, “Optimization of Decommission Strategy for Offshore Wind Farms,” *Proceedings of the 2016 IEEE Power & Energy Society General Meeting 2016*, pp. 1-5, 2016.

# CHAPTER 7. CONCLUSIONS AND FUTURE WORKS

## 7.1. CONCLUSIONS

From the thesis it can be concluded that offshore wind farm optimization aims at increasing the energy production and reducing the capital investment. The energy production is mainly affected by the wake losses and can be minimized by either optimizing the positions of WTs within wind farm or adopting an optimized wind farm control strategy. As one of the costly parts in offshore wind farm, the electrical system cost is decided by several factors as voltage levels of collection and transmission system, OSs' locations and quantities, electrical equipment type and cable connection scheme, these factors are interrelated and contribute to the delivery of a cost effective wind farm. It is also found that the LPC of wind farm can be further minimized if the co-optimization concepts can be adopted, that is, WFLO considering either optimized control strategy or electrical system optimization simultaneously. Moreover, the profitability of an offshore wind farm can be further improved by repowering the wind farm. The detailed conclusions are listed as follows:

### **1. Wake losses estimation for offshore wind farm**

Presently, there are many models can be used for wake losses estimation. Jensen model is not the accurate model for describing the wake effect of a single WT. However, for the energy production estimation of whole wind farm and WFLOP, it is a good choice considering both accuracy and computational speed. A binary matrix method is proposed and demonstrated to be effective for the wake losses estimation in this work. In this method, any irregular wind farm layout can be regarded as a regular shaped wind farm and shaped by the binary matrix. Thus, the calculation process for irregular wind farm layout can be simplified. The results obtained by the binary matrix have been compared with the results obtained by WAsP and shows only 2.84% and 0.55% errors respectively in two cases.

### **2. Optimization methods for different problems**

In this work, analytical algorithm as interior point method and sequential quadratic programming method and heuristic algorithms as PSO including GPSO, non-linear weight PSO, APSO, PSO-MAM and GA are adopted and compared in offshore wind farm optimization work. The analytical optimization method can ensure the robustness of solution, but needs the gradient information of the objective function. It could be a good choice for solving non-linear optimization problem. However, the



objectives of WFLOP or wind farm control optimization problem concern the wake losses calculation of whole wind farm which is a complex process and thus makes the problem extremely non-convex. It is hard to obtain the gradient information from wind farm energy production model. So does the CCLOP. Therefore, heuristic algorithms are applied instead. From simulation, it can be concluded that PSO-MAM outperforms than other algorithms in solving continuous optimization problem. However, it needs more computational time than other versions of PSO while APSO is the best choice in solving integer or mixed integer optimization problem.

### **3. Optimization methods of offshore wind farm micro-siting**

The WFLOP can be solved based on grid model or coordinate model. The recent research works use coordinate model more since it can give a better solution for WFLOP. Due to the complexity of WFLOP, most of works used heuristic optimization method to solve the problem while PSO is the most frequently adopted algorithm. Some new research has been proposed using mathematical programming method based on grid model, no evidence showed that the classic optimization method outperformed than heuristic optimization methods in finding a lower cost wind farm layout. The regular/irregular WFLO programs are completed by optimizing the position of each WT in this work. The concept of restriction regions in the sea is also proposed and implemented using penalty function method in the program. The non-linear weight control PSO can help find an optimized regular shape wind farm which minimizes the LPC by 6.72% while saving more than 50% of occupation sea area. The layout optimized by PSO-MAM has a 3.83% higher energy production while using GA can only increase the energy production by 0.8% compared with NRW layout. In addition, two co-optimization methods which optimize the wind farm layout and either cable connection layout or control strategy are proposed. Compared with separate optimization methods (optimizing the wind farm layout at first and then optimize the cable connection layout or control strategy), it can find a better layout which reduce the LPC by 0.29% and 0.19% respectively.

### **4. An optimized power dispatch method for offshore wind farm**

The optimal control strategy for single WT is the MPPT control strategy while for wind farm control; the overall energy production can be further enhanced by optimizing the power reference setting point for each WT compared with using the MPPT control strategy. Essentially, the optimized control strategy aims at redistributing the wake losses among the WTs within the wind farm. The optimized power reference setting point is reached by controlling the pitch angle of WT. Based on the heuristic method; an optimized power dispatch method is proposed which can reduce the LPC of the regular shaped and irregular shaped wind farm by 2.2% and 0.15% respectively compared with the MPPT control strategy. It is an effective

control strategy of minimizing the LPC of offshore wind farm. However, it can be seen from simulation that the optimized control strategy is close to the MPPT strategy and very sensitive to the searching start solution (initial solution). Also, it depends on the estimation of the wind speed reached at each WT which means that the accuracy of wake model have a great impact on this strategy. Hence, no evidence shows that this method can be applied for real application.

### **5. Optimization platform of electrical system design for offshore wind farm**

An optimization platform is designed in this work which can help the wind farm owner optimize the electrical system configuration including voltage selection of both collection system and transmission system, electrical component type selection, OS quantity and locations' determination as well as the cable connection layout optimization. Several deterministic and heuristic algorithms have been adopted for constructing this platform. Compared with the existing works, the proposed APSO-MST algorithm has more flexibility in finding a radial cable connection layout which outperformed than some deterministic method as MST and DMST in reducing investment by 4.7% and 4.5% when the OS location is taken into account. From simulation, it is also found that if OS location optimization is taken into account the overall investment on cables can be significantly reduced by 11.27% compared with the near shore located OS scenario.

### **6. Proposals for end of life offshore wind farm**

When the wind farm comes to its life end, it can be dismantled, partial repowering or fully repowering. Lots of factors can affect this decision as the possibility of obtaining the old spares, cost of repairs and upgrades, foundation types, weather conditions, seabed conditions, local legislation, etc. These factors are exclusive and unique for each wind farm and thus there is no general rule for offshore wind farm decommissioning yet. The proposed repowering optimization method is a preferable strategy which can make best use of the existing facilities and reduce the impact to the marine ecosystem, it helps wind farm owner to decide where to install and which type of WT should be selected to repower the offshore wind farm. The simulation results show that the proposed repowering strategy can help reduce LCoE of wind farm by 14.03% with a 16.23% lower overall investment compared with the traditional method of replacing the “break” WTs with the same type new WTs. It is more profitable to invest using this strategy.

## **7.2. FUTURE WORKS**

Although many aspects have been documented in this thesis for large scale offshore wind farm optimization, there are still a lot of possibilities for theoretical and

technology improvement. Some issues of high interest for future investigations are listed below:

- 1) Presently, the WFLO work is done by maximizing the energy production or minimizing the cost of energy by a simplified wind farm cost model. In reality, the foundation cost, which is a costly component in offshore wind farm, is related to the seabed condition and water depth. The energy production considering wake effect and foundation costs are both related to the WT positions. Those two aspects should be considered simultaneously in the WFLOP so that a comprehensive decision could be made.
- 2) Fatigue load cause the reduction of wind farm lifetime due to the wake turbulence. If closer spacing is arranged between a pair of WTs then the fatigue load will be increase. In contrary to that, larger distance will result in a smaller fatigue load. This problem is never addressed in any WFLO paper and should be considered in future work.
- 3) Reliability is an important factor for offshore wind farm performance. Since the O&M is very expensive and time-consuming for offshore wind farm, it would nice to have a safe electrical system, however, more reliable always responds to more invest. Hence, the electrical system design should concern about both aspects and find the tradeoff according to the practical requirement. Though some works has addressed reliability problem in wind farm design [33][34], it could be more interesting if the quantitative relations between reliability and economy can be done within large scale offshore wind farm optimization.
- 4) Some classic algorithms like linear programming could be used in solving both WFLOP and CCLOP. Those methods could be investigated and compared with the heuristic optimization methods.

# LITERATURE LIST

- [1] GWEC report 2015, Online: <http://www.gwec.net/publications/global-wind-report-2/global-wind-report-2015-annual-market-update/>; 2015.
- [2] World's first offshore wind farm on its last turn, Online: <http://www.dongenergy.com/en/media/newsroom/news/articles/worlds-first-offshore-wind-farm-on-its-last-turn>.
- [3] S. Anderson, "Comparing Offshore and Onshore Wind," HAS 10-5 The Economics of Oil and Energy, April 30, 2013.
- [4] P. Enevoldsen, "Onshore wind energy in Northern European forests: Reviewing the risks," *Renewable & Sustainable Energy Reviews*, Vol. 60, pp. 1251–1262, 2016.
- [5] EMD International A/S, Available from: <http://www.emd.dk/WindPRO/>.
- [6] A. Peña, P.-E. Réthoré, M. P. van der Laan, "On the application of the Jensen wake model using a turbulence-dependent wake decay coefficient: the Sexbierum case," *Wind Energy*, Vol. 19, pp. 763–776, 2016. doi: [10.1002/we.1863](https://doi.org/10.1002/we.1863).
- [7] J. Yang, R. Zhang, Q. Sun, and H. Zhang, "Optimal Wind Turbines Micrositing in Onshore Wind Farms Using Fuzzy Genetic Algorithm," *Mathematical Problems in Engineering*, vol. 2015, Article ID 324203, 9 pages, 2015. doi:10.1155/2015/324203
- [8] J. S. González, M. B. Payán, J. M. R. Santos, F. González-Longatt, "A review and recent developments in the optimal wind turbine micro-siting problem," *Renewable and Sustainable Energy Reviews*, 18 October 2013.
- [9] H. M. Junginger, W. C. Turkenburg, A. Faaij, "Cost reduction prospects for offshore wind farms," *Wind Engineering*, vol. 28, pp. 97–118, 2004.
- [10] A. Peeters, "Cost analysis of the electrical infrastructure that is required for offshore wind energy: an experience curve based survey," Final report, Utrecht University, Utrecht (The Netherlands), 2003.
- [11] S. Benjamin, P. Enevoldsen, "One style to build them all: Corporate culture and innovation in the offshore wind industry," *Energy Policy*, Vol. 86, no. 11, pp. 402–415, 2015.
- [12] Y. Ma, H. Yang, X. Zhou, and L. Ji, "The dynamic modeling of wind farms considering wake effects and its optimal distribution," in *Proc. World Non-Grid-Connected Wind Power Energy Conf. (WNWEC'09)*, Nanjing, China, pp. 1–4, Sep. 2009.
- [13] R. Shakoor, M. Y. Hassan, A. Raheem, and Y.-K. Wu, "Wake effect modeling: A review of wind farm layout optimization using Jensen's model," *Renewable and Sustainable Energy Reviews*, vol. 58, pp. 1048–1059, 2016.
- [14] E. W. Weisstein, "NP-Hard Problem," From MathWorld—A Wolfram Web Resource. <http://mathworld.wolfram.com/NP-Problem.html>.

- [15] R. Archer, G. Nates, S. Donovan, H. Waterer, "Wind turbine interference in a wind farm layout optimization mixed integer linear programming model," *Wind Energy*, vol. 35, pp. 165–75, 2011.
- [16] D. E. Goldberg, J. H. Holland. "Genetic algorithms and machine learning," *Mach Learn*, vol. 3, pp. 95–99, 1988.
- [17] Holland H John, "Adaptation in natural and artificial systems," *Cambridge, MA, MIT Press*, 1992.
- [18] J. Kennedy, R. Eberhart, "Particle swarm optimization," *Proc. IEEE Int. Conf. Neural Networks*, pp. 1942–1948, Apr. 1995.
- [19] J. Kennedy, "The particle swarm: social adaptation of knowledge," *Proc. IEEE Int. Conf. Evolution of Computing*, Indianapolis, IN, pp. 303–308, 1997.
- [20] M. Hu, T. Wu, J. D. Weir, "An adaptive particle swarm optimization with multiple adaptive methods," *IEEE Transactions on Evolutionary Computation*, Vol. 17, pp. 705–720, 10 Dec. 2012.
- [21] Y. Shi, R. C. Eberhart, "Empirical study of particle swarm optimization," in *Proc. Congr. Evol. Comput.*, pp. 1950–1955, 1999.
- [22] B. Jiao, Z. Lian, X. Gu, "A dynamic inertia weight particle swarm optimization algorithm," *Chaos, Solitons Fractals*, vol. 37, pp. 698–705, Aug. 2008.
- [23] Y. Shi, R. C. Eberhart, "Fuzzy adaptive particle swarm optimization," in *Proc. Congr. Evol. Comput.*, 2001, pp. 101–106.
- [24] R. C. Eberhart, Y. Shi, "Tracking and optimizing dynamic systems with particle swarms," in *Proc. Congr. Evol. Comput.*, pp. 94–100, 2001.
- [25] Z.-H. Zhan, J. Zhang, Y. Li, H. S.-H. Chung, "Adaptive particle swarm optimization," *IEEE Trans. Syst., Man, Cybern. B, Cybern.*, vol. 39, no. 6, pp. 1362–1381, Apr. 2009.
- [26] J. Zhang, H. S.-H. Chung, W.-L. Lo, "Clustering-based adaptive crossover and mutation probabilities for genetic algorithms," *IEEE Trans. Evol. Comput.*, vol. 11, no. 3, pp. 326–335, Jun. 2007.
- [27] A. Chatterjee, P. Siarry, "Nonlinear inertia weight variation for dynamic adaptation in particle swarm optimization," *Comput. Oper. Res.*, vol. 33, pp. 859–871, Mar. 2006.
- [28] S. Kirkpatrick, M. Vecchi, "Optimization by simulated annealing," *Science*, vol. 220, pp. 671–680, 1983.
- [29] A. Colomi, M. Dorigo, V. Maniezzo, "Distributed optimization by ant colonies," In *Proceedings of the first European conference on artificial life*, pp.134-142, 1991.
- [30] D. J. Bryg, "Comparison of NEVADA Simulation to Monte Carlo Simulation," *Simulation Conference Proceedings*, pp. 471-476, 11-14 Dec. 1994.
- [31] N. Chen, "Large-scale offshore wind farm electrical collection systems optimization," *master thesis, Shanghai University of Electric Power*, 2011.
- [32] S. Lundberg, "Configuration study of larger wind park," *Thesis for the degree of Licentiate Engineering, Dept. Electr. Power Eng., Chalmers Univ. Technol., Goteborg, Sweden*, 2003.

- [33] M. Zhao, Z. Chen, F. Blaabjerg, "Application of genetic algorithm in electrical system optimization for offshore wind farms," *Int. Conf. on Electric Utility Deregulation and Restructuring and Power Technologies (DRPT)*, Nanjing, China, 2008.
- [34] M. Zhao, Z. Chen, F. Blaabjerg, "Optimisation of electrical system for offshore wind farms via genetic algorithm," *IET Renewable Power Generation*, pp. 205-216, 2009.
- [35] H. J. Bahirat, B. A. Mork, H. K. Hoidalén, "Comparison of wind farm topologies for offshore applications," *2012 IEEE Power and Energy Society General Meeting*, pp. 1-8, 2012.
- [36] L.-L. Huang, N. Chen, H. Zhang, Y. Fu, "Optimization of large-scale offshore wind farm electrical collection systems based on improved FCM," *International Conference on Sustainable Power Generation and Supply (SUPERGEN 2012)*, Hangzhou, 2012.
- [37] S. Dutta, T. J. Overbye, "Optimal Wind Farm Collector System Topology Design Considering Total Trenching Length," in *IEEE Trans. Sustainable Energy*, vol. 3, pp. 339-348, 2012.
- [38] A. M. Jenkins, M. Scutariu, K. S. Smith, "Offshore wind farm inter-array cable layout," *PowerTech (POWERTECH), 2013 IEEE Grenoble*, pp. 1-6, 2013.
- [39] F. M. Gonzalez-Longatt, P. Wall, P. Regulski, V. Terzija, "Optimal electric network design for a large offshore wind farm based on a modified genetic algorithm approach," *IEEE Syst. J.*, vol. 6, pp. 164-172, 2012.
- [40] L.-L. Huang, Y. Fu, X. M. Guo, "Optimization of electrical connection scheme for large offshore wind farm with genetic algorithm," *International Conference on Sustainable Power Generation and Supply, 2009. SUPERGEN '09*, pp. 1-4, 2009.
- [41] D. D. Li, C. He, Y. Fu, "Optimization of electric distribution system of large offshore wind farm with improved genetic algorithm," *2008 IEEE Power and Energy Society General Meeting - Conversion and Delivery of Electrical Energy in the 21st Century*, pp. 1-6, 2008.
- [42] O. Dahmani, S. Bourguet, P. Guerin, M. Machmoum, P. Rhein, L. Josse, "Optimization of the internal grid of an offshore wind farm using Genetic algorithm," *2013 IEEE Grenoble PowerTech (POWERTECH)*, pp. 1-6, 2013.
- [43] J. S. Gonzalez, M. B. Payan, J.R. Santos, "A New and Efficient Method for Optimal Design of Large Offshore Wind Power Plants," *IEEE Transactions on Power Systems*, vol. 28, pp. 3075-3084, 2013.
- [44] S. Dutta, T. J. Overbye, "A clustering based wind farm collector system cable layout design," *2011 IEEE Power and Energy Conference at Illinois (PECI)*, pp. 1-6, 2011.
- [45] Y. Wu, C. Lee, C. Chen, K. Hsu, H. Tseng, "Optimization of the wind turbine layout and transmission system planning for a large-scale offshore wind farm by AI technology," *IEEE Transactions on Industry Application*, vol. 50, pp. 2071-2080, 2014.

- [46] C. N. Elkinton, "Offshore wind farm layout optimization," Doctoral Dissertations, 2007, Online: <http://scholarworks.umass.edu/dissertations/AAI3289248>.
- [47] S. Lumbreras and A. Ramos, "Optimal design of the electrical layout of an offshore wind farm applying decomposition strategies," *IEEE Trans. Power Syst.*, Vol. 28, pp. 1434-1441, 2013.
- [48] P. D. Hopewell, F. Castro-Sayas, D. I. Bailey, "Optimising the Design of Offshore Wind Farm Collection Networks," *UPEC '06. Proceedings of the 4-1st International Universities Power Engineering Conference*, vol. 1, pp. 84-88, 2006.
- [49] P. Hou, W. Hu, Z. Chen, "Offshore Substation Locating in Wind Farms Based on Prim Algorithm," *IEEE Power & Energy Society General Meeting*, pp. 1-5, 2015.
- [50] P. Hou, W. Hu, Z. Chen, "Optimization for Offshore Wind Farm Cable Connection Layout using Adaptive Particle Swarm Optimization Minimum Spanning Tree Method," *IET Renewable Power Generation*, vol. 10, pp. 175-183, 2016.
- [51] P. Hou, W. Hu, C. Chen, Z. Chen, "Overall Optimization for Offshore Wind Farm Electrical System" *Wind Energy*, 2016.
- [52] J. Bauer, J. Lysgaard, "The Offshore Wind Farm Array Cable Layout Problem—A Planar Open Vehicle Routing Problem," *Department of Informatics, University of Bergen*, pp. 1–16, Norway.
- [53] A. C. Pillai, J. Chick, L. Johanning, M. Khorasanchi, V. de Laleu, "Offshore wind farm electrical cable layout optimization," *Engineering optimization*, 2015. DOI: 10.1080/0305215X.2014.992892.
- [54] R. A. Devore, V. N. Temlyakov, "Some remarks on greedy algorithm," *Adv. Comp. Math.*, pp. 173–187, 1996.
- [55] T. Bektas, "The multiple traveling salesman problem: An overview of formulations and solution procedures," *Omega*, vol. 34, no. 3, pp. 209–219, Jun. 2006.
- [56] W. H. Press, S. A. Teukolsky, W. T. Vetterling, B. P. Flannery, "Numerical recipes in fortran 77: The art of scientific computing (2nd edition)," Cambridge University Press, Vol. 10, no. 9, pp. 438-444, 1997.
- [57] F. Li, B. Golden, E. Wasil, "The open vehicle routing problem: Algorithms, large-scale test problems, and computational results," *Computers & Operations Research*, vol. 34, pp. 2918-2930, 2007.
- [58] J. A. Bondy, U. S. R. Murty, "Graph theory with applications," Macmillan Press Ltd., 1976.
- [59] WAsP-the wind Atlas analysis and application program, Available from: <http://risoe.dtu.dk/WAsP.aspx>.
- [60] WindSim technical brochure, Available from: [http://www.windsim.com/documentation/windsim\\_brochure\\_WEB.pdf](http://www.windsim.com/documentation/windsim_brochure_WEB.pdf).
- [61] Meteodyn meteorology and dynamics, Available from: [http://www.meteodyn.com/en/wind\\_energy.html](http://www.meteodyn.com/en/wind_energy.html).

- [62] WindFarmer, Available from: <http://www.gl-garradhassan.com/en/software/GHWindFarmer.php>.
- [63] AWS Truepower, LLC, OpenWind, Available from: <http://www.awsopenwind.org/>.
- [64] R. J. Barthelmie, G. C. Larsen, S. T. Frandsen, "Comparison of wake model simulations with offshore wind turbine wake profiles measured by sodar," *Journal of Atmospheric and Oceanic Technology* 2006, vol. 23:888–901.
- [65] S. J. Andersen, J. N. Sørensen, S. Ivanell, R. F. Mikkelsen, "Comparison of Engineering Wake Models with CFD Simulations," *Journal of Physics*, 2014.
- [66] WindPRO/PARK, "Introduction wind Turbine Wake Modelling and Wake Generated Turbulence," *EMD International A/S*, Niels Jernes Vej 10, DK-9220 Aalborg, Denmark, 1 Apr. 2005.
- [67] G. C. Larsen, J. Højstrup, H.A. Madsen, "Wind Fields in Wakes," *EUWEC '96*, Gothenburg, 1996, pp. 764-768.
- [68] S. Frandsen, R. Barthelmie, S. Pryor, O. Rathmann, S. Larsen, J. Højstrup, M. Thøgersen, "Analytical modelling of wind speed deficit in large offshore wind farms," *Wind Energy*, vol. 9, pp. 39-53, January-April 2006.
- [69] F. González-Longatt, P. Wall, V. Terzija, "Wake effect in wind farm performance: Steady-state and dynamic behavior," *Renewable Energy*, vol. 39, pp. 329-338, Sep. 2011.
- [70] P. Hou, W. Hu, M. Soltani, Z. Chen, "A Novel Energy Yields Calculation Method for Irregular Wind Farm Layout", *41th Annual Conference of the IEEE Industrial Electronics Society (IECON 2015)*, pp. 000380 - 000385, Yokohama, Japan, 9-12 Nov. 2015.
- [71] M. R. Patel, "Wind and Solar Power Systems," *CRC Press*, 1999.
- [72] Beatriz Pérez, Roberto Mínguez, Raúl Guanche, "Offshore wind farm layout optimization using mathematical programming techniques," *Renewable Energy*, vol. 53, pp. 389-399, May 2013.
- [73] G. Mosetti, C. Poloni, B. Diviacco, "Optimization of wind turbine positioning in large wind farms by means of a genetic algorithm," *Journal of Wind Engineering and Industrial Aerodynamics*, vol. 51(1), pp.105-116, 1994.
- [74] S. Grady, M. Hussaini, and M. Abdullah, "Placement of wind turbines using genetic algorithms," *Renewable Energy*, vol. 30, no. 2, pp. 259 – 270, 2005.
- [75] G. Marmidis, S. Lazarou, E. Pyrgioti, "Optimal placement of wind turbines in a wind park using Monte Carlo simulation," *Renewable Energy*, vol. 33 (7), pp. 1455–1460, 2008.
- [76] N. P. Prabhu, P. Yadav, B. P. and S. K. Panda, "Optimal placement of off-shore wind turbines and subsequent micro-siting using Intelligently Tuned Harmony Search algorithm," *Power and Energy Society General Meeting (PES)*, 2013 IEEE, pp. 1-7, Vancouver, BC, Jul. 2013.
- [77] S. Pookpant, W. Ongsakul, "Optimal placement of wind turbines within wind farm using binary particle swarm optimization with time-varying acceleration coefficients," *Renewable Energy*, vol. 55, pp. 266-276, Jul. 2013.



- [78] T. G. do Couto, B. Farias, A. Carlos G. C. Diniz and M. Vinicius G. de Morais, "Optimization of Wind Farm Layout Using Genetic Algorithm," *10th World Congress on Structural and Multidisciplinary Optimization*, Orlando, Florida, USA, May 2013.
- [79] S. Salcedo-Sanz, D. Gallo-Marazuela, A. Pastor-Sánchez, L. Carro-Calvo, A. Portilla-Figueras, L. Prieto, "Evolutionary computation approaches for real offshore wind farm layout: A case study in northern Europe," *Expert Systems with Applications*, vol. 40, no. 16, pp. 6292-6297, 2013.
- [80] S. Salcedo-Sanz, D. Gallo-Marazuela, A. Pastor-Sánchez, L. Carro-Calvo, A. Portilla-Figueras, L. Prieto, "Offshore wind farm design with the Coral Reefs Optimization algorithm," *Renewable Energy*, vol. 63, pp. 109-115, 2014.
- [81] S. D. O. Turner, D. A. Romero, P. Y. Zhang, C. H. Amon, T. C. Y. Chan, "A new mathematical programming approach to optimize wind farm layouts," *Renewable Energy*, vol. 63, pp. 674-680, 2014.
- [82] J. Gonzalez, M. Burgos Payan, and J. Riquelme Santos, "A new and efficient method for optimal design of large offshore wind power plants," *IEEE Transactions on Power Systems*, vol. 28, no. 3, pp. 3075-3084, 2013.
- [83] A. Kusiak and Z. Song, "Design of wind farm layout for maximum wind energy capture," *Renewable Energy*, vol. 35, no. 3, pp. 685-694, 2010.
- [84] E. Y. S. SU, "Design of wind farm layout using ant colony algorithm," *Renewable Energy*, pp. 53-62, vol. 44, Aug. 2012.
- [85] C. Wan, J. Wang, G. Yang, H. Gu, and X. Zhang, "Wind farm micro-siting by Gaussian particle swarm optimization with local search strategy," *Renewable Energy*, vol. 48, pp. 276-286, 2012.
- [86] S. Chowdhury, J. Zhang, A. Messa, L. Castillo, "Optimizing the arrangement and the selection of turbines for wind farms subject to varying wind conditions," *Renew Energy*, vol. 52, pp. 273-282, 2013.
- [87] O. Rahbari, M. Vafaeipour, F. Fazelpour, M. Feidt, M. A. Rosen, "Towards realistic designs of wind farm layouts: Application of a novel placement selector approach," *Energy Conversion and Management*, vol. 81, pp. 242-254, 2014.
- [88] X. Gao, H. Yang, and L. Lu, "Investigation into the optimal wind turbine layout patterns for a Hong Kong offshore wind farm," *Energy*, vol. 73, pp. 430-442, 2014.
- [89] J. Park, K. Law, "Layout optimization for maximizing wind farm power production using sequential convex programming," *Applied Energy*, vol. 151, pp. 320-334, 2015.
- [90] J. Feng, W.Z. Shen, "Solving the wind farm layout optimization problem using random search algorithm," *Renewable Energy*, vol. 78, pp. 182-192, Jun. 2015.
- [91] B. Pérez, R. Mínguez, R. Guanche, "Offshore wind farm layout optimization using mathematical programming techniques," *Renewable Energy*, vol. 53, pp. 389-399, 2013.

- [92] L. Wang, A. C. C. Tan, Y. Gu, "Comparative study on optimizing the wind farm layout using different design methods and cost models," *Journal of Wind Engineering and Industrial Aerodynamics*, vol. 146, pp. 1–10, 2015.
- [93] Y. Chen, "Commercial Wind Farm Layout Design and Optimization," *Texas A&M University*, Kingsville, Ann Arbor, pp.47, 2013.
- [94] P. Hou, W. Hu, C. Chen, M. Soltani, Z. Chen, "Optimization of offshore wind farm layout in restricted zones," *Energy*, vol. 113, pp. 487–496, 15 Oct. 2016.
- [95] L.Y. Pao, K.E. Johnson, "Control of wind turbines", *IEEE Control Syst. Mag.*, vol. 31, (2), pp. 44–62, 2011.
- [96] J. Lee, E. Son, B. Hwang, S. Lee, "Blade pitch angle control for aerodynamic performance optimization of a wind farm," *Renewable Energy*, vol. 54, pp. 124–130, 2012.
- [97] J.S. González, M.B. Payán, J.R. Santos, et al., "Maximizing the overall production of wind farms by setting the individual operating point of wind turbines," *Renewable Energy*, vol. 80, pp. 219–229, 2015.
- [98] A. Behnood, H. Gharavi, B. Vahidi, et al. "Optimal output power of not properly designed wind farms, considering wake effects," *Int. J. Electr. Power Energy Syst.*, vol. 63, pp. 44–50, 2014.
- [99] J.-S. Shin, W.-W. Kim, J.-O Kim, "Study on Designing for Inner Grid of Offshore Wind Farm," *Journal of Clean Energy Technologies*, Vol. 3, No. 4, July 2015.
- [100] S. Dutta, T. J. Overbye, "A Graph-theoretic Approach for Addressing Trenching Constraints in Wind Farm Collector System Design," *Power and Energy Conference at Illinois (PECI)*, 2013.
- [101] R. Hassan, B. Cohanim, O. de Weck, "A comparison of particle swarm optimization and the genetic algorithm," in *Proceedings of the 46th AIAA/ASME/ASCE/AHS/ASC structures, structural dynamics and materials conference*, 2005.
- [102] S. Lundberg, "Performance comparison of wind park configurations," *master thesis, Chalmers university of technology, department of electric power engineering*, Gothenburg, Sweden, 2003.
- [103] G. Quinonez-Varela, G. W. Ault, O. Anaya-Lara, J. R. McDonald, "Electrical collector system options for large offshore wind farms," *IET Renewable Generation*, pp. 107–114, vol. 1, July 2007.
- [104] M. Zhao, Z. Chen, and F. Blaabjerg, "Loss of Generation Ratio Analysis for Offshore Wind Farms," *IECON 2006 - 32nd Annual Conference on IEEE Industrial Electronics*, pp. 2844–2849, 2006.
- [105] M. Zhao, Z. Chen, and F. Blaabjerg, "Generation Ratio Availability Assessment of Electrical Systems for Offshore Wind Farms," *IEEE trans. on Energy Conversion*, pp. 755–763, Vol. 22, 2007.
- [106] M. Zhao, Z. Chen, and J. Hjerrild, "Analysis of the Behaviour of Genetic Algorithm Applied in Optimization of Electrical System Design for Offshore Wind Farms," *IECON 2006*, pp.2335–2340, 2006.

- [107] Wu, Y.-K., et al.: ‘Optimization of the wind turbine layout and transmission system planning for a large-scale offshore wind farm by AI technology’, *IEEE Trans. Ind.*, vol. 50, (3), pp. 2071–2080, Appl. 2014.
- [108] Energistyrelsen, “www.ens.dk,” 2016. Available: <http://www.ens.dk/sites/ens.dk/files/info/tal-kort/statistik-noegletal/oversigt-energisektoren/stamdataregister-vindmoeller/anlaegprodtilnettet.xls>.
- [109] P. C. S. A. & I. G. G. del Río, “Policies and design elements for the repowering of wind farms: A qualitative analysis of different options,” *Energy Policy*, vol. 39, pp. 1897 - 1908, 2011.
- [110] K. Smyth, N. Christie, D. Burdon, J. P. B. R. Atkins and M. Elliott, “Renewables-to-reefs? – Decommissioning options for the offshore wind power industry,” *Marine Pollution Bulletin*, vol. 90, p. 247–258, 2015.
- [111] P. Hou, W. Hu, M. Soltani, B. Zhang, Z. Chen, “Optimization of Decommission Strategy for Offshore Wind Farms,” *Proceedings of the 2016 IEEE Power & Energy Society General Meeting*, 2016.
- [112] S. Mathew, “Fundamentals, Resource Analysis and Economics,” *Wind Energy*, 1<sup>st</sup> edition, New York: Springer, 2006.
- [113] P. Hou, W. Hu, M. Soltani and Z. Chen, “A New Approach for Offshore Wind Farm Energy Yields Calculation with Mixed Hub Height Wind Turbines,” *Proceedings of the 2016 IEEE Power & Energy Society General Meeting 2016*, pp. 1-5, 2016.
- [114] “V90-1.8/2.0 MW Maximum output at medium-wind and low-wind sites,” *Vestas Wind Systems A/S*, Alsvej 21, 8940 Randers SV, Denmark.
- [115] C. Bak, F. Zahle, R. Bitsche, T. Kim, A. Yde, L. C. Henriksen, A. Natarajan, M. H. Hansen, “Description of the DTU 10 MW Reference Wind Turbine,” *DTU Wind Energy*, July 2013.
- [116] J. S. González, M. B. Payán and J. R. Santos, “Optimal Control of Wind Turbines for Minimizing Overall Wake Effect Losses in Offshore Wind Farms,” *EuroCon 2013*, 1st - 4th, July 2013.
- [117] M. Hu, T. Wu, and J. D. Weir, “An intelligent augmentation of particle swarm optimization with multiple adaptive methods,” *Inform. Sci.*, vol. 213, pp. 68–83, Dec. 2012.
- [118] K. Chen, P. Delarue, A. Bouscayrol, et al., “Minimum copper loss and power distribution control strategies of double-inverter-fed wound-rotor induction machines using energetic macroscopic representation,” *IEEE Trans. Energy Convers.*, Vol. 25, (3), pp. 642–651, 2010.
- [119] F. D. Bianchi, H. D. Battista, and R. J. Mantz, “Wind Turbine Control Systems,” Springer, 2007.
- [120] L. Y. Pao and K. E. Johnson, “Control of wind turbines,” *IEEE Control Syst. Mag.*, vol. 31, no. 2, pp. 44–62, 2011.
- [121] Norwegian Centre for Offshore Wind Energy (NORCOWE). (2014, Sep. 9). WP2014-Froysa-NRWF NORCOWE Reference Wind Farm.
- [122] F. Thomsen, “Anholt Offshore Wind Farm,” Dong Energy, link: [www.anholtoffshorewindfarm.com](http://www.anholtoffshorewindfarm.com).

- [123] J. Welstead, R. Hirst, D. Keogh, G. Robb, R. Bainsfair, "Scottish Natural Heritage Commissioned Report No. 591," Research and guidance on restoration and decommissioning of onshore wind farms, 2013. [Online]. Available: [http://www.snh.org.uk/pdfs/publications/commissioned\\_reports/591.pdf](http://www.snh.org.uk/pdfs/publications/commissioned_reports/591.pdf).
- [124] The First Offshore Wind Farm Decommissioning Complete, 2016. The Maritime Executive. MarEx, [Online]. Available: <http://www.maritime-executive.com/article/firstoffshore-wind-farm-decommissioning-complete>.
- [125] Vattenfall starts first ever offshore wind farm dismantling, OffshoreWIND.biz, 2016. [Online]. Available: <http://www.offshorewind.biz/2015/12/04/vattenfall-starts-first-ever-offshore-wind-farm-dismantling/>.
- [126] United Nations Convention on the Law of the Sea, 1958. [http://www.un.org/depts/los/convention\\_agreements/texts/unclos/unclos\\_e.pdf](http://www.un.org/depts/los/convention_agreements/texts/unclos/unclos_e.pdf).
- [127] "Decommissioning of Offshore Renewable Energy Installations under the Energy Act 2004," Department of Energy and Climate Change, 2011. [Online]. Available: [https://www.gov.uk/government/uploads/system/uploads/attachment\\_data/file/80786/orei\\_guide.pdf](https://www.gov.uk/government/uploads/system/uploads/attachment_data/file/80786/orei_guide.pdf).
- [128] S. Bradley, "End of Life Opportunities," Energy Technology Institute, 2014.
- [129] O. Yanguas Minambres, "Assessment of Current Offshore Wind Support Structures Concepts: Challenges and Technological Requirements by 2020," Karlshochschule International University, 2012.
- [130] Heba Hashem, "Offshore decommissioning market is emerging, but is wind industry prepared," Wind Energy Update, 2017. [Online]. Available: <http://analysis.windenergyupdate.com/operations-maintenance/offshore-decommissioning-market-emerging-wind-industry-prepared>.
- [131] Hans Kerkvliet, Heracles Polatidis, "Offshore wind farms' decommissioning: a semi quantitative Multi-Criteria Decision Aid framework," Sustainable Energy Technologies and Assessments, vol. 18, pp.69-79, 2016.
- [132] Eva Topham, David McMillan, "Sustainable decommissioning of an offshore wind farm," Renewable energy, vol. 102, pp. 470-480, 2017.
- [133] K. Smyth, N. Christie, D. Burdon, J. P. B. R. Atkins and M. Elliott, "Renewables-to-reefs? – Decommissioning options for the offshore wind power industry," Marine Pollution Bulletin , vol. 90 , p. 247–258, 2015.
- [134] C. Birkeland, "Assessing the Life Cycle Environmental Impacts of Offshore Wind Power Generation and Power Transmission in the North Sea," Norwegian University of Science and Technology Department of Energy and Process Engineering, 2011.
- [135] "Life Cycle Assessment of Offshore and Onshore Sited Wind Farms," Elsam Engineering, 2004. <http://www.apere.org/manager/>.
- [136] Eric Lantz, Michael Leventhal, Ian Baring-Gould, "Wind Power Project Repowering: Financial Feasibility, Decision Drivers, and Supply Chain Effects," Technical report, National renewable energy laboratory, 2013.

## **APPENDIX PAPER A1~A15**

# A Novel Energy Yields Calculation Method for Irregular Wind Farm Layout

Peng Hou, Weihao Hu, Mohsen Soltani, Zhe Chen,

Department of Energy Technology  
Aalborg University

Pontoppidanstraede 101, Aalborg DK-9220, Denmark  
[pho@et.aau.dk](mailto:pho@et.aau.dk), [whu@et.aau.dk](mailto:whu@et.aau.dk), [sms@et.aau.dk](mailto:sms@et.aau.dk), [zch@et.aau.dk](mailto:zch@et.aau.dk)

**Abstract**— Due to the increasing size of offshore wind farm, the impact of the wake effect on energy yields become more and more evident. The seafloor topography would limit the layout of the wind farm so that irregular layout is usually adopted in large scale offshore wind farm. However, the calculation for the energy yields in irregular wind farm considering wake effect would be difficult. In this paper, a mathematical model which includes the impacts of the variation of both wind direction and velocity on wake effect is established. Based on the wake model, a binary matrix method is proposed for the energy yields calculation for irregular wind farms. The results show that the proposed wake model is effective in calculating the wind speed deficit. The calculation framework is applicable for energy yields calculation in irregular wind farms.

**Index Terms**—binary matrix method; calculation framework; energy yields; irregular wind farm; wake model.

## Nomenclature

$C_{p,opt}$	Power coefficient at $\lambda_{opt}$
$d_{ji}$	Distance from $O_i$ to $O_j$
$E_{tot}$	Total energy yields
$h_{ji}$	Length of diagonal line in blue quadrangle
$L_{-ji}$	Distance from the center of upstream wind turbine (WT) to downstream WT's center
$M(i, j)$	Element of matrix $M$ at row $i$ , column $j$
$N_{col}$	Total number of WTs in a column
$N_{row}$	Total number of WTs in a row
$O_i$	Center of the downstream WT
$O_j$	Center of the wake that developed from the upstream WT
$P_{m,ij}$	Mechanical power generated by WT at row $i$ , column $j$
$P_{tot,t}$	Wind farm power production within the corresponding sample time interval $t$
$R$	Rotor radius
$R_i$	Radius of the downstream WT's rotor
$R_j$	Radius of the wake that generated from the upstream WT rotor
$R_0$	Radius of the upstream WT's rotor
$R(x)$	Generated wake radius at $x$ distance along the wind direction

$S_i$	Fan shaped area of the sweeping area that in downstream WT rotor
$S_j$	Fan shaped area of the wake area
$S_0$	Sweeping area of WT's rotor with radius $R_0$
$S_{partial}$	Blue area in Figure 1(b) which shows the wake effect region of downstream WT
$S_q$	Blue quadrangle area in Figure 1
$v$	Injected wind speed
$V_{ij}$	Wind speed deficit generated by the WT at $i^{th}$ row, $j^{th}$ column of wind farm
$V_j(\alpha, V_0)$	Wind speed of the upstream WT when the inflow wind direction angle is $\alpha$ and velocity is $V_0$
$V_{n,m}$	Wind velocity at WT at row $n$ , column $m$
$V_{n,m}(\alpha, V_0)$	Wind speed of the upstream WT when free wind direction angle is $\alpha$ and velocity is $V_0$
$V_0$	Free wind velocity or the input wind velocity of the upstream WT
$V_w$	Wind velocity in the wake at a distance $x$ downstream of the upstream WT
$x_i, y_i$	Position of the downstream WT in coordinate system
$\lambda_{opt}$	Optimal tip speed ratio for the pitch angle $\beta'$ , at which the power coefficient will be maximum
$\beta'$	Pitch angle
$\gamma$	Chord angle corresponding to $S_j$
$\mu$	Chord angle corresponding to $S_i$
$\rho$	Air density, 1.225kg/m <sup>3</sup> in standard condition

## I. INTRODUCTION

The wake effect can be defined as the impact of the upstream WT to the downstream ones which incurs the reduction of the total energy production of the wind farm [1]. Since the development of wind energy technology, the capacity of the wind farm is increasing a lot. In such a big wind farm, the wake effect becomes particularly evident. The overestimation of energy yields means a higher voltage level selection of electrical equipment and higher capacity of cables are required. This will induce the waste of investment on components' redundancy. Moreover, the wind farm control strategy and operating reserve will be influenced as well [2], [3]. In 1983, Jensen created a wake model which assumes a linear expansion of the wake after the upstream WT based on momentum conservation theory. After that, several wake

This work has been (partially) funded by Norwegian Centre for Offshore Wind Energy (NORCOWE) under grant 193821/S60 from Research Council of Norway (RCN). NORCOWE is a consortium with partners from industry and science, hosted by Christian Michelsen Research.

models are proposed for the wake calculation [4]. In [5], a method to calculate the wake losses by Jensen model is proposed while the Larsen eddy viscosity model is specified in [6]. Presently, there are three wake models that are widely used in Wind Farm Layout Optimization Problem (WFLOP) [7]. The objective of the WFLOP is to find an optimal layout which can meet the requirement of minimizing the investment while maximizing the energy yields [8]. In order to foresee the energy yields better, some works have been done on the wake effect losses calculations by using CFD (Computational Fluid Dynamics) [9]. The authors tried to accurately describe the wake effect by solving differential equations, however, the calculation time is quite long so that it is not an expected way for energy yields calculation. In this paper, a wake model with varying wind speed is established at first. Then, a binary matrix method for calculating the irregular wind farm yields by taking wake effect into account is proposed. The results show that the proposed method is an effective and efficient way for irregular wind farm energy yields calculation.

The analytical equations for the wake model are specified in section II, the calculation framework is presented in Section III. The FINO3 reference wind farm is chosen as the study case to demonstrate the proposed method in Section IV. Finally, conclusions and future work are given In Section V.

## II. WIND FARM MODEL

In this section, the Jensen wake model is firstly introduced. Based on which, the wind speed varying wake model which concerns the total wake effects from neighboring WT's as well as the varying wind speed's impacts are proposed. The energy model and calculation framework are presented at last.

### A. Wake Effect Model

In this simulation, the Jensen wake model is adopted as the basic wake model to analyze the wake effect for its simplicity.

#### 1) Jensen wake model

The formula for Jensen single wake model can be expressed as [4]:

$$V_w = V_0 + V_0(\sqrt{1-C_t} - 1) \left( \frac{R_0}{R(x)} \right)^2 \quad (1)$$

$$R(x) = R_0 + kx \quad (2)$$

Where,  $C_t$  is the thrust coefficient of the WT and  $k$  is the wake decay constant. The recommended value of  $k$  is 0.04 for offshore environment which is suitable for a free wind condition (turbulence-free, that is to say not affected by any upstream turbine) [10].

In some cases, the center of downstream WT is not aligned with wind velocity. The wind velocity at downstream WT's will be determined by the overlapped area generated by the evolved wake which can be seen in Figure 1 (b). Then equation (1) can be modified as [11]:

$$V_w = V_0 - V_0 \left( 1 - \sqrt{1-C_t} \right) \left( \frac{R_0}{R(x)} \right)^2 \left( \frac{S_{\text{partial}}}{S_0} \right) \quad (3)$$

### B. Multiple wakes

Within the wind farm, there is a probability that one downstream WT would be in the affected region of wake that generated by several upstream WT's. The problem has been solved by sum of squares of velocity deficits method [7]. As a consequence, the wind velocity at WT in row  $n$ , column  $m$  can be expressed as:

$$V_{n,m} = V_0 \left[ 1 - \sqrt{\sum_{i=1}^{N_{\text{row}}} \sum_{j=1}^{N_{\text{col}}} \left[ 1 - \left( \frac{V_{ij}}{V_0} \right) \right]^2} \right] \quad (4)$$

### C. Wind speed varying wake model

In reality, the wind direction changed from time to time. The WT would change its nacelle until it faced to the wind direction so that more wind energy can be absorbed. The variation of the wind velocity as well as the direction will both influence the wind speed deficit so does the energy yields. This change can be described by using a modified model with coordinate system. In this model, the wind is considered to be existed in 4 quadrants. In each quadrant two cases are required to be specified as shown in Figure 1. In which, the red line is the distance from the center of the upstream WT to downstream WT. The green area, denoted as  $S_{\text{overlap}}$  is the overlapped area. The blue quadrangle area is denoted as  $S_q$ .

A series of analytical equations for wake velocity calculation in case (a) can be derived as:

$$L_{ji} = \sqrt{(x_j - x_i)^2 + (y_j - y_i)^2} \quad (5)$$

$$d_{ji} = L_{ji} |\sin(\alpha + \beta)| \quad (6)$$

$$R_j = R_i + kL_{ji} |\cos(\alpha + \beta)| \quad (7)$$

$$\gamma = 2\cos^{-1} \frac{R_j^2 + d_{ji}^2 - R_i^2}{2R_j d_{ji}} \quad (8)$$

$$\mu = 2\cos^{-1} \frac{R_i^2 + d_{ji}^2 - R_j^2}{2R_i d_{ji}} \quad (9)$$

$$h_{ji} = 2R_i |\sin(\mu/2)| \quad (10)$$

$$S_0 = \pi R_i^2 \quad (11)$$

$$S_j = \frac{\gamma(R_j)^2}{2} \quad (12)$$

$$S_i = \frac{\mu R_i^2}{2} \quad (13)$$

$$S_q = 0.5h_{ji}d_{ji} \quad (14)$$

$$S_{\text{overlap}} = S_j + S_i - S_q \quad (15)$$

The above equations are derived step by step to calculate the green area as illustrated in Figure 1 which is the effective

area that used to calculate the speed at the downstream WT's blade. Then the wind velocity at  $j^{\text{th}}$  WT can be rewritten as:

$$V_j(\alpha, V_0) = V_0 \left[ 1 - \left( 1 - \sqrt{1 - C_t} \right) \left( \frac{R_0}{R_j} \right)^2 \left( \frac{S_{\text{overlap}}}{S_r} \right) \right] \quad (16)$$

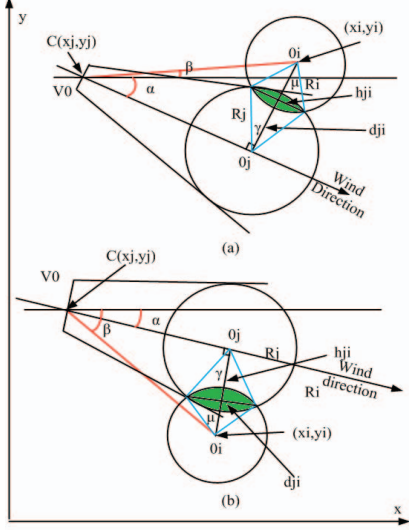


Figure 1. Wind speed varying wake model

Where  $\alpha$  is the angle between line  $CO_j$  and x axis, in other words, the wind direction while  $\beta$  is the angle between line  $CO_j$  and x axis. In case (b), the analytical equations is merely modified by changing all (6) and (7) into  $(\beta - \alpha)$  while keeping all other terms the same.

The model proposed above is valid when the wake and the rotor sweeping area are intersected. In general, three cases should be considered in energy yields calculation as shown in Figure 2.

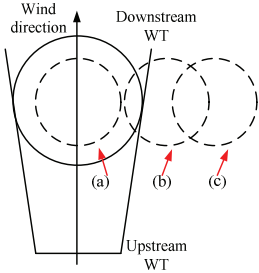


Figure 2. Three cases in wake losses calculation

The dotted circle represents the location of the downwind WT. The wake effect will be receded gradually if the downwind WT is moving from position (a) to (c). As a result, three cases should be specified. The specifications of three cases are summarized in Table I as follow:

TABLE I. JUDGEMENT SPECIFICATIONS

Case	Category	Condition	Analytical equations
(a)	full wake effect	$0 \leq d_{ji} \leq R_j - R_i$	(1) (2) (4)
(b)	partial wake effect	$R_j - R_i \leq d_{ji} \leq R_j + R_i$	(5) - (16)
(c)	non-wake effect	$d_{ji} \geq R_j + R_i$	$V_j = V_0$

#### D. Energy model

The power produced by WT can be calculated using the following equations [12], [13]:

$$P_{m,ij} = 0.5 C_{p, \text{opt}} (\beta', \lambda_{\text{opt}}) \rho \pi R^2 v^3 \quad (17)$$

In the simulation, the power production of each WT is found by assuming a maximum power point tracking (MPPT) control strategy [14]. Hence, the total power production that generated by the WTs at row  $i$ , column  $j$  can be written as:

$$P_{\text{tot}} = \sum_{j=1}^{N_{\text{col}}} \sum_{i=1}^{N_{\text{row}}} P_{m, ij} \quad (18)$$

### III. BINARY MATRIX METHOD FOR IRREGULAR WIND FARM ENERGY CALCULATION

The energy yields calculation for irregular wind farm is difficult since there is no explicit rule to define the distance between the WTs. The problem is solved by introducing a binary matrix in this paper so that the energy calculation can be simplified by using the ordinary way combing this shaping matrix.

#### A. Binary matrix and modification of equations

As it is known, the wind speed deficit is a function of distance from upstream WT to downstream WT along wind direction. In irregular wind farm it is quite complex to define this distance for each turbine. Hence, a binary matrix is introduced as shown below.

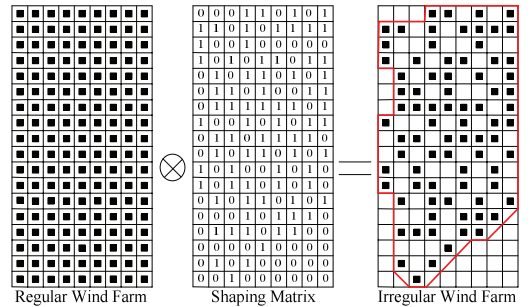


Figure 3. Binary matrix method

The black solid square in Figure 3 represents the WT. Number 1 means there is a WT in this position while 0 means the position is empty. By using the binary matrix, the original full occupied wind farm can be shaped into an irregular wind farm. Combing (4) - (16), the wind velocity and total energy yields can be calculated as:



$$V_{n,m}(\alpha, V_0) = V_0 \left[ 1 - \sqrt{\sum_{i=1}^{N_{row}} \sum_{j=1}^m \left[ 1 - M(i, j) \cdot \left( \frac{V_{ij}}{V_0} \right) \left( \frac{S_{overlap,ij}}{S_r} \right)^2 \right]} \right] \quad (19)$$

$$E_{tot} = \sum_{t=1}^{TE} P_{tot,t} T \quad (20)$$

Where, TE is the sample time for energy yields calculation. The wind velocity and direction for the calculation is obtained from the Norwegian Meteorological Institute [15], [16]. In their work, the wind speed is sampled every 3 hours. Hence, in this paper, TE is taken as 365\*8 which is also the maximum iteration and T is 3 hours in the following simulation.

### B. Calculation framework

The energy yields calculation for irregular wind farm should be easier solved with the binary matrix method as mentioned above. The calculation framework can be seen in Figure 4.

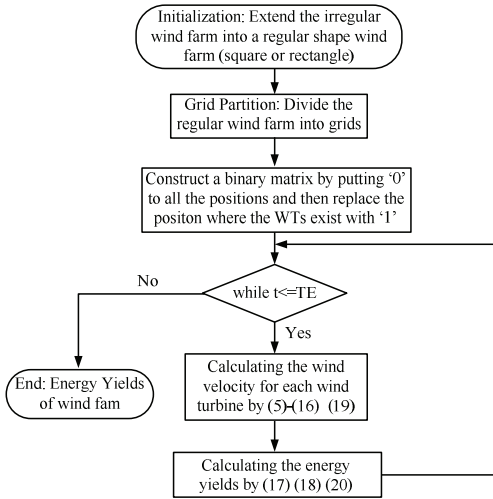


Figure 4. Calculation framework

The wind farm will be partitioned into small grids. Each grid could have one WT or not. The length of the grid is decided by the shortest distance's projection on wind farm side length direction between two WTs.

## IV. CASE STUDY

The simulation is implemented on the platform of Matlab R2013a. Two study cases are adopted to verify the feasibility of the proposed method.

### A. Case I

FINO3 reference wind farm is sited 80km west of German island of Sylt. In the first case, the irregular layout is assumed to be as shown in Figure 5 [17].

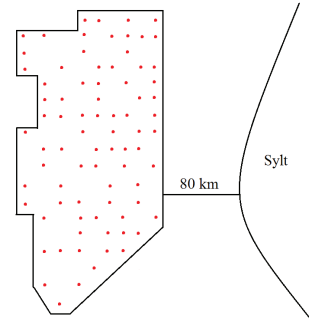


Figure 5. Case I Wind Farm Layout

### 1) DTU 10 MW WT

The DTU 10MW WT is considered as the reference WT in this paper. The specification of which is listed in Table II. The detailed information of  $C_p$  and  $C_t$  is listed as a lookup table in [18].

TABLE II. DTU 10MW WT SPECIFICATION [15]

Parameter	10 MW DTU WT
Cut-in Wind Speed	4 m/s
Cut-out Wind Speed	25 m/s
Rated Wind Speed	11.4 m/s
Rotor Diameter	178.3 m
Rated Power	10 MW

### 2) Simulation and results

According to the binary matrix method, the layout transformation process is the same as illustrated in Figure 3. The input wind velocity and direction distribution for the simulation are illustrated in Figure 6.

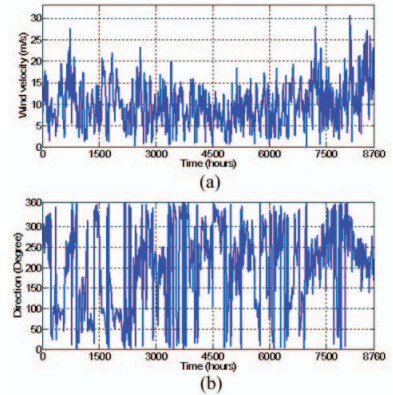


Figure 6. (a) Wind velocity variation every 3 hours (b) Wind direction variation every 3 hours

Following the calculation framework, the energy yields for this case are obtained as in Table III. The energy yields for one year are illustrated in Figure 7.

TABLE III. SIMULATION RESULTS

Name	Binary Matrix Calculation
Duration	8760 h
Wind farm capacity	800 MW
Energy yields	3460.70 GWh
Capacity Factor	49.38%
Energy yields without wake effect	4164.91 GWh
Capacity Factor (no wakes)	59.43%
Wake losses efficiency	16.91%
Simulation time	162.87 seconds

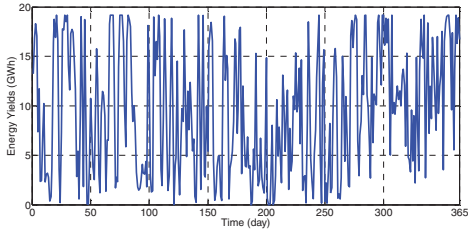


Figure 7. Daily energy yields for irregular wind farm layout in one year

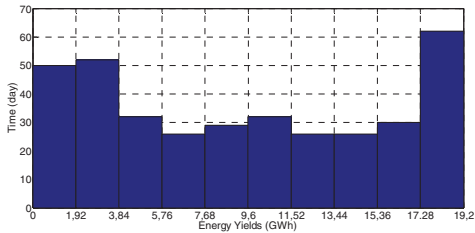


Figure 8. Energy yields distribution for irregular wind farm layout in one year

The program is performed on a computer which is an Intel(R) Core(TM) i7-4800MQ CPU @ 2.70 GHz processor with 8 GB RAM. As illustrated in Figure 7 and 8, in most of time of a year, about 62 days, the wind farm can supply 17.28 to 19.2 GWh electricity to main grid per day. The total energy yields for this case is 3460.70 GWh. Table III shows that the wake effect reduced the energy production by 16.19% and the computational time is around 177 seconds.

### B. Case II

In this case, the wind farm layout is assumed to be elliptical as shown in Figure 9. The red stars show the WT locations. Different from case I, the distances between WTs in horizontal or vertical direction are totally different. If the shortest distance's projection on wind farm side length direction between two WTs is still adopted as the length of the grid. Then the energy yields of this wind farm cannot be calculated instance due to out of memory reasons. In order to conquer this problem, the grid partition process could be modified by partitioning grids into different length rectangular instead of square while binary matrix method will be still effective.

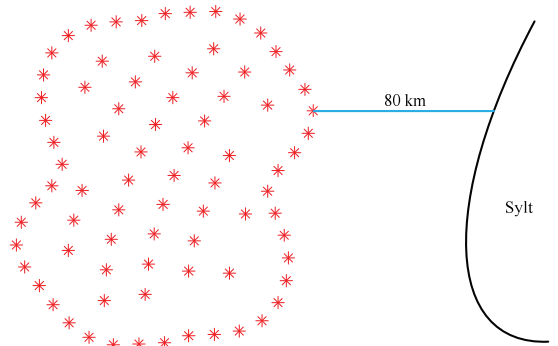


Figure 9. Case II Wind Farm Layout

The energy yields considering either wake effect or not are listed in Table IV. In this case, the wake effect reduced the energy production by 9.03% and the computational time is around 2915 seconds.

TABLE IV. SIMULATION RESULTS

Name	Binary Matrix Calculation
Duration	8760 h
Wind farm capacity	800 MW
Energy yields	3789.00 GWh
Capacity Factor	54.07%
Energy yields without wake effect	4164.91 GWh
Capacity Factor (no wakes)	59.43%
Wake losses efficiency	9.03%
Simulation time	2915.25 seconds

The energy yields with and without considering wake effects for both cases are also calculated by WASP (Wind Atlas Analysis and Application software) [19]. The results are included in Table V. The error shows the difference between proposed method and WASP. It can be seen the results is close to that obtained with WASP.

TABLE V. ENERGY YIELDS COMPARISON OF TWO CASES

		Energy Yields by Matlab (GWh)	Energy Yields by WASP (GWh)	Error (%)
Case I	Without considering wake effect	4164.91	4214.40	1.17%
	Considering wake effect	3460.70	3394.46	2.84%
Case II	Without considering wake effect	4164.91	4219.09	0.045%
	Considering wake effect	3789.00	3926.71	3.51%

## V. CONCLUSIONS AND FUTURE WORK

The wake effect has a significant contribution to the reduction of offshore wind farms energy yields. The variation in both wind velocity and direction will have impacts on the calculation of wake losses. Since the wind farm layout is usually irregular, it is difficult to calculate the energy yields

considering wake effect by traditional ways. In this paper, a new wake model which includes the multiple wakes and the wind speed varying wake is established. Based on which, a new binary matrix method is applied in an irregular wind farm energy yields calculation. The studied cases demonstrate that it is an effective way to calculate any shape wind farm energy yields considering wake effect. In future, the method could be used in finding the optimal locations of WTs in offshore wind farm by taking the components' cost into consideration.

#### ACKNOWLEDGMENT

Authors would like to thank Norwegian Centre for Offshore Wind Energy (NORCOWE) under grant 193821/S60 from Research Council of Norway (RCN).

#### REFERENCES

- [1] Youjie Ma, Haishan Yang, Xuesong Zhou, Li Ji, "The dynamic modeling of wind farms considering wake effects and its optimal distribution," World Non-Grid-Connected Wind Power and Energy Conference, 2009. WNWEC 2009, pp. 1-4, Nanjing, 24-26 Sept. 2009.
- [2] Peng Wang, Goel, L., Yi Ding, Loh Poh Chang, Andrew, A., "Reliability-based long term hydro/thermal reserve allocation of power systems with high wind power penetration," Power & Energy Society General Meeting, 2009. PES '09. IEEE, pp. 1-7, Calgary, AB, 26-30 July 2009.
- [3] Erik Ela, Brendan Kirby, Eamonn Lannoye, Michael Milligan, Damian Flynn, Bob Zavadil, "Evolution of Operating Reserve Determination in Wind Power Integration Studies," 2010 IEEE Power & Energy Society General Meeting, 25-29 July, 2010.
- [4] N.O. Jensen, "A Note on Wind Generator Interaction," Risø National Laboratory, DK-4000 Roskilde, Denmark, November 1983.
- [5] F. González-Longatt, P. Wall, V. Terzija, "Wake effect in wind farm performance: Steady-state and dynamic behavior," Renewable Energy 39 (2012) 329e338, 16 September 2011.
- [6] G. C. Larsen, J. Højstrup, H.A. Madsen, "Wind Fields in Wakes," EUWEC '96, Gothenburg, 1996.
- [7] WindPRO/PARK, "Introduction wind Turbine Wake Modelling and Wake Generated Turbulence," EMD International A/S.
- [8] Serrano Gonzalez, J., Burgos Payan, M. and Riquelme Santos, J. M., "An improved evolutive algorithm for large offshore wind farm optimum turbines layout," PowerTech, 2011 IEEE Trondheim, pp. 1-6, Trondheim, June 2011.
- [9] Annette Westerhellweg, Thomas Neumann, "CFD simulations of wake effects at the alpha ventus offshore wind farm," EWEA 2011, Brussels.
- [10] Philippe Beauceage, Michael Brower, Nick Robinson, Chuck Alonge, "Overview of six commercial and research wake models for large offshore wind farms," Proceedings EWEA 2012, Copenhagen, 2012.
- [11] F. González-Longatt, P. Wall, V. Terzija, "Wake effect in wind farm performance: Steady-state and dynamic behavior," Renewable Energy 39 (2012) 329e338, 16 September 2011.
- [12] Serrano Gonzalez, J., Burgos Payan, M., Riquelme Santos, J., "Optimum Wind Turbines Operation for Minimizing Wake Effect Losses in Offshore Wind Farms," 2013 13th International Conference on Environment and Electrical Engineering (EEEIC), pp. 188-192, Wroclaw, 1-3 November 2010.
- [13] P. Flores, A. Tapia, G. Tapia, "Application of a control algorithm for wind speed prediction and active power generation," Renewable Energy, Vol. 30, Issue 4, pp. 523-536, April 2005.
- [14] Wei Qiao, "Intelligent mechanical sensorless MPPT control for wind energy systems," Power and Energy Society General Meeting, 2012 IEEE, pp. 1-8, San Diego, CA, 22-26 July 2012.
- [15] Christian Bak, Frederik Zahle, Robert Bitsche, Taeseong Kim, Anders Yde, Lars Christian Henriksen, Anand Natarajan, Morten Hartvig Hansen, "Description of the DTU 10 MW Reference Wind Turbine," DTU Wind Energy, July 2013.
- [16] Birgitte R. Furevik and Hilde Haakenstad, "Near-surface marine wind profiles from rawinsonde and NORA10 hindcast," Journal of Geophysical Research, Vol. 117, 7 Dec. 2012.
- [17] FINO3 - research platform in the North Sea and the Baltic No. 3 [Online]. Available: <http://www.fino3.de/en/>.
- [18] <http://met.no/English/>, the Norwegian Meteorological Institute.
- [19] <http://www.wasp.dk/>, DTU Wind Energy.

# A New Approach for Offshore Wind Farm Energy Yields Calculation with Mixed Hub Height Wind Turbines

Peng Hou, Weihao Hu, Mohsen Soltani, Zhe Chen,

Department of Energy Technology

Aalborg University

Pontoppidanstraede 101, Aalborg DK-9220, Denmark

pho@et.aau.dk, whu@et.aau.dk, sms@et.aau.dk, zch@et.aau.dk

**Abstract**— In this paper, a mathematical model for calculating the energy yields of offshore wind farm with mixed types of wind turbines is proposed. The Jensen model is selected as the base and developed to a three dimension wake model to estimate the energy yields. Since the wind turbines are with different hub heights, the wind shear effect is also taken into consideration. The results show that the proposed wake model is effective in calculating the wind speed deficit. The calculation framework is applicable for energy yields calculation in offshore wind farms.

**Index Terms**—different hub heights; shear effect; calculation framework; energy yields; wake model.

## Nomenclature

$C_{opt}$	Power coefficient at $\lambda_{opt}$
$d_{ij}$	Distance from $O_i$ to $O_j$
$E_{tot}$	Total energy yields
$h_{ij}$	Length of diagonal line in blue quadrangle
Hub(i, j)	Hub height matrix
k	Decay constant
$L_{ij}$	Distance from the center of upstream WT to downstream WT's center
$M(i, j)$	Element of matrix M at row I, column j
$N_{col}$	Total number of WTs in a column
$N_{row}$	Total number of WTs in a row
$O_i$	Center of the downstream WT
$O_j$	Center of the wake that developed from the upstream WT
$P_{m,ij}$	Mechanical power generated by WT at row I, column j
$P_{tot,t}$	Wind farm power production within the corresponding sample time interval t
R	Rotor radius
$R_i$	Radius of the downstream WT's rotor
$R_j$	Radius of the wake that generated from the upstream WT rotor
$R_0$	Radius of the upstream WT's rotor
$R(x)$	Generated wake radius at x distance along the wind direction

$S_i$	Fan shaped area of the sweeping area that in downstream WT rotor
$S_j$	Fan shaped area of the wake area
$S_0$	Sweeping area of WT's rotor with radius $R_0$
$S_{ol}$	Blue area in Figure 3(b) which shows the wake effect region of downstream WT
$S_q$	Blue quadrangle area in Figure 3
$V_{ij}$	Wind speed deficit generated by the WT at $i^{th}$ row, $j^{th}$ column of wind farm
$V_{ij}(\alpha, V_{0,ij})$	Wind speed of the upstream wind turbine (WT) when the inflow wind direction angle is $\alpha$ and velocity is $V_{0,ij}$
$V_{nm}$	Wind velocity at WT at row n, column m.
$V_{nm}(\alpha, V_{0,ij})$	Wind speed of the upstream WT when free wind direction angle is $\alpha$ and velocity is $V_{0,ij}$
$V_{0,ij}$	Wind velocity at the blade of WT at $i^{th}$ row, $j^{th}$ column of wind farm
$x_i, y_i$	Position of the downstream WT in coordinate system
$z_0$	Surface roughness
$z_{ref}$	Reference height for the measured wind speed
$z_{ij}$	Hub height of WT at row i, column j
$\lambda_{opt}$	Optimal tip speed ratio for the pitch angle $\beta'$ , at which the power coefficient will be maximum
$\beta'$	Pitch angle
$\gamma$	Chord angle corresponding to $S_j$
$\mu$	Chord angle corresponding to $S_i$
$\rho$	Air density, 1.225kg/m <sup>3</sup> in standard condition

## I. INTRODUCTION

The WTs extracts the power from the wind which incurs the wind speed reduction and turbulence increase at downstream WT. The physic change of speed and turbulence for the wind is called wake effect [1]. With the development of the capacity of the wind farm, the wake losses estimation becomes particularly evident. Because the overestimation of energy yields means a higher voltage level selection of electrical equipment and higher capacity of cables are required, this will induce the waste of investment on components' redundancy. In addition, the wind farm control strategy and operating reserve will be influenced as well [2], [3]. Presently, there are three wake models that are widely

This work has been (partially) funded by Norwegian Centre for Offshore Wind Energy (NORCOWE) under grant 193821/S60 from Research Council of Norway (RCN). NORCOWE is a consortium with partners from industry and science, hosted by Christian Michelsen Research.

used in solving the Wind Farm Optimization Problem (WFOP) as: Jensen model, Ainslie model and G.C. Larsen model [4]. Based on momentum conservation theory, Jensen proposed a wake model which assumes a linear expansion of the wake after the upstream WT in 1983. After that, several wake models are proposed for the wake calculation [5]. In [6], a method to calculate the wake losses by Jensen model is proposed while the Larsen eddy viscosity model is specified in [7]. Besides using analytical model to predict the energy yields of the wind farm, some works have been done on the wake effect simulation by using CFD (Computational Fluid Dynamics) which is a more precise way to estimate the wake losses [8]. The authors tried to accurately describe the wake effect by solving differential equations, however, the calculation time is quite long so that it is not an expected way for energy yields calculation in WFOP.

In this paper, a 3D wake model which considers the wake losses within an offshore wind farm with different hub height WTs is proposed. The proposed model is used for the energy yields calculation of two reference wind farm and the results show that the proposed method is an effective and efficient way for regular and irregular wind farm energy yields calculation.

The analytical equations for the wake model are specified in section II, the calculation framework is presented in Section III. The FINO3 reference wind farm is chosen as the study case to demonstrate the proposed method in Section IV. Finally, conclusions and future work are given in Section V.

## II. WIND FARM MODEL

In this section, the Jensen wake model is firstly introduced. Based on which, the wake model which concerns the total wake effects from different height WTs are proposed. The energy model is presented at last.

### A. Jensen Model

In this simulation, the Jensen wake model is adopted as the basic wake model to analyze the wake effect for its simplicity. The formula for Jensen single wake model is [9]:

$$V_{ij} = V_0 - V_0 \left( 1 - \sqrt{1 - C_{t,ij}} \right) \left( \frac{R_i}{R_j(x)} \right)^2 \quad (1)$$

$$R_j(x) = R_i + kx \quad (2)$$

The recommended value of  $k$  is 0.04 for offshore environment which is suitable for a free wind condition (turbulence-free, that is to say not affected by any upstream turbine) [10].

### B. Multiple Wakes

Within the wind farm, there is a probability that one downstream WT would be in the affected region of wake that generated by several upstream WTs. The problem has been solved by sum of squares of velocity deficits method [4]. As a consequence, the wind velocity at WT in row  $n$ , column  $m$  can be expressed as:

$$V_{nm} = V_0 \left[ 1 - \sqrt{\sum_{i=1}^{N_{row} N_{col}} \sum_{j=1} \left[ 1 - \left( \frac{V_{ij}}{V_0} \right) \right]^2} \right] \quad (3)$$

### C. Shear Effect

When the height is above 1 km, atmosphere is hardly influenced by the friction against the ground. However, in the lower layers, wind speed increases as the height of air goes up. This is called wind shear effect [10]. So if the height of some WTs is different, this effect should be also incorporated. Then, the wind speed can be rewritten as:

$$V_{0,ij} = V_{ref} \frac{\ln \left( \frac{z_{ij}}{h_0} \right)}{\ln \left( \frac{z_{ref}}{z_0} \right)} \quad (4)$$

### D. Wake Model for Mixed WT Offshore Wind Farm

In this work, it is assumed that there are two types of WTs with different heights exist in one offshore wind farm. The wake model for this wind farm should take shear effect into consideration. The effected wake area that contributes to the wind speed deficit when two WTs are in a line is illustrated in Figure 1.

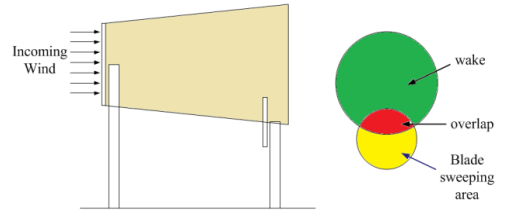


Figure 1. Illustration of wake overlapping with two wind turbines in a line.

As can be seen in Figure 1, the downstream WT are partial within the wake that generated by the upstream WT due to the hub height difference. If two WTs are not in a line, then four conditions should be considered as shown in Figure 2.

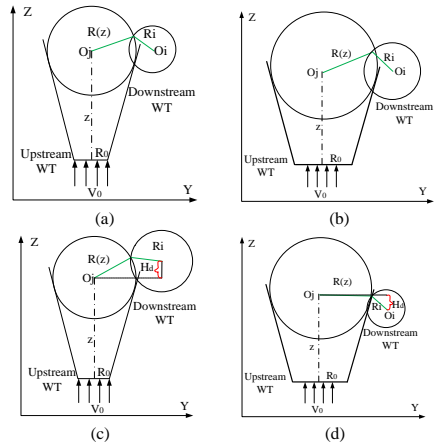


Figure 2. Wake model with mixed WT wind farm in y-z coordinate. (a) Upstream and downstream WTs are both WT type 1. (b) Upstream WT is WT type 1 and downstream WT is WT type 2. (c) Upstream WT is WT type 1 and downstream WT is WT type 2. (d) Upstream and downstream WTs are both WT type 2.

The affected wake area in four conditions is shown in y-z coordinate in Figure 2 (a) and (d) are the cases when upstream and downstream WT are in the same type. So the circle centers are in the same height. If the WTs are with different height, then the affected wake area will be reduced because of the height difference,  $H_d$ , as shown in Figure 2. (b) and (c). In this model, the wind is considered to be existed in 4 quadrants. In each quadrant two cases are required to be specified as shown in Figure 3. In which, the red line is the distance from the center of the upstream WT to downstream WT. The green area, denoted as  $S_{ol}$  is the overlapped area. The blue quadrangle area is denoted as  $S_q$ . If all the WTs are with same height, then a 2 dimension (2D) wake model will be used to wake losses estimation while the 3D wake model is the updating version by taking the hub height difference's impact on the wake affected area into consideration.

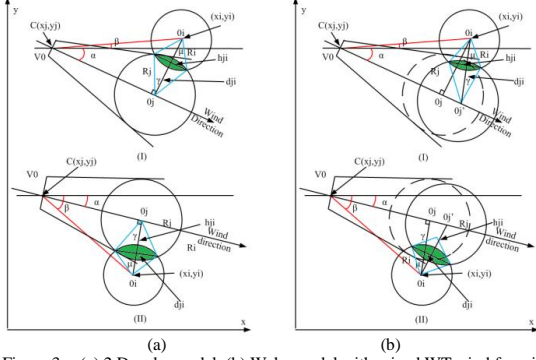


Figure 3. (a) 2 D wake model. (b) Wake model with mixed WT wind farm in x-y coordinate.

The 2D wake model is shown in Figure. 3 (a) while (b) indicates the proposed model. A series of analytical equations for wake velocity calculation of 3D wake model in case (I) can be derived as:

$$L_{ij} = \sqrt{(x_j - x_i)^2 + (y_j - y_i)^2} \quad (5)$$

$$L_d = \overline{O_j O_i} = H_b - H_s \quad (6)$$

$$d_{ij} = \sqrt{(L_{ij} |\sin(\alpha + \beta)|)^2 + (L_d)^2} \quad (7)$$

$$R_j = R_i + kL_{ij} |\cos(\alpha + \beta)| \quad (8)$$

$$\gamma = 2\cos^{-1} \frac{R_i^2 + d_{ij}^2 - R_j^2}{2R_j d_{ij}} \quad (9)$$

$$\mu = 2\cos^{-1} \frac{R_i^2 + d_{ij}^2 - R_j^2}{2R_i d_{ij}} \quad (10)$$

$$h_{ij} = 2R_i |\sin(\mu/2)| \quad (11)$$

$$S_0 = \pi R_i^2 \quad (12)$$

$$S_j = \frac{\gamma(R_j)^2}{2} \quad (13)$$

$$S_i = \frac{\mu R_i^2}{2} \quad (14)$$

$$S_q = 0.5h_{ij}d_{ij} \quad (15)$$

$$S_{ol} = S_j + S_i - S_q \quad (16)$$

Then the wind velocity at  $j^{\text{th}}$  WT can be rewritten as:

$$V_{ij}(\alpha, V_{0,ij}) = V_{0,ij} [1 - (1 - \sqrt{1 - C_{t,ij}}) \left( \frac{R_0}{R_j} \right)^2 \left( \frac{S_{ol}}{S_0} \right)] \quad (17)$$

In case (II), the analytical equations is merely modified by changing all (6) and (7) into  $(\beta - \alpha)$  while keeping all other terms the same.

The model proposed above is valid when the wake and the rotor sweeping area are intersected. The general principle of intersection judgement is shown in Figure 4.

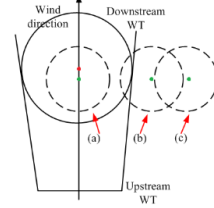


Figure 4. Three cases in wake losses calculation

The dotted circle represents the location of the downwind WT. The red dot and green dot show the circle centers for the generated wake at downstream WT and downstream WT itself. The wake effect will be receded gradually if the downwind WT is moving from position (a) to (c). The specifications of three cases are summarized in Table I as follow:

TABLE I. JUDGEMENT SPECIFICATIONS

Case	Category	Condition	Analytical equations
(a)	full wake effect	$0 \leq d_{ji} \leq R_j - R_i$	(1) - (4)
(b)	partial wake effect	$R_j - R_i \leq d_{ji} \leq R_j + R_i$	(5) - (17)
(c)	non-wake effect	$d_{ji} \geq R_j + R_i$	$V_j = V_0$

### E. Energy model

The power produced by WT can be calculated using the following equations [11], [12]:

$$P_{m,ij} = 0.5C_{p,opt}(\beta', \lambda_{opt}) \rho \pi R^2 V_{ij}^3 \quad (18)$$

In the simulation, the power production of each WT is found by assuming a maximum power point tracking (MPPT) control strategy [13]. Hence, the total power production that generated by the WTs at row  $i$ , column  $j$  can be written as:

$$P_{\text{tot}} = \sum_{j=1}^{N_{\text{col}}} \sum_{i=1}^{N_{\text{row}}} P_{m,ij} \quad (19)$$

### III. BINARY MATRIX METHOD FOR IRREGULAR WIND FARM ENERGY CALCULATION

The energy yields calculation for irregular wind farm is difficult since there is no explicit rule to define the distance between the WTs. The problem is solved by introducing a binary matrix,  $M(i, j)$  as shown in Figure 5.

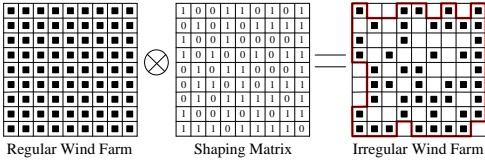


Figure 5. Binary matrix method

The black solid square in Figure 5 represents the WT. Number 1 means there is a WT in this position while 0 means the position is empty. By using the binary matrix, the original full occupied wind farm can be shaped into an irregular wind farm. Then, the wake speed as well as the energy yields of wind farm can be calculated as follow:

$$V_{nm}(\alpha, V_{0,ij}) = V_{0,ij} \left[ 1 - \sqrt{\sum_{i=1}^{N_{row}} \sum_{j=1}^m [1 - M(i, j) \cdot \left( \frac{V_{ij}}{V_{0,ij}} \right) \left( \frac{S_{0,ij}}{S_0} \right)^2]} \right] \quad (20)$$

$$E_{tot} = \sum_{t=1}^{TE} P_{tot,t} T \quad (21)$$

In order to evaluate the wake interaction between WTs with different hub height, a hub height matrix,  $Hub(i, j)$ , is defined according to  $M(i, j)$ . The positions which the type 2 WTs are in will be indicated as number '10' instead of '1' in  $M(i, j)$ . Then the original binary matrix will be changed into a '0-1-10' matrix while 0 means no WT in this position, 1 means there is a type 1 WT in this position and 10 means there is a type 2 WT in this position.

#### A. Calculation framework

The energy yields calculation for irregular wind farm should be easier solved with the binary matrix method as mentioned above. The calculation framework can be seen in Figure 6.

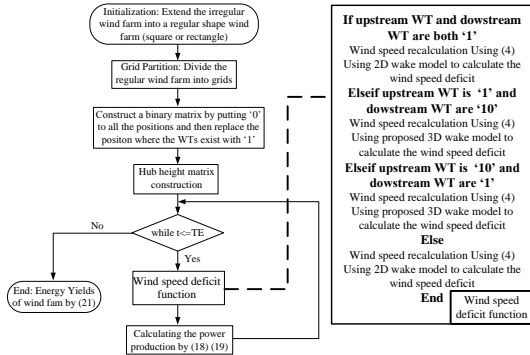


Figure 6. Calculation framework

Firstly, the binary matrix will be used to help identify the distance between each pair of WT by partitioning the wind farm into small grids. Each grid could have one WT or not. Then the hub height matrix will help decide which condition (as shown in Figure 2) should be considered at this moment. If both turbines are with same type then 2D wake model will be

used to estimate the wake losses otherwise the energy yields of the wind farm will be calculated base on 3D wake model.

## IV. CASE STUDY

The simulation is implemented on the platform of Matlab R2013a. Two study cases are adopted to verify the feasibility of the proposed method.

### A. Case I

FINO3 reference wind farm is sited 80km west of German island of Sylt. In the first case, the wind farm layout is assumed to be as shown in Figure 7 [14].

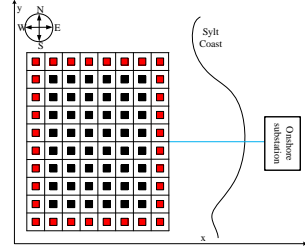


Figure 7. Case I Wind Farm Layout

Two types of WTs (Vestas V90-2.0 [15] and DTU 10MW reference WT [16]) are considered as the reference WTs in this paper. The distance between each pair of WT is 630m (7 rotor diameter of 2MW WT, 7D). As shown in Figure 7, the red squares show the positions of 10 MW WT while black squares indicate the 2 MW WT.

The input wind velocity and direction distribution for the simulation are illustrated in Figure 8. The input time series wind speed for the calculation is obtained from the Norwegian Meteorological Institute [14]. Following the calculation framework, the energy yields for this case are obtained as in Table II.

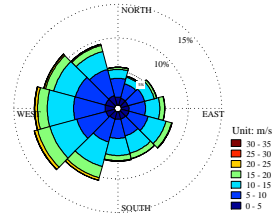


Figure 8. Wind Rose of FINO3 [17]

TABLE II. SIMULATION RESULTS

Name	Mixed WT farm	10MW WT farm	2MW WT farm
Wind farm capacity	416 MW	800 MW	160 MW
Energy yields	1813.4 GWh	3393.29 GWh	704.97 GWh
Capacity Factor	49.76%	48.42%	50.30%
Energy yields without wake effect	2220.3 GWh	4386.12 GWh	776.38 GWh
Capacity Factor (no wakes)	60.93%	62.59%	55.39%
Wake losses	18.33%	22.64%	9.20%
Simulation time	964seconds	959seconds	960seconds



The program is performed on a computer which is an Intel(R) Core(TM) i7-4800MQ CPU @ 2.70 GHz processor with 8 GB RAM. The wake losses take up to 18.33% of total energy extracted from the wind. The energy yields of this wind farm with mixed WT (Mixed WT farm) was compared with the results obtained from 10MW WT farm (wind farm composed by 10MW WTs) and 2MW WT farm (composed by 2MW WTs). It can be seen that the wake losses in Mixed WT farm and 10MW WT farm is relatively higher than 2MW WT farm. This is because that the designed reference wind farm is with a smaller separation between each pair of WT, which makes the wake effect more obvious when the bigger size WTs are adopted.

### B. Case II

In this case, the reference wind farm layout is assumed to be elliptical as shown in Figure 9. The red stars show the 10MW WT locations while the blue stars shows the locations of 2MW WT locations.

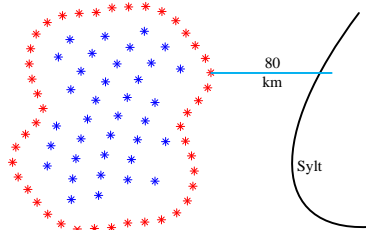


Figure 9. Case II Wind Farm Layout

Based on the same wind input as illustrated in Figure 8, the energy yields considering either wake effect or not are listed in Table III. In this case, the wake effect reduced the energy production to 15.95%.

TABLE III. SIMULATION RESULTS

Name	Mixed WT farm	10MW WT farm	2MW WT farm
Wind farm capacity	512 MW	800	160
Energy yields	2321.3 GWh	3870.68 GWh	684.57 GWh
Capacity Factor	51.76%	55.23%	48.84%
Energy yields without wake effect	2761.7 GWh	4386.12 GWh	776.38 GWh
Capacity Factor (no wakes)	61.58%	62.59%	55.39%
Wake losses	15.95%	11.75%	11.83%
Simulation time	1782s	1773	1765

### V. CONCLUSIONS AND FUTURE WORK

In this paper, a new wake model which is applicable of calculating the wind speed in the wakes generated by WTs with different hub heights is proposed. The shear effect is considered to estimate the wind speed difference in different height and incorporated into the Jensen model so that a 3D wake model can be generated to evaluate the wind speed deficit in a wind farm with different hub height WTs. The studied cases demonstrate that it is an effective way to calculate any shape wind farm energy yields considering wake effect. In the future, the proposed model may be used for layout optimization work of the wind farm with different hub

height and power curve WTs to build up a more cost-effective wind farm.

### ACKNOWLEDGMENT

Authors would like to thank Norwegian Centre for Offshore Wind Energy (NORCOWE) under grant 193821/S60 from Research Council of Norway (RCN).

### REFERENCES

- [1] Youjie Ma, Haishan Yang, Xuesong Zhou, Li Ji, "The dynamic modeling of wind farms considering wake effects and its optimal distribution," World Non-Grid-Connected Wind Power and Energy Conference, 2009. WNWEC 2009, pp. 1-4, Nanjing, 24-26 Sept. 2009.
- [2] Peng Wang, Goel, L., Yi Ding, Loh Poh Chang, Andrew, A., "Reliability-based long term hydro/thermal reserve allocation of power systems with high wind power penetration," Power & Energy Society General Meeting, 2009. PES '09. IEEE, pp. 1-7, Calgary, AB, 26-30 July 2009.
- [3] Erik Ela, Brendan Kirby, Eamonn Lannoye, Michael Milligan, Damian Flynn, Bob Zavadil, "Evolution of Operating Reserve Determination in Wind Power Integration Studies," 2010 IEEE Power & Energy Society General Meeting, 25-29 July, 2010.
- [4] WindPRO/PARK, "Introduction wind Turbine Wake Modelling and Wake Generated Turbulence," EMD International A/S.
- [5] N.O. Jensen, "A Note on Wind Generator Interaction," Risø National Laboratory, DK-4000 Roskilde, Denmark, November 1983.
- [6] F. González-Longatt, P. Wall, V. Terzija, "Wake effect in wind farm performance: Steady-state and dynamic behavior," Renewable Energy 39 (2012) 329e338, 16 September 2011.
- [7] G. C. Larsen, J. Hojstrup, H.A. Madsen, "Wind Fields in Wakes," EUWEC '96, Gothenburg, 1996.
- [8] Annette Westerhellweg, Thomas Neumann, "CFD simulations of wake effects at the alpha ventus offshore wind farm," EWEA 2011, Brussels.
- [9] F. González-Longatt, P. Wall, V. Terzija, "Wake effect in wind farm performance: Steady-state and dynamic behavior," Renewable Energy 39 (2012) 329e338, 16 September 2011.
- [10] S. Mathew, "Fundamentals, Resource Analysis and Economics," Wind Energy: 1st ed. New York: Springer, 2006.
- [11] Serrano Gonzalez, J., Burgos Payan, M., Riquelme Santos, J., "Optimum Wind Turbines Operation for Minimizing Wake Effect Losses in Offshore Wind Farms," 2013 13th International Conference on Environment and Electrical Engineering (EEEIC), pp. 188-192, Wroclaw, 1-3 November 2010.
- [12] P. Flores, A. Tapia, G. Tapia, "Application of a control algorithm for wind speed prediction and active power generation," Renewable Energy, Vol. 30, Issue 4, pp. 523-536, April 2005.
- [13] Wei Qiao, "Intelligent mechanical sensorless MPPT control for wind energy systems," Power and Energy Society General Meeting, 2012 IEEE, pp. 1-8, San Diego, CA, 22-26 July 2012.
- [14] <http://met.no/English/>, the Norwegian Meteorological Institute.
- [15] "V90-1.8/2.0 MW Maximum output at medium-wind and low-wind sites," Vestas Wind Systems A/S, Alsvej 21, 8940 Randers SV, Denmark.
- [16] Christian Bak, Frederik Zahle, Robert Bitsche, Taeseong Kim, Anders Yde, Lars Christian Henriksen, Anand Natarajan, Morten Hartvig Hansen, "Description of the DTU 10 MW Reference Wind Turbine," DTU Wind Energy, July 2013.
- [17] Birgitte R. Furevik and Hilde Haakenstad, "Near-surface marine wind profiles from rawinsonde and NORA10 hindcast," Journal of Geophysical Research, Vol. 117, 7 Dec. 2012.
- [18] R&D centre Kiel University of Applied Sciences GmbH, FINO3—Research Platform in the North Sea and the Baltic No. 3 [Online]. Available: <http://www.fino3.de/en/>.



# Optimised power dispatch strategy for offshore wind farms

ISSN 1752-1416


Received on 19th April 2015

Revised on 11th September 2015

Accepted on 29th September 2015

doi: 10.1049/iet-rpg.2015.0176

www.ietdl.org

Peng Hou, Weihao Hu , Baohua Zhang, Mohsen Soltani, Cong Chen, Zhe Chen

Department of Energy Technology, Aalborg University, Pontoppidanstraede 101, Aalborg DK-9220, Denmark

✉ E-mail: whu@et.aau.dk

**Abstract:** Maximising the power production of offshore wind farms using proper control strategy has become an important issue for wind farm operators. However, the power transmitted to the onshore substation is not only related to the power production of each wind turbine but also the power losses which are related to electrical system topology. This study proposed an optimised power dispatch strategy for minimising the levelised production cost of a wind farm. Particle swarm optimisation (PSO) is employed to obtain final solution for the optimisation problem. Both regular shape and irregular shape wind farm are chosen for the case study. The proposed dispatch strategy is compared with two other control strategies. The simulation results show the effectiveness of the proposed strategy.

## Nomenclature

$V_0$ [m/s]	input wind velocity at upstream WT
$R_0$ [m]	WT's rotor blade radius
$S_0$ [m <sup>2</sup> ]	area that WT's rotor swept
$R_{ij}$ [m]	generated wake radius by the WT at row $i$ , column $j$ along the wind direction
$S_{\text{overlap},ij}$ [m <sup>2</sup> ]	overlapped area generated by upstream WT to affected downstream WT at row $i$ , column $j$
$V_{ij}$ [m/s]	wake velocity generated by the WT at $i$ th row, $j$ th column of wind farm
$L_{ij}$ [m]	distance from upstream WT at row $i$ , column $j$ to the affected downstream WT
$C_t$	thrust coefficient of WT
$d_c$	wake decay constant
$V_{nm}$ [m/s]	wind velocity at the WT at row $n$ , column $m$
$N_{\text{row}}$	number of WTs in a row
$N_{\text{col}}$	number of WTs in a column
$P_{\text{mec}}$ [MW]	power extracted from the wind
$V$ [m/s]	inflow wind speed
$\rho$ [kg/m <sup>3</sup> ]	air density
$R$ [m]	blade radius
$\lambda$	tip speed ratio
$\beta$ [°]	blade pitch angle
$V$ [m/s]	wind velocity
$\omega_{\text{rot}}$ [r/min]	rotor speed of generator
$C_{p,nm}$	power coefficient of WT at row $n$ , column $m$ which is a function of the pitch angle $\beta$ and the tip speed ratio $\lambda$
$V_{\text{cut-in}}$ [m/s]	cut-in wind speed of WT
$V_{\text{rated}}$ [m/s]	rated wind speed of WT
$V_{\text{cut-out}}$ [m/s]	cut-out wind speed of WT
$P_{\text{mec}}^{\text{rated}}$ [MW]	rated power that can be generated by WT
$P_{\text{mec},nm}$ [MW]	power generated by WT at row $n$ , column $m$
$P_{\text{tot}}$ [MW]	total power production of wind farm
$P_{\text{loss},ij}$ [MW]	power losses of cable at row $i$ , column $j$
$I_{ij}$ [kA]	current in cable at row $i$ , column $j$
$R_{e,ij}$ [ohm/m]	resistance of cable at row $i$ , column $j$
$\rho_{R,ij}$ [ohm*mm/m]	resistivity of selected cable at row $i$ , column $j$
$l_{R,ij}$ [m]	length of cable at row $i$ , column $j$
$S_{R,ij}$ [m <sup>2</sup> ]	sectional area of cable at row $i$ , column $j$
$U_{0,ij}$ [kV]	voltage to earth of cable at row $i$ , column $j$
$E_{\text{tot}}$ [MWh]	energy yields of wind farm in one year

$TE$	total number of time interval for energy yields calculation
$P_{\text{tot},i}$ [MW]	total power production of wind farm at time interval $i$
$P_{\text{tot,loss},i}$ [MW]	total power losses of wind farm at time interval $i$
$C_i$ [MDKK/km]	the unit cost of cable $i$
$S_{n,i}$ [W]	the rated apparent power of cable in line $i$
$N$	total number of cables in a wind farm
$A_p, B_p, C_p$	the coefficient of cable cost model
$I_{i,\text{rated}}$ [A]	the rated current of cable in line $i$
$U_{i,\text{rated}}$ [V]	the rated voltage of cable in line $i$
$L_i$ [km]	the length of cable $i$
$l_1, l_2$	learning factors
$r_1, r_2$	stochastic numbers which can generate some random numbers within [0, 1]
$x_i^k, x_i^{k+1}$ [m]	position of particle $i$ at iteration $k$ and $k+1$ respectively
$v_i^k, v_i^{k+1}$ [m]	speed of particle $i$ at iteration $k$ and $k+1$ respectively
$P_{\text{best}}^k$ [m]	best position of particle $i$ at iteration $k$
$G_{\text{best}}^k$ [m]	best position of all particles at iteration $k$
$n$	non-linear modulation index
$w$	inertia weight
$w_{\text{initial}}$	initial inertia weight at the start of a given run
$w_{\text{final}}$	final inertia weight at the end of a given run
$t$	iteration sequence number
$C_{\text{max}}$	maximum iteration

## 1 Introduction

The world market continuously has an increasing demand for wind energy. It is expected that more than 25% of world's electricity will be generated by renewables while one fourth of which is supplied by wind energy by 2035 [1]. The wind farm can be established onshore or offshore. The offshore wind farm (OWF) draws more and more attention recently mainly due to relatively more wind with less turbulence in offshore as well as low environmental impact [2]. Since the investment on OWF is higher, optimisation work is quite essential to be conducted for OWF to make the energy production more competitive in the electricity market.

A cost-effective OWF concerns two aspects: the energy yields and investment. Many works have been done on the layout design to maximise the energy production while getting a minimum investment.

Since the optimisation problem is usually non-linear, heuristic algorithms are usually required for solving optimisation problems. In [3–8], genetic algorithm (GA) is adopted to find the optimal locations of wind turbine (WTs) within the wind farm to minimise the wake losses.

In addition to optimise the wind farm layout in design phase, the control strategy is also critical to the economic efficiency of an existing wind farm. Maximum power point tracking strategy (MPPT) [9] can ensure the maximum power captured of each WT and is widely used for WT control. The principle is tracking the maximum power coefficient ( $C_p$ ) and the maximum power corresponding to the wind flow through rotor [10]. Due to the impact of wake effect, the wind at downstream WTs will be reduced. Hence, there is a possibility to reduce the total wake losses by controlling the operation point of each WT so that the total power production of the wind farm may be increased. Using pitch angle control method to improve the wind farm power production has already been reported in [11]. The Blade element momentum theory and eddy viscosity model were adopted to predict the power production and the methods were validated through a regular shape wind farm using GA. At the same time, a new method of optimising tip speed ratio and blade pitch angle to make up an individual control method for WT was presented in [12], the simulation was done using Horns Rev wind farm layout considering different wind directions. The simulation results showed that the power production can be increased with the new control method if the inflow wind speed was between cut-in and rated wind speed. In [13], the pitch angle of each WT was optimised to maximise the energy yields of the wind farm considering varying wind direction, however, the wind farm and wake model is simplified. In addition to meta-heuristic method, a gradient based optimisation techniques has been used in [14] using measured wind data in an irregular array layout. It can be seen that Jensen model is used for most of the wind farm optimisation work [3–8, 12, 13]. The main reason is that calculation of energy yields using Jensen model requires the least computation time in comparison with the other models. Moreover, it was observed that the sophisticated models have a similar level of accuracy as Jensen model for such kind of studies in [15]. Taking into account the reasons mentioned above, Jensen model is selected in this paper.

In [9–14], it is shown that the existing control methods can improve the power production of regular shape wind farm or irregular array layout which still has a regular layout. However, a cost-effective wind farm concerns three aspects: investment, power production and power losses which can be expressed using levelised production cost (LPC) [16]. In this paper, a new method of individual control for each WT to minimise the LPC of wind farm is proposed. The new contributions of this paper are now summarised as the following: (i) by properly distributing the power production reference of each WT, the LPC of the OWF can be reduced. The LPC is minimised instead of maximising power production of whole wind farm. The final solution is found by PSO optimisation program. (ii) The proposed power dispatch strategy can be used in any irregular shaped wind farms for the whole operation range. A regular wind farm with 400 MW capacities and the irregular shaped Norwegian Centre for Offshore Wind Energy (NORCOWE) reference wind farm are chosen as case studies to demonstrate the effectiveness of the proposed method.

The paper is organised as follows. The analytical equations for calculating the wake velocity with varying wind speed and the MPPT control strategy are presented in Section 2. The optimised power dispatch strategy (OPD) and the optimisation framework are presented in Section 3. The simulation results and analysis for regular shape and totally irregular shaped wind farms are presented and discussed in Sections 4 and 5 respectively. Finally, conclusions are given in Section 6.

## 2 Wind farm models

The wake model and the traditional control strategy (TCS) are specified in this section. The power production model which is the baseline for comparison is also built up in this section.

### 2.1 Jensen wake model

In 1983, Jensen proposed a simplified wake model which assuming a linear wake expanding behind the upstream WT [17, 18]

$$V_{ij} = V_0 - V_0 \left(1 - \sqrt{1 - C_t}\right) \left(\frac{R_0}{R_{ij}}\right)^2 \left(\frac{S_{\text{Overlap}_{ij}}}{S_0}\right) \quad (1)$$

$$R_{ij} = R_0 + d_c L_{ij} \quad (2)$$

The recommended value of  $d_c$  is 0.04 for offshore environment [19].

In a large wind farm, the downstream WT will be affected by several upstream WTs. To evaluate all the contributions to wind speed deficit at downstream WTs, the authors in [19] proposed a method in which the multiple wakes are calculated by using the 'sum of squares of velocity deficits'. Hence, the wind velocity at the WT at row  $n$ , column  $m$  can be derived as

$$V_{nm} = V_0 \left[1 - \sqrt{\sum_{i=1}^{N_{\text{row}}} \sum_{j=1}^{N_{\text{col}}} \left[1 - \left(\frac{V_{ij}}{V_0}\right)^2\right]}\right] \quad (3)$$

Besides the full shadowing condition, partial shadowing takes place as frequently as full shadowing. It is necessary to estimate the wake losses of the wind farm considering partial wake effect. The wake model with varying wind velocity and direction was described in [21].

### 2.2 Power captured model

The mechanical power extracted from the wind at WT can be expressed as follows [22]

$$P_{\text{mec}} = \frac{1}{2} \rho \pi R^2 V^3 C_p(\beta, \lambda) / 10^6 \quad (4)$$

The wind power captured by a WT in the whole operation region can be expressed as a power curve [23], which is shown in Fig. 1. In different wind speed region, the WT control methods are different. The control strategies in different regions are presented in this section.

(i) *Region 1*: If the wind speed is lower than the cut-in speed, as in region 1. The wind power available is lower than losses in the turbine system. Hence, the turbine does not produce power.

(ii) *Region 2*: The primary objective of the strategy in Region 2 is to maximise the energy capture by tracking the maximum power coefficient  $C_p^{\text{max}}(\beta_{\text{opt}}, \lambda_{\text{opt}})$ , known as MPPT [24]. In this region, the pitch angle is set to the optimal pitch angle  $\beta_{\text{opt}}$  and the tip speed ratio is tuned to its optimal value  $\lambda_{\text{opt}}$  by adapting the rotor speed  $\omega_{\text{rot}}$  to its reference [32].

(iii) *Region 3*: If the wind speed is higher than the rated wind speed, the reference rotor speed should be the nominal rotor speed  $\omega_{\text{rot}}^{\text{nom}}$  [32]. The tip speed ratio  $\lambda$  can be calculated by (5) and then the power coefficient  $C_p(\beta, \lambda)$  can be derived from (4)

$$\lambda = \frac{\omega_{\text{rot}}^{\text{nom}} R}{V} \quad (5)$$

$$C_p(\beta, \lambda) = \frac{2 \times 10^6 P_{\text{mec}}^{\text{rated}}}{\rho \pi R^2 V^3} \quad (6)$$

Once  $C_p(\beta, \lambda)$  and  $\lambda$  are known, the pitch angle,  $\beta$ , can then be determined by interpolation in the power coefficient table  $C_p(\beta, \lambda)$ .

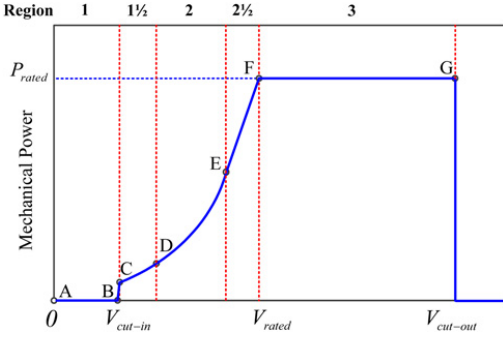


Fig. 1 Power curve of a WT

(iv) *Transition regions*: 1(1/2) and 2(1/2): Region 1(1/2) and Region 2(1/2) are transition regions between Region 1 and Region 2 and between Region 2 and Region 3, respectively. In both regions, the generator rotational speed is kept at a fixed value: the lower limit  $\omega_{rot}^{min}$  for Region 1(1/2) and the nominal value  $\omega_{rot}^{min}$  for Region 2(1/2). At a certain wind speed, the tip speed ratio  $\lambda$  can be determined by (5). For each determined tip speed ratio  $\lambda$ , the optimal power coefficient value  $C_p^{opt}(\beta, \lambda)$  and then the corresponding pitch angle  $\beta$  can be found in the look-up table  $C_p(\beta, \lambda)$  [32].

The power production of each WT is calculated by (4), and the total power production that is generated by the WTs can be written as

$$P_{tot} = \sum_{m=1}^{N_{col}} \sum_{n=1}^{N_{row}} P_{mec, mn} \quad (7)$$

### 2.3 Power losses and energy yields

The power losses of AC cable can be expressed as

$$P_{loss, ij} = 3I_{ij}^2 R_{e, ij} \quad (8)$$

where

$$R_{e, ij} = \rho_{R, ij} \frac{L_{R, ij}}{S_{R, ij}} \quad (9)$$

Then the total losses within the wind farm can be written as

$$P_{loss, tot} = \sum_{j=1}^{N_{col}} \sum_{i=1}^{N_{row}} P_{loss, ij} \quad (10)$$

From (7) to (10), the energy yield of the wind farm can be formulated as

$$E_{tot} = \sum_{i=1}^{TE} (P_{tot, i} - P_{tot, loss, i}) T_i \quad (11)$$

## 3 Problem formulation and optimisation

The objective function and constraints are built to analyse how the minimum LPC can be obtained with the proposed OPD. The PSO algorithm is adopted as optimisation method. The mathematical model and assumptions are presented in the section.

### 3.1 Levelised production cost

In this simulation, the objective function is constructed using LPC index which takes capital investment discounted costs during the life-cycle into account. In this project, the capital cost is calculated by the total cable cost using the model proposed in [16].

$$C_i = A_p + B_p \exp\left(\frac{C_p S_{n, i}}{10^8}\right) \quad (12)$$

$$S_{n, i} = \sqrt{3} I_{i, rated} U_{i, rated} \quad (13)$$

$$CAP_t = \sum_i^N C_i L_i Q_i \quad (14)$$

$$C_0 = \sum_{i=1}^{Ny} CAP_t (1+r)^{-i} \quad (15)$$

$$LPC = \left[ \frac{C_0 r (1+r)^{Ny}}{(1+r)^{Ny} - 1} + OAM_t \right] \frac{1}{E_{tot, av}} \quad (16)$$

As it can be seen from above equations, LPC is determined by two parts: total discounted costs and the total discounted energy output. The total investment  $C_0$  is assumed to be made in the first year and paid off during the lifetime of the wind farm. The generated energy  $E_{tot, av}$  is the average energy yield per year.

### 3.2 Optimised power dispatch strategy

As discussed above, the power extracted by each WT is determined by  $C_p$  while the  $C_t$  has an impact on the wind speed of downwind WTs. The pitch angle and tip speed ratio decide the  $C_p$  and  $C_t$ . Hence, it is possible to change the blade pitch angle of each WT to change the power production which is the basic concept of [11–13]. However, the power that really can bring in profit is the power that reached at the onshore substation (OS) or PCC point which also related to the power losses within the wind farm. Hence, LPC is selected as the evaluation index to evaluate the performance of OPD in this simulation and only the power losses along the cables are considered. The objective function of the problem can be expressed as

$$\text{Objective: } \min_{\beta_{mn}} \left\{ LPC = \left[ \frac{C_0 r (1+r)^{Ny}}{(1+r)^{Ny} - 1} + OAM_t \right] \right. \quad (17)$$

$$\left. \frac{1}{\sum_n \text{Num}_{col} \sum_m \text{Num}_{row} 0.5 \rho C_{p, mn} (\beta_{mn}, \lambda_{mn}) \pi R^2 v_{mn}^3} \right\}$$

$$\text{Constraints : } \beta_{min} \leq \beta_{ij} \leq \beta_{max} \quad (18)$$

$$P_{ij} \leq P_{rated} \quad (19)$$

$$\omega \leq \omega_{max} \quad (20)$$

$$\frac{\partial C_p(\beta_{mn}, \lambda)}{\partial \lambda} \leq 0 \quad (21)$$

The  $v_{mn}$  is calculated by (1)–(3). To ensure the WT not to fall into stall region, the  $\lambda$  has to limit to be in the right-hand side of  $C_p$ - $\lambda$  curve. This condition can be expressed as (12).

When the wind direction changes, the WT's nacelle will change its position as well, however, the yaw speed cannot follow the wind direction changing speed. That is so-called yaw misalignment [25]. In this project, the yaw misalignment impacts on the final energy yields are neglected.

### 3.3 Optimisation method

Since the problem is expected to be non-linear and non-convex, heuristic algorithm should be a good choice to solve this problem. Based on the social behaviour of fish schooling and bird flocking, Kennedy and Eberhart [26] proposed an evolutionary algorithm which has a good performance of solving non-linear optimisation problem. In this paper, the PSO algorithm is adopted.

In PSO, each possible solution is defined as a particle. The searching space is called particle swarm and the particle position is updated by giving each particle with a predefined speed and the speed is updated according to the particle's position as well. Then, all the particles will tend to move to their adjacent best positions which are the local optimal position and the results at those positions are called local optimal solutions. The best position among those local optimal positions is called global optimal position and the result at this position is called global optimal solution. The algorithm can be expressed in following equations [27].

$$v_i^{k+1} = wv_i^k + I_1 \text{rand}_1(\text{Pbest}_i^k - x_i^k) + I_2 \text{rand}_2(\text{Gbest}^k - x_i^k) \quad (22)$$

$$x_i^{k+1} = x_i^k + v_i^{k+1} \quad (23)$$

A larger  $\omega$  means the algorithm has a stronger global searching ability while smaller  $\omega$  ensures the local searching ability. In this project, the non-linear inertia weight [28] control method is adopted. The expression of non-linear inertia weight is as follows

$$w = w_{\text{final}} + (w_{\text{initial}} - w_{\text{final}}) \left( \frac{I_{\text{max}} - t}{I_{\text{max}}} \right)^n \quad (24)$$

### 3.4 Optimisation framework

As proposed above, the LPC is used to evaluate the proposed control method. The simulation procedure to access the OPD by PSO is shown in Fig. 2. The parameters of PSO are initialised in the first step. The LPC will be initially calculated by a series of randomly

given  $\beta$  (particle) which is the initial particle population and will be used for comparison later. Then the  $\beta$  will be updated and transmitted into the fitness function where the wind speed at each WT will be first calculated according to climatological information and Jensen wake model. After that,  $\lambda$  will be calculated according to (5), then  $C_i$  and  $C_p$  of each WT will be calculated with the given  $\beta$  and  $\lambda$ . Then, the energy yields of the whole wind farm can be obtained using power captured model based on the given cable connection layout. After that, LPC will be calculated using cable cost model and send out to the PSO main function for comparison. In fitness evaluation step, the particle which can generate the minimal LPC will be saved. This process will not be terminated if the maximum iteration is reached. Finally, a series of the optimised  $\beta$  for each WT which contribute to the minimal LPC will be selected.

Climatological information: The data is obtained from the work of Norwegian Meteorological Institute [29], in which the wind speeds are sampled per 3 h, for the convenience of calculation, the raw data is formulated into wind rose which is used for the energy production calculation of a year.

## 4 Simulation results for regular shaped wind farm

Initially, the optimised dispatch strategy is tested in a 8 row and 10 columns rectangular layout wind farm with 80 (National Renewable Energy Laboratory) NREL 5 MW WTs. The distance between each two WTs is 7 rotor diameter. Three scenarios are presented and the results are compared with TCS at first. Then the LPC reduction corresponding to different wind speeds and directions are specified. Finally, a calculation of regular wind farm LPC is done to analyse how much improvement will be achieved with the new method.

### 4.1 Regular shaped wind farm

The wind farm layout is assumed to be designed as in Fig. 3. In which, the black squares represent the WT positions while the blue lines show the cable connection configuration.

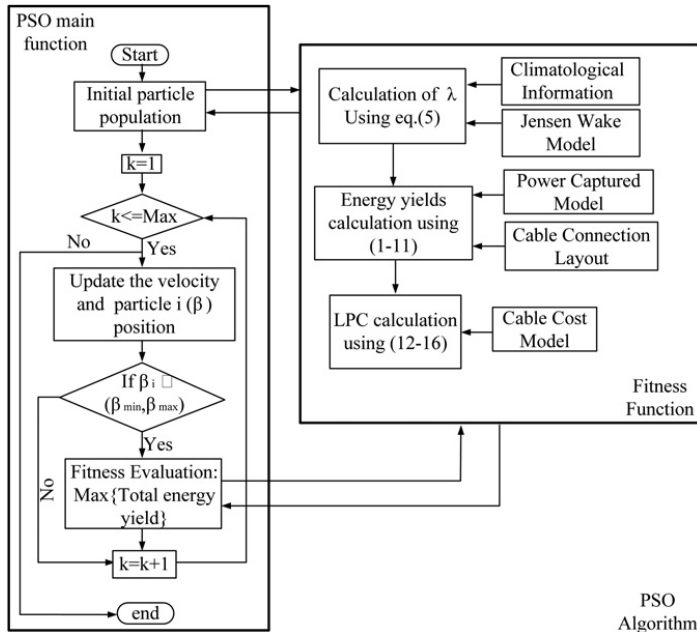
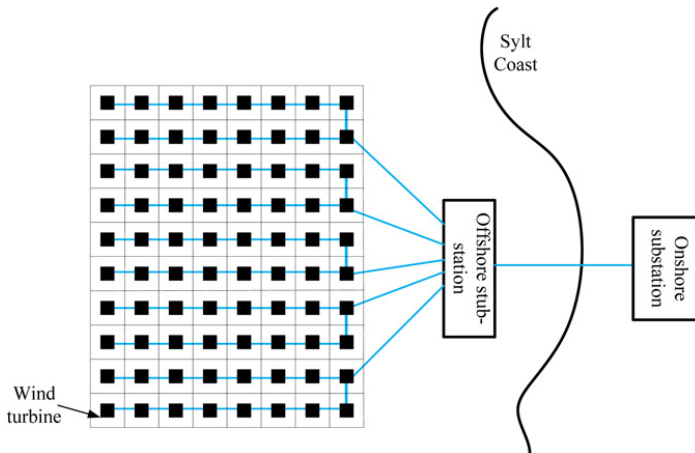


Fig. 2 Optimisation procedure



**Fig. 3** Layout of Regular Shaped Wind Farm

In this simulation, the fictive 5-MW NREL reference WT is adopted as the reference WT. The specification can be obtained in Table 1.

#### 4.2 OPD strategy for constant wind direction

The wind come from North to South is defined as the zero angle and then four scenarios are implemented in the proposed regular wind farm. The results are listed in Tables 2–4. LPC of each scenario is compared with the result obtained by TCS as illustrated in Figs. 4a–c. Finally, the LPC curve of whole wind farm with two methods are compared. In this section, the wind direction is zero and the space between WTs is large enough to avoid wake intersection, in other words, there will be no wake effect between rows. In practice, the upwind speed of each row is different. In our simulation, an assumption is made that the wind speed reached at the first WT of each row is same. Thus, only one line WT’s power production is presented. Since PSO is a stochastic optimisation method, each optimisation program is running 10 times with random initial start solution and the final solution is selected as the one with minimum LPC.

(i) *Scenario 1:  $V = 6$  m/s, Wind direction =  $0^\circ$* : Though the WTs in first line extract less wind energy, there is still a 16.7% power production increase with OPD which results in 14.3% LPC reduction compared with MPPT strategy. The WT power production for one line is illustrated in Fig. 4a. The distribution of fitness values using PSO are illustrated in Fig. 5a and the solution which have the minimal LPC is selected as the final result. The relations of the iteration and results (fitness value) are studied and shown in Fig. 5b.

(ii) *Scenario 2:  $V = 11$  m/s, Wind direction =  $0^\circ$* : If the wind speed is increasing to a value that is a little bit higher than  $V_{NRS}$ , then there is a possibility that some WTs’ rotor speed does not reach  $\omega_{rot}^{nom}$  yet while some does. As can be seen in Table 3, the rotor speed of the first line WTs reach  $\omega_{rot}^{nom}$  in both strategies in this scenario. In TCS, the pitch angle has to be manipulated to ensure the maximum wind energy captured. From (6), the  $V_{NRS}$  of NREL 5 MW WT can be calculated as 10.864 m/s. By using the new strategy the power can be increased by 15.78% and LPC can be reduced by 13.51% in this scenario. The WT power production for one line is illustrated in Fig. 4b.

(iii) *Scenario 3:  $V = 12$  m/s, Wind direction =  $0^\circ$* : When the inflow wind speed at first line WTs is reaching to 12 m/s, the WTs within the wind farm can be operated both in Region 2 as well as Region 3. The results in Table 4 show that 14.26% power increase and

12.32% LPC can be obtained in this scenario. The WT power production for one line is illustrated in Fig. 4c.

(iv) *Comparison of two methods*: The LPC reduction and LPC reduction rate for each sample speed are drawn as a curve as shown in Figs. 6a and b. It can be seen that there is a significant LPC reduction when inflow wind speed is lower and if the speed increases above 14 m/s, no improvement can be achieved with the new strategy. The maximum LPC reduction happens around 10.5 m/s, which is near the point where rotor speed reaches its maxima.

In low speed situation, the LPC reduction is high which leads to the higher LPC reduction rate. While in higher wind speed situation in which the wind speed is still in region 2, the power increase more with new strategy, however, the total power generation is larger which incurs the reduction of the LPC reduction rate. When the wind speed is above 14 m/s, the wind

**Table 1** Nrel 5 MW WT specification [30]

Parameter	5 MW NREL WT
cut-in wind speed	3 m/s
rated wind speed	11.4 m/s
cut-out wind speed	25 m/s
rotor diameter	126 m
rated power	5 MW
rated rotor speed	12.1 rpm

**Table 2** Simulation results for scenario 1

Sequence No. of WT column	TCS				OPD			
	$\lambda$	$\beta$	$\Omega$	V	$\lambda$	$\beta$	$\Omega$	V
1	7.5	0	6.82	6	7.5	3.12	6.82	6
2	7.5	0	5.32	4.68	7.5	3.16	5.78	5.09
3	7.5	0	5.12	4.50	7.5	3.14	5.74	5.05
4	7.5	0	5.04	4.44	7.5	3.03	5.67	4.99
5	7.5	0	5.01	4.41	7.5	3.51	5.69	5.00
6	7.5	0	4.99	4.39	7.5	2.97	5.70	5.02
7	7.5	0	4.98	4.38	7.5	2.96	5.69	5.01
8	7.5	0	4.98	4.38	7.5	3.40	5.69	5.00
9	7.5	0	4.97	4.37	7.5	3.97	5.64	4.96
10	7.5	0	4.07	4.37	7.5	3.69	5.59	4.91
$P_{tot}$ (MW)	29.70				34.66			
LPC (Dkk/MW)	2794.7				2395.8			

**Table 3** Simulation results for scenario 2

TCS					OPD				
Sequence No. of WT column	$\lambda$	$\beta$	$\Omega$	V	$\lambda$	B	$\Omega$	V	
1	7.25	0.0043	12.1	11	7.25	4.7285	12.1	11	
2	7.5	0	9.85	8.66	7.5	4.7285	11.0033	9.67	
3	7.5	0	9.41	8.27	7.5	4.7285	10.60	9.32	
4	7.5	0	9.26	8.14	7.5	4.7285	10.47	9.21	
5	7.5	0	9.19	8.08	7.5	4.7285	10.44	9.18	
6	7.5	0	9.16	8.05	7.5	4.7285	10.46	9.19	
7	7.5	0	9.14	8.03	7.5	4.7285	10.42	9.16	
8	7.5	0	9.13	8.02	7.5	4.7285	10.43	9.17	
9	7.5	0	9.12	8.02	7.5	3.8394	10.40	9.14	
10	7.5	0	9.11	8.01	7.5	3.9334	10.29	9.05	
$P_{tot}(MW)$		183.68					212.67		
LPC(Dkk/MW)		456.28					394.65		

**Table 4** Simulation results for scenario 3

TCS					OPD			
Sequence No. of WT column	$\lambda$	$\beta$	$\Omega$	V	$\lambda$	$\beta$	$\Omega$	V
1	6.6	4.7	12.1	12	6.6	4.73	12.1	12
2	7.5	0	11.40	10.58	7.5	4.73	12.04	10.58
3	7.5	0	9.21	9.25	7.5	4.73	11.63	10.22
4	7.5	0	8.55	8.96	7.5	4.73	11.44	10.05
5	7.5	0	8.25	8.85	7.5	4.73	11.11	9.77
6	7.5	0	8.10	8.80	7.5	4.73	10.93	9.61
7	7.5	0	8.00	8.78	7.5	4.73	11.09	9.75
8	7.5	0	7.94	8.76	7.5	4.73	11.27	9.91
9	7.5	0	7.91	8.75	7.5	4.09	11.44	10.06
10	7.5	0	7.88	8.74	7.5	3.96	11.00	9.67
$P_{tot}(MW)$		240.38					274.65	
LPC(Dkk/MW)		349.83					306.74	

farm will be operated in full load condition and no more energy can be generated in that case. Hence, the higher the inflow wind speed, the less LPC reduction rate can be realised using new control strategy.

### 4.3 OPD strategy for varying wind direction

In the above scenarios, the wake effect can only affect the downstream WTs in a line. If the coming wind is not in line with the WTs, the wakes from neighbouring rows will merge, in other words, the downstream WTs will be under the affected region of the other rows WTs. In the fourth scenario, the wind is assumed from Northeast to Southwest. The power distribution using TCS can be seen in Fig. 7a while b is obtained using new control strategy.

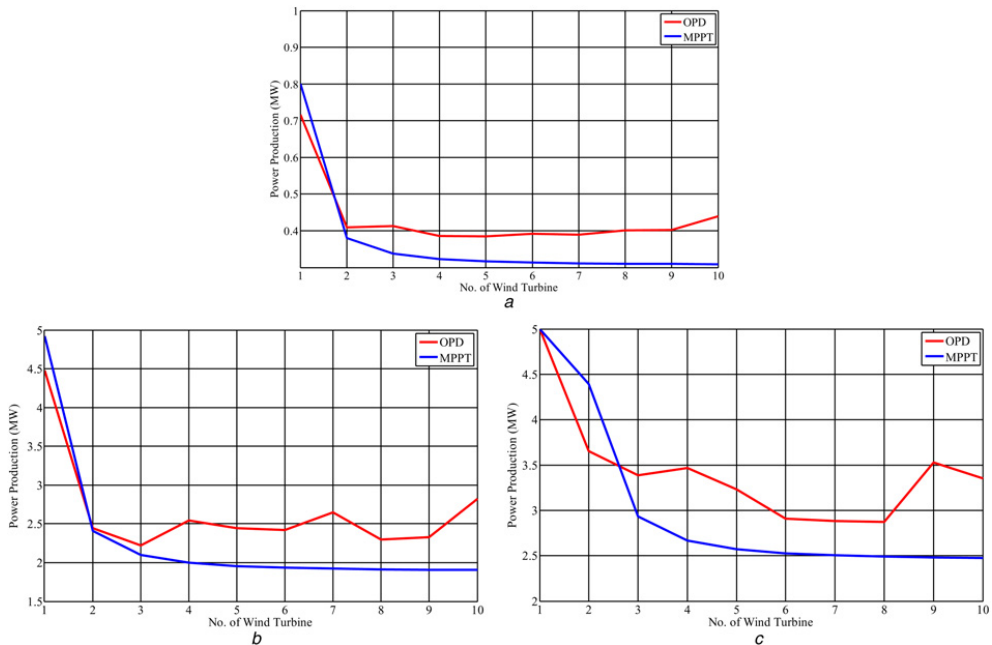


**Fig. 4** WT power production

a Power production comparison between two methods when inflow wind speed is 6 m/s and wind direction equals 0°

b Power production comparison between two methods when inflow wind speed is 11 m/s and wind direction equals 0°

c Power production comparison between two methods when inflow wind speed is 12 m/s and wind direction equals 0°



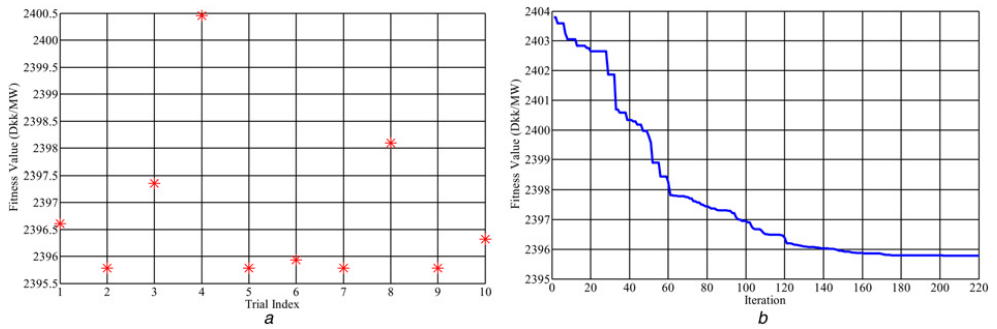


**Fig. 5** Distribution of fitness values using PSO  
*a* 10 trials for scenario 1  
*b* Fitness value corresponding to each iteration for scenario 1

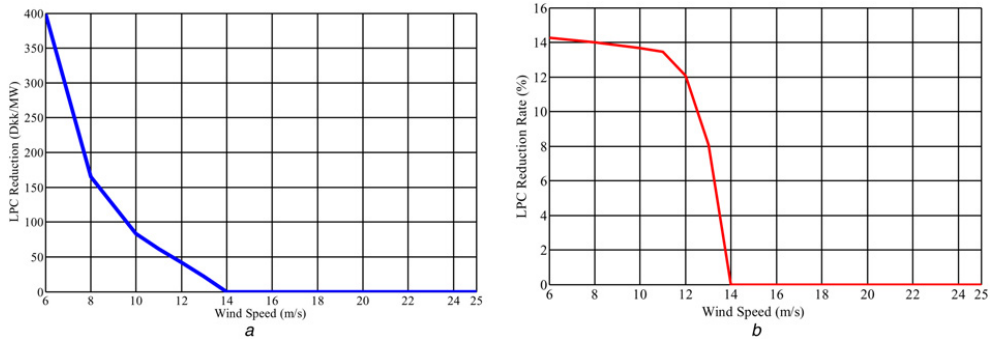


**Fig. 6** LPC reduction and LPC reduction rate for each sample speed are drawn as a curve  
*a* LPC reduction curve for regular shaped wind farm  
*b* LPC reduction rate curve for regular shaped wind farm

The total power productions for two control strategies are 96.96 MW and 101.92 MW respectively while LPCs are 859.6 Dkk/MW and 817.0 Dkk/MW. It is due to the fact that the distance between WTs is enlarged if the wind direction changed to 45°. In such case, the wake effect on the downstream WTs has already been reduced. Hence, the new method can only increase the power by only 5.12% while LPC can be reduced by 4.96% in this scenario.

In this part, the total power productions corresponding to several selected wind speeds and directions using two methods are obtained and compared in Table 5.

It can be seen that the power production will be significant increased if the wind is in line with WT. When the angle increases, the distance along the wind direction from the upwind WT to downwind WT is also increased which incurs the reduction

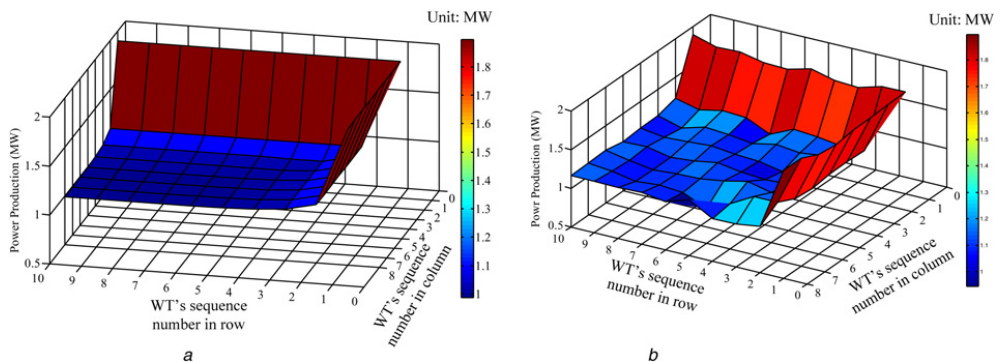


**Fig. 7** Power production comparison between two methods when inflow wind speed is 8 m/s and wind direction equals 45°  
*a* Power production distribution using TCS  
*b* Power production distribution using OPD

**Table 5** LPC comparison of two methods

Wind direction	Wind speed									
	4		8		11		12		14	
	TCS (Dkk/MW)	OPD (Dkk/MW)	TCS (Dkk/MW)	OPD (Dkk/MW)	TCS (Dkk/MW)	OPD (Dkk/MW)	TCS (Dkk/MW)	OPD (Dkk/MW)	TCS & OPD (Dkk/MW)	
0	23,037.2	8121.7	1182.0	1016.6	456.3	394.9	349.8	307.6	212.2	
15	4877.7	4866.5	614.1	613.1	238.9	238.7	212.2	212.2	212.2	
30	5156.7	5133.5	649.0	645.5	252.3	251.3	212.1	209.4	212.2	
45	6842.1	6509.9	859.6	817.0	332.7	317.0	260.9	253.8	212.2	
60	5116.2	5094.8	643.9	641.0	250.4	249.5	212.1	209.1	212.2	
75	4810.7	4803.8	605.8	604.9	235.7	235.6	212.2	212.2	212.2	
90	18,428.8	7916.5	1134.9	993.4	437.9	385.9	335.4	300.3	212.2	

of wake deficit. Hence, the new control strategy can only reduce the LPC rate less than 1%.

**4.4 LPC reduction for a regular wind farm in a year**

For the convenient of calculation, the average wind velocity and direction for one day is calculated, in other words, the energy production is calculated over a year with an average wind velocity and direction for each day in this simulation. The wind direction and speed is shown as a wind rose in Fig. 8a. The LPC for 12 main directions and the LPC reduction with the new strategy are illustrated in Figs. 8 b and c respectively. The LPC comparisons are listed in Table 6.

There are 12 directions which are shown in Fig. 8a. The colours indicate the speed interval which is shown with coloured

rectangle. The percentage figure means the occurrence rate of the wind speed in that direction. It can be seen that in the vicinity of FINO3, most of the wind is coming from southwest to northeast and the main wind speed is between 10 to 15 m/s.

As can be seen in Table 6, the new strategy succeeds in reducing the LPC by 2.20%. The LPC for 12 main directions with new strategy are illustrated in Fig. 8b. The coloured squares are the LPC interval in unit of Dkk/MW while the percentage figure shows the LPC occurrence rate in each direction. The LPC reduction with new strategy is also shown in Fig. 8c.

From Fig. 8b it can be seen that the minimal LPC direction is from southwest which corresponds to the prevailing wind direction, however, the minimal LPC increment happen in direction of west, east and south as can be seen in Fig. 8c. This is due to the fact that if the wind direction is in line with the WT's row or column the wake effect will be stronger than the other directions.

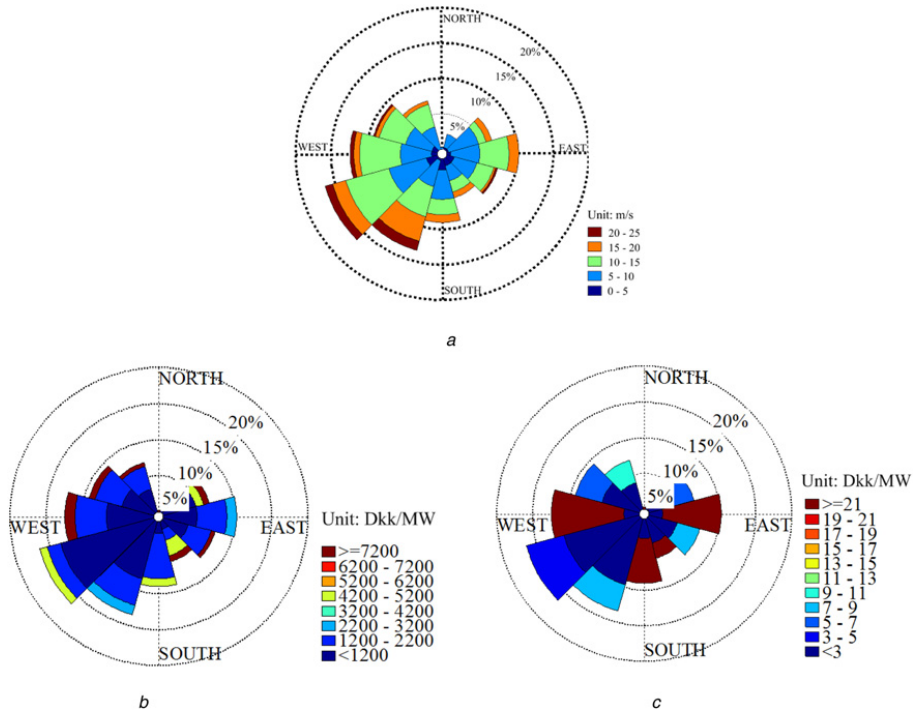


**Fig. 8** Wind direction and speed is shown as a wind rose

- a Wind rose for the wind climate in the vicinity of FINO3
- b LPC of 12 main directions for regular shape wind farm layout in one year
- c LPC reduction for regular shape wind farm layout in one year



**Table 6** LPC comparison of two methods for regular wind farm

Duration	Energy yields		
	MPPT control	OPD method	LPC reduction proportion
1 year	375.37 (Dkk/MW)	367.13 (Dkk/MW)	2.20%

## 5 Simulation results for NORCOWE reference wind farm

In this section, the NORCOWE reference wind farm (NRWF) is first introduced. The LPC for the selected wind farm are also calculated at last.

### 5.1 NORCOWE reference wind farm

The NRWF is assumed to be at the location of the FINO3 met mast-80 km west of German island of Sylt. In this work, the NRWF layout is adopted to implement the optimised control strategy [31]. The layout is shown in Fig. 9.

### 5.2 LPC comparison with OPD

In this part, the total power productions corresponding to several selected wind speeds and directions using two methods are

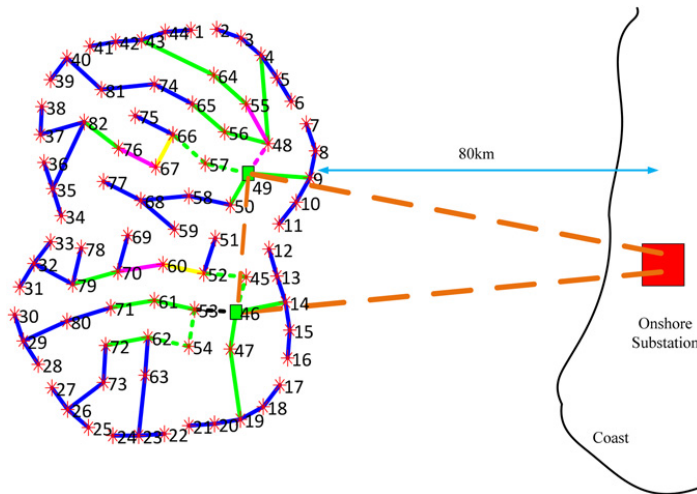


**Fig. 9** NRWF layout

**Table 7** LPC comparison of two methods

Wind direction	Wind Speed									
	4		8		11		12		14	
	TCS (Dkk/MW)	OPD (Dkk/MW)	TCS (Dkk/MW)	OPD (Dkk/MW)	TCS (Dkk/MW)	OPD (Dkk/MW)	TCS (Dkk/MW)	OPD (Dkk/MW)	TCS & OPD (Dkk/MW)	
0	5130.2	5037.6	637.4	634.5	247.4	246.4	209.1	208.9	206.9	
15	7198.9	6102.9	788.8	767.1	306.1	296.5	231.8	231.2	206.9	
30	5652.8	5347.4	682.6	675.5	264.9	262.9	217.2	214.8	206.9	
45	5250.8	5207.3	660.4	654.5	256.4	254.9	210.6	208.4	206.9	
60	5222.8	5128.5	648.7	644.8	251.8	250.6	210.3	208.9	206.9	
75	5419.8	5321.6	673.9	667.8	261.5	259.6	216.4	215.9	206.9	
90	4984.5	4923.3	614.4	613.1	239.0	238.6	213.7	213.5	206.9	

obtained and compared in Table 7. The distribution of fitness values using PSO when inflow wind speed is 6 m/s and wind direction equals 0° are illustrated in Fig. 10a. The relations of the iteration and results for final solution are studied and shown in Fig. 10b. The LPCs using MPPT and OPD are 1504.4 and 1411.2 respectively. It can be known that LPC can be reduced by 6.2% in this wind farm.

It can be seen that the LPC cannot be significantly increased in this case. This is because that the NRWF has already designed to minimise the wake losses. In such a wind farm, the proposed optimised control strategy cannot reduce the LPC so much.

### 5.3 LPC reduction for NRWF in a year

The LPC for NRWF is calculated by using the same wind data as showed in Fig. 11. The results are listed in Table 8.

Compared with regular shape wind farm, by TCS, the LPC have already been reduced in NRWF as shown in Table 8. The new strategy further reduces the LPC of the NRWF 0.15%. The LPC for 12 main directions with the new strategy are illustrated in Fig. 11a. The LPC reduction with the new strategy is also shown in Fig. 11b.

It can be seen that the LPC of regular and irregular wind farms are reduced with the new strategy while the LPC reduction of the regular wind farm was higher than that of the irregular wind farm. Compared Fig. 11a with b, it can be seen that in south, north and east the LPC reduction for regular shape wind farm are higher than the LPC reduction in irregular shape wind farm. This is due to the fact that

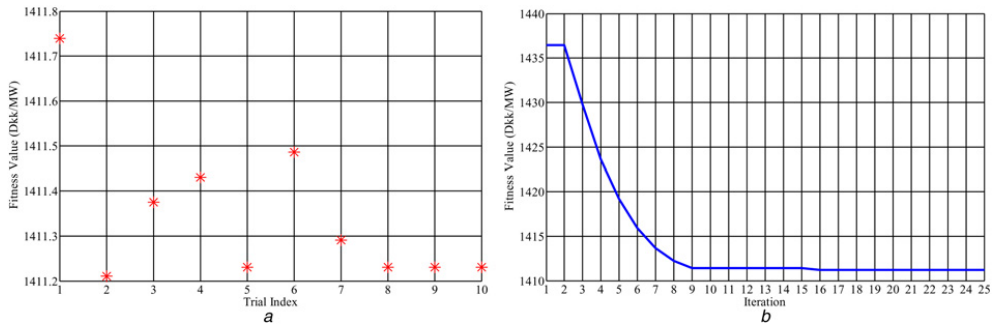


**Fig. 10** Distribution of fitness values using PSO when inflow wind speed is 6 m/s and wind direction equals 0°  
 a 10 trials for NRWF when inflow wind speed is 6 m/s and wind direction equals 0°  
 b Fitness value corresponding to each iteration for NRWF when inflow wind speed is 6 m/s and wind direction equals 0°

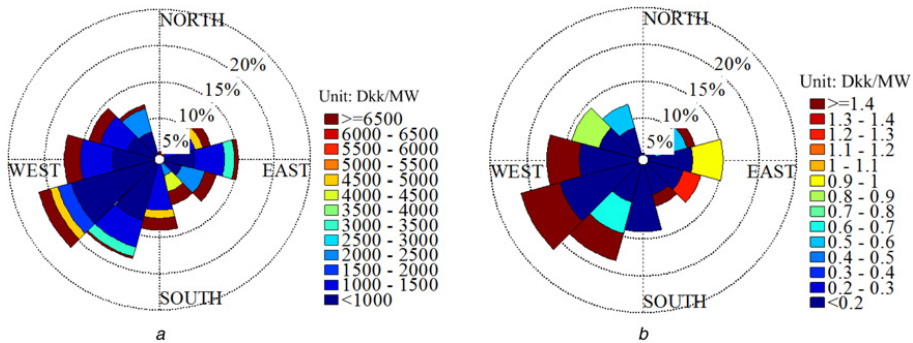


**Fig. 11** LPC for 12 main directions with the new strategy and the LPC reduction with the new strategy is also shown  
 a LPC of 12 main directions for NRWF in one year  
 b LPC reduction for NRWF in one year

the wake effect has already been reduced in irregular wind farm (see Tables 6 and 8), in other words, the wake losses among the irregular wind farm are less in this case.

#### 5.4 Computational effort comparison

The program is performed on a computer which is an Intel(R) Core (TM) i7-4800MQ CPU @ 2.70 GHz processor with 8 GB RAM. The simulation time spent by the algorithm to reach the optimal solution for each individual turbine in the regular wind farm or

**Table 8** LPC comparison of two methods for NRWF

Duration	Energy yields		
	MPPT control	OPD	LPC Reduction proportion
1 year	338.5788	338.0733	0.15%

**Table 9** Simulation time using PSO

When inflow wind speed is 8 m/s and wind direction equals 0°	Time (s)	
	Regular Shaped Wind Farm	NRWF
	1566.49	2099.96

NRWF when inflow wind speed is 8 m/s and wind direction equals 0° is concluded in Table 9.

## 6 Conclusions

Wake effect reduces the power production of wind farms. To minimise the wake losses, the layout optimisation of wind farm should be done in design phase. While for an existing wind farm, it is still possible to maximise the energy yields by properly setting the power production reference of each WT within the wind farm. However, the power that can really bring in benefits is the power that transmitted to the OS. In this paper, an OPD of minimising LPC of regular and irregular OWFs is proposed. The optimised pitch angle in each scenario is found by PSO. The effectiveness of the new strategy was well verified by study cases. In comparison with traditional MPPT control strategy, the proposed method can reduce the LPC of OWFs.

In the future, the proposed dispatch strategy can be applied in the optimisation of wind farm layout design to get a more cost-effective wind farm.

## 7 Acknowledgment

Authors thank Norwegian Centre for Offshore Wind Energy (NORCOWE) under grant 193821/S60 from Research Council of Norway (RCN).

## 8 References

- 1 Kalyan: 'Global Wind Report', available at <http://www.gwec.net/>
- 2 Perveen, R., Kishor, N., Mohanty, S.R.: 'Off-shore wind farm development: Present status and challenges', *Renew. Sustain. Energy Rev.*, 2013, **29**, pp. 780–792
- 3 González, J.S., Payán, M.B., Riquelme Santos, J.M.: 'An improved evolutionary algorithm for large offshore wind farm optimum turbines layout'. PowerTech, 2011 IEEE Trondheim, IET, 19–23 June 2011, pp. 1–6
- 4 Huang, H.-S.: 'Efficient hybrid distributed genetic algorithms for wind turbine positioning in large wind farms'. IEEE Int. Symp. on Industrial Electronics, 5–8 July 2009, pp. 2196–2201
- 5 do Couto, T.G., Farias, B., Diniz, A.C.G.C., et al.: 'Optimization of wind farm layout using genetic algorithm'. Tenth World Congress on Structural and Multidisciplinary Optimization, Orlando, Florida, USA, 19–24, May 2013
- 6 Gonzalez, J.S., Gonzalez Rodriguez, A.G., Mora, J.C., et al.: 'Optimization of wind farm turbines layout using an evolutionary algorithm'. *Renew. Energy*, 2010, **35**, (8), pp. 1671–1681
- 7 Grady, S.A., Hussaini, M.Y., Abdullah, M.M.: 'Placement of wind turbines using genetic algorithms', *Renew. Energy*, 2005, **30**, (12), pp. 259–270
- 8 Mosetti, G., Poloni, C., Diviacco, B.: 'Optimization of wind turbine positioning in large wind farms by means of a genetic algorithm', *J. Wind Eng. Ind. Aerodyn.*, 194, **51**, pp. 105–116
- 9 Errami, Y., Benchagra, M., Hilal, M., et al.: 'Control strategy for PMSG wind farm based on MPPT and direct power control'. 2012 Int. Conf. on Multimedia Computing and Systems (ICMCS) 10th–12th May 2012, pp. 1125–1130
- 10 Errami, Y., Maaroufi, M., Cherkaoui, M., et al.: 'Maximum power point tracking strategy and direct torque control of permanent magnet synchronous generator wind farm'. 2012 Int. Conf. on Complex Systems (ICCS), 5–6 November 2012, pp. 1–6
- 11 Lee, J., Son, E., Hwang, B., Lee, S.: 'Blade pitch angle control for aerodynamic performance optimization of a wind farm', *Renew. Energy*, 2012, **54**, pp. 124–130
- 12 González, J.S., Payán, M.B., Santos, J.R., et al.: 'Maximizing the overall production of wind farms by setting the individual operating point of wind turbines', *Renew. Energy*, 2015, **80**, pp. 219–229
- 13 Behnood, A., Gharavi, H., Vahidi, B., et al.: 'Optimal output power of not properly designed wind farms, considering wake effects', *Int. J. Electr. Power Energy Syst.*, 2014, **63**, pp. 44–50
- 14 Gebraad, P. M. O., Wingerden, J. W.: 'Maximum power point tracking control for wind farms', *Wind Energy*, 2014, **18**, (3), pp. 429–447
- 15 Barthelme, R.J., Folkerts, L., Larsen, G.C., et al.: 'Comparison of wake model simulations with offshore wind turbine wake profiles measured by sodar', *J. Atmos. Ocean. Technol.*, 2005, **23**, pp. 888–901
- 16 Lundberg, S.: 'Performance comparison of wind park configurations'. Technical Report 30R, Department of Electric Power Engineering, Chalmers University of Technology, Department of Electric Power Engineering, Göteborg, Sweden, August 2003
- 17 Jensen, N.O.: 'A Note on Wind Generator Interaction', 1983, p. 5
- 18 González-Longatt, F., Wall, P., Terzija, V.: 'Wake effect in wind farm performance: Steady-state and dynamic behavior', *Renew. Energy*, 2011, **39**, (1), pp. 329–338
- 19 Beaucage, P., Brower, M., Robinson, N., et al.: 'Overview of six commercial and research wake models for large offshore wind farms'. Proc. EWEA 2012, Copenhagen, 2012
- 20 Porté-Agel, F., Wu, Y.-T., Chen, C.-H.: 'A numerical study of the effects of wind direction on turbine wakes and power losses in a large wind farm', *Energies*, 2013, **6**, pp. 5297–5313, MDPI
- 21 Hou, P., Hu, W., Soltani, M., et al.: 'Optimized placement of wind turbines in large scale offshore wind farm using particle swarm optimization algorithm', *IEEE Trans. Sustain. Energy*, 2015, **99**, pp. 1–11
- 22 Chen, K., Delarue, P., Bouscayrol, A., et al.: 'Minimum copper loss and power distribution control strategies of double-inverter-fed wound-rotor induction machines using energetic macroscopic representation', *IEEE Trans. Energy Convers.*, 2010, **25**, (3), pp. 642–651
- 23 Bianchi, F.D., Battista, H.D., Mantz, R.J.: 'Wind turbine control systems' (Springer, 2007)
- 24 Pao, L.Y., Johnson, K.E.: 'Control of wind turbines', *IEEE Control Syst. Mag.*, 2011, **31**, (2), pp. 44–62
- 25 Choi, J., Shan, M.: 'Advancement of Jensen (Park) wake model'. EWEA Conf., Wien, February 2013
- 26 Kennedy, J., Eberhart, R.: 'Particle swarm optimization'. Proc. IEEE Int. Conf. Neural Networks, April 1995, pp. 1942–1948
- 27 Kennedy, J.: 'The particle swarm: social adaptation of knowledge'. Proc. IEEE Int. Conf. Evolution of Computing, Indianapolis, IN, 1997, pp. 303–308
- 28 Shi, Y., Eberhart, R. C.: 'Empirical study of particle swarm optimization'. Proc. Congress on Evolutionary Computation, 1999, pp. 1950–1955
- 29 Furevik, B.R., Haakenstad, H.: 'Near-surface marine wind profiles from rawinsonde and NORA10 hindcast', *J. Geophys. Res.*, 2012, **117**, (23)
- 30 Jonkman, J., Butterfield, S., Musial, W., et al.: 'Definition of a 5-MW reference wind turbine for offshore system development', February 2009. Available at <http://www.nrel.gov/wind/pdfs/38060.pdf>
- 31 Norwegian Centre for Offshore Wind Energy (NORCOWE). (9 September 2014). WP2014-Froya-NRWF NORCOWE Reference Wind Farm
- 32 Hansen, A.D., Jauch, C., Sorensen, P., et al.: 'Dynamic wind turbine models in power system simulation tool DlgSILENT', Riso-R-1400(EN), 2003

# Optimized Placement of Wind Turbines in Large-Scale Offshore Wind Farm Using Particle Swarm Optimization Algorithm

Peng Hou, *Student Member, IEEE*, Weihao Hu, *Member, IEEE*, Mohsen Soltani, *Member, IEEE*, and Zhe Chen, *Senior Member, IEEE*

**Abstract**—With the increasing size of wind farms, the impact of the wake effect on wind farm energy yields become more and more evident. The arrangement of locations of the wind turbines (WTs) will influence the capital investment and contribute to the wake losses, which incur the reduction of energy production. As a consequence, the optimized placement of the WT's may be done by considering the wake effect as well as the components cost within the wind farm. In this paper, a mathematical model which includes the variation of both wind direction and wake deficit is proposed. The problem is formulated by using leveled production cost (LPC) as the objective function. The optimization procedure is performed by a particle swarm optimization (PSO) algorithm with the purpose of maximizing the energy yields while minimizing the total investment. The simulation results indicate that the proposed method is effective to find the optimized layout, which minimizes the LPC. The optimization procedure is applicable for optimized placement of WT's within wind farms and extendible for different wind conditions and capacity of wind farms.

**Index Terms**—Energy yields, leveled production cost (LPC), optimized placement, particle swarm optimization (PSO), wake effect, wake model.

## NOMENCLATURE

$V_0$ (m/s)	Input wind speed at the first line wind turbine (WT).
$V_x$ (m/s)	Wind speed in the wake at a distance $x$ downstream of the upstream WT.
$R_0$ (m)	Radius of the WT's rotor.
$R_x$ (m)	Generated wake radius at $x$ distance along the wind direction.
$S_{\text{overlap}}$ (m <sup>2</sup> )	Affect wake region.
$V_{ij}$ (m/s)	Wake velocity generated by the WT at $i$ th row, $j$ th column of wind farm.
$V_{nm}$ (m/s)	Wind velocity at the WT at row $n$ , column $m$ .
$N_{\text{row}}$	Number of WT's in a row.

Manuscript received October 16, 2014; revised February 13, 2015; accepted April 28, 2015. Date of publication June 01, 2015; date of current version September 16, 2015. This work was supported by the Norwegian Centre for Offshore Wind Energy (NORCOWE) under Grant 193821/S60 from Research Council of Norway (RCN). NORCOWE is a consortium with partners from industry and science, hosted by Christian Michelsen Research. Paper no. TSTE-00582-2014.

The authors are with the Department of Energy Technology, Aalborg University, Aalborg 9220, Denmark (e-mail: pho@et.aau.dk; whu@et.aau.dk; sms@et.aau.dk; zch@et.aau.dk).

Color versions of one or more of the figures in this paper are available online at <http://ieeexplore.ieee.org>.

Digital Object Identifier 10.1109/TSTE.2015.2429912

$N_{\text{col}}$	Number of WT's in a column.
$x_{nm}, y_{nm}$ (m)	Position of the downstream WT at row $n$ , column $m$ in coordinate system.
$x_{ij}, y_{ij}$ (m)	Position of the upstream WT at row $i$ , column $j$ in coordinate system.
$C$	Center of the upstream WT.
$O_{nm}$	Center of the downstream WT at row $n$ , column $m$ .
$O_{ij}$	Center of the wake that developed from the upstream WT at row $i$ , column $j$ .
$\alpha$ (°)	Wind deviation angle, which is the angle between line $C - O_{ij}$ and $x$ -axis.
$\beta$ (°)	Angle between line $C - O_{nm}$ and $x$ -axis.
$\beta'$ (°)	Angle between $C - O_{nm}$ and $x$ -axis in second case.
$R_{ij}$ (m)	Radius of the wake that generated from the upstream WT rotor at row $i$ , column $j$ .
$S_{ij}$ (m <sup>2</sup> )	Fan-shaped area of the wake area generated by upstream WT at row $i$ , column $j$ .
$S_{nm}$ (m <sup>2</sup> )	Fan-shaped area of the sweeping area that generated by the downstream WT rotor at row $n$ , column $m$ .
$\mu$ (°)	Chord angle corresponding to $S_{nm}$ .
$\gamma$ (°)	Chord angle corresponding to $S_{ij}$ .
$L_{ij}$ (m)	Distance between upstream WT at row $i$ , column $j$ and downstream WT at row $n$ , column $m$ .
$S_{\text{overlap},ij}$ (m <sup>2</sup> )	Overlapped area in Fig. 1.
$S_{q,ij}$ (m <sup>2</sup> )	Temporary variable that is needed in the deviation process.
$h_{ji}$ (m)	Length of diagonal line in green quadrangle.
$d_{ji}$ (m)	Distance from $O_{ij}$ to $O_{nm}$
$S_r$ (m <sup>2</sup> )	Sweeping area generated by the rotor downstream WT.
$\beta''$ (°)	Pitch angle.
$\lambda_{\text{opt}}$	Optimal tip speed ratio for the pitch angle $\beta'$ , at which the power coefficient will be maximum.
$\rho$ (kg/m <sup>3</sup> )	Air density.
$C_{p,\text{opt}}$	Power coefficient at $\lambda_{\text{opt}}$ .

$P_{m,ij}$ (MW)	Mechanical power generated by WT at row $i$ , column $j$ .
$v$ (m/s)	Injected wind speed.
$R$ (m)	Rotor radius.
$P_{\text{tot},t}$ (MW)	Total power production during interval $t$ .
$P_{\text{tot,loss},t}$ (MW)	Total power losses during interval $t$ .
$T_E$ (day)	Duration interval for energy yields calculation.
$T_t$ (h)	Duration when the wind farm generating power of $P_{\text{tot},t}$ .
$E_{\text{tot}}$ (MWh)	Energy yields of the wind farm.
$t$ (h)	Energy yields calculation time.
$P_{\text{loss},i}$ (MW)	Power losses of cable $i$ .
$I_i$ (kA)	Current in cable $i$ .
$R_{e,i}$ (ohm/m)	Resistance of cable $i$ .
$\rho_{R,i}$ (ohm*m/mm <sup>2</sup> )	Resistivity of selected cable $i$ .
$l_{R,ij}$ (m)	Length of cable $i$ .
$S_{R,i}$ (m <sup>2</sup> )	Sectional area of cable $i$ .
$d_x$ (m)	Interval of WTs in $x$ direction or rather the distance between WTs in a row.
$d_y$	(m)Interval of WTs in $y$ direction or rather the distance between each row of WTs.
$C_i$ (MDKK/km)	Unit cost of cable $i$ .
$S_{n,i}$ (W)	Rated apparent power of cable in line $i$ .
$N$	Total number of cables in a wind farm.
$A_p, B_p, C_p$	Coefficient of cable cost model.
$I_{i,\text{rated}}$ (A)	Rated current of cable in line $i$ .
$U_{i,\text{rated}}$ (V)	Rated voltage of cable in line $i$ .
$L_i$ (km)	Length of cable $i$ .
$w$	Inertia weight.
$w_{\text{initial}}$	Initial inertia weight at the start of a given run.
$w_{\text{final}}$	Final inertia weight at the end of a given run.
$n$	Nonlinear modulation index.
$l_1, l_2$	Learning factors.
$\text{rand}_1, \text{rand}_2$	Stochastic numbers that can generate some random numbers within [0,1].
$x_i^k, x_i^{k+1}$ (m)	Position of particle $i$ at iteration $k$ and $k + 1$ , respectively.
$v_i^k, v_i^{k+1}$ (m)	Speed of particle $i$ at iteration $k$ and $k + 1$ , respectively.
$\text{local}_i^k$ (m)	Best position of particle $i$ at iteration $k$ .
$\text{global}^k$ (m)	Best position of all particles at iteration $k$ .

I. INTRODUCTION

ACCORDING to the Wind Report 2013 of Global Wind Energy Council (GWEC), wind energy has become the second largest renewable energy source and will take up to 25% of total renewable energy by 2035 [1]. Compared to onshore wind farm, offshore wind farm always has higher energy production efficiency and is not limited by land occupation problem; however, the investment is relatively larger. In order to maximize the energy production while getting the

minimum investment, more and more researchers are concentrating on solving the wind farm layout optimization (WFLO) problem with evolutionary algorithms. Since the scale of wind farms in early stage are relatively small, the initial attempts focus on maximizing energy yields or minimizing total losses within the wind farm using evolutionary algorithms without considering the wake effect. In [2], a multiobjective particle swarm optimization (PSO) algorithm is used to minimize the layout costs and maximize the energy output without considering the wake effect and the discounted costs of wind farm during life-cycle. The optimization for offshore wind farm electrical system is done in [3], in which the configuration with minimal LPC under required reliability is found via genetic algorithm (GA) while similar work is also presented by considering the cost and losses of each main component within wind farm [4].

The wake deficit can be explained as the impact of upstream WT to the downstream ones which incur the reduction of the total energy yields of the wind farm due to the wind speed drop downstream [5]. With the development of wind energy technology, both the capacity of the WT and wind farm increases a lot. Since the size of WT is larger, the wake effect's impact on energy yields becomes evident [6]. Three wake models commonly are the Jensen model, Ainslie model and G.C. Larsen model [7]. In Jensen model, the wakes behind the WTs are assumed to expand linearly and the wind speed within the wake of different heights is regarded to be the same. Ainslie developed a parabolic eddy viscosity model in which the wake turbulent mixing and ambient turbulence on wake are included. Since the results are obtained by solving the differential equations, it needs more time to get the solution and is more suitable for dynamic analysis of WT. The semianalytic wake model is constructed by Larsen. As reported in [8], the model is recommended for solving wake loading problem. In addition, some works of developing new model to help forecasting the energy yields of wind farm has been done in Risø National Laboratory [9], [10]. In [9], an analytical model that divided the wake into three regimes and the phenomena of multiple wakes merging, wake expanding, and wake hitting ground are all specified. The developed wake models provide researchers with the basic tool to continue the optimization work within the wind farm considering wake effect. All the models can be used for energy yields calculation; however, most of the wind farm layout design work are using Jensen model [11]–[15]. The main reason is that the calculation of energy yields using Jensen model requires the least computation time in comparison with the other models. Moreover, Jensen model shows better performance on the accuracy of energy yields calculation, which is demonstrated through a case study in [7] and [14]. Considering the reasons mentioned above, Jensen model is selected in this paper.

As it is known, the wake would recover and expand before encountering the other WTs. The wind direction is of particular importance for deciding the distance for wake to recover; in other words, the placement of WTs should consider the wake effect along with the varying wind speed's influence [16]. In order to reduce the wake losses and make the wind farm more cost-efficient, some works have been done on the planning of wind farm by comparing the energy yields from different

layouts using some commercial software as LENA-tool [16] or MaWind [18]. In [19], Patel proposed that the beneficial distance between WTs in prevailing wind direction is 8 rotor diameter (RD) to 12RD, whereas in the direction perpendicular to prevailing wind direction, the distance should be 3RD to 5RD. The placements of WTs are based on this empirical conclusion. In [20], the impact of wind directions on the energy production is studied. The energy yields are calculated by considering the wake effect with varying wind speed; however, the spacing of WT to the neighboring WTs is not in the optimization procedure. In fact, the optimal spacing for WTs is different for various wind farms and even in the same wind farm the optimal spacing for different types of WTs should be different as well. The authors are proposing more advanced method for wake rather than the simple models and we believe that if the spacing of the WTs is obtained as a result of an optimization problem, the annual power production will increase compared to the production of the wind farms whose layouts are designed based on some empirical methods.

In order to get the solution, some evolutionary algorithms are also widely used. In [21] and [22], the layouts are found by GA and the results are also compared with those obtained in commercial software WindFarmer as well as in the work of Moseetti *et al.* in [21] while net present value (NPV) is adopted to evaluate the cost variables in the wind farm and the foundation cost model is proposed that is suitable for wind farm optimization [14]. The optimized locations of WTs and the most economical way to lay the cables within the wind farm are presented in [23], in which the wind direction is considered from northeast–southwest. The optimized layout is found at the maximum energy yields efficiency with given number of WTs and five times the diameter of WTs' blade's spacing between the WTs in a row and the same distance between the rows. In [24], a developed algorithm, binary PSO, is presented, which is more efficient to fulfill the same target compared with GA. As indicated in [25], evolutionary algorithms such as GA and PSO have a good performance of finding the near optimal solution for the constrained nonlinear optimization problem. In this project, the PSO algorithm is adopted to implement the simulation since it has higher computation efficiency in solving nonlinear problems with continuous design variables compared to GA [26]. In [27]–[29], the PSO algorithm was adopted to find the near optimal WT positions.

In this paper, there are two main contributions: one is setting up a new wake model based on Jensen model, which considers both varying wind velocity and direction for calculating the wind speed at each WT within the offshore wind farm. The other is to find the optimized distances between WTs in a line and distances between each WT row with minimal LPC. The power losses as well as the wake deficit are considered, so that the optimized layout can be found. Since the problem is nonlinear, the heuristic algorithm (PSO) is adopted to get these optimized distances. The parameters such as the size of particle and iteration times are carefully designed to get the near optimal result while saving the computation time. The FINO3 reference wind farm with 800-MW capacity is chosen to demonstrate the effectiveness of the new method.

This paper is organized as follows. The analytical equations for calculating the wake velocity with varying wind speed are proposed in Section II. The objective function, which is based on the LPC, is specified in Section III. The theory of nonlinearly inertia weight PSO and the optimization framework are discussed in Section IV. The simulation results and analysis are presented in Section V and conclusion is given in Section VI.

## II. WIND FARM MODEL

First, a comprehensive model is set up. Both the wake effect impact from all upstream WTs as well as the impact of the wind speed variation on wake effect itself is included in this model. Then, the energy yields calculation model is described in this section.

### A. Wake Model

In this paper, the Jensen model is chosen as the baseline to develop a comprehensive wake model. The analytical equations for calculating the wake velocity considering varying wind speed is derived as follows.

1) *Jensen Wake Model*: In Jensen model, the wind speed of the downstream WT is formulated as [30], [31]

$$V_x = V_0 - V_0 \left(1 - \sqrt{1 - C_t}\right) \left(\frac{R_0}{R_x}\right)^2 \left(\frac{S_{\text{overlap}}}{S_0}\right) \quad (1)$$

$$R_x = R_0 + kx \quad (2)$$

where  $C_t$  is the thrust coefficient of the WT and  $k$  is the wake decay constant. The recommended value of  $k$  is 0.04 for offshore environment [32].

2) *Wake Combination*: In a large wind farm, the downstream WT would be affected by several upstream WTs. In order to evaluate wake effects of corresponding turbines, Katic *et al.* proposed a method in which the multiple wakes are calculated using the “sum of squares of velocity deficits.” Hence, the wind velocity at the WT at row  $n$ , column  $m$  can be derived as [16]

$$V_{n,m} = V_0 \left[1 - \sqrt{\sum_{i=1}^{N_{\text{row}}} \sum_{j=1}^{N_{\text{col}}} \left[1 - \left(\frac{V_{ij}}{V_0}\right)\right]^2}\right] \quad (3)$$

3) *Wake Model With Varying Wind Direction*: If the wind direction changes, the WT would change its nacelle so that the normal vector to the rotor plane is aligned with the wind direction. The variation of the wind velocity as well as the direction will both influence the wind speed deficit. This change can be described using a modified model with coordinate system illustrated in Fig. 1. The wind direction is defined as the wind deviation angle to north clockwise.

As can be seen in Fig. 1, the wind can come from four quadrants. In each quadrant, two cases should be considered. The turbine is overlapped with the right half or the left half of the wake plane. The green area is  $S_{\text{overlap},ij}$  and the blue quadrangle area is  $S_{q,ij}$ . The solid line represents the first case and



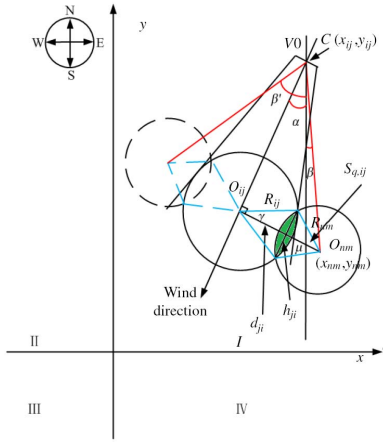


Fig. 1. Wake model with varying wind speed.

the dotted line corresponding to the second case. The derivation process for the analytical equations of condition one can be seen below

$$L_{ij} = \sqrt{(x_{ij} - x_{nm})^2 + (y_{ij} - y_{nm})^2} \quad (4)$$

$$d_{ji} = L_{ji} |\sin(\alpha + \beta)| \quad (5)$$

$$R_{ij} = R_0 + kL_{ji} |\cos(\alpha + \beta)| \quad (6)$$

$$\mu = 2\cos^{-1} \frac{R_{nm}^2 + d_{ji}^2 - R_{ij}^2}{2 * R_{nm} * d_{ji}} \quad (7)$$

$$\gamma = 2\cos^{-1} \frac{R_{ij}^2 + d_{ji}^2 - R_{nm}^2}{2 * R_{ij} * d_{ji}} \quad (8)$$

$$h_{ji} = 2R_i |\sin(\mu/2)| \quad (9)$$

$$S_r = \pi R_{nm}^2 \quad (10)$$

$$S_{ij} = \frac{\gamma(R_{ij})^2}{2} \quad (11)$$

$$S_{nm} = \frac{\mu R_{nm}^2}{2} \quad (12)$$

$$S_{q,ij} = h_{ji}d_{ji} \quad (13)$$

$$S_{\text{overlap},ij} = S_{ij} + S_{nm} - S_q. \quad (14)$$

Combining (2) to (14), the wind velocity at the downstream WT at row  $n$ , column  $m$  with wind speed  $V_0$  and wind angle  $\alpha$  in quadrant (I) can be rewritten as

$$V_{n,m} = V_0 \left\{ 1 - \sqrt{\sum_{i=1}^{N_{\text{row}}} \sum_{j=1}^{N_{\text{col}}} \left\{ 1 - \left[ \left( \frac{V_{ij}}{V_0} \right) \left( \frac{S_{\text{overlap},ij}}{S_r} \right) \right]^2 \right\}} \right\}. \quad (15)$$

If the WT is in the dotted line circle location, i.e., the second condition, then the analytical equations should be modified by substituting the  $(\alpha + \beta)$  term in (5) and (6) with  $(\beta' - \alpha)$  while keeping all the other parts the same.

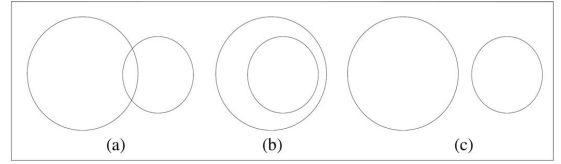


Fig. 2. (a) Partial wake effect. (b) Full wake effect. (c) Nonwake effect.

TABLE I  
WAKE EFFECT REGION JUDGMENT FOR WAKE MODEL WITH VARYING WIND DIRECTION

Case	Condition	Analytical equations
(a)	$R_j - R_i < d_{ji} < R_j + R_i$	(4)–(15)
(b)	$0 \leq d_{ji} \leq R_j - R_i$	(1)–(3)
(c)	$d_{ji} \geq R_j + R_i$	$V_j = V_0$

4) *Wake Effect Region Judgment*: There are three cases that should be considered in the wake velocity calculation, i.e., full wake effect, partial wake effect, and nonwake effect as illustrated in Fig. 2.

The judgment process can be summarized in Table I as follows.

### B. Energy Model

The energy yields calculation concerns three elements: 1) the power production; 2) the power losses; and 3) the duration. The analytical equations for calculating energy production are derived step by step in the following.

1) *Power Production*: The power produced by WT at row  $i$ , column  $j$  can be calculated using the following equation [33], [34]:

$$P_{m,ij} = 0.5\rho C_{p,\text{opt}}(\beta'', \lambda_{\text{opt}})\pi R^2 v^3 / 10^6. \quad (16)$$

In the simulation, the power production of each WT is found by assuming a maximum power point tracking (MPPT) control strategy, so (16) is valid when the wind speed is between cut-in wind speed and rated wind speed [35]. The relationship between wind speed and power output  $C_p$  and  $C_t$  is listed as a look-up table in [36]. Therefore, the total power production generated by the WTs can be written as

$$P_{\text{tot}} = \sum_{j=1}^{N_{\text{col}}} \sum_{i=1}^{N_{\text{row}}} P_{m,ij}. \quad (17)$$

2) *Power Losses and Energy Yields*: The power losses of ac cable can be expressed as

$$P_{\text{loss},i} = 3I_{R,i}^2 R_{e,i} \quad (18)$$

where

$$R_{e,i} = \rho_{R,i} \frac{l_{R,i}}{S_{R,i}}. \quad (19)$$

The length of the cable is related to the distance between WTs. As can be seen in Fig. 3, the cable connection layout

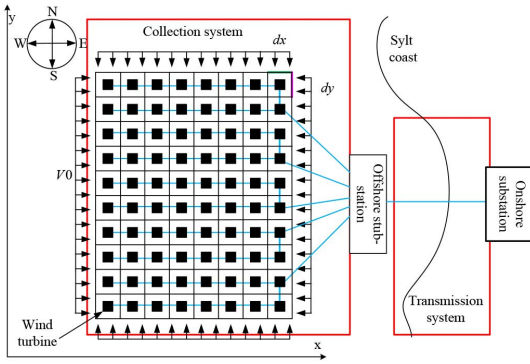


Fig. 3. Proposed wind farm layout for simulation.

is illustrated with blue lines. Hence, if the WTs are placed in a large interval, the energy yields will be increased; however, longer cables are required. Then, the total losses within the wind farm should be written as

$$P_{\text{tol,loss}} = \sum_{i=1}^N P_{\text{loss},i}. \quad (20)$$

Considering (16)–(20), the energy yields of the wind farm can be formulated as

$$E_{\text{tol,av}} = \sum_{t=1}^{T_E} (P_{\text{tot},t} - P_{\text{tol,loss},t}) T_t \quad (21)$$

### III. PROBLEM FORMULATION

The investment for an offshore wind farm is large in which the electrical system takes a high proportion. It is beneficial to maximize the energy production while investing as little as possible. The mathematical model is built to evaluate how to optimize the layout of the wind farm and the assumptions are described at the end of this section.

#### A. Levelized Production Cost

In this simulation, the objective function is constructed using LPC index which considers the capital investment, operating, and maintenance discounted costs during the life-cycle. The mathematical equations for LPC regarding offshore wind farm are formulated in [37]. In this project, the capital cost is calculated by the total cable cost using the model proposed in [38]

$$C_i = A_p + B_p \exp\left(\frac{C_p S_{n,i}}{10^8}\right)^2 \quad (22)$$

$$S_{n,i} = \sqrt{3} I_{i,\text{rated}} U_{i,\text{rated}} \quad (23)$$

$$CAP_t = \sum_i^N C_i L_i Q_i \quad (24)$$

$$C_0 = \sum_{t=1}^{N_y} CAP_t (1+r)^{-t} \quad (25)$$

$$LPC = \left[ \frac{C_0 r (1+r)^{N_y}}{(1+r)^{N_y} - 1} + OAM_t \right] \frac{1}{E_{\text{tol,av}}}. \quad (26)$$

As it can be seen from above equations, LPC is determined by two parts: 1) total discounted costs; and 2) the total discounted energy output. The total investment  $C_0$  is assumed to be made in the first year and paid off during the lifetime of the wind farm. The generated energy  $E_{\text{tol,av}}$  is the average energy yield per year.

#### B. Objective Function

The wind farm could be divided into a grid of the areas in the center of which a WT is placed. The wind farm layout is assumed to be designed as in Fig. 3.

In Fig. 3, each solid square represents a WT. The blue lines represent the cable connection. The problem can be expressed as

$$\text{Obj: } \min \{LPC(d_x, d_y)\} = \min$$

$$\left\{ \left[ \frac{C_0 (d_x, d_y) r (1+r)^{N_y}}{(1+r)^{N_y} - 1} + OAM \right] \frac{1}{E_{\text{tol,av}}(d_x, d_y)} \right\} \quad (27)$$

$$\text{Constraint: } 8R \leq d_x \leq 40R, 8R \leq d_y \leq 40R. \quad (28)$$

$C_0$  should be related to the types as well as the length of each cable, so its value is related to  $d_x$  and  $d_y$  of the wind farm,  $E_{\text{tol}}$  will be related to the wake effect as described in Section I and wind speed deficit is highly dependent on  $d_x$  and  $d_y$ , so that the changing of optimization variable  $d_x$  and  $d_y$  will induce the changing of  $E_{\text{tol}}$ .

#### C. Assumptions and Constraints

In this simulation, some assumptions are made as follows.

- 1) The reference wind farm is assumed to be a regular-shaped wind farm with a rectangle or square shape.
- 2) All cables in the collection system are assumed to be 3-core cross-linked polyethylene (XLPE) ac cable; the cables' length is selected according to the geometrical distance without considering detailed practical situations, such as the barriers, restriction in sea, and the length from WT foundation to sea bottom. The HVDC light cable is adopted for transmitting power from offshore substation to onshore substation because of the long distance.
- 3) When the wind direction changes, the WT's nacelle will change its position as well; however, the yaw speed cannot follow the wind direction changing speed. That is the so-called yaw misalignment [39]. In this project, the yaw misalignment impacts on the final energy yields are neglected.
- 4) As mentioned in Section II, there should be a trade-off which concerns the energy output as well as the



cable investment. However, the costs of the other components within the wind farm are not highly related to this distance. In this simulation, only the costs and losses of cables are considered.

- 5)  $d_x$  and  $d_y$  is restricted in the range of  $8R_0$  to  $-40R_0$ , as the lifetime of the turbine will decrease a lot due to turbulence if they are closer than  $8R_0$  [14].

#### IV. WFLO METHOD

A numerical solution is needed to help the construction of the optimized layout. In this paper, PSO method is adopted as the optimization method. The theory and the optimization procedure are presented in the following.

##### A. Particle Swarm Optimization

Based on the social behavior of fish schooling and bird flocking, Kennedy and Eberhart [40] proposed an evolutionary algorithm, which has a good performance of solving nonlinear optimization problem. In PSO, each possible solution is defined as a particle. The searching space is called particle size and the particle position is updated by giving each particle with a predefined speed. Then, all the particles will tend to move to their best positions, which are the local optimal solutions. The updating process will not be terminated until it reaches the maximum iteration or an acceptable value. The final value should be stabilized after a number of iterations. Then, this best value that is found by PSO is called the global optimal solution. The algorithm can be expressed in following equations [41]:

$$v_i^{k+1} = wv_i^k + l_1 \text{rand}_1 \left( \text{local}_i^k - x_i^k \right) + l_2 \text{rand}_2 \left( \text{global}^k - x_i^k \right) \quad (29)$$

$$x_i^{k+1} = x_i^k + v_i^{k+1} \quad (30)$$

where  $w$  is the inertia weight and  $\text{rand}$  is a function that can generate a random number which is in the range of  $[0,1]$ . A larger  $w$  means the algorithm has a stronger global searching ability while smaller  $w$  ensures the local searching ability. The parameter control methods for  $w$  can be concluded into two categories [42]: 1) the time-varying control strategy [43]–[46]; and 2) adaptive parameter control strategy [47]. The first strategy indicates that the PSO performance can be improved using linear, nonlinear, or fuzzy adaptive inertia weight, whereas the other introduce evolutionary state estimation (ESE) technique [48] to further improve the performance of PSO. In this project, the nonlinear inertia weight [49] control method is adopted since the optimization variables are only the distances between each WT row and column. The time-varying control strategy could find the optima when the problem is not so complex [43]. The expression of nonlinear inertia weight is as follows:

$$w = w_{\text{final}} + (w_{\text{initial}} - w_{\text{final}}) \left( \frac{I_{\text{max}} - t}{I_{\text{max}}} \right)^n \quad (31)$$

where  $t$  is the current iteration number and  $l_{\text{max}}$  is the maximum iteration.

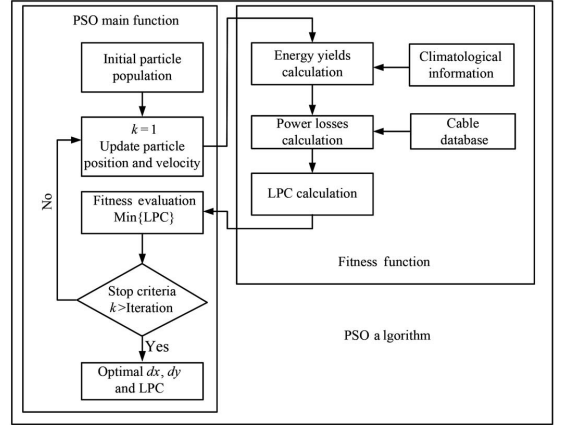


Fig. 4. Optimization procedure of finding optimized wind farm layout.

##### B. WFLO by PSO

As proposed above, the LPC index is used to evaluate the wind farm layout. The simulation procedure to access the wind farm layout by PSO is shown in Fig. 4. The parameters of PSO are initialized in the first step. The LPC will be calculated by a random generated particle position  $d_x$  and  $d_y$ . Then, the position will be updated to find the minimum LPC. The LPC is calculated in a fitness function. The function will be run when a new position is loaded. The above-mentioned procedure would not stop the PSO main function until it is run beyond the maximum iteration time. Finally, the optimized  $d_x$  and  $d_y$  will be selected which generated the minimum LPC.

1) *Climatological Information*: The data are obtained from the work of Norwegian Meteorological Institute [49], in which the wind speeds are sampled per 3 h. For the convenience of calculation, the raw data are formulated into wind rose, which is used for the energy production calculation of a year.

2) *Cable Database*: In [51], various voltage levels' cables with different conducting sectional areas could be found. In this simulation, the cables in the wind farm are 500 or 630 mm<sup>2</sup> XLPE-Cu HVAC cables operated at 66 kV nominal voltage for the collection system and 1000 mm<sup>2</sup> Cu 300 kV HVDC light cable [52] is selected for the transmission system.

#### V. CASE STUDY

In this section, a reference wind farm is first introduced and then four study cases are presented. The relations between parameters of PSO and the final results are also discussed to assure the accuracy of the algorithm in this section.

##### A. FINO3 Reference Wind Farm

The reference wind farm is located in vicinity of FINO3—80 km west of German island of Sylt. The installed capacity of the wind farm is 800 MW [53], [54].



Fig. 5. FINO3 reference wind farm siting.

TABLE II  
DTU 10-MW WT SPECIFICATION [36]

Parameter	10 MW DTU wind turbine
Cut-in wind speed	4 m/s
Rated wind speed	11.4 m/s
Cut-out wind speed	25 m/s
Rotor diameter	178.3 m
Rated power	10 MW

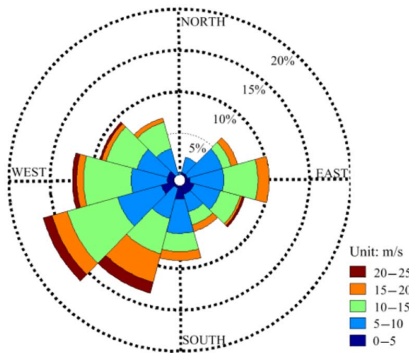


Fig. 6. Wind rose for wind climate in the vicinity of FINO3.

The site of the reference wind farm can be seen in Fig. 5. The wind farm is assumed to be with a rectangular shape with 8 rows and 10 columns layout.

In this simulation, the 10 MW DTU WT is adopted as the reference WT, the specification of which is listed in Table II and the wind velocity and direction is shown as a wind rose in Fig. 6 which is the climatological information as described in Section IV.

The power production of a wind farm can be estimated using probabilistic models such as Weibull distribution function for a number of wind speed ranges, which is a stochastic approach,

TABLE III  
SAMPLE DATASHEET

Sample	Wind direction (°)	Wind velocity (m/s)	X (m)	Y (m)
(a)	0	12	800	1000
(b)	45			
(c)	90			
(d)	135			

whereas in this paper, the wind rose is adopted to calculate the wind farm energy yields during optimization process.

Based on the measured wind data in the vicinity of FINO3, the wind rose is generated by dividing the wind direction into 12 sections with  $30^\circ$  per section. Furthermore, in each section, the wind velocity is divided into five ranges with each interval of 5 m/s. So the used wind rose likes the Weibull distribution with a number of wind speed ranges, plus wind direction. Consequently, the uncertainties have been considered. The approach could be able to give more detailed results than Weibull distribution, since it may have a probabilistic distribution model in each direction if more data available.

### B. Wake Effect Calculation

Four samples, which is the wind from northeast, north, east, and southwest, are selected from wind datasheet to validate the effectiveness of the new wake model. The information of the input parameters is listed in Table III.

The wind speed distributions at WTs considering the wake effect are illustrated in Fig. 7.  $X$  and  $Y$  indicate the spacing of WTs between rows and columns, respectively. The wind distribution is changed with the wind velocity and direction, which is corresponding to the expected results, i.e., the wake effect will incur the reduction of the wind velocity at the downstream WTs.

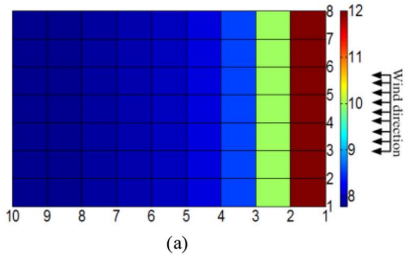
### C. Case Study

1) *Case 1: Optimized Layout for Constant  $d_x$  and  $d_y$ :* The relations of the iteration and results (fitness value) are studied and shown in Fig. 8.

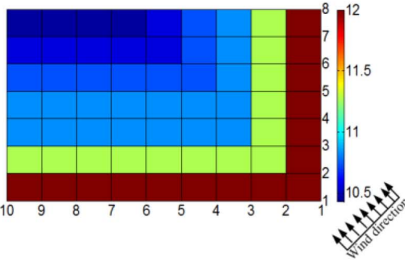
The optimized length and width of the FINO3 reference wind farm are found by PSO. The energy yields and total cable costs for this layout is calculated and listed in Table IV.

The wake losses percentage is 19.53% in this case, which demonstrates the necessity of considering the wake effect in energy yields calculation. The optimized layout for this case should be  $d_x$  equal to 713.2 m while  $d_y$  is 981.82 m. The results correspond to the fact that in vicinity of FINO3, the prevailing wind is from southwest, which has been shown in Fig. 6(b). The increase in  $d_y$  means to increase the width of the wind farm from north to south by which the energy yields will be increased. Moreover, the number of cables laying on that direction is less than those in  $x$  direction. As a consequence,  $d_x$  is relatively smaller than  $d_y$ .

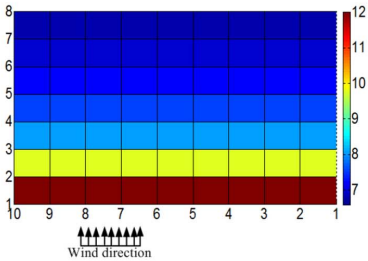
2) *Case 2: Optimized Sparse Layout:* In this case, the spacing between WTs in a row and the spacing between each WT column in reference FINO3 wind farm is assumed to be



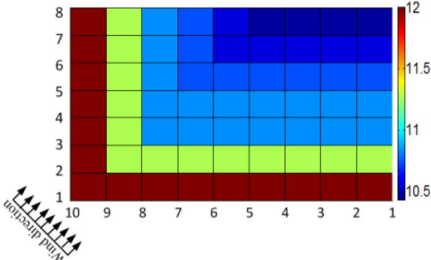
(a)



(b)



(c)



(d)

Fig. 7. Wind speed distribution of wind farm considering wake effect. (a) Wind speed distribution considering wind effect when wind direction is 0°. (b) Wind speed distribution considering wind effect when wind direction is 45°. (c) Wind speed distribution considering wind effect when wind direction is 90°. (d) Wind speed distribution considering wind effect when wind direction is 135°.

different. In other words, the optimization variable will be changed as

$$d_x = [d_{x,1}, \dots, d_{x,i}], i \in [1, N\_row - 1]$$

$$d_y = [d_{y,1}, \dots, d_{y,j}], j \in [1, N\_col - 1]$$

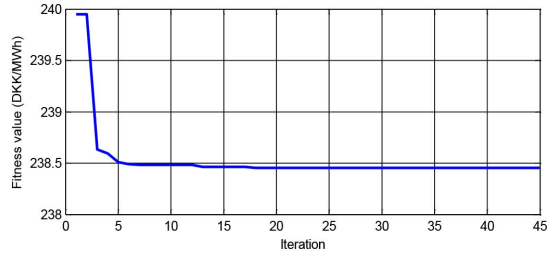


Fig. 8. Fitness value corresponding to each iteration for constant  $d_x$  and  $d_y$  layout.

TABLE IV  
LAYOUT RESULTS FOR CONSTANT  $D_x$  AND  $D_y$

Duration	365 days
$d_x$ (m)	713.2
$d_y$ (m)	981.82
LPC (DKK/MWh)	238.4549
Annual cable power losses (GWh)	45.28
Annual energy yields (GWh)	3556.46
Cable cost (MDKK)	837.01
Annual energy yields without considering wake effect (GWh)	4419.36
Wake losses percentage (%)	19.53
Iteration	45

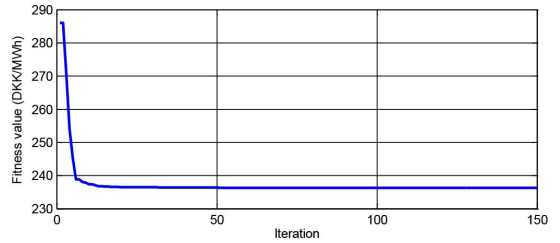


Fig. 9. Fitness value corresponding to each iteration for optimized sparse layout.

where  $N\_row$  is the total number of rows and  $N\_col$  is the total number of columns. The relations of the iteration and results are shown in Fig. 9 and the results of optimized sparse layout are listed in Table V.

For the optimized sparse layout, the wake losses decreased to 17.68%; however, the power losses and the investment on cables are both increased.

The results are also compared with a regular wind farm layout with 7 rotor diameter (7RD) distance (1248.1 m) between two WTs and 7RD spacing for rows which is concluded in Table VI.

As can be seen in Table VI, the cable costs and power losses is reduced by sparse layout and further reduced by constant  $d_x$  and  $d_y$  layout. The energy yields of optimized layout for constant  $d_x$  and  $d_y$  is minimal while minimal LPC is obtained by optimized sparse layout. The 7RD layout has the largest energy yields and occupies the largest sea area, while optimized layout with  $d_x$  and  $d_y$  is converse. The proposed method is succeeded

TABLE V  
LAYOUT RESULTS FOR OPTIMIZED SPARSE LAYOUT

Duration	365 days
$d_{x,i}$ (m)	713.2
$d_{y,j}$ (m)	1750.66
	1945.90
	713.20
	1004.81
	713.20
	1700.96
	713.20
	1954.65
	1950.83
LPC (DKK/MWh)	236.3054
Annual cable power losses (GWh)	46.80
Annual energy yields (GWh)	3637.96
Cable cost (MDKK)	848.36
Annual energy yields without Considering wake effect (GWh)	4419.36
Wake losses percentage (%)	17.68
Iteration	150

TABLE VI  
LAYOUT COMPARISONS OF TWO OPTIMIZED LAYOUTS

Name	Optimized layout for constant $d_x$ and $d_y$	Optimized sparse layout	7RD layout
Annual cable power losses (GWh)	45.28	46.80	51.71
Annual energy yields (GWh)	3556.46	3637.96	3839.94
Cable cost (MDKK)	837.01	848.36	959.41
LPC (DKK/MWh)	238.4549	236.3054	253.3376
Layout (km <sup>2</sup> )	4.99km × 8.84km = 44.11	4.99km × 12.45km = 62.13	8.73km × 11.23 km = 98.04

in finding optimized layouts, which improves the LPC with 5.87% for constant  $d_x$  and  $d_y$  layout, while optimized sparse layout reduces the LPC with 6.72% comparing with 7RD layout; however, the optimized layout with constant  $d_x$  and  $d_y$  saves 55% area occupation, while optimized sparse layout only saves 36.63%. The best layout in the simulation should be optimized sparse layout, whereas in practical, the optimized layout for constant  $d_x$  and  $d_y$  maybe drawn more attention since the less area occupation means less installation cost.

## VI. CONCLUSION

The wind flow within a wind farm would be disturbed by the wake effect. This incurs the reduction of energy production. In large-scale wind farms, the wake losses that depend on the spacing of the WTs are obvious. In this paper, the wake model for calculating the wake losses has been developed. The effectiveness of the model was well demonstrated by a study case. The results show that the proposed model can be used for wake losses calculation with varying wind direction and velocity. The optimized layouts are found using PSO algorithm. From comparison, it can be concluded that the proposed method may be used for the regular-shaped wind farm layout design.

The method proposed in this paper is under the assumption that the wind farm is under MPPT control strategy all the time. If the wind farm is under power regulation mode, then the problem may become a reserve dispatch issue, which may be considered in future work. Actually, the offshore wind farms are mostly running in MPPT, due to being expensive to run in regulation.

This paper focused on the regular-shaped wind farm layout optimization which should be rectangular or square shape. All other shaped wind farm layouts are classified into irregular shaped wind farm. In the future, the optimization of irregular shaped wind farm layout considering wake effect will be addressed. In that case, other optimization variables such as the locations of each WT within the wind farm instead of the spacing between each pair of WTs would be introduced. In order to place the WTs optimally, binary PSO will be adopted to decide the suitable locations to arrange the WTs. The robustness of PSO will be illustrated for this type of study. Since the energy yields calculation of irregular-shaped wind farm layout is more complex compared with regular shaped wind farm layout, the optimization process will be more time-consuming.

## REFERENCES

- [1] global wind energy council, *Global Wind Report*, 2014 [Online]. Available: <http://www.gwec.net/>
- [2] K. Veeramachaneni, M. Wagner, U.-M. O'Reilly, and F. Neumann, "Optimizing energy output and layout costs for large wind farms using particle swarm optimization," in *Proc. IEEE Congr. Evol. Comput. (CEC)*, Jun. 2012, pp. 1–7.
- [3] M. Zhao, Z. Chen, and F. Blaabjerg, "Optimization of electrical system for offshore wind farm via genetic algorithm," *IET Renew. Power Gener.*, vol. 3, no. 2, pp. 205–216, Jun. 2009.
- [4] M. B. Nandigam and S. K. Dhali, "Optimal design of an offshore wind farm layout," in *Proc. Int. Symp. Power Electron. Electr. Drives Autom. Motion (SPEEDAM'08)*, Jun. 2008, pp. 1470–1474.
- [5] Y. Ma, H. Yang, X. Zhou, and L. Ji, "The dynamic modeling of wind farms considering wake effects and its optimal distribution," in *Proc. World Non-Grid-Connected Wind Power Energy Conf. (WNWEC'09)*, Nanjing, China, Sep. 2009, pp. 1–4.
- [6] A. Tahavorgar and J. E. Quaiocoe, "Estimation of wake effect in wind farms using design of experiment methodology," in *Proc. IEEE Energy Convers. Congr. Expo. (ECCE)*, Sep. 2013, pp. 3317–3324.
- [7] WindPRO/PARK, "Introduction wind turbine wake modelling and wake generated turbulence," EMD Int. A/S, Aalborg, Denmark, 2005.
- [8] G. C. Larsen, J. Højstrup, and H. A. Madsen, "Wind fields in wakes," in *Proc. Eur. Union Wind Energy Conf. (EUWEC'96)*, Gothenburg, Sweden, 1996, pp. 764–768.
- [9] S. Frandsen *et al.*, "Analytical modelling of wind speed deficit in large offshore wind farms," in *Proc. Wind Energy*, Jan. 2006, pp. 39–53.
- [10] S. Frandsen *et al.*, "The necessary distance between large wind farms offshore—Study," Risø National Laboratory, Roskilde, Denmark, Tech. Rep. Risø-R-1518(EN), 2005, 29 p.
- [11] Y.-K. Wu, C.-Y. Lee, C.-R. Chen, K.-W. Hsu, and H.-T. Tseng, "Optimization of the wind turbine layout and transmission system planning for a large-scale offshore wind farm by AI technology," in *Proc. IEEE Ind. Appl. Soc. Annu. Meeting (IAS)*, Oct. 7–11, 2012, pp. 1–9.
- [12] A. Kusiak and H. Zheng, "Optimization of wind turbine energy and power factor with an evolutionary computation algorithm," *Renew. Energy*, vol. 35, pp. 685–694, Mar. 2010.
- [13] Y. Eroğlu and S. U. Seçkiner, "Design of wind farm layout using ant colony algorithm," *Renew. Energy*, vol. 44, pp. 53–62, Aug. 2012.
- [14] B. Pérez, R. Minguez, and R. Guanche, "Offshore wind farm layout optimization using mathematical programming techniques," *Renew. Energy*, vol. 53, pp. 389–399, May 2013.
- [15] S. Pookpant and W. Ongsakul, "Optimal placement of wind turbines within wind farm using binary particle swarm optimization with time-varying acceleration coefficients," *Renew. Energy*, vol. 55, pp. 266–276, Jul. 2013.

[16] F. Portáe-Agel, Y.-T. Wu, and C.-H. Chen, "A numerical study of the effects of wind direction on turbine wakes and power losses in a large wind farm," *Energies*, vol. 6, pp. 5297–5313, 2013.

[17] K. Rudion, Z. A. Styczynski, A. Orths, and O. Ruhle, "MaWind - Tool for the aggregation of wind farm models," in *Proc. IEEE Power Energy Soc. Gen. Meeting Convers. Del. Electr. Energy 21st Century*, Pittsburgh, PA, USA, Jul. 2008, pp. 1–8.

[18] N. Moskalenko, K. Rudion, and A. Orths, "Study of wake effects for offshore wind farm planning," in *Proc. Int. Symp. Mod. Electr. Power Syst. (MEPS)*, Wroclaw, Poland, Sep. 2010, pp. 1–7.

[19] M. R. Patel, *Wind and Solar Power Systems*. Boca Raton, FL, USA: CRC Press, 1999.

[20] N. P. Prabhu, P. Yadav, B. Prasad, and S. K. Panda, "Optimal placement of off-shore wind turbines and subsequent micro-siting using Intelligently Tuned Harmony Search algorithm," in *Proc. IEEE Power Energy Soc. Gen. Meeting (PES)*, Vancouver, BC, Canada, Jul. 2013, pp. 1–7.

[21] T. G. do Couto, B. Farias, A. C. G. C. Diniz, and M. V. G. de Moraes, "Optimization of wind farm layout using genetic algorithm," in *Proc. 10th World Congr. Struct. Multi. Optim.*, Orlando, FL, USA, May 2013.

[22] J. Serrano Gonzalez, M. Burgos Payan, and J. M. Riquelme Santos, "An improved evolutionary algorithm for large offshore wind farm optimum turbines layout," in *Proc. IEEE Trondheim PowerTech*, Trondheim, Norway, Jun. 2011, pp. 1–6.

[23] Y. Wu, C. Lee, C. Chen, K. Hsu, and H. Tseng, "Optimization of the wind turbine layout and transmission system planning for a large-scale offshore wind farm by AI technology," *IEEE Trans. Ind. Appl.*, vol. 50, no. 3, pp. 2071–2080, Sep. 24, 2013.

[24] M. A. Khanesar, M. Teshnehlab, and M. A. Shoorehdeli, "A novel binary particle swarm optimization," in *Proc. Mediterr. Conf. Control Autom.*, Athens, Greece, Jun. 27–29, 2007, pp. 1–6.

[25] P. Y. Zhang, "Topics in wind farm layout optimization: Analytical wake models, noise propagation, and energy production," M.S. Thesis, Univ. Toronto, Toronto, ON, Canada, Jul. 17, 2013.

[26] R. Hassan, B. Cohanin, and O. de Weck, "A comparison of particle swarm optimization and the genetic algorithm," in *Proc. 46th AIAA/ASME/ASCE/AHS/ASC Struct. Struct. Dyn. Mater. Conf.*, 2005.

[27] R. Rahmani, A. Khairuddin, S. M. Cherati, and H. A. M. Pesaran, "A novel method for optimal placing wind turbines in a wind farm using particle swarm optimization (PSO)," in *Proc. Int. Power Electron. Conf. (IPEC)*, Oct. 27–29, 2010, pp. 134–139.

[28] C. Wan, J. Wang, G. Yang, H. Gu, and X. Zhang, "Wind farm micro-siting by Gaussian particle swarm optimization with local search strategy," *Renew. Energy*, vol. 48, pp. 276–286, 2012.

[29] C. Wan, J. Wang, G. Yang, and X. Zhang, "Optimal micro-siting of wind farms by particle swarm optimization," *Adv. Swarm Intell.*, vol. 6145, pp. 198–205, 2010.

[30] N. O. Jensen, "A note on wind generator interaction," Risø National Laboratory, Roskilde, Denmark, Tech. Rep. RISØ-M-2411/1983, p. 5.

[31] F. González-Longatt, P. Wall, and V. Terzija, "Wake effect in wind farm performance: Steady-state and dynamic behavior," *Renew. Energy*, vol. 39, pp. 329–338, Sep. 2011.

[32] P. Beaucauge, M. Brower, N. Robinson, and C. Alonge, "Overview of six commercial and research wake models for large offshore wind farms," in *Proc. Eur. Wind Energy Assoc. (EWEA'12)*, Copenhagen, Denmark, 2012, pp. 95–99.

[33] J. S. González, A. G. Gonzalez Rodriguez, J. C. Morac, J. R. Santosa, and M. B. Payana, "Optimum wind turbines operation for minimizing wake effect losses in offshore wind farms," *Renew. Energy*, vol. 35, no. 8, pp. 1671–1681, Aug. 2010.

[34] P. Flores, A. Tapia, and G. Tapia, "Application of a control algorithm for wind speed prediction and active power generation," *Renew. Energy*, vol. 30, no. 4, pp. 523–536, Apr. 2005.

[35] W. Qiao, "Intelligent mechanical sensorless MPPT control for wind energy systems," in *Proc. IEEE Power Energy Soc. Gen. Meeting*, San Diego, CA, USA, Jul. 2012, pp. 1–8.

[36] C. Bak *et al.*, "Description of the DTU 10 MW reference wind turbine," DTU Wind Energy, Fredericia, Denmark, Jul. 2013.

[37] M. Zhao, "Optimization of electrical system for offshore wind farms via a genetic algorithm approach," Ph.D. Dissertation, Faculty Eng. Sci. Med., Aalborg Univ., Aalborg, Denmark, Oct. 2006.

[38] S. Lundberg, "Performance comparison of wind park configurations," Dep. Electr. Power Eng., Chalmers Univ. Technol., Goteborg, Sweden, Tech. Rep. 30R, Aug. 2003.

[39] J. Choi and M. Shan, "Advancement of Jensen (Park) wake model," in *Proc. Eur. Wind Energy Assoc. (EWEA) Conf.*, Wien, Austria, Feb. 2013, pp. 1–8.

[40] J. Kennedy and R. Eberhart, "Particle swarm optimization," in *Proc. IEEE Int. Conf. Neural Netw.*, Apr. 1995, pp. 1942–1948.

[41] J. Kennedy, "The particle swarm: Social adaptation of knowledge," in *Proc. IEEE Int. Conf. Evol. Comput.*, Indianapolis, IN, USA, 1997, pp. 303–308.

[42] M. Hu, T. Wu, and J. D. Weir, "An adaptive particle swarm optimization with multiple adaptive methods," *IEEE Trans. Evol. Comput.*, vol. 17, no. 5, pp. 705–720, Dec. 10, 2012.

[43] Y. Shi and R. C. Eberhart, "Empirical study of particle swarm optimization," in *Proc. Congr. Evol. Comput.*, 1999, pp. 1950–1955.

[44] B. Jiao, Z. Lian, and X. Gu, "A dynamic inertia weight particle swarm optimization algorithm," *Chaos, Solitons Fractals*, vol. 37, pp. 698–705, Aug. 2008.

[45] Y. Shi and R. C. Eberhart, "Fuzzy adaptive particle swarm optimization," in *Proc. Congr. Evol. Comput.*, 2001, pp. 101–106.

[46] R. C. Eberhart and Y. Shi, "Tracking and optimizing dynamic systems with particle swarms," in *Proc. Congr. Evol. Comput.*, 2001, pp. 94–100.

[47] Z.-H. Zhan, J. Zhang, Y. Li, and H. S.-H. Chung, "Adaptive particle swarm optimization," *IEEE Trans. Syst. Man Cybern. B, Cybern.*, vol. 39, no. 6, pp. 1362–1381, Apr. 2009.

[48] J. Zhang, H. S.-H. Chung, and W.-L. Lo, "Clustering-based adaptive crossover and mutation probabilities for genetic algorithms," *IEEE Trans. Evol. Comput.*, vol. 11, no. 3, pp. 326–335, Jun. 2007.

[49] A. Chatterjee and P. Siarry, "Nonlinear inertia weight variation for dynamic adaptation in particle swarm optimization," *Comput. Oper. Res.*, vol. 33, pp. 859–871, Mar. 2006.

[50] B. R. Furevik and H. Haakenstad, "Near-surface marine wind profiles from rawinsonde and NORA10 hindcast," *J. Geophys. Res.*, vol. 117, Dec. 7, 2012.

[51] *XLPE Submarine Cable Systems Attachment to XLPE Land Cable Systems-User's Guide*. Fredericia, Denmark: ABB Corporation, 2013.

[52] *HVDC Light Cables-Submarine and Land Power Cables*. Fredericia, Denmark: ABB Corporation, 2013.

[53] R&D centre Kiel University of Applied Sciences GmbH, *FINO3—Research Platform in the North Sea and the Baltic No. 3* [Online]. Available: <http://www.fino3.de/en/>

[54] Norwegian Centre for Offshore Wind Energy (NORCOWE). (2014, Sep. 9). *WP2014-Froysa-NRWF NORCOWE Reference Wind Farm* [Online]. Available: <http://www.norcowe.no/>



**Peng Hou** (S'14) received the B.Eng. degree in electrical engineering from Hebei University of Technology, Tianjin, China, in 2008, and the M.Sc. degree in electrical engineering from Chalmers University of Technology, Gothenburg, Sweden, in 2010. He is currently pursuing the Ph.D. degree at the Department of Energy Technology, Aalborg University, Aalborg, Denmark.

His research interests include wind farm layout design and optimization algorithm applications.



**Weihao Hu** (S'06–M'13) received the B.Eng. and M.Sc. degrees in electrical engineering from Xi'an Jiaotong University, Xi'an, China, in 2004 and 2007, respectively, and the Ph.D. degree in energy technology from Aalborg University, Aalborg, Denmark, in 2012.

He is currently an Associate Professor with the Department of Energy Technology, Aalborg University. He is the Vice Program Leader of Wind Power System Research Program, Department of Energy Technology, Aalborg University. He has participated in several national and international research projects and he has more than 50 publications in his technical field. His research interests include wind power generation and intelligent energy systems.





**Mohsen Soltani** (S'05–M'08) received the M.Sc. degree in electrical engineering from Sharif University of Technology and the Ph.D. degree in electrical and electronic engineering from Aalborg University, Aalborg, Denmark, in 2004 and 2008, respectively.

He was a Visiting Researcher at Eindhoven University of Technology, Eindhoven, The Netherlands, in 2007. He fulfilled a Postdoctoral and an Assistant Professor program with Aalborg University in 2008–2012. In 2010, he was granted a Visiting Scholar at Stanford University, Stanford, CA, USA. He is now an Associate Professor with the Department of Energy Technology, Aalborg University. His research interests include modeling, control, estimation, fault detection, and their applications to electromechanical and energy conversion systems, wind turbines, and wind farms.



**Zhe Chen** (M'95–SM'98) received the B.Eng. and M.Sc. degrees in electrical engineering from the Northeast China Institute of Electric Power Engineering, Jilin City, China, in 1982 and 1986, respectively, and the Ph.D. degree in electrical engineering from the University of Durham, Durham, U.K, in 1997.

He is a full Professor with the Department of Energy Technology, Aalborg University, Aalborg, Denmark. He is the Leader of Wind Power System Research Program, Department of Energy Technology, Aalborg University and the Danish Principle Investigator for Wind Energy of Sino-Danish Centre for Education and Research. He has led many research projects and has more than 400 publications in his technical field. His research interests include power systems, power electronics and electric machines, wind energy, and modern power systems.

Dr. Chen is an Editor of the IEEE TRANSACTIONS ON POWER SYSTEMS, an Associate Editor of the IEEE TRANSACTIONS ON POWER ELECTRONICS, a Fellow of the Institution of Engineering and Technology (London, U.K.), and a Chartered Engineer in the U.K.



# Optimization of offshore wind farm layout in restricted zones



Peng Hou, Weihao Hu<sup>\*</sup>, Cong Chen, Mohsen Soltani, Zhe Chen

Department of Energy Technology, Aalborg University, Pontoppidanstraede 111, Aalborg DK-9220, Denmark

## ARTICLE INFO

### Article history:

Received 19 November 2015

Received in revised form

9 July 2016

Accepted 12 July 2016

Available online 22 July 2016

### Index terms:

Offshore wind farm

Layout optimization

Restricted offshore area

Particle swarm optimization

Irregular wind farm layout

## ABSTRACT

In this research, an optimization method for offshore wind farm layout design is proposed. With the purpose of maximizing the energy production of the wind farm, the wind turbine (WT) positions are optimized. Due to the limitations of seabed conditions, marine traffic limitations or shipwrecks, etc., the WTs are expected to be placed outside specific areas. Based on this fact, a restriction zone concept is proposed in this paper and implemented with the penalty function method. In order to find a feasible solution, a recent proposed stochastic algorithm, particle swarm optimization algorithm with multiple adaptive methods (PSO-MAM) is adopted. The simulation results indicate that the proposed method can find a layout which outperforms a baseline layout of a reference wind farm (RWF) by increasing the energy yield by 3.84%.

© 2016 Elsevier Ltd. All rights reserved.

## 1. Introduction

An offshore wind farm (OWF) shows more benefits at higher wind speeds, less turbulence and less impact on residents compared with an onshore wind farm; however, the construction and maintenance cost is high. In order to get a cost-effective wind farm, the layout of the wind farm should be optimized.

The wake effect will cause a wind speed deficit at the downstream wind turbines (WTs). As a result, the energy production of the wind farm will be reduced. Hence, it is necessary to optimize a wind farm layout design which can minimize the wake losses so that the rate of return on investment can be increased. In Ref. [1], Mosetti et al. used a genetic algorithm (GA) to optimize the OWF layout, this is the initial work of OWF layout design. The construction area is partitioned into 100 squares and the WTs can be placed at the center of each square. Later, the authors of [2] improved this method which can get a layout with more power production considering the possibility of installing more WTs in the same area. Many researchers have worked on the wind farm layout optimization problem (WFLOP) and the results have been compared with the above two layouts [3–6]. Reference [3] demonstrated that the Monte Carlo algorithm was outperformed by the GA in finding a higher value of the objective function under

the assumption that the wind direction is constant, while [4] showed the advantages of using an Intelligently Tuned Harmony Search algorithm for WFLOP. In Ref. [5], a binary particle swarm optimization method with time-varying acceleration coefficients (BPSO-TVAC) is proposed and the obtained results are compared with other 5 meta-heuristic algorithms. In Ref. [6], another wake and energy production model was considered to conduct the work and the obtained result was compared with that of the commercial software WindFarmer. Different from previous work, [7] proposed a sequential optimization method which shows better performance in finding a near optimal solution in calculation precision. In Ref. [8], an evolutionary computational approach to optimize the layout for a real offshore wind farm in northern Europe was proposed. Though the final wind farm was irregularly shaped, the WTs inside the wind farm were still placed with an array layout. One year later, the authors in Ref. [9] introduced another heuristic method, coral reefs optimization algorithm, to solve the WFLOP, the simulation results showed that the proposed method outperformed evolutionary approaches, differential evolution and harmony search algorithms in finding a better layout with more power generation. It can be seen that the works mentioned above are focused on solving the WFLOP using meta-heuristic algorithm based on grid partition methods. Since the problem is pre-simplified by partitioning the whole area into grids, some possible solutions have already been neglected.

In order to conquer this drawback, the works [10–18] optimize the WT locations using Cartesian coordinate form which permits the WTs to move within a predefined region freely. This increases

<sup>\*</sup> Corresponding author.

E-mail addresses: [pho@et.aau.dk](mailto:pho@et.aau.dk) (P. Hou), [whu@et.aau.dk](mailto:whu@et.aau.dk) (W. Hu), [cchen12@googlemail.com](mailto:cchen12@googlemail.com) (C. Chen), [sms@et.aau.dk](mailto:sms@et.aau.dk) (M. Soltani), [zch@et.aau.dk](mailto:zch@et.aau.dk) (Z. Chen).

Nomenclature	
$V_0$ [m/s]	input wind speed at the WT
$V_x$ [m/s]	wind speed in the wake at a distance $x$ downstream of the upstream WT
$R_0$ [m]	radius of the WT's rotor
$R_x$ [m]	generated wake radius at $x$ distance along the wind direction
$S_{overlap}$ [m <sup>2</sup> ]	affected wake region
$C_t$	thrust coefficient
$k_d$	decay constant
$\rho$ [kg/m <sup>3</sup> ]	air density,
$C_{p,i}$	power coefficient of WT $i$
$P_{m,i}$ [W]	mechanical power generated by WT $i$
$v_i$ [m/s]	wind speed at WT $i$
$N$	total number of WTs in a wind farm
$P_{tot,t}$ [W]	total power production during interval $t$
$T_E$ [day]	duration interval for energy yields calculation
$T_t$ [h]	duration when the wind farm generating power of $P_{tot,t}$
$E_{tot,av}$ [Wh]	mean energy yields in one year
$t$ [h]	energy yields calculation time
$L$	vector of WT positions
$F$	construction area of wind farm
$E_{tot,av}(L)$ [Wh]	mean energy yields in one year when the wind farm layout is $L$
$x_i, y_i$	coordinate of WT $i$
$x_k, y_k$	coordinate of WT $k$
$d_{min}$	minimal distance between any pair of WT
$R$	index of constraint function
$N$	total number of WTs
$C$	total number of penalty functions that should be used in the problem for unrestricted sea area
$C_1$	total number of penalty function that should be used in the problem for restricted sea area
$R$	restriction zone in $F$
$C_F R$	complementary set of restriction zone, $R$ , in predefined sea area, $F$ .
$\varphi(L_i)$	penalty function for WT $i$
$W$	inertia weight
$l_1, l_2$	learning factors
$r_1, r_2$	stochastic numbers which can generate some random numbers within [0, 1]
$q_i^k, q_i^{k+1}$ [m]	position of $i^{th}$ particle at iteration $k$ and $k+1$ respectively, in other words, the $i^{th}$ solution generated randomly at iteration $k$ and $k+1$ respectively
$v_i^k, v_i^{k+1}$ [m]	speed of $i^{th}$ particle at iteration $k$ and $k+1$ respectively, in other words, the updating step length for the $i^{th}$ solution at iteration $k$ and $k+1$ respectively
$Q_i^k$ [m]	best position found by the $i^{th}$ particle before iteration $k$ , in other words, the best solution obtained in position $i^{th}$ till iteration $k$ which is also called as personal best solution till iteration $k$
$Q_g^k$ [m]	best position found by all particles (the swarm) before iteration $k$ , in other words, the best solution obtained till iteration $k$ which is also called as global best solution till iteration $k$
$Q_i$	best position found so far by the $i^{th}$ particle
$Q_g$	best position found so far by all the particles
$I$	swarm size
$O$	maximum iteration

the freedom of the search space and gives more chances for the meta-heuristic method to find a near optimal solution. In Ref. [10], the wind farm is assumed to have a circular shape. Several wind turbines are placed optimally within this area which is an initial attempt to solve WFLOP based on a coordinate system. Similarly, [11] used colony optimization algorithm to optimize the WT positions, which was demonstrated to be outperformed by Ref. [10] in increasing the wind farm power production which was the objective function in this paper. Furthermore, a particle filtering approach is proposed to solve WFLOP in Ref. [12]. From the comparison, it can be seen that it is an alternative way of optimizing the WFLO compared with evolutionary strategy algorithm [10] and ant colony optimization method [11]. In Ref. [13], the wind farm layout was optimized by seeding an evolutionary algorithm heuristically considering the wind farm orography, while PSO was adopted in Refs. [14, 15] to design the wind farm. In Ref. [14], the WFLOP was solved considering three aspects: the location of each WT, the number of WT as well as the type selection of WT using mixed-discrete PSO while [15] adopted Gaussian PSO with local search strategy to optimize the WT positions. Besides, there were also some attempts to use mathematical programming to solve WFLOP as specified in Refs. [16–18]. In Ref. [16], a random search (RS) algorithm which showed better performance than the heuristic algorithm in computational time is proposed, the RS algorithm was demonstrated by using the Horns Rev I wind farm as the case study. Also, Horns Rev I wind farm layout was selected as the benchmark and compared with the optimized layout obtained by sequential convex programming in Ref. [17]. Since the WFLOP is non-convex, a

global optimal solution cannot be guaranteed. In order to get a near optimal solution, a mathematical programming method was adopted in Ref. [18] that used heuristic methods to set an initial layout then used nonlinear mathematical programming techniques to get a local optimal solution. However, due to the offshore topology limitation, some predefined zone may not be available to install WTs or could be costly for installation in practice. In Ref. [19], the Dogger Bank Reference Wind Farm layout (DRW) was designed by avoiding installing WTs within the highest foundation cost region which resulted a blank area in the wind farm. In Ref. [20], three types of offshore wind farm configurations in Hong Kong (aligned, staggered, scattered) were investigated using GA. The simulation results showed that the scattered layout was the best choice in terms of levelised cost of energy (LCOE). The works mentioned above are concentrated on the WFLOP within a predefined area without considering the impact of the restriction area to the design of the WFLO. Though the WTs were placed away from the higher cost foundation zone in Ref. [19], the wind turbine locations are chosen manually. Thus, it is still possible to increase the energy yields of the wind farm layout in Ref. [19] by adopting optimization methods.

The LCOE is the most interesting parameter in many cases, while in this paper we try to address the problem of layout optimization for harvesting total energy production under the assumption that the size and number of turbines are given. The contributions of this paper are twofold: 1) WFLOP is solved by taking the offshore restricted area into consideration. 2) PSO with multiple adaptive methods (PSO-MAM), is arranged to solve the WFLOP. The



NORCOWE reference wind farm with 800 MW capacities is chosen to demonstrate the effectiveness of the new method.

The paper is organized as follows. In Section 1, the wind farm models are first proposed. The models of problem and constraints are explained in Section 2. The theory of PSO-MAM is discussed in Section 3. The simulation results and analysis are presented in Section 4, and conclusions are given in Section 5.

## 2. Modeling of wind farm

The wind speed deficit can be explained as the shadow impact of the upstream WTs to the downstream ones, i.e., the wind speed, reached at the downstream WTs, will be reduced. In order to maximize the energy yields of the whole wind farm, the wake losses should be accurately estimated. The analytical equations for wind speed calculation considering wake effect is presented first in this section. Based on it, the energy yields of the wind farm can be obtained assuming a maximum power point tracking (MPPT) control strategy.

### 2.1. Wake model

Currently, there are three models widely used in estimating the wind farm wake losses, known as N. O. Jensen wake model, Ainslie wake model and G.C. Larsen wake model [21] while Jensen wake model was selected as the wake model for the wind farm layout optimization problem (WFLOP) in most of the layout design works ([1–18]) for the sake of saving computational time and reducing prediction errors [18]. Hence, the Jensen model is selected to model the wind speed deficit. The analytical equations for calculating the wake velocity are as follows [22].

$$V_x = V_0 - V_0 \left(1 - \sqrt{1 - C_t}\right) \left(\frac{R_0}{R_x}\right)^2 \left(\frac{S_{overlap}}{S_0}\right) \quad (1)$$

$$R_x = R_0 + kx \quad (2)$$

The decay constant,  $k$ , describes the feature of the wake expansion rate, the recommended value for an offshore environment is 0.04 [22]. Due to the wake effect, the upstream WT can cause the wind speed reduction of several downstream WTs' and the wind speed at one downstream WT can be affected by several upstream WTs as well. In order to calculate the wake losses of the wind farm, Katic et al. proposed a method in which the multiple wakes are calculated by using the 'sum of squares of velocity deficits'. The analytical equation is as follows [23]:

$$V_n = V_0 \left[1 - \sqrt{\sum_{i=1}^N \left[\left(\frac{V_i}{V_0}\right)^2}\right]}\right] \quad (3)$$

The energy yield calculation considering variation of both wind velocity and wind direction has been done in a previous work. The detailed modeling can be seen in Ref. [24].

### 2.2. Energy production of offshore wind farm

In Ref. [25], the power extracted by each individual WT is given as:

$$P_{m,i} = 0.5\rho C_{p,i} \pi R^2 v_i^3 \quad (4)$$

By MPPT control strategy, the power production of each WT can be found by (4) [26]. The relationship between the wind speed and the power output,  $C_p$  is listed as a lookup table in Ref. [27]. The velocity at each WT is related to the OWF layout or the WTs'

positions ( $L$ ). Hence, the total power production that is generated by the WTs can be written as:

$$P_{tot} = \sum_{i=1}^N P_{m,i}(L_i) \quad (5)$$

Considering (1)–(5), the energy yields of the wind farm can be rewritten as:

$$E_{tot,av} = \frac{\sum_{t=1}^{T_E} (P_{tot,t}) T_t}{T_t T_E} 8760 \quad (6)$$

### 2.3. Objective functions and constraints

The purpose of this work is to maximize the energy yields of the wind farm by optimizing the positions of WTs. Two optimization problems which correspond to the unrestricted and restricted sea area problems are specified mathematically below.

#### 2.3.1. Model of problem for unrestricted sea area

The WTs are required to be placed within a predefined sea area,  $F$ , using an optimized strategy so that the energy yields can be maximized. Besides, the distance between any two WTs within the wind farm should also be constrained. By considering the above reasons, the objective function can be set up as:

$$\text{Objective: } \max(E_{tot,av}(L))$$

Subject to:

$$F_r(L_i) = \sqrt{(x_i - x_k)^2 + (y_i - y_k)^2} - d_{min} \geq 0, \quad \forall i \neq k \quad (7)$$

$$L_i = (x_i, y_i) \in F \quad (8)$$

where  $r \in [1, 2 \dots C]$ ,  $i, k \in [1, 2 \dots N]$  and  $C$  is the total number of constraints which is equal to  $N(N-1)/2$ .

#### 2.3.2. Model of problem for restricted sea area

As mentioned in Section 1, the foundation cost as well as installation cost will be greatly increased in some cases related to the sea bed condition. Alternatively, due to the limitation of some existing facilities such as oil wells or shipwrecks, etc., the WTs cannot be installed in specified zones [19]. In order to ensure the feasibility of the solution, a restriction zone,  $R$ , is defined in this work. Then, the problem can be rewritten as:

$$\text{Objective: } \max(E_{tot,av}(L))$$

Subject to:

$$\begin{cases} F_r(L_i) = \sqrt{(x_i - x_k)^2 + (y_i - y_k)^2} - d_{min} \geq 0, \quad \forall i \neq k \\ L_i = (x_i, y_i) \in C_{rF} \end{cases} \quad (9)$$

where  $C_{rF}$  is the complement of the restriction zone,  $R$ , in the predefined sea area,  $F$ . The definition of  $C_{rF}$  and  $F$  will be more understandable using a simple example as illustrated in Fig. 1.

In Fig. 1, the construction area is shown on left which is the white area that refines by the black rectangle while the yellow circular area on right is the restriction area. The feasible solution of the problem for restricted sea area should be found within  $C_{rF}$ .

## 3. Methodology

Presently, heuristic algorithms are widely used in solving the non-linear problem, which is a good way to save computational cost while retaining the ability to find a global optimal solution to

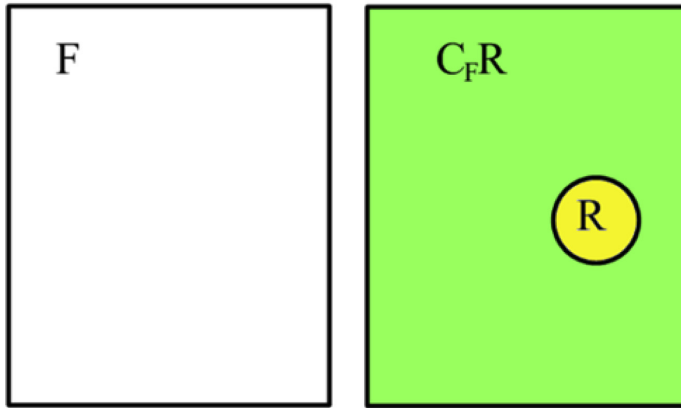


Fig. 1. Illustration of the restriction zone.

some extent. However, if the objective function is quite complex and plenty of nonlinear constraints are included, it may be locked into a locally optimal solution. In order to conquer this drawback, a recently proposed method, PSO-MAM, is adopted as the optimization method in this paper. The restriction area is implemented using penalty function in this paper. The description of penalty function for realizing the restriction area is first introduced. Then, the theory of PSO-MAM and the optimization procedure are presented.

### 3.1. Penalty function

In order to satisfy all the constraints and get a feasible solution, a penalty function method is adopted in this paper and the analytical models for unrestricted and restricted sea areas respectively are described in detail in this part.

#### 3.1.1. Penalty function of problem for unrestricted sea area

As mentioned in Section 3.1, the heuristic algorithm as PSO can be used to solve the unconstrained optimization problem which means it can limit the particles (solution) to moving into the pre-defined area. In this case, (7) can be satisfied by PSO. However, (8) can be violated if no specific condition is defined. Conversely, if the particle is limited to follow (8) in the particle update process then there is a possibility of violating (7). In order to get a feasible solution and simplify the numerical calculation, a penalty function is defined as follows:

$$\phi(L_i) = |\min\{0, F_r(L_i)\}| \quad (10)$$

Then, the objective function for wind farm layout optimization with unrestricted sea area can be rewritten as:

$$\max \left( E_{tot}(L) - PF \sum_{i=1}^C \phi(L_i) \right) \quad (11)$$

In (11),  $F_r(L_i)$  represents the distance between any pair of WTs.  $\phi(L_i) = 0$  means that every distance between each pair of WTs is larger than 4 rotor diameters, in other words, the solution is feasible, while  $\phi(L_i) > 0$  indicates that some WTs are placed so close that the penalty function will be triggered.

If no penalty function is adopted, (7)–(9) can also be satisfied in an iterative way. Taking the problem described in 2.3.1 as an

example, the algorithm procedure can be expressed as follows.

---

#### Algorithm 1: Constraint

---

```

1. function constrain (x);
   Counter: Start=2; the initial value of Start can be any except 1
   Input: The optimization variable (WT position) x
2. While Start=1
3.     Start=1;
4.     for i=1:N (total number of WTs)
5.         for j=1: N
6.             if j=i then
7.                 Check (7) and (8)
8.                 While (7) or (8) is not satisfied
9.                     Set L(j) which can satisfy (7) and (8)
10.                    Start=Start+1;
11.                end
12.            end
13.        end
14.    end
15. end

```

---

As can be seen in algorithm 1, (7) and (8) can also be satisfied without using a penalty function. However, iterative processes must then be included. Initially, the optimization variable will enter into algorithm 1 to avoid violating (7) and (8), and then the PSO-MAM algorithm will be triggered. As a result, the computational time would be increased. Superior to that, the penalty function method has good synergy with PSO. It can be known from (10) and (11) that once the particles of PSO move into a position where (7) or (8) is not satisfied then the fitness value will be reduced greatly, so the positions of particles will be spontaneously updated to avoid entering into this penalized region and seek more beneficial positions. Finally, the constrained optimization problem can be transformed into an unconstrained one with the help of the penalty function. In this paper, the penalty factor,  $PF$ , is set at 10000. A larger  $PF$  (for instance 100000 in this case) will put the final value below zero, while if the value of  $PF$  is too small then the penalty function cannot ensure the final result is feasible.

#### 3.1.2. Penalty function of problem for restricted sea area

Similarly, the penalty function can be defined inside a restriction sea area as:

$$\phi'(L_i) = |\min\{0, D_r(L_i)\}| \tag{12}$$

where,  $D_r(L_i)$  indicates the nearest distance of infeasible solution to the predefined restriction zone boundary. The calculation of  $D_r(L_i)$  is illustrated in Fig. 2.

As illustrated in Fig. 2, there are a total of 4 red dots in this graphic which represent the locations of WTs. The area bounded by the green lines and red circle shows the restriction zones. If the red dot is within the restriction zones then the nearest distance between the WT and restriction zone boundary should be calculated.  $l_1$  and  $l_2$  show the distance between WT 1 and WT 2 to their respective nearest boundaries, which is a simple example to identify the  $D_r(L_i)$ .

In the simulation, not all the WTs positions will enter into this penalty function. The judgement principles are as follows:

- (1) If  $x \in [x1, x2]$ ,  $y \in [y1, y2]$ , then enter into penalty function.
- (2) If  $x \in [x2, x3]$ ,  $y \in [0, y2]$ , then enter into penalty function.
- (3) If  $x \in [x3, x4]$ ,  $y \in [0, y2]$  or  $y$  is inside the domain of  $f3$ , then enter into penalty function.
- (4) If  $x \in [x4, x5]$ ,  $y$  is inside the domain of  $f3$ , then enter into penalty function.
- (5) Otherwise, the penalty function will not be used.

Then, the objective function for restriction zone wind farm layout optimization can be written as:

$$\max \left( E_{tot}(L) - PF \left( \sum_{i=1}^C \phi(L) + \sum_{i=1}^{C_1} \phi'(L) \right) \right) \tag{13}$$

where  $C_1$  is the total number of penalty function that should be used in the problem for restricted sea area. It can be seen from Fig. 2 that the value of  $C_1$  is not deterministic. It will change with the number of WTs that falls into the restriction zone during the simulation process.

In practice, the restricted sea area or wind farm can be defined as any shape. This can be realized by revising the functions in judgement principles.

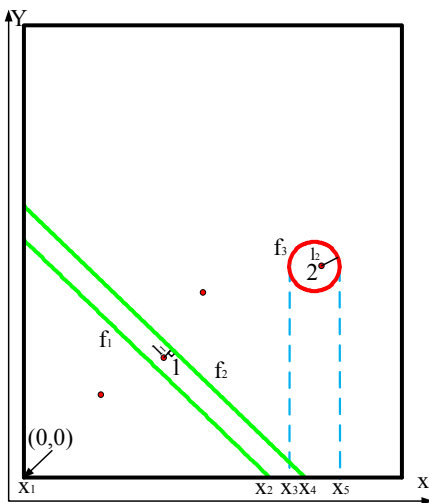


Fig. 2. Illustration of calculation of  $D_r(L_i)$ .

### 3.2. PSO

Mimicking the process of fish hunting for prey, the PSO algorithm was firstly proposed by Kennedy and Eberhart [28] in 1995. As one of the evolutionary algorithms, PSO has good performance in finding the optimal solution for continuous nonlinear optimization problems while GA is good at solving integer optimization problems. Although there are some revised versions of GA which enable the GA to solve continuous problems, PSO is still a better choice which has higher computational efficiency and can get a result which benefits the objective function more compared with GA [29]. The global version PSO (GPSO) can be expressed in the following equations [30].

$$v_i^{k+1} = wv_i^k + l_1r_1(Q_i^k - q_i^k) + l_2r_2(Q_g^k - q_i^k) \tag{14}$$

$$q_i^{k+1} = q_i^k + v_i^{k+1} \tag{15}$$

In PSO, one possible solution is called a particle and the particle population or swarm size is the number of the particles, in other words, the number of possible solutions in a swarm is decided by the swarm size. As can be seen in (10), there are three parts. The first part represents the velocity of previous particle. A larger inertial weight ensures a stronger global searching ability while smaller  $w$  ensures the local searching ability. The other two parts are used to ensure the local convergence ability of the algorithm. Hence, the final result is sensitive to the setting of the control parameters ( $l_1$ ,  $l_2$  and  $w$ ).

In order to reduce the sensitivity of the final result to control parameters, many works have been carried out on parameter control methods for  $w$  which can be summarised into two categories [31]: simple rule based parameter control [32–35] and adaptive parameter control strategy [36]. The first strategy indicates that the PSO performance can be improved by using linear, non-linear or fuzzy rule inertia weight while the other introduces evolutionary state estimation (ESE) technique [37] to further improve the performance of PSO. Recently, a PSO-MAM method was proposed which has been proven to have an outstanding performance in finding a near optimal solution [38].

### 3.3. Optimization framework

To optimize the locations of WTs, the PSO-MAM is adopted in this paper, which improves the performance of PSO by using multiple search methods. The simulation procedure to access the wind farm layout by PSO is shown in Fig. 3.

In Fig. 3, the parameters of PSO are initialized in the first step. After that, the initial particle positions (solution) will be transferred into the fitness function to calculate the energy yield (fitness value). The initial particle-specific and global best solutions will be picked up by comparing the fitness value of each solution. Then the initial positions will be updated in different module. In PSO-MAM, there are totally three modules [38]:

- (1) PSO module (M1): In module 1, the initialized positions and corresponding velocities will be updated by the employed PSO operator. If the updated solution is feasible, then the fitness function will be run otherwise it will enter into module 2.
- (2) Intelligent multiple search methods module (M2): In order to improve the searching ability of PSO, two search methods (non-uniform mutation-based method [39] and sub-gradient method [40]) are implemented in this module. Once the program is in module 2, one of the two search

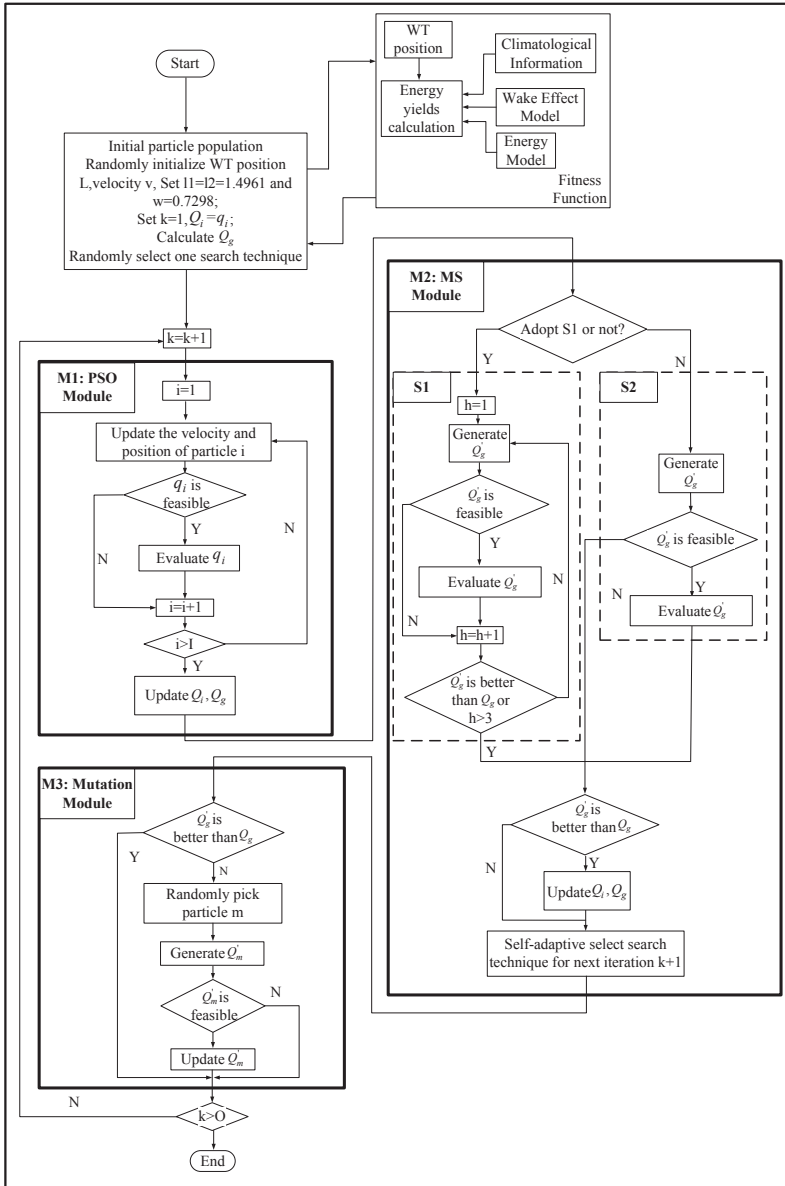


Fig. 3. Optimization flowchart based on PSO-MAM (S1: non-uniform mutation-based method and S2: sub-gradient method) [38].

methods will be determined using the roulette wheel selection [41] based on the search method's execution probability. The updated solution will be updated by the selected method so that the diversity of the population can be increased, in other words, the probability of the program falling into local optimal solution will be reduced. The solution which can get a better fitness value will be kept

otherwise the original solution in M1 will be kept and entered into M3.  
 (3) Mutation module (M3): In this module, one randomly selected particle will be updated using a mutation operator. The above procedure does not stop until the maximum iteration is reached.

3.4. Assumptions

In this work, a constant number of WTs are expected to be placed within a predefined construction area to harvest the wind farm. Some assumptions are made as follows:

- (1) The WT positions are regarded as the sites where foundations are built. Hence, the boundary condition means the foundations are built within the construction area while the rotor blades are permitted outside the boundary.
- (2) The distance for each pair of WT cannot be smaller than 4 rotor diameters as otherwise the lifetime of the turbine will decrease a lot due to turbulence [18].

4. Case study

First a Reference Wind Farm (RWF) is introduced and then the input wind speed is shown as a wind rose. Thereafter, two scenarios, which are the optimization of offshore wind farm layout with and without considering restriction area, are presented respectively. In order to increase the possibility of getting the global optimal solution, the PSO-MAM based program was run 10 times. The GA in MATLAB's optimization toolbox is adopted to find the results as a comparison in this work.

4.1. RWF

The reference wind farm has been designed at the location of the FINO3 met mast- 80 km west of the German island of Sylt. The installed capacity of the wind farm is 800 MW with 80, 10 MW reference WTs and two substations [42]. In this paper, the RWF is selected as the benchmark and the performance of the optimized wind farm will be compared with that of the RWF layout which is shown in Fig. 4.

As can be seen in Fig. 4, the blue circles indicate the WT positions while the green rectangle shows the construction area. In this simulation, the DTU 10 MW WT is adopted as the reference WT. The specification for this is listed in Table 1.

4.2. Wind rose

The wind resource has the stochastic characteristic. The power production of a wind farm can be estimated using probabilistic models such as a Weibull distribution function for a number of wind speed ranges, which is a stochastic approach, whereas in this paper, the wind rose is adopted to calculate the wind farm energy yields during the optimization process (see Fig. 5).

**Table 1**  
DTU 10 MW wind turbine specification [43].

Parameter	10 MW DTU wind turbine
Cut-in Wind Speed	4 m/s
Rated Wind Speed	11.4 m/s
Cut-out Wind Speed	25 m/s
Rotor Diameter	178.3 m
Rated Power	10 MW

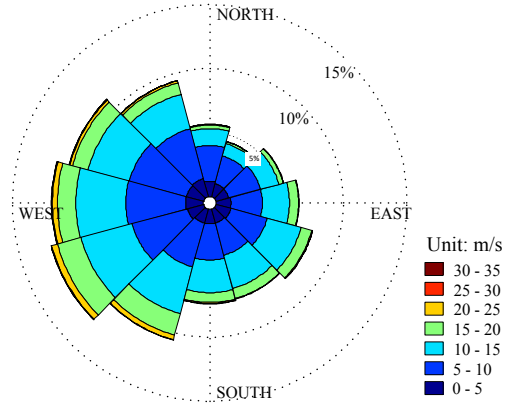


Fig. 5. Wind rose for wind climate in the vicinity of FINO3.

The data is obtained from the work of the Norwegian Meteorological Institute [44], in which the wind speeds are sampled per 3 h. For the convenience of calculation, the raw data is formulated into a wind rose which is used for the energy production calculation for a year.

Based on the measured wind data in the vicinity of FINO3, the wind rose is generated by dividing the wind direction into 12 sections with 30° per section. Furthermore, in each section the wind velocity is divided into 5 ranges at intervals of 5 m/s. So the used wind rose is similar to the Weibull distribution with a number of wind speed ranges, plus wind direction. The approach may be able to give more detailed results than Weibull distribution, since it may provide a probabilistic distribution model in each direction if more data is available.

4.3. Scenario I: optimization of wind farm layout without considering restriction sea area

In order to get a near global optimal solution, the PSO-MAM program is run 10 times and the final solution is selected as the one with minimal LPC. Following the same procedure, the problem is also solved using GA algorithm for comparison. The energy yields of each trial for scenario I using PSO-MAM is shown in Figs. 7(a) and 11(a) shows the results for scenario II. The results obtained by GA is shown in Figs. 7(b) and 11(b) shows the results for scenario II.

In this scenario, the WT positions are expected to be optimized within the same predefined area as shown in Fig. 4. The RWF layout is coded into the PSO particle and regarded as one of the initial solutions. The optimized layout found by PSO-MAM is shown in Fig. 6 while the fitness value of the best trial using PSO-MAM algorithm is shown in Fig. 8.

As can be seen from Fig. 6, the blue circles represent the WTs' positions while the green lines show the boundary of the

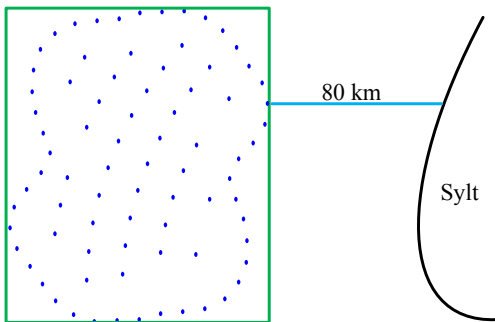


Fig. 4. The illustration of FINO3 reference wind farm layout [42].

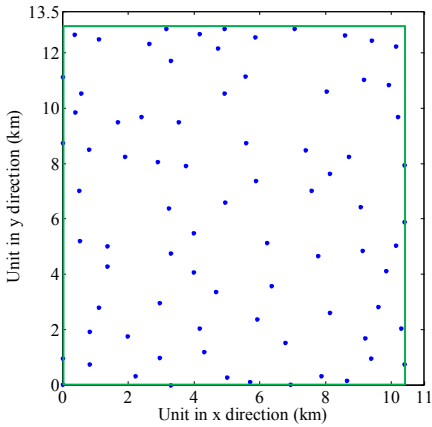


Fig. 6. The WT position illustration for scenario I using PSO-MAM.

predefined wind farm construction zone. Due to the area limitation, some WT's locations are already at the boundary, but no WT is outside this boundary which means that the penalty function limits all the possible solutions to inside this predefined domain. In Fig. 7(a), it can be seen that the PSO-MAM can find the same result 5 out of 10 times and the final solution is stabilized around 4161 after the 820<sup>th</sup> iteration as can be seen in Fig. 8. The GA algorithm can also find a layout with higher energy yield compared with the manually designed layout. Compared with the results found by PSO-MAM in Fig. 7(a), it can also be seen that the GA is not robust as can be seen in Fig. 7(b).

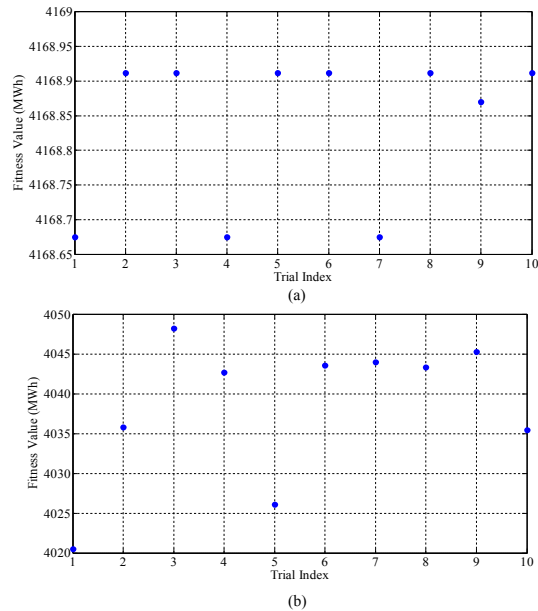


Fig. 7. The fitness value distribution by running the program 10 times for scenario I. (a) PSO-MAM. (b) GA.

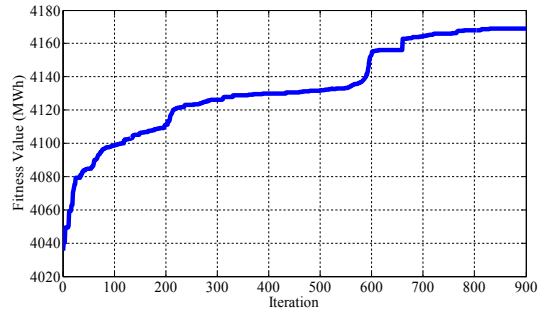


Fig. 8. The relation between fitness value and iteration for scenario I using PSO-MAM.

#### 4.4. Scenario II: optimization of wind farm layout considering restriction sea area

In this scenario, two restriction zones are set up within the construction sea area as shown in Fig. 9. The WTs are expected to be placed outside these restriction zones and generate as much as power as possible. The optimized layout for this scenario using PSO-MAM is shown in Fig. 10. The best trial is selected as the final result for this scenario. The fitness value which corresponds to each iteration of this trial is shown in Fig. 12.

As can be seen from Fig. 10, all WTs are located outside the restriction area and no WT is out of the construction area boundary. The final solution is stabilized around 4169 after the 1180<sup>th</sup> iteration which can be seen in Fig. 12.

#### 4.5. Results and discussion

The performances of optimized layouts and RWF layout are concluded in Table 2 as follow.

From Table 2, it can be seen that the optimized layout in the simulation can increase the energy yield by 3.84%. Even if a restriction area is assumed as in scenario II, the energy yield is still 3.41% larger than RWF layout. In scenario II, only the polygonal restriction area is added into the construction region. It can also be seen that the layout found by PSO-MAM outperformed that of the GA by finding a layout which generated 2.99% and 6.68% more energy in the respective scenarios.

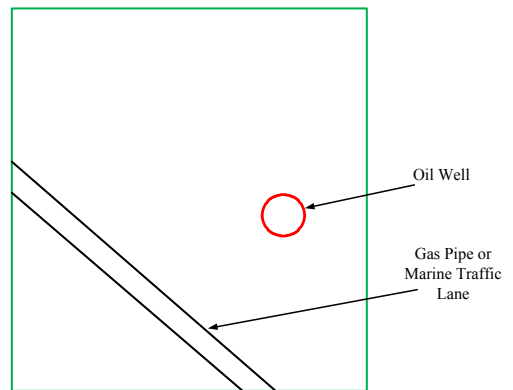


Fig. 9. The construction area of scenario II.

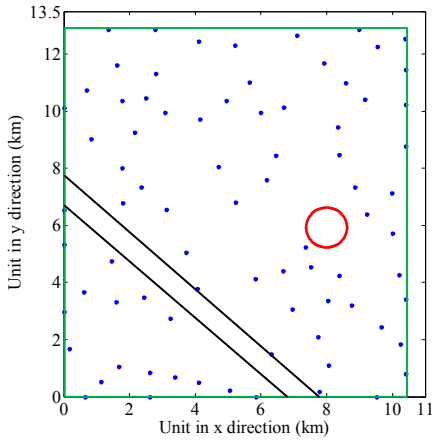


Fig. 10. The WT position illustration for scenario II using PSO-MAM.

**Table 2**  
Specification of wind farm layout performance.

	Energy yields (Gwh)		Capacity factor (%)	
	PSO	GA	PSO	GA
NRWF	4015.17		57.29	
Scenario I	4169.24	4048.23	59.49	57.76
Scenario II	4151.95	3892.02	59.25	55.54

**5. Conclusions**

In this paper, a heuristic optimization method is proposed to solve the WFLOP considering the restriction area within the pre-defined construction area. Compared with GA, it can be seen that the PSO-MAM algorithm is a better choice for solving WFLOP. It can find a layout which can generate 3.83% more energy than manually designed layout. Due to the restriction of seabed condition, marine traffic, etc., some area within the planning area is forbidden to place WT. The restriction area concept is proposed and implemented successfully by using the penalty function method. Although, only

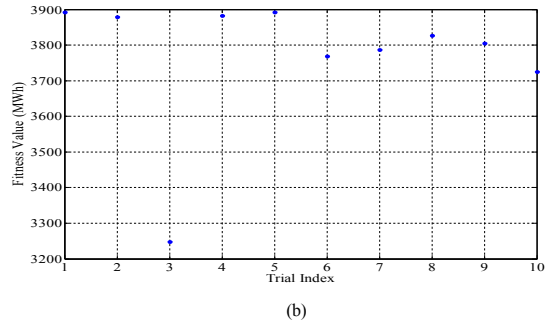
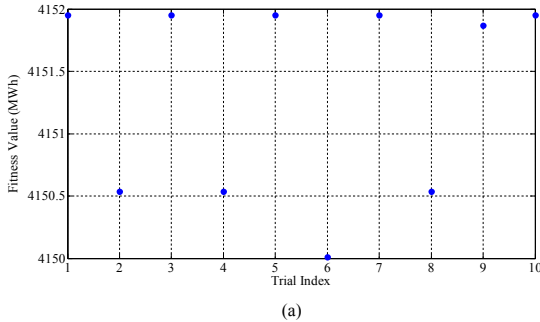


Fig. 11. The fitness value distribution by running PSO-MAM 10 times for scenario II. (a) PSO-MAM. (b) GA.

In the future, the work of optimizing offshore wind farm layout can be updated by considering an overall optimization of WTs' locations as well as the electrical system layout. The optimization variables should then be integer or discrete. Hence, a mixed-integer optimization method must be adopted to solve the problem.

two simple situations are illustrated (the oil well and gas pipe line which are assumed to be circular and rectangular respectively) the proposed method and algorithm can be fitted into any shaped restriction area by identifying the contour of the restriction area using some methods, such as curve fitting.

**Acknowledgments**

Authors would like to thank Norwegian Centre for Offshore Wind Energy (NORCOWE) under grant 193821/S60 from Research Council of Norway (RCN).

**References**

- [1] Mosetti G, Poloni C, Diviacco B. Optimization of wind turbine positioning in large wind farms by means of a genetic algorithm. *J Wind Eng Ind Aerodyn* 1994;51(1):105–16.
- [2] Grady S, Hussaini M, Abdullah M. Placement of wind turbines using genetic algorithms. *Renew Energy* 2005;30(2):259–70.
- [3] Marmidis G, Lazarou S, Pyrgioti E. Optimal placement of wind turbines in a wind park using Monte Carlo simulation. *Renew Energy* 2008;33(7):1455–60.
- [4] Prasad Prabhu N, Yadav P, Prasad B, Kumar Panda S. Optimal placement of offshore wind turbines and subsequent micro-siting using intelligently tuned harmony search algorithm. In: *Power and Energy Society General Meeting (PES), 2013 IEEE*; Jul. 2013. p. 1–7. Vancouver, BC.
- [5] Pookpunt S, Ongsakul W. Optimal placement of wind turbines within wind farm using binary particle swarm optimization with time-varying acceleration

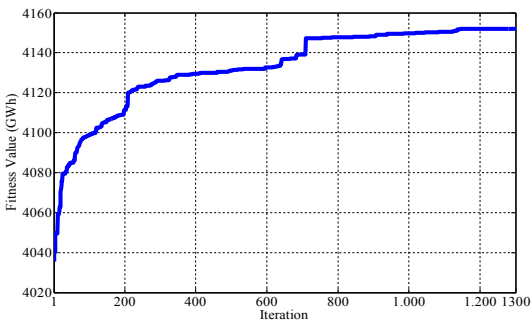


Fig. 12. The relation between fitness value and iteration for scenario II using PSO-MAM.

- coefficients. *Renew Energy* Jul. 2013;55:266–76.
- [6] Couto TG, Farias B, Carlos A, Diniz GC, Vinicius M, de Morais G. Optimization of wind farm layout using genetic algorithm. In: 10th World Congress on Structural and Multidisciplinary Optimization, Orlando, Florida, USA; May 2013.
- [7] Gonzalez J, Burgos Payan M, Riquelme Santos J. A new and efficient method for optimal design of large offshore wind power plants. *IEEE Trans Power Syst* 2013;28(3):3075–84.
- [8] Salcedo-Sanz S, Gallo-Marazuela D, Pastor-Sánchez A, Carro-Calvo L, Portilla-Figueras A, Prieto L. Evolutionary computation approaches for real offshore wind farm layout: a case study in northern Europe. *Expert Syst Appl* 2013;40(16):6292–7.
- [9] Salcedo-Sanz S, Gallo-Marazuela D, Pastor-Sánchez A, Carro-Calvo L, Portilla-Figueras A, Prieto L. Offshore wind farm design with the coral reefs optimization algorithm. *Renew Energy* 2014;63:109–15.
- [10] Kusiak A, Song Z. Design of wind farm layout for maximum wind energy capture. *Renew Energy* 2010;35(3):685–94.
- [11] Eroglu Y, Seçkiner SU. Design of wind farm layout using ant colony algorithm. *Renew Energy* 2012;44:53–62.
- [12] Eroglu Y, Seçkiner SU. Wind farm layout optimization using particle filtering approach. *Renew Energy* 2013;58:95–107.
- [13] Saavedra-Moreno B, Salcedo-Sanz S, Paniagua-Tineo A, Prieto L, Portilla-Figueras A. Seeding evolutionary algorithms with heuristics for optimal wind turbines positioning in wind farms. *Renew Energy* 2011;36:2838–44.
- [14] Chowdhury S, Zhang J, Messa A, Castillo L. Optimizing the arrangement and the selection of turbines for wind farms subject to varying wind conditions. *Renew Energy* 2013;52:273–82.
- [15] Wan C, Wang J, Yang G, Gu H, Zhang X. Wind farm micro-siting by Gaussian particle swarm optimization with local search strategy. *Renew Energy* 2012;48:276–86.
- [16] Feng J, Shen WZ. Solving the wind farm layout optimization problem using random search algorithm. *Renew Energy* Jun. 2015;78:182–92.
- [17] Park J, Law KH. Layout optimization for maximizing wind farm power production using sequential convex programming. *Renew Energy* Aug. 2015;151:182–92.
- [18] Pérez B, Mínguez R, Guanche R. Offshore wind farm layout optimization using mathematical programming techniques. *Renew Energy* 2013;53:389–99.
- [19] Kirkeby H, Merz KO. Layout and electrical design of a 1.2 GW wind farm for research on the next generation of offshore wind energy technologies. Trondheim, Norway: Sintef Energy Research; April 1, 2014.
- [20] Gao X, Yang H, Lin L, Koo P. Wind turbine layout optimization using multi-population genetic algorithm and a case study in Hong Kong offshore. *J Wind Eng Ind Aerodyn* 2015;139:89–99.
- [21] WindPRO/PARK: 'Introduction wind turbine wake modelling and wake generated turbulence'. EMD International A/S.
- [22] Beaucage P, Brower M, Robinson N, Alonge C. Overview of six commercial and research wake models for large offshore wind farms. In: Proc. Eur. Wind Energy Assoc. (EWEA'12), Copenhagen, Denmark; 2012. p. 95–9.
- [23] Porte-Agel F, Wu Y, Chen C. A numerical study of the effects of wind direction on turbine wakes and power losses in a large wind farm. *Energies* 2013;6:5297–313. MDPI.
- [24] Hou P, Hu W, Soltani M, Chen Z. Optimized placement of wind turbines in large scale offshore wind farm using particle swarm optimization algorithm. *IEEE Trans Sustain Energy* 2015;6(4):1272–82.
- [25] Serrano González J, González Rodríguez AG, Castro Morac J, Riquelme Santosa J, Burgos Payana M. Optimum wind turbines operation for minimizing wake effect losses in offshore wind farms. *Renew Energy* Aug. 2010;35(8):1671–81.
- [26] Qiao Wei. Intelligent mechanical sensorless MPPT control for wind energy systems. In: Power and Energy Society General Meeting, 2012 IEEE; Jul. 2012. p. 1–8. San Diego, CA.
- [27] Bak C, Zahle F, Bitsche R, Kim T, Yde A, Christian Henriksen L, et al. Description of the DTU 10 MW Reference wind turbine. Fredericia, Denmark: DTU Wind Energy; Jul. 2013.
- [28] Kennedy J, Eberhart R. Particle swarm optimization. In: Proc. IEEE Int. Conf. Neural networks; Apr. 1995. p. 1942–8.
- [29] Hassan R, Cohanim B, de Weck O. A comparison of particle swarm optimization and the genetic algorithm. In: Proceedings of the 46th AIAA/ASME/ASCE/AHS/ASC Structures, Structural Dynamics and Materials Conference; 2005.
- [30] Kennedy J. The particle swarm: social adaptation of knowledge. In: Proc. IEEE Int. Conf. Evolution of Computing, Indianapolis, IN; 1997. p. 303–8.
- [31] Hu M, Wu T, Weir JD. An adaptive particle swarm optimization with multiple adaptive methods. *IEEE Trans Evol Comput* 10 Dec. 2012;17:705–20.
- [32] Shi Y, Eberhart RC. Empirical study of particle swarm optimization. In: Proc. Congr. Evol. Comput; 1999. p. 1950–5.
- [33] Jiao B, Lian Z, Gu X. A dynamic inertia weight particle swarm optimization algorithm. *Chaos Solit Fractals* Aug. 2008;37:698–705.
- [34] Shi Y, Eberhart RC. Fuzzy adaptive particle swarm optimization. In: Proc. Congr. Evol. Comput; 2001. p. 101–6.
- [35] Eberhart RC, Shi Y. Tracking and optimizing dynamic systems with particle swarms. In: Proc. Congr. Evol. Comput; 2001. p. 94–100.
- [36] Zhan Z-H, Zhang J, Li Y, Chung HS-H. Adaptive particle swarm optimization. *IEEE Trans Syst, Man Cybern B, Cybern* Apr. 2009;39(6):1362–81.
- [37] Zhang J, Chung HS-H, Lo W-L. Clustering-based adaptive crossover and mutation probabilities for genetic algorithms. *IEEE Trans Evol Comput* Jun. 2007;11(3):326–35.
- [38] Hu M, Wu T, Weir JD. An intelligent augmentation of particle swarm optimization with multiple adaptive methods. *Inf Sci Dec.* 2012;213:68–83.
- [39] Michalewicz Z. Genetic algorithms + data structures = evolution programs. 3rd ed. London, UK: Springer-Verlag; 1996.
- [40] Boyd S. EE364b course notes: sub-gradient methods. Stanford, CA: Stanford University; 2010.
- [41] Zhang L, Chang H, Xu R. Equal-width partitioning roulette wheel selection in genetic algorithm. In: IEEE International Conference on Technologies and Applications of Artificial Intelligence; 2012. p. 62–7.
- [42] Norwegian Centre for Offshore Wind Energy (NORCOWE). (2014, Sep. 9). WP2014—Froya-NRWF NORCOWE reference wind farm.
- [43] Bak C, Zahle F, Bitsche R, Kim T, Yde A, Henriksen LC, et al. Description of the DTU 10 MW reference wind turbine. Fredericia, Denmark: DTU Wind Energy; Jul. 2013.
- [44] Furevik BR, Haakenstad H. Near-surface marine wind profiles from rawinsonde and NORA10 hindcast. *J Geophys Res* 7 Dec. 2012;117.



# Offshore Wind Farm Layout Design Considering Optimized Power Dispatch Strategy

Peng Hou, *Student Member, IEEE*, Weihao Hu, *Member, IEEE*, Mohsen Soltani, *Member, IEEE*, Cong Chen, Baohua Zhang, *Student Member, IEEE*, Zhe Chen, *Senior Member, IEEE*

**Abstract**— Offshore wind farm has drawn more and more attention recently due to its higher energy capacity and more freedom to occupy area. However, the investment is higher. In order to make a cost-effective wind farm, the wind farm layout should be optimized. The wake effect is one of the dominant factors leading to energy losses. It is expected that the optimized placement of wind turbines (WT) over a large sea area can lead to the best tradeoff between energy yields and capital investment. This paper proposes a novel way to position offshore WTs for a regular shaped wind farm. In addition to optimizing the direction of wind farm placement and the spacing between WTs, the control strategy's impact on energy yields is also discussed. Since the problem is non-convex and lots of optimization variables are involved, an evolutionary algorithm, the particle swarm optimization algorithm (PSO), is adopted to find the solution. In order to increase the probability of finding the global optimal solution, the adaptive parameter control strategy is utilized. Simulation results are given to verify the proposed approach and comparison is made with results obtained using other methods.

**Index Terms**— Wake effect, optimized placement of wind turbines, direction of wind farm placement, non-convex, Particle Swarm Optimization (PSO), Optimized power dispatch control strategy.

## Nomenclature

$V_0$ [m/s]	Incoming wind speed
$V_{ij}$ [m/s]	Wind speed reached at the blade of WT at row $i$ , column $j$
$k_d$	Decay constant, for an offshore environment the recommended value is 0.04 [21]
$C_{p,mn,k}$	Power coefficient of WT at row $m$ , column $n$ for control interval $k$
$R_0$ [m]	WT's rotor radius
$R_{y,j}$ [m]	Generated wake radius at at row $m$ , column $n$
$S_{overlap}$ [m <sup>2</sup> ]	Affect wake region
$S_0$ [m <sup>2</sup> ]	Area swept by WT blade
$C_t$	Thrust coefficient
$\beta_{mn}$ [°]	Pitch angle of WT at row $m$ , column $n$

$\lambda_{mn}$	Optimal tip speed ratio for the pitch angle $\beta_{mn}$ at which the power coefficient will be maximum
$\rho$ [kg/m <sup>3</sup> ]	Air density
$P_{m,mn}$ [MW]	Mechanical power generated by WT at row $m$ , column $n$
$v_{mn}$ [m/s]	Wind speed at WT in row $m$ , column $n$
$N_{row}$	Number of WTs in a row
$N_{col}$	Number of WTs in a column
$P_{loss,i}$ [MW]	Power losses of cable $i$
$I_i$ [kA]	Current in cable $i$
$R_{e,i}$ [ohm/m]	Resistance of cable $i$
$\rho_{R,i}$ [ohm*m/mm <sup>2</sup> ]	Resistivity of selected cable $i$
$l_{R,i,j}$ [m]	Length of cable $i$
$S_{R,i}$ [m <sup>2</sup> ]	Sectional area of cable $i$
$N$	Total number of cables in a wind farm
$P_{tot,t}$ [MW]	Total power production during interval $t$
$P_{tot,loss,t}$ [MW]	Total power losses during interval $t$
$T_E$ [day]	Duration interval for energy yields calculation
$T_t$ [h]	Duration when the wind farm generating power of $P_{tot,t}$
$E_{tot,av}$ [MWh]	Mean energy yields in one year
$t$ [hour]	Energy yields calculation time
$C_i$ [MDKK/km]	Unit cost of cable $i$
$S_{rated,i}$ [W]	Rated apparent power of cable in line $i$
$A_p, B_p, C_p$	Coefficients of cable cost model
$I_{i,rated}$ [A]	Rated current of cable in line $i$
$U_{i,rated}$ [V]	Rated voltage of cable in line $i$
$l_i$ [km]	Length of cable $i$
$Q_i$	Quantity of cable $i$
$CAP_t$ [Dkk]	Capital cost in year $t$
$C_0$ [Dkk]	Present value of capital cost
$N_y$	Economic lifetime
$r$	Discount ratio
$d_{x,i}$ [m]	Interval $i$ of WTs in $x$ direction or rather the distance between WTs rows
$d_{y,j}$ [m]	Interval $j$ of WTs in $y$ direction or rather the distance between WTs columns
$Num\_c$	Total number of control strategy
$\theta$ [°]	Wind farm direction
$\beta_{mn,k}$ [°]	Pitch angle of WT in row $m$ , column $n$ for time interval $k$
$\omega_{mn,t}, \omega_{max}$	Rotor speed of WT in row $m$ , column $n$ for time interval $k$ , and maximum rotor speed limitation
$w$	Inertia weight
$l_1, l_2$	Learning factors
$r_1, r_2$	Stochastic numbers which can generate some random numbers within [0, 1]
$x_i^k, x_i^{k+1}$ [m]	Position of particle $i$ at iteration $k$ and

This work has been funded by Norwegian Centre for Offshore Wind Energy (NORCOWE) under grant 193821/S60 from Research Council of Norway (RCN). NORCOWE is a consortium with partners from industry and science, hosted by Christian Michelsen Research.

The authors are with the Department of Energy Technology, Aalborg University, Aalborg, Denmark (e-mail: pho@et.aau.dk; whu@et.aau.dk; sms@et.aau.dk; cchen12@googlemail.com; bzh@et.aau.dk; zch@et.aau.dk).

$v_i^k, v_i^{k+1}$ [m]	k+1 respectively Speed of particle i at iteration k and k+1 respectively
$local_i^k$ [m]	Best position of particle i at iteration k
$global^k$ [m]	Best position of all particles at iteration k
$d_{x,i}, d_{y,j}$	WTs' spacing in x and y direction respectively
G	maximum number of evolutionary generation

## I. INTRODUCTION

Though large investment is required for constructing an offshore wind farm, it is still a favorable renewable resource with respect to its dominant advantages as: high energy density and no noise pollution to residences. Once the wind farm construction area is determined, the WT's can be placed optimally according to the statistic wind resources measured within the construction area. Since the wake effect will induce a reduction of wind speed at the downstream WT's, it is expected that the optimized layout minimize the wake losses as much as possible. The initial work maximizing the offshore wind energy yields for the minimum investment within a given area is presented in [1], the solution is found through a simplified wind farm cost model using a genetic algorithm (GA). [2] indicated that the results found by [1] can be further improved by adjusting the parameters of the GA. Similarly, [3] presented a Monte Carlo method for solving wind farm layout optimization problem (WFLOP) and the results was demonstrated to be more beneficial than [2] while [4] addressed the same problem using intelligently tuned harmony search (ITHS) method which was proved to be outperformed than GA in finding a layout which can generate more energy. HS and improved HS (IHS) methods in most of the studied cases. Using binary particle swarm optimization with time-varying acceleration coefficients (BPSO-TVAC) algorithm to solve the WFLOP is presented in [5] and the result is compared with those of 5 other heuristic algorithms. Instead of relying on heuristic algorithms, mathematical programming (quadratic integer program (QIP) and mix-integer linear program (MILP)) were adopted in [6] to solve WFLOP which ensure the optimality or local optimal result in some extent, the optimized layouts were compared with the work of [1][2] and demonstrated to be more cost-effective in most of cases.

In the above papers, the WT positions are optimized by partitioning the area into a small grid where each grid point represents a possible WT position. In order to increase the freedom of movement of the WT's, several works have used coordinate form instead of grid form to express the location of the WT's [7]-[9]. [7] used an evolutionary algorithm to place WT's within a circular boundary wind farm under the assumption that the distance between each pair of WT cannot be smaller than 4 WT rotor diameters. Two years later, Yunus Eroglu et al. [8] adopted an ant colony algorithm to further improve the performance of this round shaped wind farm, the results also showed that it is possible to install up to 9 WT's within this wind farm, which is different from the conclusion of [7] that no feasible solution can be found when more than 6 WT's are installed. [9] optimized the WT layout using a Gaussian PSO algorithm which showed better performance than both Grady's and an empirical layout in energy yields and computational time. The number of WT's was optimized together with the WT layout through the mixed-discrete

particle swarm optimization (MDPSO) algorithm in [10]. In [11], GA was adopted to optimize the layout, some practical constraints as load-bearing capacity, turbine hub height, soil condition and prohibited restrictions were considered to make the final result more realistic. In [12], three types of offshore wind farm configurations in Hong Kong (aligned, staggered, scattered) were investigate using GA, the simulation results showed that the scattered layout was the best choice in terms of levelised cost of energy (LCOE). The above works show more interests in harvesting the offshore wind farm without considering the impacts of the optimized WT locations on the cost increase while the investment is in fact another critical factor that decides the economy of the wind farm. The overall optimization in terms of WT positions as well as the cable connection layout was conducted in [13] to reach the target of a cost-effective wind farm.

From literature study, it can be seen that there are some common points among the above works: 1) Using a stochastic approach (the Weibull distribution) to simulate renewable production. 2) Different optimization algorithms are adopted to optimize the problem. 3) The WT's are always assumed to be operated under the Maximum power point tracking strategy (MPPT) [14] in the wind farm design phase.

Besides the WFLO, the control strategy is also critical to the performance of the wind farm. Traditionally, all WT's are assumed to be operated under MPPT control strategy. Based on it, the wind farm layout was designed to minimize the wake losses. In order to get more profits, some new control strategy has also been proposed to harvest the existing wind farm which is normally conducted by changing the tip speed ratio ( $\lambda$ ) and blade pitch angle ( $\beta$ ) of each WT [15]-[18]. In one of our previous work [19], an optimized power dispatch control strategy was proposed to minimize the levelized production cost (LPC) of an offshore wind farm. From previous experience, it can be known that the optimized control strategy varies with wind farm layout which means that these factors are interdependent. To the best of our knowledge, no research work has been done by taking optimized control strategy into consideration in the wind farm design phase. Hence, the main contributions of this paper can be two folders: 1) Different from literature [15]-[19], the optimized control strategy is taken into consideration in the wind farm design phase in this work. 2) Overall optimization of a regular shaped wind farm considering three aspects: the direction of the wind farm placement, the spacing of each pair of WT's and the wind farm control strategy.

Similar to previous work, LPC is also chosen as the evaluation index in this work; this considers the power losses, total power production of WT's as well as the capital investment. To increase the possibility of finding the global optimum, an adaptive PSO (APSO) is adopted to optimize the WT layout. The FINO3 reference wind farm is chosen as the study case to verify the effectiveness of the new method.

The paper is organized as follows. Section II presents the mathematic models of the wind farm. Section III describes the formulation of objective function while APSO algorithm and the optimization framework are specified in Section IV. Test cases are given in Section V. Eventually, conclusions are discussed in Section VI.

## II. MATHEMATICAL MODELS OF WIND FARM

Due to the wake effect, there would be energy losses inside

wind farm. The wind farm layout optimization (WFLO) should be done by considering the wake effect so that more benefits can be obtained by the wind farm owner. In this section, the wake model which is used to calculate the wind speed reached at each WT of the offshore wind farm is firstly described then the energy model is presented to calculate the energy production considering the wake losses.

#### A. Wake Model

The wind speed arrived at the blade of the downstream WTs could be affected, partial affected or non-affected by the wakes that generated by the upstream WTs. The multiple wake interaction within the wind farm is illustrated in Fig. 1.

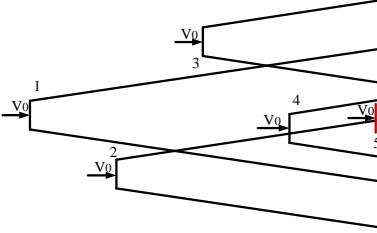


Fig. 1. Schematic of multiple wake.

In Fig.1, the number shows the sequence number of each WT and it can be seen that WT 5 (highlighted with brown color) is totally affected by the wake that generated by WT 1, 4 and partially affected by the wake that generated by WT 2 while there are no wake effects on WT 2 and 3. This simple example indicates that the wind speed deficit calculation will involve superposition procedure; moreover, this process will be changed with different wind speed which will make the wake losses estimation more complex. In [7], a detailed mathematical wake model has been described which is a good way of solving the above problem. However, due to the discretization of the wind speed and wind direction, there may occur “free wake” areas. The authors in [20] pointed out this drawback and succeeded in fixing this problem by introducing a smooth transition between different wind directions. In [21], a wake model which is similar to [7] has been proposed and through comparison with the result obtained from commercial software WAsP (Wind energy industry-standard software) [22], it showed a good agreement for wake loss estimation. Hence, the same model in [21] has been adopted to calculate the energy yields of the wind farm. The energy yields of the whole wind farm can be derived step by step in the following:

$$V_{ij} = V_0 - V_0 \left( 1 - \sqrt{1 - C_t} \right) \left( \frac{R_0}{R_{ij}} \right)^2 \left( \frac{S_{overlap,ij}}{S_0} \right) \quad (1)$$

$$R_{ij} = R_0 + k_d x_{ij} \quad (2)$$

$$V_{mn} = V_0 \left[ 1 - \sqrt{\sum_{i=1}^{N_{row}} \sum_{j=1}^{N_{col}} \left[ 1 - \left( \frac{V_{ij}}{V_0} \right) \right]^2} \right] \quad (3)$$

#### B. Energy Model

In [1]-[13], the MPPT control strategy is adopted as the wind farm control strategy to conduct the wind farm layout optimization work while in this work the power production of each WT is obtained by an optimized pitch angle control method which has been done in a previous work [19]. The

total power production can then be obtained as follows:

$$P_{m,mn} = 0.5 \rho C_{p,mn} (\beta_{mn}, \lambda_{mn}) \pi R_0^2 v_{mn}^3 / 10^6 \quad (4)$$

$$P_{tol} = \sum_{m=1}^{N_{col}} \sum_{n=1}^{N_{row}} P_{m,mn} \quad (5)$$

The power losses in three phase AC cable can be calculated using the following equations:

$$P_{loss,i} = 3 I_i^2 R_{e,i} \quad (6)$$

$$R_{e,i} = \rho_{R,i} \frac{L_{R,i}}{S_{R,i}} \quad (7)$$

Compared to [21], a new way to calculate the power losses along the cables is proposed and illustrated in Fig. 2.

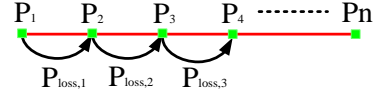


Fig. 2. The illustration of power losses calculation.

Assume the power losses of  $n$  WTs in a line are to be calculated as shown in Fig. 2. Each green square represents a WT while the red line indicated the cable connection layout. Here, the power losses along the cables between each pair of WTs can be expressed as:

$$P_{loss,n} = \left( \frac{\sum_{n=1}^N P_n - \sum_{n=1}^{N-1} P_{loss,n}}{\sqrt{3} U_{n, rated}} \right)^2 R_{e,n} \quad (8)$$

As can be seen from the (1)-(8), the precise power losses calculation should be a hierarchical process rather than independent calculation. The total losses within the wind farm can be calculated by summing up all the power losses along each cable as follow:

$$P_{tol, loss} = \sum_{j=1}^N P_{loss,j} \quad (9)$$

From (1) to (9), the average energy production of the wind farm can be expressed as follow:

$$E_{tol, av} = \sum_{t=1}^{T_E} (P_{tol,t} - P_{tol, loss,t}) T_t / T_E \quad (10)$$

### III. PROBLEM FORMULATION

A good WT layout design will satisfy both the maximization of energy yields and minimization of corresponding investment. In this section, the formulation of evaluation index, *LPC*, is specified at first then the assumptions are presented.

#### A. LPC

*LPC* index which includes both total discounted costs and the total discounted energy output is adopted to set up the objective function. In this work, only the cost of cables is included which is obtained by the model in [25]. The analytical equations are listed as follows:

$$C_i = A_p + B_p \exp \left( \frac{C_p S_{rated,i}}{10^8} \right)^2 \quad (11)$$

$$S_{rated,i} = \sqrt{3} I_{i,rated} U_{i,rated} \quad (12)$$

Then, the *LPC* of the offshore wind farm can be derived step by step based on the analytical equations in [24].

$$CAP_i = \sum_i^N C_i L_i Q_i \quad (13)$$

$$C_0 = \sum_{t=1}^{Ny} CAP_t (1+r)^{-t} \quad (14)$$

$$LPC = \left[ \frac{C_0 r (1+r)^{Ny}}{(1+r)^{Ny} - 1} + OAM_t \right] \frac{1}{E_{tot,av}} \quad (15)$$

### B. Wind Farm Direction

The wind direction is defined as the bearing of the wind source while the wind farm direction is defined in the opposite, anticlockwise, direction, as illustrated in Fig. 3. The black squares represent the WTs while the purple dotted line shows the central axis. In the simulation, the wind farm is assumed to be rotated around its geometric center.

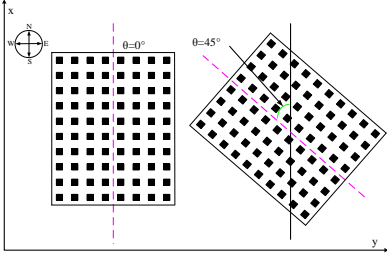


Fig. 3. Illustration of wind farm direction.

### C. Objective Function

In order to optimize the WT layout, four factors are considered in this paper, that is, the spacing of WTs in the *x* direction ( $Opt_1$ ) and in the *y* direction ( $Opt_2$ ), the wind farm direction ( $Opt_3$ ) as well as the pitch angle of each WT corresponding to a different wind speed ( $Opt_4$ ).

$$\text{Objective: } \min \{LPC(Opt_{1-4})\} \quad (16)$$

$$\text{Variables: } Opt_1 : d_{x,i} \dots d_{x,Num\_row-1} \quad (17)$$

$$Opt_2 : d_{y,j} \dots d_{y,Num\_col-1} \quad (18)$$

$$Opt_3 : \theta \quad (19)$$

$$Opt_4 : \beta_{mn,t} \dots \beta_{Num\_rowNum\_col,T_E} \quad (20)$$

$$\text{Constraints: } 8R \leq Opt_1 \leq 40R, 8R \leq Opt_2 \leq 40R \quad (21)$$

$$-90 \leq Opt_3 \leq 90 \quad (22)$$

$$0 \leq Opt_4 \leq \beta_{mn,max} \quad (23)$$

$$\omega_{mn,k} \leq \omega_{max} \quad (24)$$

$$\frac{\partial C_{p,mn,k}(\beta_{mn,k}, \lambda_{mn,k})}{\partial \lambda_{mn,k}} \leq 0 \quad (25)$$

In order to ensure the WT does not fall into the stall region, the tip speed ratio,  $\lambda$ , has to be limited to the right side of  $C_p-\lambda$  curve. This condition is expressed as (25).

### D. Assumptions

In this simulation, some assumptions are made as follows:

- 1) Each cable is assumed to be operating at nominal voltage.
- 2)  $d_{x,i}$  and  $d_{y,j}$  as illustrated in Fig. 5,  $\in [8R_0, 40R_0]$ . For the sake that the lifetime of the turbine will decrease greatly due to turbulence if they are closer than  $8R_0$  [26].

## IV. PROPOSED METHODOLOGY

Heuristic algorithms are widely used in solving the nonlinear problems. In this paper, an adaptive control strategy is adopted to further improve the performance of PSO. The mechanism of this algorithm is introduced at first and the optimization flowchart for this problem is specified in the end.

### A. APSO

For a non-convex problem, evolutionary algorithms as GA and PSO should be a good choice, with a good chance of finding the optimal solution for the nonlinear optimization problem. In this project, the PSO algorithm is adopted to implement the simulation since it has higher computational efficiency for solving nonlinear problems with continuous design variables compared with GA [27]. The PSO algorithm was first proposed by Kennedy and Eberhart [28] in 1995. In order to increase the global searching ability of PSO, the algorithm is further modified into a global version (GPSO) as follows [29].

$$v_i^{k+1} = wv_i^k + l_1 r_1 (local_i^k - x_i^k) + l_2 r_2 (global^k - x_i^k) \quad (26)$$

$$x_i^{k+1} = x_i^k + v_i^{k+1} \quad (27)$$

For PSO, the final result is sensitive to the settings of the parameters. A larger  $w$  ensures a stronger global searching ability while smaller  $w$  will increase the local searching ability of algorithm. In order to conquer this drawback, much work has been conducted on parameter control methods which can be divided into two categories [30]: time-varying control strategies [31]-[34] and an adaptive parameter control strategy [35]. The first strategy indicate that the PSO performance can be improved by using linear, non-linear or fuzzy adaptive inertia weight while the other introduces an evolutionary state estimation (ESE) technique [36] to further improve the performance of PSO. In this project, the adaptive parameter control method is adopted to further improve the final solution. The specification of APSO can be found in [35].

### B. Penalty Function

As mentioned in section IV.A, the APSO algorithm can be used to get a near optimal solution of the unconstrained optimization problem, in other words, the *LPC* can be minimized by APSO. However, not all solutions are feasible. In order to satisfy (25), a penalty function [37] is defined as follow:

$$\phi(\beta_{mn,k}) = \max\left(\frac{\partial C_{p,mn,k}(\beta_{mn,k}, \lambda_{mn,k})}{\partial \lambda_{mn,k}}, 0\right) \quad (28)$$

Then, the objective function can be written as follows:

$$\min(LPC) = \min \left\{ \frac{(C_0 + \sum_{m,n,k} \phi(\beta_{mn,k})PF)r(1+r)^{Ny}}{(1+r)^{Ny} - 1} + OAM_t \left[ \frac{1}{E_{tol,av}} \right] \right\} \quad (29)$$

The penalty factor, PF, is 1000000 in this simulation which is decided by trial and error. In (28), the function will be greater than zero if (25) is not satisfied. Then the objective function will be penalized by using this infeasible solution. In PSO, the particle will tend to move to find the best solution to benefit the objective function. The utilization of penalty function will give the particles in PSO a direction or signal of not moving into that infeasible region which is a common way of transferring constrained optimization problem into an unconstrained optimization problem so that the computational time can be saved.

### C. Optimization Flowchart

As proposed above, the *LPC* index is used to evaluate the wind farm layout. The optimization flowchart of wind farm layout by PSO is shown in Fig. 4. The parameters for the PSO are initialized in the first step. A randomly generated particle which contains two parts information: wind farm layout,  $d_x$  and  $d_y$  as well as the control strategy will be used to get the power production from all WTs at first. Then the power losses and cost will be calculated based on the predefined cable connection layout. After that, the *LPC* will be calculated based on the energy yields and total cost obtained above. The penalty function is the last step that will be activated in this fitness function. If the condition (25) is not satisfied, the objective function will be penalized as described in section IV.B which will result in a higher value of *LPC*. Then the position will be updated to find the minimum *LPC*. The *LPC* is calculated in a Fitness function. The function will be run when a new position is loaded. The above procedure does not stop the PSO main function until the objective value become intact for 50 iterations. Finally, the optimal  $d_{x,i}$  and spacing in the y direction  $d_{y,j}$  as well as the wind farm control strategy which contributes to the minimum *LPC*, will be selected.

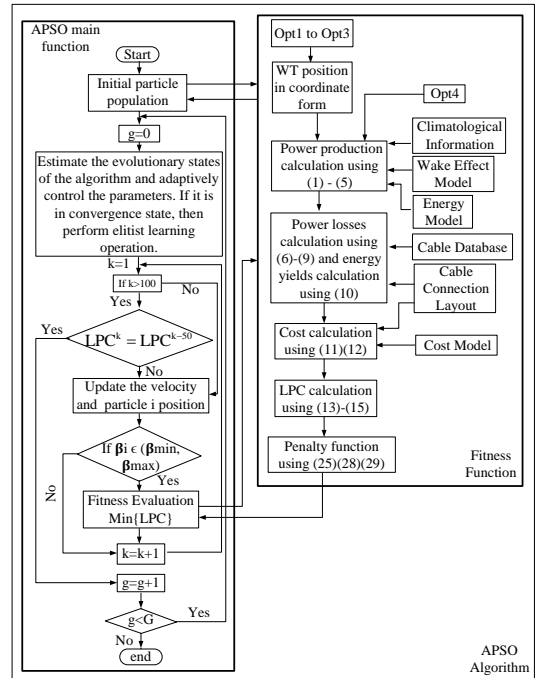


Fig. 4. The optimization flowchart for solving the proposed method.

The climatological information and cable database are the same as what we used in a previous work [21].

## V. CASE STUDY

In this section, a reference wind farm is first introduced and then two study cases are presented. Several trials have been done in PSO to increase the possibility of getting the global optimal solution in this section.

### A. Modified FINO3 Reference Wind Farm

The reference wind farm is assumed to be located in the vicinity of FINO3 to the west of the German island of Sylt. The installed capacity of the wind farm is 400MW [38][39]. The OS is assumed to be located 55km from the onshore substation. The cable connection layout and the WT layout before optimization are assumed to be as in Fig. 5.

TABLE I

NREL 5MW WT SPECIFICATION [40]	
Parameter	5 MW NREL WT
Cut-in Wind Speed	3 m/s
Rated Wind Speed	11.4 m/s
Cut-out Wind Speed	25 m/s
Rotor Diameter	126 m
Rated Power	5 MW

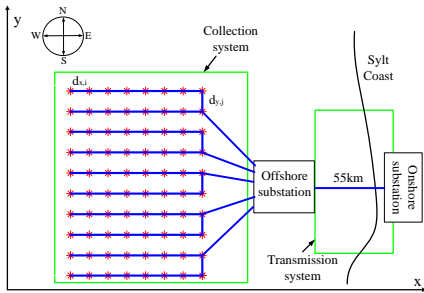


Fig. 5. The cable connection layout and WT's positions.

As listed in Table I, the NREL 5MW WT is selected as the reference WT. The input wind speed is illustrated in Fig. 6 in the format of wind rose.

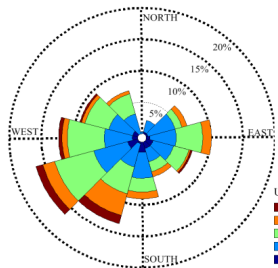


Fig. 6. Statistic wind speed illustration for wind climate near FINO3.

Instead of using probabilistic models, such as a Weibull distribution function to estimate the power production of a wind farm, the wind rose is adopted to calculate the wind farm energy yields during the optimization process in this paper. The wind rose is generated statistically based on the measured time series wind speed. Detailed information about the wind rose is specified in [21].

### B. Wind Farm Direction Optimization

In order to see the impact of the wind farm direction on the final result, the distance between WTs in the x direction or y direction as indicated in Fig. 5 is assumed to be 7 rotor diameters (7D) in this case. The optimization variable is the wind farm direction. As can be seen from Fig. 7, the wind farm is assumed to be rotated around the center. (a) is the original layout, (b) is the designed layout according to the wind speed distribution which means that the longer side of the wind farm should face towards or, in other words, the wind farm direction should be perpendicular to the maximum wind resource distribution direction as can be seen from Fig. 6 and (c) is the optimized WT layout. The final layout is compared with the other two layouts as shown in Fig. 7 and the specifications are listed in Table 2. In this optimization problem, only one optimization variable, that is the wind farm direction, is included. Hence, the population size is defined as 15.

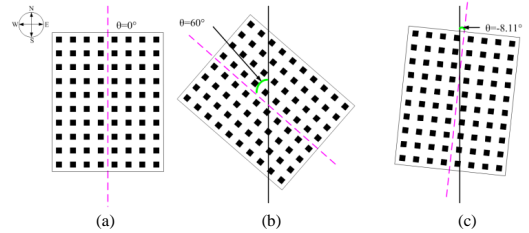


Fig. 7. The wind farm directions illustrated of different WT layout. (a) The original layout. (b) Industrial designed layout. (c) Optimized WT layout considering wind farm direction.

TABLE II  
SPECIFICATION OF WIND FARM DIRECTION OPTIMIZATION

	Wind farm direction (°)	Energy yields without considering Power losses (GWh)	Power losses (GWh)	Cost of cables (MDkk)	LPC (Dkk/MWh)
(a)	0	1972.9	34.24	345.25	178.14
(b)	60	1981.6	35.69	372.95	191.71
(c)	-8.11	2172.9	39.17	345.15	161.80

It can be seen from Table II that the optimized layout, (c), can reduce the LPC by 9.17% and 15.60% respectively compared with layouts (a) and (b). Empirically, the regular shaped wind farm should be established facing the most abundant wind resource direction. As can be seen from Fig. 6, the wind resource from the left lower corner takes the highest proportion. Hence, the wind farm in Fig. 7. (b) is placed facing to this direction. The result shows that (b) can only increase the energy by 0.69% , however, due to the increase in power losses and cost of cables, the LPC is increased by 7.63% compared with (a). Clearly, wind farm direction optimization can improve the wind farm performance significantly. In order to increase the possibility of getting the global optimal solution, the PSO program is run 10 times and the final solution is selected as the one with minimal LPC. The distributions of objective values using either GPSO or APSO are illustrated in Fig. 8.

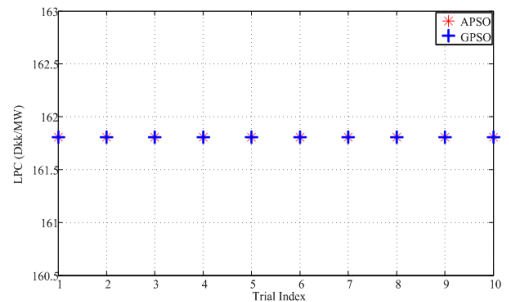


Fig. 8. The objective value distribution from running two types of PSO 10 times.

From Fig. 8, it can be seen that the final results are all stabilized around 161.8 for 10 trials using either APSO or GPSO. There is no difference between using APSO and GPSO if the optimization problem is simple.

The interval search method is also adopted here to help find the optimal solution. The results are illustrated in Fig. 9 and redrawn as a spider net plot in Fig. 10.

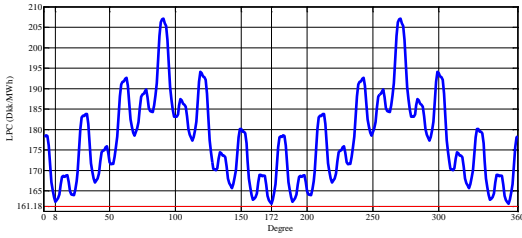


Fig. 9. LPC value corresponds to each degree.

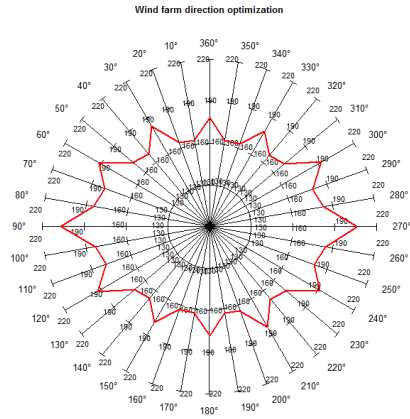


Fig. 10. The spider net plot for the wind farm direction optimization.

It can be seen from Fig. 9 that the lowest objective value happens a little bit over 352 degree which is close to the result (-8.18 degree) found by PSO.

### C. WT Siting Optimization

Three scenarios are presented in this part. The detailed information is specified as follows:

- Scenario I: WT interval optimization (In this scenario, the optimization variables are  $Opt_1$  and  $Opt_2$ )
- Scenario II: WT interval and wind farm direction optimization (In this scenario, the optimization variables are  $Opt_1$  to  $Opt_3$ )
- Scenario III: Pitch angle optimization based on layout obtained in Scenario II (In this scenario, the optimization variable is  $Opt_4$ )
- Scenario IV: WT position optimization under optimized control method (In this scenario, the optimization variables are  $Opt_1$  to  $Opt_4$ ),

In order to increase the visualization, the WTs' positions in different layouts (Because Scenario III's layout is the same as Scenario II, only three layouts are presented in Fig. 9.) are drawn in one figure as Fig. 9.

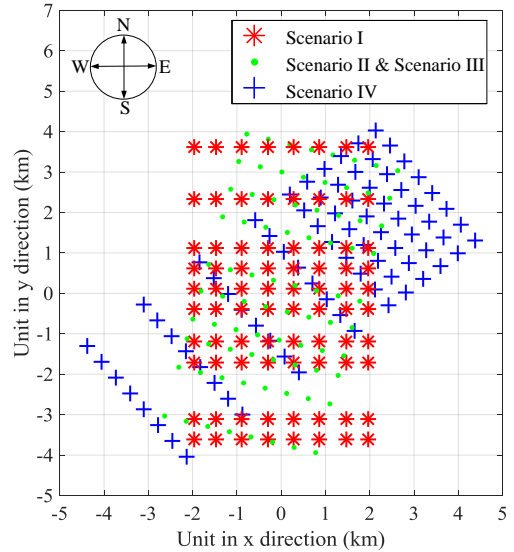


Fig. 11. The WT position illustration for each scenario.

As can be seen in Fig. 11, the red stars shows the WT positions for Scenario I, green dots are the WT positions for Scenario II and the WT positions for Scenario IV are indicated with the blue plus signs. It can be noticed that not only the difference of wind turbine spacing among each scenario exists, but also the wind farm direction varies.

In order to get a near optimal solution, the PSO program is run 20 times. The objective values for each optimized layout are compared in Fig. 12 through Fig. 15 respectively.

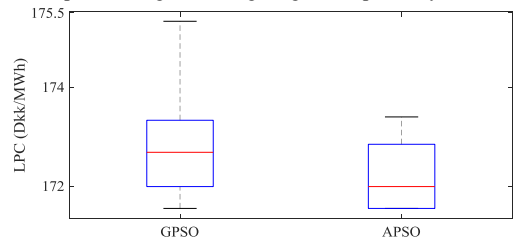


Fig. 12. Boxplot for WT spacing optimization using PSO.

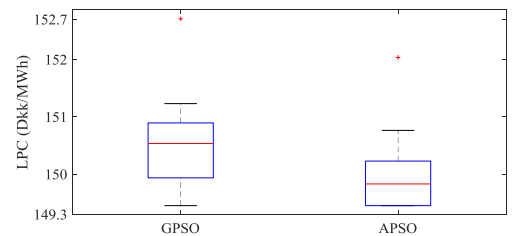


Fig. 13. Boxplot for WT spacing and wind farm direction optimization using PSO.

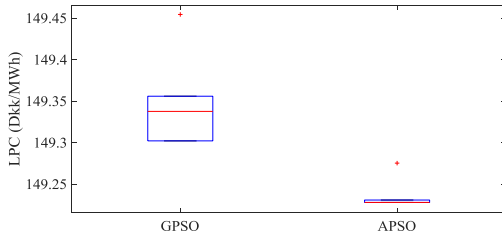


Fig. 14. Boxplot for pitch angle optimization based on layout obtained in Scenario II using PSO.

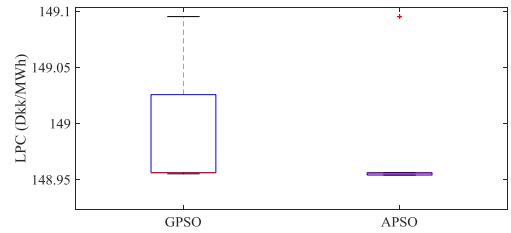


Fig. 15. Boxplot for overall WT position optimization using PSO.

The performance of GPSO and APSO is compared in Table III.

TABLE III  
COMPARISON BETWEEN GPSO AND APSO

	Best Solution (Dkk/MWh)		Average value of 10 trial Solution (Dkk/MWh)		Computation Time for best trial (s)		Population size of PSO		Iteration	
	GPSO	APSO	GPSO	APSO	GPSO	APSO	GPSO	APSO	GPSO	APSO
<b>Scenario I</b>	171.5471	171.5471	172.7273	172.1280	2226	3729	30			50
<b>Scenario II</b>	149.4544	149.4544	150.5313	149.9669	8421	10396	35			70
<b>Scenario III</b>	149.3021	149.2279	149.3356	149.2314	80852	83983	100			120
<b>Scenario IV</b>	148.9563	148.9542	148.9910	148.9832	113170	124605	120			230

#### D. Results and Discussion

The performances of optimized layouts from the four scenarios are summarized in Table IV as follows.

TABLE IV  
SPECIFICATION OF WIND FARM DIRECTION OPTIMIZATION

	Wind farm direction (°)	Energy yields (GWh)	Power losses (GWh)	Cost of cables (MDkk)	LPC (Dkk/MWh)
Scenario I	0	1884.3	31.50	317.75	171.55
Scenario II	-14.89	2143.9	37.85	314.67	149.45
Scenario III	-14.89	2147.2	37.94	314.67	149.23
Scenario IV	-50.63	2096.4	36.74	306.70	148.95

It can be seen in Table IV that the optimized layouts in Fig. 7. (c) and Scenarios I through IV can reduce the *LPC* by 9.17%, 3.70%, 16.10%, 16.23% and 16.38% respectively compared with the original layout as illustrated in Fig. 7. (a). By simply optimizing the wind farm direction, the *LPC* can be further reduced by 5.68% compared with the  $d_x$  and  $d_y$  optimized layout (Scenario I) while the  $d_x$  and  $d_y$  optimized layout considering wind farm direction optimization (Scenario II) outperforms the wind farm direction optimization layout by further reducing *LPC* by 7.63%. Essentially, the purposes of optimizing the wind farm direction or spacing between WTs are both finding the tradeoff between reducing wake losses and reducing investment on cables. From the simulation, it can be concluded that wind farm direction optimization is an important factor of wind farm layout design and sometimes even more importance than optimizing the spacing between WTs.

When the wind farm's control strategy is also optimized as in Scenario III and IV, the *LPC* can only be improved 0.15% and 0.33% compared with Scenario II. This is because the optimized control strategy aims at redistributing the wake losses among the WTs within the wind farm. This strategy would have a greater effect if the wind farm is poorly-designed and the wake effects between the WTs are strong; however, in our case, the WT layout has already been well

designed. There should not be so much wake effect for the optimized control strategy to play with. As a result, there is no significant improvement from using the optimized wind farm control strategy. This result also corresponds to our previous work [19] in which the *LPC* reduction of offshore wind farm using optimized power dispatch strategy was not significant as well.

The best layout in this simulation should arise from Scenario IV. The wind farm direction is around -50 degrees which is contrary to the empirically designed layout as shown in Fig. 7. (b) and the *LPC* is 22.30% better than in the empirically designed layout.

For this optimization work, APSO is adopted to help find a near optimal solution. From simulation, it can be seen that the APSO can find a better solution when there are more optimization variables as in Scenarios I through IV. For simpler problems such as the wind farm direction optimization, APSO and GPSO find the same final solution, but APSO needs more computation time.

In reality, the performance of wind farm is also related to the submarine topography which decides the cost of installation as well as the feasibility of cable and wind turbine installation, and can be used as constraint conditions. However, this kind of data is often difficult to obtain. Hence, this work is concentrated on the wind farm layout optimization together with wind farm control strategy design without considering the influence of land configuration.

#### VI. CONCLUSIONS AND FUTURE WORK

A cost-effective wind farm should harvest energy with less investment which make both wind farm layout design as well as control strategy critical. Moreover, the wind farm direction for a regular shaped wind farm has been proved to have a great impact on the energy yield as well. Here it is possible to differ from the traditional design method which optimized the control strategy after the wind farm is established. The results show that the proposed method can benefit the wind farm better than the other proposed layout design methods. However, there is still a limitation on the application of the proposed method, that is, the control strategy can only be

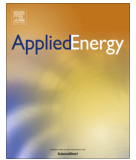


applicable based on an exact wake model which can predict the wind speed at each WT accurately.

In the future, the proposed optimization method will be applied into the WFLO of irregular shaped wind farm considering the cable connection layout optimization.

## REFERENCES

- [1] Mosetti G, Poloni C, Diviacco B., "Optimization of wind turbine positioning in large wind farms by means of a genetic algorithm," *Journal of Wind Engineering and Industrial Aerodynamics*, vol. 51(1), pp.105-116, 1994.
- [2] S. Grady, M. Hussaini, and M. Abdullah, "Placement of wind turbines using genetic algorithms," *Renewable Energy*, vol. 30, no. 2, pp. 259 – 270, 2005.
- [3] G. Marmidis, S. Lazarou, E. Pyrgioti, "Optimal placement of wind turbines in a wind park using Monte Carlo simulation," *Renewable Energy*, 33 (7), pp. 1455–1460, 2008
- [4] Narasimha Prasad Prabhu, Parikshit Yadav, Bhuneshwar Prasad and Sanjib Kumar Panda, "Optimal placement of off-shore wind turbines and subsequent micro-siting using Intelligently Tuned Harmony Search algorithm," *Power and Energy Society General Meeting (PES)*, 2013 IEEE, pp. 1-7, Vancouver, BC, Jul. 2013.
- [5] Sittichoke Pookpant, Weerakorn Ongsakul, "Optimal placement of wind turbines within wind farm using binary particle swarm optimization with time-varying acceleration coefficients," *Renewable Energy*, Vol. 55, pp. 266-276, Jul. 2013.
- [6] S.D.O. Turner, D.A. Romero, P.Y. Zhang, C.H. Amon, T.C.Y. Chan, "A new mathematical programming approach to optimize wind farm layouts," *Renewable Energy* 63 (2014), pp. 674-680.
- [7] A. Kusiak and Z. Song, "Design of wind farm layout for maximum wind energy capture," *Renewable Energy*, Vol. 35, No. 3, pp. 685-694, 2010.
- [8] Yunus Eroglu, Serap Ulusam Seçkiner, "Design of wind farm layout using ant colony algorithm," *Renewable Energy*, Vol. 44, pp. 53-62, Aug. 2012.
- [9] C.Wan, J.Wang, G. Yang, H. Gu, and X. Zhang, "Wind farm micro-siting by Gaussian particle swarm optimization with local search strategy," *Renewable Energy*, vol. 48, pp. 276–286, 2012.
- [10] S. Chowdhury, J. Zhang, A. Messa, L. Castillo, "Optimizing the arrangement and the selection of turbines for wind farms subject to varying wind conditions," *Renew Energy*, vol. 52, pp. 273–282, 2013.
- [11] Omid Rahbari, Majid Vafaeipour, Farivar Fazelpour, Michel Feidt, Marc A. Rosen, "Towards realistic designs of wind farm layouts: Application of a novel placement selector approach," *Energy Conversion and Management* 81, pp. 242–254, 2014.
- [12] X. Gao, H. Yang, and L. Lu, "Investigation into the optimal wind turbine layout patterns for a Hong Kong offshore wind farm," *Energy*, vol. 73, pp. 430–442, 2014.
- [13] Wu Yuan-Kang, Lee Ching-Yin, Chen Chao-Rong, Hsu Kun-Wei, Tseng Huang-Tien, Optimization of the wind turbine layout and transmission system planning for a large-scale offshore wind farm by AI technology," *IEEE Trans. on Industry Applications*, Vol. 50, Issue 3, pp. 2071-2080, 24 Sep. 2013.
- [14] Whei-Min Lin, Chih-Ming Hong, Intelligent approach to maximum power point tracking control strategy for variable-speed wind turbine generation system, *Energy*, 35 (6), pp. 2440–2447, 2010.
- [15] Javier Serrano González, Angel G. Gonzalez Rodriguez, José Castro Morac, Jesús Riquelme Santosa, Manuel Burgos Payana, "Optimum Wind Turbines Operation for Minimizing Wake Effect Losses in Offshore Wind Farms," *Renewable Energy*, Vol. 35, Issue 8, pp. 1671-1681, Aug. 2010.
- [16] Jaejoon Lee, Eunkuk Son, Byungho Hwang, Soogab Lee, "Blade pitch angle control for aerodynamic performance optimization of a wind farm," *Renewable Energy*, pp. 124-130, 10th Sep. 2012.
- [17] A. Behnood, H. Gharavi, B. Vahidi, G.H. Riahy, "Optimal output power of not properly designed wind farms, considering wake effects," *Electrical Power and Energy Systems*, Vol. 63, pp. 44-50, Dec. 2014.
- [18] Javier Serrano González a, Manuel Burgos Payán, Jesús Riquelme Santos, Angel Gaspar González Rodriguez, "Maximizing the overall production of wind farms by setting the individual operating point of wind turbines," *Renewable Energy* 80, pp. 219-229, 2015.
- [19] Peng Hou, Weihao Hu, Baohua Zhang, Mohsen Soltani, Cong Chen, Zhe Chen, "Optimised power dispatch strategy for offshore wind farms," *IET Renewable Power Generation*, pp. 11, 2015.
- [20] Daniel Lückehe, Markus Wagner, Oliver Kramer, "On Evolutionary Approaches to Wind Turbine Placement with Geo-Constraints," *Proceedings of the 2015 Annual Conference on Genetic and Evolutionary Computation (GECCO '15)*, pp. 1223-1230, 2015.
- [21] Peng Hou, Weihao Hu, Mohsen Soltani, Zhe Chen, "Optimized Placement of Wind Turbines in Large Scale Offshore Wind Farm using Particle Swarm Optimization Algorithm," *IEEE Transactions on Sustainable Energy*, Vol: 6, Issue: 4, pp.1272-1282, 2015.
- [22] Link: <http://www.wasp.dk/>
- [23] Fernando Port e-Agel, Yu-TingWu, Chang-Hung Chen, "A Numerical Study of the Effects of Wind Direction on Turbine Wakes and Power Losses in a large Wind Farm," *Energies*, vol. 6, pp. 5297-5313, MDPI, 2013.
- [24] M. Zhao, Z. Chen, F. Blaabjerg, "Optimization of Electrical System for Offshore Wind Farms via Genetic Algorithm," *IET Proc. – Renewable Power Generation*, Vol. 3, Iss. 2, June 2009, pp. 205-216.
- [25] S. Lundberg, "Performance comparison of wind park configurations," Department of Electric Power Engineering, Chalmers University of Technology, Department of Electric Power Engineering, Goteborg, Sweden, Tech. Rep. 30R, Aug. 2003.
- [26] Beatriz Pérez, Roberto Mínguez, Raúl Guanche, "Offshore wind farm layout optimization using mathematical programming techniques," *Renewable Energy*, Vol. 53, pp. 389-399, May 2013.
- [27] R. Hassan, B. Cohanim, O. de Weck, "A comparison of particle swarm optimization and the genetic algorithm," in *Proceedings of the 46th AIAA/ASME/ASCE/AHS/ASC structures, structural dynamics and materials conference*, 2005.
- [28] Kennedy, J., Eberhart, R., "Particle swarm optimization," *Proc. IEEE Int. Conf. Neural Networks*, pp. 1942–1948, Apr. 1995.
- [29] Kennedy, J., "The particle swarm: social adaptation of knowledge," *Proc. IEEE Int. Conf. Evolution of Computing*, Indianapolis, IN, pp. 303–308, 1997.
- [30] Mengqi Hu, Wu, T., Weir, J.D., "An adaptive particle swarm optimization with multiple adaptive methods," *IEEE Transactions on Evolutionary Computation*, Vol. 17, pp. 705-720, 10 Dec. 2012.
- [31] Y. Shi and R. C. Eberhart, "Empirical study of particle swarm optimization," in *Proc. Congr. Evol. Comput.*, 1999, pp. 1950–1955.
- [32] B. Jiao, Z. Lian, and X. Gu, "A dynamic inertia weight particle swarm optimization algorithm," *Chaos, Solitons Fractals*, vol. 37, pp. 698–705, Aug. 2008.
- [33] Y. Shi and R. C. Eberhart, "Fuzzy adaptive particle swarm optimization," in *Proc. Congr. Evol. Comput.*, pp. 101–106, 2001.
- [34] R. C. Eberhart and Y. Shi, "Tracking and optimizing dynamic systems with particle swarms," in *Proc. Congr. Evol. Comput.*, 2001, pp. 94–100.
- [35] Z.-H. Zhan, J. Zhang, Y. Li, and H. S.-H. Chung, "Adaptive particle swarm optimization," *IEEE Trans. Syst., Man, Cybern. B, Cybern.*, vol. 39, no. 6, pp. 1362–1381, Apr. 2009.
- [36] J. Zhang, H. S.-H. Chung, and W.-L. Lo, "Clustering-based adaptive crossover and mutation probabilities for genetic algorithms," *IEEE Trans. Evol. Comput.*, vol. 11, no. 3, pp. 326–335, Jun. 2007.
- [37] S.P. Neill, M.R. Hashemi, M.J. Lewis, Optimal phasing of the European tidal-stream resource using the greedy algorithm with penalty function, *Energy*, 73, pp. 997–1006, 2014.
- [38] FINO3 - research platform in the North Sea and the Baltic No. 3. [Online]. Available: <http://www.fino3.de/en/>.
- [39] WP2014-Froya-NRWF NORCOWE Reference Wind Farm. [Online]. Available: <http://www.norcowe.no/>.
- [40] J. Jonkman, S. Butterfield, W. Musial, and G. Scott, "Definition of a 5-MW Reference Wind Turbine for Offshore System Development," Technical Report, NREL/TP-500-38060, Feb. 2009.



# Combined optimization for offshore wind turbine micro siting



Peng Hou, Weihao Hu\*, Mohsen Soltani, Cong Chen, Zhe Chen

Department of Energy Technology, Aalborg University, Pontoppidanstraede 101, Aalborg, Denmark

## HIGHLIGHTS

- The uncrossed cable connection layout (UCCL) was found by heuristic method.
- The UCCL was optimized simultaneously with the wind turbines' positions.
- The proposed method outperformed than traditional method by getting a lower LPC.
- The optimized layout reduced LPC by 5.00% than reference wind farm.

## ARTICLE INFO

### Article history:

Received 8 August 2016

Received in revised form 10 November 2016

Accepted 24 November 2016

### Keywords:

Mixed integer particle swarm optimization (MIPSO)

Wind farm layout optimization

Offshore substation (OS) locating

Cable connection configuration optimization

Levelized production cost (LPC)

## ABSTRACT

In order to minimize the wake loss, wind turbines (WT) should be separated with large intervening spaces. However, this will incur an increase in the capital expenditure on electrical systems and even in the operation and maintenance costs. In order to realize a cost-effective wind farm, an integrated optimization method in which the positions of the WTs and offshore substations (OS) and the cable connection configuration are optimized simultaneously is proposed in this paper. Since the optimization variables are both continuous and discrete, the mixed integer particle swarm optimization (MIPSO) algorithm is adopted to minimize the levelized production cost (LPC) of the wind farm. Simulation results are given for validating the proposed approach and comparison is made with results obtained using other methods. It is found that the proposed method can reduce the levelized production cost (LPC) by 5.00% and increase the energy yields by 3.82% compared with the Norwegian centre for offshore wind energy (NORCOWE) reference wind farm layout. This is better than the traditional method which only achieves a 1.45% LPC reduction although it increases the energy yields by 3.95%.

© 2016 Elsevier Ltd. All rights reserved.

## 1. Introduction

Offshore wind farms have some advantages, such as higher energy production, less wake turbulence and lower environmental impact compared with onshore wind farms. However, the investment is higher. More and more research is concentrating on the optimization of offshore wind farms to establish a cost-effective wind farm. This involves two sorts of optimization: the optimization of WT positions and the optimization of the electrical system.

Generally, the wind farm construction zone will be chosen according to statistical data of measured wind speed. After that, the WTs' positions should be determined within that construction zone with the purpose of minimizing the wake losses. In [1], a review in optimal wind-turbine-micro-siting problem was performed comparing the latest research and highlighting the main factors that should be considered when solving the wind farm lay-

out optimization problem (WFLOP). It [1] indicated that the WFLOP can be solved using two models: one is a grid model which discretizes the sea area into grids, so the grid size or the number of the cells the sea is divided into decides the size of the solution space; the other is the continuous model which uses coordinates to represent the positions of the WT. In the earlier research, the offshore WFLOP was solved by partitioning the construction zone, assumed to be square, into identical grid squares so that the WT placement problem can be transferred into a combinatory optimization problem. As earliest mentioned in [2], the WFLOP can be solved using a genetic algorithm (GA) with the purpose of minimizing the cost of energy while [3] proposed a better result compared with [2] by tuning the GA parameters. Since then, different algorithms were adopted to solve the problem proposed in [1]: the results obtained by the Monte Carlo method in [4] was demonstrated to be more effective than [3] in finding a cost effective layout. Ref. [5] selected an intelligently tuned harmony search (ITHS) method which proved to be the best choice among GA, harmony search (HS) and improved harmony search (IHS) methods in most

\* Corresponding author.

E-mail addresses: [whu@et.aau.dk](mailto:whu@et.aau.dk) (W. Hu), [zch@et.aau.dk](mailto:zch@et.aau.dk) (Z. Chen).

## Nomenclature

$V_{at}$	input wind speed at the first line WT [m/s]	$N$	total number of wind turbines in a wind farm
$R_0$	radius of the WT's rotor [m]	$P_{tot,t}$	total power production during interval $t$ [MW]
$\beta$	pitch angle of WT [ $^\circ$ ]	$P_{tot,loss,t}$	total power losses during interval $t$ [MW]
$\lambda$	optimal tip speed ratio for the pitch angle $\beta$ , at which the power coefficient will be maximum	$TE$	the generated section of the wind rose
$\rho$	air density [kg/m <sup>3</sup> ]	$T_t$	duration when the wind farm generates power of $P_{tot,t}$ [h]
$V_{cut-in}, V_{cut-out}$	the cut-in and cut out wind speeds, the speeds at which the WT begins to generate power or shut down [m/s]	$E_{tot,av}$	mean energy yield in one year [MWh]
$V_{rated}$	the rated wind speed at which the WT reaches its rated power [m/s]	$t$	energy yields calculation time [h]
$C_p$	power coefficient of WT	$M_i$	unit cost of cable $i$ [MDkk/km]
$S_0$	the swept area of the WT rotor blade [m <sup>2</sup> ]	$S_{rated,i}$	rated apparent power of cable in line $i$ [W]
$S_{overlap}$	affect wake region [m <sup>2</sup> ]	$A_q, B_q, C_q$	coefficients in the cable cost model
$C_t$	thrust coefficient	$L_i$	length of cable $i$ [km]
$k_c$	decay constant	$Q_i$	quantity of cable $i$
$D$	diameter of WT rotor blade [m]	$CAP_t$	capital cost in year $t$ [Dkk]
$x$	the distance between the upstream and downstream WT along the wind direction [m]	$CAP_p$	present value of the capital cost [Dkk]
$P_{loss,1}$	power loss of cable 1 [MW]	$N_y$	economic lifetime of wind farm [year]
$I_1$	current in cable 1 [kA]	$r$	discount ratio
$R_{e,i}$	resistance of cable $i$ [ohm/m]	$Z$	the predefined area for constructing offshore wind farm
$\rho_R$	resistivity of cables [ohm * m]	$H_r$	test function for the distance constraint
$L_{R,i}$	length of cable $i$ [m]	$w$	inertia weight
$S_{R,i}$	sectional area of cable $i$ [m <sup>2</sup> ]	$l_1, l_2$	learning factors
$P_{loss,i}$	power losses of cable $i$ [MW]	$r_1, r_2$	random variables distributed uniformly on [0, 1]
$I_{i,rated}$	rated current of cable $i$ [A]	$x_i^k, x_i^{k+1}$	position of particle $i$ at iterations $k$ and $k+1$ respectively [m]
$U_{i,rated}$	rated voltage of cable $i$ [V]	$v_i^k, v_i^{k+1}$	speed of particle $i$ at iterations $k$ and $k+1$ respectively [m]
		$Lo_i^k$	best position of particle $i$ at iteration $k$ [m]
		$Go_i^k$	best position of any particle at iteration $k$ [m]

of the studied cases while the binary particle swarm optimization with time-varying acceleration coefficients (BPSO-TVAC) algorithm was presented in [6] and the obtained result was outperformed than 5 other heuristic algorithms at finding a better solution. Similarly, the WFLOP can also be solved by classic optimization methods. In [7], the quadratic integer programming (QIP) and mix-integer linear programming (MILP) method were adopted and the results were also compared with [2,3]. This was demonstrated to be an alternative method [7] to get a more cost-effective wind farm while saving computational time.

Using a grid model as in [2–7] to solve the WFLOP can simplify the problem. However, some potential solutions may be missed. In order to conquer this problem, a coordinate model was adopted to solve the WFLOP in [8–10]. An evolutionary algorithm was presented in [8] to optimize the WTs' positions within a circular construction zone under the constraint that the minimum distance between each pair is 4 WT rotor diameters. Later, the authors in [9] proposed an ant colony algorithm to place the WTs within the same wind farm as [8]. The paper [9] obtains an optimized wind farm layout utilizing a Gaussian PSO algorithm which proved to be outperformed than Grady's work by generating more energy yields and using less computational time. In [11], a mixed-discrete particle swarm optimization (MDPSO) algorithm was proposed to optimize the installation positions as well as the number of WTs. More realistic optimization work was done in [12], which used a GA to place the WTs while considering of load-bearing capacity, turbine hub height, soil conditions and prohibited locations. A wind farm layout investigation for Hong Kong was undertaken in [13]; a GA was adopted to implement the simulation and from the results it can be seen that the scattered layout has the minimal levelized cost of energy (LCOE) out of aligned, staggered and scattered layouts. Mathematical programming was used to solve WFLOP with a coordinate model to guarantee optimality. The

Horns Rev I wind farm layout was selected as the benchmark in [14,15] to compare with the optimal layout obtained using random search (RS) algorithm [14] and sequential convex programming (SQP) [15] respectively. A continuous wake model was proposed in [15] to formulate the wind farm power function and calibrated using CFD simulation data; the WFLOP was also solved using sequential convex programming which proved to be an efficient and fast approach to wind farm layout design. A hybrid optimization method was presented in [16] which used a heuristic method to set an initial layout and then used nonlinear mathematical programming techniques to find a local optimal solution in order to obtain a result closer to the global optimum. The differences between using various layout models (the grid model and the coordinate model) and cost models (the Masetti et al. model and Chen's model [17]) to solve the WFLOP based on GA were presented in [18] in a comparative study. Recently, a non-linear mathematical programming method (the interior point method) was presented to solve the WFLOP based on the grid model in [19]; this demonstrated that such a method had a higher efficiency than the GA.

From the above literature, it can be concluded that (1) Meta-heuristic or stochastic methods are mostly used to solve the WFLOP, due to the fact that WFLOP cannot be completely described using analytical equations. (2) Some recent published work used PSO frequently instead of GA to optimize the wind farm layout and obtained better solutions, which is in line with the conclusion in [1]. (3) The energy production of an offshore wind farm is estimated based on probabilistic models based on a large set of wind speed time series (for instance 10 years' wind speed measured at intervals of 3 h). However, due to the uncertainties in wind conditions, the energy generated over specific years may vary. Since the energy production is one of the dominant factors deciding the wind turbines' positions, the risk that wind farm investors must meet should be analyzed. This has been done in

[20–22]. In [20], the uncertainty about wind in both velocity and direction are mathematically expressed by a set of uncertainty scenarios with probabilities of occurrence. Then the expected value of the net present value (NPV) and the corresponding risk can be calculated based on the given wind turbine positions. A robust wind farm layout optimization was presented in [21]. Two models, non-parametric wind uncertainty (NPWU) and parametric wind uncertainty (PWU) model were proposed in [21] to characterize the uncertainties in estimated annual wind distributions. The PSO was adopted to find an optimized wind farm layout that minimizing the cost of energy (COE) while reducing uncertainties in the COE as much as possible. Besides uncertainties from variation in wind, that in demand for electricity also generates risk for the wind farm investors. Those two aspects were considered simultaneously with wind farm layout optimization in [22] with the purpose of minimizing the COE of the wind farm with a specified upper bound for risk. The above works focused on maximizing the annual energy production or minimizing the cost of energy using various simplified cost models, as specified in [1], by intelligent placement of the WTs. However, the investment into the electrical system, in particular the relation between electrical system design and the final investment was not taken into consideration.

When the WTs' locations have been determined, the electrical system layout should then be designed. The offshore wind farm electrical system (OWFES) optimization problem can be categorized into three parts, namely the combinatory optimization of the electrical equipment [23–26], the design of cable connection configuration and determining the number and location of OSs. In [25], the electrical system was designed by finding the best combination from the available database, which contains information on voltage level, electrical equipment and offshore wind farm type. The wind farm layout design comparisons regarding losses, reliability and total investment were performed in [26]. In the above works, the cable connection layout was designed empirically while the cost of cables can be reduced a lot if an appropriate method could be used in cable connection layout design. Imagining that the WTs are spread wide in sea, the power generated from each WT should be collected and transmitted to the onshore substation. If the WTs are regarded as vertices, then the problem can be reformulated into a mathematical problem of finding the minimum spanning tree (MST) of a given weighted graph [27]. Using the greedy algorithm [28] to minimize the cost of collection system (CS) of an offshore wind farm has been done in [29,30] which set the cost of cable in each branch as the weight so that a MST layout could be formulated. The Travelling Salesman Problem (TSP) [31] is another model that can be used to optimize the CS layout as presented in [32,33]. MST and TSP methods can be used to generate a deterministic result, but some potential solutions are omitted. In order to get a better result for this non-convex problem, GA was widely used in cable connection layout design [33–37]. The GA-TSP algorithm to optimize the cable connection layout of a large scale offshore wind farm with 4 OSs was presented in [33] and the results indicated that it has better performance than the method proposed in [35]. However, the method of [33] cannot ensure an entire uncrossed layout. Instead of using heuristic optimization method, a mixed integer linear programming (MILP) method was proposed in [38] to optimize the cable connection layout and cable cross-section simultaneously. Similarly, different methods such as clustering based algorithms, ant colony system algorithms and linear programming were also adopted to find a layout with minimal overall cost [39–41]. Traditionally, the OSs are centrally located as indicated in [42] from the practical point, while the best position to construct the OS is selected from a series of given locations in [41]. In [34], an overall optimization of the cable connection layout, OS location was investigated as well as the selection of electrical equipment, however, some assumptions

were made, such as centrally located OSs and an identical number of WTs in each cluster. In one of our previous works, [43], a more flexible cable connection layout design method was presented which can minimize the investment on cables while retaining an uncrossed scheme. Usually, the WTs' locations are optimized first and then the electrical system design will be done based on this optimized layout.

Through this literature study, it can be seen that many works have been written on optimizing wind farm layout or offshore wind farm electrical systems, in the order that the offshore wind farm layout is always first optimized to harvest the power output and the electrical system design work is based on the optimized layout. Though the authors in [44] tried to solve the WFLOP together with the cable connection layout design so that an overall cost-effective wind farm could be established, for that wind farm only had one offshore substation and the WFLOP was solved based on a grid model, which is not the real case in offshore wind farm construction planning. Besides, the proposed cable connection configurations [44] are crossed, which is impractical since such a layout will incur a higher cost of installation and maintenance.

In this paper, the wind farm optimization work is also focused on the overall offshore wind farm optimization like [44]. However, more improvement have been made, as follows: (1) Instead of a grid model, the coordinate model is used in this paper to solve the WFLOP together with the design scheme of cable connections. (2) The cable connection configuration was optimized with a heuristic method which can ensure an uncrossed layout. (3) The locations of 2 OSs were also expressed in the coordinate system and optimized simultaneously with the wind farm layout and cable connection configuration. The above three factors are actually synergistic, which have a combined influence on the performance of the planned offshore wind farm. Though [44] tried to make a breakthrough, the crossed cable connection layout as well as the grid based WFLO both makes the method in that paper unrealistic. The proposed integrated optimization method aims at solving the existing problem and makes the method applicable. It is expected that the designed wind farm should be more efficient than the layout obtained by the two-stage optimization method (firstly optimizing the wind farm layout and the designing the cable connection layout based on the optimized wind farm layout). In order to demonstrate our hypothesis, the Norwegian centre for offshore wind energy (NORCOWE) reference wind farm is chosen as a comparison case study.

The paper is organized as follows: The analytical equations for calculating the wind farm energy yields are derived first. Based on these, the WFLOP is then described in Section 2. Section 3 specifies the methodology that is used to implement the simulation, and simulation results and discussion are provided in Section 4. Conclusions are presented last.

## 2. Modelling of offshore wind farms

Wake speed deficits will reduce the energy efficiency of the wind farm. In order to estimate the energy yields of the wind farm accurately, the wake effect should be taken into consideration. The power production of a single WT is described first, and then the wake model is introduced. The energy yield calculation which is based on the above two models is proposed at the end.

### 2.1. Power production model of WTs

The output power of an individual WT can be changed by tuning its pitch angle or tip speed ratio. If the WTs are tuned to get the maximum power coefficient, then this control strategy is called the maximum power point tracking strategy (MPPT) method. In

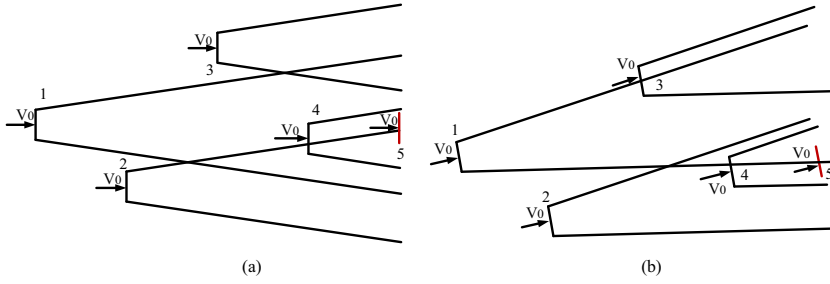


Fig. 1. Schematic of multiple wake. (a) Wind direction from west to east and (b) wind direction from southwest to northeast.

this work, the MPPT method is selected as the wind farm control strategy. Hence, the power production of each WT can be expressed as follows [45]:

$$P = \begin{cases} 0 & 0 \leq V_{at} \leq V_{cut-in} \\ 0.5\rho C_p(\beta, \lambda)\pi R_0^2 V_{at}^3 / 10^6 & V_{cut-in} < V_{at} \leq V_{rated} \\ P_{rated} & V_{rated} < V_{at} \leq V_{cut-out} \\ 0 & V_{cut-out} < V_{at} \end{cases} \quad (1)$$

## 2.2. Wake model

Presently, there are three widely used wake models: the Jensen model, the Ainslie model and the G.C. Larsen model [46]. The Jensen model is chosen in [2–17] as well as in this work. This is because the Jensen model needs less computational time to evaluate the energy losses [16] while permitting a high accuracy estimation of the power production [46]. On the assumption that the wake diameter develops linearly, the wind speed deficit can be obtained analytically with the following equation [47]:

$$U = V_0 \left( 1 - \frac{(1 - \sqrt{1 - C_t}) \left( \frac{S_{overlap}}{S_0} \right)}{\left( 1 + \frac{2k_x x}{D} \right)^2} \right) \quad (2)$$

In reality, the downstream WT's power production can be affected by wakes that are generated by several upstream WTs. In addition to this, the changing wind speed makes the wind speed deficit calculation even more complex. The multiple wake interaction considering wind speed variation is illustrated in Fig. 1.

This simple example indicates that the wind speed deficit calculation will require superposition and judgement procedures to solve this problem. An analytical model of wake loss estimation established based on the well-known Jensen model has been proposed in one of our previous works [48].

## 2.3. Energy yields considering power losses

The energy generated by each WT will be collected through a series of AC or DC submarine cables which are usually spread in the sea in a tree shaped layout. The power will flow from the end node of each WT cluster to the OS and then all the power will be transmitted to the onshore substation (in some cases, the power will be collected and then transmitted to the onshore substation directly). The power flow process is illustrated in Fig. 2.

In Fig. 2, the WTs are represented with red<sup>1</sup> stars while the blue lines show the cable connection layout. The dotted line indicates that the layout may be extended. Assuming the power losses of n

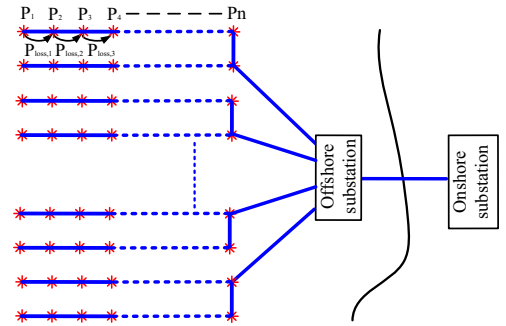


Fig. 2. The illustration of power losses along AC cables within the offshore wind farm.

wind turbines in a line are to be calculated, then the power losses along the cables can be calculated from the following equations:

$$P_{loss,1} = 3I_1^2 R_{e,1} \quad (3)$$

$$R_{e,i} = \rho_R \frac{I_{R,i}}{S_{R,i}} \quad (4)$$

$$P_{loss,i} = \left( \frac{\sum_{j=1}^N P_n - \sum_{j=1}^{N-1} P_{loss,j}}{\sqrt{3}U_{i,rated}} \right)^2 R_{e,i} \quad (5)$$

From this example, it can be seen that the power losses can be more accurately calculated by such a hierarchical process. Then the total losses within the wind farm can be obtained by summing all the losses along the cables as follows:

$$P_{tot,loss} = \sum_{j=1}^N P_{loss,j} \quad (6)$$

The total power production is the summation of output power from each WT which can be calculated by the wake model and power production model mentioned above.

$$P_{tot} = \sum_{n=1}^N P_{m,n} \quad (7)$$

Considering the variation in energy yield in different years, the average energy yield of the wind farm can be derived by the following equation:

$$E_{tot,av} = \sum_{t=1}^{T_E} (P_{tot,t} - P_{tot,loss,t}) T_t \quad (8)$$

<sup>1</sup> For interpretation of color in Figs. 2, 4 and 8, the reader is referred to the web version of this article.

### 2.4. Cost model

Theoretically, if there is enough space to install the WTs, the wake losses can be minimized, but this will increase the investment in the electrical system. The optimized layout should consider both impacts on the cost-effectiveness of the wind farm. In this work, only the cable cost is considered which can be expressed as follows [49]:

$$M_i = A_q + B_q \exp\left(\frac{C_q S_{rated,i}}{10^8}\right)^2 \quad (9)$$

$$S_{rated,i} = \sqrt{3} I_{i,rated} U_{i,rated} \quad (10)$$

$$CAP_t = \sum_i^N M_i L_i Q_i \quad (11)$$

### 3. Wind farm layout optimization

Heuristic algorithms are widely used to solve non-linear problems. In this paper, the APSO method is adopted as the optimization method. First the objective function is derived on the basis of leveled production cost (LPC). The methodology and the optimization procedure are presented.

#### 3.1. Problem formulation

From the economic point of view, a well-designed wind farm should generate more and pay less. If we take the whole wind farm lifetime into account, then the performance of the planned wind farm can be evaluated with the LPC index. The LPC for offshore wind farm has already been derived in [50] as:

$$CAP_p = \sum_{t=1}^{Ny} CAP_t (1+r)^{-t} \quad (12)$$

$$LPC = \frac{CAP_p r (1+r)^{Ny}}{(1+r)^{Ny} - 1} \frac{1}{E_{tol,av}} \quad (13)$$

In this work, the objective function is constructed on the basis of LPC. The optimization method will update the solution again and again until an acceptable LPC is found. It is easy to ensure all the solutions are found without crossing the predefined boundary condition. However, not all solutions are feasible. Because the turbulence is so severe if the WTs are placed closer than 4 rotor diameter (4D) as to incur a reduction in the life time of the wind farm [16], the WTs are expected to be placed within a predefined area, Z, under the constraint that the distance between each pair of WTs should be over 4D. In order to solve this problem, a penalty function is defined in this work. Then the optimization problem can be expressed mathematically as follows:

Objective:

$$\phi_f = |\min(0, H_r(x_i))| \quad (14)$$

$$\min \left\{ \frac{C_0(x)r(1+r)^{Ny}}{(1+r)^{Ny} - 1} \frac{1}{E_{tol,av}} - P_f \phi_f \right\} \quad (15)$$

Variables:

$$x_1 : X_1 \dots X_{N+2} \quad (16)$$

$$x_2 : Y_1 \dots Y_{N+2} \quad (17)$$

$$x_3 : B_1 \dots B_{N-1} \quad (18)$$

Subject to:

$$X_{min} \leq x_1 \leq X_{max} \quad (19)$$

$$Y_{min} \leq x_2 \leq Y_{max} \quad (20)$$

$$H_r(x_i) = \sqrt{(X_i - x_k)^2 + (Y_i - y_k)^2} - d_{min} \geq 0, \quad \forall i \neq k, i \in (1, N) \quad (21)$$

where  $r \in [1, 2, \dots, C]$ ,  $i, k \in [1, 2, \dots, N]$ . C equals  $N(N-1)/2$  which represents the total number of constraints and  $P_f$  is the penalty factor. The last two positions,  $x_1$  and  $x_2$ , represent the location of two OSs which are confined by (19) and (20). It can be seen that if the final result does not satisfy (21) then (14) will be greater than zero. In that case, the objective (15) will be penalized by finding this infeasible solution. The selection of the penalty factor is significant to the final result. If too large a magnitude of results under a trial and error method. Under the help of the penalty function, the optimization method will try to update the results to avoid falling into this infeasible region.

#### 3.2. APSO

For a non-convex problem, it is possible to use a gradient-based optimization algorithm to get a local optimal solution. However, for some complex problem, these classic algorithms easily fall into

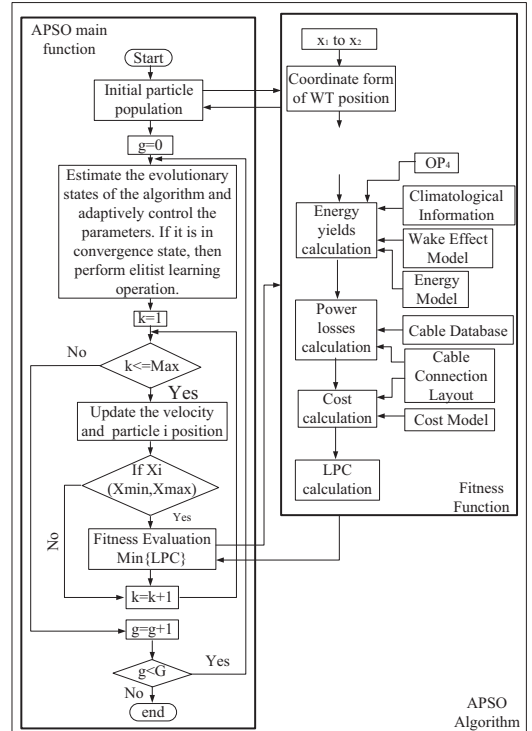


Fig. 3. Optimization flowchart.



**Table 1**  
DTU 10 MW WT specification [66].

Parameter	10 MW DTU WT
Cut-in Wind Speed	4 m/s
Rated Wind Speed	11.4 m/s
Cut-out Wind Speed	25 m/s
Rotor Diameter	178.3 m
Rated Power	10 MW

a local optimal solution and thus sometimes give a worse result compared with a manually designed solution. Though they cannot ensure optimality as well, heuristic algorithms as GA and PSO have good performance when it comes to finding a better solution that can benefit the fitness function. PSO is selected to implement this work, because it gives better performance for efficiently solving a continuously nonlinear problem compared with GA [51]. The global version of the PSO (GPSO) proposed by Kennedy and Eberhart is expressed as follows [52]:

$$v_i^{k+1} = wv_i^k + l_1r_1(local_i^k - x_i^k) + l_2r_2(global^k - x_i^k) \quad (22)$$

$$x_i^{k+1} = x_i^k + v_i^{k+1} \quad (23)$$

The GPSO can be further modified to cope with integer optimization problems by taking the integer value of the updated solution in each iteration as follows:

$$x_i^{k+1} = \text{int}(x_i^k + v_i^{k+1}) \quad (24)$$

In PSO, the parameters' value is critical to the final solution. Generally, a larger inertia weight,  $w$ , ensures a stronger global searching ability while smaller  $w$  ensures local searching ability and the learning factors are designed to ensure the algorithm's local convergence. These parameters can be controlled linearly or non-linearly [53–56] or intelligently controlled [57–60]. In [57], a comprehensive learning PSO (CLPSO) was presented which updated the particle positions by selecting a different local best particle in each iteration, and this was demonstrated to have a good performance for solving multimodal problems. The pattern search technology was combined with PSO in [58] to ensure an identical final result even with arbitrary starting points. In order to tune the value intelligently, an adaptive parameter tuning method was presented in [59]. Recently, the performance of PSO

to solve discrete optimization problem was presented and tested in [60], using a discrete PSO (DPSO). In this project, the method presented in [59] is selected to help find a near-optimal solution.

### 3.3. APSO-MST

As mentioned in Section 1, the cable connection configuration can be optimized using deterministic, stochastic or hybrid methods. In this work, the cable connection configuration and the OS locations are expected to be optimized with the method in [43] which is a heuristic method and demonstrated to have a better performance for finding a lower cost cable connection layout compared with some deterministic methods such as a minimum spanning tree (MST) algorithm.

### 3.4. Optimization framework

The problem studied in this work can be described as follows: Within a predefined construction area in the sea, a constant number of WTs and OSs are to be installed and connected through a series of submarine cables intelligently so that the LPC of this offshore wind farm can be minimized. The APSO algorithm is selected to optimize the WT locations while the APSO-MST method is adopted to connect the WTs. The optimization flow chart is shown in Fig. 3.

As can be seen in Fig. 3, the parameters for the PSO are initialized in the first step. The symbols on arrays represent the results that from the arrays' start blocks which will be transferred into the arrays' pointed blocks. In the beginning, a randomly generated particle which contains two pieces of information: the WTs and the OSs' positions in coordinate form ( $X_1$ ) as well as the cable connection layout, which is built by indicating the selected branch sequence number in each layout formation step ( $X_2$ ), will be transferred into the fitness function. In the fitness function, the power production of the present wind farm layout will first be calculated considering the wake effect based on  $X_1$ . Then the power losses will be calculated based on the output of each WT ( $P_{m,n}$ ) and the cable connection layout ( $X_2$ ). It should be noticed that the penalty function will be triggered if (14) is not satisfied. After that, the cable cost will be calculated with the initial cable connection configuration. Eventually, the LPC will be calculated using (12), (13), and (15) according to the calculated power production, the power losses along the cables and total cost of the cables. Following the same

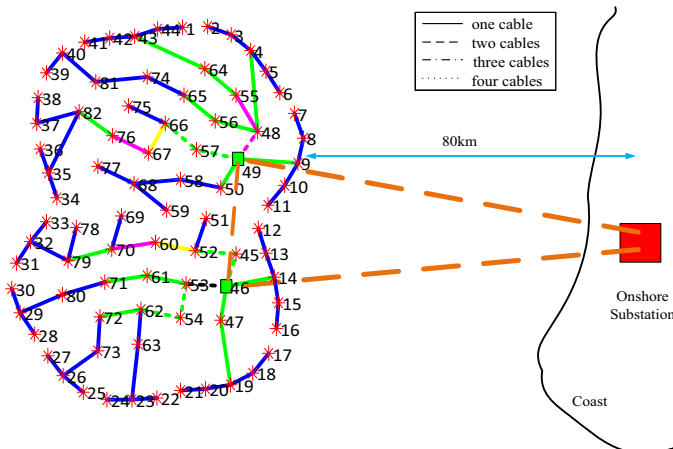


**Fig. 4.** The illustration of NRWF layout.

**Table 2**  
Specification of cables by color.

	Collection line					Transmission line
Voltage	66 kV					220 kV
Type	AC					AC
Color	Blue	Green	Purple	Yellow	Black	Brown
Cable sectional area (mm <sup>2</sup> )	95/150	240/300	400/500	630/800	1000	300

procedure, the function will be run when a new solution is loaded. The APSO main function will not terminate until the maximum iteration time is exceeded. The climatological information is the wind speed which is measured each 3 h by the staff in [61] and the cable database is generated based on the ABB cable manual [62].

3.5. Assumptions

Some assumptions are made in this paper and described in the following:

- Normally, the voltage level of the collection system of offshore wind farm can be 33 kV, 66 kV or even higher while the transmission cable voltage level ranges from 132 kV to 400 kV [63]. The voltage level for the collection system is assumed to be 66 kV while the transmission cables are assumed to be operated at 220 kV. This assumption is made by considering the situation when the offshore substation is 80 km away from the shore, which needs requires higher voltage level transmission cables. For calculation simplicity, the cables are assumed to be operated under one per unit voltage at all times which is a common assumption in cable layout optimization work as [30,33,35,37–44].
- In [49], the cost model for a WT is only related to its capacity while the cost of foundations is described as a constant cost regardless of location and water depth. Hence, only the costs of cables are considered in this paper to have a significant impact on the selection of the positions of the WTs.

- According to the cost model in [49], the installation cost is proportional to the installation distance. On this assumption, the installation cost will not change the final cable connection layout.

4. Case studies

In this section, two study cases are presented which are based on NORCOWE reference wind farm and Horns Rev 1 wind farm. The simulation results are stated and discussed at the end.

4.1. Case study I: NRWF

The NRWF is assumed to be located in the vicinity of FINO3 to the west of the German island of Sylt [64,65]. The wind farm is composed by 80 10 MW DTU WTs as specified in Table 1. The cable

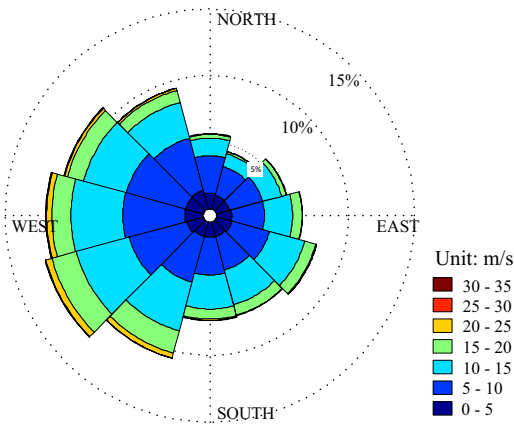


Fig. 5. Wind rose for wind climate in the vicinity of FINO3.

**Table 3**  
Distribution of solutions over 20 runs.

	Worst solution (Dkk/MWh)	Average value of solutions (Dkk/MWh)	Best solution (Dkk/MWh)
Scenario I	360.18	356.23	354.59
Scenario II	363.54	356.98	355.67
Scenario III	350.13	345.44	342.89

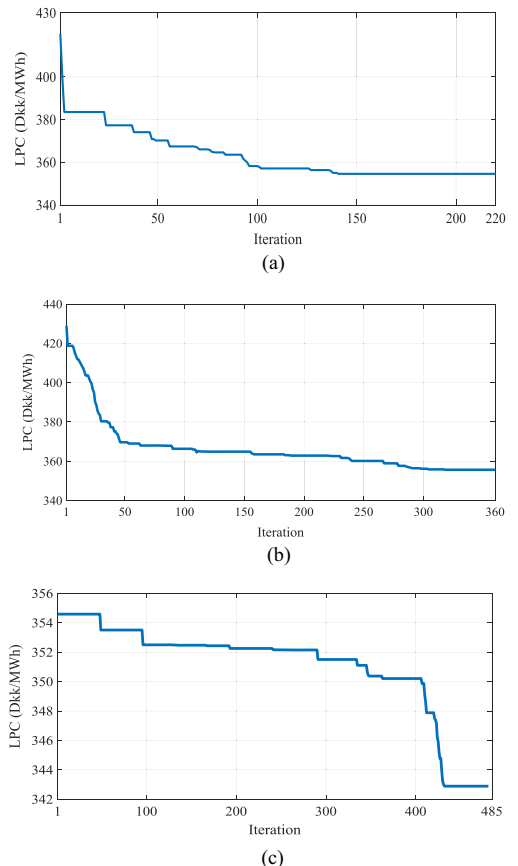


Fig. 6. The fitness value vs. each generation for different scenario. (a) For Scenario I. (b) For Scenario II. (c) For Scenario III.



connection layout and wind farm layout of this wind farm are shown in Fig. 4.

As can be seen in Fig. 4, the red stars show the WT's positions while the colored line represents the different cables that are specified in Table 2 by sectional area. The wind speed used for energy yield calculation is shown as a wind rose in Fig. 5.

4.1.1. Simulation results

In this work, three scenarios were presented and compared with the NRWF layout which means that two OSs were expected to be constructed so that the power captured by 80 WTs can be collected and transmitted to the onshore substation. Scenario I was done by only optimizing the cable connection layout for the NRWF layout. Similarly, the cable connection layout was obtained based on the optimized wind farm layout proposed in [67] respectively using the method mentioned in Section 3.3 while Scenario III was the combined optimization result which optimized the cable connection configuration and wind farm layout at the same time.

The layout in [67] was obtained with the purpose of minimizing the wake losses by optimizing the WT's positions which means that the overall design for Scenario II is done by two separate optimizations. The reason for comparing with [67] is to show the benefit of the simultaneous optimization of the layout and cable compared to the traditional way as Scenario II.

For this non-convex optimization problem, the solution cannot be proved optimally. In order to get a near-optimal solution, the program is run for 20 times and the best solution is selected as the final solution. The results from the 20 runs are collected and listed in Table 3 while the fitness values corresponding to each iteration for each scenario are illustrated in Fig. 6.

The optimized layout for each scenario is illustrated in Fig. 7. The detailed locations of each WT in Scenarios II and III are specified in Tables 6 and 7 which are listed in Appendix A.

It can be seen from Fig. 7 that the optimized wind farm layout is more scattered than the benchmark, which corresponds to the common sense that a scattered layout usually has a higher capacity

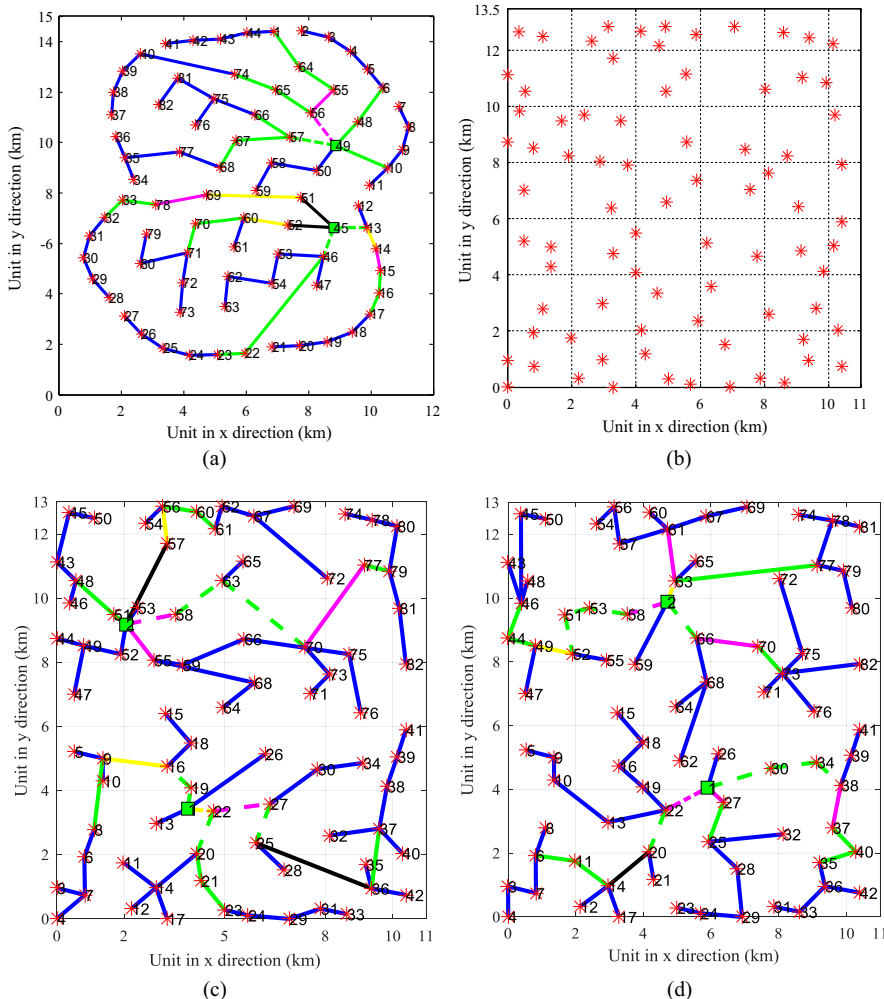


Fig. 7. The wind farm cable connection scheme. (a) Scenario I: The optimized cable connection scheme based on the NRWF wind farm layout. (b) The optimized wind farm layout in [66]. (c) Scenario II: The optimized cable connection scheme based on (b). (d) Scenario III: The overall optimization of the wind farm by the proposed method.

**Table 4**  
Specification of optimized wind farm configurations for Case I.

	Cost of connecting cables (MDkk)	Cost of collection system cables (MDkk)	Cost total (MDkk)	Energy yields of wind farm (GWh)	Energy reaching the onshore substation (GWh)	LPC (Dkk/MWh)
NRWF layout	30.86	229.25	1417.18	4010.93	3927.68	360.92
Scenario I	22.85	215.24	1392.60	4010.93	3928.56	354.59
Scenario II	42.37	250.99	1450.18	4169.24	4078.53	355.67
Scenario III	41.69	230.30	1397.14	4164.08	4075.84	342.89

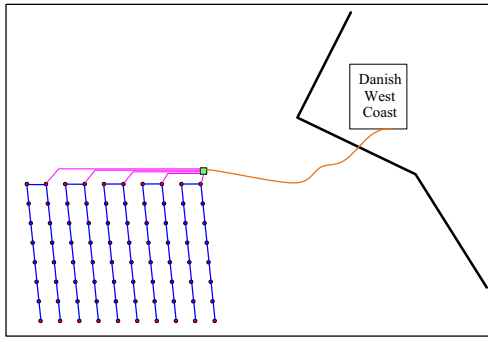


Fig. 8. The Horns Rev I offshore wind farm.

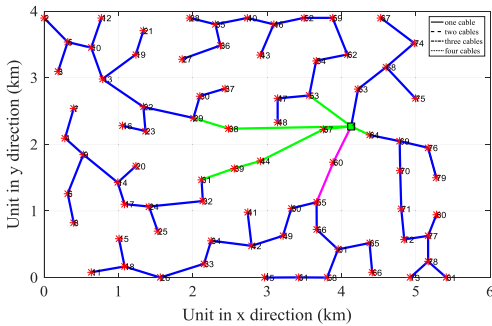


Fig. 9. The illustration of optimized Horns Rev I wind farm layout.

factor. The performances of the optimized layouts from the four scenarios are summarized in Table 4 as follows.

In Table 4, the cost of connecting cables shows the cost of cables between two OSS while the cost of collection system cables means the total cable cost for connecting WTs. From Table 4, it can be seen that the optimized layouts in Scenarios I through III can reduce the LPC by 1.75%, 1.45% and 5.00% respectively compared with the NRWF layout as illustrated in Fig. 4. Though the energy yields have been increased by 3.95% when optimizing the positions of WTs in Scenario II, the total cost increases by 2.33% as well which results

in a 1.45% reduction in the LPC. In contrast to that, Scenario III gained a 3.59% reduction in LPC compared with Scenario II. Scenario II is where the maximum total energy yield from the WTs can be obtained. However, the investment increase on the cables of the collection system resulted in the lower LPC compared with Scenarios I and III. The lowest LPC occurred in Scenario III, which optimized the cable connection scheme and wind farm locations at the same time with the proposed method.

4.1.2. Discussion

Scenarios I and II follow the traditional way of wind farm layout design, in which the WT positions will be decided first aiming at maximizing the power production of whole wind farm while the cable connection scheme is optimized in the next step to minimize the total investment as far as possible. However, it can be seen that even when the WTs were placed optimally as in Scenario II, the LPC will be higher than the manually designed wind farm layout in Scenario I. The overall performance of the wind farm can be further improved by considering the wind farm layout and cable connection configuration at the same time as in Scenario III.

4.2. Case study II: Horns Rev I wind farm

The Horns Rev I wind farm is located around 20 km offshore in the North Sea and is composed of 80 2 MW Vestas 2.0-V80 WTs [68]. The wind farm layout and cable connection scheme are shown in Fig. 8.

In Fig. 8, the green square shows the location of the offshore substation while the cable connection scheme was shown using the same color described in Case I. The only differences are the voltage levels for collection system and transmission system in this case are 34 kV and 132 kV respectively. The proposed method is expected to find a layout which will be more economic than the present design. The optimized layout is shown in Fig. 9.

Based on the proposed optimization method, a real case study is proposed in this part. The cable connection layout with different sectional areas is presented in Fig. 9 which is illustrated in the same way as specified in Table 2. The final results are summarized in Table 5.

Based on the proposed optimization method, a real case study is proposed in this part. It can be seen that by using the proposed method, the LPC has been reduced by 14.53%. The cost is significantly reduced by 12.28% while the energy production is 2.49% increased. The offshore substation is located within the wind farm area, unlike in the original design.

**Table 5**  
Specification of optimized wind farm configurations for Case II.

	Cost of collection system cables (MDkk)	Cost total (MDkk)	Energy yields of wind farm (MWh)	Energy reached at the onshore substation (GWh)	LPC (Dkk/MWh)
Horn Rev I layout	86.34	189.88	737.78	730.45	260.03
Optimized layout	56.03	166.56	756.16	749.66	222.25

## 5. Conclusion

Wind farm layout optimization and cable connection scheme design are two critical parts to deciding the economy of wind farm performance. Traditionally, the WT positions will be optimized first to maximize the wind farm power production. The cable connection configuration and OS locations will be determined, after the well-designed wind farm layout is fixed, to realize a cost-effective wind farm.

In this paper, an overall design methodology for offshore wind farm which included the optimization of wind farm layout, OS locations as well as the cable connection configuration was proposed. The simulation results indicate that the traditional method, which harvests the wind as much as possible and then optimizes the cable connection configuration, is not the best approach to overall wind farm optimization. The proposed method can further reduce the LPC of the wind farm by 5% compared with NRWF which is 3.55% higher than the result found by traditional method. Even worse the traditional method may conclude a worse performance wind farm which has a 0.3% higher LPC compared with manually designed wind farm layout. The proposed method was

shown to be an effective way to further improve the wind farm compared with the traditional design method. It can be used for overall evaluation of a planned wind farm and to help the investor make a good decision.

In the future, the installation cost and foundation cost which are related to the sea bed condition and water depth will be considered in the wind farm layout optimization. Moreover, the relation between wind farm layout (scattered irregular distribution layout or regular array arranged layout) and installation cost should be investigated so that a comprehensive optimization work can be done for the wind farm planning.

## Acknowledgments

The authors would like to thank the Norwegian Centre for Offshore Wind Energy (NORCOWE) under grant 193821/S60 from the Research Council of Norway (RCN).

## Appendix A

See Tables 6–8.

**Table 6**  
The WT locations in Scenario II.

WT sequence no.	x	y	WT sequence no.	x	y	WT sequence no.	X	y
1	5864.28	12563.76	28	818.51	1930.99	55	7390.73	8482.83
2	9393.52	12441.84	29	0.01	965.27	56	5882.85	7364.42
3	7060.01	12863.99	30	0.01	8749.60	57	366.31	12673.37
4	10142.50	12245.92	31	3991.69	4081.74	58	4949.50	6594.88
5	5552.51	11159.25	32	525.07	5212.24	59	4661.10	3358.96
6	9909.19	10843.79	33	1107.72	2787.34	60	4722.95	12157.56
7	10142.51	5056.11	34	1366.88	5005.91	61	4170.87	2038.81
8	10,401	5897.57	35	8121.44	7624.88	62	6773.42	1525.01
9	10400.99	7951.14	36	805.81	8518.61	63	4933.76	10542.92
10	10293.88	2049.59	37	2405.64	9699.40	64	5579.27	8728.40
11	9158.00	11035.23	38	569.26	10542.89	65	1906.90	8254.52
12	8708.36	8254.68	39	0	11126.01	66	4299.03	1186.85
13	9121.99	4862.23	40	1688.58	9494.46	67	3743.43	7918.88
14	9837.09	4134.06	41	2632.42	12331.23	68	3287.81	4754.30
15	9607.04	2816.44	42	3151.03	12863.97	69	3230.35	6398.05
16	10,401	747.38	43	8581.75	12635.44	70	2954.91	2970.77
17	9201.77	1693.83	44	4913.38	12,864	71	2955.09	975.67
18	8639.01	149.45	45	7769.31	4671.21	72	3286.83	11712.73
19	7860.23	321.19	46	8129.59	2599.51	73	4160.39	12697.78
20	6924.86	0.02	47	9056.36	6427.93	74	3529.36	9495.52
21	5694.32	111.59	48	7556.17	7029.18	75	2891.02	8068.38
22	5002.50	280.57	49	2222.47	321.81	76	1978.72	1756.85
23	9375.83	949.60	50	6210.97	5141.72	77	1107.31	12495.62
24	3288.52	0.02	51	6359.29	3591.90	78	513.81	7009.62
25	7.03	14.14	52	5929.81	2371.17	79	3991.65	5481.82
26	1368.87	4293.39	53	8057.66	10620.44	80	390.61	9852.72
27	834.92	747.37	54	10205.42	9690.60			

**Table 7**  
The WT locations in Scenario III.

WT sequence no.	x	y	WT sequence no.	x	y	WT sequence no.	x	y
1	5856.31	12564.86	28	819.04	1930.61	55	7393.22	8489.09
2	9585.97	12435.11	29	1.2712	958.86	56	5872.02	7366.04
3	7068.56	12863.98	30	1.92	8742.31	57	382.62	12651.29
4	1101.19	12486.07	31	3988.38	4074.18	58	4953.00	6594.94
5	5553.09	11164.23	32	547.33	5229.28	59	4656.97	3349.23
6	9911.63	10861.14	33	1103.97	2792.30	60	4723.88	12164.48
7	10150.01	5064.17	34	1358.00	5007.02	61	4160.74	2034.57
8	10,401	5881.56	35	8114.64	7641.82	62	6777.62	1515.92
9	10,401	7939.08	36	810.49	8506.19	63	4933.51	10533.83
10	10276.57	2053.87	37	2405.25	9691.049	64	5570.86	8740.53
11	9149.66	11038.64	38	571.17	10532.21	65	1909.71	8254.67
12	8705.15	8256.40	39	0	11114.54	66	4303.81	1169.51

Table 7 (continued)

WT sequence no.	x	y	WT sequence no.	x	y	WT sequence no.	x	y
13	9128.14	4853.77	40	1682.62	9483.37	67	3747.28	7925.96
14	9839.80	4135.53	41	2620.97	12334.98	68	3283.22	4732.62
15	9596.01	2799.48	42	3136.57	12863.70	69	3226.31	6405.07
16	10.401	758.41	43	8595.16	12619.84	70	2954.60	2969.64
17	9209.55	1696.11	44	4916.65	4891.58	71	2954.61	971.64
18	8620.01	161.66	45	7770.06	4670.45	72	3294.65	11707.27
19	7851.70	323.61	46	8132.88	2594.71	73	4178.02	12697.81
20	6920.73	0	47	9048.25	6446.26	74	3528.62	9491.08
21	5684.62	116.42	48	7565.85	7067.95	75	2900.35	8060.83
22	4993.86	289.14	49	2130.45	323.62	76	1976.40	1753.67
23	9371.60	964.56	50	6210.38	5130.72	77	10400.98	12246.21
24	3283.70	0	51	6370.65	3598.40	78	512.22	6998.98
25	5.32	9.21	52	5931.37	2357.99	79	3988.10	5473.69
26	1361.01	4287.80	53	8029.15	10603.68	80	390.04	9841.37
27	825.10	745.11	54	10170.11	9686.86			

Table 8  
Value of coefficients.

Name	Value	Name	Value	Name	Value	Name	Value
$\rho$	1.225 kg/m <sup>3</sup> at sea level and at 15 °C	$k_c$	0.4	$\rho_R$	75 × 1e-8 ohm × m at 20 °C	TE	60
$N_y$		r	0.05	w	0.8 at the initial stage	$l_1, l_2$	Both equal to 2 at the initial stage

References

[1] González JS, Payán MB, Santos JMR, González-Longatt F. A review and recent developments in the optimal wind-turbine micro-siting problem. *Renew Sustain Energy Rev* 2014;30:133–44.

[2] Mosetti G, Poloni C, Diviacco B. Optimization of wind turbine positioning in large wind farms by means of a genetic algorithm. *J Wind Eng Ind Aerodyn* 1994;51(1):105–16.

[3] Grady S, Hussaini M, Abdullah M. Placement of wind turbines using genetic algorithms. *Renewable Energy* 2005;30(2):259–70.

[4] Marmidis G, Lazarou S, Pyrgioti E. Optimal placement of wind turbines in a wind park using Monte Carlo simulation. *Renewable Energy* 2008;33(7):1455–60.

[5] Prabhu NP, Yadav P, Prasad, B., Panda SK. Optimal placement of off-shore wind turbines and subsequent micro-siting using intelligently tuned harmony search algorithm. *Power and Energy Society General Meeting (PES), Vancouver, BC, IEEE; Jul. 2013. p. 1–7.*

[6] Pookpant S, Ongsakul W. Optimal placement of wind turbines within wind farm using binary particle swarm optimization with time-varying acceleration coefficients. *Renewable Energy* 2013;55:266–76.

[7] Turner SDO, Romero DA, Zhang PY, Amon CH, Chan TCY. A new mathematical programming approach to optimize wind farm layouts. *Renewable Energy* 2014;63:674–80.

[8] Kusiak A, Song Z. Design of wind farm layout for maximum wind energy capture. *Renewable Energy* 2010;35(3):685–94.

[9] Eroglu Y, Seckiner SJ. Design of wind farm layout using ant colony algorithm. *Renewable Energy* 2012;44:53–62.

[10] Wan C, Wang J, Yang G, Gu H, Zhang X. Wind farm micro-siting by Gaussian particle swarm optimization with local search strategy. *Renewable Energy* 2012;48:276–86.

[11] Chowdhury S, Zhang J, Messa A, Castillo L. Optimizing the arrangement and the selection of turbines for wind farms subject to varying wind conditions. *Renewable Energy* 2013;52:273–82.

[12] Rahbari O, Vafaeipour M, Fazelpour F, Feidt M, Rosen MA. Towards realistic designs of wind farm layouts: application of a novel placement selector approach. *Energy Convers Manage* 2014;81:242–54.

[13] Gao X, Yang H, Lu L. Investigation into the optimal wind turbine layout patterns for a Hong Kong offshore wind farm. *Energy* 2014;73:430–42.

[14] Feng J, Wen ZS. Solving the wind farm layout optimization problem using random search algorithm. *Renewable Energy* 2015;78:182–92.

[15] Park J, Law K. Layout optimization for maximizing wind farm power production using sequential convex programming. *Appl Energy* 2015;151:320–34.

[16] Pérez B, Mínguez R, Guanache R. Offshore wind farm layout optimization using mathematical programming techniques. *Renewable Energy* 2013;53:389–99.

[17] Chen Y. Commercial wind farm layout design and optimization. Kingsville, Ann Arbor: Texas A&M University; 2013. p. 47.

[18] Wang L, Tan ACC, Gu Y. Comparative study on optimizing the wind farm layout using different design methods and cost models. *J Wind Eng Ind Aerodyn* 2015;146:1–10.

[19] Guirguis D, Romero DA, Amon CH. Toward efficient optimization of wind farm layouts: utilizing exact gradient information. *Appl Energy* 2016;179:110–23.

[20] Messac A, Chowdhury S, Zhang J. Characterizing and mitigating the wind resource-based uncertainty in farm performance. *J Turbul* 2012. 131–26.

[21] González JS, Payán MB, Santos JMR. Optimization of wind farm turbine layout including decision making under risk. *IEEE Syst J* 2012;6:94–102.

[22] Yin PY, Wu TH, Hsu PY. A power-deficiency and risk-management model for wind farm micro-siting using cyber swarm algorithm. *Appl Math Model* 2016;40:2177–89.

[23] Lundberg S. Configuration study of larger wind park. Göteborg, Sweden: Dept Electr Power Eng, Chalmers Univ Technol; 2003 [Thesis for the degree of Licentiate Engineering].

[24] Zhao M, Chen Z, Blaabjerg F. Application of genetic algorithm in electrical system optimization for offshore wind farms. In: Presented at the int conf on electric utility deregulation and restructuring and power technologies (DRPT), Nanjing, China; 2008.

[25] Zhao M, Chen Z, Blaabjerg F. Optimisation of electrical system for offshore wind farms via genetic algorithm. *IET Renew Power Gener* 2009;205–16.

[26] Bahirat HJ, Mork BA, Hoidalun HK. Comparison of wind farm topologies for offshore applications. In: 2012 IEEE power and energy society general meeting. p. 1–8.

[27] Bondy JA, Murty USR. Graph theory with applications. The Macmillan Press Ltd.; 1976.

[28] Devore RA, Temlyakov VN. Some remarks on greedy algorithm. *Adv Comput Math* 1996:173–87.

[29] Huang L, Chen N, Zhang H, Fu Y. Optimization of large-scale offshore wind farm electrical collection systems based on improved FCM. In: International conference on sustainable power generation and supply (SUPERGEN 2012), Hangzhou, 8–9 Sept.; 2012.

[30] Dutta S, Overbye TJ. Optimal wind farm collector system topology design considering total trenching length. *IEEE Trans Sustain Energy* 2012;3(3):339–48.

[31] Press WH, Teukolsky SA, Vetterling WT, Flannery BP. Numerical recipes in fortran 77: the art of scientific computing. 2nd ed. Cambridge University Press; 1992. p. 438–444 [chapter 10.9].

[32] Jenkins AM, Scutarium M, Smith KS. Offshore wind farm inter-array cable layout. *PowerTech (POWERTECH), 2013 IEEE Grenoble, 16–20 June; 2013. p. 1–6.*

[33] Gonzalez-Longatt FM, Wall P, Regulski P, Terzija V. Optimal electric network design for a large offshore wind farm based on a modified genetic algorithm approach. *IEEE Syst J* 2012;6(1):164–72.

[34] Huang L, Fu Y, Guo X. Optimization of electrical connection scheme for large offshore wind farm with genetic algorithm. In: International conference on sustainable power generation and supply. SUPERGEN '09; Apr. 2009. p. 1–4, 6–7.

[35] Li DD, He C, Fu Y. Optimization of electric distribution system of large offshore wind farm with improved genetic algorithm. In: 2008 IEEE power and energy society general meeting - conversion and delivery of electrical energy in the 21st century, 20–24 July; 2008. p. 1–6.

[36] Dahmani O, Bourquet S, Guerin P, Machmoum M, Rhein P, Josse L. Optimization of the internal grid of an offshore wind farm using Genetic algorithm. In: 2013 IEEE Grenoble PowerTech (POWERTECH), 16–20 Jun.; 2013. p. 1–6.

[37] Gonzalez JS, Payan MB, Santos JR. A new and efficient method for optimal design of large offshore wind power plants. *IEEE Trans Power Syst* 2013;28(3):3075–84.

- [38] Wedzik A, Siewierski T, Szykowski M. A new method for simultaneous optimization of wind farm's network layout and cable cross-sections by MILP optimization. *Appl Energy* 2016;182:525–38.
- [39] Dutta S, Overbye TJ. A clustering based wind farm collector system cable layout design. In: 2011 IEEE power and energy conference at Illinois (PECI), Champaign, IL, 25–26 Feb.; 2011. p. 1–6.
- [40] Wu Y, Lee C, Chen C, Hsu K, Tseng H. Optimization of the wind turbine layout and transmission system planning for a large-scale offshore wind farm by AI technology. *IEEE Trans Ind Appl* 2014;50(3):2071–80.
- [41] Lumberras S, Ramos A. Optimal design of the electrical layout of an offshore wind farm applying decomposition strategies. *IEEE Trans Power Syst* 2013;28(2):1434–41.
- [42] Hopewell PD, Castro-Sayas F, Bailey DI. Optimising the design of offshore wind farm collection networks. In: UPEC '06, Proceedings of the 4–1st international universities power engineering conference, vol. 1, 6–8 Sept.; 2006. p. 84–8.
- [43] Hou P, Hu W, Chen Z. Optimization for offshore wind farm cable connection layout using APSO-MST method. *IET Renew Power Gener* 2016;10(5):694–702.
- [44] Wu YK, Lee CY, Chen CR, Kun-Wei Hsu, Huang-Tien Tseng. Optimization of the wind turbine layout and transmission system planning for a large-scale offshore wind farm by AI technology. *IEEE Trans Ind Appl* 2013;50(3):2071–80.
- [45] Pao LY, Johson KE. A tutorial on the dynamics and control of wind turbines and wind farms. In: Proceedings of 2009 American control conference.
- [46] WindPRO/PARK. Introduction wind turbine wake modelling and wake generated turbulence. EMD International A/S.
- [47] Beaucage P, Brower M, Robinson N, Alonge C. Overview of six commercial and research wake models for large offshore wind farms. In: Proceedings EWEA 2012, Copenhagen; 2012.
- [48] Hou P, Hu W, Soltani M, Chen Z. Optimized placement of wind turbines in large scale offshore wind farm using particle swarm optimization algorithm. *IEEE Trans Sustain Energy* 2015;6(4):1272–82.
- [49] Lundberg S. Performance comparison of wind park configurations. Goteborg, Sweden: Department of Electric Power Engineering, Chalmers University of Technology, Department of Electric Power Engineering. Tech. Rep. 30R; Aug. 2003.
- [50] Zhao M. Optimization of electrical system for offshore wind farms via a genetic algorithm approach Dissertation submitted to the. Denmark: Faculty of Engineering, Science and Medicine at Aalborg University; 2006.
- [51] Hassan R, Cohanim B, de Weck O. A comparison of particle swarm optimization and the genetic algorithm". In: Proceedings of the 46th AIAA ASME/ASCE/AHS/ASC structures, structural dynamics and materials conference.
- [52] Kennedy J. The particle swarm: social adaptation of knowledge. In: Proc. IEEE int conf evolution of computing, Indianapolis, IN. p. 303–8.
- [53] Shi Y, Eberhart RC. Empirical study of particle swarm optimization. In: Proc Congr Evol Comput. p. 1950–5.
- [54] Jiao B, Lian Z, Gu X. A dynamic inertia weight particle swarm optimization algorithm. *Chaos Solitons Fractals* 2008;37:698–705.
- [55] Shi Y, Eberhart RC. Fuzzy adaptive particle swarm optimization. In: Proc Congr Evol Comput. p. 101–6.
- [56] Eberhart RC, Shi Y. Tracking and optimizing dynamic systems with particle swarms. In: Proc Congr Evol Comput. p. 94–100.
- [57] Liang JJ, Qin AK, Suganthan PN, Baskar S. Comprehensive learning particle swarm optimizer for global optimization of multimodal functions. *IEEE Trans Evol Comput* 2006;10(3).
- [58] Vaz AIF, Vicente LN. A particle swarm pattern search method for bound constrained global optimization. *J Global Optim* 2006;39:197–219.
- [59] Zhan Z-H, Zhang J, Li Y, Chung HS-H. Adaptive particle swarm optimization. *IEEE Trans Syst Man Cybern B Cybern* 2009;39(6):1362–81.
- [60] Deroussi L, Lemoine D. Discrete particle swarm optimization for the multi-level lot-sizing problem. *Int J Appl Metaheuristic Comput* 2013;2:44–57.
- [61] Norwegian Centre for Offshore Wind Energy (NORCOWE). <<http://www.offshorewind.biz/tag/norcowe/>>.
- [62] XLPE submarine cable systems attachment to XLPE land cable systems—user's guide. A/S Håndværkervej 23, 7000 Fredericia; ABB Corporation; 2013.
- [63] Kirkeby H, Merz KO. Layout and electrical design of a 1.2 GW wind farm for research on the next generation of offshore wind energy technologies. *Sintef Energy Research* 2014.
- [64] FINO3 - research platform in the North Sea and the Baltic No. 3. <<http://www.fino3.de/en/>>.
- [65] WP2014-Froysa-NRWFF NORCOWE reference wind farm. <<http://www.norcowe.no/>>.
- [66] Bak C, Zahle F, Bitsche R, Kim T, Yde A, Henriksen LC, et al. Description of the DTU 10 MW reference wind turbine. Fredericia, Denmark: DTU Wind Energy; 2013.
- [67] Hou P, Hu W, Chen C, Soltani M, Chen Z. Optimization of offshore wind farm layout considering restriction zone. *Energy* 2016;113:487–96.
- [68] Schachner J. Power connections for offshore wind farms. TU Delft University; 2004 [Diploma thesis].

# Optimisation of offshore wind farm cable connection layout considering levelised production cost using dynamic minimum spanning tree algorithm

Peng Hou, Weihao Hu ✉, Cong Chen, Zhe Chen

Department of Energy Technology, Aalborg University, Pontoppidanstraede 101, Aalborg DK-9220, Denmark

✉ E-mail: whu@et.aau.dk

ISSN 1752-1416

Received on 12th February 2015

Revised on 15th June 2015

Accepted on 5th August 2015

doi: 10.1049/iet-rpg.2015.0052

www.ietdl.org

**Abstract:** The approach in this study has been developed to optimise the cable connection layout of large-scale offshore wind farms. The objective is to minimise the levelised production cost (LPC) of an offshore wind farm by optimising the cable connection configuration. On the basis of the minimum spanning tree (MST) algorithm, an improved algorithm, the dynamic MST algorithm is proposed. The current carrying capacity of the cable is considered to be the main constraint and the cable sectional area is changed dynamically. An irregular shaped wind farm is chosen as the studied case and the results are compared with the layout obtained by a traditional MST algorithm. Simulation results show that the proposed method is an effective way for offshore wind farm collection system layout design.

## Nomenclature

$V_0$ [m/s]	input wind velocity at upstream WT	$\rho$ [kg/m <sup>3</sup> ]	air density
$R_0$ [m]	WT's rotor blade radius	$\lambda_{opt}$	tip speed ratio
$S_0$ [m <sup>2</sup> ]	area swept by the WT's rotor	$\beta$ [°]	blade pitch angle
$R_{ij}$ [m]	generated wake radius by the WT at row $i$ , column $j$ along the wind direction	$V$ [m/s]	wind velocity
$S_{overlap,ij}$ [m <sup>2</sup> ]	overlapped area generated by upstream WT to affected downstream WT at row $i$ , column $j$ of wind farm	$C_{p,opt}$	optimal value of power coefficient
$V_{ij}$ [m/s]	wake velocity generated by the WT at row $i$ , column $j$ of wind farm	$P_{loss,ij}$ [MW]	power losses of cable at row $i$ , column $j$
$L_{ij}$ [m]	distance from upstream WT at row $i$ , column $j$ to the affected downstream WT	$I_{ij}$ [kA]	current in cable at row $i$ , column $j$
$V_{nm}$ [m/s]	wind velocity at the WT at row $n$ , column $m$	$R_{e,ij}$ [Ω/m]	resistance of cable at row $i$ , column $j$
N_row	number of WTs in a row	$\rho_{R,ij}$ [Ωm/mm <sup>2</sup> ]	resistivity of selected cable at row $i$ , column $j$
N_col	number of WTs in a column	$l_{R,ij}$ [m]	length of cable at row $i$ , column $j$
$C_i$ [MDkk/km]	unit cost of cable $i$	$S_{R,ij}$ [m <sup>2</sup> ]	sectional area of cable at row $i$ , column $j$
$A_p, B_p, C_p$	coefficients of the cable cost model	$U_{0,ij}$ [kV]	voltage to earth of cable at row $i$ , column $j$
$S_{n,i}$ [MW]	rated apparent power of cable in line $i$	$E_{tot}$ [MWh]	energy yields of wind farm in one year
$I_{i,rated}$ [kA]	rated current of cable in line $i$	TE	total number of time interval for energy yields calculation
$U_{i,rated}$ [kV]	rated voltage of cable in line $i$	$P_{tot,i}$ [MW]	total power production of wind farm at time interval $i$
$x, y$	position of offshore substation (OS) in the form of coordinate	$P_{tot,loss,i}$ [MW]	total power losses of wind farm at time interval $i$
cost <sub><math>i</math></sub> [MDkk]	cost of cables that was used in branch $i$	$T_i$ [h]	duration of time interval $i$
$Q_i$	number of cables that was used in branch $i$	$C_0$ [DKK]	initial capital investment on cables
$L_i(x, y)$ [km]	length of cable $i$ when OS location is $(x, y)$	$E_y$	economic lifetime, 20–25 year
$C_i(x, y)$ [MDkk/km]	unit cost of cable $i$ when OS location is $(x, y)$	$x, y$	position of OS in the form of coordinate
$P_{m,ij}$ [MW]	power extracted from the wind by WT at row $i$ , column $j$	$I_i$ [A]	current going through the cable $i$
$v$ [m/s]	inflow wind speed	$L_x$ [km]	width of wind farm in horizontal direction
		$L_y$ [km]	length of wind farm in vertical direction
		$N_G$	total number of vertices in a graph
		$C_0^{GT}(x, y)$ [DKK]	initial capital investment on cables when OS location is $(x, y)$ and the cable connection layout is $G_T$

$E_{\text{tot}}^{G_T}(x, y)$  [MWh]

energy yields of wind farm when OS location is  $(x, y)$  and the cable connection layout is  $G_T$

$LPC^{G_T}(x, y)$  [DKK/MWh]

LPC of wind farm when OS location is  $(x, y)$  and the cable connection layout is  $G_T$

## 1 Introduction

As a form of renewable energy, wind power has recently drawn more and more attention. Compared with an onshore wind farm, an offshore wind farm always has a higher efficiency and no noise pollution for surrounding residents. However, the cost of constructing an offshore wind farm is greater. Since it usually consists of a large quantity of wind turbines (WTs) and is spread out in the sea, a lot of expensive cables and electrical equipment are needed. With the gradual improvement of the equipment's voltage level, the proportion of the construction investment used on the collection system (CS) of an offshore wind farm steps up to 18% which is much higher than for an onshore wind farm [1]. Hence, it is advantageous to optimise the electrical system of the offshore wind farm to get a cost-effective wind farm.

The electrical system of the offshore wind farm can be divided into two parts: the CS and the transmission system as shown in Fig. 1.

The power generated from each WT is first collected through a series of medium-voltage (MV) cables and transmitted to the offshore substation (OS) by one or several MV integration cables. The voltage is transformed to a transmission voltage level so that all the power can be transmitted to the onshore substation through the transmission system. Owing to the limitation of cable current carrying capacity, the cable size should be carefully selected. Since the location of the substation has significant impact on the CS layout, which contributes to the total cost of the electrical system, it is necessary to design the cable connection layout considering OS location to save investment on cables while meeting the operating requirements.

The optimisation of an offshore wind farm electrical system was considered in [2] which compares AC and/or DC (CSs) corresponding to different voltage levels. Furthermore, CSs with different topologies were compared in [3], where the electrical system is optimised with respect to both the levelised production cost (LPC) as well as reliability. In addition to the optimisation work of finding a combination of different types of electrical components to minimise the LPC, optimising the cable connection layout has also been considered in [4–8]. In [4], a new algorithm to minimise system power losses and improve reliability was proposed and validated through a small reference wind farm. On

the basis of a practical wind farm project, the fuzzy C-means clustering algorithm was adopted in [5] to partition the whole system into several subsets. The substation was regarded to be located in the centre of each subset and the cable connection layout in each part was optimised with the minimum spanning tree (MST) algorithm. The MST was also utilised and modified in [6] with the purpose of minimising the total trenching length. In addition, genetic algorithms (GAs) have also been widely used in the optimisation of cable connection layouts [7, 8]. The cable connection layout was designed with the objective of minimising total cable length, capital cost as well as power losses in [7]. In [8], the minimal cost cable connection layout for a four substation offshore wind farm was presented. The travelling salesman problem algorithm was adopted to improve the standard GA to find a minimal cost layout. From the cables' rated current, the number of WTs in each cluster were calculated and assumed to be the same. The results were also compared with similar work which has been done using a hybrid GA and immune algorithm and showed better performance in [9]. Similarly, [10] proposed a method to optimise the offshore wind farm cable connection layout based on planar open vehicle routing. However, [8, 10] have some limitations of cable sectional area and the number of WTs in one cluster, while our algorithm has greater flexibility to generate a branching layout and the selection of cable sectional area is dynamically changed according to the number of WTs connected to the branch without defining the starting point and the end point (the depot and the client). All the above works assumed that the cable type for connecting every two WTs was already known without thinking of dynamic changes in cable type during the layout formulation process. The present cable connection layout design work has been done with three main objectives: minimising the total cost of electrical components, minimising the trenching distance and minimising operational losses. It would be more beneficial if the cost of cables and the power losses could be optimised at the same time to get an enhanced electrical system layout with higher energy yields and less investment. Moreover, the OS location optimisation problem, which should be a key variable in the electrical system optimisation problem, is not discussed in [2–10].

In this paper, the offshore wind farm CS layout is optimised by a modified MST algorithm. Since the location of the OS is highly related to the CS layout, the siting of the OS is optimised together with the system layout. To meet the system operation requirements, the cable current carrying capacity is considered in the cable selection process during the simulation. Instead of minimising the total cable cost, LPC is selected as the evaluation index. The wake effect, power losses along the cables as well as cable cost are considered to optimise the cable layout. The

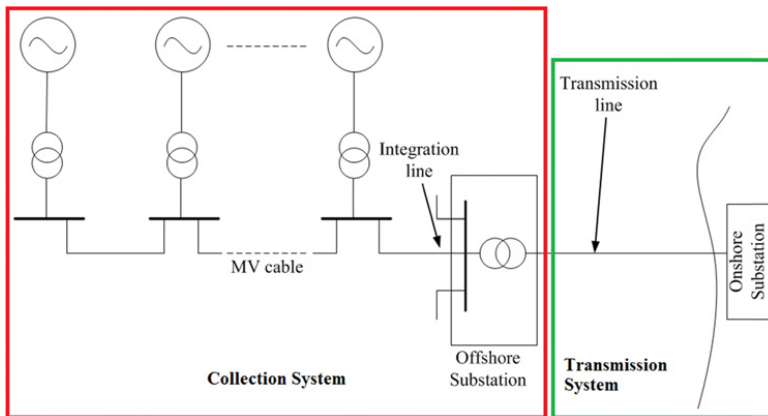


Fig. 1 Typical offshore wind farm configuration



proposed method is implemented in an irregular shaped wind farm and the results show that it is an effective way for offshore wind farm cable connection layout design.

This paper is organised as follows. Section 2 provides the following models of the wind farm: cable cost model, wake effect model and energy model. The problem description and objective function are presented in Section 3. Section 4 presents the dynamic MST (DMST) algorithm and optimisation framework. An irregular shaped wind farm is chosen as the study case to demonstrate the proposed method in Section 5. Section 6 summarises the main conclusions.

## 2 Wind farm models

The wake model which includes the variation of both wind direction and velocity is introduced first in this chapter and then the cable cost model is presented. The energy yields model is specified last in this section.

### 2.1 Jensen wake model

The wake deficit can be explained as the impact of upstream WTs on downstream ones which reduce the total energy yield of the wind farm due to the wind speed drop downstream [11]. Three commonly used wake models are the Jensen model, Ainslie model and G.C. Larsen model [12]. In this paper, the Jensen model, which was proposed by Jensen in 1983, is adopted since it is not time-consuming and can introduce fewer prediction errors in energy yield calculations [13]. In this model, the wake is assumed to expand linearly behind the upstream WT. The mathematical description of this model can be written [14, 15]

$$V_{ij} = V_0 - V_0 \left(1 - \sqrt{1 - C_t}\right) \left(\frac{R_0}{R_{ij}}\right)^2 \left(\frac{S_{\text{overlap},ij}}{S_0}\right) \quad (1)$$

$$R_{ij} = R_0 + kL_{ij} \quad (2)$$

where  $C_t$  is the thrust coefficient of the WT and  $k$  is the wake decay constant. The recommended value of  $k$  is 0.04 for an offshore environment [16].

In a large wind farm, a downstream WT can be affected by several upstream WTs. To evaluate all these contributions to wind speed deficit at downstream WTs, Porté-Agel *et al.* [17] proposed a method in which the multiple wakes are calculated by using the 'sum of squares of velocity deficits'. Hence, the wind velocity at the WT at row  $n$ , column  $m$  can be expressed as

$$V_{nm} = V_0 \left[1 - \sqrt{\sum_{i=1}^{N_{\text{row}}} \sum_{j=1}^{N_{\text{col}}} \left[1 - \left(\frac{V_{ij}}{V_0}\right)^2\right]}\right] \quad (3)$$

### 2.2 Cost model

The cost model is set up according to the cables' rated power. The mathematical equations can be written as in [18]

$$C_i = A_p + B_p \exp\left(\frac{C_p S_{n,i}}{10^8}\right)^2 \quad (4)$$

$$S_{n,i} = \sqrt{3}I_{i,\text{rated}}U_{i,\text{rated}} \quad (5)$$

The cables are selected according to their rated current which is correlated to the sectional area in this paper. In some cases, more cables are required between two WTs if many WTs are connected in one branch. Hence, the cost of cabling between each pair of

WTs can be rewritten as

$$\text{cost}_i = Q_i C_i(x, y) L_i(x, y) \quad (6)$$

### 2.3 Energy yields model

The energy yields calculation concerns three elements: power production, power losses and duration. The analytical equations for calculating energy production are derived step by step as the follows.

**2.3.1 Power production:** The power produced by the WT at row  $i$ , column  $j$  can be calculated using the following equation [19, 20]:

$$P_{m,ij} = 0.5 \rho C_{p,\text{opt}}(\beta, \lambda_{\text{opt}}) \pi R_0^2 v^3 / 10^6 \quad (7)$$

In the simulation, the power production of each WT is found by assuming a maximum power point tracking control strategy, so (7) is valid when the wind speed is between the cut-in wind speed and rated wind speed [21]. The relationship between wind speed and power output,  $C_p$  and  $C_t$ , is listed as a lookup table in [22]. Thus the total power generated by the WTs can be written as

$$P_{\text{tot}} = \sum_{j=1}^{N_{\text{col}}} \sum_{i=1}^{N_{\text{row}}} P_{m,ij} \quad (8)$$

**2.3.2 Power losses and energy yields:** The power losses of AC cable can be expressed as

$$P_{\text{loss},ij} = 3I_{ij}^2 R_{e,ij} \quad (9)$$

where

$$R_{e,ij} = \rho_{R,ij} \frac{L_{R,ij}}{S_{R,ij}} \quad (10)$$

The length of the cable is related to the distance between WTs. Then the total losses within the wind farm can be written as

$$P_{\text{loss,tot}} = \sum_{j=1}^{N_{\text{col}}} \sum_{i=1}^{N_{\text{row}}} P_{\text{loss},ij} \quad (11)$$

From (7) to (11), the energy yield of the wind farm can be formulated as

$$E_{\text{tot}} = \sum_{i=1}^{\text{TE}} (P_{\text{tot},i} - P_{\text{tot,loss},i}) T_i \quad (12)$$

## 3 Problem formulation

The evaluation index, LPC, is introduced first in this section, and then the cable connection layout design problem is discussed and formulated into a mathematical problem. The objective function is presented at the end.

### 3.1 Levelised production cost

In this simulation, the objective function is constructed using an LPC index which takes capital discounted costs during the life-cycle into account. The mathematical equation for LPC for an offshore wind farm can be written as [23]

$$\text{LPC} = \frac{C_0 r (1+r)^{Ny} - 1}{(1+r)^{Ny} - 1} \frac{1}{E_{\text{tot}}} \quad (13)$$

$$C_0 = \sum_{i=1}^{My} \sum_{j=1}^N \text{cost}_i (1+r)^{-i} \quad (14)$$



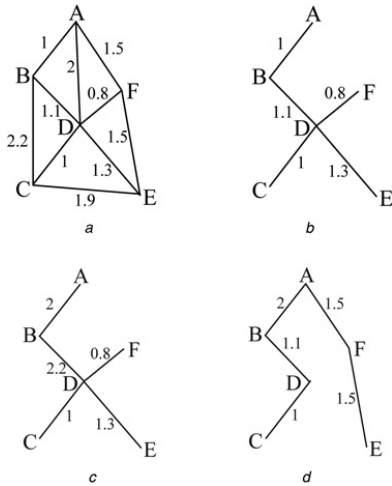


**Fig. 2** Illustration of MST and DMST algorithm  
*a* Undirected graph with six vertices and the different weights of each branch  
*b* Layout found by MST with minimal total weight  
*c* Layout found by MST with the weights updated from the previous arrangement  
*d* Layout found by DMST with updated weights from the previous arrangement

The cables' costs are considered separately by dividing the whole system into two parts: the CS and transmission system which are illustrated in Fig. 1 as the red and green blocks, respectively. The generated power is transmitted through a different type of cable in each part.

### 3.2 Objective function

Within the large region of the wind farm, it is desirable to find the most economical way to collect power under the technical requirements. Given the increased cost of cable crossing, an uncrossed cable connection layout is preferable in practice. The problem is similar to the classic mathematical problem of finding the MST of a given graph, expressed as [24]

$$G_T = (V, B_T, W_T) \quad G_T \leq G, B_T \leq B, W_T \leq W \quad (15)$$

where  $G$  is the undirected weighted graph and  $G_T$  is a subgraph of  $G$  representing the MST of  $G$ .  $V$  represents the vertices in graph  $G$ , which are the locations of WTs and substations in this paper.  $B$  shows all the possible paths between vertices in  $V$ , whereas  $B_T$  gives the branches that connect  $V$  in  $G_T$ .  $W$  is the weight of each edge in  $G$  and  $W_T$  is the weight of each branch in  $G_T$ . In this paper, the weight is defined as the LPC which includes the cable cost, energy production of the vertices on each end of the branch as well as energy losses from the branch and then the problem can be written as follows.

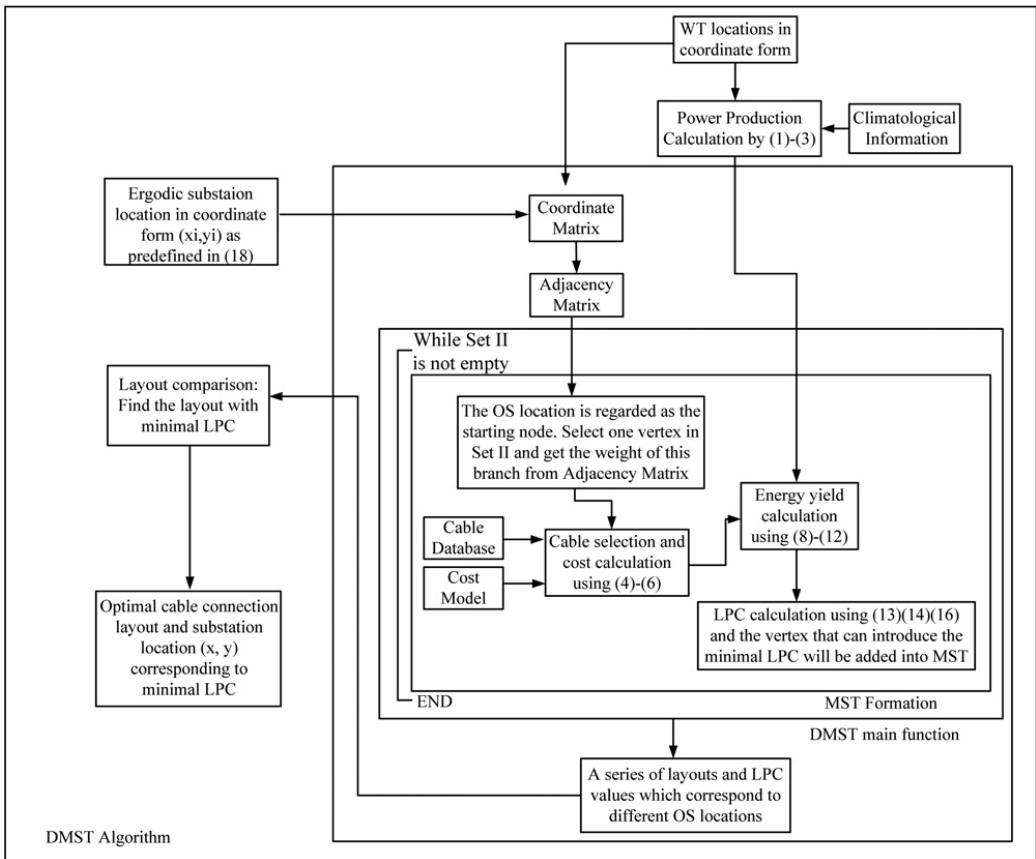


**Fig. 3** Optimisation framework with DMST algorithm

## Objective

$$\min \{LPC^{G_T}(x, y)\} = \min \left\{ \left[ \frac{C_0^{G_T}(x, y)r(1+r)^{N_y}}{(1+r)^{N_y} - 1} \right] \frac{1}{E_{tot}^{G_T}(x, y)} \right\} \quad (16)$$

## Constraints

$$I_i \leq I_{i,rated}; \quad i \in [1, N_G] \quad (17)$$

$$x \in [0, L_x]; \quad y \in [0, L_y] \quad (18)$$

The number  $N$  is the total number of vertices which is, in this paper, the total number of WTs plus the number of OSs.

## 4 Methodology

The cable connection problem can be solved by the DMST algorithm. The improved MST algorithm is proposed first. Then, modified algorithms which can optimise the OS location as well as the cable connection layout are specified in the optimisation framework.

### 4.1 DMST algorithm

As mentioned in Section 2, the optimised cable connection layout should be a tree which only permits one path between any two vertices. If the distance between each pair of WTs is regarded to be the weight, then the traditional MST algorithm can be used to find a  $G_T$  which has a minimal total weight (distance). However, due to limitations of current carrying capacity, the number of WTs that can be connected to one arc is proportional to the cable sectional area. If more WTs are connected to one branch, the cables in a previous arrangement may have to be changed in order to satisfy the change of operational requirements. Hence, if the LPC is regarded to be the weight, then the weight (LPC) will be changed each time a new vertex is added. The traditional MST can only find the layout with minimal distances to connect all the WTs rather than the minimal LPC. To solve this problem, a DMST algorithm is proposed and compared with the traditional MST algorithm. Fig. 2 shows a simple example.

As can be seen in Fig. 2, assuming six nodes are to be connected (a) is the undirected graph and the number shows the weight for each branch. The tree graph is formulated by assuming that A is the start point for the search. The layout found by the traditional MST algorithm is as illustrated in (b). The total weight for this method is  $1 + 1.1 + 0.8 + 1 + 1.3 = 5.2$ . However, if it is assumed that the original weights will be doubled when more than two nodes are connected after one branch, then the weight should be updated as shown in (c) and the total weight becomes  $2 + 2.2 + 0.8 + 1 + 1.3 = 7.3$ . Since the DMST considers the impact of the node that is about to be added into the MST to the previous structure's weight, the layout obtained by using DMST is as in (d) and the total weight obtained in this method is  $2 + 1.1 + 1 + 1.5 + 1.5 = 7.1$ . The DMST can find a better layout compared with the MST.

In this paper, the DMST is applied to optimise the layout. Six sets and one matrix are created as follows [11]:

Set I: Containing the vertices added into the MST.

Set II: Containing the vertices that have not yet been added into the MST.

Set III: Containing the weights of the branches in the MST, in other words, the branches chosen to connect the vertices in set I.

Set IV: Containing the total number of WTs connected after each branch in the MST.

Set V: Containing the sectional area of each cable or edge of the MST.

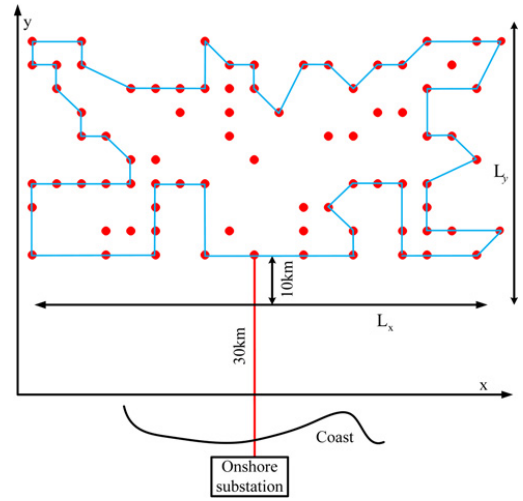


Fig. 4 Irregular shaped wind farm layout

Set VI: Containing the total energy yield of WTs connected to each branch in the MST, in other words, in set I.

*Adjacency matrix:* Containing all the weights between two adjacent vertices.

Initially, the sets I, III and IV will be empty and all the vertices are in Set II. Then vertex  $V_1$  is selected as the starting point which represents the OS from Set II and moved to Set I and all the branches that connect to  $V_1$  are compared. The branch that introduces total minimal LPC will be added to Set III and the selected vertex will be added to Set I and deleted from Set II. The number of the WTs connected to arc is incremented as WTs are added to the branch leading off it, and recorded in Set IV. If the number of WTs after a certain cable is over its limit when a new vertex is added, the cable sectional area should be updated and recorded in Set V and then the energy yields transmitted to the vertex in Set I can be calculated based on the information in Sets II, III and V. This process will stop when Set II is empty.

### 4.2 Cable connection layout optimisation framework

In this project, the location of the OS should be found together with the CS layout. The OS is regarded as the starting point and introduced into the adjacency matrix. Hence, the MST is generated from the OS until all the WTs are connected. The optimisation framework is shown in Fig. 3.

*Cable database:* In [25], various voltage levels' cables with different sectional areas can be found. In this simulation, the cables in the wind farm are XLPE-Cu AC cables operated at 33 kV nominal voltage for the CS and one 132 kV 630 mm<sup>2</sup> high voltage alternating current (HVAC) cable is selected for the transmission system.

Table 1 Specification of cable colour

CS					
voltage level type	33 kV AC				
colour*	yellow	green	purple	blue	black
cable sectional area, mm <sup>2</sup>	70/95/120/150	185/240/300	400/500	630/800	1000

\*Colour figures can be found online

*Climatological information:* The data is obtained from the work of the Norwegian Meteorological Institute [26], in which the wind speeds are sampled per 3 h. For convenience of calculation, the raw data is formulated into a wind rose which is used to calculate the energy production over a year.

The locations of WTs and the onshore substation are assumed to be fixed in this project. Therefore, the power extracted from the wind by each WT can be calculated according to the climatological information at the beginning. Since the wind resource information of a given wind farm is constant, this step will be run only one time.

The optimised location of the substation is expected to be found within the predefined area as described in (18). Each time a new OS location is loaded, it will be transferred into the DMST main function. In this, a new coordinate matrix which contains the coordinates of WTs and the OS will be created. On the basis of this, the adjacency matrix will be generated by taking the distance between every two locations as the branch's weight. Then the optimised layout of the wind farm, the weight of selected branches

and the number of WTs that connect to any selected branches will be found and calculated in the MST formulation step according to the process described in Section 4. A. Owing to the transmission capacity limitation, the cable size of each branch should be carefully selected. The cable database contains the available cable sizes. From the number of WTs connected to the branch, the maximum current going through the cable can be calculated. Then the corresponding cable sectional area can be found in the cable database. After that the total cost can be calculated using (4)–(6). When all the matched cables' sizes are selected, the energy yields which includes power production as well as power losses along the cables can be calculated using (8)–(12). Then the LPC will be calculated using (13), (14) and (16), the vertex that introduces the minimal LPC will be added into the MST. The MST formation step will not stop until Set II is empty. Finally, a series of LPCs corresponding to each loaded OS location will be transferred into the LPC comparison step.

In LPC comparison step, the optimised cable connection layout could be selected according to the results that obtained in DMST

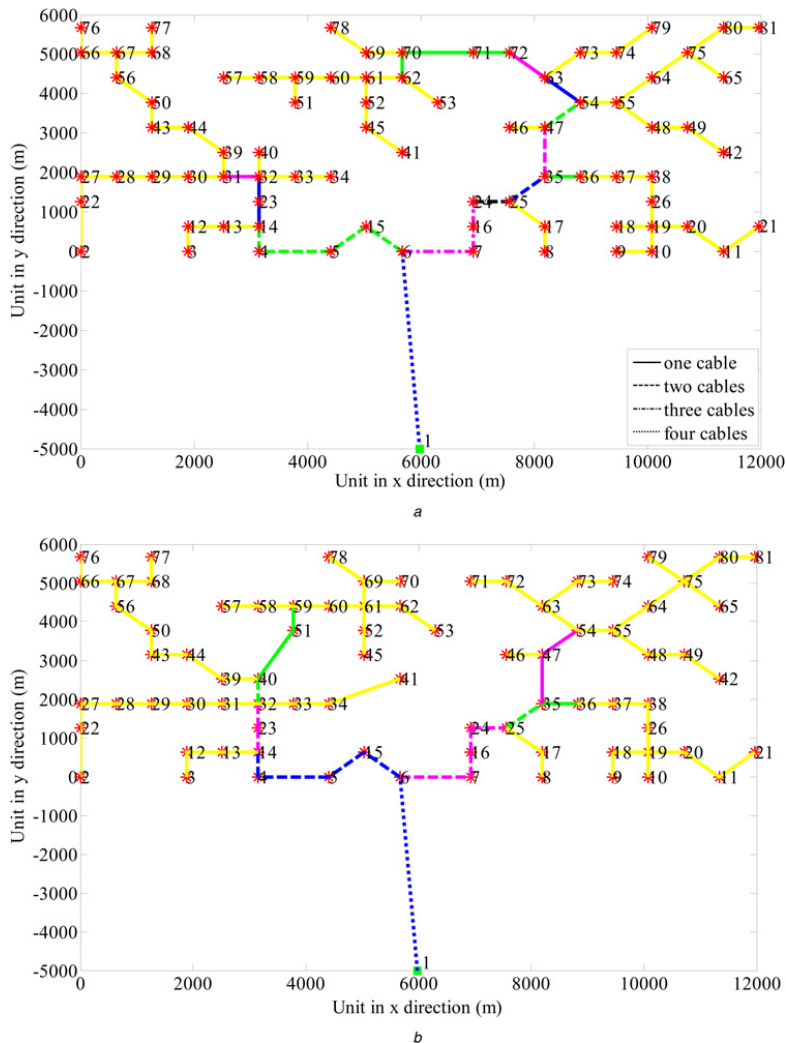


**Fig. 5** Layout optimisation for scenarios 1

a Optimised layout for OS near shore found by the MST  
 b Optimised layout for OS near shore found by the DMST

main function which is the layout with minimal LPC. Finally, the minimal LPC cable connection layout as well as the location of the OS will be decided.

## 5 Case study

The simulation is implemented on the MATLAB software platform. An irregular wind farm is chosen as the study case to verify the feasibility of the proposed method.

### 5.1 Irregular shaped wind farm

A wind farm configuration with 80 Vestas V90-2.0 MW (90 m rotor diameter) [27] WT<sub>s</sub> as shown in Fig. 4 is used as the study case. It is assumed to be set up 30 km away from the coast. The locations of the WT<sub>s</sub> are predefined and the nearest distance between each pair of WT<sub>s</sub> is seven rotor diameters (7Ds). The detailed locations of WT<sub>s</sub> are given in the Appendix. Three scenarios are presented and compared with the obtained optimised layout.

In Fig. 4, the red dots show the locations of the WT<sub>s</sub>. The blue lines are the boundary of the predefined wind farm. In this paper, the voltage level of the CS is assumed to be 33 kV while the transmission system is at 132 kV. Three scenarios are presented and the results are compared in a later paragraph.

**5.1.1 Scenario I: OS near shore:** In this scenario, the OS is assumed to be constructed 25 km away from the coast. Then the cable connection layout can be found by the proposed method.

The red stars are WT<sub>s</sub> and green square is the OS. The lines show the cable connection layout and the colour of the line represents the rating of the cable which is explained in Table 1. Since multiple cables might be adopted between some pairs of WT<sub>s</sub>, the number of cables utilised between each pair of WT<sub>s</sub> is indicated with different types of lines, which may be solid lines (one cable), dashed lines (two cables), dashed-and-dotted lines (three cables) and dotted lines (four cables), as shown in the lower right box of Fig. 5a. The colours and lines in the following figures are defined the same way. The input to the coordinate matrix in this case is just one given location for the OS instead of a series of locations. The optimised layouts found by the MST and DMST are illustrated in Figs. 5a and b, respectively.

**5.1.2 Scenario II: OS in the centre of the wind farm:** In this scenario, the OS is assumed to be constructed in the middle of the wind farm. The optimised cable connection layouts found by the MST and DMST for this scenario are illustrated in Figs. 6a and b, respectively.

**5.1.3 Scenario III: optimised CS layout:** In this scenario, the OS location is expected to be found together with the optimised cable connection layout. Using the traditional MST, the layout can be found as shown in Fig. 7a, whereas the optimised layout obtained following the proposed optimisation framework is as in Fig. 7b.

To see the performance of the proposed method, the layouts are also compared in Table 1. The trenching length indicates the total single line distance between WT<sub>s</sub> while cable length is the total length of cable that should be laid in this layout.

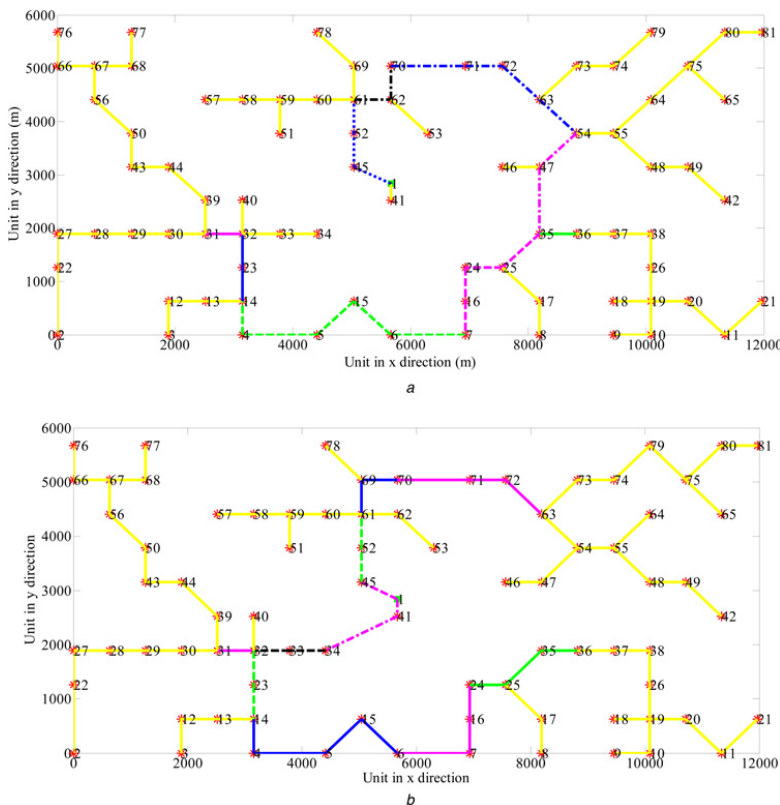


**Fig. 6** Layout optimisation for scenarios II

a Optimised layout for OS in the centre found by the MST  
 b Optimised layout for OS in the centre found by the DMST

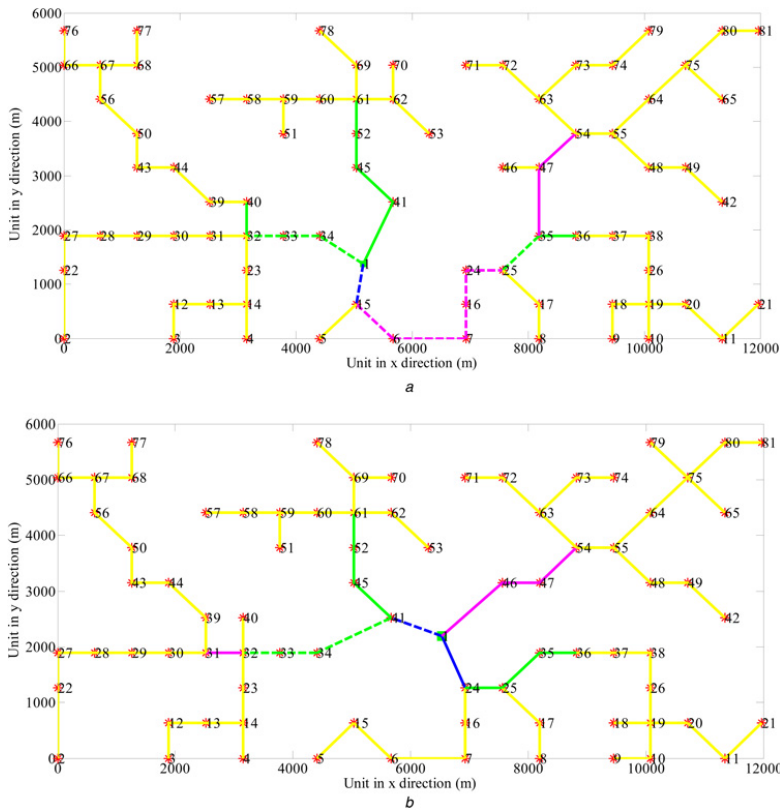


**Fig. 7** Layout optimisation for scenarios III

- a Optimised CS layout found by the MST
- b Optimised CS layout found by the DMST

As can be seen in Table 2, the DMST method can find a layout with smaller LPC compared with the MST method in all scenarios. In each scenario, the DMST method can find a layout which needs less investment in cables and generates more energy. It can reduce the LPC by 0.63, 18.54 and 3.14% in the three scenarios compared with the MST method. Scenario III, which considers the optimised location to set up the OS, always gives the best layout compared with scenarios I and II. In scenario III, the LPC from the MST can be reduced by 16.39 and 24.69%, respectively, compared with scenarios I and II. While using the DMST, the LPC in scenario III is 18.85 and 10.21% lower than in scenarios I and II. There is also an abnormal phenomenon occurring when the MST algorithm is adopted to find the optimised cable connection layout in scenario II. It can be seen that the total cable cost for the OS as well as the LPC is much higher than the values obtained by the DMST and this result is also the worst result in all scenarios using either method. As can be seen in Fig. 6a, there are actually two feeders coming out from the OS in this layout. One is collecting the power from merely one WT while the generated power from the other 79 is collected by the other feeder. Hence, four 630 mm<sup>2</sup> cables are needed in this feeder and multiple cable operation is always required in this case which increases the total cost of cables. This worst case also proves that the MST can only identify the nearest WT to connect to achieve the target of getting the shortest total cable length instead of getting a minimal cost layout. The best layout in this paper is illustrated in Fig. 7b and is obtained using the DMST algorithm by taking OS location optimisation into consideration. However, constructing the offshore wind farm far away from the

shore increases the cost of foundations. Hence, more factors such as varying foundation cost with water depth, cable installation costs, operation and maintenance costs etc. should be considered to make the layout more practical so that a comprehensive decision can be made.

**Table 2** Layout comparisons of MST and DMST

	Scenario I		Scenario II		Scenario III	
	MST	DMST	MST	DMST	MST	DMST
total cable length for CS, km	91.08	87.38	86.56	66.87	66.92	63.22
trenching length for CS, km	63.67	64.23	58.79	58.94	59.06	59.63
cable to shore, km	25	25	32.84	32.84	31.38	32.22
cable costs for CS, MDkk	178.61	176.83	175.65	117.83	105.86	95.06
cable costs for TS, MDkk	103.75	103.75	136.27	136.27	130.23	133.61
total Cable invest, MDkk	282.36	280.58	311.93	254.1	236.09	228.67
energy losses, GWh	16.51	15.66	17.08	13.88	13.07	11.99
energy yields, GWh	859.69	860.53	859.12	862.34	863.12	864.21
substation location	(5.99, -5)	(5.67, 2.84)	(5.16, 1.37)	(6.53, 2.19)	-	-
LPC, Dkk/MWh	328.54	326.15	363.19	294.77	273.52	264.68

## 6 Conclusions and future work

This paper describes a new way of finding an optimised offshore wind farm electrical system layout with minimal LPC using a DMST. The wake effect and power losses along the cables are two main concerns in LPC evaluation. Since the optimised layout problem is similar to the classic MST problem in graph theory, the new method proposed is based on this idea. Some factors such as the best location to build the OS and suitable cable sectional areas for each line between two WT are considered during the layout formulation process in this paper. The proposed method is applied to an irregular shaped wind farm. The results demonstrate that the proposed method is an effective way to find the electrical system layout with minimal LPC. Moreover, the OS location indeed has a significant impact on the final layout and total costs, the optimised layout considering the placement of the OS has the lowest cost compared with the other layouts.

In future, the number of OSs and the availability of electrical equipment should be included into the cable connection layout design problem and the transformers, circuit breakers, cable installation and OS platform foundation costs should be considered to make a more practical layout.

## 7 Acknowledgment

The authors thank the Norwegian Centre for Offshore Wind Energy (NORCOWE) under grant 193821/S60 from the Research Council of Norway (RCN).

## 8 References

- 1 Chen, Z., Blaabjerg, F.: 'Wind farm – a power source in future power systems', *Renew. Sustain. Energy Rev.*, 2009, **13**, pp. 1288–1300
- 2 Zhao, M., Chen, Z., Blaabjerg, F.: 'Application of genetic algorithm in electrical system optimization for offshore wind farms'. Presented at the Int. Conf. Electric Utility Deregulation and Restructuring and Power Technologies (DRPT), Nanjing, China, 2008
- 3 Zhao, M., Chen, Z., Blaabjerg, F.: 'Optimization of electrical system for a large DC offshore wind farm by genetic algorithm'. Proc. of NORPIE'04, 14–16 June 2004
- 4 Dutta, S., Overbye, T.J.: 'A clustering based wind farm collector system cable layout design'. 2011 IEEE Power and Energy Conf. at Illinois (PECI), Champaign, IL, 25–26 February 2011, pp. 1–6
- 5 Ling-Ling, H., Ning, C., Hongyue, Z., *et al.*: 'Optimization of large-scale offshore wind farm electrical collection systems based on improved FCM'. Int. Conf. on Sustainable Power Generation and Supply (SUPERGEN 2012), Hangzhou, 8–9 September 2012
- 6 Dutta, S., Overbye, T.J.: 'Optimal wind farm collector system topology design considering total trenching length', *IEEE Trans. Sustain. Energy*, 2012, **3**, (3), pp. 339–348. S.
- 7 Jenkins A.M., Scutariu, M., Smith, K.S.: 'Offshore wind farm inter-array cable layout'. PowerTech (POWERTECH), 2013 IEEE Grenoble, 16–20 June 2013, pp. 1–6

- 8 Gonzalez-Longatt, F.M., Wall, P., Regulski, P., *et al.*: 'Optimal electric network design for a large offshore wind farm based on a modified genetic algorithm approach', *IEEE Syst. J.*, 2012, **6**, (1), pp. 164–172
- 9 Li, D.D., He, C., Fu, Y.: 'Optimization of internal electric connection system of large offshore wind farm with hybrid genetic and immune algorithm'. Proc. Third Int. Conf. Electric Utility DRPT, April 2008, pp. 2476–2481
- 10 Bauer, J., Lysgaard, J.: 'The offshore wind farm array cable layout problem – a planar open vehicle routing problem', *J. Oper. Res. Soc.*, 2015, **66**, pp. 360–368, doi: 10.1057/jors.2013.188
- 11 Ma, Y., Yang, H., Zhou, X., *et al.*: 'The dynamic modeling of wind farms considering wake effects and its optimal distribution'. World Non-Grid-Connected Wind Power and Energy Conf., 2009. WNVEC 2009, Nanjing, September 2009, pp. 1–4
- 12 WindPRO/PARK: 'Introduction wind turbine wake modelling and wake generated turbulence'. EMD International A/S
- 13 Pérez, B., Minguez, R., Guanche, R.: 'Offshore wind farm layout optimization using mathematical programming techniques', *Renew. Energy*, 2013, **53**, pp. 389–399
- 14 Jensen, N.O.: 'A note on wind generator interaction', 1983, p. 5
- 15 González-Longatt, F., Wall, P., Terzija, V.: 'Wake effect in wind farm performance: Steady-state and dynamic behavior', *Renew. Energy*, 2011, pp. 329–338, September
- 16 Beaucage, P., Brower, M., Robinson, N., *et al.*: 'Overview of six commercial and research wake models for large offshore wind farms'. Proc. EWEA 2012, Copenhagen, 2012
- 17 Porté-Agel, F., Wu, Y.-T., Chen, C.-H.: 'A numerical study of the effects of wind direction on turbine wakes and power losses in a large wind farm', *Energies*, 2013, **6**, pp. 5297–5313, MDPI
- 18 Lundberg, S.: 'Performance comparison of wind park configurations'. Technical Report, 30R, Department of Electric Power Engineering, Chalmers University of Technology, Department of Electric Power Engineering, Goteborg, Sweden, August 2003
- 19 González, J.S., Gonzalez Rodriguez, A.G., Morac, J.C., *et al.*: 'Optimum wind turbines operation for minimizing wake effect losses in offshore wind farms', *Renew. Energy*, 2010, **35**, (8), pp. 1671–1681
- 20 Flores, P., Tapia, A., Tapia, G.: 'Application of a control algorithm for wind speed prediction and active power generation', *Renew. Energy*, 2005, **30**, (4), pp. 523–536
- 21 Qiao, W.: 'Intelligent mechanical sensorless MPPT control for wind energy systems'. 2012 IEEE Power and Energy Society General Meeting, San Diego, CA, July 2012, pp. 1–8
- 22 'General specification V90-1.8/2.0 MW 50 Hz VCS'. Vestas Wind Systems A/S, Technology R&D, 19 November 2010
- 23 Zhao, M.: 'Optimization of electrical system for offshore wind farms via a genetic algorithm approach'. Dissertation, Faculty of Engineering, Science and Medicine at Aalborg University, Denmark, October 2006
- 24 Bondy, J.A., Murty, U.S.R.: 'Graph theory with applications' (The Macmillan Press Ltd., 1976)
- 25 'XLPE submarine cable systems attachment to XLPE land cable systems-user's guide'. ABB corporation
- 26 Furevik, B.R., Haakenstad, H.: 'Near-surface marine wind profiles from rawinsonde and NORA10 hindcast', *J. Geophys. Res.*, 2012, **117**, pp. 1–14
- 27 'General SPECIFICATION V90-1.8/2.9 MW 50 Hz VCS'. Vestas Technology R&D, 19 November 2010

## 9 Appendix

The WT locations are listed in Table 3 in the coordinate form.

**Table 3** Location of WT in coordinate form

WT no.	X(m)	Y(m)	WT no.	X(m)	Y(m)	WT no.	X(m)	Y(m)	WT no.	X(m)	Y(m)
1	0	0	21	11,970	630	41	5670	2520	61	5040	4410
2	0	0	22	0	1260	42	11,340	2520	62	5670	4410
3	1890	0	23	3150	1260	43	1260	3150	63	8190	4410
4	3150	0	24	6930	1260	44	1890	3150	64	10,080	4410
5	4410	0	25	7560	1260	45	5040	3150	65	11,340	4410
6	5670	0	26	10,080	1260	46	7560	3150	66	0	5040
7	6930	0	27	0	1890	47	8190	3150	67	630	5040
8	8190	0	28	630	1890	48	10,080	3150	68	1260	5040
9	9450	0	29	1260	1890	49	10,710	3150	69	5040	5040
10	10,080	0	30	1890	1890	50	1260	3780	70	5670	5040
11	11,340	0	31	2520	1890	51	3780	3780	71	6930	5040
12	1890	630	32	3150	1890	52	5040	3780	72	7560	5040
13	2520	630	33	3780	1890	53	6300	3780	73	8820	5040
14	3150	630	34	4410	1890	54	8820	3780	74	9450	5040
15	5040	630	35	8190	1890	55	9450	3780	75	10,710	5040
16	6930	630	36	8820	1890	56	630	4410	76	0	5670
17	8190	630	37	9450	1890	57	2520	4410	77	1260	5670
18	9450	630	38	10,080	1890	58	3150	4410	78	4410	5670
19	10,080	630	39	2520	2520	59	3780	4410	79	10,080	5670
20	10,710	630	40	3150	2520	60	4410	4410	80	11,340	5670



# Optimisation for offshore wind farm cable connection layout using adaptive particle swarm optimisation minimum spanning tree method

Peng Hou, Weihao Hu ✉, Zhe Chen

Department of Energy Technology, Aalborg University, Pontoppidanstraede 101, Aalborg DK-9220, Denmark

✉ E-mail: whu@et.aau.dk

**Abstract:** The wind farm layout optimisation problem is similar to the classic mathematical problem of finding the minimum spanning tree (MST) of a weighted undirected graph. Due to the cable current-carrying capacity limitation, the cable sectional area should be carefully selected to meet the system operational requirement and this constraint should be considered during the MST formulation process. Hence, traditional MST algorithm cannot ensure a minimal cable investment layout. In this study, a new method to optimise the offshore wind farm cable connection layout is presented. The algorithm is formulated based on the concept of MST and further improved by adaptive particle swarm optimisation algorithm. Since the location of the offshore substation (OS) has a significant impact on both the layout formulation and total cost of cables, the optimised location of OS is expected to be found together with the optimised cable connection layout. The proposed method is compared with the MST and dynamic MST methods and simulation results show the effectiveness of the proposed method.

## Nomenclature

$C_i$	unit cost of cable $i$ (MDkk/km)
$A_p, B_p, C_p$	coefficients of cable cost model
$S_{\text{rated},i}$	rated apparent power of cable in line $i$ (MW)
$I_{i,\text{rated}}$	rated current of cable in line $i$ (kA)
$U_{i,\text{rated}}$	rated voltage of cable in line $i$ (kV)
$x, y$	position of OS in the form of coordinate
$\text{Cost}_{\text{min}}$	minimum cost of total cables for optimised cable connection layout (MDkk)
$G_T$	sub-graph in $G$ which represents one possible spanning tree of $G$
$C_i^{G_T}(x, y)$	cost of cable $i$ for $G_T$ when OS location is $(x, y)$
$L_i^{G_T}(x, y)$	length of cables $i$ for $G_T$ when OS location is $(x, y)$
$L_x, L_y$	predefined area for constructing OS in $x$ direction and $y$ direction, respectively
$I_i$	current going through the cable $i$ (kA)
$N$	total number of vertices in a graph
$k$	sequence number of iteration
$w$	inertia weight
$l_1, l_2$	learning factors
rand	random number in the range $[0, 1]$
$x_i^k, x_i^{k+1}$	position of particle $i$ at iteration $k$ and $k+1$ , respectively (m)
$v_i^k, v_i^{k+1}$	speed of particle $i$ at iteration $k$ and $k+1$ , respectively (m)
$Lb_i^k$	best position of particle $i$ at iteration $k$ (m)
$Gb^k$	best position of all particles at iteration $k$ (m)
$I_p$	quantity of particles
$k_{\text{max}}$	quantity of iterations
$f$	evolutionary factor
$d_g$	mean distance from global best particle to the others
$d_{\text{min}}$	minimal mean distance from one particle to the others
$d_{\text{max}}$	maximum mean distance from one particle to the others

## 1 Introduction

Offshore wind farm has become focus of wind power development recently due to its higher wind energy resources density and stability. Since the wind turbines (WTs) are distributed in a wide area, a large number of submarine cables and electrical components are needed to collect the power captured by WTs and transmit the energy to onshore substation. As mentioned in [1], the cost of offshore wind farm electrical system can take up to 15–30% of total investment in which the cost of cables take a large proportion. It is desirable to optimise the cable connection layout to make a cost-effective offshore wind farm.

The existing work of optimisation of offshore wind farm layout can be divided into two parts: the WT location optimisation [2–8] and the optimisation of offshore wind farm electrical system design [9–20]. In [2], the initial WT positions were randomly generated using heuristic method and then the local optimal layout was found using non-linear mathematical programming techniques. An optimisation of a real offshore wind farm is done in [3] using evolutionary algorithms, the regular turbines layout and design strategies of free turbines disposition with fixed number of turbines are presented and simulation results have shown that the free design with fixed number of turbines method can benefit offshore wind farm more. A recent work of optimising WTs positions has been done in [4] using multi-population genetic algorithm (GA). Instead of partitioning whole construction area into grids, the coordinate form was used to locate WTs in [4] and the algorithm was demonstrated to be outperformed than some previous methods [5–8].

The optimisation of offshore wind farm electrical system can also be further divided into two sorts: the optimised selection of electrical components and optimised cable connection layout design. In [9, 10], a large database which contains various types of electrical components with common voltages and industrial design cable connection topologies are produced. The optimised electrical system layout is decided by comparing the total cost of different

electrical components' composition. Finally, the selected voltage level, the suitable type of equipment as well as the cable connection topology can be obtained. Similar work has also been done in [11] which compared a variety of wind farm designs with respect to losses, reliability and cost. The method can be used to save the investment on electrical system, however, the cable connection layout is actually decided from the designer's experience. There is still a possibility of further reducing the cost of submarine cables. In [12], the collection system power losses were minimised and the reliability is also considered using a cluster-based algorithm. Based on the concept of minimum spanning tree (MST) in the graphic theory, some works have been done using greedy algorithm [13] to get a minimal cost collection system layout [14, 15]. Besides, GA is also widely used for solving these problems [16, 17]. In [16], the collection system layout was designed with the purpose of minimising total cable length, capital cost as well as power losses. The results were also compared with the optimised layout that obtained by prim algorithm while the minimal cost cable connection layout for a four substation offshore wind farm was presented in [17]. The travelling salesman problem algorithm was adopted to improve the standard GA to find a minimal cost layout. From the cable rated current, the number of WT in each cluster were calculated and assumed to be the same. The optimised layout was compared with a similar work [18] which used hybrid GA and immune algorithm to optimise the system layout and showed better performance.

Moreover, the offshore substation (OS) location has a significant impact on the formulation of collection system layout [19]. For engineering consideration, Hopewell *et al.* [19] proposed a method to locate OS which shows that the most favourable location for OS should be in central area while in [20], the optimised OS location is selected from a series of given positions. In sum, it would be beneficial if the optimisation of OS location and the collection system layout can be done at the same time to make a comprehensive optimisation work. As indicated in [21], evolutionary algorithms such as GA and particle swarm optimisation (PSO) have a good performance of finding the final solution for the constrained non-linear optimisation problem. In this project, the PSO algorithm is adopted to implement the simulation since it has higher computation efficiency in solving non-linear problems with continuous design variables compared with GA [22].

The WTs' positions may be decided at first and then the cable connection configuration will be designed based on this wind farm layout. It is also the reason why the optimisation work of offshore wind farms is usually divided into two parts as mentioned above. However, there is also a possibility to optimise the WT positions as well as the cable connection layout at the same time. In [23], an artificial intelligent method to find the feasible scheme for the WT location and internal cable connection of a wind farm was proposed. In which, the locations of WTs are found by GA algorithm and then the optimised cable connection layout is decided by ant colony system. The possibility of using different sectional area's cable is considered in this paper, however, the final cable connection layout was crossed which would increase the cost of installation and maintenance while in our work the uncrossed cable connection layout can be ensured.

In this paper, a new method, adaptive PSO (APSO)-MST is proposed to get an optimised cable connection layout. To ensure an uncrossed cable connection layout, the tree concept in graphic theory is preserved in this algorithm while the generation of the tree graphic is guide by APSO algorithm. Since the location of OS is highly related to the collection system layout, the siting of the OS is optimised together with the system layout. To meet the system operation requirement, the cable current carrying capacity is considered during the layout formulation process. The proposed method is implemented in an irregular shaped wind farm and the results are compared with other two existing methods.

The paper is organised as follows. Section 2 provides some related models at first and then the objective function is presented. The methodology for solving the problem is specified in Section 3. An irregular shaped wind farm is chosen as the study case to

demonstrate the proposed method in Section 4. Section 5 summarises the main conclusions.

## 2 Mathematical model

In this section, the concept of MST is first introduced, and then followed by the cost model. The objective function is presented at last.

### 2.1 Minimum spanning tree

In graphic theory [24], the spanning tree is defined as a sub-graph of an undirected graph which contains all the vertices in that graph and permits only one path between every two vertices. For a given graph, the spanning tree will not be unique which means that there are a number of ways to formulate a tree graph to connect all the vertices. Based on it, the MST is defined as a spanning tree with minimum weights which can be expressed as

$$G_T = (V, B_T, W_T), \quad G_T \in G, \quad B_T \in B, \quad W_T \in W \quad (1)$$

where  $G$  means the undirected weighted graph and  $G_T$  is the sub-graph in  $G$  which represents one possible spanning tree of  $G$ .  $V$  represents the vertices in graphic  $G$ .  $B$  shows all the possible paths or rather the branches that connect  $V$  while  $B_T$  is all the branches that connect  $V$  in  $G_T$ .  $W$  is the weight of each branch in  $G$  and  $W_T$  is the weight of each branch in  $G_T$ . In a given  $G$ , the MST can be described as a  $G_T$  with minimum total  $W_T$ .

### 2.2 Cost model

The cost models are set up according to cables' rated power. The mathematical equations can be written as [25]

$$C_i = A_p + B_p \exp\left(\frac{C_p S_{\text{rated},i}}{10^8}\right)^2 \quad (2)$$

$$S_{\text{rated},i} = \sqrt{3} I_{i,\text{rated}} U_{i,\text{rated}} \quad (3)$$

After the voltage level is decided, the cables are selected according to its rated current which is correlated to the sectional area. The cable types are selected according to an existing cable list in [26]. In some cases, more cables are required between two WTs if many WTs are connected after this branch.

### 2.3 Objective function

If the location of WTs and OS can be regarded as vertices while the costs of the cables are regarded as the weight of branches. Then, the problem can be converted into a classic mathematical problem as finding the MST of a given graph. As a consequence, the mathematical expression of the problem can be written as

*Obj.*

$$\text{Cost}_{\min} = \min\left(\sum_{i=1}^{N-1} C_i^{G_T}(x, y) L_i^{G_T}(x, y)\right), \quad G_T \in G \quad (4)$$

*Constraints*

$$I_i \leq I_{i,\text{rated}}; \quad i \in (1, N-1) \quad (5)$$

$$x \in (0, L_x); \quad y \in (0, L_y) \quad (6)$$

As mentioned before,  $G$  is undirected weighted graph which represents all possible cable connection layouts.  $G_T$  is one layout of  $G$  which contains a number of vertices ( $V$ , WT location) with different weight ( $W$ , cable cost) between them.  $B$  is the branch that connected vertices. The  $N$  is the total number of vertices which is



the total number of WT's plus the number of OS in this work. Once the tree shape layout ( $G_T$ ) is determined, the total cost of cables can be calculated using (1)–(6).

The location of substation will influence the collection system layout so that the costs will be changed as well. In this paper, the cable connection layout and the location of OS are expected to be optimised at the same time. The optimised layout should be a tree graph connecting all WT's with minimum total costs.

### 3 Methodology

The prim and dynamic MST (DMST) algorithms are presented at first. After that PSO algorithm is specified. Based on the existing algorithms, the APSO-MST algorithm, which concerns both the optimisation of substation location as well as electrical system layout are proposed. The optimisation framework is presented last.

#### 3.1 Prim algorithm

Due to the higher cost of crossed cable connection layout, the offshore wind farm collection system should be an uncrossed configuration with minimised total cost. This description corresponds to the classic mathematical problem of finding MST in an undirected weighted graph [24]. Currently, prim algorithm and kruskal algorithm are widely used to solve MST problem which are both based on the idea of greedy algorithm [13]. In this work, the prim algorithm [27] is modified to optimise the collection system layout and OS location together. The results found by MST will be regarded as the baseline and compared with another two proposed algorithms.

#### 3.2 DMST algorithm

The prim algorithm can be used to find an optimised layout under the assumption that the weight in each branch is constant, however, during the design of an offshore wind farm if more WT's are connected to one string, the cables in a previous arrangement may have to be changed in order to satisfy the change of the operational requirement. In other words, the weight (cost of cable) will be changed during the layout formulation process. To find a better layout, a DMST algorithm has already proposed in a previous work [28] which was demonstrated to outperform prim algorithm.

#### 3.3 PSO algorithm

In 1995, Kennedy and Eberhart [29] got an inspiration from the social behaviour of fish schooling and bird flocking and developed an evolutionary algorithm, PSO algorithm, which has a good performance of solving non-linear optimisation problem. After that, a modified PSO which is the so-called global PSO (GPSO) is proposed to increase the possibility of finding a global optimal solution by same authors. The algorithm can be expressed in following equations [30]

$$v_i^{k+1} = wv_i^k + l_1 \text{rand}(Lb_i^k - x_i^k) + l_2 \text{rand}(Gb^k - x_i^k) \quad (7)$$

$$x_i^{k+1} = x_i^k + v_i^{k+1} \quad (8)$$

$$i \in (1, I_p), \quad k \in (1, k_{\max}) \quad (9)$$

For the heuristic algorithms, the parameter setting is critical to the final solution. To increase the possibility of finding a global optimal solution, many works have been done to control the inertia weight. Presently, two sorts of parameter control methods are widely used: the time-varying control strategy [31–34] and adaptive parameter control strategy [35]. The first strategy indicate

that the PSO performance can be improved by using linear, non-linear or fuzzy adaptive inertia weight while the other introduce evolutionary state estimation technique [36] to further improve the performance of PSO. In this project, the adaptive PSO control method is adopted to increase the global optimal result searching ability, in which the inertia weight is expressed as [35]

$$w = 1/(1 + 1.5e^{-2.6f}) \in [0.4, 0.9], \quad \forall f \in [0, 1] \quad (10)$$

$$f = \frac{d_g - d_{\min}}{d_{\max} - d_{\min}} \quad (11)$$

where  $f$  is the evolutionary factor which is defined to control the parameters in PSO adaptively.

#### 3.4 APSO-MST algorithm

Essentially, the greedy algorithm for solving MST problem is a decision-making process which provides solutions to multi-step problems by indicating the best choice in each step. In greedy algorithm, the decision which can bring the most benefit in each step, in other words, local optimal solution is selected. The final result, global optimal solution, is actually the combination of these local optimal solutions in each step. Hence, the basic idea of greedy algorithm can be described as the choice of the best option at each moment. Once the decision is made in each step, it would never be considered again. The mathematical proof is specified in [24].

However, for cable connection layout design problem, the weight (cost of cable) is always changing during the layout formulation process. The traditional algorithm can only find the layout with minimal distances to connect all the WT's rather than minimum cable costs. The DMST provides another better strategy to find a cheaper cable connection layout compared with prim algorithm, however, it also followed the idea that the decision made in each step will not be considered again. Hence, it cannot ensure the result to be an optimal solution. To find a better layout, an APSO-MST algorithm is proposed so that a spanning tree with minimum total weight, which considered dynamic changing process during the tree formulation process, can be found. Different from greedy algorithm, the decision-making task in each step is done by APSO in this algorithm. In other words, the spanning tree's formulation is guided by APSO. Since the decision in each step is regarded as a whole in APSO, it can be reconsidered so that it can avoid the constraints of decision making in greedy and DMST algorithms. Moreover, because the layout is also formulated based on the idea of finding a MST, the uncrossed cable connection layout can also be preserved. Fig. 1 shows a simple example of using different methods.

As can be seen in Fig. 1, assuming six nodes are to be connected, Fig. 1a is the undirected graph and the number shows the weight for each branch. The tree graphic is formulated by assuming that A is the searching start point. To simulate the condition that the cable sectional area should be changed if more WT's are connected after this branch, it is assumed that the weight in previous arrangement will be doubled when more than two nodes are connected after one branch. The layout found by traditional MST algorithm is shown in Fig. 1b. The total weight for this method is  $1.6 \times 2 + 1.4 \times 2 + 1.4 \times 2 + 2 + 1.9 = 12.7$ . The DMST consider the impact of the node that is about to be added into the MST to the previous structure's weight. The layout obtained by using DMST is shown in Fig. 1c and the total weight obtained by this method is  $2.2 \times 2 + 2 + 1.9 + 1.6 + 1.4 = 11.3$ . The total weight obtained by APSO-MST is  $2.2 + 1.6 + 1.4 + 3 + 1.9 = 10.1$ . The Greek numerals I–V represent the tree graphic formulation sequence. Since the result obtained by MST or DMST are deterministic, the tree graphic formulation process is unique as shown in Figs. 1e and f. As a heuristic method, PSO will randomly select a branch in each tree formulation step. Hence, there will be more freedom for the layout formulation. As shown in Figs. 1g and h, two tree

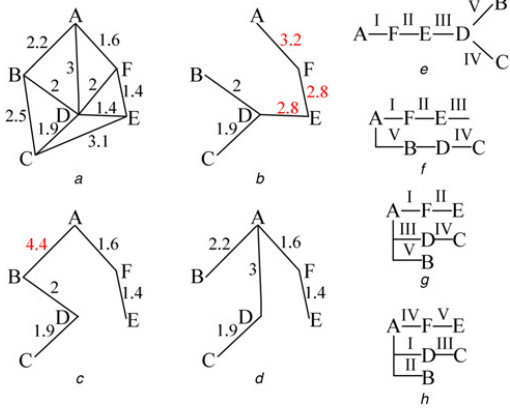


**Fig. 1** Illustration of different method

- a Undirected graph with six vertices and different weight of each branch
- b Layout found by MST with updating the weight of previous arrangement
- c Layout found by DMST with updating the weight of previous arrangement
- d Layout found by APSO-MST with updating the weight of previous arrangement
- e Procedure of tree formulation using MST
- f Procedure of tree formulation using DMST
- g, h Procedure of tree formulation using APSO-MST

formulation processes are presented. It can be seen that the tree formulation sequence can be varied though the final layout is the same. Due to this release in the freedom of branch selection, the APSO-MST can find the lowest weight layout compared with the other two methods in this simple example.

In APSO-MST, four sets and one matrix are created as follows:

- Set I*: Containing the vertices that added into the MST.
- Set II*: Containing the vertices that have not yet added into the MST.
- Set III*: Containing the weights of the branches connecting the vertices in the MST, in other words, in set I.
- Set IV*: Containing the total number of WTs that connected to each branch in MST, in other words, the number of WT that is undertaken by each branch in MST.

*Adjacency matrix*: Containing all the weights between two adjacent vertices. In this work, the weight is the cost of the cable for this branch. Initially, all the cables are assumed to be with 70 mm<sup>2</sup> sectional area which is the minimal sectional area in [26]. Then the cost can be updated by (2).

Initially, the sets I, III and IV will be put empty and all the vertices are stored in set II. Then the minimum cost spanning tree formulation process will start with a given vertex ( $V_1$ , in this paper is the OS location) and it will be deleted from set II and added to set I, then the APSO will select a vertex randomly from set II. The selected vertex must meet the requirement that the new formulated branch that connect to vertex in set I (in this step is  $V_1$ ) could not cross the other branches in MST. The selected vertex will be added to set I and deleted from set II. The weight of this branch will be found from adjacency matrix and added to set III. The number of the WTs connected to this branch will be added 1 in set IV at this time. For a certain type of cable, the maximum number of WTs that it can undertake is limited. Hence, if the number of WTs after a certain branch (cable) in set IV is over this limit when a new vertex is added, the cable sectional area or rather the weight of this branch (cable cost) should be updated. This process will stop when set II is empty which means a spanning tree is formulated, however, since the vertex that is selected in each step is picked up randomly. It needs iterative calculation to get an optimised result which is accomplished by APSO in this work.

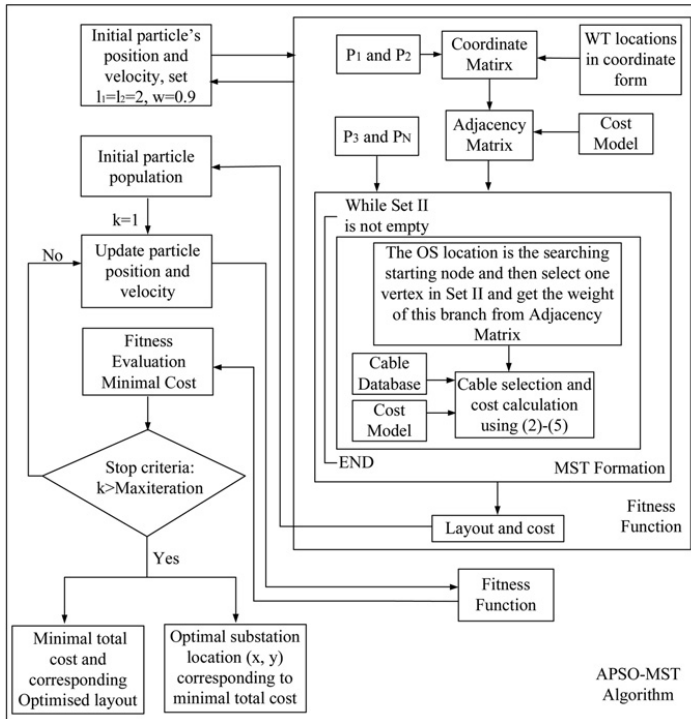


**Fig. 2** Optimisation framework for proposed method

### 3.5 Coding of particle

Each particle (each solution) contains two parts of information: the coordinate of OS location as well as the branch sequence number. All potential solutions are required to be coded into particles which are the initial step in PSO. The detailed information of coding is as follows

$$P\{p_1, p_2, p_3, \dots, p_N\}$$

$p_1, p_2$  represent the coordinate of OS location.  
 $p_3 \dots p_N$  represent the vertex sequence number.

### 3.6 Optimisation framework

As proposed above, the proposed algorithm is expected to find an optimised layout with minimum cable costs in consideration of OS placement. The simulation procedure to access the optimised cable connection layout by APSO-MST is shown in Fig. 2.

The parameters of APSO are initialised in the first step. As described above, the initial particles' position would include two parts of information: randomly selected vertices in each step and randomly given OS location which is limited by (6). The particles will be transferred into fitness function and will be utilised to generate the coordinate matrix with the given WT locations. Then the adjacency matrix will be formed using cost model. The first calculated total cost and cable connection layout will be obtained after the MST is generated in MST formation step as described in Section 4.4. The result from the first calculation will be saved as the initial particle population which is the basis for comparison later. Then the particles will be updated and transferred into the fitness function by following the same procedure. The calculated cost and its corresponding layout can be obtained and send out to the fitness evaluation step for comparison. Or it may stop if the maximum iteration is reached. Finally, a series of vertices number as well as the optimised location for OS will be selected.

## 4 Case study

An irregular wind farm is chosen as the study case to verify the feasibility of the proposed method in this section. The layout of the reference wind farm is introduced first. Then the results obtained by the proposed method is presented and compared with the other two methods.

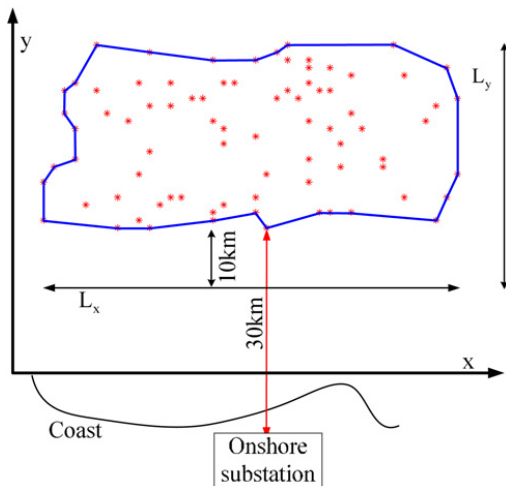


Fig. 3 Layout of irregular shaped wind farm

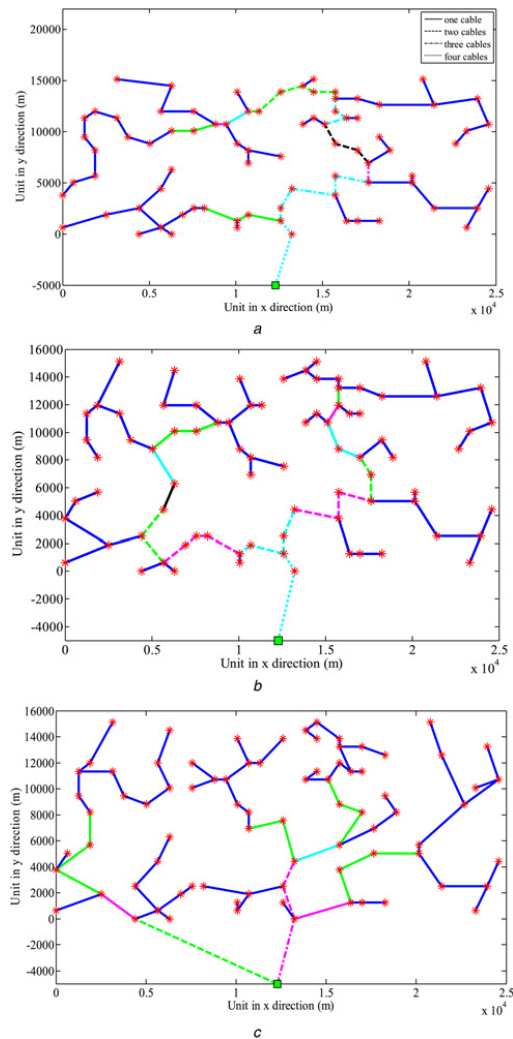


Fig. 4 Cable connection layout comparison using different methods when OS is near shore

- a Optimised layout with OS near shore obtained by MST
- b Optimised layout with OS near shore obtained by DMST
- c Optimised layout with OS near shore obtained by APSO-MST

### 4.1 Irregular shaped wind farm

The wind farm is assumed to be set up 30 km away from the onshore substation with 80, Vestas V90-2.0 MW (90 m rotor diameter) WTs which is shown in Fig. 3.

Table 1 Specification of cable colour

Collection system					
voltage level	33 kV				
type	AC				
colour	blue	green	purple	cyan	black
cable sectional area, mm <sup>2</sup>	70, 95, 120, 150	185, 240, 300	400, 500	630, 800	1000

The onshore substation is also assumed to be constructed 30 km away from wind farm and the OS is permitted to be constructed within the area that indicated by  $L_x$  and  $L_y$ .

#### 4.2 Optimised collection system layout

To show the performance of the proposed method, the layout obtained by MST algorithm and APSO-MST algorithm are compared through three scenarios which are presented as follows.

**4.2.1 Scenario I: near shore OS layout:** As can be seen in Fig. 4, the offshore WTs and OS location are represented in a coordinate system. The OS are assumed to be located 5 km away from wind farm lower boundary which is 25 km away from the coast. The red stars are WTs and green square is OS. The lines show the cable connection layout and the colour of the line represents the rating of the cable which is explained in Table 1. Since multiple

cables might be adopted between some pair of WTs, the number of cables that utilised between each two WTs is indicated with different types of lines, which are solid line (one cable), dash line (two cables), dash dotted line (three cables) and dotted line (four cables), and are shown in upper right box of Fig. 4a. The colours and lines in the following figures have the same meaning in this work.

**4.2.2 Scenario II: central placement OS layout:** In this scenario, the OS is assumed to be constructed in the middle of the wind farm. The optimised layout obtained using MST, DMST and APSO-MST algorithm is shown in Figs. 5a–c, respectively.

**4.2.3 Scenario III: optimised layout considering OS siting:** In scenario III, the OS location is optimised together with the collection system layout. With different OS location, the cost of transmission cables are varying. The optimised layouts are shown in Figs. 6a–c.

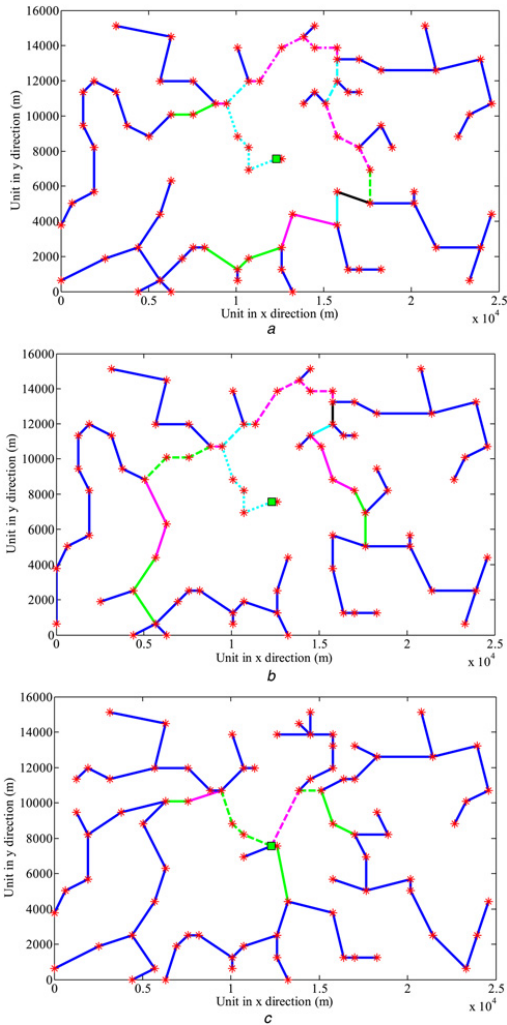


**Fig. 5** Cable connection layout comparison using different methods when OS is in centre

- a Optimised layout with central OS obtained by MST
- b Optimised layout with central OS obtained by DMST
- c Optimised layout with central OS obtained by APSO-MST

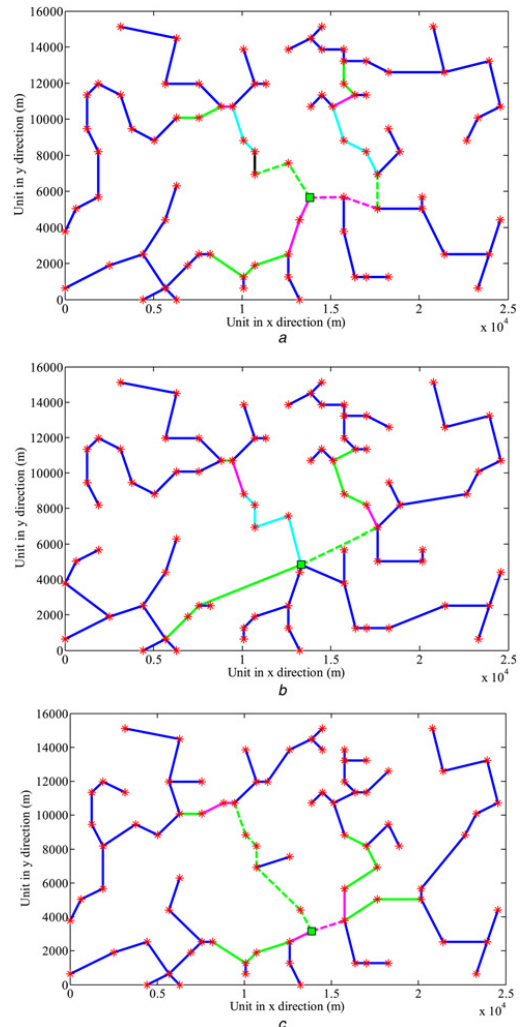


**Fig. 6** Overall cable connection layout optimisation

- a Optimised collection system layout obtained by MST
- b Optimised collection system layout obtained by DMST
- c Optimised collection system layout obtained by APSO-MST

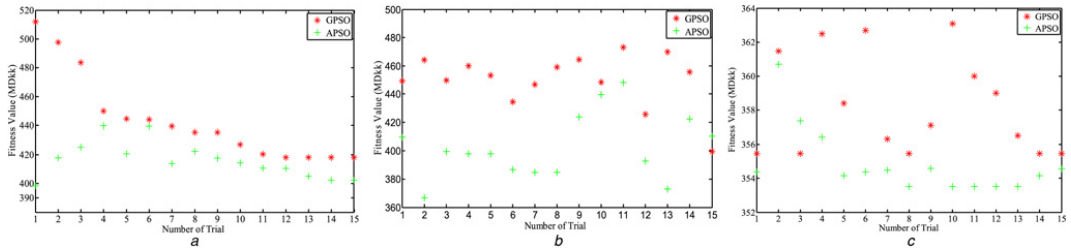


**Fig. 7** Fifteen trails for optimised cable connection layout

- a Fifteen trails for optimised cable connection layout with OS near shore obtained by APSO-MST
- b Fifteen trails for optimised cable connection layout with central OS obtained by APSO-MST
- c Fifteen trails for optimised cable connection layout with overall optimised cable connection layout obtained by APSO-MST

### 4.3 Results and discussion

As the APSO algorithm is used to find a minimal cost layout, to increase the possibility of obtaining a global optimal solution, the program is run 15 times and the most favourite solution is selected as the final result. The statistical distribution of the final results for each scenario is illustrated in Fig. 7.

In Fig. 7, the red stars show the final result that is found by GPSO each trial and green plus means the obtained result using APSO. Additionally, the relations of the generation and cable cost (fitness value) for each scenario with the best trial are studied and shown in Fig. 8. It can be seen that the cable cost stabilised at a fixed value at 100th iteration in all scenarios.

The obtained layouts are compared in Table 2. One 630 mm<sup>2</sup>, 132 kV high-voltage AC submarine cable, transmission line, is selected to connect OS to onshore substation. The total trenching length is the distance for laying the cables. The total cable length is larger than trenching length means more than one cable is needed between two WTs in some part of the wind farm.

It can be seen from Table 2 that DMST algorithm can find a cheaper layout compared with MST algorithm no matter where the OS location is and APSO-MST can provide the best layout in each scenario. The APSO-MST algorithm finds a layout which can

reduce the cost 19.4 and 12.1% compared with MST and DMST, respectively, in scenario I, 24.6 and 18.8% in scenario II, 4.7 and 4.5% in scenario III. In scenarios I and II, the DMST will always try to find a layout with longer trenching length and shorter cable length while APSO-MST finds an even longer trenching length which means that the less cost cable connection layout should use parallel cable operation as little as possible. As it is known, the location of OS will decide the length transmission line and has a significant impact on collection system layout. Compared with scenarios I and II, the total cost of cables is less in scenario II no matter which algorithm is adopted which means that it is more beneficial to construct the OS within the wind farm instead of near shore if only the cost of cables are considered. In scenario III, DMST and APSO-MST find a longer trenching length and cable length layout compared with MST, however, the total cable cost is also reduced step by step using DMST and APSO-MST. As can be seen from Figs. 6a–c, more purple and blue coloured cables are adopted in MST compared with the other two layouts which means that in this scenario though the total cable length is increased by two proposed algorithms, the thickness of cables are reduced which reduce the total cost of cables finally. It can also be seen that the APSO-MST can only reduce the cable cost <5% compared with the other two methods in scenario III. Hence, it

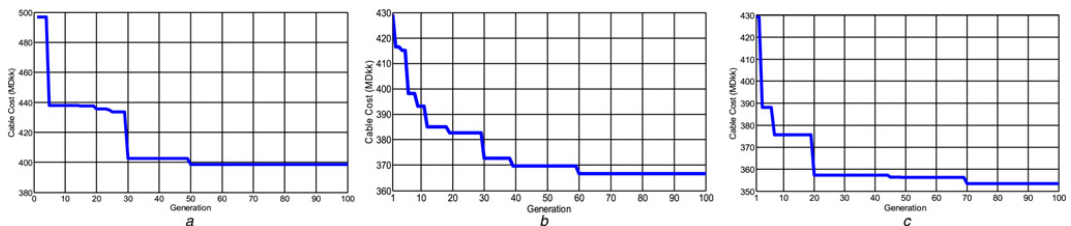


**Fig. 8** Cable cost corresponding to each generation

- a Cable cost corresponding to each generation for optimised layout with OS near shore obtained by APSO-MST
- b Cable cost corresponding to each generation for optimised layout with central OS obtained by APSO-MST
- c Cable cost corresponding to each generation for optimised collection system layout obtained by APSO-MST

**Table 2** Optimised layout comparison

	Scenario I			Scenario II			Scenario III		
	MST	DMST	APSO-MST	MST	DMST	APSO-MST	MST	DMST	APSO-MST
total cable length for CS, km	193.20	181.88	185.22	174.57	161.96	149.80	140.70	144.37	146.35
total trenching length for CS, km	135	136.36	161.12	129.93	130.94	140.44	130.61	139.58	135.24
cable to shore, km	25	25	25	37.56	37.56	37.56	35.67	37.30	33.19
cable costs for CS, MDkk	390.79	349.71	294.68	330.50	295.94	210.89	222.99	215.38	215.79
cable costs for TS, MDkk	103.75	103.75	103.75	155.87	155.87	155.87	148.04	154.80	137.73
total cable invest, MDkk	494.54	453.46	398.43	486.37	451.81	366.76	371.03	370.18	353.52
substation location		(12.29, -5)			(12.29, 7.56)		(13.81, 5.64)	(13.7, 5.26)	(13.86, 3.15)



can be concluded that it is very important to consider the optimised location of OS in the cable connection layout design work.

The minimal cost layout in this simulation is the layout found by APSTO-MST in scenario III as illustrated in Fig. 6c. The OS is expected to be constructed within wind farm, however, constructing the offshore wind farm far away from the shore may increase the cost of foundations. Hence, more factors such as varying foundation cost with water depth, cable installation cost, operation and maintenance cost, and so on should be considered to make the layout more practical so that a comprehensive decision can be made.

## 5 Conclusions

The cable connection layout has a significant impact on the investment of wind farm electrical system. Some deterministic methods as DMST or MST can only ensure an optimal solution under some particular assumptions while the actual cable connection configuration is more flexible. In this paper, a new method, APSTO-MST, is proposed to optimise the cable connection configuration for offshore wind farms. Some factors such as the siting of the OS and the suitable cable sectional area for each line between two WTs are considered in this paper. To increase the searching ability of PSO, adaptive control parameter technology is used and compared with GPSO. The results show that APSTO outperforms GPSO in finding a more beneficial solution. From the studied cases, it can be seen that the proposed method is an effective way to find the minimal cost cable connection layout considering cable power capacity limitation for irregular shaped wind farm compared with the other two deterministic methods.

In future, the work can be further improved from the following aspects. (i) The transmission loss, financial income for selling electricity and submarine topography limitation may be taken into consideration to evaluate the performance of an entire offshore wind farm. (ii) Optimisation work of WT locations and inter-cable connection layout could be done at the same time. The WT positions which will be represented by Cartesian coordinate form as well as cable connection layout will be considered as the optimisation variables together. Since the energy yields calculation considering the wake effect is required, the computational time could be longer. (iii) The optimisation variables, as the number of OSs and the voltage levels of various electrical equipment could be included into the optimised layout design problem to get more comprehensive results.

## 6 Acknowledgment

The authors thank the Norwegian Centre for Offshore Wind Energy (NORCOWE) under grant 193821/S60 from the Research Council of Norway (RCN).

## 7 References

- Ling-Ling, H., Ning, C., Hongyue, Z., *et al.*: 'Optimization of large-scale offshore wind farm electrical collection systems based on improved FCM'. Int. Conf. on Sustainable Power Generation and Supply (SUPERGEN 2012), 8–9 September 2012, pp. 1–6
- Pérez, B., Mínguez, R., Guanche, R.: 'Offshore wind farm layout optimization using mathematical programming techniques'. *Renew. Energy*, 2013, **53**, pp. 389–399
- Salcedo-Sanz, S., Gallo-Marazuela, D., Pastor-Sánchez, A., *et al.*: 'Evolutionary computation approaches for real offshore wind farm layout: a case study in northern Europe'. *Expert Syst. Appl.*, 2013, **40**, (16), pp. 6292–6297
- Gao, X., Yang, H., Lin, L., *et al.*: 'Wind turbine layout optimization using multi-population genetic algorithm and a case study in Hong Kong offshore'. *J. Wind Eng. Ind. Aerodyn.*, 2015, **139**, pp. 89–99
- González, J.S., Gonzalez Rodriguez, A.G., Castro Mora, J., *et al.*: 'Optimization of wind farm turbines layout using an evolutionary algorithm'. *Renew. Energy*, 2010b, **35**, (8), pp. 1671–1681
- Grady, S.A., Hussaini, M.Y., Abdullah, M.M.: 'Placement of wind turbines using genetic algorithms'. *Renew. Energy*, 2005, **30**, (2), pp. 259–270
- Pookpant, S., Ongsakul, W.: 'Optimal placement of wind turbines within wind farm using binary particles swarm optimization with time-varying acceleration coefficients'. *Renew. Energy*, 2013, **55**, pp. 266–276

- Zhang, C., Hou, G., Wang, J.: 'A fast algorithm based on the sub modular property for optimization of wind turbine positioning'. *Renew. Energy*, 2011, **36**, (11), pp. 2951–2958
- Lundberg, S.: 'Configuration study of larger wind park'. Thesis for the degree of Licentiate Engineering, Department of Electric Power Engineering, Chalmers University of Technology, Göteborg, Sweden, 2003
- Zhao, M., Chen, Z., Blaabjerg, F.: 'Application of genetic algorithm in electrical system optimization for offshore wind farms'. Presented at the Int. Conf. on Electric Utility Deregulation and Restructuring and Power Technologies (DRPT), Nanjing, China, 2008
- Bahirat, H.J., Mork, B.A., Hoidalén, H.K.: 'Comparison of wind farm topologies for offshore applications'. 2012 IEEE Power and Energy Society General Meeting, 22–26 July 2012, pp. 1–8
- Dutta, S., Overbye, T.J.: 'A clustering based wind farm collector system cable layout design'. 2011 IEEE Power and Energy Conf. at Illinois (PECI), Champaign, IL, 25–26 February 2011, pp. 1–6
- Devore, R.A., Temlyakov, V.N.: 'Some remarks on greedy algorithm'. *Adv. Comp. Math.*, 1996, **5**, pp. 173–187
- Ling-Ling, H., Ning, C., Hongyue, Z., *et al.*: 'Optimization of large-scale offshore wind farm electrical collection systems based on improved FCM'. Int. Conf. on Sustainable Power Generation and Supply (SUPERGEN 2012), Hangzhou, 8–9 September 2012
- Dutta, S., Overbye, T.J.: 'Optimal wind farm collector system topology design considering total trenching length'. *IEEE Trans. Sustain. Energy*, 2012, **3**, (3), pp. 339–348
- Jenkins, A.M., Scutari, M., Smith, K.S.: 'Offshore wind farm inter-array cable layout'. 2013 IEEE Grenoble PowerTech (POWERTECH), 16–20 June 2013, pp. 1–6
- Gonzalez-Longatt, F.M., Wall, P., Regulski, P., *et al.*: 'Optimal electric network design for a large offshore wind farm based on a modified genetic algorithm approach'. *IEEE Syst. J.*, 2012, **6**, (1), pp. 164–172
- Li, D.D., He, C., Fu, Y.: 'Optimization of internal electric connection system of large offshore wind farm with hybrid genetic and immune algorithm'. Proc. 3rd Int. Conf. on Electric Utility DRPT, April 2008, pp. 2476–2481
- Hopewell, P.D., Castro-Sayas, F., Bailey, D.L.: 'Optimising the design of offshore wind farm collection networks'. Proc. 41st Int. Universities Power Engineering Conf., UPEC '06, 6–8 September 2006, vol. 1, pp. 84–88
- Lumbreras, S., Ramos, A.: 'Optimal design of the electrical layout of an offshore wind farm applying decomposition strategies'. *IEEE Trans. Power Syst.*, 2013, **28**, (2), pp. 1434–1441
- Zhang, P.Y.: 'Topics in wind farm layout optimization: analytical wake models, noise propagation, and energy production'. Master Thesis, University of Toronto, 17 July 2013
- Hassan, R., Cohaním, B., de Weck, O.: 'A comparison of particle swarm optimization and the genetic algorithm'. Proc. 46th AIAA/ASME/ASCE/AHS/ASC Structures, Structural Dynamics and Materials Conf., 2005
- Wu, Y.-K., Lee, C.-Y., Chen, C.-R., *et al.*: 'Optimization of the wind turbine layout and transmission system planning for a large-scale offshore wind farm by AI technology'. *IEEE Trans. Ind. Appl.*, 2014, **50**, (3), pp. 2071–2080
- Bondy, J.A., Murty, U.S.R.: 'Graph theory with applications' (Macmillan Press Ltd., 1976)
- Lundberg, S.: 'Performance comparison of wind park configurations'. Technical Report 30R, Department of Electric Power Engineering, Chalmers University of Technology, Department of Electric Power Engineering, Göteborg, Sweden, August 2003
- ABB corporation. 'XLPE submarine cable systems attachment to XLPE land cable systems-user's guide' (ABB corporation, 2013)
- Vandervalk, B.P., McCarthy, E.L., Wilkinson, M.D.: 'Optimization of distributed SPARQL queries using Edmonds' algorithm and prim's algorithm'. Int. Conf. on Computational Science and Engineering, 2009, CSE '09, 29–31 August 2009, vol. 1, pp. 330–337
- Hou, P., Hu, W., Chen, Z.: 'Offshore wind farm electrical system layout optimization using dynamic minimum spinning tree algorithm'. 50th IEEE International Universities Power Engineering Conference, UPEC 2015, England, UK, 2015, pp. 1–5
- Kennedy, J., Eberhart, R.: 'Particle swarm optimization'. Proc. IEEE Int. Conf. on Neural Networks, April 1995, pp. 1942–1948
- Kennedy, J.: 'The particle swarm: social adaptation of knowledge'. Proc. IEEE Int. Conf. on Evolution of Computing, Indianapolis, IN, 1997, pp. 303–308
- Shi, Y., Eberhart, R.C.: 'Empirical study of particle swarm optimization'. Proc. Congress on Evolutionary Computation, 1999, pp. 1950–1955
- Jiao, B., Lian, Z., Gu, X.: 'A dynamic inertia weight particle swarm optimization algorithm'. *Chaos Solitons Fractals*, 2008, **37**, pp. 698–705
- Shi, Y., Eberhart, R.C.: 'Fuzzy adaptive particle swarm optimization'. Proc. Congress on Evolutionary Computation, 2001, pp. 101–106
- Eberhart, R.C., Shi, Y.: 'Tracking and optimizing dynamic systems with particle swarms'. Proc. Congress on Evolutionary Computation, 2001, pp. 94–100
- Zhan, Z.-H., Zhang, J., Li, Y., *et al.*: 'Adaptive particle swarm optimization'. *IEEE Trans. Syst. Man Cybern. B, Cybern.*, 2009, **39**, (6), pp. 1362–1381
- Zhang, J., Chung, H.S.-H., Lo, W.-L.: 'Clustering-based adaptive crossover and mutation probabilities for genetic algorithms'. *IEEE Trans. Evol. Comput.*, 2007, **11**, (3), pp. 326–335

## 8 Appendix

The WTs locations are listed in Table 3 in the coordinate form.

**Table 3** Location of WTs in coordinate form

WT No.	X, m	Y, m	WT No.	X, m	Y, m	WT No.	X, m	Y, m	WT No.	X, m	Y, m
1	4410	0	21	23 940	2520	41	5040	8820	61	1890	11 970
2	6300	0	22	0	3780	42	10 080	8820	62	5670	11 970
3	13 230	0	23	15 750	3780	43	15 750	8820	63	7560	11 970
4	0	630	24	5670	4410	44	22 680	8820	64	10 710	11 970
5	5670	630	25	13 230	4410	45	1260	9450	65	11 340	11 970
6	10 080	630	26	24 570	4410	46	3780	9450	66	15 750	11 970
7	23 310	630	27	630	5040	47	18 270	9450	67	18 270	12 600
8	10 080	1260	28	17 640	5040	48	6300	10 080	68	21 420	12 600
9	12 600	1260	29	20 160	5040	49	7560	10 080	69	15 750	13 230
10	16 380	1260	30	1890	5670	50	23 310	10 080	70	17 010	13 230
11	17 010	1260	31	15 750	5670	51	8820	10 710	71	23 940	13 230
12	18 270	1260	32	20 160	5670	52	9450	10 710	72	10 080	13 860
13	2520	1890	33	6300	6300	53	13 860	10 710	73	12 600	13 860
14	6930	1890	34	10 710	6930	54	15 120	10 710	74	14 490	13 860
15	10 710	1890	35	17 640	6930	55	24 570	10 710	75	15 750	13 860
16	4410	2520	36	12 600	7560	56	1260	11 340	76	6300	14 490
17	7560	2520	37	1890	8190	57	3150	11 340	77	13 860	14 490
18	8190	2520	38	10 710	8190	58	14 490	11 340	78	3150	15 120
19	12 600	2520	39	17 010	8190	59	16 380	11 340	79	14 490	15 120
20	21 420	2520	40	18 900	8190	60	17 010	11 340	80	20 790	15 120

# A Novel Way for Offshore Wind Farm Cable Connection Layout Design with Meta-heuristic Optimization

Peng Hou, Weihao Hu\*, Cong Chen, Mohsen Soltani, Zhe Chen,

Department of Energy Technology, Aalborg University, Pontoppidanstraede 101, Aalborg, Denmark

\*[whu@et.aau.dk](mailto:whu@et.aau.dk)

**Abstract:** Offshore wind farms have drawn more and more attention recently due to higher energy capacity and more freedom of area occupation. However, the investment of offshore wind farms is high. As one of the main expenses, the electrical system can take up more than 15% of the total investment while cable costs take a large proportion. In order to make a cost-effective wind farm, the cable connection layout should be optimized. This paper proposes a novel way for offshore wind farm cable connection layout design. The levelised production cost (LPC), which concerns three aspects: electrical power losses, power captured by wind turbines (WT) and investment, is selected as the evaluation index. In order to get an uncrossed cable connection layout, some idea of computational geometry is adopted. Since all the optimization variables are integers, an evolutionary algorithm, integer particle swarm optimization algorithm (IPSO), is adopted to find a near optimal solution. To improve the performance of the IPSO, the adaptive parameter control strategy is utilized to help find a better solution. Simulation results are given to validate the proposed approach and comparisons are made with results obtained by the Norwegian centre for offshore wind energy (NORCOWE) reference wind farm.

*Index Terms*— wake effect, levelised production cost (LPC), uncrossed cable connection layout, computational geometry, integer particle swarm optimization (IPSO), adaptive parameter control strategy.

## NOMENCLATURE

$V_0$ [m/s]	incoming wind speed
$V_x$ [m/s]	wind speed in the wake at a distance $x$ along the wind direction
$R_0$ [m]	WT's rotor radius
$S_{eff}$ [m <sup>2</sup> ]	effective wake region
$C_t$	thrust coefficient
$V_{def,ij}$ [m/s]	the wind speed deficit for WT at row $i$ , column $j$
$k_d$	decay constant
$P_{m,mn}$ [MW]	power extracted from the wind by WT at row $m$ , column $n$
$N_{row}$	quantity of WTs in a row
$N_{col}$	quantity of WTs in a column
$P_{loss,i}$ [MW]	power losses along cable $i$
$I_i$ [kA]	current in cable $i$
$R_{res,i}$ [ohm/m]	resistance of cable $i$
$\rho_{res,i}$ [ohm*m/mm <sup>2</sup> ]	resistivity of selected cable $i$
$l_{res,i}$ [m]	length of cable $i$
$S_{res,i}$ [m <sup>2</sup> ]	sectional area of cable $i$
$N$	total quantity of cables that connect wind turbines in a wind farm
$P_{tot,t}$ [MW]	total power production during interval $t$
$P_{tot,loss,t}$ [MW]	total power losses during interval $t$
$T_E$ [day]	duration interval for energy yields calculation



$T_t$ [h]	duration when the wind farm generating power of $P_{tol,t}$
$E_{tol,av}$ [MWh]	mean energy yields in one year
$t$ [hour]	energy yields calculation time
$C_i$ [MDKK/km]	$i^{th}$ cable's unitary cost
$A_1, A_2, A_3$	coefficient of cable cost model
$I_{i,rated}$ [A]	$i^{th}$ cable's rated current
$U_{i,rated}$ [V]	$i^{th}$ cable's rated voltage
$H_i$ [km]	$i^{th}$ cable's length
$Q_i$	quantity of cable $i$
$x_i$	the selected WT's sequence
$Cal_t$ [Dkk]	capital cost in year $t$
$C_{og}$ [Dkk]	present value of capital cost
$N_y$	economic lifetime
$R$	discount ratio
$w$	inertia weight
$l_1, l_2$	learning factors
$r_1, r_2$	stochastic variables in the range of [0, 1]
$x_i^k, x_i^{k+1}$ [m]	position of particle $i$ at iteration $k$ and $k+1$ respectively
$v_i^k, v_i^{k+1}$ [m]	speed of particle $i$ at iteration $k$ and $k+1$ respectively
$lc_i^k$ [m]	best solution obtained from particle $i$ at iteration $k$
$gl^k$ [m]	best solution obtained from all particles at iteration $k$

## 28 1. Introduction

29 Offshore wind farms have become a focus recently mainly due to their higher wind energy resource  
30 density and stability. Since the WTs are distributed over a wide sea area, a large number of submarine  
31 cables and electrical components are needed to collect the power captured by the wind turbines (WT) and  
32 transmit the energy to an onshore substation. As mentioned in [1], the cost of an offshore wind farm  
33 electrical system can be more than 15% of the total investment in which the cost of cables takes a large  
34 proportion. It is desirable to optimize the cable connection layout to make a cost-effective offshore wind  
35 farm.

36 The optimization of the offshore wind farm electrical system layout can be divided into two  
37 categories: the combinatory optimization of electrical components of wind farm as well as cable  
38 connection layout design. In [2], the offshore wind farm electrical system was optimized using a genetic  
39 algorithm (GA), a large database which contains a variety of types of electrical components with common  
40 voltages and different industrial design cable connection topologies is created. The electrical system layout  
41 is optimized by comparing the total cost of different combination from this database. The final solution  
42 which introduces the lowest investment was decided as the final result. Similar work has also been done in  
43 [3] which compared a variety of wind farm designs with respect to losses, reliability and cost. These two  
44 works can be used to reduce the investment in the electrical system. However, the cable connection layout  
45 is actually decided from the designer's experience. There is still the possibility of further reducing the cost

46 of submarine cables. In [4], the cable connection layout of collection system was optimized using a cluster  
47 based algorithm with the purpose of minimizing the total power losses. The greedy algorithm [5] is the  
48 common way to find the minimum spanning tree (MST) for a given weighted graphic. Based on the  
49 concept of MST, some work was done to obtain a minimal cost collection system layout [6][7]. In addition  
50 to that, GA is also widely used to make a good cable connection layout design for offshore wind farm  
51 [8][9]. In [8], the collection system layout was optimized with multi-objective: minimizing total cable  
52 length, minimizing capital investment or power losses minimization and the results were compared with  
53 the optimal layout obtained by prim's algorithm. In [9], a method of minimizing the cost of the cable  
54 connection layout for a 4 substation offshore wind farm was presented. In order to find a minimal cost  
55 layout, the travelling salesman problem (TSP) algorithm was adopted to improve the standard GA [9], the  
56 number of WT in each cluster was calculated and assumed to be uniform based on the cable rated current.  
57 The optimized layout in [9] was also compared with a similar work [10] which used hybrid GA and  
58 immune algorithm to optimize the system layout and showed better performance.

59 As is known, the location of the offshore substation (OS) has a significant impact on the formulated  
60 collection system layout [11]. For engineering considerations, reference [11] proposed a method to locate  
61 the OS which shows that the most favorable location for the OS should be in a central area while in [12],  
62 the optimal OS location is selected from a series of given positions. From [11][12], it can be known that it  
63 will be beneficial if the optimization of OS location and the collection system layout can be done at the  
64 same time.

65 Besides investment, energy production, which can really generate benefits, is another point that  
66 should be considered when designing an offshore wind farm. However, in [5] through [12], the cable  
67 connection layout was optimized only by minimizing the total cable cost without considering the power  
68 losses. Though power losses were considered in [3] and [4], the wake effect is not included. In one of our  
69 previous work [13], a method to calculate the energy yields regarding various wind velocity and direction  
70 has already been proposed which is the basis of wake losses estimation in this paper. Based on the previous  
71 work, a new method is proposed to get an optimized cable connection layout with the minimal levelized  
72 production cost (LPC) in this paper. The main contributions are as follows: 1) Based on the concept of  
73 cross product in computational geometry, a method of ensuing the uncrossed layout formulation is  
74 proposed which is not mentioned in the above papers [1]-[12]. 2) The location of OS construction is  
75 optimized together with the cable connection layout and it is selected from a number of given locations  
76 using heuristics method in this work. 3) LPC, which combines energy yields and investment, is chosen as  
77 the optimization objective. The proposed method is implemented in the Norwegian Centre for Offshore

78 Wind Energy (NORCOWE) reference wind farm and the results show that 1.75% LPC reduction can be  
 79 realized by using the proposed method.

80 The paper is organized as follows. Section 2 first provides some related models, then the objective  
 81 function is presented in section 3. The methodology for solving the problem is specified in Section 4. The  
 82 NOCOWE reference offshore wind farm (NRWF) is chosen as the study case to demonstrate the proposed  
 83 method in Section 5. Section 6 summarizes the main conclusions.

## 84 2. Mathematical Models

85 In this section, three models, namely wake model, power production model as well as cable cost  
 86 model that are required for solving this optimization problem are proposed one by one.

### 87 2.1. Wake Model

88 In 1983, Jensen proposed a model which is now widely used to describe the attribute of wind when it  
 89 encounters the WT blades quantitatively [14]. Based on the momentum conservation, the wake is assumed  
 90 to be expanded linearly in this model. Then the wind speed in the wake can be expressed as follow [15].

$$91 \quad V_x = V_0 - V_0 \left( I - \sqrt{I - C_t} \right) \left( \frac{R_0}{R_0 + k_d x} \right)^2 \left( \frac{S_{eff}}{S_0} \right) \quad (1)$$

92 The decay constant,  $k_d$ , is the slope rate of wake expansion. For offshore environment, the suggested  
 93 value is 0.04 [16]. Compared with other models, Jensen model is actually a simplified wake model,  
 94 however, the energy yields calculation of the whole wind farm is based on the ‘sum of square’ method [17]  
 95 which makes the Jensen model show less prediction error. In addition, this simplicity in calculation results  
 96 in less computational time [18]. Hence, Jensen model is selected in most of work related to optimization.

97 The downstream WT may be affected by the wakes that generated by several upstream WTs. In order  
 98 to estimate all the contributions to the wake losses accurately, the distance between each pair of WT as  
 99 well as the affected wake area should be carefully calculated which involves lots of superposition and  
 100 judgement procedures. In a previous work, an efficient method of wake losses estimation has already been  
 101 proposed [13]. Based on that, the wind speed reached at the blade of the WT at row  $n$ , column  $m$  can be  
 102 written as:

$$103 \quad V_{n,m} = V_0 - \sqrt{\sum_{i=1}^{N_{row}} \sum_{j=1}^{N_{col}} [V_{def,ij}]^2} \quad (2)$$

### 104 2.2. Wake Model

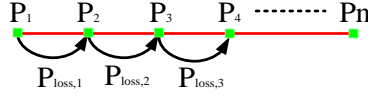
105 The power extracted from each WT is calculated by assuming a maximum power point tracking  
 106 (MPPT) control strategy [20] which is the same model that we used in [13]. After the wind speed arrived at

107 the downstream WT was calculated using (2), the power production of this WT will be calculated by  
 108 interpolating the  $C_p$  v.s. wind speed lookup table in [21]. Finally, the total power production can be  
 109 summarized as follow.

$$110 \quad P_{tol} = \sum_{m=1}^{N_{col}} \sum_{n=1}^{N_{row}} P_{m, mn} \quad (3)$$

111 In this work, the power losses is calculated by a more precise way which is illustrated in Fig. 1.

112



113

114

115

116

117

118

119

120

121

122

123

124

125

126

127

128

129

*Fig. 1. An illustration of power losses calculation.*

Assume the power losses of  $n$  WTs in a line are to be calculated as shown in Fig. 1. Each green square represents a WT while the red line indicates the cable connection layout. Hence, the power losses along the cables between each pair of WTs can be expressed as:

$$P_{loss,1} = \left( \frac{P_1}{\sqrt{3}U_{1,rated}} \right)^2 R_{res,1} \quad (4)$$

$$P_{loss,2} = \left( \frac{P_1 + P_2 - P_{loss,1}}{\sqrt{3}U_{2,rated}} \right)^2 R_{res,2} \quad (5)$$

$$P_{loss,i} = \left( \frac{\sum_{i=1}^n P_i - \sum_{i=1}^{i-1} P_{loss,i}}{\sqrt{3}U_{i,rated}} \right)^2 R_{res,i} \quad (6)$$

Where

$$R_{res,i} = \rho_{res,i} \frac{l_{res,i}}{S_{res,i}} \quad (7)$$

$$P_{loss,n,13} = \left( \frac{\sum_{n=1}^N P_n}{\sqrt{3}U_{n,rated}} \right)^2 R_{res,n} \quad (8)$$

As can be seen from (4) to (7), the precise power losses calculation should be a hierarchical process rather than independent calculations as (8) which was the method that we used in previous work [13]. Then the total losses within the wind farm should be written as:

$$P_{tol,loss} = \sum_{i=1}^N P_{loss,i} \quad (9)$$

Considering (3) to (7) and (9), the energy yields of the wind farm can be formulated as:

$$E_{tol,av} = \sum_{t=1}^{T_E} (P_{tol,t} - P_{tol,loss,t}) T_t / T_E \quad (10)$$

### 2.3. Cost Model

In this work, the cost models proposed in [22] is adopted. Then the cost of each cable can be expressed as:

$$C_i = A_1 + A_2 \exp\left(\frac{A_3 \sqrt{3} I_{i,rated} U_{i,rated}}{10^8}\right)^2 \quad (11)$$

The cable' sectional area is decided under the limitation of cable current carrying density. The maximum current that each cable would undertake will be decided by the selected voltage level as well as the number of WTs that connected after it. Once the maximum current is calculated, the sectional area will be decided according to its current carrying ability which can be found as a lookup table in [23].

## 3. Methods for Cable Connection Layout Design

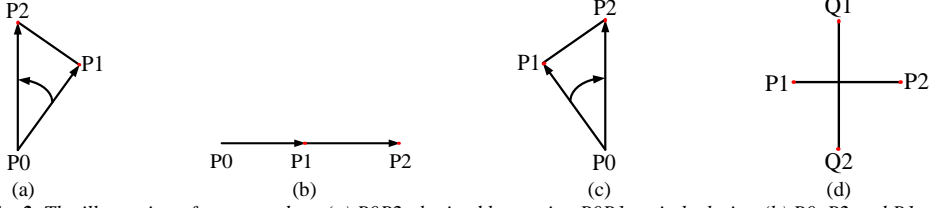
In this section, the line segments judgement method which is used to ensure the uncrossed cable connection layout is introduced at first. After that, a heuristic algorithm, integer PSO (IPSO) which is widely used to solve non-linear problems is specified.

### 3.1. Spanning Tree

In graph theory, a tree is defined as a connected graph with no circuit while the spanning tree can be defined as a sub tree of a graph containing all vertices [24]. For the offshore wind farm case, an uncrossed configuration is desirable since lower investment can be realized. Hence, the cable connection layout problem can be described mathematically as finding an uncrossed spanning tree layout for offshore wind farm with minimum LPC.

### 3.2. Judgement of Line Segments Intersection

The classic method to determine whether two line segments intersect is to check whether each segment straddles the line containing the other or not [25]. The realization of this line segment judgement method is based on the concept of cross product. The general idea can be explained using a simple example as illustrated in Fig. 2.



156  
 157  
 158 **Fig. 2.** The illustration of cross product. (a)  $P0P2$  obtained by moving  $P0P1$  anti-clockwise. (b)  $P0$ ,  $P2$  and  $P1$  are in a  
 159 line. (c)  $P0P2$  obtained by moving  $P0P1$  clockwise. (d)  $P1P2$  and  $Q1Q2$  are intersected.  
 160

161 Assume there are two line segments  $P1P2$  and  $Q1Q2$  which are required to be judged. The red dots in  
 162 Fig. 2 show the end points of these line segments. To determine whether each segment straddles the other,  
 163 in other words, whether they are intersected, the cross product can be used as is shown with a simple  
 164 example as Fig. 2 (a) to (c).

165 Fig. 2 (a) shows that if  $(P2-P0) \times (P1-P0) < 0$ , then  $P2P0$  can be obtained by rotating  $P1P0$  anti-  
 166 clockwise. (b) shows that if  $(P2-P0) \times (P1-P0) = 0$ , then  $P1$ ,  $P2$  and  $P0$  are on the same line. (c) shows that  
 167 if  $(P2-P0) \times (P1-P0) > 0$ , then  $P2P0$  can be obtained by rotating  $P1P0$  clockwise. By using this method, it  
 168 can be easily known whether two points ( $P2$  and  $P1$  or  $Q2$  and  $Q1$ ) are on the same side of one segment  
 169 ( $P1P2$  or  $Q1Q2$ ).

170 Based on the theory mentioned above, the intersection judgement of two line segments can be  
 171 determined as follow.

$$\begin{cases} (P_1 - Q_1) \times (Q_2 - Q_1)(Q_2 - Q_1) \times (P_2 - Q_1) \geq 0 \\ (Q_1 - P_1) \times (P_2 - P_1)(P_2 - P_1) \times (Q_2 - P_1) \geq 0 \end{cases} \quad (12)$$

173 Where  $\times$  is the symbol of cross product.

174 Simply speaking, if the two end points of one line segment are not on the same side of the other line  
 175 segment, then the two lines are intersected as shown in Fig. 2 (d). The uncrossed cable connection layout  
 176 obtained in this paper is based on this method.

### 177 3.3. IPSO

178 Stochastic optimization algorithms such as GA or PSO give a good choice of solving a non-convex  
 179 problem [26]. Initially, GA is proposed for solving integer optimization problems while PSO aims at  
 180 solving discrete optimization problems. In order to increase the adaptation of these algorithms, some  
 181 modified versions have been proposed which can cope with integer or mixed-integer optimization  
 182 problems. In this project, the IPSO is adopted to implement the simulation since it requires less  
 183 computation time compared with GA [27]. The mathematical expression is as follows.

$$v_i^{k+1} = \text{int}(wv_i^k + l_1r_1(lc_i^k - x_i^k) + l_2r_2(gl^k - x_i^k)) \quad (13)$$

$$x_i^{k+1} = x_i^k + v_i^{k+1} \quad (14)$$

In PSO, inertia weight is a control parameter which can provide a balance between global and local explorations. In order to reduce the sensitivity of the final solution to inertia weight, an adaptive parameter control strategy is adopted to help find a near optimal solution. The specification of APSO can be found in [28].

#### 4. Mathematical Formulation of the Problem

In this section, the mathematical model is built to evaluate how to optimize the cable connection layout of the wind farm using LPC and the optimization framework is described at the end.

##### 4.1. Heuristic Method for Cable Connection Layout Design

In an offshore wind farm, there could be hundreds of WTs. If the WT and OS locations can be regarded as vertices, then the number of spanning trees of this graph will be huge and it is impossible for computer to exhaust all the solutions to find the optimal one. In order to solve this problem, a heuristic method is proposed in this paper. Fig. 3 shows a simple example.

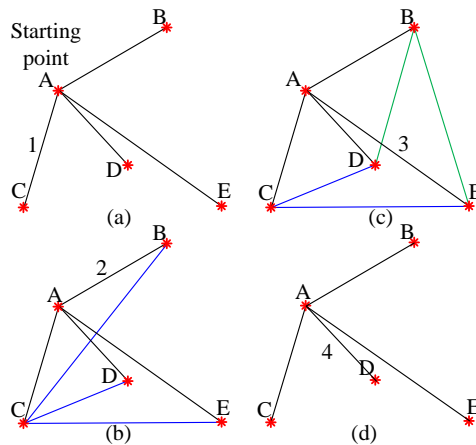


Fig. 3. Illustration of the proposed method. (a) - (d) are respectively the first, second, third and last steps when generating a spanning tree for a graph with 5 vertices.

For this heuristic method, the layout is stochastically given at the beginning by indicating the branch number in each layout formulation step. A simple example is made here to make the layout formulation process understandable. In this example, the final layout as shown in Fig. 3 (d) is given at the beginning stochastically. It is assumed that five vertices (A to E) represented by red stars are to be connected which means 4 decisions (the number of decisions equals the total number of vertices in the graph minus one) have to be made. The number besides the line show the order of decision making and the nearest branch to

208 this number is the selected branch in this decision making step. Point A is assumed to be the start point for  
 209 the search (in the simulation, the start point is always the OS). In Fig. 3. (a), the possible branches that can  
 210 be chosen in this step is illustrated with black line. For a 5-vertex graph, there are  $4*1=4$  options at the first  
 211 step of the spanning tree formulation process; it is assumed that C is selected in this step. (b) shows the  
 212 possible branches that can be chosen in this next step. In this step, two start points (A and C) can be  
 213 selected. The possible branches that can be selected associated with A and C are illustrated with black and  
 214 blue lines respectively. It can be seen that there are  $3*2=6$  options which can be chosen in this step. By  
 215 following the same procedure, (c) uses black, blue and green lines to illustrate all the possible branches that  
 216 can be selected. (d) shows the final layout and there are  $1*4=4$  options in this case. One thing that should  
 217 be noticed that line BD intersects AE which is already in the formulated tree. Hence, if this line is selected,  
 218 then the penalty function which will be introduced in section 4. 3 will be applied.

219 From the above example, it can be concluded as follows: the complete graph on N vertices has  $(N-1)!$   
 220 spanning trees. Since the number of self-intersecting spanning trees varies with the positions of vertices, it  
 221 is hard to conclude how many spanning trees of a graph that do not self-intersect there are. Hence, there are  
 222 two problems that should be solved with the proposed method. One is to reduce the computation cost for  
 223 the computer (The complexity of this problem is  $O(n!^2)$  which means that it is an NP hard problem [29].  
 224 Even though these intersecting spanning trees can reduce the number of potential solutions, the problem  
 225 could still be NP hard), the other is to eliminate every spanning tree with intersecting line segments but  
 226 these depend on the specific layout and are impractical to enumerate.

#### 227 4.2. Objective Function

228 In this simulation, an LPC index is adopted to set up the objective function. In this, both total  
 229 discounted costs and the total discounted energy output are included. The expression for LPC for an  
 230 offshore wind farm is formulated in [30]. The capital cost is calculated by the total cable cost using the  
 231 model proposed in section 2. 3.

$$232 \quad Cal_t = \sum_i^N C_i(x_i) H_i(x_i) Q_i(x_i) \quad (15)$$

233 As can be seen from (15), the cable cost is decided by the selected spanning tree (cable connection  
 234 layout) as introduced in section 4.1 and this spanning tree is formulated by the decided optimization  
 235 variable,  $x_i$ .

$$236 \quad C_{og} = \sum_{t=1}^{N_y} Cal_t (1+r)^{-t} \quad (16)$$



$$LPC = \frac{C_{og}(x_i)r(1+r)^{Ny}}{\left[(1+r)^{Ny} - 1\right]E_{rol,av}} \quad (17)$$

Then the objective function can be expressed as:

$$\text{Objective:} \quad \min(LPC(x)) \quad (18)$$

$$\text{Constraint:} \quad 1 \leq x_i \leq i(N_w - i) \quad (19)$$

#### 4.3. Penalty Function

As mentioned in section 3. 2 and 3. 3, the uncrossed layout problem can be solved using knowledge of computational geometry [31] while PSO algorithm can be used to get a near optimal solution of the unconstrained optimization problem when the problem is NP hard. However, if the spanning trees with intersecting line segments are merely deleted from the simulation, the particles will not have explicit directions to move in. As a result, the PSO will easily fall into a local optimal solution and never get out. In order to conquer this problem, a penalty function is defined as follows:

$$\phi(Q) = I_N \quad (20)$$

If one set of crossed lines is found then the penalty function will be triggered and thus the objective function will be penalized by adding additional cost. Then, the objective function can be written as follows:

$$\min(LPC) = \min \left[ \frac{(C_0 + I_N PF)r(1+r)^{Ny}}{(1+r)^{Ny} - 1} \frac{1}{E_{rol,av}} \right] \quad (21)$$

The penalty factor,  $PF$ , is 1000000 in this simulation which is decided by trial and error.

#### 4.4. Assumptions and Constraints

In this simulation, some assumptions are made as follows

1) The voltage levels for the collection system (CS) and the transmission system (TS) are assumed to be 66kV and 220kV respectively.

2) Yaw misalignment [32] which is the phenomenon that the rotating speed of yaw cannot follow the speed changing of wind direction, as a result the nacelle will not be able to face to the wind flowing direction all the time. In this project, the yaw misalignment is not considered when calculating the energy yields of wind farm.

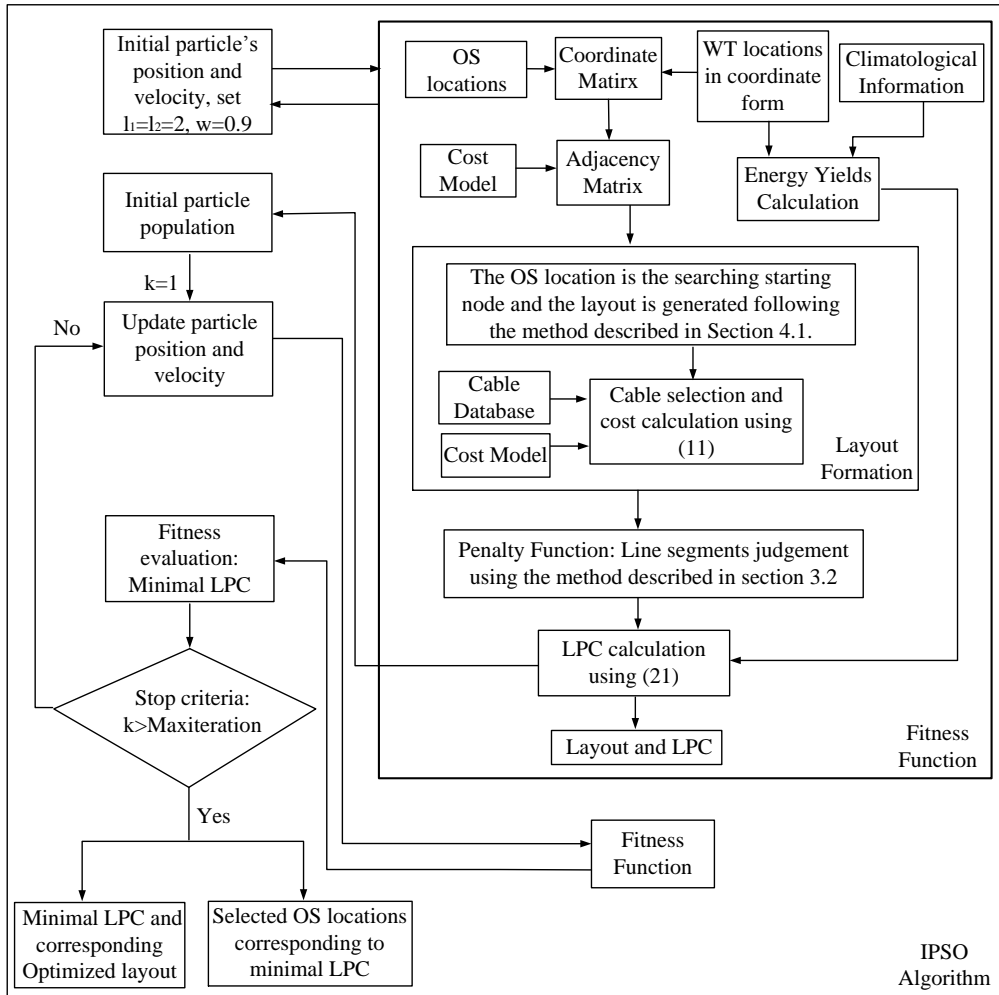
3) The voltage for each cable is assumed to be operating at nominal voltage.

#### 4.5. Optimization Framework

In this work, the optimized layout with minimum LPC in consideration of OS placement is found by

265 proposed method. The simulation procedure to reach the optimized cable connection layout by proposed  
 266 method is shown in Fig. 4.

267 Climatological Information: Instead of using probabilistic models, such as the Weibull distribution to  
 268 estimate the power production of a wind farm, the wind rose is adopted to calculate the wind farm energy  
 269 yields during the optimization process in this paper. Based on the time series for measured wind speed, the  
 270 wind rose is generated statistically. The detailed information for the wind rose and how to use it for wake  
 271 losses evaluation is specified in a previous work [13].



272  
 273 **Fig. 4.** The optimization framework for the proposed method.

274 The parameters of the IPSO are initialized in the first step. The initial particles' position includes two  
 275 parts of information: one is a series of randomly selected branches at each step as described above, the  
 276

277 other is two randomly given OS location sequence numbers from the given available positions. The  
 278 particles will be transferred to the Fitness Function and be utilized to generate the coordinate matrix with  
 279 the given WT locations. Then the adjacency matrix will be formed using the cost model. The energy yields  
 280 of each WT can be calculated based on the coordinate matrix as well as the Climatological Information  
 281 [33] which is generated based on the time series wind speed. The cable connection layout will be generated  
 282 in the Layout Formation step as described in Section 4.1. After that, the layout will be checked in the  
 283 penalty function and then the LPC will be obtained using (21). The result from the first calculation will be  
 284 saved as the initial particle population which will be the basis for comparison later.

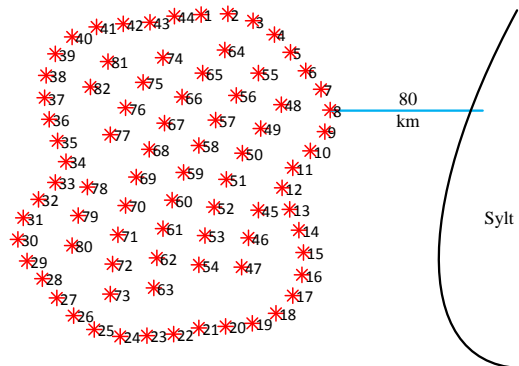
285 The particles containing the information of the selected branch sequence number at each step as well  
 286 as the OS location will be updated and transferred into the fitness function one by one. By following the  
 287 same procedure as in the first calculation, the calculated LPC and its corresponding layout can be obtained  
 288 and send to the Fitness Evaluation step for comparison. Or this process may stop if the maximum iteration  
 289 is reached. Finally, a series of branch sequence numbers as well as the selected locations for OSs which  
 290 contribute to the minimum LPC will be selected. The optimized layout is formulated according to the  
 291 selected branch number in each step during the layout formulation process.

## 292 5. Case Study

293 In this section, a reference wind farm is first introduced and then two study cases are presented.  
 294 Several trials have been done in IPSO to increase the possibility of getting the global optimal solution in  
 295 this section.

### 296 5.1. NRWF

297 The NRWF [34] is assumed to be at the location of the FINO3 met mast- 80km west of the German  
 298 island of Sylt. The installed capacity of the wind farm is 800MW. The OS is assumed to be located 80 km  
 299 from the onshore substation. The illustration of WT positions is shown in Fig. 5.



300  
 301 *Fig. 5. The illustration of the NRWF WT layout.*

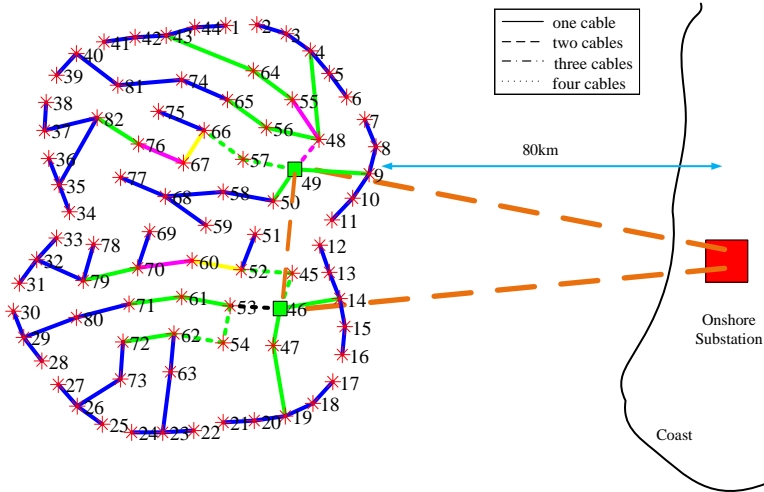
302

303

304

305

As can be seen in Fig. 5, the red stars represent the WTs while the number besides each WT is the sequence number. There are 82 positions in total which can be used to install WT or establish OS. In the NRWF layout, the OS locations have been selected and the cable connection layout is shown in Fig. 6.



306

307

308

**Fig.6. NRWF Cable Connection Layout.**

309

310

311

312

313

314

315

As it can be seen in Fig. 6, the two offshore substations (OS) are assumed to be located in positions No. 46 and 49 respectively. The green squares are OSs. The lines show the cable connection layout while the line colors show the ratings of the cables as listed in Table I. Since multiple cables are used between some WTs, the number of cables is illustrated with different types of lines.

**Table 1** Specification of Cables Color

		Collection System					Transmission System
Voltage		66kV					220kV
Type		AC					AC
Color	blue green purple yellow black						Brown
Cable							
Sectional Area	95/150 240/300 400/500 630/800 1000						300

316

317

318

319

In this simulation, the 10 MW DTU WT is adopted as the reference WT. The specification of this are listed in Table II and the distribution of wind velocity and direction is shown as a wind rose in Fig. 7 using is the climatological information as described in section 4.

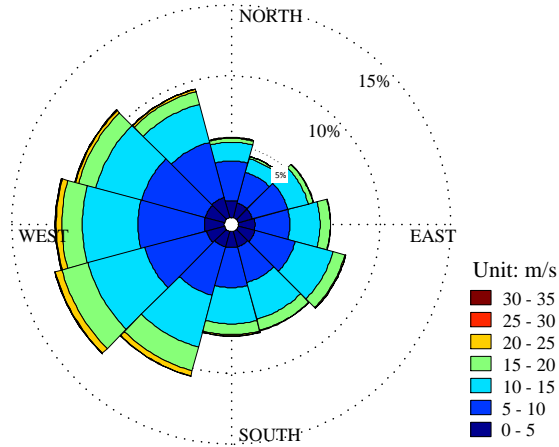
320

321

322  
323  
324**Table 2** DTU 10MW Wind Turbine Specification [35]

Parameter	10 MW DTU Wind Turbine
Cut-in Wind Speed	4 m/s
Rated Wind Speed	11.4 m/s
Cut-out Wind Speed	25 m/s
Rotor Diameter	178.3 m
Rated Power	10MW

325

326  
327  
328*Fig. 7. Wind rose generated based on the measured data near FINO3.*

### 329 5.2. Scenario I: Optimized Layout without Considering OS Siting

330 In this scenario, the cable connection layout is optimized by assuming that No. 46 and 49 are the OSs  
 331 which transmit power to the onshore substation. The optimized layout using the proposed method is shown  
 332 in Fig. 8. In order to find a near optimal solution, the program is run 10 times and the best solution is  
 333 selected as the final solution. The 10 trials are illustrated in Fig. 9 while the fitness values corresponding to  
 334 each iteration for the final solution are shown in Fig. 10.

335

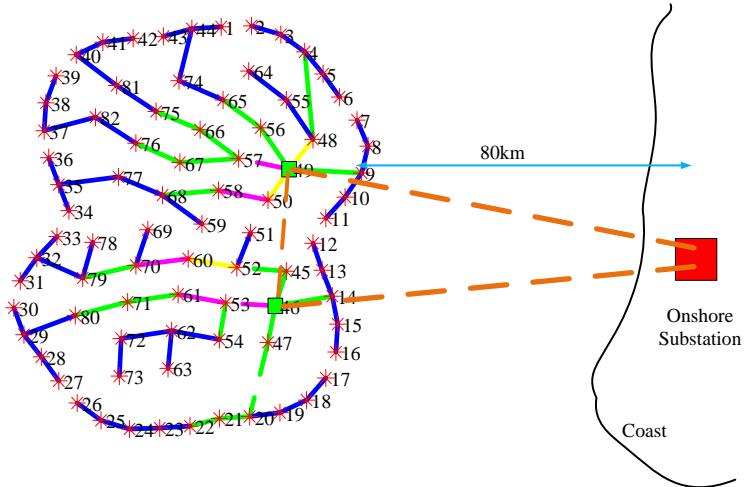


Fig. 8. The optimized cable connection layout for scenario I.

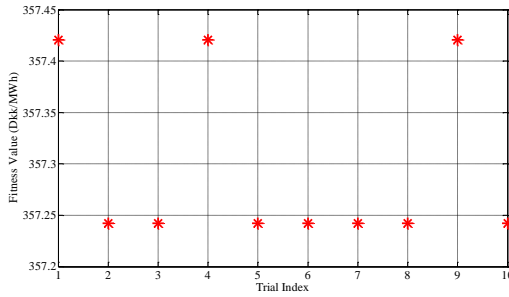


Fig. 9. 10 trials using IPSO for scenario I.

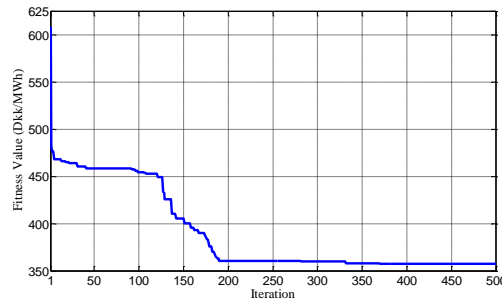


Fig. 10. Fitness values corresponding to each iteration for scenario I.

From Fig. 9, it can be seen that the IPSO with adaptive parameter control method can find the same value 6 out of 10 times and the final results are stabilized around 360 after the 400<sup>th</sup> iteration as shown in Fig. 10.

### 5.3. Scenario II: Optimized Layout Considering OS Siting

In this scenario, the positions of the OSs are optimized together with the cable connection layout. The two OS positions are expected to be selected from the predefined 82 positions and the other positions will be used to install WTs. The cable details regarding voltage level as well as sectional area for transmission lines are the same as in the NRWF. The optimized cable connection layout using IPSO is shown in Fig. 11.

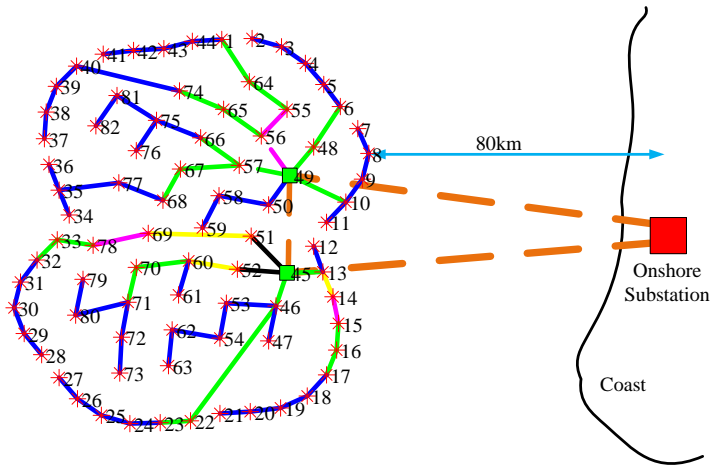


Fig. 11. The WT position illustration for each scenario.

As can be seen in Fig. 11, positions No. 49 and 45 are selected to construct the OSs instead of 49 and 46 in this scenario. The 10 trials of using IPSO to minimize the LPC of this layout are shown in Fig. 12 while the fitness value corresponding to each iteration is shown in Fig. 13.

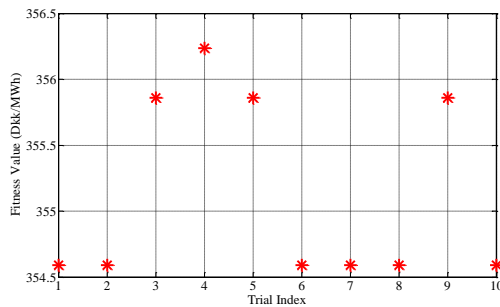


Fig. 12. 10 trials using IPSO for scenario II.

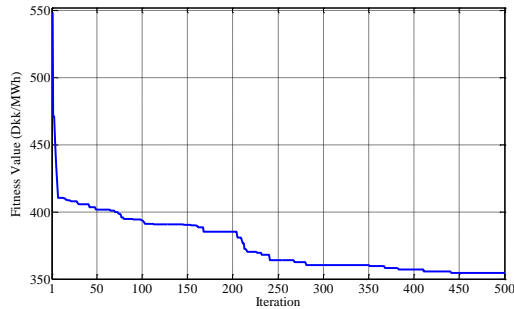


Fig. 13. Fitness value corresponding to each iteration for scenario II.

The robustness of IPSO in this scenario is shown in Fig. 13. It can be seen that the final results stabilize around 360 after the 440th iteration. It can be seen in Fig. 10 and 13 that the initial fitness value started at a very high value. This is because the NRWF layout solution was not loaded into the optimization algorithm until the 180<sup>th</sup> iteration which ensures the diversity of the population to some extent.

#### 5.4. Results and discussion

The performances of the optimized layouts are compared with the NRWF layout in Table III as follows.

**Table 3** Specification of Optimized Cable Connection Layout

	Energy yield (GWh)	Energy losses (GWh)	Energy yields at PCC (GWh)	Cost of collection cables (MDkk)	Cost of transmission cables (MDkk)	Total Cost of cables (MDkk)	LPC (DKK/MWh)
NRWF	4015.17	87.5	3927.67	229.25	1187.93	1417.18	360.92
Scenario I	4015.17	87.01	3928.16	214.93	1187.93	1402.86	357.24
Scenario II	4015.67	87.04	3928.63	215.24	1177.40	1392.64	354.59

In Table III, the cost of connecting cables means the cable used to connect OSs. The optimized layouts in scenario I and II can reduce the LPC by 1.02% and 1.75% respectively compared with the NRWF layout. By taking the OS locations into the optimization, the optimized layout in scenario II can further reduce the LPC by 0.74% compared with scenario I. The best layout in this simulation is scenario II, which can reduce the energy losses and cable cost by 0.53% and 1.73% respectively compared with the NRWF layout while the energy reached at PCC can be increased only by 0.02%. Hence, the dominant factor in the reduction of LPC is the cable cost.



## 385 6. Conclusions

386 In order to realize a cost-effective wind farm, the cable connection layout should be carefully  
 387 designed. An uncrossed cable connection layout which requires less investment on cables while  
 388 transmitting more power to the onshore substation is desirable. In this paper, a new method which can  
 389 minimize the LPC of an offshore wind farm while ensuring an uncrossed cable connection configuration is  
 390 proposed. The optimized cable connection layouts in scenario I and II outperformed the NRWF layout by  
 391 1.02% and 1.75% which demonstrates the effectiveness of the proposed method for cable connection  
 392 layout design.

393 In future, the work can be improved in the following aspects: introducing an optimization variable  
 394 for the number of OSs and including the voltage levels of kinds of electrical equipment into the cable  
 395 connection layout design problem to get a more comprehensive result.

## 396 7. Acknowledgment

397 The authors would like to thank the Danish Council for Strategic Research to support the project  
 398 "Authors would like to thank Norwegian Centre for Offshore Wind Energy (NORCOWE) under grant  
 399 193821/S60 from Research Council of Norway (RCN).

## 400 8. References

- 401 [1] Huang Ling-Ling, Chen Ning, Zhang Hongyue, Fu Yang, "Optimization of large-scale offshore wind farm  
 402 electrical collection systems based on improved FCM," *International Conference on Sustainable Power  
 403 Generation and Supply (SUPERGEN 2012)*, pp. 1-6, 8-9 Sept. 2012.
- 404 [2] M. Zhao, Z. Chen, and F. Blaabjerg, "Application of genetic algorithm in electrical system optimization for  
 405 offshore wind farms," *presented at the Int. Conf. on Electric Utility Deregulation and Restructuring and Power  
 406 Technologies (DRPT)*, Nanjing, China, 2008.
- 407 [3] Bahirat, H.J., Mork, B.A., Hoidalén, H.K., "Comparison of wind farm topologies for offshore applications,"  
 408 *2012 IEEE Power and Energy Society General Meeting*, pp. 1-8, 22-26 Jul. 2012.
- 409 [4] Dutta, S., Overbye, T.J., "A clustering based wind farm collector system cable layout design," *2011 IEEE Power  
 410 and Energy Conference at Illinois (PECI)*, pp. 1-6, Champaign, IL, 25-26 Feb. 2011.
- 411 [5] R. A. Devore, V. N. Temlyakov, "Some remarks on greedy algorithm," *Adv. Comp. Math.*, pp. 173-187, 1996.
- 412 [6] Huang Ling-Ling, Chen Ning, Zhang Hongyue, Fu Yang, "Optimization of large-scale offshore wind farm  
 413 electrical collection systems based on improved FCM," *International Conference on Sustainable Power  
 414 Generation and Supply (SUPERGEN 2012)*, Hangzhou, 8-9 Sept. 2012.
- 415 [7] S. Dutta, T. J. Overbye, "Optimal Wind Farm Collector System Topology Design Considering Total Trenching  
 416 Length," in *IEEE Trans. Sustainable Energy*, vol. 3, no. 3, pp. 339-348, July 2012.
- 417 [8] Jenkins, A.M., Scutariu, M., Smith, K.S., "Offshore wind farm inter-array cable layout," *PowerTech  
 418 (POWERTECH), 2013 IEEE Grenoble*, pp. 1-6, 16-20 June 2013.
- 419 [9] F. M. Gonzalez-Longatt, P. Wall, P. Regulski, and V. Terzija, "Optimal electric network design for a large  
 420 offshore wind farm based on a modified genetic algorithm approach," *IEEE Syst. J.*, vol. 6, no. 1, pp. 164-172,  
 421 Mar. 2012.

- 422 [10] D. D. Li, C. He, and Y. Fu, "Optimization of internal electric connection system of large offshore wind farm  
423 with hybrid genetic and immune algorithm," in *Proc. 3rd Int. Conf. Electr. Utility DRPT*, pp. 2476–2481, Apr.  
424 2008.
- 425 [11] Hopewell, P.D., Castro-Sayas, F., Bailey, D.I., "Optimising the Design of Offshore Wind Farm Collection  
426 Networks," *UPEC '06. Proceedings of the 4-1st International Universities Power Engineering Conference*, vol.  
427 1, pp. 84-88, 6-8 Sept. 2006.
- 428 [12] Lumbreras, S.; Ramos, A. "Optimal Design of the Electrical Layout of an Offshore Wind Farm Applying  
429 Decomposition Strategies", *Power Systems, IEEE Transactions on*, pp. 1434 - 1441 vol. 28, Issue 2, May 2013.
- 430 [13] Peng Hou, Weihao Hu, Mohsen Soltani, Zhe Chen, "Optimized Placement of Wind Turbines in Large Scale  
431 Offshore Wind Farm using Particle Swarm Optimization Algorithm," *IEEE Transactions on Sustainable Energy*,  
432 vol. 6, Issue 4, pp.1272-1282, 2015.
- 433 [14] F. González-Longatt, P. Wall and V. Terzija, "Wake effect in wind farm performance: Steady-state and  
434 dynamic behavior," *Renewable Energy*, vol. 39, pp. 329-338, Sep. 2011.
- 435 [15] WindPRO/PARK, "Introduction wind Turbine Wake Modelling and Wake Generated Turbulence," *EMD  
436 International A/S*, Niels Jernes Vej 10, DK-9220 Aalborg, Denmark, 1 Apr. 2005.
- 437 [16] Philippe Beaucage, Michael Brower, Nick Robinson, Chuck Alonge, "Overview of six commercial and research  
438 wake models for large offshore wind farms," *Proceedings EWEA 2012*, Copenhagen, pp. 95-99, 2012.
- 439 [17] Fernando Porté-Agel, Yu-TingWu, Chang-Hung Chen, "A Numerical Study of the Effects of Wind Direction  
440 on Turbine Wakes and Power Losses in a large Wind Farm," *Energies*, vol. 6, pp. 5297-5313, MDPI, 2013.
- 441 [18] Beatriz Pérez, Roberto Minguez, Raúl Guanache, "Offshore wind farm layout optimization using mathematical  
442 programming techniques," *Renewable Energy*, vol. 53, pp. 389-399, May 2013.
- 443 [19] P. Flores, A. Tapia, G. Tapia, "Application of a control algorithm for wind speed prediction and active power  
444 generation," *Renewable Energy*, vol. 30, Issue 4, pp. 523-536, Apr. 2005.
- 445 [20] Wei Qiao, "Intelligent mechanical sensorless MPPT control for wind energy systems," *Power and Energy  
446 Society General Meeting, 2012 IEEE*, pp. 1-8, San Diego, CA, Jul. 2012.
- 447 [21] Christian Bak, Frederik Zahle, Robert Bitsche, Taeseong Kim, Anders Yde, Lars Christian Henriksen, Anand  
448 Natarajan and Morten Hartvig Hansen, "Description of the DTU 10 MW Reference Wind Turbine," *DTU Wind  
449 Energy*, Fredericia, Denmark, Jul. 2013.
- 450 [22] S. Lundberg, "Performance comparison of wind park configurations," *Department of Electric Power  
451 Engineering, Chalmers University of Technology, Department of Electric Power Engineering*, Goteborg,  
452 Sweden, Tech. Rep. 30R, Aug. 2003.
- 453 [23] "XLPE Submarine Cable Systems Attachment to XLPE Land Cable Systems-User's Guide," *ABB corporation*.
- 454 [24] J. A. Bondy and U. S. R. Murty, "Graph theory with applications," *the Macmillan Press Ltd.*, 1976.
- 455 [25] Thomas H Cormen, Charles E Leiserson, Ronald L Rivest, Clifford Stein, "Introduction to algorithms," third  
456 edition, MIT Press, 2001 – 1180.
- 457 [26] Zhang, P. Y., "Topics in wind farm layout optimization: Analytical wake models, noise propagation, and energy  
458 production," *master thesis, University of Toronto*, 17 Jul. 2013.
- 459 [27] R. Hassan, B. Cohanin, O. de Weck, "A comparison of particle swarm optimization and the genetic algorithm,"  
460 in *Proceedings of the 46th AIAA/ASME/ASCE/AHS/ASC structures, structural dynamics and materials  
461 conference*, 2005.
- 462 [28] Z.-H. Zhan, J. Zhang, Y. Li, and H. S.-H. Chung, "Adaptive particle swarm optimization," *IEEE Trans. Syst.,  
463 Man, Cybern. B, Cybern.*, vol. 39, no. 6, pp. 1362–1381, Apr. 2009.
- 464 [29] Eric W. Weisstein, "NP-Hard Problem," From MathWorld-A Wolfram Web Resource.  
465 <http://mathworld.wolfram.com/NP-Problem.html>.
- 466 [30] Menghua Zhao, "Optimization of Electrical System for Offshore Wind Farms via a Genetic Algorithm  
467 Approach," *Dissertation submitted to the Faculty of Engineering, Science and Medicine at Aalborg University*,  
468 Denmark, Oct. 2006.
- 469 [31] Coello Coello, C.A., "Theoretical and numerical constraint-handling techniques used with evolutionary  
470 algorithms: a survey of the state of the art," *Computer Methods in Applied Mechanics and Engineering*, 191(11-  
471 12), pp. 1245–1287, 2002.
- 472 [32] J. Choi, M. Shan, "Advancement of Jensen (Park) wake model," *EWEA Conference*, Wien, pp. 1-8, Feb. 2013.
- 473 [33] Birgitte R. Furevik and Hilde Haakenstad, "Near-surface marine wind profiles from rawinsonde and NORA10  
474 hindcast," *Journal of Geophysical Research*, vol. 117, 7 Dec. 2012.

- 475 [34] “Norcowe annual report 2015,” Norwegian Centre for Offshore Wind Energy (NORCOWE), 2015.
- 476 [35] C. Bak et al., “Description of the DTU 10 MW reference wind turbine,” DTU Wind Energy, Fredericia,
- 477 Denmark, Jul. 2013.

## RESEARCH ARTICLE

**Overall Optimization for Offshore Wind Farm Electrical System**

Peng Hou, Weihao Hu, Cong Chen and Zhe Chen

Department of Energy Technology, Aalborg University, Aalborg, Denmark

**ABSTRACT**

Based on particle swarm optimization (PSO), an optimization platform for offshore wind farm electrical system (OWFES) is proposed in this paper, where the main components of an offshore wind farm and key technical constraints are considered as input parameters. The offshore wind farm electrical system is optimized in accordance with initial investment by considering three aspects: the number and siting of offshore substations (OS), the cable connection layout of both collection system (CS) and transmission system (TS) as well as the selection of electrical components in terms of voltage level and capacity. Because hundreds of optimization variables, continuous or discrete, are involved in the problem, a mix integer PSO (MIPSO) is required to obtain the solution. The fuzzy C-means clustering (FCM) algorithm is used to partition the wind farm into several sub regions. The collection system layout in each sub region as well as the connection scheme between offshore substations are optimized by an adaptive PSO-minimum spanning tree algorithm (APSO-MST) which has been proposed in a previous work. The simulation results show that the proposed optimization platform can find an optimized layout that save 3.01% total cost compared with the industrial layout, and can be a useful tool for OWFES design and evaluation. Copyright © 2016 John Wiley & Sons, Ltd.

**KEYWORDS**

adaptive PSO-minimum spanning tree algorithm (APSO-MST); cable connection layout; Design Optimization; fuzzy C-means clustering (FCM) algorithm; mix integer PSO (MIPSO); offshore substations (OS); offshore wind farm electrical system (OWFES); Particle Swarm Optimization (PSO)

**Correspondence**

W. Hu, Department of Energy Technology, Aalborg University, Aalborg Denmark.  
E-mail: whu@et.aau.dk

Received 14 January 2016; Revised 7 October 2016; Accepted 13 November 2016

**NOMENCLATURE**

$Cost_{TF,i}$ [MEUR]	total cost of transformer on OS platform $i$
$A_p, B_p, C_p, \beta$	coefficients of cost model
$P_{TF,i}$ [MW]	rated power of transformer on OS platform $i$
$N_{TF,i}$	number of transformer on OS platform $i$
$S_{ij, rated}$ [MVA]	rated apparent power of cable in sub region $i$ , line $j$
$I_{ij, rated}$ [kA]	rated current of cable in sub region $i$ , line $j$
$U_{ij, rated}$ [kV]	rated voltage of cable in sub region $i$ , line $j$
$C_{ij}$ [MEUR]	cost of cable in sub region $i$ , line $j$
$Cost_{plat,i}$ [MEUR]	cost of OS platform $i$
$N_{sub}$	number of OS platform
$C_{dig}$ [MEUR/m]	unit cost of laying cables
$C_{total}$ [MEUR]	total cost of electrical system
$L_{ij}$	length of cable in sub region $i$ , line $j$
$G_T$	sub-graph in $G$ which represents one possible spanning tree of $G$

$C_{ij}^{G_T, v}(x, y)$	cost of cable that used in sub region $i$ , line $j$ for $G_T$ when OS location is $(x, y)$ and voltage level is $v$
$L_{ij}^{G_T, v}(x, y)$	length of cables that used in sub region $i$ , line $j$ for $G_T$ when OS location is $(x, y)$ and voltage level is $v$
$Cost_{CS}^v$ [MEUR]	cost of collection systems when voltage level is $v$
$Cost_{TF}^v$ [MEUR]	cost of transformers when voltage level is $v$
$L_x, L_y$	predefined area for constructing OS in $x$ direction and $y$ direction respectively
$N_{sub}$	total number of sub region
$v$	voltage level
$i$	sequence number of particle
$w$	inertia weight
$l_1, l_2$	learning factors
$rand$	random number in the range $[0, 1]$
$x_i^k, x_i^{k+1}$ [m]	position of particle $i$ at iteration $k$ and $k + 1$ respectively
$v_i^k, v_i^{k+1}$ [m]	speed of particle $i$ at iteration $k$ and $k + 1$ respectively
$L_i^k$ [m]	best position of particle $i$ at iteration $k$
$G^k$ [m]	best position of all particles at iteration $k$
$I_p$	quantity of particles
$k_{max}$	quantity of iterations
$I_{max}$	number of maximum iteration
$N_{S1}$	number of sub regions (offshore substations)
$N_{WT}$	number of total wind turbines

## 1. INTRODUCTION

Offshore wind farm shows its superiority in higher wind energy resources density and less impact on surrounding residents; however, the cost of establishing offshore wind farm is much higher than onshore wind farm. Because the cost of offshore wind farm collection system (CS) can take up to 15%–30%<sup>1</sup> of total investment, more and more research works have been performed in optimizing the offshore wind farm electrical system (OWFES) to obtain a cost-effective wind farm.

The optimization of OWFES concerns mainly three aspects: the combinational selection of electrical equipment regarding voltage level and type, the cable connection layout as well as the number and location of offshore substations (OS). In,<sup>2–5</sup> the optimization electrical equipment selection regarding voltage level and type for offshore wind farm was studied. An optimization platform for OWFES design was proposed in,<sup>4</sup> which used main components of wind farm and key technical specifications as input parameters and the enhanced electrical system layout is decided by comparing the total cost of different electrical components' composition. Similarly, a variety of wind farm designs with respect to losses, reliability and cost was compared in.<sup>5</sup> The CS layouts studied in aforementioned literatures were designed empirically. Actually, the cost of cables can be saved if proper cable connection layout is adopted. Presently, two classic mathematical models were utilized to optimize the cable connection layout: Minimum Spanning Tree (MST)<sup>6</sup> and Travelling Salesman Problem (TSP).<sup>7</sup> The common way to solve MST is the greedy algorithm<sup>8</sup> which has been utilized to minimize the cost of CS in reference.<sup>9,10</sup> the MST layout is formulated by regarding the cost of cable in each branch as the weight while the CS layout was also optimized using TSP in reference.<sup>11,12</sup> Because the problem are complex and non-convex, genetic algorithm (GA) or some improved GAs were widely used in cable connection layout design.<sup>12–16</sup> In,<sup>12</sup> the cable connection scheme of a four substation offshore wind farm was optimized using GA-TSP algorithm and the result was cheaper than the optimized layout in reference,<sup>14</sup> however, the cable connection layout was sometimes crossed. Besides, some other methods as clustering based algorithm, ant colony system algorithm as well as linear programming were also utilized to reduce the cost of electrical system.<sup>17–19</sup> The impact of OS location on the cost of CS was first presented in reference,<sup>20</sup> which proposed a method to locate OS from engineering perspective and indicated that the most favorable location for OS should be in central area. Similarly, the OS location is decided from a series of given positions in reference.<sup>21</sup> The existing works optimized the OWFES in consideration of one or two aspects are as indicated earlier. Although an overall optimization work considering three aspects has been made in reference,<sup>13</sup> the OS was located in the center of each region that was partitioned using Fuzzy C-Means clustering (FCM) algorithm and the number of wind turbines (WTs) in one cluster was assumed to be the same. There should be a more flexible cable connection layout that satisfy the system operation requirement and preserve the uncrossed layout so that a lower investment can be made.

In one piece of our previous work,<sup>22</sup> the impact of OS location on the final investment of wind farm electrical system has already been investigated; however, cable connection layout was merely formulated by MST which is a deterministic algorithm. Recently, an adaptive PSO-minimum spanning tree (APSO-MST) algorithm<sup>23</sup> was also presented which used heuristic method to connect WTs. This method<sup>23</sup> outperformed<sup>22</sup> by finding a lower cost cable connection layout. In the aforementioned two papers, there is only one OS position is expected to be optimized and the voltage level is not regarded

as an optimization variables. Actually, there are mainly the following factors that have significant impacts on OWFES investment, that is, the voltage level selection (for CS and TS), the number of OSs and their locations as well as the cable connection layout of CS and TS. Because these variables are discrete or continuous and interconnected with each other by a group of constraints, the problem is expected to be non-convex. To solve such a complex problem, an optimization platform, which is based on PSO algorithm, to optimize OWFES is established in this paper. The main contributions of this paper are three folders: (i) FCM algorithm is adopted to partition the wind farm into several sub regions. Instead of using the clustering center as the OS location as reference,<sup>13</sup> the OS location in each sub region is optimized. (ii) APSO-MST is used to generate the uncrossed cable connection layout not only for CS as reference<sup>23</sup> but also for TS. (iii) Voltage selection has a critical impact for the selection of cable sectional area so does the location of OSs, this relation has been modelled and the factors mentioned earlier are considered at the same time in this paper. The proposed method is implemented in an irregular shaped wind farm and the results show that the proposed method can generate a layout that reduces the total cost 3.01% compared with an industrial layout.

The paper is organized as follows. Section 2 provides some related models at first, then the objective function is presented. The methodology for solving the problem is specified in Section 3. An irregular shaped wind farm is chosen as the study case to demonstrate the proposed method in Section 4. Section 5 summarizes the main conclusions.

## 2. OPTIMIZATION MODEL

In this section, the cost model of the electrical system is described at first, and then followed by the objective function.

### 2.1. Cost model

The cost of the electrical system is calculated by summing up the cost of all components. The cost models of all common electrical components specified in reference,<sup>24</sup> are adopted in this work. For this optimization problem, only the cost of OS platform, OS transformers, cables for CS and TS as well as cost of laying the cables are considered and the original currency unit in reference<sup>24</sup> was converted into EUR considering the current currency rate. The mathematical expressions of the aforementioned components' costs are expressed as follows.

$$Cost_{TF, j} = A_p + B_p (P_{TF, j} N_{TF, j})^\beta \quad (1)$$

$$C_{ij} = A_p + B_p \exp\left(\frac{C_p S_{ij, rated}}{10^8}\right)^2 \quad (2)$$

$$S_{ij, rated} = \sqrt{3} I_{ij, rated} U_{ij, rated} \quad (3)$$

The cable type selection procedure is the same as what we did in reference<sup>22</sup> that is based on the cable database provided by reference.<sup>25</sup> If too many WTs are connected after one cable, then more than one cable is required in the same route. The maximum number of cable that can be operated in parallel is assumed to be four in this work.

$$Cost_{plat, i} = A_p + B_p P_{TF, i} N_{TF, i} \quad (4)$$

The cost of laying cable is assumed to be 261 EUR/m for sea. Hence, the total cost of the electrical system can be written as follows:

$$Cost_{tot} = \sum_{i=1}^{N_{sub}} \left[ Cost_{TF, i} + \sum_{j=1}^{N_{WT, i}} (C_{ij} + C_{dig}) L_{ij} + Cost_{plat, i} \right] \quad (5)$$

### 2.2. Objective function

The objective of the optimization is to find the best design regarding cost. In order to further reduce the cost, the CS layout is expected to be optimized using a modified MST algorithm that is specified in a previous work.<sup>23</sup> Considering the voltage level's impact on the cable type selection, the cost of the CS in reference<sup>23</sup> can be rewritten as follows:

$$Cost_{CS}^k = \sum_{i=1}^{N_{sub}} \sum_{j=1}^{N_{WT, i}} C_{ij}^{G_T, k}(x, y) L_{ij}^{G_T, k}(x, y) \quad (6)$$

$$G_T \in G, k \in (33kV, 45kV, 66kV) \quad (7)$$

G is undirected weighted graph, a  $G_T$  represents one tree graph in G. The optimized CS layout is a  $G_T$  that has minimal total cost. Similarly, the cost of TS can be expressed as follows:

$$Cost_{TS}^k = \sum_{j=1}^{N\_sub} Cost_{TF,j}^{G_T,k}(x,y) \quad (8)$$

Considering (6)–(8), the optimization problem can be described as following:  
Objective:

$$\min(Cost_{tot}) = \min \sum_{i=1}^{N\_sub} \left[ Cost_{TF,i} + \sum_{j=1}^{N_{WT,i}-1} \left( C_{ij}^{G_T,k}(x,y) + C_{dig} \right) L_{ij}^{G_T,k}(x,y) + C_{plat,i} \right] \quad (9)$$

Subject to:

$$I_{ij} \leq I_{ij,rated}; j \in (1, N_{WT,i} - 1) \quad (11)$$

$$x \in (0, L_x); y \in (0, L_y) \quad (12)$$

$$N\_sub \in (0, 3) \quad (13)$$

$$v \in (132kV, 150kV, 220kV) \quad (14)$$

### 2.3. Assumptions

In this simulation, some assumptions are made as follows:

- 1 Usually, the number of OS is no more than 4, in this project, the limitation of number of OS is assumed to be 3 because the wind farm in the study case will not require more than 3 OSs.
- 2 The conductors of adopted cables are assumed to be copper and the voltage level of CS and TS are assumed to be selected from 33, 45, 66 kV and 132, 150, 220 kV, respectively.
- 3 The number of transmission cables could be 1 ~ 4. More than 4 cables are not considered due to the high cost of installation of buried cables.
- 4 The WTs' locations are assumed to be already known.
- 5 If more than one OS is required in the wind farm, then the cable voltage level between OSs and the voltage level of each CS are assumed to be the same.
- 6 Considering the redundancy, two transformers are chosen to be used on each platform. The capacity of transformer is decided as 110% of the maximum power generated from the turbines.<sup>26</sup>
- 7 Because of the low probability of cable fault and the heavy cost of cable system, normally no back-up connection system in practice now. Hence, this paper is focus on the minimization of total investment of electrical equipment without considering cable reliability issue.

## 3. METHODOLOGY

The whole wind farm can be divided into several sub-regions by FCM algorithm. The algorithm is presented first. After that, PSO algorithm and several technologies to improve the performance of PSO are introduced. Then, the mix integer PSO-MST algorithm, which is utilized to implement the overall OWFES optimization, is proposed. The optimization framework is presented last.

### 3.1. Fuzzy C-means clustering

The FCM algorithm is first proposed in 1984<sup>27</sup> which is applicable to geostatistical data analysis problem. Any set of numerical data can be partitioned into several clusters and the center of each cluster will also be found using FCM. If the locations of WTs are regarded as a set of data, then the OS zoning problem can be solved by FCM. As proposed in reference,<sup>9</sup> the FCM algorithm has already been used to partition the wind farm into several zones and the center of each zone is the OS location; however, the central placement layout is just one practical way of OS locating as described in

reference,<sup>20</sup> the cost can be further reduced if the OS location can be properly selected which was one of the conclusions from our previous work.<sup>22</sup> In this project, the FCM algorithm is adopted to partition the wind farm into several zones and the OS locations are optimized by PSO algorithm.

### 3.2. Mix integer PSO Algorithm

Mimicking the social behavior of fish schooling and bird flocking Kennedy and Eberhart<sup>28</sup> developed an evolutionary algorithm, PSO algorithm, which has a good performance of solving non-linear optimization problem; however, the initial version of PSO is applicable to continuous optimization variables. In order to solve the integer problem, the algorithm is modified in reference.<sup>29</sup> To ensure the integer value of each solution, the position will be updated by taking the integer value of the particle's speed. The integer PSO can be expressed in following equations<sup>30</sup> and the MIPSO is constructed by adding the following part into the original format of PSO.

$$v_i^{k+1} = \text{int}(wv_i^k + l_1 \text{rand}(L_i^k - x_i^k) + l_2 \text{rand}(G^k - x_i^k)) \tag{14}$$

$$x_i^{k+1} = x_i^k + v_i^{k+1} \tag{15}$$

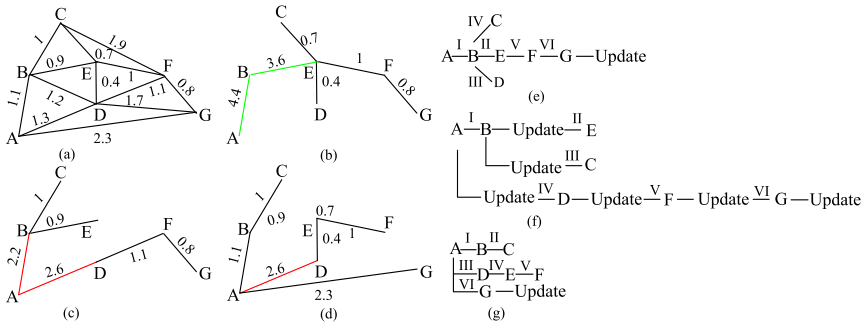


**Figure 1.** A simple example. (a) Undirected graph with 6 vertices and different weight of each branch. (b) Cable scheme using MST with updating the cost of previous decision. (c) Cable scheme using DMST with updating the cost of previous decision. (d) Cable scheme using APSO-MST with updating the cost of previous decision. (e) The sequence of decision making by MST. (f) The sequence of decision making by DMST. (g) The sequence of decision making by APSO-MST.

**Table I.** Cable information for simple example.

Type	a	b	c
Color	black	red	green
Number of WTs that can be connected to	≤2	3	≥4
Cost per unit	1	2	4

$$S_i \begin{bmatrix} S_1 & S_2 & S_3 & S_4 & \dots & S_n \end{bmatrix}$$

- $S_1$ : The number of OS or rather the sub region of wind farm
- $S_2$ : The voltage level of CS
- $S_3$ : The voltage level of TS
- $S_4 - S_{3+2N_{WT}}$ : The locations of Oss in coordinate form
- $S_{3+2N_{WT}} - S_{3+2N_{WT}+N_{WT}}$ : The cable connection layout of CS
- $S_{4+2N_{WT}} - S_{3+3N_{WT}+N_{WT}}$ : The cable connection layout of TS

**Figure 2.** Coding of particle  $S_i$ .



$$i \in (1, I_p), k \in (1, k_{max}) \tag{16}$$

The inertia weight,  $w$ , is the parameter that indicates the searching ability of the particle. The larger the  $w$  is the stronger global searching ability the particle has. Inversely, the smaller  $w$  ensures a relatively better local searching ability. For different problem, the best solution would be found with different parameter setting of PSO, in other words, the final solution is very sensitive to the parameter setting. Hence, the parameters should be changed by trial and error to obtain the best solution at early times.

In order to overcome this drawback, many researchers have been performed to establish a method of changing the control parameters automatically so that the performance of PSO can be efficiently enhanced.<sup>31–34</sup> From the perspective of parameter control mechanism, the existing work can be divided into two sorts: control strategy based on time-varying principle<sup>31–33</sup> and adaptive parameter control strategy.<sup>34</sup> Some common ways as linear increasing or decreasing  $w$ , changing  $w$  nonlinearly as well as adapting control parameters fuzzily were utilized to optimize the PSO performance in the first category. For the adaptive parameter control strategy, the parameters are controlled according to the present evolution state so that the performance of PSO can be further improved. Recently, a PSO with multiple adaptive methods (PSO-MAM) method was proposed in reference<sup>35</sup> and demonstrated to have an outstanding performance of finding a near global optimal solution; however, it can only be used to solve continuous optimization problem. In this project, MIPSO algorithm is adopted to implement the optimization work. In order to improve the searching ability of PSO, adaptive PSO (APSO)<sup>34</sup> is investigated to obtain a near optimal solution.

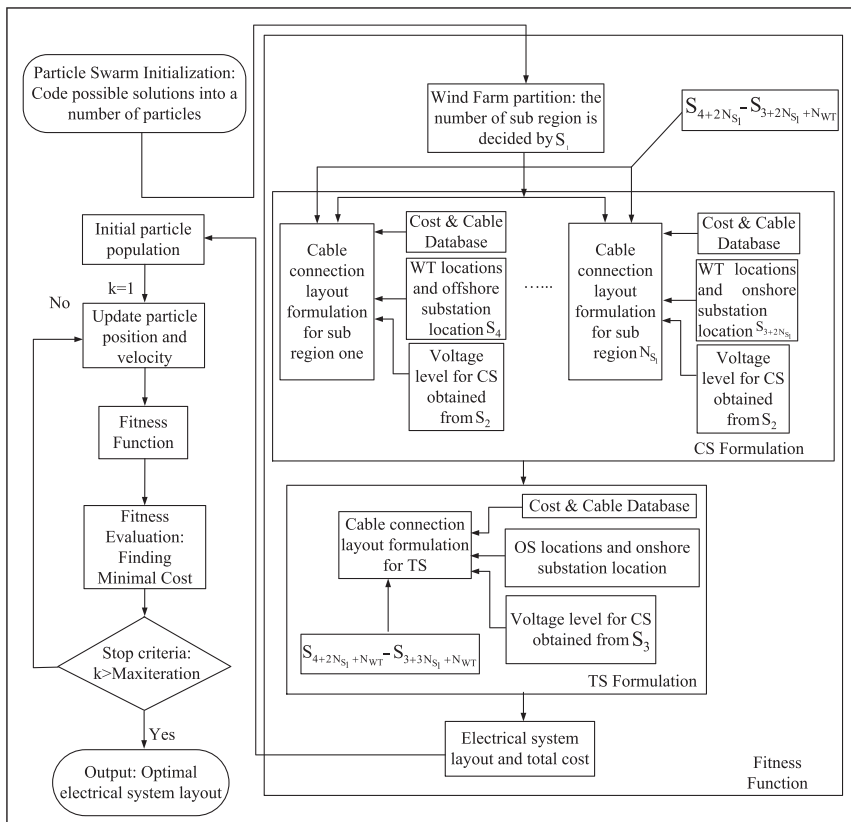


Figure 3. The optimization framework for proposed method.

### 3.3. Adaptive PSO-minimum spanning tree algorithm

In,<sup>23</sup> the cable connection layout optimization work considering OS locating was performed. In which an APSO-MST algorithm is proposed. The proposed algorithm is a stochastic algorithm that is proposed based on the tree concept in graphic theory.<sup>36</sup> Hence, it cannot only ensure the uncrossed cable connection layout but also a lower cost compared with two other deterministic methods as prim algorithm and dynamic minimal spanning tree algorithm (DMST). In this paper, the APSO-MST algorithm is adopted to design the cable connection layout to reach a cost-effective wind farm layout. The differences among three cable connection algorithms can be easier understood through a simple example as illustrated in Figure 1.

It is assumed that 6 WTs (indicated by B to G) are required to be connected to the offshore substation (indicated by A) which are shown in Figure 1 (a). The number in Figure 1 (a) represents the distance between each pair of WT while the cable cost is actually decided by two factors: the length and type of the cable. In order to obtain a simulation in this aspect, three cables are assumed to be available in this example. The information of three cables are listed in Table I.

As can be seen in Table I, the cost increases with the number of WTs connected after one cable. For simplicity, the distance and the cable cost are assumed to be non-dimensional. Then, in Figure 1 (b) to (d) the number shows the cost of each cable instead of merely distance in (a). Different colors are used to represent different types of cables. The cable scheme found by MST is as (b) and the total cost is  $1.1*4 + 0.9*4 + 0.7 + 0.4 + 1 + 0.8 = 10.9$  while the cost of cable connection scheme using DMAT and APSO-MST are  $1.1*2 + 1.3*2 + 0.9 + 1.1 + 0.8 + 1 = 8.6$  and  $1.1 + 1 + 1.3*2 + 0.4 + 2.3 + 1 = 8.4$ , respectively. This MST algorithm find the most expensive scheme because two biggest cables are adopted which are illustrated with green in (b). The greek numerals I to VI indicate the scheme formulation sequence. Because the result obtained by MST or DMST are deterministic, the tree graphic formulation process is unique as shown in Figure 1. (e) and (f) and the difference is that DMST update the cost of cables after each decision is made while MST only concerns the distance and update the cost after the final layout is formulated. Compared with those, heuristic method, APSO-MST, will random make a decision in each formulation step. Hence, there will be more freedom for the scheme to be formulated. Show (g) shows one possible solution while it can also be A-D-E-F, A-G, A-B-C then G-U, etc. Different decision-making sequence are allowed in APSO-MST that can contribute to the same cable scheme whereas similar to MST, the cost will be updated after the final layout is formulated. For the sake that APSO-MST permits this freedom of branch selection, it can find the lowest cost cable connection scheme compared with the other two methods in this simple example.

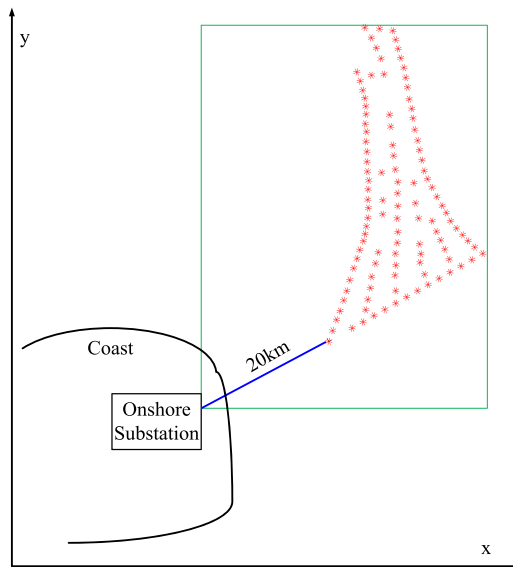


Figure 4. The layout of irregular shaped wind farm.

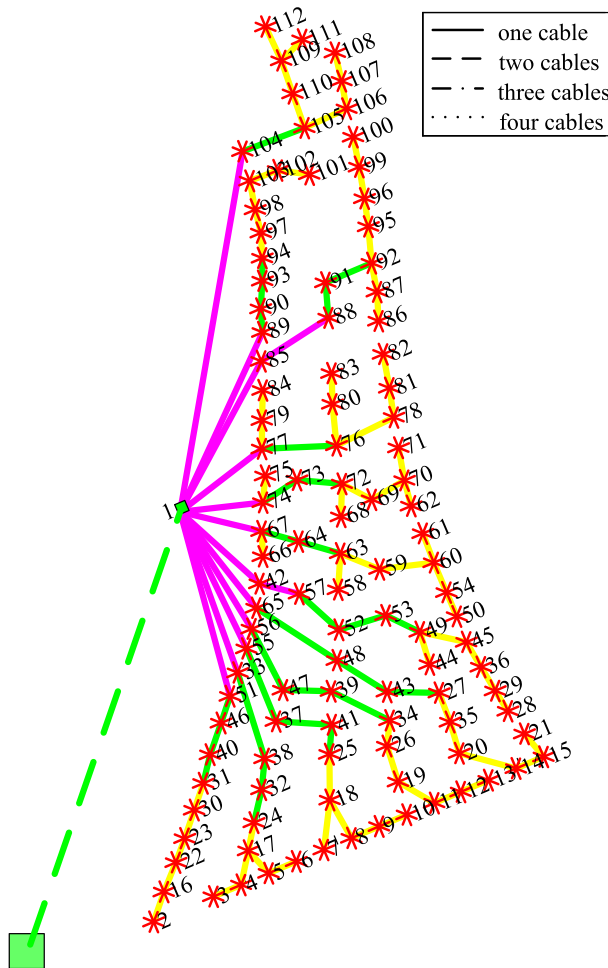


Figure 5. Industrial layout for irregular shaped wind farm (Layout 1).

### 3.4. Coding of particle $N_{S1}$

The selection of different voltage level will have an impact on the selection of cables sectional area as well as the type of transformers. Different types of components lead to different ratings, different costs and also different cable connection layout. There are correlations among aforementioned choices. In order to solve the problem, all potential solutions are

Table II. Specification of cable color.

Type	Collection system/transmission system				
	AC				
Color	Yellow	Green	Purple	Blue	Black
Cable sectional area (mm <sup>2</sup> )	70,95,120,150	185,240,300	400,500	630,800	1000

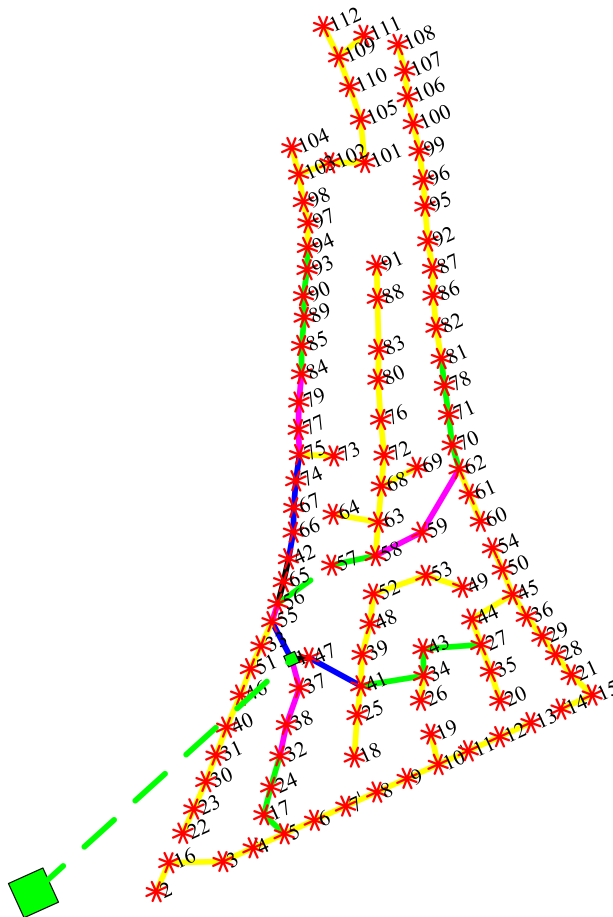


**Figure 6.** Optimized cable connection layout with one OS obtained by APSO-MST (Layout 2).

required to be coded into the particle swarm that is the initial step in PSO. The particle swarm  $S$  represents all the possible electrical system design and each design is defined in particle  $S_i$  as shown in Figure 2.

As can be seen in Figure 2, the control variables are discrete or continuous. Hence, the MIPSO is adopted to find the solution. Different from continuous PSO, the value of control variables are required to be rounded in update process if it is integer.<sup>37</sup> The first particle or position  $S_1$  in the particle defines the number of OS. Based on it, FCM will divide the wind farm into  $N_{S1}$  sub regions and the voltage level of CS and TS will then be decided by position  $S_2$  and  $S_3$ . Instead of using the center of each sub region as the OS location, the location of OS is in position  $S_4$  to  $S_3 + 2N_{S1}$  and will be used to generate the adjacency matrix.<sup>23</sup> The last two terms as shown in Figure 2 represent the connection layout of CS and TS, respectively. In APSO-MST, the cable connection layout is randomly given initially and updated with the factors described earlier until the optimized layout is found.

### 3.5. Optimization framework

The proposed algorithm is expected to find a near optimal electrical system layout with minimum total costs in consideration of OS placement as well as voltage level of each part. The simulation procedure to access the optimized cable connection layout by PSO-MST is shown in Figure 3.

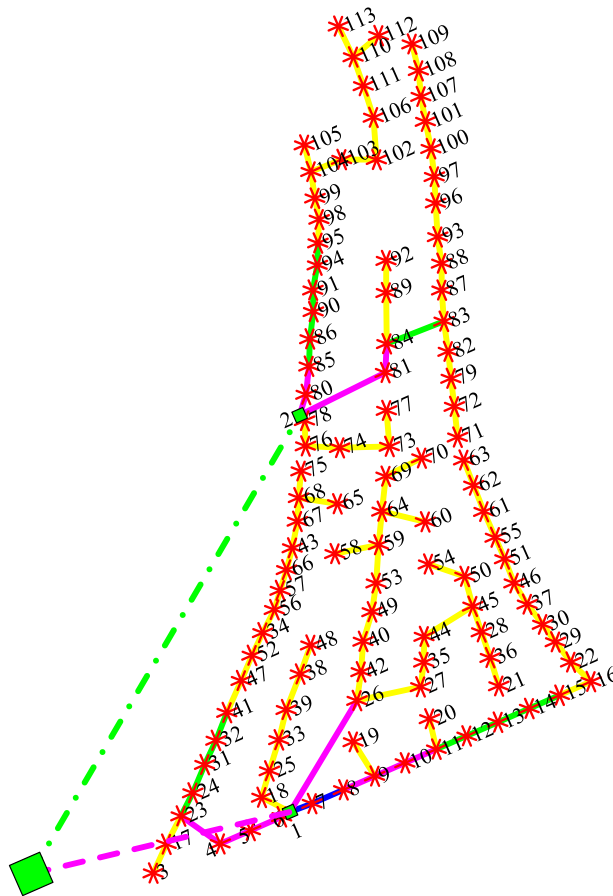


**Figure 7.** Optimized cable connection layout with two OSs obtained by APSO-MST (Layout 3).

The particles of PSO are initialized with a series of randomly given values in the first step and then transferred into Fitness Function. In which, the wind farm will be partitioned into several sub regions corresponding to the value of  $S_1$  using FCM. Then, the transformer as well as OS platform's rating will be decided according to the number of WTs in each region. In each sub region, the location of OS is determined by  $S_4$  to  $S_{3+2NS_1}$ . After that, the cable connection layout for each sub region as well as cable connection scheme for OSs will be formulated using the method proposed in reference<sup>23</sup> based on the information provided by  $S_{4+2NS_1}$  to  $S_{3+2NS_1+NWT}$ . Finally, the cable current carrying limitation and its cost corresponding to different sectional area will be decided based on the formulated cable connection layout as well as the voltage of each system given by  $S_2$  and  $S_3$  using the cost model presented in Section 2.1. The first calculated total cost and cable connection layouts will be obtained after the cable connection layouts for CS and TS are generated respectively in CS and TS Formation step. The result from the first calculation will be saved as the initial particle population that is the basis for comparison later. Then, the particles which contain the information as described in Figure 2 will be updated and transferred into the fitness function. By following the same procedure as the first calculation does, the calculated cost and its corresponding layout can be obtained and send out to the Fitness Evaluation step for comparison. This updating process will be ceased if the maximum iteration is reached. Finally, the optimized electrical system layout that is the minimum total cost design that found by program will be output.

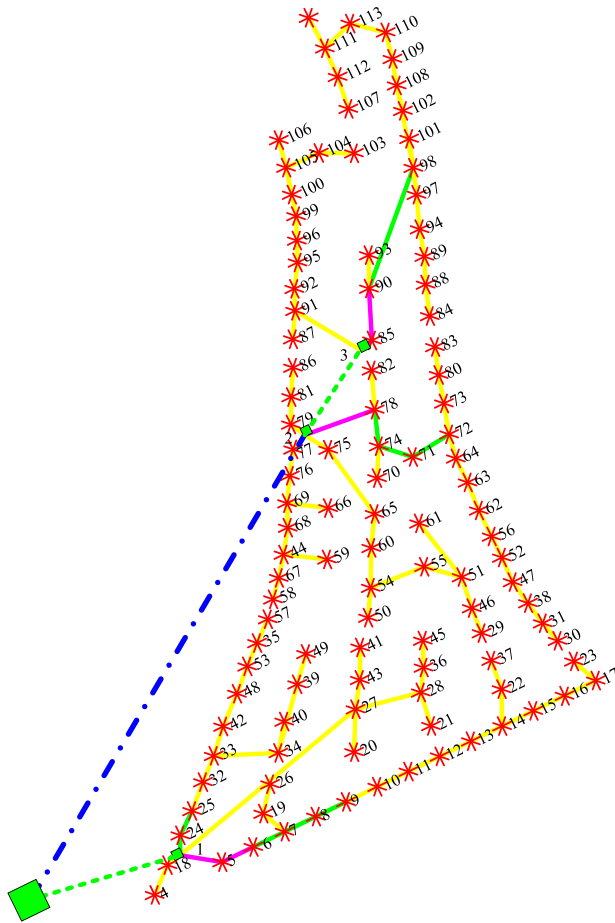


Figure 8. Optimized cable connection layout with three OSs obtained by APSO-MST (Layout 4).

#### 4. CASE STUDY

An irregular wind farm is chosen as the study case to verify the feasibility of the proposed method in this section. The layout of the reference wind farm is introduced first. Then, the results obtained by the proposed method are presented and compared.

##### 4.1. Irregular shaped wind farm

In this work, the industrial layout is designed similar to Anholt offshore wind farm<sup>38</sup> is selected and defined as the industrial layout. In this wind farm, the distance from the onshore substation to the nearest WT in the wind farm is assumed to be 20 km. There are totally 111, Siemens SWT-3.6-107<sup>39</sup> (107 m rotor diameter) WTs in this wind farm which is shown in Figure 4. The red stars show the WT locations while the green rectangular indicates the area that the OS can be located.

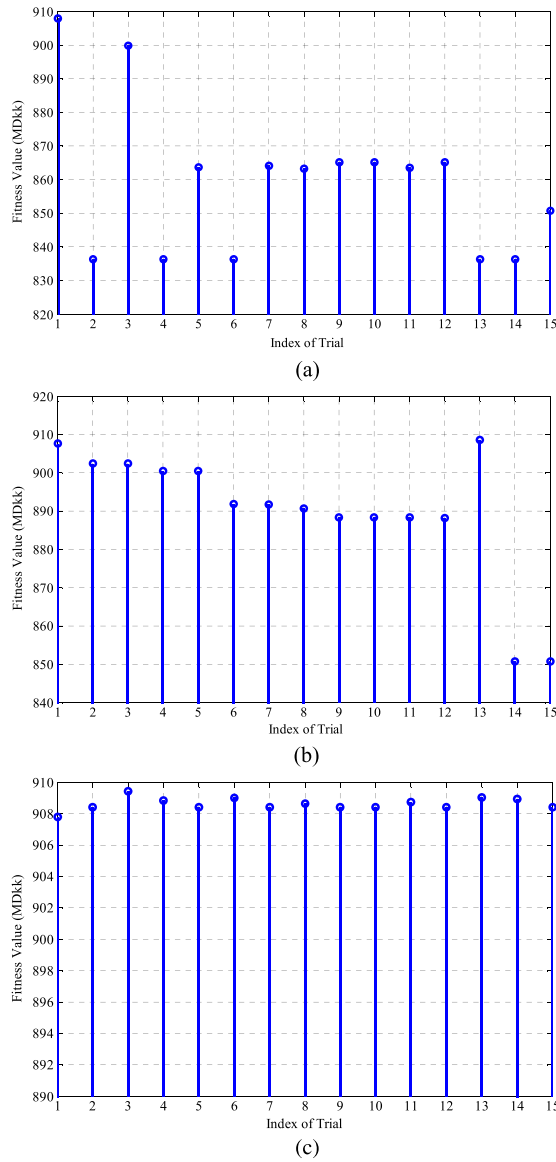


**Figure 9.** (a) The fitness value of each trial for Layout 2. (b) The fitness value of each trial for Layout 3. (c) The fitness value of each trial for Layout 4.

**4.2. Optimization of electrical system**

As can be seen in Figure 5, the offshore WTs, OS as well as onshore substation location are represented in a coordinate system. The red stars are WTs and small green square is OS. Considering the visualization, the onshore substation is illustrated with a bigger green square and the location's x coordinate is diminished to one-tenth of its original value.

The lines show the cable connection layout and the color of the line represents the rating of the cable that is explained in Table II. The number besides the red star (WT) indicates the sequence number of WT and No. 1 shows the sequence number of OS. Because multiple cables might be adopted between some pair of WTs, the number of cables that utilized between each two WTs is indicated with different types of lines, which are solid line (one cable), dash line (two cables), dash dotted line (three cables) and dotted line (four cables), and showed in upper right box of Figure 2. The colors and lines in the following figures have the same meaning in this work.

The optimized layout with 1 to 3 OSs is shown in Figures 6–8 respectively. The OS is permitted to be optimized within the area that showed in Figure 4.

### 4.3. Results and discussion

For the stochastic algorithm, the results are highly related to the parameter setting. Although the APSO is adopted in this paper, it cannot ensure the result is deterministic. The program is running 15 times to increase the possibility of finding the global optimal solution. The 15 times trails for each layout are illustrated in Figure 9(a) (b) and (c), respectively.

Because the PSO algorithm is used to find a minimal cost layout, the robustness of the best result within the 15 trials is shown below. The relations of the generation and cable cost (fitness value) for each layout are studied and shown in Figures 10–12. It can be seen that the cable cost stabilized at a fixed value at 300th generation in all layouts.

The obtained layouts are compared in Table III. The energy yields are calculated considering wake effect as well as the losses along the cables. The detailed energy yields calculation process considering wake effect is specified in another work.<sup>40</sup> The cost of energy is calculated by using total cost over energy yields.

As can be seen in Table III, Layout 2 to 4 is the optimized electrical system that can be obtained by the proposed method when the quantity of OS is 1, 2 and 3, respectively. The Layout 2 and 3 can reduce the total cost 3.01% and 1.33%

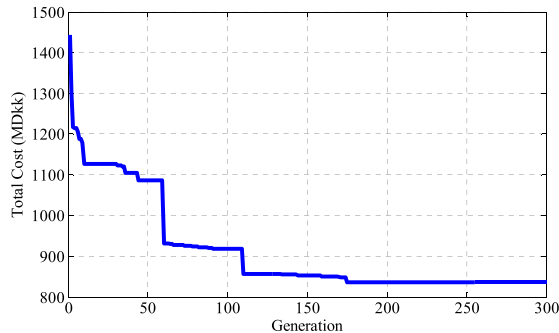


Figure 10. The total cost corresponding to each generation for layout 2.

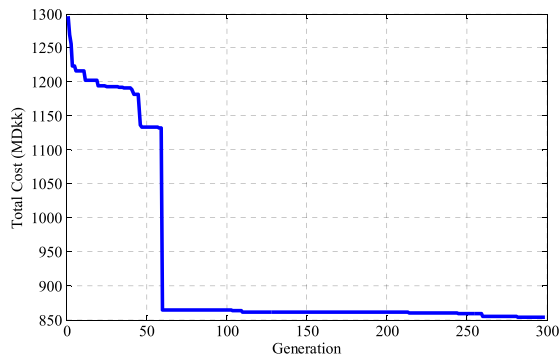
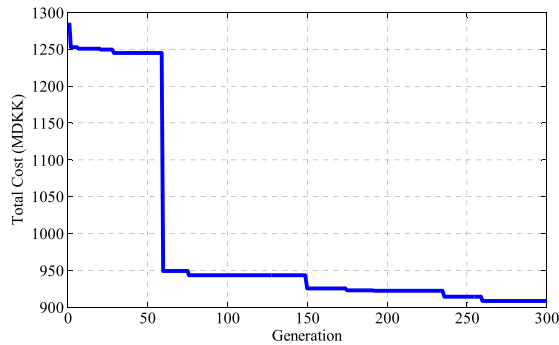


Figure 11. The total cost corresponding to each generation for layout 3.





**Figure 12.** The total cost corresponding to each generation for layout 4.

**Table III.** Specification of wind farm.

	Layout 1	Layout 2	Layout 3	Layout 4
Transformer type	33/220 kV, 220 MVA	66/220 kV, 220 MVA	66/220 kV, 140, 85 MVA	66/220, 60, 80, 85 MVA
Quantity of platform	1	1	2	3
Cost of CS (MEUR)	26.25	19.81	17.36	18.56
Cost of TS (MEUR)	23.02	22.63	23.98	25.47
Cost of cable installation (MEUR)	28.70	32.05	31.22	33.42
Total length of cables (km)	14.77	16.48	16.06	17.19
Cost of transformer (MEUR)	2.25	2.25	3.17	3.86
Cost of platform (MEUR)	35.73	35.73	38.67	40.85
Total cost (MEUR)	115.95	112.46	114.40	122.16
Energy losses along cables (GWh)	23.42	15.89	9.64	1.92
Energy yields at onshore substation(GWh)	1887.89	1895.42	1901.67	1902.39
Cost of energy (EUR/MWh)	61.42	59.33	60.16	64.21

compared with layout 1 (industrial layout), however, the Layout 4 increase the cost 5.35%. This is because the savings on the cables cannot compensate for the big increase on the cost of platforms and transformers. Higher energy yield can be obtained by using Layout 3 and 4 compared with Layout 1 and 2, however, the minimal cost of energy layout is also Layout 2 followed by Layout 3 and industrial layout. In sum, the best electrical system design of the wind farm should be Layout 2 with only one platform. For one thing, it can increase the energy yield, for another the total cost can be reduced compared with the other layouts.

## 5. CONCLUSIONS

This paper proposes a novel way for wind farm electrical system design. The algorithm improves the previous work on cable connection layout design by taking into account of more impact factors as number of OS as well as each OS location, the cable connection layout among OSs, the voltage level of TS and CS. Results show that the algorithm proposed in this paper can be used to generate a design that has lower total cost and also lower cost of energy compared with industrial layout. The proposed optimization platform can help design wind farm electrical system with the aim of reducing total cost. Actually, it can be easily modified to cope with different objectives, such as minimal Levelised cost of energy (LCoE), etc. In practice, the repair times are very long for offshore wind farm. If this fact is considered into the layout formulation, then a close loop cluster may be adopted. The proposed algorithm can be modified to include some general layout as loop cluster layout by making some assumptions or constraints.

In future, the work will be further improved by taking into account some other constraints as trenching restrictions, the cost of foundation to obtain a more realistic wind farm electrical system design. Moreover, the WT's locations could also be selected as the optimization variables and studied together with offshore wind farm electrical system design.

## ACKNOWLEDGEMENTS

Authors would like to thank Norwegian Centre for Offshore Wind Energy (NORCOWE) under grant 193821/S60 from Research Council of Norway (RCN).

## REFERENCES

1. Chen N. *Large-Scale Offshore Wind Farm Electrical Collection Systems Optimization*. Shanghai University of Electric Power: Shanghai, 2011.
2. Lundberg S. *Configuration Study of Larger Wind Park. Thesis for the Degree of Licentiate Engineering, Dept. Electr. Power Eng., Chalmers Univ. Technol.*: Goteborg, Sweden, 2003.
3. Zhao M, Chen Z, Blaabjerg F. Application of genetic algorithm in electrical system optimization for offshore wind farms. *Int. Conf. on Electric Utility Deregulation and Restructuring and Power Technologies (DRPT)*, Nanjing, China, 2008.
4. Zhao M, Chen Z, Blaabjerg F. Optimisation of electrical system for offshore wind farms via genetic algorithm. *Renewable Power Generation, IET* 2009; **205-216**.
5. Bahirat HJ, Mork BA, Hoidalen HK. Comparison of wind farm topologies for offshore applications. *IEEE Power and Energy Society General Meeting* 2012; **2012**: 1–8.
6. Bondy JA, Murty USR. *Graph Theory with Applications*. the Macmillan Press Ltd: Ontario, 1976.
7. Press WH, Teukolsky SA, Vetterling WT, Flannery BP. *Numerical Recipes in Fortran 77: the Art of Scientific Computing* (2nd edn), vol. **10.9**. Cambridge University Press: Cambridge; 438–444.
8. Devore RA, Temlyakov VN. Some remarks on greedy algorithm. *Advances in Computational Mathematics* 1996; **173-187**.
9. Ling-Ling H, Ning C, Hongyue Z, Yang F. Optimization of large-scale offshore wind farm electrical collection systems based on improved FCM. *International Conference on Sustainable Power Generation and Supply (SUPERGEN 2012)*, Hangzhou: 2012.
10. Dutta S, Overbye TJ. Optimal wind farm collector system topology design considering total trenching length. *IEEE Transactions on Sustainable Energy* 2012; **3**: 339–348.
11. Jenkins AM, Scutariu M, Smith KS. Offshore wind farm inter-array cable layout. *PowerTech (POWERTECH), 2013 IEEE Grenoble* 2013: 1–6.
12. Gonzalez-Longatt FM, Wall P, Regulski P, Terzija V. Optimal electric network design for a large offshore wind farm based on a modified genetic algorithm approach. *IEEE Systems Journal* 2012; **6**: 164–172.
13. Lingling H, Yang F, Xiaoming G. Optimization of electrical connection scheme for large offshore wind farm with genetic algorithm. *International Conference on Sustainable Power Generation and Supply, 2009. SUPERGEN '09*; 2009; 1–4.
14. Li DD, He C, Fu Y. of large offshore wind farm with improved genetic algorithm. *2008 IEEE Power and Energy Society General Meeting - Conversion and Delivery of Electrical Energy in the 21st Century*; 2008; 1–6.
15. Dahmani O, Bourguet S, Guerin P, Machmoum M, Rhein P, Josse L. Optimization of the internal grid of an offshore wind farm using Genetic algorithm. *IEEE Grenoble PowerTech (POWERTECH) 2013*; **2013**: 1–6.
16. Serrano Gonzalez J, Burgos Payan M, Riquelme Santos J. A new and efficient method for optimal design of large offshore wind power plants. *IEEE Transactions on Power Systems* 2013; **28**: 3075–3084.
17. Dutta S, Overbye TJ. A clustering based wind farm collector system cable layout design. *IEEE Power and Energy Conference at Illinois (PECI) 2011*; **2011**: 1–6.
18. Wu Y, Lee C, Chen C, Hsu K, Tseng H. Optimization of the wind turbine layout and transmission system planning for a large-scale offshore wind farm by AI technology. *IEEE Transactions on Industry Applications* 2014; **50**: 2071–2080.
19. Lumbreras S, Ramos A. Optimal design of the electrical layout of an offshore wind farm applying decomposition strategies. *IEEE Transactions on Power Apparatus and Systems* 2013; **28**: 1434–1441.
20. Hopewell PD, Castro-Sayas F, Bailey DI. Optimising the design of offshore wind farm collection networks. *UPEC '06. Proceedings of the 4-1st International Universities Power Engineering Conference*; 2006; **1**: 84–88.
21. Lumbreras S, Ramos A. Optimal design of the electrical layout of an offshore wind farm applying decomposition strategies. *Power Systems, IEEE Transactions on* 2013; **28**: 1434–1441.
22. Hou P, Hu W, Chen Z. Offshore substation locating in wind farms based on prim algorithm. *IEEE Power & Energy Society General Meeting*; 2015.

23. Hou P, Hu W, Chen Z. Optimization for offshore wind farm cable connection layout using APSO-MST method. *IET Renewable Power Generation* 2016; **10**: 694–702.
24. Lundberg S. Performance comparison of wind park configurations, *Department of Electric Power Engineering, Chalmers University of Technology, Department of Electric Power Engineering, Goteborg, Sweden, Tech.*; 2003.
25. XLPE submarine cable systems attachment to XLPE Land cable systems-user's guide. ABB corporation.
26. Kirkeby H, Merz KO. Layout and electrical design of a 1.2 GW wind farm for research on the next generation of offshore wind energy technologies. *Sintef Energy Research, Trondheim*; 2014.
27. Bezdek JC, Ehrlich R, Full W. The fuzzy c-means clustering algorithm. *Computers & Geosciences* 1984; **10**: 191–203.
28. Kennedy J, Eberhart R. Particle swarm optimization. *Proc. IEEE Int. Conf. Neural Networks*; 1995; 1942–1948.
29. Laskari EC, Parsopoulos KE, Vrahatis MN. Particle swarm optimization for integer programming. *IEEE Congress on Evolutionary Computation* 2002; **2**: 1582–1587.
30. Gaing ZL. Constrained optimal power flow by mixed-integer particle swarm optimization, in *Proc. IEEE Power Eng. Soc. General Meeting*; 2005; 243–250.
31. Shi Y, Eberhart RC. Empirical study of particle swarm optimization. *CEC 99. Proceedings of the 1999 Congress on Evolutionary Computation*; 1999; **3**.
32. Jiao B, Lian Z, Gu X. A dynamic inertia weight particle swarm optimization algorithm. *Chaos, Solitons & Fractals* 2008; **37**: 698–705.
33. Shi Y, Eberhart RC. Fuzzy adaptive particle swarm optimization. *Proceedings of the 2001 Congress on Evolutionary Computation* 2001; **1**: 101–106.
34. Zhan Z-H, Zhang J, Li Y, Chung HS-H. Adaptive particle swarm optimization. *IEEE Transactions on Systems, Man, and Cybernetics. Part B, Cybernetics* 2009; **39**: 1362–1381.
35. Hu M, Wu T, Weir JD. An intelligent augmentation of particle swarm optimization with multiple adaptive methods. *Information Sciences* 2012; **213**: 68–83.
36. Bondy JA, Murty USR. Graph theory with applications, *the Macmillan Press Ltd*, 1976.
37. Matsui T, Kato K, Sakawa M, Uno T, Matsumoto K. Particle swarm optimization for nonlinear integer programming problems. *Proceedings of the International Multi Conference of Engineers and Computer Scientists 2008*; 2008; **II**.
38. Thomsen F, Anholt offshore wind farm, *Dong Energy*, Available: [www.anholtoffshorewindfarm.com](http://www.anholtoffshorewindfarm.com).
39. New dimension. Available: [www.siemens.com/wind](http://www.siemens.com/wind).
40. Hou P, Hu W, Soltani M, Chen Z. Optimized placement of wind turbines in large scale offshore wind farm using particle swarm optimization algorithm. *IEEE Transactions on Sustainable Energy* 2015; **6**: 1–11.

# Offshore Substation Locating in Wind Farms Based on Prim Algorithm

Peng Hou, Weihao Hu, Zhe Chen,  
 Department of Energy Technology  
 Aalborg University  
 Pontoppidanstraede 101, Aalborg DK-9220, Denmark  
[pho@et.aau.dk](mailto:pho@et.aau.dk), [whu@et.aau.dk](mailto:whu@et.aau.dk), [zch@et.aau.dk](mailto:zch@et.aau.dk)

**Abstract**— The investment of offshore wind farm is large while the cost on electrical system can take up to 15% of the total costs. In order to reduce the cost, it is desirable to optimize the electrical system layout in design phase. Since the location of offshore substation (OS) is highly related to the electrical system layout, the optimal layout design work should be done with the consideration of the impact of the location of offshore substation on the submarine cable connection layout to minimize the investment of cables. This paper addresses a new method to optimize the OS location together with the cable connection layout. The results show that the proposed method is an effective way for offshore wind farm cable connection layout design.

**Index Terms**—electrical system layout; offshore substation (OS); submarine cable.

## Nomenclature

$C_i$ [MDKK/km]	the unit cost of cable $i$
$S_{n,i}$ [W]	the rated apparent power of cable in line $i$
$A_p, B_p, C_p$	the coefficient of cable cost model
$I_{i,rated}$ [A]	the rated current of cable in line $i$
$U_{i,rated}$ [V]	the rated voltage of cable in line $i$
$x, y$	the position of OS in the form of coordinate
$C_i(x, y)$	the unit cost of cable $i$ when OS location is $(x, y)$
$L_i(x, y)$ [km]	the length of cable $i$ when OS location is $(x, y)$
$Q_i(x, y)$	the number of cable $i$ when OS location is $(x, y)$
$C_{tot}(x, y)$	the total cost of cables when OS location is $(x, y)$
$N$	total number of vertices in a graph
$I_i$ [A]	the current going through the cable $i$
$L_x$ [km]	the width of wind farm in horizontal direction
$L_y$ [km]	the length of wind farm in vertical direction

## I. INTRODUCTION

The offshore wind farm has a larger power capacity factor and occupies larger area compared with onshore wind farm. In

such a wide region, the power generated from each Wind Turbine (WT) is first collected through a series of medium voltage (MV) cables and be transmitted to the OS by one or several MV integration cables. The voltage is transferred to a transmission voltage level so that all the power can be transmitted to the onshore substation through transmission system. Due to the limitation of cable current carrying capacity, the cable size should be carefully selected. Since the location of the substation would have a significant impact on the collection system layout which contributes to the total investment of electrical system, it is necessary to design the cable connection layout considering OS location to save investment on cables while meet the operating requirement.

The assessment of offshore wind farm layout has been done in [1] for comparing AC and/or DC collection systems (CS) corresponding to different voltage levels. Further, the collection system with different topology was compared in [1]. The electrical system is optimized concerns both the production cost as well as reliability in this paper. In [3], a new algorithm to minimize the system power losses and improve the reliability was proposed and validated through a small reference wind farm. Based on a practical wind farm project, the Fuzzy C-means clustering algorithm was adopted in [4] to partition the whole system into several subsets. The substation was regarded to be located in the center of each subset and the cable connection layout in each part was optimized with Minimum Spanning Tree (MST) algorithm to get a minimal investment of collection system. The MST is also utilized and modified in [6]. The layout with minimal trenching length is found. The maximum number of WTs that can be connected after one cable is considered. The power flow is also computed to help assign the cable size. In addition, Generic algorithm (GA) was also widely used in finding optimal cable connection layout [6][7]. The topology design, electrical system voltage level as well as key components selection are included in [6]. It succeeded in optimizing the electrical system layout with the minimal Levelised Production Cost (LPC) while reaching the reliability requirement. The optimal collection system is also presented in [7]. It attempt to use GA to find the minimal cost cable connection layout for a 4 substation offshore wind farm and several layouts are compared to demonstrate the effectiveness of the new method.

This work has been (partially) funded by Norwegian Centre for Offshore Wind Energy (NORCOWE) under grant 193821/S60 from Research Council of Norway (RCN). NORCOWE is a consortium with partners from industry and science, hosted by Christian Michelsen Research.

In this paper, the offshore wind farm collection system layout is optimized by prim algorithm. Since the location of OS is highly related to the collection system layout, the siting of the OS is optimized together with the system layout to minimize the total investment on electrical system. In order to meet the system operation requirement, the cable current carrying capacity is considered in cable selection process during the simulation. The proposed method is implemented in a regular and an irregular shaped wind farm and the results show that it is an effective way for offshore wind farm electrical system layout design.

The prim algorithm for the optimization problem, cost models and optimization framework are specified in section II. A regular and an irregular shaped wind farm both with 80, 2MW WT are chosen as the study cases to demonstrate the proposed method in Section III. Finally, conclusions and future work are given In Section IV.

## II. PROBLEM FORMULATION

In this section, the MST problem and prime algorithm are firstly introduced. Then the cost model which is used in this work is specified. Finally, the optimization framework and some assumptions are proposed.

### A. Minimum Spanning Tree

A tree is defined as a connected acyclic graph [7] which is one sub graph of the undirected graph. The spanning tree can be defined as a sub graph of an undirected weighted graph which connects all the vertices with merely one path between every two nodes while the minimum spanning tree is one of the spanning trees with minimum weight [8]. If the location of WTs and OS can be regarded as vertices while the costs of the cables are regarded as the weight of branches. Then, the problem can be converted into a classic mathematical problem as finding the MST of a weighted graph.

### B. Prim Algorithm

Presently, prim algorithm and kruskal algorithm, which are both based on the idea of greedy algorithm, are commonly used in solving MST problem [9]. In this work, the prim algorithm is adopted to get the collection system layout and modified to include the optimization of OS location. Generally, the prim algorithm proceeds as follows [10]:

- (1) Selecting any node V in the graph as the searching starting point.
- (2) Constructing two sets, A and B. Adding the rest vertices in the graph into Set A which stores unvisited vertices within the graph.
- (3) Comparing the weight of all the branches that connect to V and select the minimum-weight branch as the generated tree branch in this step. The other vertices of this branch will be added to Set B and deleted from Set A.
- (4) If Set A is empty, the program will stop. Otherwise, go to step 3 until the MST is completed.

### C. Cost model

The cost models are set up according to cables' rated power. The mathematical equations can be written as [11]:

$$C_i = A_p + B_p \exp\left(\frac{C_p S_{n,i}}{10^8}\right)^2 \quad (1)$$

$$S_{n,i} = \sqrt{3} I_{i,rated} U_{i,rated} \quad (2)$$

The cables are selected according to its rated current which is correlated to the sectional area in this paper. In some cases, more cables are required between two WTs if too many WTs are connected after this branch. Then the total cost of cables can be calculated by the following equation.

$$C_{tot}(x, y) = \sum_i^N C_i(x, y) L_i(x, y) Q_i(x, y) \quad (3)$$

### D. Optimal cable connection layout by modified Prim algorithm

In this project, the optimal location of OS should be found together with the optimal collection system layout. It can be solved by introducing one more element of substation location into the graph and the location of OS is selected as the searching starting point. The optimization framework is shown in Fig. 1.

**Cable Database:** In [12], various voltage levels' cables with different sectional areas can be found. In this simulation, the cables in the wind farm are XLPE-Cu AC cables operated at 33kV nominal voltage for collection system and one 132kV 715 mm<sup>2</sup> HVAC cable is selected for transmission system.

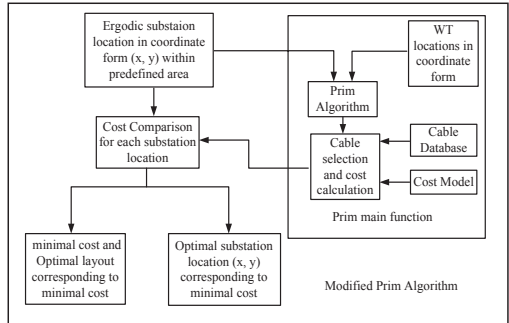


Figure 1. Optimization framework

The locations of WTs and onshore substation are assumed to be fixed in this project. The optimal location of substation is expected to be found within the predefined area. Each time, a new OS location is loaded, a new coordinate matrix which contains the coordinate of WTs and OS will be created. Based on it, the optimal cable connection layout will be found by using prim algorithm which is discussed in Section II.B. Since the transmission capacity limitation, the cable size of each branch should be carefully selected. The Cable Database contains the available cable size. From the number of WTs connected to the branch, the maximum current going through the cable could be calculated. After that, the total cost could be calculated using (1), (2) and (3).

Since the location of OS is given ergodically. A series of costs should be compared in cost comparison step so that the minimum cost layout could be selected which is the optimal cable connection layout. Finally, the minimal cost electrical system layout as well as the location of OS will be found at the same time.

### E. Assumptions

Some necessary assumptions for the optimization problems are:

- The lengths of the cables are selected according to the geometrical distance without thinking of practical usage, such as the barriers, restriction in sea, etc.
- The position of OS ( $x, y$ ) is permitted to be constructed within a prespecified area, that is,  $x \in (0, L_x)$ ;  $y \in (-10, L_y)$ .
- Due to the cable current carrying capacity limitation, the current in each cable cannot over its limit, that is,  $I_i \leq I_{i, \text{rated}}$ ,  $i \in (1, N)$ .

## III. CASE STUDY

The simulation is implemented on the platform of Matlab software. Two study cases are adopted to verify the feasibility of the proposed method.

### A. Case I: Regular shaped wind farm

The wind farm is assumed to be set up 30km away from the coast with 80, Vestas V90-2.0 MW (90m rotor diameter) WT's which can be seen in Fig. 2. The locations of WT's are predefined within a 7D\*7D regular shaped wind farm which means that the distance between each two WT's are 7 rotor diameters. Four scenarios are presented and compared with obtained optimal layout.

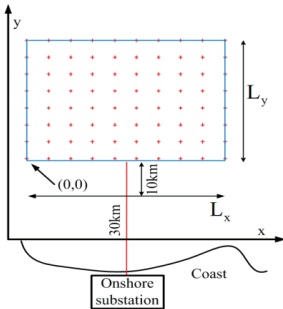


Figure 2. Regular shaped wind farm

In Fig. 2, the red star shows the locations of WT's. The blue square is the boundary of the predefined wind farm area. The substation is permitted to move from 0 to  $L_x$  in  $x$  direction and  $-10$  to  $L_y$  in  $y$  direction. The cable within the blue square area and the cable which transmit the power collected from all WT's to OS constitute the collection system. It can be seen that if the OS is moving closer to the coast, the investment on HVAC cable will be reduced, however, the investment on

collection system's cables should be higher and it will be just contrary if the substation is constructed inside the blue square area. There should be a tradeoff between these two parts' costs.

1) *Scenario I: Industrial offshore wind farm layout:* In this scenario, the industrial 7D layout is introduced. As can be seen in Fig. 3, the red stars indicate the WT's location and the green lines show the integration cables which transmit the power from WT's to OS (the blue square) while the black lines show the cable connection layout. There are totally 5 integration cables in this layout. Each integration cable has the capability of transmitting the power generated by 16 WT's in full load condition. The WT's are placed with 7 rotor diameters interval in both  $x$  and  $y$  direction and the OS is 25 km away from coast.

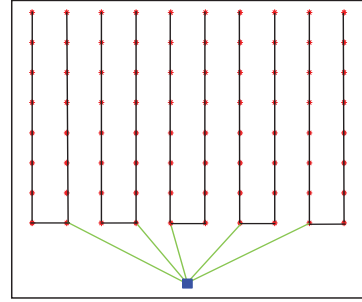


Figure 3. Industrial 7D layout

2) *Scenario II: OS near shore layout:* In this scenario, the OS is assumed to be constructed 25km away from coast. Then the cable connection layout could be found by the proposed method. The input to the coordinate matrix is just one given location of OS instead of a series of locations in this case. The optimal layout is illustrated in Fig. 4.

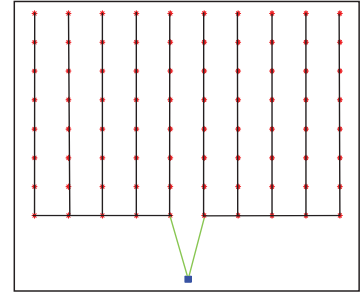


Figure 4. Optimal layout for OS near shore

3) *Scenario III: OS in the center layout:* In this scenario, the OS is assumed to be constructed in the middle of wind farm. The optimal cable connection layout found by the proposed method for this scenario is illustrated in Fig. 5.

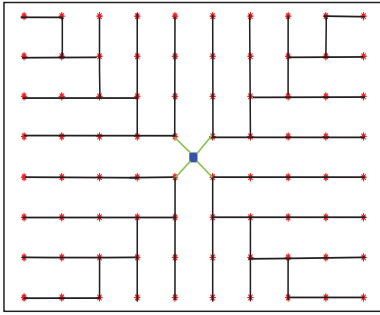


Figure 5. Optimal layout for OS in the center of wind farm

4) *Scenario IV: Optimal collection system layout:* In this scenario, the OS location is expected to be found together with the optimal cable connection layout. Following the proposed optimization framework in Section II. D, the optimal layout is shown in Fig. 6. In order to see the performance of the proposed method, the layouts are also compared in Table I.

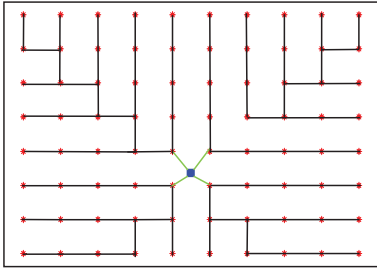


Figure 6. Optimal collection system layout for regular shaped wind farm

TABLE I. LAYOUT COMPARISONS FOR REGULAR SHAPED WIND FARM

	Scenario I	Scenario II	Scenario III	Scenario IV
Total cable length for CS (km)	73.37	72.96	49.67	50.95
Trenching length for CS (km)	73.37	54.78	49.67	49.75
Cable to shore (km)	25	25	32.21	31.38
Cable costs for CS (MDKK)	118.10	131.31	68.39	137.64
Cable costs for TS (MDKK)	103.75	103.75	133.65	135.91
Total Cable invest (MDKK)	221.85	235.06	202.04	199.02
Substation location	(2.84,-5)	(2.84,-5)	(2.84,2.21)	(2.84,1.38)

In Table I, the trenching length indicates the total single line distance between WTs while cable length is the total cables that should be laying in this layout. It can be seen that

the cheaper layouts should be Scenario III and IV. The cable length is longer than trenching length for Scenario II and IV which means that more than one cable is needed between two WTs in some parts in these layouts.

Compared with Scenario I, Scenario II is more expensive. In spite of saving the invest on the cables which collect all the power from WTs and transmit it to the OS, in the layout of Scenario II, more than one cable has to be utilized between WTs to meet the operational requirement which increases the total cost eventually.

The minimal cost layout is Scenario IV. However, it is preferable to have only one cable between WTs as Scenario I and III layout in practical. Since more cables operating in parallel means the invest on trenching and electrical components will be doubled.

#### B. Case II: Irregular shaped wind farm

In this section, an irregular wind farm with 7 rows and 14 columns is chosen as the studied wind farm. In this wind farm, there are totally 80, Vestas V90-2.0 MW WTs which are placed with a nearly rhombus shape. The distance between WTs in both x and y direction are 7 rotor diameter (7D) as well which can be seen in Fig. 7.

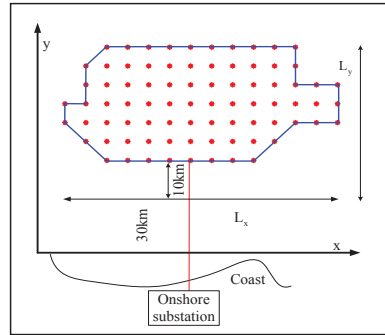


Figure 7. Irregular shaped wind farm

The onshore substation is also assumed to be 30 km away from wind farm. Three optimal layouts for this case are shown in Fig. 8, 9 and 10. The specifications of these optimal layouts are concluded in table II.

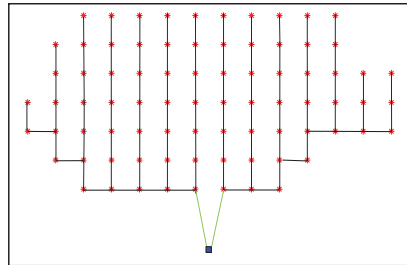


Figure 8. Optimal layout for OS near shore for irregular wind farm



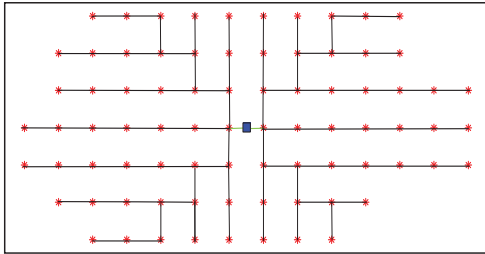


Figure 9. Optimal layout for OS in the center of irregular wind farm

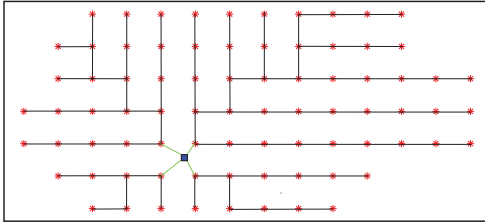


Figure 10. Optimal collection system layout for irregular shaped wind farm

TABLE II. LAYOUT COMPARISONS FOR IRREGULAR SHAPED WIND FARM

	Scenario I	Scenario II	Scenario III
Total cable length for CS (km)	72.96	50.4	51.26
Trenching length for CS (km)	54.78	49.77	49.74
Cable to shore (km)	25	31.89	31.10
Cable costs for CS (MDKK)	136.21	70.12	70.27
Cable costs for TS (MDKK)	103.75	132.35	129.07
Cable invest (MDKK)	239.96	202.47	199.34
Substation location	(4.1,-5)	(4.1,3.78)	(2.96, 1.08)

The graphic in Fig. 8 is the obtained optimal layout when OS is planned to be constructed near shore, while Fig. 9 and 10 represent the optimal layout with central placement of OS and optimal layout with optimal OS location. Similar conclusion can be made that the layout should be more cheap if the substation is constructed somewhere within the wind farm. The Scenario III save the investment of cables for 16.93% and 1.55% compared with Scenario I and II, however, constructing the offshore wind farm far away from the shore may increase the cost of foundations. Hence, more factors as varying foundation cost with water depth, cable installation cost, operation and maintenance cost, etc. should be considered to make the layout more practical so that a comprehensive decision can be made.

#### IV. CONCLUSIONS AND FUTURE WORK

In order to reduce the cost and make the wind farm more competitive in electricity market, it is necessary to make a cost-effective electrical system layout under the system

operational requirement. Within numbers of cable connection layouts, it is expected to find the minimal cost one with no cross cables. This description corresponds to the classic MST problem in graphic theory. Based on it, a new method is proposed to find the optimal electrical system layout for offshore wind farm. Some factors such as the best location to build up the OS and the suitable cable sectional area for each line between two WT's are considered in this paper. The studied cases demonstrate that the proposed method is an effective way to find the minimal cost collection system layout considering cable power transmitting limitation for regular/irregular shaped wind farm. In future, the work can be extended from two aspects: one is to include variable of the number of OSs into the optimal layout design problem to get a more optimal result, the other is to taking the energy yields as well power losses along the cables into consideration to evaluate the layout performance.

#### ACKNOWLEDGMENT

Authors would like to thank Norwegian Centre for Offshore Wind Energy (NORCOWE) under grant 193821/S60 from Research Council of Norway (RCN).

#### REFERENCES

- [1] S. Lundberg, "Configuration study of larger wind park," Thesis for the degree of Licentiate Engineering, Dept. Electr. Power Eng., Chalmers Univ. Technol., Goteborg, Sweden, 2003.
- [2] M. Zhao, Z. Chen, and F. Blaabjerg, "Application of genetic algorithm in electrical system optimization for offshore wind farms," presented at the Int. Conf. on Electric Utility Deregulation and Restructuring and Power Technologies (DRPT), Nanjing, China, 2008.
- [3] Dutta, S., Overbye, T.J., "A clustering based wind farm collector system cable layout design," 2011 IEEE Power and Energy Conference at Illinois (PECI), pp. 1-6, Champaign, IL, 25-26 Feb. 2011.
- [4] Huang Ling-Ling, Chen Ning, Zhang Hongyue, Fu Yang, "Optimization of large-scale offshore wind farm electrical collection systems based on improved FCM," International Conference on Sustainable Power Generation and Supply (SUPERGEN 2012), Hangzhou 8-9 Sept. 2012.
- [5] S. Dutta, T. J. Overbye, "Optimal Wind Farm Collector System Topology Design Considering Total Trenching Length," in IEEE Trans. Sustainable Energy, vol.3, no.3, pp.339-348, July 2012.S.
- [6] M. Zhao, Z. Chen, F. Blaabjerg, "Optimization of electrical system for a large DC offshore wind farm by genetic algorithm," Proc. Of NORPIE'04, June 14-16.
- [7] F. M. Gonzalez-Longatt, P. Wall, P. Regulski, and V. Terzija, "Optimal electric network design for a large offshore wind farm based on a modified genetic algorithm approach," IEEE Syst. J., vol. 6, no. 1, pp. 164-172, Mar. 2012.
- [8] J. A. Bondy and U. S. R. Murty, "Graph theory with applications," the Macmillan Press Ltd., 1976.
- [9] R. A. Devore, V. N. Temlyakov, "Some remarks on greedy algorithm," Adv. Comp. Math., 1996, pp. 173-187.
- [10] Vandervalk, B.P., McCarthy, E.L., Wilkinson, M.D., "Optimization of Distributed SPARQL Queries Using Edmonds' Algorithm and Prim's Algorithm," International Conference on Computational Science and Engineering, 2009. CSE '09, Vol. 1, pp. 330-337, 29-31 Aug. 2009.
- [11] S. Lundberg, "Performance comparison of wind park configurations," Department of Electric Power Engineering, Chalmers University of Technology, Department of Electric Power Engineering, Goteborg, Sweden, Tech. Rep. 30R, Aug. 2003.
- [12] "XLPE Submarine Cable Systems Attachment to XLPE Land Cable Systems-User's Guide," ABB corporation.



# Offshore Wind Farm Cable Connection Configuration Optimization using Dynamic Minimum Spanning Tree Algorithm

Peng Hou, Weihao Hu and Zhe Chen

Department of Energy Technology  
Aalborg University  
Aalborg, Denmark

[pho@et.aau.dk](mailto:pho@et.aau.dk), [whu@et.aau.dk](mailto:whu@et.aau.dk) and [zch@et.aau.dk](mailto:zch@et.aau.dk)

**Abstract**— A new approach, Dynamic Minimal Spanning Tree (DMST) algorithm, which is based on the MST algorithm is proposed in this paper to optimize the cable connection layout for large scale offshore wind farm collection system. The current carrying capacity of the cable is considered as the main constraint. The dynamic changing of the cable capacity, therefore, the cost during the searching process is presented in this work. Two wind farms are chosen as the studied case and the final results show that the proposed method can save the investment on cables 1.07% and 6.10% respectively compared with MST method. It is a more economical way for cable connection configuration design of offshore wind farm collection system.

**Index Terms**— Dynamic Minimal Spanning Tree (DMST), current carrying capacity, cable connection configuration design

## Nomenclature

$G$	Undirected graph
$G_T$	One tree graph in $G$
$V, B, W$	Vertices, branches and weight of each branch in graph $G_T$
$C_i$	Unit cost of cable $i$
[MDKK/km]	
$L_i$ [km]	Length of cable $i$
$N$	Total number of vertices in a graph
$I_i$ [A]	Current going through the cable $i$
$A_p, B_p, C_p$	Coefficient of cable cost model
$S_{rated,i}$ [MW]	Rated apparent power of cable $i$
$I_{i,rated}$ [kA]	Rated current of cable $i$
$U_{i,rated}$ [kV]	Rated voltage of cable $i$

## I. INTRODUCTION

Wind energy industry has undertaken a rapid development during the last decade. From the 2013 wind report of Global Wind Energy Council (GWEC), it is expected that over one quarter of world's electricity would be generated by renewables, in which, 25% is expected to be supplied by wind energy by 2035 [1]. As an important part of offshore wind farm, the investment of electrical system can take up to 15% of the total costs while the cost of cables takes a large proportion. It is desirable to connect the Wind Turbines (WT) economically so that a more economical competitive wind farm could be realized.

The offshore wind farm electrical system can be divided into two parts: collection system and transmission system. All the generated power are collected from each WT to offshore substation (OS) through a collection system and then transmitted to the onshore substation through the transmission system. The optimization of offshore wind farm electrical system has been done in using Genetic Algorithm (GA) [2]. Various types of components with different voltage levels, the typical WT cluster configuration (collection system configuration) and wind farm configuration was formulated into an input database and the optimal topology with optimal voltage level, components types and configurations was found to make a minimal production cost wind farm. It was a good way to make a decision from the existing data; however, since the cluster configurations were designed by experience, there were still some spaces for further optimization on collection system. GA was also adopted in and modified by considering open-multiple traveling salesmen problem (omTSP) to find the minimal cost of collection system layout for an offshore wind farm with 4 substations [3]. From the cable rated current, the number of WT in each

cluster were calculated and assumed to be the same. The results were also compared with a similar work which has been done using hybrid GA and immune algorithm and showed better performance [4]. Besides using heuristic algorithm, some work has also been done using MST algorithm [5], [6]. In [5], the locations of OS were decided by Fuzzy C-means clustering algorithm which partitioned the whole system into several subsets and then MST was adopted to optimize the cable connection layout in each part to get a minimal investment of the collection system while [6] introduced splice node into the MST algorithm to optimize the collection system layout with the purpose of minimizing total trenching length. Moreover, the limitation of maximum WTs that can connect to one feeder was considered so that the cable size for each branch can be determined. However, all the works above assumed that the cable type for connecting every two WTs was already known without thinking of the dynamic cable type changing during the layout formulation process.

The contribution of this paper is two fold: 1) A new approach, DMST method, to optimize the offshore wind farm collection system cable connection layout is proposed. 2) Different from the MST method which selected the cables for each branch after the cable configuration is formulated. The cables were selected during the cable configuration formulation process according to the cable current carrying density, so that the system operation requirement will be met. The effectiveness of the proposed method is demonstrated in case study and it shows better performance in cost reduction compared with the MST method.

## II. PROBLEM FORMULATION

As described in [7], the offshore wind farm collection system design problem is similar to the classic mathematical problem of finding MST in a given graph. Considering using the cable cost to indicate the weight between nodes instead of using merely distance, the problem can be described as:

$$\text{Variables: } G_T = (V, B, W) \quad (1)$$

Objective:

$$\text{Cost}_{\min} = \min \left( \sum_{i=1}^{N-1} C_i G_T L_i G_T \right), G_T \in G \quad (2)$$

$$\text{Constraints: } I_i \leq I_{i, \text{rated}}; i \in (1, N-1) \quad (3)$$

Where  $G$  is undirected graph and  $G_T$  represents one tree graph in  $G$  which contains a number of vertices ( $V$ , WT location) with different weight ( $W$ , cable cost) between them.  $B$  is the branch that connected vertices. It is expected that a  $G_T$  with minimum total  $W$  should be found, that is the optimized collection system layout. The  $N$  is the total number of vertices which is the total number of WTs plus OS in this work.

The costs of cables are calculated using the model which has been presented in [8]. The mathematic expression can be written as:

$$C_i = A_p + B_p \exp \left( \frac{C_p S_{\text{rated},i}}{10^8} \right)^2 \quad (4)$$

$$S_{\text{rated},i} = \sqrt{3} I_{i, \text{rated}} U_{i, \text{rated}} \quad (5)$$

The cable sectional area is selected by comparing the maximum current that would go through this cable as well as the cables rated current. In some cases, more cables may be required between two WTs if too many WTs are connected after this branch.

## III. OPTIMIZATION METHOD

The MST problem can be solved by prim algorithm, however, the traditional MST algorithm can only find the optimized cable connection layout with minimal total cable length instead of minimal cost. In this section, the modified algorithm of optimizing the wind farm collection system layout is specified at first. Followed by which is the optimization framework.

### A. Dynamic MST Algorithm

According to graphic theory, a tree can be defined as a connected acyclic graph within a pre-specified graph [9]. Only one path is allowed between every two nodes in a tree. The MST is one possible layout that connects all the nodes with the minimum total weights. Presently, prim algorithm and kruskal algorithm are commonly used in solving MST problem which are both based on the idea of Greedy Algorithm [10]. This method can be used when all the weights are given.

However, if more WTs are connected to one string, the cables in a previous arrangement may have to be changed in order to satisfy the change of the operational requirement. In other words, the weight (cost of cable) will be changed during the simulation. The traditional MST can only find the layout with minimal distances to connect all the WTs rather than minimum cable costs. In order to solve this problem, a dynamic MST algorithm is proposed and compared with traditional MST algorithm, Fig. 1 shows a simple example.

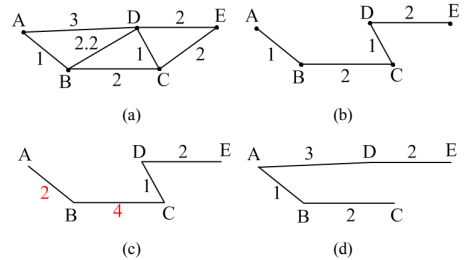


Fig. 1. (a) Undirected graph. (b) Layout found by MST. (c) Layout found by MST with updated weights. (d) Layout found by dynamic MST.

As can be seen in Fig. 1, assuming five nodes are to be connected and A is the starting point. (a) is the undirected graph and the number shows the weight for each branch. The layout found by traditional MST algorithm is illustrated as (b).

The total weight for this method is  $1+2+1+2=6$ . However, if assuming that the weight in previous arrangement will be doubled when more than 2 nodes are connected after one branch. Then the weight in layout (b) should be updated as shown in (c) and the total weight is  $2+4+1+2=9$ . The dynamic MST considers the impact of the vertex that is about to be added into the MST to the previous structure's weight. Hence, it can find a layout that has less total weight which is shown in (d) and the total weight by this method is  $1+3+2+2=8$ .

In this work, the dynamic MST is applied to find the optimized layout. Four sets and one matrix are created as follow [10]:

Set I: Containing the vertices that added into the MST.

Set II: Containing the vertices that have not yet added into the MST.

Set III: Containing the weights of the branches connecting the vertices in the MST, in other words, in set I.

Set IV: Containing the total number of WTs that connected to each branch in MST, in other words, in set I.

Adjacency Matrix: Containing all the weights between two adjacent vertices. In this work, the weight is the cost of the cable for this branch. Initially all the cables are assumed to be with 70 mm<sup>2</sup> sectional area which is the minimal sectional area in [11]. Then the cost can be updated by (2).

Initially, the Set I, III and IV will be put empty and all the vertices are stored in Set II. Then a random vertex ( $V_1$ ) is selected from Set II and add to Set I, then all the braches that connect to  $V_1$  will be compared. The vertex that could introduce total minimal cost will be added to Set III and the selected vertex will be added to Set I and deleted from Set II. The number of the WTs connected to this branch will be added 1 at this time. If the number of WTs after a certain cable is over it limit when a new vertex is added, the cable or rather the weight of this branch should be updated. This process will stop when Set II is empty.

### B. Optimization Framework

The proposed method is expected to find a less cost cable connection layout compared with traditional MST algorithm. The optimization procedure of DMST is shown in Fig. 2.

**Cable Database:** In [11], various voltage levels' cables with different sectional areas can be found. In this simulation, the cables in the wind farm are XLPE-Cu AC cables operated at 33kV nominal voltage for collection system and one 132kV 630 mm<sup>2</sup> HVAC cable is selected for transmission system.

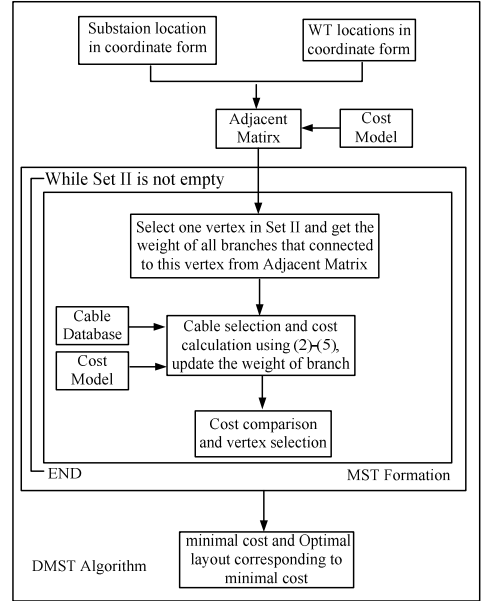


Fig. 2. DMST optimization framework.

With the given WTs and OS locations, the adjacent matrix which contains all the weights between two adjacent vertices is calculated at first. Then the cable connection layout will be formulation in MST formulation step. Initially, a random vertex in Set II will be selected and the weight of branches that can connect to this vertex will be calculated. If the current of a certain branch (cable) exceed its operation limit. The cable sectional area as well as the cost of this cable will be updated using (2)-(5) in cable selection step. After that, the vertex that could introduce the less cost will be selected and deleted from Set II as described in Section III. A. This process will not stop until Set II is empty. Finally, the calculated minimal cost and its corresponding optimized layout can be obtained.

## IV. SIMULATION AND RESULTS

The simulation is implemented on the platform of Matlab software. Two study cases are adopted to verify the feasibility of the proposed method. Both wind farms are assumed to be irregular shaped. This is because that the cable connection layout design for regular shaped wind farm would be easier. Actually, the proposed method can be used for any shaped wind farm cable connection configuration design while this paper focused on the cable configuration design of irregular shaped wind farm.

### A. Case I: OS in the Center of An Irregular Wind Farm

In this case, the irregular shaped wind farm is assumed to be set up 30km away from the coast with 80, Vestas V90-2.0 MW (90m rotor diameter) WTs. The locations of OS

are predefined in the center of the wind farm and the distance between WTs in both x and y direction is 7 rotor diameter (7D) as well which can be seen in Fig. 3.

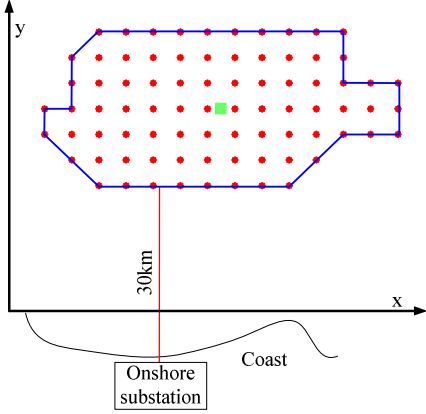


Fig. 3. Irregular shaped wind farm layout.

As can be seen in Fig. 3, the red dots are the WTs locations and the green square shows the substation location. The onshore substation is assumed to be constructed 30 km away from the wind farm.

TABLE I  
SPECIFICATION OF CABLE COLOR

Collection system					
Voltage level	33kV				
Type	AC				
Color	yellow	green	purple	blue	black
Cable Sectional area (mm <sup>2</sup> )	70,95, 120,150	185,240, 300	400,500	630,800	1000

The optimized cable connection layouts are shown in Fig. 4. In which, the lines outline the cable connection layout and the color of the line represents the rating of the cable which is explained in Table I. Since multiple cables might be adopted between some pair of WTs, the number of cables that utilized between each two WTs is indicated with different types of lines, which are solid line (one cable), dash line (two cables), dash dotted line (three cables) and dotted line (four cables), and showed in upper right box of Fig. 4. The number besides the red star (WT) shows the sequence number of the corresponding WT.

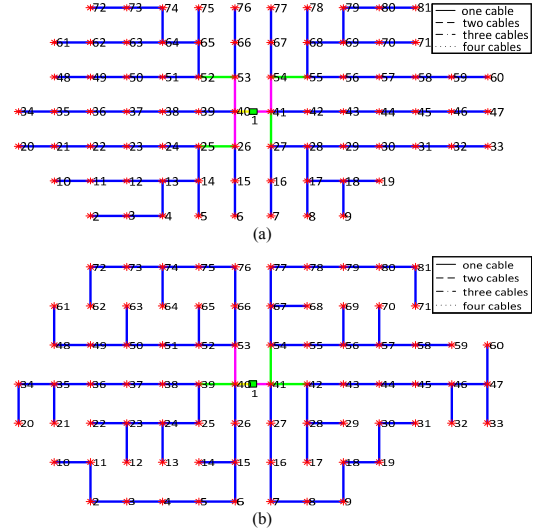


Fig. 4. The illustration of cable connection configuration for case I. (a) Optimized cable connection layout using MST. (b) Optimized cable connection layout using DMST.

TABLE II  
LAYOUT COMPARISONS FOR IRREGULAR SHAPED WIND FARM

	MST	DMST
Cable invest (MDKK)	202.47	200.31
Total cable length for CS (km)	50.4	50.4
Trenching length for CS (km)	49.77	49.77

As can be seen in Table II, the optimized collection system layout obtained by DMST can save the investment of cables for 1.07% compared with MST. The trenching length means the total single line distance of connecting all WTs in the wind farm. Though the total trenching length as well as total cable length are the same by using two methods, the invest on cables is different. Since the cable sectional areas are reduced by using dynamic MST which can be seen from the line colors of branch 26-40, 27-41, 54-41, 55-54, 52-53 by comparing Fig. 4 (a) and (b), the total cable cost is saved finally.

#### B. Case II: Extremely Irregular Wind Farm (OS near shore)

In this case, the cable connection layout design is expected to be done for an extremely irregular layout wind farm. The OS, denoted with a green square, is assumed to be constructed 20km away from the coast. There are totally 111, Vestas V90-2.0 MW (90m rotor diameter) WTs within this wind farm. The distance between WTs is 600m at the edge while inside the wind farm the distance between WTs is 900 to 1300m which is shown in Fig. 5.

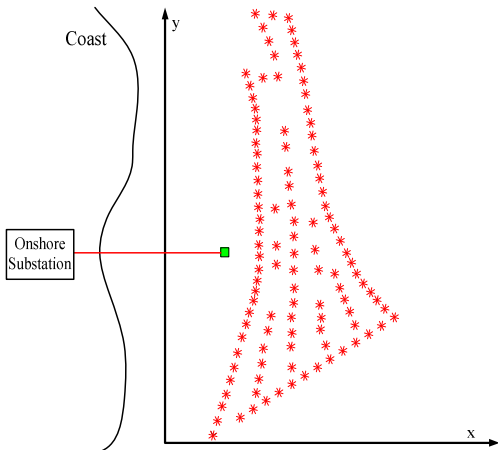
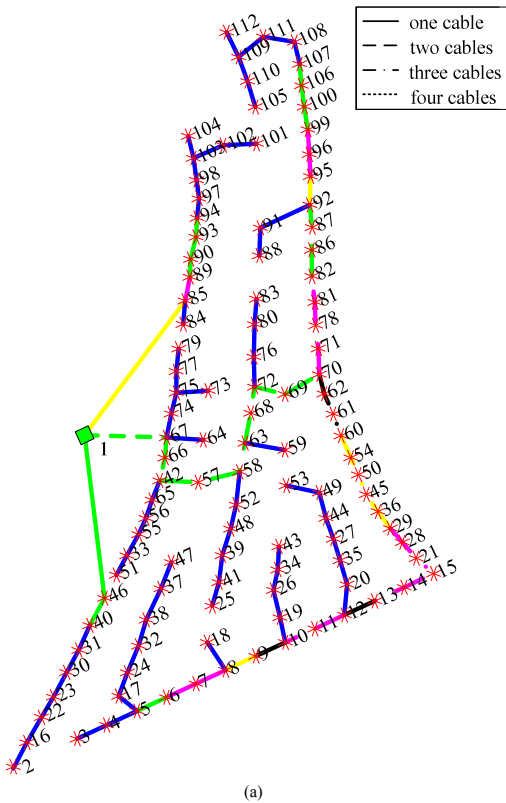
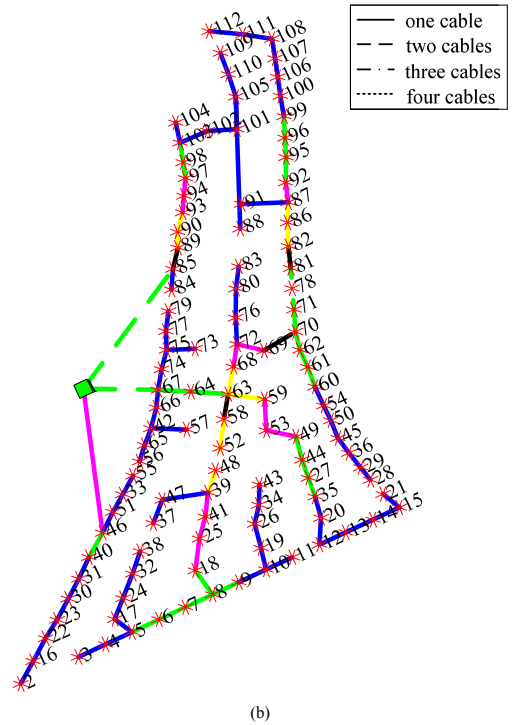


Fig. 5. Extremely irregular wind farm layout.



(a)



(b)

Fig. 6. The illustration of cable connection configuration for case II. (a) Optimized cable connection layout using MST. (b) Optimized cable connection layout using DMST.

As shown in Fig. 6, there are three feeders in each layout. By using different method to collect the power generated from WTs, the total cost will be different. The detailed information is listed in Table III.

TABLE III  
LAYOUT COMPARISONS FOR EXTREMELY IRREGULAR SHAPED WIND FARM

	MST	DMST
Cable invest (MDKK)	399.06	374.70
Total cable length for CS (km)	99.215	98.785
Trenching length for CS (km)	69.741	78.214

As can be seen in Table III, the optimized collection system layout obtained by DMST can save the investment of cables for 6.10% compared with MST. The MST method can find a layout with minimal trenching length which is 10.83% shorter than the layout found by DMST method, however, since the total cable length is longer and the adopted cables in some part are thicker in MST layout the total cost of cables is higher as a result. In reality, some factors which related to the trenching length as, cable installation cost, operation and maintenance cost, etc. should be considered to make the layout more practical so

that a comprehensive decision can be made in wind farm layout design phase.

## V. CONCLUSIONS

Traditional MST algorithm can be used to minimize the total connection distance for an offshore wind farm. However, due to the current carrying limitation, the cable costs would be changed if more WTs are connected to one string which always happens during the optimization of layout formulation process. The layout with minimal connection distance may not be the layout with minimal costs. This paper proposed a new method to find the optimized cable connection layout for offshore wind farm considering the dynamic changing cable costs during the optimization. The studied cases demonstrate that it is an effective way to minimize the collection system cost for irregular shape wind farm.

## ACKNOWLEDGEMENTS

Authors would like to thank Norwegian Centre for Offshore Wind Energy (NORCOWE) under grant 193821/S60 from Research Council of Norway (RCN).

## REFERENCES

- [1] Kalyan, "Global Wind Report," <http://www.gwec.net/>.
- [2] M. Zhao , Z. Chen and F. Blaabjerg "Optimization of electrical system for a large DC offshore wind farm by genetic algorithm", *Nordic Workshop on Power and Industrial Electronics 2004-037*, 2004.
- [3] F. M. Gonzalez-Longatt, P. Wall, P. Regulski, and V. Terzija, "Optimal electric network design for a large offshore wind farm based on a modified genetic algorithm approach," *IEEE Syst. J.*, vol. 6, no. 1, pp. 164-172, Mar. 2012.
- [4] D. D. Li, C. He, and Y. Fu, "Optimization of internal electric connection system of large offshore wind farm with hybrid genetic and immune algorithm," in *Proc. 3rd Int. Conf. Electr. Utility DRPT*, Apr. 2008, pp. 2476-2481.
- [5] Huang Ling-Ling, Chen Ning, Zhang Hongyue, Fu Yang, "Optimization of large-scale offshore wind farm electrical collection systems based on improved FCM," *International Conference on Sustainable Power Generation and Supply (SUPERGEN 2012)*, Hangzhou 8-9 Sept. 2012.
- [6] S. Dutta, T. J. Overbye, "Optimal Wind Farm Collector System Topology Design Considering Total Trenching Length," in *IEEE Trans. Sustainable Energy*, vol.3, no.3, pp.339-348, July 2012.S.
- [7] J. A. Bondy and U. S. R. Murty, "Graph theory with applications," the Macmillan Press Ltd., 1976.
- [8] S. Lundberg, "Performance comparison of wind park configurations," Department of Electric Power Engineering, Chalmers University of Technology, Department of Electric Power Engineering, Goteborg, Sweden, Tech. Rep. 30R, Aug. 2003.
- [9] F. M. Gonzalez-Longatt, P. Wall, P. Regulski, and V. Terzija, "Optimal electric network design for a large offshore wind farm based on a modified genetic algorithm approach," *IEEE Syst. J.*, vol. 6, no. 1, pp. 164-172, Mar. 2012.
- [10] R. A. Devore, V. N. Temlyakov, "Some remarks on greedy algorithm," *Adv. Comp. Math.*, 1996, pp. 173-187.
- [11] "XLPE Submarine Cable Systems Attachment to XLPE Land Cable Systems-User's Guide," ABB corporation.

# Optimization of Decommission Strategy for Offshore Wind Farms

Peng Hou, Weihao Hu, Mohsen Soltani, Baohua Zhang, Zhe Chen,

Department of Energy Technology  
Aalborg University

Pontoppidanstraede 101, Aalborg DK-9220, Denmark

[pho@et.aau.dk](mailto:pho@et.aau.dk), [whu@et.aau.dk](mailto:whu@et.aau.dk), [sms@et.aau.dk](mailto:sms@et.aau.dk), [bzh@et.aau.dk](mailto:bzh@et.aau.dk), [zch@et.aau.dk](mailto:zch@et.aau.dk)

**Abstract**— The life time of offshore wind farm is around 20 years. After that, the whole farm should be decommissioned which is also one of the main factors that contribute to the high investment. In order to make a cost-effective wind farm, a novel optimization method for decommission is addressed in this paper. Instead of abandoning the foundations after the wind farm is running out of its life cycle, the proposed method can make good use of the existing facilities so that the cost of energy (COE) can be reduced. The results show that 12.93% reduction of COE can be realized by using the proposed method.

**Index Terms**— offshore wind farm; optimization; decommission strategy, cost of energy (COE).

## Nomenclature

$V_0$ [m/s]	input wind speed at the wind turbine (WT)
$V_x$ [m/s]	wind speed in the wake at a distance $x$ downstream of the upstream WT
$R_0$ [m]	radius of the WT's rotor
$R_x$ [m]	generated wake radius at $x$ distance along the wind direction
$S_{overlap}$ [m <sup>2</sup> ]	affect wake region
$C_t$	thrust coefficient
$k_d$	decay constant
$V_n$ [m/s]	wind speed at the blade of downstream WT considering the impacts of several upstream WTs
$\rho$ [kg/m <sup>3</sup> ]	air density,
$C_{p,i}$	power coefficient of WT $i$
$P_{m,i}$ [MW]	mechanical power generated by WT $i$
$v_i$ [m/s]	wind speed at WT $i$
$P_{tot,i}$ [MW]	total power production during interval $t$
$T_E$ [day]	duration interval for energy yields calculation
$T_t$ [h]	duration when the wind farm generating power of $P_{tot,t}$
$E_{tot,av}$ [MWh]	mean energy yields in one year
$t$ [hour]	energy yields calculation time
$(x_i, y_i), (x_k, y_k)$	coordinate of WT $i$ and $k$
$E_{tot,av}(x_i, y_i)$ [MWh]	mean energy yields in one year when the WTs' positions are $(x_i, y_i)$

$A_p, B_p$	coefficient of WT cost model
$C_{WT}, C_f$	cost coefficient of WT and foundation
$x_{min}, y_{min}$	minimum boundary of wind farm
$x_{max}, y_{max}$	maximum boundary of wind farm
$d_{min}$	minimal distance between any pair of WT
$R$	index of constraint function
$N_{WT}, N_f$	total number of WTs and foundations
$C$	total number of penalty functions that should be used in the problem for unrestricted sea area
$\varphi(x_i, y_i)$	penalty function for WT $i$
$w$	inertia weight
$l_1, l_2$	learning factors
$r_1, r_2$	stochastic numbers which can generate some random numbers within [0, 1]
$q_i^k, q_i^{k+1}$ [m]	position of $i^{\text{th}}$ particle at iteration $k$ and $k+1$ respectively
$v_i^k, v_i^{k+1}$ [m]	speed of $i^{\text{th}}$ particle at iteration $k$ and $k+1$ respectively
$Q_i^k$ [m]	best position of $i^{\text{th}}$ particle at iteration $k$
$Q_g^k$ [m]	best position of all particles (the swarm) at iteration $k$
$Q_i$	best position found so far by the $i^{\text{th}}$ particle
$Q_g$	best position found so far by the swarm

## I. INTRODUCTION

Offshore wind farms have advantages of higher energy efficiency and less impact on residents compared with onshore wind farms, however, the investment is high. In order to make more profits, many works have been done on optimization of offshore wind farm layout.

Due to the impact of wake effect, the wind speed reached at the downstream WTs will be reduced which incurs the energy losses of whole wind farm. To optimize the wind farm layout, two models are widely used. The first model is grid model which partition the whole wind farm into numbers of grids and the WT positions are selected from the center of some of these grids [1]-[5]. The other is coordinate model which used Cartesian coordinate system to represent the position of each WT [6]-[11]. The initial work to minimize the wake losses by placing the WTs in an optimized way is done by Mosetti et al who used genetic algorithm (GA) to optimize the WT layout [1]. Later, the authors of [2] improve this method by considering the possibility of installing more WTs in the same

This work has been (partially) funded by Norwegian Centre for Offshore Wind Energy (NORCOWE) under grant 193821/S60 from Research Council of Norway (RCN). NORCOWE is a consortium with partners from industry and science, hosted by Christian Michelsen Research.

area. Many researches have been done on WT position optimization and the results were compared with the above two layouts [3]-[5]. The Monte Carlo algorithm was demonstrated to be outperformed by GA in solving this problem by assuming the wind direction is constant in [3] while [4] shows the advantages of using Intelligently Tuned Harmony Search algorithm for WT locating. In [5] a binary particle swarm optimization method with time-varying acceleration coefficients (BPSO-TVAC) is proposed and the obtained results are compared with other 5 meta-heuristic algorithms. The above methods were proved to be effective in increasing the power production, however, some possible solutions have already been neglected using grid model. The layout was expected to be further optimized by giving WTs more freedom to move within predefined area.

The first paper that used coordinate model to solve wind farm layout optimization problem (WFLOP) was addressed in [6]. Several WTs are optimized placed within a predefined circular shape wind farm. Similarly, [7] used colony optimization algorithm to solve the WFLOP and was demonstrated to be outperformed than [6]. A particle filtering approach was presented in [8] and the optimized layout was compared with the obtained layout in [6] and [7]. In addition to heuristic optimization, some attempts to use mathematical programming to solve WFLO problem were done in [9]-[11]. In [9], a random search (RS) algorithm was proposed which showed better performance by GA on computational time, moreover, the RS algorithm was also applied to design the Horns Rev I wind farm layout so that the energy yields can be increased. Also, Horns Rev I wind farm layout was selected as the benchmark and compared with the optimized layout obtained by sequential convex programming in [10]. Since the WFLOP is non-convex, global optimal solution cannot be guaranteed. In order to get an even near optimal solution, a mathematical programming method was adopted in [11] which used heuristic method to set an initial layout then used nonlinear mathematical programming techniques to get a local optimal solution.

As it is known, the life time of offshore wind farm is around 20 years [12]. After that, the WT cannot be used. The above works focused on maximizing the energy yields of wind farm without considering the decommission cost. In consideration of marine ecological environment and ensure the safety of navigation and other marine function, offshore wind farm should be decommissioned after stop production [13], however, the foundation of WT can still be used at that time. It is possible to use the existing foundations to establish a new wind farm so that the cost of decommission as well as the cost of installing new WTs can both be saved.

In this paper, a new decommission strategy is proposed which can reduce the cost of energy of the wind farm compared with the cost of establishing a new one. Instead of abandoning the foundations, new WTs can be installed on the original location. In consideration of the reduction of the foundation intensity after the wind farm life cycle, smaller WTs were selected to install on the original place. In order to have the same wind farm capacity, more WTs were elected on new locations and the locations were decided using adaptive PSO (APSO). A regular shape reference wind farm is chose as

the study case and the result show that the proposed method is an effective way to reduce the cost of energy.

The paper is organized as follows. In Section II, the wind farm models are proposed at first. Followed by which is the objective function. The methodology is discussed in Section III. The simulation results and analysis are presented in Section IV and Conclusions are given in Section V.

## I. MODELLING OF WIND FARM

In this section, the model of calculating energy yields considering wind speed deficit is introduced at first. Then the cost model and objective function are specified.

### A. Wake Model

In this paper, Jensen model is selected to estimate the wind speed deficit. The analytical equations for calculating the wake velocity are in the following [14].

$$V_x = V_0 - V_0 \left( I - \sqrt{I - C_t} \right) \left( \frac{R_0}{R_x} \right)^2 \left( \frac{S_{overlap}}{S_0} \right) \quad (1)$$

$$R_x = R_0 + k_d x \quad (2)$$

The decay constant,  $k_d$ , describes the feature of the wake expansion, the recommended value for offshore environment should be 0.04 [14].

The above equations described how to calculate the wind speed behind one WT. The interaction of WTs within whole wind farm could also be described based on Katic et al's 'sum of squares of velocity deficits' method. The analytical equation is as follow [15]:

$$V_n = V_0 \left[ I - \sqrt{\sum_{i=1}^N \left[ I - \left( \frac{V_i}{V_0} \right) \right]^2} \right] \quad (3)$$

The energy yields calculation considering variation of both wind velocity and wind direction has been done in a previous work. The detailed information can be seen in [16].

### B. Energy Production of Offshore Wind Farm

In [17], the power extracted by individual WT is given as:

$$P_{m,i} = 0.5 \rho C_{p,i} \pi R^2 v_i^3 / 10^6 \quad (4)$$

By assuming a maximum power point tracking (MPPT) control strategy [18], the power production of each WT can be found by (4). The velocity at each WT is related to the WTs' positions  $(x_i, y_i)$ . Hence, the total power production that generated by the WTs can be written as:

$$P_{tot} = \sum_{i=1}^N P_{m,i}(x_i, y_i) \quad (5)$$

Considering (1) to (5), the energy yields of the wind farm can be rewritten as:

$$E_{tot,av} = \frac{\sum_{t=1}^{T_E} (P_{tot,t}) T_t}{T_t T_E} 8760 \quad (6)$$



### C. Cost Model

In this paper, the cost of WT which includes a 33kV transformer is set up according to its rated power. The mathematical equations can be written as [19]:

$$C_{WT} = A_p + B_p P_{rated} \quad (7)$$

In this model, the cost of the WT is assumed to be increased linearly and the cost of foundation for each WT is 6.075 MDKK, which is assumed independent of water depth and size and type of WT [19].

### D. Objective Function

In this work, the performance of the new wind farm using existing foundations will be compared with the ordinary one based on the evaluation index, cost of energy (COE) as follow:

$$\text{Obj: } \min(\text{COE}) = \frac{E_{tot,av}}{C_{WT} N_{WT} + C_f N_f} \quad (8)$$

$$\text{Constraints: } x_{\min} \leq x_i \leq x_{\max}, i \in (1, N_{WT}) \quad (9)$$

$$y_{\min} \leq y_i \leq y_{\max}, i \in (1, N_{WT}) \quad (10)$$

$$F_r(x_i, y_i) = \sqrt{(x_i - x_k)^2 + (y_i - y_k)^2} - d_{\min} \geq 0, \forall i \neq k \quad (11)$$

## II. METHODOLOGY

Presently, heuristic algorithms are widely used in solving the non-linear problem. In this paper, APSO is selected as the optimization method. The theory and the optimization procedure are presented in the following.

### A. PSO

The PSO algorithm was firstly proposed by Kennedy and Eberhart [20] in 1995. As one of the evolutionary algorithms, it has a good performance of finding a near optimal solution for the nonlinear optimization problem. The global version PSO (GPSO) can be expressed in following equations [21].

$$v_i^{k+1} = wv_i^k + l_1 r_1 (Q_i^k - q_i^k) + l_2 r_2 (Q_g^k - q_i^k) \quad (12)$$

$$q_i^{k+1} = q_i^k + v_i^{k+1} \quad (13)$$

In PSO, the possible solutions (particles) will be coded into swarm and the size of swarm means the number of the particles, in other words, the number of possible solutions in a swarm is decided by the swarm size. As can be seen in (12), there are three parts. The first part represents the velocity of previous particle. A larger  $w$  ensures a stronger global searching ability while smaller  $w$  ensures the local searching ability. The other two parts are used to ensure the local convergence ability of the algorithm. Hence, the final result is sensitive to the setting of the control parameters ( $l_1$ ,  $l_2$  and  $w$ ). In order to reduce the sensitivity of final result to control parameters, many works have been done on the parameter control methods for  $w$  which can be concluded into two categories [22]: simple rule based parameter control [23]-[26] and adaptive parameter control strategy [27]. The first strategy indicate that the PSO performance can be improved by using linear, non-linear or fuzzy rule inertia weight while the other introduce evolutionary state estimation (ESE) technique [28]

to further improve the performance of PSO. In this project, the WT positions were decided using the method in [27].

### B. Penalty Function

The heuristic algorithm as PSO can be used to solve the unconstrained optimization problem within the predefined area. In this case, (9) and (10) can be satisfied by PSO, however, (11) can be violated if no specific condition are defined. Conversely, if the particle is limited to follow (11) then the particles might be out of predefined boundary. In order to ensure the feasibility of the solution and simplify the numerical calculation, a penalty function method is used and defined as follow:

$$\phi(x_i, y_i) = \left| \min \{0, F_r(x_i, y_i)\} \right| \quad (14)$$

Then, the objective function for unrestricted sea area wind farm layout optimization can be rewritten as:

$$\max(\text{COE} - \text{PF} \sum_{i=1}^C \phi(x_i, y_i)) \quad (15)$$

The penalty function (11) represents the distance between the infeasible solution and the feasible region.  $\phi(x_i, y_i) = 0$  means that all the WT's positions are found within the predefined area,  $F_r$  in other words, the solution is feasible, while  $\phi(x_i, y_i) > 0$  indicates that some WT's positions are out of construction area boundary. By using this method, (11) can be easily realized. The advantage of using penalty function is that the constrained optimization problem could be transformed into an unconstrained one so that the computational time can be reduced. In this paper, the penalty factor,  $PF$ , is determined as 1000. The value of this factor is selected by trial and error.

### C. Optimization Framework

The optimization framework is shown in Fig.1.

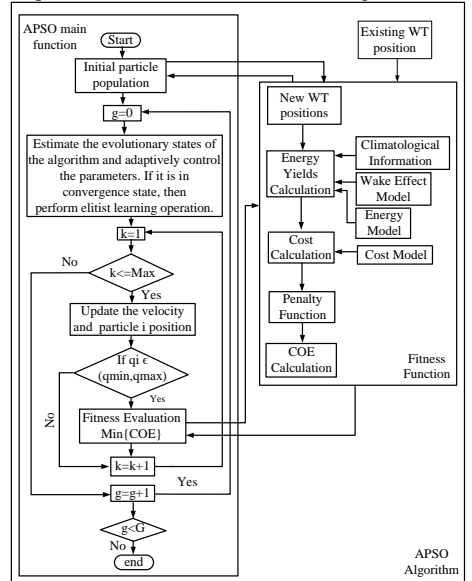


Figure. 1. Optimization flowchart based on APSO

The parameters of APSO are initialized in the first step. The existing WT and the new optimized WT positions will be integrated in Fitness Function and then the energy yields as well as the cost was calculated based on this wind farm layout. The penalty function will be used to ensure (11). After that, the COE will be calculated based on (4)-(8). The first calculated COEs as well as the corresponding particles (solutions) will be saved as the initial particle population which is the basis for comparison later. Then the particles will be updated and transferred into the fitness function by following the same procedure. The calculated result can be obtained and send out to the Fitness Function for comparison. Or it may stop if the maximum iteration is reached. Finally, a series of new installed WT positions will be decided.

Climatological information: The data is obtained from the work of the Norwegian Meteorological Institute [29], in which the wind speeds are sampled per 3 hours. For convenience of calculation, the raw data is formulated into a wind rose which is used to calculate the energy production over a year.

## II. CASE STUDY

The simulation is implemented on the platform of Matlab software. One study case was adopted to verify the feasibility of the proposed method.

### A. Scenario I: Rebuild on the Original Locations

The reference wind farm was established with 80, Vestas V80-2.0 MW (80m rotor diameter) [30] WTs which can be seen in Fig. 2. The total power capacity is 160MW. The locations of WTs are predefined within a 7D\*7D regular shaped wind farm which means that the distance between each two WTs are 7 rotor diameters.

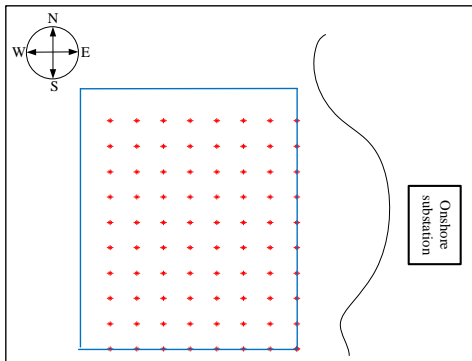


Figure 2. Reference wind farm layout

The red stars show the WT positions while the blue line is the boundary for installing new WTs to rebuild the wind farm. Monopile foundation was adopted since the average water depth is assumed to be 10m. Since the design of WT has been developed during the decades of wind farm operating period, the present 2MW WT which has a lower cut-in speed can generating more power when the incoming wind speed is lower compared with the old version WT. Hence, the wind farm was rebuilt using the original locations with 2MW Vestas V90-2.0MW WT [31]. Since the foundation has been used for more than 20 years, strengthen cost is required. It is assumed that the cost for strengthening foundation is 10% of the foundation cost.

### B. Scenario II: Decommission Optimization for Reference Wind Farm Wind Farm

In this work, the existing foundation will be used. For safety consideration, the Vestas V90-1.8MW WT [31] will be installed on the original place instead of 2MW WT. In order to have the same power capacity as original one has. 9 WTs will be installed and the new installed WT positions will be optimized considering the wake effect using APSO. Since smaller WTs are adopted in this case. The cost of strengthening foundation is assumed to be only 5%. The optimized layout is shown in Fig. 3.

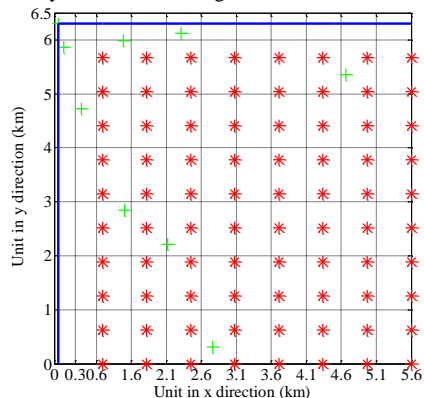


Figure 3. Optimized wind farm layout

In Fig. 3, the red stars showed the original WT which has been replaced using 1.8 MW WTs while green plus indicated the nine new installed WT positions. The optimized WT positions are found by APSO and the fitness value corresponds to each iteration is illustrated in Fig. 4.

TABLE I. RESULTS COMPARISON

	Benchmark	Scenario I	Scenario II
Costs of WTs (MDKK)	991.44	991.44	982.15
Costs of renovation/bulid foundations (MDKK)	486	48.6	79.0
Total cost (MDKK)	1477.4	1040.04	1061.2
Energy yields (GWh)	764.90	764.90	806.32
CoE (DKK/MWh)	1931.0	1359.7	1316.1

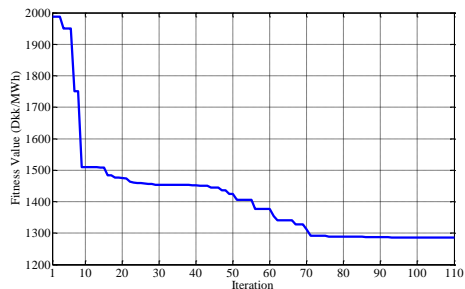


Figure 4. Fitness Value corresponds to each iteration

In Fig. 4, the fitness value was stabilized around 810 after 90<sup>th</sup> iteration using APSO algorithm. In Table I, the

benchmark is the common way of decommissioning which rebuild all the foundations on original place. It can be seen that the total cost of scenario II is decreased by 33.32% compared with benchmark while the cost will be increased by 2.03% compared with scenario I, however, by installing 9 more WTs with optimized locations, the total energy yields can be increased by 5.42% compared with benchmark. The COE is reduced by 31.84% and 29.59% by scenario II and I respectively compared with benchmark.

### III. CONCLUSIONS AND FUTURE WORK

The offshore wind farm will be decommissioned in order to protect marine ecological environment after approximately 20 years' operation. This is mainly due to the fact that the WT cannot be used after this period. However, the foundation is always oversized. In order to make best use of the foundation and save the investment, a new decommission strategy is proposed in this paper. Instead of paying for abandoning the foundations, a new wind farm can be established using the original foundations. From simulation results, it can be seen that the decommission strategy can help reduce the cost of energy a lot (36.74% in the study case) and by merely installing 9 more WTs, the energy yields of whole wind farm can be significantly increased by 5.42%. The potential value of this method will not merely on foundations since the life time of parts of the WTs, such as tower body can also be longer than 20 years. The recycling idea in offshore wind farm proposed in this paper could show more commercial benefits in future.

### ACKNOWLEDGMENT

Authors would like to thank Norwegian Centre for Offshore Wind Energy (NORCOWE) under grant 193821/S60 from Research Council of Norway (RCN).

### REFERENCES

- [1] Moseiti G, Poloni C, Diviaco B., "Optimization of wind turbine positioning in large wind farms by means of a genetic algorithm," *Journal of Wind Engineering and Industrial Aerodynamics*. vol. 51(1), pp.105-116, 1994.
- [2] S. Grady, M. Hussaini, and M. Abdullah, "Placement of wind turbines using genetic algorithms," *Renewable Energy*, vol. 30, no. 2, pp. 259 – 270, 2005.
- [3] G. Marmidis, S. Lazarou, E. Pyrgioti, "Optimal placement of wind turbines in a wind park using Monte Carlo simulation," *Renewable Energy*, 33 (7) (2008), pp. 1455–1460.
- [4] Narasimha Prasad Prabh, Parikshit Yadav, Bhuneshwar Prasad and Sanjib Kumar Panda, "Optimal placement of off-shore wind turbines and subsequent micro-siting using Intelligently Tuned Harmony Search algorithm," *Power and Energy Society General Meeting (PES)*, 2013 IEEE, pp. 1-7, Vancouver, BC, Jul. 2013.
- [5] Sittichoke Pookpant, Weerakorn Ongsakul, "Optimal placement of wind turbines within wind farm using binary particle swarm optimization with time-varying acceleration coefficients," *Renewable Energy*, Vol. 55, pp. 266-276, Jul. 2013.
- [6] B Saavedra-Moreno, S Salcedo-Sanz, A Paniagua-Tineo, L Prieto, A. Portilla-Figuera, "Seeding evolutionary algorithms with heuristics for optimal wind turbines positioning in wind farms," *Renewable Energy*, vol. 36, pp. 2838–2844, 2011.
- [7] S. Chowdhury, J. Zhang, A. Messa, L. Castillo, "Optimizing the arrangement and the selection of turbines for wind farms subject to varying wind conditions," *Renew Energy*, vol. 52, pp. 273–282, 2013.
- [8] C.Wan, J.Wang, G. Yang, H. Gu, and X. Zhang, "Wind farm micro-siting by Gaussian particle swarm optimization with local search strategy," *Renewable Energy*, vol. 48, pp. 276–286, 2012.

- [9] Feng, J.; Shen, W.Z., "Solving the wind farm layout optimization problem using random search algorithm," *Renewable Energy*, vol. 78, pp. 182–192, Jun. 2015.
- [10] Jinkyoo Park, Kincho H. Law, "Layout optimization for maximizing wind farm power production using sequential convex programming," *Renewable Energy*, vol. 151, pp. 182–192, Aug. 2015.
- [11] B. Pérez, R. Mínguez, R. Guanche, "Offshore wind farm layout optimization using mathematical programming techniques," *Renew Energy*, vol. 53, pp. 389–399, 2013.
- [12] M. Zhao, Z. Chen, J. Hjerrild, "Analysis of the behaviour of genetic algorithm applied in optimization of electrical system design for offshore wind farms," *Proc. Of the 32nd IEEE Conference on Industrial Electronics*, pp. 2335–2340, 2006.
- [13] Fei Wu, Xu Jia, Jiali Sun, Chunjie Yu, Hongsheng Ci, "Offshore oil and gas platform decommissioning research," *OCEANS 2014*, Taipei, pp. 1-4.
- [14] P. Beaucage, M. Brower, N. Robinson, and C. Alonge, "Overview of six commercial and research wake models for large offshore wind farms," in *Proc. Eur. Wind Energy Assoc. (EWEA'12)*, Copenhagen, Denmark, 2012, pp. 95–99.
- [15] Fernando Port'e-Agel, Yu-TingWu, Chang-Hung Chen, "A Numerical Study of the Effects of Wind Direction on Turbine Wakes and Power Losses in a large Wind Farm," *Energies*, vol. 6, pp. 5297-5313, MDPI, 2013.
- [16] Peng Hou, Weihao Hu, Soltani, Mohsen, Zhe Chen, "Optimized Placement of Wind Turbines in Large Scale Offshore Wind Farm using Particle Swarm Optimization Algorithm," *IEEE Transactions on Sustainable Energy*, Vol. PP, Nr. 99, 2015.
- [17] Javier Serrano González, Angel G. Gonzalez Rodriguez, José Castro Morac, Jesús Riquelme Santosa, Manuel Burgos Payana, "Optimum Wind Turbines Operation for Minimizing Wake Effect Losses in Offshore Wind Farms," *Renewable Energy*, Vol. 35, Issue 8, pp. 1671-1681, Aug. 2010.
- [18] Wei Qiao, "Intelligent mechanical sensorless MPPT control for wind energy systems," *Power and Energy Society General Meeting*, 2012 IEEE, pp. 1-8, San Diego, CA, Jul. 2012.
- [19] S. Lundberg, "Performance comparison of wind park configurations," *Department of Electric Power Engineering, Chalmers University of Technology, Department of Electric Power Engineering, Goteborg, Sweden*, Tech. Rep. 30R, Aug. 2003.
- [20] Kennedy, J., Eberhart, R., "Particle swarm optimization," *Proc. IEEE Int. Conf. Neural Networks*, pp. 1942–1948, Apr. 1995.
- [21] Kennedy, J., "The particle swarm: social adaptation of knowledge," *Proc. IEEE Int. Conf. Evolution of Computing*, Indianapolis, IN, pp. 303–308, 1997.
- [22] Mengqi Hu, Wu, T., Weir, J.D., "An adaptive particle swarm optimization with multiple adaptive methods," *IEEE Transactions on Evolutionary Computation*, Vol. 17, pp. 705-720, 10 Dec. 2012.
- [23] Y. Shi and R. C. Eberhart, "Empirical study of particle swarm optimization," in *Proc. Congr. Evol. Comput.*, 1999, pp. 1950–1955.
- [24] B. Jiao, Z. Lian, and X. Gu, "A dynamic inertia weight particle swarm optimization algorithm," *Chaos, Solitons Fractals*, vol. 37, pp. 698–705, Aug. 2008.
- [25] Y. Shi and R. C. Eberhart, "Fuzzy adaptive particle swarm optimization," in *Proc. Congr. Evol. Comput.*, 2001, pp. 101–106.
- [26] R. C. Eberhart and Y. Shi, "Tracking and optimizing dynamic systems with particle swarms," in *Proc. Congr. Evol. Comput.*, 2001, pp. 94–100.
- [27] Z.-H. Zhan, J. Zhang, Y. Li, and H. S.-H. Chung, "Adaptive particle swarm optimization," *IEEE Trans. Syst., Man, Cybern. B, Cybern.*, vol. 39, no. 6, pp. 1362–1381, Apr. 2009.
- [28] J. Zhang, H. S.-H. Chung, and W.-L. Lo, "Clustering-based adaptive crossover and mutation probabilities for genetic algorithms," *IEEE Trans. Evol. Comput.*, vol. 11, no. 3, pp. 326–335, Jun. 2007.
- [29] Birgitte R. Furevik and Hilde Haakenstad, "Near-surface marine wind profiles from rawinsonde and NORA10 hindcast," *Journal of Geophysical Research*, Vol. 117, 7 Dec. 2012.
- [30] "Never Installed Turbine-technical brochure," *Blue Planet Wind NV, Sint Aldegondiskaai 18, 2000 Antwerpen, Belgium*.
- [31] "V90-1.8/2.0 MW Maximum output at medium-wind and low-wind sites," *Vestas Wind Systems A/S, Alsvej 21, 8940 Randers SV, Denmark*.

# Improving the Next Generation of Offshore Wind Energy Investments: Offshore Wind Farm Repowering Optimization

Peng Hou<sup>\*^</sup>, Peter Enevoldsen<sup>⌘</sup>, Weihao Hu<sup>^</sup>, Zhe Chen<sup>^</sup>

<sup>^</sup>Department of Energy Technology, Aalborg University

<sup>⌘</sup>Center for Energy Technologies, BTECH Aarhus University

**\*Corresponding Author:** Department of Energy Technology, Aalborg University, Pontoppidanstræde  
111, 9220, Aalborg, Denmark  
Email: [pho@et.aau.dk](mailto:pho@et.aau.dk) Tel: +4552704312

**ABSTRACT:** The offshore wind farm decommissioning is usually the last stage of the offshore wind farm life cycle. Due to the challenges in the decommissioning process, such as impact on marine environment, severe weather conditions, vessel limitations and lack of operational experience, the decommissioning strategy should be planned initially to avoid such complications, which ultimately can cause radical changes to the levelized cost of energy and the wind farm owner's business case. Despite these challenges, less attention has been paid to the decommissioning compared with the efforts that have been made in launching a new wind farm project. In this paper, the research is focused on optimization of offshore wind farm repowering which is one of the choices of wind farm owner when the offshore wind farm comes to its life time end. The net present value (NPV) is selected as the evaluation index to identify whether it is economical to invest in such way. From the simulations performed in this research, it is revealed that the reconstructed wind farm, which is composed by multiple types of wind turbines has a higher NPV (139.1%) compared to the ordinary replacing approach, which shows the advantage of the proposed method. This research is hereby contributing with an optimization tool to the wind industry, which consequently drives down the cost of energy produced by offshore wind turbines.

**Key Words:** Offshore Wind Power, Decommissioning, Optimization, Repowering

## 1. INTRODUCTION:

The history of offshore wind power can be traced back to 1991 when the first offshore wind farm, Vindeby, was installed in Denmark [1]. Compared with onshore wind farms, it is still a novel energy technology and thus more attentions have been paid on the increasing energy production efficiency or improving installation technology while wind farm owners seem to be oblivious to the significance of the decommissioning [2]. Also, most of the present research has concentrated on the development, construction, and operational stages of offshore wind farms [3]. However, considering the increasing demand for the decommissioning in the near future, the decommissioning should be studied and planned at the very beginning of the project to prevent the complications which would incur the unexpected higher costs and environmental impacts [4].

Decommissioning is considered to be the last step of the project. According to [5], decommissioning can be defined as the reverse of the installation phase, the objective of decommissioning is to return the site to the condition before the project deployment as far as possible. The first offshore wind farm decommissioning in record (Yttre Stengrud wind project) happened in 2016 [7]. This project was only operated for 15 years [6]. However, due to the difficulty in finding the spare parts and huge cost of repairs and upgrades, the wind farm owner decided to dismantle it [7]. Recently, several decommissioning plans were also announced as Vindeby, and Lely. In addition, it is expected that the number of offshore wind farm decommissioning will surge in the next decade since many offshore projects commercialized in the early 2000s. The information in Table 1 shows the operating offshore wind farms that have been in commission for more than 10 years, including the installed capacity for each wind farm (MW).

**Table 1 Offshore Projects with more than 10 years of operation [8]**

<b>Project Name</b>	<b>Country</b>	<b>Wind Farm Size</b>	<b>Wind Turbines</b>
Arklow Bank 1	Ireland	25.2 MW	7
Barrow	United Kingdom	90 MW	30
Blyth	United Kingdom	4 MW	2
Bockstigen	Sweden	2.5 MW	5
Breitling Demonstration	Germany	2.5 MW	1
Ems Emden	Germany	4.5 MW	1
Frederikshavn	Denmark	7.6 MW	3
Horns Rev 1	Denmark	160 MW	80
Irene Vorrink	Netherlands	16.8 MW	28
Kentish Flats 1	United Kingdom	90 MW	30
Lely	Netherlands	2 MW	4
Middelgrunden	Denmark	40 MW	20
North Hoyle	United Kingdom	60 MW	30
Nysted 1	Denmark	165.6 MW	72
Ronland	Denmark	17.2 MW	8
Sakata	Japan	16 MW	8
Samso	Denmark	23 MW	10
Scroby Sands	United Kingdom	60 MW	30
Setana	Japan	1.32 MW	2
Tuno Knob	Denmark	5 MW	10
Utgrunden 1	Sweden	10.5 MW	7
Vindeby	Denmark	4.95 MW	11
Yttre Stengrund	Sweden	10 MW	5

50 From table 1, it can easily be derived that the decommissioning era is coming, and even with great variety  
51 in the number of wind turbines and capacity for each wind farm. Taken into account the difference in the  
52 foundation type, weather conditions, seabed conditions, etc. of each site, the decommissioning scheme are  
53 expected to be exclusive and unique for each wind farm. In other words, it seems impossible to enact a  
54 general method for offshore wind farm decommissioning [4]. In order to reduce the impacts of the  
55 offshore wind farm on the local marine environment, the wind farm developer should follow the legal  
56 obligation, as UNCLOS (United Nations Convention on the Law of the Sea) [9], Energy Act [10], and  
57 Coast Protection Act [11]. All the obligations emphasize on the responsibility of the wind farm owner to  
58 make a complete dismantling which including removing the foundation and cables (sometimes cable can  
59 be left in situ) to minimize the project's impacts on the marine ecosystem, despite findings from the oil  
60 and gas industry revealing that keeping concrete foundations would harm the ecosystem less than  
61 removing it [12]. As a reaction to the environmental impact of constructing and dismantling offshore  
62 wind turbines, research have been conducted on the increased environmental cost for decommissioning  
63 of offshore wind turbines, when compared to the onshore counterpart [13][14]. Further studies have even  
64 included strategies for decommissioning of foundations and cables, in order to limit the impact on the  
65 local marine life [15]. As an example, Northern America is expected to become a large offshore wind  
66 market, and a study is already estimating decommissioning costs and proposing strategies, which ensures  
67 the decommissioning of wind turbines, foundations, and cables [16].

68 The offshore wind farm usually has a life time of 20 years, after that, the wind farm owner has to make a  
69 decision on how to decommission the wind farm, yet some wind turbines have been in operation for more  
70 than 25-30 years [17]. In the above statement, the decommissioning is defined as the process of  
71 dismantling entire wind farm including the cutting off the foundation, removal of the wind turbine and  
72 cables, etc. However, the some components within the wind farm usually have a longer life time. For  
73 instance, the life time of the foundations can be lasted over 100 years (for gravity based foundations) [18],

74 the internal array and transmission cables could be operated for more than 40 years [19]. Based on this,  
75 some wind farm decided to repower the offshore wind farm which use the majority of the original  
76 electrical system (or foundations) to installing bigger wind turbines so that the capital cost of the new  
77 project can be reduced. Presently, there are two repowering strategies that are available as partial  
78 repowering (refurbishment) or full repowering [4]. The partial repowering is considered to be the process  
79 of installing minor components within the wind farm as rotors, blades, gearboxes, etc. while full  
80 repowering indicates replacing the old turbines with newer, bigger ones to obtain higher energy  
81 efficiency. The repowering is regarded one end-of-life decision for offshore wind farm in [2]-[4], [9],  
82 [15], [18]-[21], it has the sustainable characteristic and there is also a potential value to recycle or reuse  
83 the dismantled spares. However, the profitability of the repowering option was not demonstrated until the  
84 work of [22]. In [22], the analysis of profitability regarding the full and partial repowering was done using  
85 evaluation index net present value (NPV). It can be concluded that the full repowering will be lucrative  
86 until 20-25 years of operation. Before this time, the impacts of repowering become inconspicuous.  
87 Moreover, partial repowering shows only about 10% cost savings compared with full repowering which  
88 indicates that it is not a preferable choice unless advanced technology can be applied to promote the  
89 generation efficiency or minimize operating costs. Nevertheless, not all wind turbines will be  
90 decommissioned at the exact same time as [22] assumed. The replacement of merely one wind turbine  
91 within a wind farm will cause changes in the wind conditions observed for the other wind turbines, due to  
92 changes in wakes. It can therefore be considered, which wind turbine to remove first, in order to  
93 maximize the energy output of the remaining wind turbines. Also, the full repowering option can  
94 introduce a smaller or bigger wind turbine and the present research concentrated on whether a bigger  
95 foundation should be used which will bring in extra investment. However, the bigger wind turbine would  
96 have a different hub height and blade diameter compared with original one. The wake losses in such a  
97 mixed hub height wind farm should be estimated so that the profitability of the repowering decision can  
98 be well analyzed.

99 Having finalized the initial literature review, an additional search was applied for decommissioning and  
100 recycling strategies for other offshore structures for inspiration. Several studies have been conducted on  
101 the decommissioning of oil and gas rigs with a special focus on avoiding damage on the local marine  
102 environment [23][24]. However, since oil and gas is a limited energy source, the recycling part, and  
103 potential optimization of such has not been touched upon in these studies. One lesson learned is however  
104 the fact, that least damage is done to marine environment by keeping the concrete structures under sea  
105 [12], instead of removing them, which only strengthens the proposition of this research paper.

106 The contribution of this research can be summarized as follows:

- 107 1. The repowering option for offshore wind farm was formulated as a non-convex optimization  
108 problem in this research. To our knowledge, this is the first paper which quantitatively analyzes  
109 the profitability of the repowering strategy.
- 110 2. The traditional repowering option is replacing the all existing wind turbine with bigger or smaller  
111 WT while the wind farm with mixed type of wind turbines is considered as one solution in this  
112 paper to increase the efficiency of the previous wind farm
- 113 3. Mathematical derivations for wake losses estimation with mix hub height wind turbines' wind  
114 farm is given for the proposed optimized repowering method which can help the wind farm owner  
115 to create their own decommissioning strategy quantitatively.

116 Besides the above presented targets, which are benefitting the industrial stakeholders in the wind industry,  
117 this research also aims at informing researchers and academia about a novel approach of combining  
118 optimization algorithms with offshore wind farm decommissioning.

119

## 120 **2. Problem Formulation**

121 In this section, the energy production estimation using wake model and energy model is firstly  
122 introduced. After that, the objective function is presented. The assumptions are made at last.

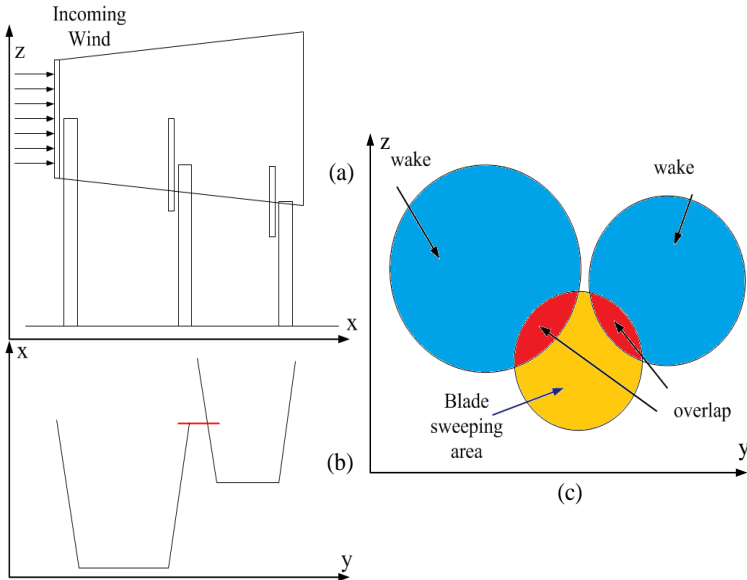
123 **2.1 Wake Model**

124 When the height is above 1 km, atmosphere is hardly influenced by the friction against the ground.  
 125 However, in the lower layers, wind speed increases as the height of air goes up. This is called wind shear  
 126 effect [25]. So if the height of some wind turbines (WT) is different, this effect should be also  
 127 incorporated. Then, the wind speed can be rewritten as:

$$V_{0,ij} = V_{ref} \frac{\ln\left(\frac{z_{ij}}{h_0}\right)}{\ln\left(\frac{z_{ref}}{z_0}\right)} \quad (1)$$

129 In order to estimate the wake losses generated within a wind farm with different types of WTs. The wake  
 130 overlapped should be calculated which is illustrated in figure 2 with a simple example.  
 131

132 **Figure 1 A simple of wake overlapped phenomenon in wind farm with mixed types of wind turbines.**



133  
 134  
 135 As can be seen in figure 2, three WTs with different hub height are shown in a simplified way with x-y, x-  
 136 z and y-z coordinate respectively. The core part for wake losses estimation is to calculate the affected  
 137 wake area which is illustrated with red color in figure 2. (c). The wind speed reached at the blade of a  
 138 wind turbine within the wind farm will be reduced by the wake generated from several wind turbines'.  
 139 The evaluation process of the wake effects of corresponding wind turbines would be a complex process.  
 140 In order to simplify the calculation, a binary matrix calculation method was proposed in [26]. Then, the  
 141 wind speed deficit calculation method for offshore wind farm with mix hub height wind turbines can be  
 142 obtained as follow:

$$V_{nm}(\alpha, V_{0,ij}) = V_{0,ij} \left[ 1 - \sqrt{\sum_{i=1}^n \sum_{j=1}^m \left[ 1 - Ma(i, j) \cdot \left( \frac{V_{ij}}{V_{0,ij}} \right) \left( \frac{S_{ol,ij}}{S_0} \right)^2 \right]} \right] \quad (2)$$

## 144 2.2 Energy Model

145 When the WTs are installed, the wind farm can be operated by a certain control strategy. In this work, the  
146 maximum power point tracking (MPPT) control strategy [27] is assumed so that power extracted by  
147 individual WT can be written as [28]:

$$148 P_{e, nm} = 0.5 \rho C_{p, nm} \pi R^2 v_{nm}^3 / 10^6 \quad (3)$$

149 In this paper, the wind farm power production output will be determined by the selected WT type in each  
150 given location. Then, the total power production of wind farm can be written as:

$$151 P_{tot} = \sum_{i=1}^N P_{e, nm} \quad (4)$$

152 Considering (1) to (4), the energy yields of the wind farm can be rewritten as:

$$153 E_{tot, av} = \frac{\sum_{t=1}^{T_E} (P_{tot, t}) T_t}{T_t T_E} 8760 \quad (5)$$

## 154 2.3 Cost Model

155 In this paper, the cost of WT which includes a 33kV transformer and foundation cost are both set up  
156 according to their rated powers respectively. The mathematical equations can be written as:

$$157 C_{WT} = A_{WT} P_{rated} \quad (6)$$

$$158 C_f = A_f P_{rated} \quad (7)$$

159 In this model, the cost of the WT is assumed to be increased linearly and the cost of foundation for each  
160 WT is 6.075 MDKK/MW, which is assumed independent of water depth and size and type of WT based  
161 on [29].

## 162 3. Methodology

164 This section introduces the methods and materials applied in the examination and optimization of a  
165 strategy for repowering offshore wind farm.

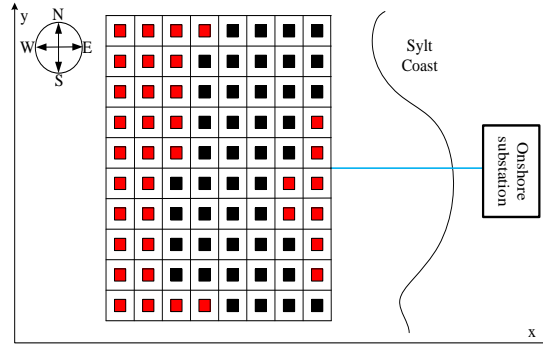
### 166 3.1 Wind Farm Repowering Optimization Realization

167 As introduced, the offshore wind farm will be in operation for approximately 20 to 25 years. After that,  
168 the wind farm owner should consider the decision of dismantling or repowering. In order to make best use  
169 of the existing facilities, repowering seems to be a better choice. However, the condition in each wind  
170 farm is different (wind condition, original wind turbine type, wind turbine distribution layout, etc). A  
171 method is required to evaluate the profitability of repowering strategy. Thus, an optimized repowering  
172 strategy is proposed in this paper to help the wind farm owner make the decision. The concept can be  
173 explained with the following simple example as shown in figure 3.

174



Figure 2 The optimization framework of proposed method.

176  
177

178 As illustrated in figure 3, the squares represent the WTs. It can be imagined that not all WTs “broken” at  
 179 the same time. In this work, it is assumed that the old WTs will be dismantled in several generations. Like  
 180 shown in figure 2, the WTs marked with red are assumed to be decommissioned (dismantle these WTs) or  
 181 repowered (replaced by new WTs) after 20 years’ operation which is the 1<sup>st</sup> decommissioning generation.  
 182 Several types of WTs can be selected to replace the original WTs presented in this research. Different  
 183 selection of WTs corresponds to different cost on foundation. If the original WT, the Vestas V80-2.0  
 184 MW, is selected, then no further costs for foundations would be spent, while implementation of bigger  
 185 WTs installation equals a higher cost of both WT, as well as foundation. Also, it is possible not to install  
 186 new WTs in some location to save the cost. This condition has been expressed with (8). After the 1<sup>st</sup>  
 187 decommissioning generation completed, the left old WTs may need to be operated together with the new  
 188 WTs which is expected to improve the production efficiency. In this research, it is also assumed that 4  
 189 years’ after the 1<sup>st</sup> decommissioning generation, the WTs that represents by black squares are required to  
 190 be replaced as well. Since a few locations exist where no new WTs were installed in the first  
 191 decommissioning generation, the optimization process of this time will involve not only the WTs  
 192 selection for the present locations but also the locations where no WTs are installed in the first  
 193 decommissioning generation. Finally, a new wind farm with mixed types of WTs may be constructed.  
 194 To sum up, repowering using bigger WTs will result in a wind farm with a higher energy production.  
 195 However, more investment should be spent, as larger wind turbines are more expensive. The optimized  
 196 repowering strategy proposed in this paper is expected to help find this tradeoff by maximizing the *NPV*  
 197 for offshore energy.

### 198 3.2 Optimization Setup

199 The research strategy applied in this paper focuses on the swarm based optimization method for  
 200 optimizing the repowering strategy of offshore wind farm. This methodology is specified in the  
 201 following.

#### 202 3.2.1 Particle Swarm Optimization (PSO)

203 For a non-convex problem, evolutionary algorithms as genetic algorithm (GA) and PSO should be a good  
 204 choice, with a good chance of finding the optimal solution for the nonlinear optimization problem.  
 205 Considering the outstanding performance of PSO in computational efficiency [30], it was selected to  
 206 implement the simulation. The integer PSO (IPSO) can be expressed mathematically as follows [31]:

$$207 \quad v_i^{k+1} = wv_i^k + l_1 r_1 (local_i^k - x_i^k) + l_2 r_2 (global^k - x_i^k) \quad (8)$$

$$208 \quad x_i^{k+1} = \text{int}(x_i^k + v_i^{k+1}) \quad (9)$$

209 The setting of parameters in PSO is critical to the final solution, since a larger inertia weight,  $w$ , ensures a  
 210 stronger global searching ability, which increases the chance of finding a better solution in global region,  
 211 while smaller  $w$  ensures local searching ability. In order to conquer this drawback, it is vital to examine  
 212 parameter control methods for  $w$ : as time varying control strategies [32][33] or adaptive parameter control  
 213 strategy [34]. Recently, a PSO with multiple adaptive methods (PSO-MAM) was proposed [35] and was  
 214 demonstrated to be outperformed by the existing common evolutionary algorithms in finding a better  
 215 solution. However, this method is valid for solving continuous optimization problem. Hence, the adaptive  
 216 PSO algorithm (APSO) [34] is selected instead to find the solution in this paper.

### 217 3.2.2 Penalty Function

218 Due to the wake turbulence, the lifetime of the WT will be significantly reduced if the distance between a  
 219 pair of WT is smaller than four rotor diameters (4D), due to increased loads on the wind turbine  
 220 components [37]. This condition can be expressed as follow:

$$221 \quad Dis_q(L_i) = \sqrt{(Wx_i - Wx_k)^2 + (Wy_i - Wy_k)^2} - \left( \frac{d_{min,k} + d_{min,i}}{2} \right) \geq 0, \forall i \neq k \quad (10)$$

222 Where  $q \in [1, 2 \dots C]$ ,  $i, k \in [1, 2 \dots N]$  and  $C$  is the total number of constraints which is equal to  $N(N-1)/2$ .  
 223  $L_i$  represents the wind turbine position which is  $(Wx_i, Wy_i)$ . Since different type of WT with different  
 224 rotor diameter has considered in this work, the minimal distance between each pair of WT is defined as  
 225 the average 4D of two calculated WTs as the last term in (10). Then the feasibility of the selected WTs will  
 226 be judged by the equation as follow:

$$227 \quad \phi_q = \left| \min \{ 0, Dis_q \} \right| \quad (11)$$

228  
229

### 230 3.2.3 Objective Function

231 Equation (11) shows that if the spacing between each pair of WTs is above the limit, then no penalty will  
 232 be applied, and vice versa. Combining (1) to (7), (10) and (11), the objective function for this problem can  
 233 be written as:

$$234 \quad \text{Obj.} \quad \min \left( \frac{\sum_{m=1}^M \sum_{i=1}^{N_{WT,m}} \max \left[ 0, (C_{f,m}(x_i) - C_{f,o}) \right] + C_{WT,m}(x_i)}{(1+r)^{N_m}} \right) \quad (12)$$

$$235 \quad \text{Constraint:} \quad \sum_{n=1}^N \frac{E_{tot,av,n}(X) - PF \sum_{q=1}^C \phi(L_i)}{(1+r)^n} \quad (13)$$

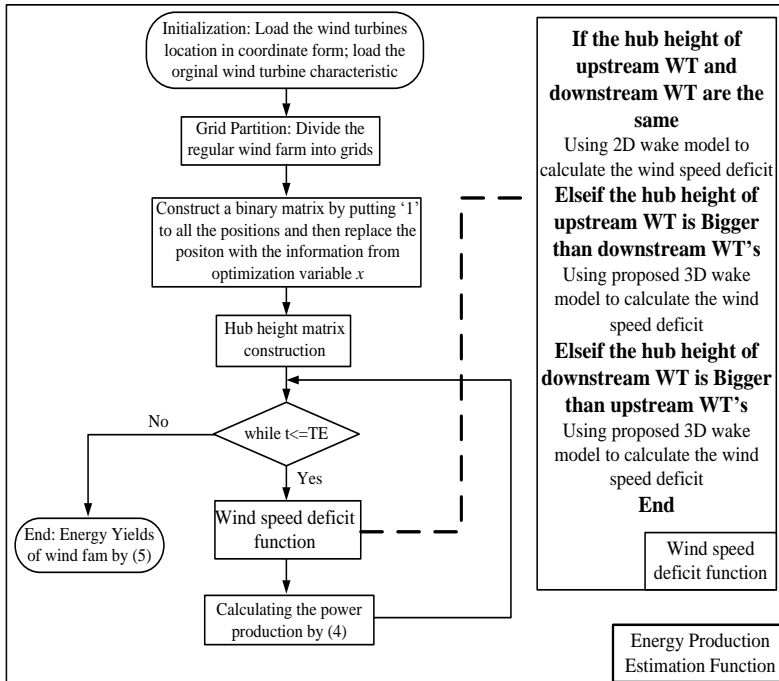
236 Where,  $X$  is the set of  $x_i$  ( $i=1,2,\dots,N_{WT}$ ).

237 In this work, if a bigger WT is installed in the original place, a cost should be included which represents  
 238 the cost of strengthening the foundation as expressed by  $C_{f,N_m}(x_i) - C_{f,o}$ . The constraint (13) shows that  
 239 there are eight options to choose in each original WT position (0 means no WT is installed in that  
 240 position).

### 241 3.2.4 Optimization Framework

242 In this research, the NPV is set up as the evaluation value so that an optimized repowering strategy can be  
 243 determined. The energy production of this wind farm with mixed types of WTs is calculated using the  
 244 model proposed in [26]. The energy production flowchart is shown in figure 4.

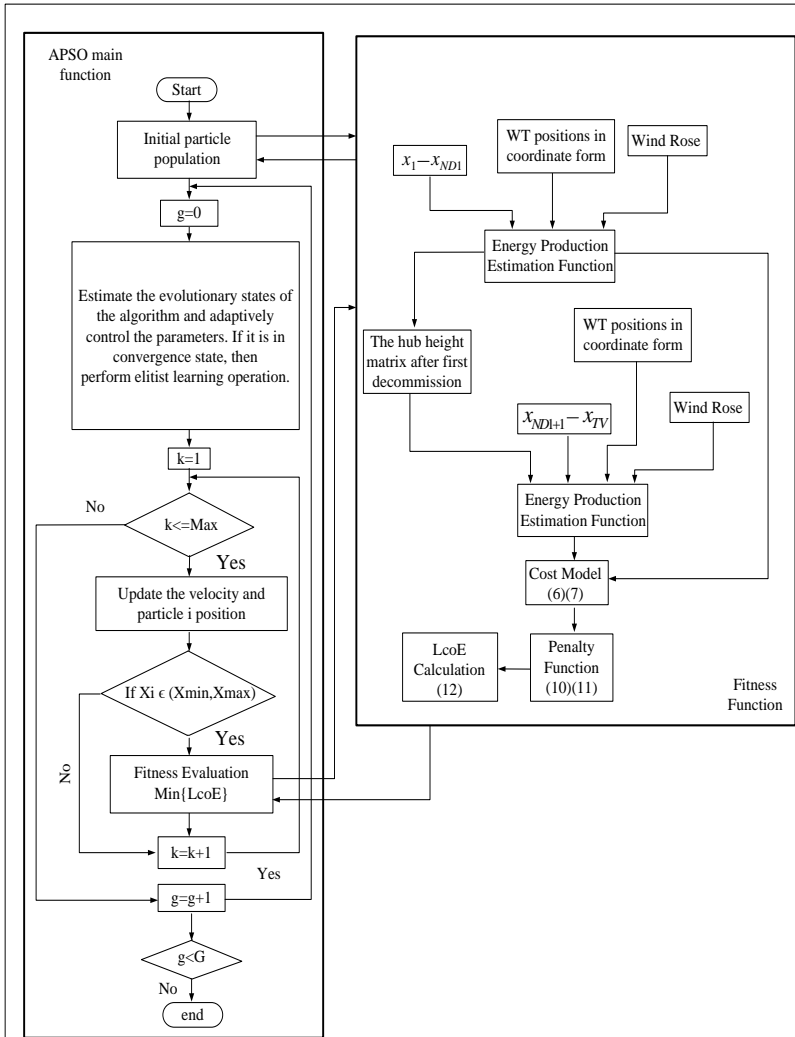
Figure 3 The flowchart of energy yields estimation.



246  
247

248 To estimate the wake losses for the wind farm with mixed types of WTs, a hub height matrix is defined.  
 249 Using the 3D wake model, the hub height and energy production is presented for each WT. Based on  
 250 these information, the proposed repowering strategy optimization framework can be concluded in figure  
 251 5.

Figure 4 The optimization framework.



253  
254

255 As can be seen in figure 4, the parameters for APSO are initialized in the first step. A randomly generated  
 256 particle, which contains two pieces of information: the selection of WT in each of the original WT  
 257 locations for both repowering processes will be generated first and transfer into Energy Production  
 258 Estimation Function where the hub height matrix ( $Ma$ ) for the first repowering process will be  
 259 recomputed according to the information in  $x_1$  through  $x_{ND1}$ . Together with the statistical model, wind rose,  
 260 and the given locations of WTs, the energy production of this wind farm can then be calculated. The  
 261 process has been illustrated in figure 3. Following the same procedure, the energy yields of the wind farm  
 262 after the second repowering process will be calculated. Consequently, the LCoE of this wind farm can be  
 263 obtained by considering the cost of these two repowering processes, which, as described earlier, is related  
 264 to the selection of WTs in each location. The first calculated LCoE as well as the corresponding  
 265 repowering strategy,  $x$ , will be saved as the initial population and used for comparison in the optimization  
 266 process. The fitness function will be triggered when a new position is loaded and  $x$  as well as its speed  $v$   
 267 will be updated according to (8) and (9) to find the minimum LCoE. The above procedure does not stop

268 the PSO main function until the fitness value does not change for 50 iterations. Finally, the optimized  
 269 repowering strategy,  $x$ , which yields the minimum LCoE, will be selected.

### 270 3.3 Assumptions

271 In order to implement the program, some assumptions are made as follows:

- 272 • In this work, it is assumed that all the wind turbines will be replaced by using the proposed  
 273 repowering strategy twice. (The second repowering happens 4 years after the first repowering.)
- 274 • The repowering period would have an impact on the energy production. This effect is neglected  
 275 to simply the problem.
- 276 • Due to the continuous enhancement of integration of wind energy, the Danish electricity price  
 277 will decrease [37]. In this work, the electricity price is assumed to be linearly decrease with  
 278 1%/year.
- 279 • The new constructed wind farm is expected to be operated for 23 years which is counted from the  
 280 time that the new wind farm is completely constructed.
- 281 • After years of operation, the WT's will not have its original performance, which means that the  
 282 old WT will generate less energy. This kind of problem is neglected in this work.
- 283 • The increased cost of foundation for installing bigger WT is assumed to be the cost difference  
 284 between the bigger foundation and the original one.

### 285 4. Case Study

286 In this section, the input database and three scenarios are presented. Hereafter, the results are collected,  
 287 analyzed and discussed.

288

#### 289 4.1 Database

290 In order to make the reused wind farm cost-effective, several wind turbines with different characteristics  
 291 are considered and specified in Table 2.

292

293

Table 2 Specification of Wind Turbines

Type	Siemens 1.3 (I)	Vestas V90-1.8 (II)	Vestas V80-2.0 (III)	Siemens 2.3 (IV)	Siemens 3.6 (V)	NREL 5MW (VI)	DTU 10 MW (VII)
Rated Power (MW)	1.3	1.8	2	2.3	3.6	5	10
Cut-in Wind Speed (m/s)	4	4	4	4	4	3	4
Rated Wind Speed (m/s)	17	13	14.5	16	17	11.4	11.4
Cut-out Wind Speed (m/s)	25	25	25	25	25	25	25
Rotor Diameter (m)	62	90	80	93	107	126	178.3
Hub Height (m)	60	80	67	80	80	90	119

294

#### 295 4.2 Wind Farm Design

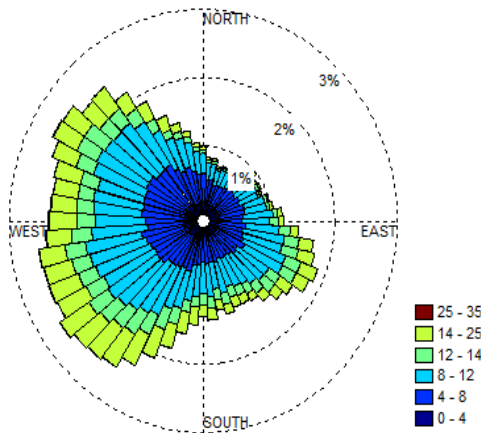
296 In order to make the optimization strategy useful in practice, the simulations have been conducted using a  
 297 real operating offshore wind farm, Horns Rev 1, located off the western shore of Denmark in the Nordic  
 298 Sea [38]. The wind farm were commissioned in 2002, why the findings in this paper very well could be  
 299 applied in a few years for this particular wind farm. The wind farm itself has a size of 160 MW based on  
 300 80 wind turbines with a hub height of 70. The layout of the wind farm is presented in figure 2 of section  
 301 3.

302 As can be seen in figure 3, the layout of the wind farm has a rectangular shape. The distances between the  
303 wind turbines are 7 rotor diameters (560m).  
304

### 305 4.3 Wind Data

306 In order to estimate the changes in energy output when removing wind turbines, wind data from a  
307 mesoscale source, EMD ConWx [39], has been applied in 75 meters height, which is comparable to the  
308 hub height of 70 meters for the currently installed wind turbines. Figure 6 presents the wind conditions at  
309 Horns Rev 1 by revealing the wind rose and the wind distribution.  
310

311 **Figure 5 Wind rose of average wind speed from year 2002 to 2015.**



312 It becomes clear that Horns Rev 1 is experiencing winds from west-southwest. Hence, it is assumed that  
313 the WTs which are distributed in this direction are more likely to be replaced in the first repowering  
314 process, due to additional loads. That being said, wake effects can have increased the loads significantly  
315 for the remaining WTs, due to increased turbulence intensity in the WT rows in the middle and at the  
316 back of the wind farm.  
317

### 318 4.4 Results and Discussion

319 The proposed repowering strategy is compared with two other repowering methods in this section in the  
320 following.

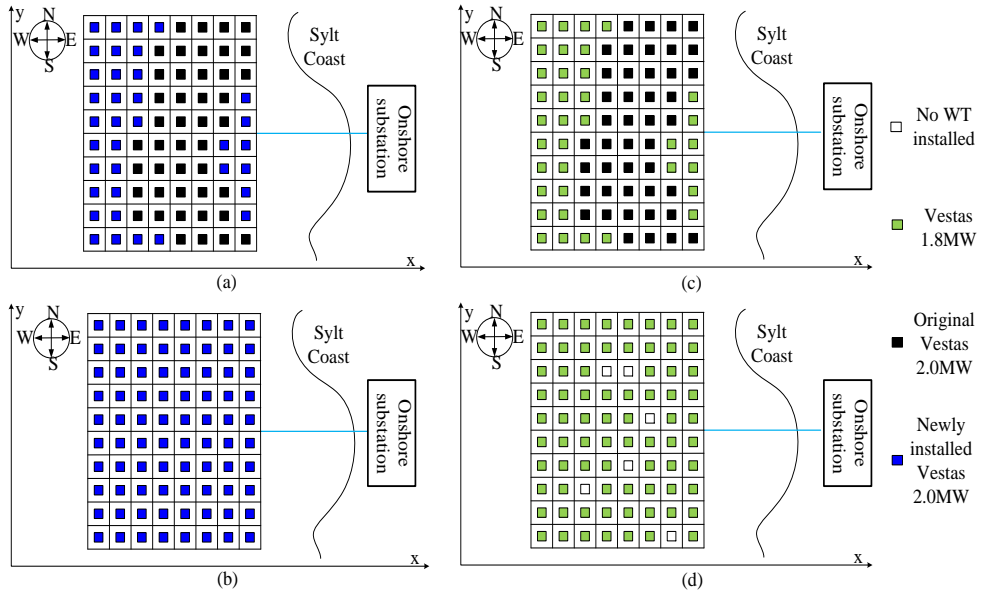
#### 321 4.4.1 Scenario I: New for Old

322 In this scenario, the WTs will be replaced with the original type of WT once they are broken. Since the  
323 foundation of WT is usually oversized, the foundation cost could be saved in this case. The result is  
324 concluded in Table 3.  
325

#### 326 4.4.2 Scenario II: Optimized Repowering Strategy

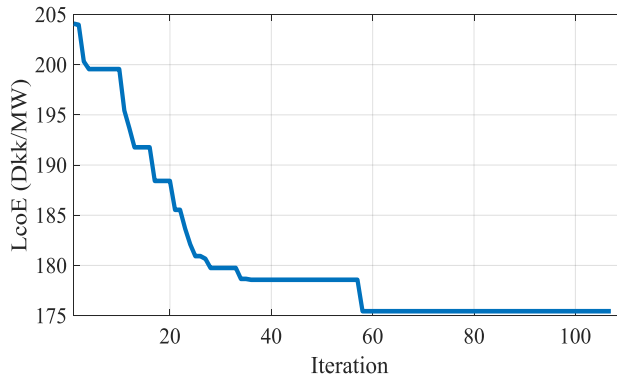
327 In this scenario, the “break” WTs in each repowering period will be replaced so that a new offshore wind  
328 farm is constructed. As mentioned in 3.1, the replacement of bigger WT will introduce some extra cost on  
329 strengthening the foundation which is specified in 3.2.3.

330 The simulation results after each replacement period are shown in figure 6. Using the stochastic  
331 optimization method given in this paper, the type of WT which can give the minimum LCoE of the  
332 offshore wind farm is selected. The simulation results are listed in Table 4. For scenario II, the objective  
333 value corresponds to each iteration is as figure 7.



334  
 335 **Figure 6 Repowering result after each replacing period. (a) the WT selection after first repowering in scenario I. (b) the**  
 336 **WT selection after second repowering in scenario I. (c) the WT selection after first repowering in scenario II. (d) the WT**  
 337 **selection after second repowering in scenario II.**

338 Figure 6 (a) and (c) shows the results after first repowering phase, the black blocks are the original WTs  
 339 and the newly installed WTs are illustrated in blue (scenario I) or green (scenario II) while figure 6 (b)  
 340 and (d) shows the result after the second repowering phase, assumed to take place 4 years after the first  
 341 repowering has been finalized.



342  
 343 **Figure 7 LCoE by iteration for scenario II.**

344 It can be seen from figure 7 that the result stabilized between the 57<sup>th</sup> and 107<sup>th</sup> iterations which is treated  
 345 as the final result obtained by APSO. The details of each repowering strategy are shown in Tables 3 and 4  
 346 while the comparisons between different scenarios are given in Table 5 as follows.  
 347

**Table 3 Specification of scenario I**

	Capacity (MW)	Number of other types of WT Newly Installed	Number of 2MW WT Newly Installed	Power Production (MW)	Capacity Factor (%)
1 <sup>st</sup> repowering	160	0	36	82.5	51.08
2 <sup>nd</sup> repowering	160	0	44	82.5	51.08

349

350

351

352

353

354

In this scenario, the performance reduction due to machine aging is neglected and the broken WTs are replaced with the same type of WTs in each repowering process so that the energy yields after each repowering optimization are the same.

**Table 4 Specification of scenario II**

	Capacity (MW)	Number of other types of WT Newly Installed	Number of 5MW WT Newly Installed	Power Production (MW)	Capacity Factor (%)
1 <sup>st</sup> repowering	268	0	36	123.1	50.64
2 <sup>nd</sup> repowering	400	0	44	183.1	55.16

355

356

357

358

359

360

361

362

363

364

365

366

367

Compared Table 4 with 3, it can be seen that after 1<sup>st</sup> repowering the capacity factor of scenario II is just a little bit lower compared with the result of scenario I while after 2<sup>nd</sup> repowering, the capacity factor of scenario II becomes 7.99% higher than scenario I. This is because in this scenario smaller WTs with a small rotor diameter are installed while the original wind farm layout is designed according to a larger WT. This results in lower wake losses and thus the capacity factor is increased. It is interesting to see that bigger WT is not selected in scenario II which contradicts with the common sense that bigger WT installation can give more cost effective wind farm. This is because the studied wind farm in this case is designed for 2.0 MW WT which means the distances between pair of WTs are relatively smaller for bigger WT. If bigger WT are adopted, then the 4D distance constraint will be violated. On the other side, the original wind farm is always designed according to the onsite wind resources while bigger WT also need higher wind speed to drive. Hence, the 1.8MW WT is selected by the program.

**Table 5 Comparison of different repowering strategies**

	LCoE (Dkk/MW)	Net Present Value of Total Cost related to foundations (MDkk)	Net Present Value of Total cost of WTs (MDkk)	Net Present Value of overall cost (MDkk)
Scenario I	204.08	0	1973.1	1973.1
Scenario II	175.44	0	1652.9	1652.9

368

369

370

371

372

## 5. Conclusions

373

374

This research introduces a novel strategy for repowering WTs in offshore wind farms, in order to maximize the value of a wind farm investment. The results are obtained using the data from an actual



375 offshore wind farm, Horns Rev 1, and by simulating various optimization scenarios in order to reveal the  
376 proper strategy. The APSO algorithm revealed the best solution after 510 iterations, where the minimum  
377 LCoE, 14.03% smaller than in the control scenario was achieved. The proposed method can be used by  
378 stakeholders in the wind industry to forecast investment opportunities by planning changes in the wind  
379 farm layout when repowering WTs.

380 The results presented in this research are based on a specific wind farm, while the method itself should be  
381 applied for other wind farms where repowering could be considered. The advantage of applying the  
382 approach presented here relies on the opportunity of comparing several WT types as input, which  
383 eventually benefits the wind project developer. Furthermore, it is assumed that an awareness of which  
384 WTs should be repowered and when will result in an increase on the return on investment in the final  
385 years of the wind farm lifetime.

386 Different from standard offshore wind farm decommissioning, the “recycling idea”, that is, repowering is  
387 quantitatively analyzed in this work. If a recycled wind farm project can be launched, it would encourage  
388 more investors to participate since the proposed strategy requires less capital investment and construction  
389 time compared with the construction of a new wind farm, which might not only be a barrier for some  
390 investors who do not have enough funds, but also not decrease the levelized cost of wind energy.

391 Besides the obvious financial benefits of applying the proposed repowering approach, which ultimately  
392 lowers the cost of wind energy, the results of this research also benefit the environment, both on a micro-  
393 and mesoscale, as the local marine life has adjusted to the foundations, and new foundations would mean  
394 additional emission of polluting gasses.

395 For further research, this approach could be extended by considering transportation between WTs, cabling,  
396 etc. so a comprehensive analysis can be conducted.

397

### 398 **Acknowledgments**

399 Authors would like to thank Norwegian Centre for Offshore Wind Energy (NORCOWE) under grant  
400 193821/S60 from Research Council of Norway (RCN).

401

402

403

404

405

406

407

408

409

410

411

412

413

414

415

416

417

418

419

420

421

422

423 **Appendices**  
 424 **Nomenclature**

Variable	Unit	Description
$h_0$	m	Hub height of WT
$Ma(i, j)$		Element of shaping matrix M at row i, column j
$R_0$		WT's rotor radius
$S_0$	m <sup>2</sup>	Swept area of WT's rotor with radius $R_0$
$S_{0l,ij}$	m <sup>2</sup>	The wake effect region of downstream WT at row i, column j
$V_{ij}$	m/s	Wind speed deficit generated by the WT at i <sup>th</sup> row, j <sup>th</sup> column of wind farm
$V_{ij}(\alpha, V_{0,ij})$	m/s	Wind speed of the upstream WT (WT) when the inflow wind direction angle is $\alpha$ and velocity is $V_{0,ij}$
$V_{nm}(\alpha, V_{0,ij})$	m/s	Wind speed of the upstream WT when free wind direction angle is $\alpha$ and velocity is $V_{0,ij}$
$V_{ref}$	m/s	Measured wind speed at height
$V_{0,ij}$	m/s	Wind velocity at the blade of WT at i <sup>th</sup> row, j <sup>th</sup> column of wind farm
$x_i, y_i$	m	Position of the downstream WT in coordinate system
$z_0$		Surface roughness
$z_{ref}$		Reference height for the measured wind speed
$z_{ij}$	m	Hub height of WT at row i, column j
$P_{e,nm}$	MW	Mechanical power generated by WT i
$v_{nm}$	m/s	Wind speed at WT i
$P_{tot,t}$	MW	Total power production during interval t
$T_E$	day	Duration interval for energy yields calculation
$T_i$	hour	Duration when the wind farm generating power of $P_{tot,t}$
$t$	hour	Energy yields calculation time
$E_{tot,av}(x_i)$	MWh	Mean energy yields in one year when the WT's positions are $(x_i, y_i)$
$M$		Sequence index of repowering
$M$		Number of replacing cycle
$N_m$		The starting time when the repowering strategy happens ( $N_1$ is 1, $N_2$ is 4)
$C_{f,m}$	Million Dkk	Cost of foundation incl. installation at year $N_m$
$C_{f,o}$	Million Dkk	Cost of original foundation incl. installation
$C_{WT,m}$	Million Dkk	Cost of new installed WT at year $N_m$
$R$		Discounted rate
$ND_1$		Number of optimization variables for the first repowering process
$TV$		Total number of optimization variables
$N$		Total number of WT's
$C_{p,nm}$		Power efficiency of WT at row m, col n

425  
 426 **Reference**

427 [1] M. Bilgili, A. Yasar and E. Simsek, "Offshore wind farm development in Europe and its comparison with  
 428 onshore counterpart," Renewable and Sustainable Energy Reviews, vol. 15, pp. 905-915, 2011.  
 429 [2] Heba Hashem, "Offshore decommissioning market is emerging, but is wind industry prepared," Wind  
 430 Energy Update, 2017. [Online]. Available: [http://analysis.windenergyupdate.com/operations-](http://analysis.windenergyupdate.com/operations-maintenance/offshore-decommissioning-market-emerging-wind-industry-prepared)  
 431 [maintenance/offshore-decommissioning-market-emerging-wind-industry-prepared](http://analysis.windenergyupdate.com/operations-maintenance/offshore-decommissioning-market-emerging-wind-industry-prepared).  
 432 [3] Hans Kerkvliet, Heraclides Polatidis, "Offshore wind farms' decommissioning: a semi quantitative Multi-  
 433 Criteria Decision Aid framework," Sustainable Energy Technologies and Assessments, vol. 18, pp.69-79,  
 434 2016.

- 435 [4] Eva Topham, David McMillan, "Sustainable decommissioning of an offshore wind farm," *Renewable*  
436 *energy*, vol. 102, pp. 470-480, 2017.
- 437 [5] J. Welstead, R. Hirst, D. Keogh, G. Robb, R. Bainsfair, Scottish Natural Heritage Commissioned Report  
438 No. 591, Research and guidance on restoration and decommissioning of onshore wind farms, 2013.  
439 [Online]. Available: [http://www.snh.org.uk/pdfs/publications/commissioned\\_reports/591.pdf](http://www.snh.org.uk/pdfs/publications/commissioned_reports/591.pdf).
- 440 [6] Vattenfall starts first ever offshore wind farm dismantling, *OffshoreWIND.biz*, 2016. [Online]. Available:  
441 <http://www.offshorewind.biz/2015/12/04/vattenfall-starts-first-ever-offshore-wind-farm-dismantling/>.
- 442 [7] The First Offshore Wind Farm Decommissioning Complete, 2016. The Maritime Executive. *MarEx*,  
443 [Online]. Available: [http://www.maritime-executive.com/article/firstoffshore-wind-farm-decommissioning-](http://www.maritime-executive.com/article/firstoffshore-wind-farm-decommissioning-complete)  
444 [complete](http://www.maritime-executive.com/article/firstoffshore-wind-farm-decommissioning-complete).
- 445 [8] LORC, "www.lorc.dk," 2016. [Online]. Available: <http://www.lorc.dk/offshore-wind-farms-map/list>.
- 446 [9] United Nations Convention on the Law of the Sea, 1958.  
447 [http://www.un.org/depts/los/convention\\_agreements/texts/unclos/unclos\\_e.pdf](http://www.un.org/depts/los/convention_agreements/texts/unclos/unclos_e.pdf).
- 448 [10] Decommissioning of Offshore Renewable Energy Installations under the Energy Act 2004, Department of  
449 Energy and Climate Change, 2011. [Online]. Available:  
450 [https://www.gov.uk/government/uploads/system/uploads/attachment\\_data/file/80786/orei\\_guide.pdf](https://www.gov.uk/government/uploads/system/uploads/attachment_data/file/80786/orei_guide.pdf).
- 451 [11] Coast Protection Act, Irish Statute Book, 1963. [Online]. Available:  
452 <http://www.irishstatutebook.ie/eli/1963/act/12/enacted/en/print>.
- 453 [12] Paul Ekins, Robin Vanner, James Firebrace, "Decommissioning of offshore oil and gas facilities: A  
454 comparative assessment of different scenarios," *Journal of Environmental Management*, Vol. 79, Issue: 4,  
455 pp. 420-438, June 2006.
- 456 [13] A. Bonou, A. Laurent and S. I. Olsen, "Life cycle assessment of onshore and offshore wind energy-from  
457 theory to application," *Applied Energy*, vol. 180, p. 327-337, 2016.
- 458 [14] J. Kaldellis, D. Apostolou, M. Kapsali and E. Kondili, "Environmental and social footprint of offshore  
459 wind energy. Comparison with onshore counterpart," *Renewable Energy*, vol. 92, pp. 543-556, 2016.
- 460 [15] K. Smyth, N. Christie, D. Burdon, J. P. B. R. Atkins and M. Elliott, "Renewables-to-reefs? –  
461 Decommissioning options for the offshore wind power industry," *Marine Pollution Bulletin*, vol. 90, p.  
462 247-258, 2015.
- 463 [16] M. J. Kaiser and B. Snyder, "Modeling the decommissioning cost of offshore wind development on the  
464 U.S. Outer Continental Shelf," *Marine Policy*, vol. 36, p. 153-164, 2012.
- 465 [17] Energistyrelsen, "www.ens.dk," 2016. [Online]. Available: [http://www.ens.dk/sites/ens.dk/files/info/tal-](http://www.ens.dk/sites/ens.dk/files/info/tal-kort/statistik-noegletal/oversigt-energisektoren/stamdataregister-vindmoeller/anlaegprodilnettet.xls)  
466 [kort/statistik-noegletal/oversigt-energisektoren/stamdataregister-vindmoeller/anlaegprodilnettet.xls](http://www.ens.dk/sites/ens.dk/files/info/tal-kort/statistik-noegletal/oversigt-energisektoren/stamdataregister-vindmoeller/anlaegprodilnettet.xls).
- 467 [18] S. Bradley, End of Life Opportunities, Energy Technology Institute, 2014.
- 468 [19] O. Yanguas Minambres, "Assessment of Current Offshore Wind Support Structures Concepts: Challenges  
469 and Technological Requirements by 2020," *Karlsruhochschule International University*, 2012.
- 470 [20] C. Birkeland, "Assessing the Life Cycle Environmental Impacts of Offshore Wind Power Generation and  
471 Power Transmission in the North Sea," *Norwegian University of Science and Technology Department of*  
472 *Energy and Process Engineering*, 2011.
- 473 [21] Life Cycle Assessment of Offshore and Onshore Sited Wind Farms, *Elsam Engineering*, 2004.  
474 <http://www.apere.org/manager/>.
- 475 [22] Eric Lantz, Michael Leventhal, Ian Baring-Gould, "Wind Power Project Repowering: Financial Feasibility,  
476 Decision Drivers, and Supply Chain Effects," Technical report, National renewable energy laboratory,  
477 2013.
- 478 [23] Jiang Luqing, Zheng Xilai, Liang Chun, Yue Feng, Zhang Junjie, "The Disposition and Management  
479 Strategy of Decommissioning Offshore Oil Platform in Chengdao, China Energy Procedia," 2010  
480 International Conference on Energy, Environment and Development - ICEED2010, Vol. 5, p. 525-528,  
481 2011.
- 482 [24] Salem Y. Lakhala, M.I. Khanb, M. Rafiqul Islamb, "An "Olympic" framework for a green  
483 decommissioning of an offshore oil platform," *Ocean & Coastal Management*, Vol. 52, Issue: 2, p. 113-  
484 123, February 2009.
- 485 [25] S. Mathew, *Wind Energy: Fundamentals, Resource Analysis and Economics*, 1st ed., New York: Springer,  
486 2006.
- 487 [26] P. Hou, W. Hu, M. Soltani and Z. Chen, "A New Approach for Offshore Wind Farm Energy Yields  
488 Calculation with Mixed Hub Height Wind Turbines," Boston, 2016.
- 489 [27] W. Qiao, "Intelligent mechanical sensorless MPPT control for wind energy systems," San Diego, 2012.

- 490 [28]J. S. González, A. G. Gonzalez Rodriguez, J. C. . Mora, J. R. Santos and M. B. Payan, "Optimum wind  
491 turbines operation for minimizing wake effect losses in offshore wind farms," *Renew. Energy*, vol. 35, p.  
492 1671–1681, 2010.
- 493 [29]Danish Wind Industry Association, "www.windpower.org," 2003. [Online]. Available: [http://xn--drmstre-  
494 64ad.dk/wp-content/wind/miller/windpower%20web/en/tour/rd/foundat.htm](http://xn--drmstre-64ad.dk/wp-content/wind/miller/windpower%20web/en/tour/rd/foundat.htm).
- 495 [30]Y. Shi and R. C. Eberhart, "Empirical study of particle swarm optimization," *Proc. Congr. Evol. Comput.*,  
496 p. 1950–1955, 1999.
- 497 [31]E. C. Laskari, K. E. Parsopoulos and M. N. Vrahatis, "Particle Swarm Optimization for Integer  
498 Programming," *Proceedings of the 2002 Congress on Evolutionary Computation*, vol. 2, pp. 1582-1587,  
499 2002.
- 500 [32]B. Jiao, Z. Lian and X. Gu, "A dynamic inertia weight particle swarm optimization algorithm," *Chaos,  
501 Solitons Fractals*, vol. 37, p. 698–705, 2008.
- 502 [33]R. C. Eberhart and Y. Shi, "Tracking and optimizing dynamic systems with particle swarms," *Proc. Congr.  
503 Evol. Comput.*, p. 94–100, 2001.
- 504 [34]Z.-H. Zhan, J. Zhang, Y. Li and H. S.-H. Chung, "Adaptive particle swarm optimization," *IEEE Trans.  
505 Syst.*, vol. 39, p. 1362–1381, 2009.
- 506 [35]Hu M, Wu T, Weir JD, "An intelligent augmentation of particle swarm optimization with multiple adaptive  
507 methods," *Inf Sci*, Vol. 213, p. 68-83, Dec. 2012.
- 508 [36]B. Pérez, R. Mínguez, and R. Guanache, "Offshore wind farm layout optimization using mathematical  
509 programming techniques," *Renew. Energy*, vol. 53, pp. 389–399, May 2013.
- 510 [37]W. Hu, Z. Chen and B. B. Jensen, "The Relationship Between Electricity Price and Wind," 2010.
- 511 [38]Dong, "www.dongenergy.com," 2016. [Online]. Available: [http://www.dongenergy.com/da/vores-  
512 forretning/wind-power/hvor-vi-er-aktive/horns-rev-1](http://www.dongenergy.com/da/vores-forretning/wind-power/hvor-vi-er-aktive/horns-rev-1).
- 513 [39]EMD, "www.emd.dk," 2016. [Online].
- 514 [40]M. R. Bøndergaard, "The Future of Wind Energy in Denmark - Reducing the Cost and Increasing the Value  
515 of Wind," IEA Report Launch: Cost Reduction for Onshore Wind – Status and Perspectives, Copenhagen ,  
516 2015.



ISSN (online): 2446-1636  
ISBN (online): 978-87-7112-900-7

AALBORG UNIVERSITY PRESS